David Taylor Research Center

Bethesda, MD 20084–5000

DTRC–92/012   December 1992

A Review of Statistical Studies of Seakeeping Qualities

by Yasufumi Yamanouchi

The Tenth David W. Taylor Lectures

93-24702

Approved for public release; distribution is unlimited.

REPORT DOCUMENTATION PAGE

1a. REPORT SECURITY CLASSIFICATION UNCLASSIFIED		1b. RESTRICTIVE MARKINGS			
2a. SECURITY CLASSIFICATION AUTHORITY		3. DISTRIBUTION/AVAILABILITY OF REPORT Approved for public release; distribution is unlimited.			
2b. DECLASSIFICATION/DOWNGRADING SCHEDULE					
4. PERFORMING ORGANIZATION REPORT NUMBER(S) DTRC–92/012		5. MONITORING ORGANIZATION REPORT NUMBER(S)			
6a. NAME OF PERFORMING ORGANIZATION David Taylor Research Center	6b. OFFICE SYMBOL *(If applicable)* Code 1540	7a. NAME OF MONITORING ORGANIZATION			
6c. ADDRESS *(City, State, and ZIP Code)* Bethesda, Maryland 20084–5000		7b. ADDRESS *(City, State, and ZIP Code)*			
8a. NAME OF FUNDING/SPONSORING ORGANIZATION	8b. OFFICE SYMBOL *(If applicable)*	9. PROCUREMENT INSTRUMENT IDENTIFICATION NUMBER			
8c. ADDRESS *(City, State, and ZIP Code)*		10. SOURCE OF FUNDING NUMBERS			
		PROGRAM ELEMENT NO.	PROJECT NO.	TASK NO.	WORK UNIT ACCESSION NO.

11. TITLE *(Include Security Classification)*
A Review of Statistical Studies of Seakeeping Qualities

12. PERSONAL AUTHOR(S)
Yamanouchi, Yasufumi

13a. TYPE OF REPORT Final	13b. TIME COVERED FROM_____ TO_____	14. DATE OF REPORT *(YEAR, MONTH, DAY)* 1992, December	15. PAGE COUNT 437

16. SUPPLEMENTARY NOTATION

17. COSATI CODES			18. SUBJECT TERMS *(Continue on reverse if necessary and identify by block number)*
FIELD	GROUP	SUB–GROUP	See reverse side.

19. ABSTRACT *(Continue on reverse if necessary and identify by block number)*

In Part I, the general procedures of the conventional method of correlation or spectrum analysis of a random process (nonparametric method) are reviewed, stressing the statistical reliability of the results. A few suggestions for improving coherencies are given. In Part II, the characteristics of AR, MA, and ARMA models are discussed. The model–fitting technique supported by AIC criteria is introduced, with the examples of application to seakeeping data. In Part III, the statistical treatments of nonlinearities in random process analysis are summarized and reviewed. Conclusions are given, and future work is proposed.

20. DISTRIBUTION/AVAILABILITY OF ABSTRACT ☒ UNCLASSIFIED/UNLIMITED ☐ SAME AS RPT ☐ DTIC USERS	21. ABSTRACT SECURITY CLASSIFICATION UNCLASSIFIED	
22a. NAME OF RESPONSIBLE INDIVIDUAL Justin H. McCarthy	22b. TELEPHONE *(Include Area Code)* (301) 227–1609	22c. OFFICE SYMBOL Code 1540

DD FORM 1473, JUN 86   *Previous editions are obsolete.*

Block 18 (Continued)

A review of statistical studies. seakeeping qualities. stochastic processes, parametric analysis of time series. nonparametric analysis of time series, spectrum analysis. nonlinear stochastic process analysis. model fitting techniques to a time series, AR model. MA model, ARMA model, and AIC criterion.

Accesion For		
NTIS CRA&I		A
DTIC TAB		☐
Unannounced		☐
Justification		
By		
Distribution /		
Availability Codes		
Dist	Avail and / or Special	
A-1		

CONTENTS

CONTENTS (Continued)

CONTENTS (Continued)

CONTENTS (Continued)

CONTENTS (Continued)

FIGURES

FIGURES (Continued)

TABLES

THIS PAGE INTENTIONALLY LEFT BLANK

FOREWORD

For several reasons, the publication of this report was postponed for several years. Its contents were summarized at the time of this author's oral presentation at DTRC in July 1985, reflecting the state–of–the–art up to 1984. The manuscript of the written version was completed in August 1987 and is now to be published five years later in 1992. During these years the state–of–the–art has made considerable progress, and this author finds the "review" to be insufficient, especially in Part III because of the recent works of several researchers. In order to update the report this author has added a "Supplement of References," (Refs. 101–124) listing publications that have appeared since 1984, together with some other publications that he had failed to refer to in the original manuscript.

THIS PAGE INTENTIONALLY LEFT BLANK

PREFACE

The David W. Taylor Lectures were initiated as a living memorial to our founder in recognition of his many contributions to naval architecture and naval hydrodynamics. Admiral Taylor was a pioneer in the use of hydrodynamic theory and mathematics for the solution of naval problems. The system of mathematical lines developed by Taylor was used to develop many ship designs for the Navy long before the computer was invented. He founded and directed the Experimental Model Basin; perhaps most important of all, he established a tradition of applied scientific research at the "Model Basin" which has been carefully nurtured through the decades and which we treasure and protect today. In the spirit of this tradition, we invite an eminent scientist in a field closely related to the Center's work to spend a few weeks with us, to consult with and advise our working staff, and to give a series of lectures on subjects of current interest.

Our tenth lecturer in this series is Dr. Yasufumi Yamanouchi who is currently Technical Advisor to Mitsui Engineering and Shipbuilding Co., Ltd. Dr. Yamanouchi graduated from the Tokyo University in 1943 and received his Dr. Eng. from there in 1962. For many years (1946–73), he served with the Governmental Research Institute on

Ship Technology, that changed its name from Railway Technical Research Institute (1946–50), then to Transportation Technical Research Institute (1950–63), and finally to Ship Research Institute, Ministry of Transport. He was Head of the Ship Performance

xxi

Division (1962–63) and Head of the Ship Dynamics Division (1963–69), then Deputy General Director (1969–72) and finally Director–General of the Ship Research Institute (1972–73), Ministry of Transport in Tokyo, Japan. He joined Mitsui Engineering and Shipbuilding Co., Ltd. as Senior Deputy Director, advancing to Technical Director upon his retirement in 1983. He contributed to the construction and organization of a new research laboratory, and was the first General Manager of the Akishima Laboratory of Mitsui from 1975 to his retirement in 1983. He was Professor at the College of Science and Technology (1982–89) of Nihon University in Tokyo, Japan.

Dr. Yamanouchi has had a long and distinguished scientific career, with pioneering publications on ship dynamics, ocean waves and stochastic processes. He is no stranger to the United States, having done research at the Davidson Laboratory of Stevens Institute of Technology from 1957–60 and having served as Visiting Professor at the U.S. Naval Academy during 1984–85. We are most honored that he agreed to be a David W. Taylor Lecturer.

ABSTRACT

In Part I, the general procedures of the conventional method of correlation or spectrum analysis of a random process (nonparametric method) are reviewed, stressing the statistical reliability of the results. A few suggestions for improving the coherencies are given. In Part II, the characteristics of AR, MA, and ARMA models are discussed. The model–fitting technique supported by AIC criteria is introduced, with the examples of application to the seakeeping data. In Part III, the statistical treatments of nonlinearities in random process analysis are summarized and reviewed. Conclusions are given, and future work is proposed.

1

CHAPTER 1

INTRODUCTION

1.1 PROLOGUE

In the summer of 1951, a group of research naval architects who were scheduled to be on board the cargo ship Nissei–Maru cruising the Pacific from Japan to the United States was discussing the design of a system for measuring, recording, and analyzing actual ship performance data. Such a system was needed for the first large–scale cooperative test,[1] organized by the Japan Towing Tank Committee (JTTC) of the Society of Naval Architects of Japan (SNAJ) and scheduled to start at the end of the year, to provide a basis for the post–World War II study of hydrodynamic ship performance in all the laboratories and universities in Japan.

To find the relationships between ship's propeller revolutions, shaft horsepower, modes of motion, rudder angle, and so on, we decided to record, simultaneously and as accurately as possible, as many elements of ship performance as possible. Such measurements would provide an overview of the response of the ship. Many practical limitations, such as budget constraints, had to be considered, however. In addition we didn't know the real limits of the accuracy of these kinds of measurements, nor did we know how to choose the proper duration of observation times. After lengthy discussion, it was decided to record each type of measurement for three minutes.

Very few naval architects at that time had a good knowledge of probability or of statistics. We did not know how to analyze the data taken at sea, and we did not know how to estimate the ensemble characteristics of performance from a single sample observation. The simultaneous records of the averages of the 3–minute responses gave us valuable knowledge of actual sea performance, but we realized that simple averages sometimes cover or conceal important information. For ship oscillations, of course, mean values are not significant, but this author could not be satisfied with merely noting the average frequency and mean amplitudes.

During the test, the author[2] was responsible for measuring the ship's relative speed and developed a new type of ship speed meter, based on an idea of Dr. Shiha. This new meter measured the frequency of Karman vortices produced behind a triangular cylinder towed by the ship and gave instant indications of speed variations. Although the towing point was selected to minimize the effects of pitching, heaving, and rolling, these motions did affect the speed of the towed body. The objective was to eliminate the effects of all motions except surging and to derive from these records, by some method, the real variations in the ship's speed relative to the water. The author later found that an advanced technique of multiple input analysis would have been useful.

After the test at sea, we continued to look for methods for analyzing the data and found a stochastic process analysis used in weather forecasting to predict temperature, humidity, precipitation, and so on. The author started at once to study time series analysis and tried first several kinds of periodogram analysis and then correlogram and spectrum analysis.[3] Because of the poor communications in the engineering and scientific fields in Japan at that time (even five years after the war) we had very little information about the outside world until 1954 and were unaware of the pioneering work of Dr. M. St. Denis

and Prof. W. J. Pierson Jr.[4] in 1953. We had to start on our own independent of the achievements in the USA.

1.2 PURSUING THE IMPROVEMENT OF COHERENCY FUNCTIONS

After the bases for the mathematical and statistical theories were established by N. Wiener,[5,6] J. L. Doob,[7] C. E. Shannon,[8] S. O. Rice,[9] and others, mostly in the 1940's, the stochastic analysis techniques were applied in many scientific and engineering fields besides communications and control engineering. These techniques were adopted rather early in the analysis of ocean waves and of a ship's response at sea. This method has been pretty well formulated by the efforts of oceanographers like G. Neumann,[10] W. J. Pierson, Jr.,[11] M. S. Longuet–Higgins,[12] D. E. Cartwright and M. S. Longuet–Higgins,[13] and by the pioneering work of M. St. Denis and W. J. Pierson, Jr.,[4] succeeded by E. V. Lewis,[14] and J. F. Dalzell and Y. Yamanouchi,[15] and is now rather popular with us. We now know that, in practical applications and when applying certain theories, a few statistical considerations are necessary in the numerical computations in order to get reliable results.

In Part I, the author tried to show the problems encountered in sample computations, in the so–called correlation method that are also closely related to the basis for model fitting techniques (that is, the parametric method treated in Part II) and reviews the conventional nonparametric method. The author did not intend to go into detail about the analysis technique.

The coherency function, if properly calculated, is a good index of the extent to which spectrum analysis, as a linear process, is valid for application to a stochastic process. A few results of this author's efforts in this field, presented later in Part I, are related to improvement of the techniques for obtaining a good estimate of coherencies.

1.3 TIME DOMAIN CHARACTERISTICS

Time series analysis is sometimes called spectrum analysis, thus showing that estimation of reliable spectral functions is very important in the analysis of time series.

Spectral functions are surely powerful functions which provide good information on a stochastic process and also resolve the tangled relations of convoluted types in the time domain. However, because of this fact, and also partly because (auto) correlation did not appear in an important way, in St. Denis and Pierson's pioneering paper,[4] rather little attention has been paid by naval architects to the time domain relations over the past few decades. From his first involvement in this study, this author has thought that time domain functions deserved more attention and has made some efforts along this line.

Of course spectral functions and correlation functions are actually the same function expressed in different ways. Sometimes, however, in sample computations, applying the time domain expression helps us understand the characteristics of the stochastic process better, because we are accustomed to expressing the physical process by differential equations that are expressions in the time domain. The time domain expression of stochastic processes helps us in the analysis to use already known characteristics of the process. Moreover, the correlation window operation in the sample computation is just a multiplying operation, whereas the spectral window operation is now an entangled convolution operation that is more complex in real sample computations. In sample computations,

consideration of the windows is very important and also a troublesome problem to get reliable results.

Parametric estimation of the spectral function, explained in Part II, is a method of fitting a certain statistical model to the process to be analyzed and then estimating the parameters of that model. This method is based on time domain characteristics, and the model fitted is closely related to the equations of motion of the process itself. The method represents a different approach to spectrum analysis and, this author believes, that is a promising one, supplementing the conventional nonparametric approach, treated in Part I. So, in Part II, several types of discrete parameter models will be introduced in detail, and then the results of application of the model fitting method to the analysis of seakeeping data will be shown. By this method, the actual response system, in which the output is fed back to the input to some extent, can also be tackled. This kind of system has been hard to be analyzed by the conventional method.

1.4   TREATMENT OF NONLINEARITIES

One of the reasons for low coherencies in linear spectral analysis is the existence of nonlinearities in the response or in the input. So in Part III, the treatment of nonlinearities in process analysis is reviewed. One of the greatest achievements in this field for the analysis of seakeeping data is due to John F. Dalzell[16,17] in the application of polyspectra. This application will not be described in detail, except the basic idea, of this treatment but another review of the treatment of nonlinearities will be given, to make clear the mutual relationships of these several different approaches to the problem. In addition, the treatment of nonlinearity in response characteristics during one trial has been introduced in Section 3.4 in Part I, as an example of multi-input single-output analysis.

1.5   SCOPE OF STUDIES

In statistical studies on seakeeping, there are roughly two kinds of applications. One is based on the invariant characteristics of a ship itself, and its behavior is studied statistically, assuming the excitement from the environment is also stationary. The other involves the macroscopic probabilistic distributions of seakeeping behavior, assuming a variety of changes in environmental conditions. The former is sometimes called short-term statistics, and the latter, long-term statistics. They are, of course, closely related, and the short-term statistics are usually used as the basis for studying the long-term statistics. Here mostly short-term statistics will be treated.

4

PART I
A REVIEW OF SPECTRAL ANALYSIS THROUGH PERIODOGRAM (NONPARAMETRIC SPECTRAL ANALYSIS)

To clarify the problems and difficulties encountered in sample computations and make them the basis for further discussions, the rough scheme of the techniques of spectrum analysis (through periodograms, the popular nonparametric method) will be reviewed first in Chapter 2. Then some ideas proposed by this author for solving these difficulties will be summarized in Chapter 3, Part I. Many text books,[18-23] especially the comprehensive one by Priestley,[23] were used as references in Chapter 2.

CHAPTER 2

BASIC PROCEDURE OF THE SPECTRAL ANALYSIS AND THE PROBLEM OF SAMPLE COMPUTATIONS

2.1 RANDOM PROCESS AND ITS CHARACTERISTICS

Here the general continuous process on t is expressed by $X(t)$, its realization as $x(t)$, and the probability density distribution function related to this process as $p_t(x)$. The general discrete process is X_t, its realization is x_t, and probability distribution density function is $p_t(x)$. Then, as expected values,

$$\text{mean } [X(t)] = E\,[X(t)] = \int_{-\infty}^{\infty} x(t)p_t(x)dx = \mu(t) \tag{2.1}$$

$$\text{var. } [X(t)] = E\left[\left\{(Xt) - \mu(t)\right\}^2\right] = \int_{-\infty}^{\infty} [x(t) - \mu(t)]^2\, p_t(x)dx = \sigma^2(t). \tag{2.2}$$

Usually, the probability density distribution function $p_t(x)$ is a function of t; accordingly, the mean $\mu(t)$ and the variance $\sigma^2(t)$ are also functions of time.

Joint probability density distribution functions, $p_{t_1 t_2 t_3 \ldots t_n}(x_1, x_2, x_3, \ldots x_n)$ exist for all $n, n = 1, 2, \ldots n, (n \to \infty)$ and all $p_{t_1}(x_1), p_{t_2}(x_2), \ldots ; p_{t_1 t_2}(x_1, x_2), \ldots ;$ $p_{t_1 t_2 t_3}(x_1, x_2, x_3), \ldots ; \ldots$ are defined as their marginal functions.

5

Theoretically, if all the joint distribution functions of all orders

$$p_{t_1}(x_1), p_{t_2}(x_2), \ \ldots$$

$$p_{t_1 t_2}(x_1, x_2), p_{t_2 t_3}(x_2, x_3), \ \ldots \ldots$$

$$p_{t_1 t_2 t_3}(x_1, x_2, x_3), \ \ldots \ldots$$

$$\cdot \ \cdot \ \cdot \ \cdot \ \cdot \ \cdot \ \cdot$$

$$p_{t_1 t_2 t_3} \ \cdots \ t_n(x_1, x_2, x_3, \ \ldots \ x_n), \ \ldots \ldots \ldots$$

are known, the probability structure of X_t is completely specified.

2.1.1 Completely Stationary

If

$$p_{t_1 t_2} \ \cdots \ t_n(x_1, x_2, \ \ldots \ x_n) = p_{t_1+k_1 t_2+k_1} \cdots \ t_n+k_1, (x_1, x_2, \ \ldots \ x_n), \quad (2.3)$$

for any $t_1, t_2, \ \ldots \ t_n$ and any k, this process is completely stationary.

2.1.2 Stationary Up to Order m

In this case, the joint moment up to order m should be the same.

$$E\left[\{X(t_1)\}^{m_1}\{X(t_2)\}^{m_2} \ \ldots \ldots \ \{X(t_n)\}^{m_n}\right]$$

$$= E\left[\{X(t_1 + k)\}^{m_1}\{X(t_2 + k)\}^{m_2} \ \ldots \ldots \ \{X(t_n + k)\}^{m_2}\right], \quad (2.4)$$

for all positive integers $m_1, \ m_2, \ \ldots \ m,$

where

$$m_1 + m_2 + \ \ldots \ m_n \leq m.$$

2.1.3 Stationary Up to Order 2

Especially when the order is $m = 2$, the process is called weakly stationary. When the probability density distribution functions are Gaussian, they are completely determined by the means, variances, and covariances of two variables, and accordingly they are completely stationary.

2.1.4 Ergodicity

When the ensemble of the averages across the processes converge to the corresponding time averages along the process over period N (when N tends toward infinity and the mean square is consistent), the process is called ergodic. The ergodicity is a more strict condition than the stationality as is shown in Fig. 2.1.
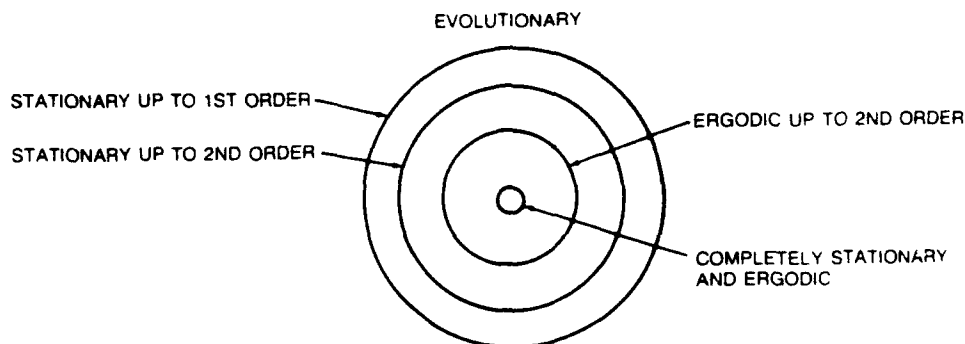
Fig. 2.1. Stationarity and ergodicity.

For example,

$$R(\tau) = F \; [X(t) \cdot X(t + \tau)]$$

$$= \int_{-\infty}^{\infty} \int_{-\infty}^{\infty} x(t)x(t + \tau)p(x_t, x_{t+\tau})dx_t dx_{t+\tau}$$

$$= \lim_{t \to \infty} \frac{1}{T} \int_{0}^{T} x(t)x(t + \tau)dt. \tag{2.5}$$

2.1.5 Summary of Gaussian (Normal) Probability Distribution Functions

For convenience, the Gaussian probability distribution functions for various numbers of variables are summarized here. For a single variable,

$$p(x) = \frac{1}{(2\pi\sigma_x^2)^{1/2}} \; \exp\left[-\frac{1}{2} \frac{(x - \mu_x)^2}{\sigma_x^2} \right]. \tag{2.6}$$

Normalized by $z = (x - \mu_x)/\sigma_x$,

$$p(z) = \frac{1}{\sqrt{2\pi}} \; e^{-\frac{z^2}{2}}. \tag{2.7}$$

For two variables X and Y

7

$$p(x,y) = \frac{1}{2\pi[\sigma_x^2\sigma_Y^2(1-\varrho^2)]^{1/2}} \exp\left[-\frac{1}{2}\left\{\frac{(x-\mu_x)^2}{(1-\varrho^2)\sigma_x^2} - \frac{2\varrho(x-\mu_x)(y-\mu_y)}{(1-\varrho^2)\sigma_x\sigma_Y} + \frac{(y-\mu_y)^2}{(1-\varrho^2)\sigma_Y^2}\right\}\right]$$

$$= \frac{1}{2\pi\Delta^{1/2}} \exp\left[-\frac{1}{2}\left\{\frac{\sigma_Y^2}{\Delta}(x-\mu_x)^2 - \frac{2\varrho\sigma_x\sigma_Y}{\Delta}(x-\mu_x)(y-\mu_Y) + \frac{\sigma_x^2}{\Delta}(y-\mu_Y)^2\right\}\right]$$

$$= \frac{1}{2\pi\Delta^{1/2}} \exp\left[-\frac{1}{2}\left\{\beta_{xx}(x-\mu_x)^2 - 2\beta_{xy}(x-\mu_x)(y-\mu_Y) + \beta_{YY}(y-\mu_Y)^2\right\}\right]. \tag{2.8}$$

Here,

$$\Delta = \left\|\begin{bmatrix}\gamma_{xx} & \gamma_{xy} \\ \gamma_{yx} & \gamma_{yy}\end{bmatrix}\right\| = \left\|\begin{bmatrix}\sigma_x^2 & \varrho\sigma_x\sigma_y \\ \varrho\sigma_x\sigma_y & \sigma_y^2\end{bmatrix}\right\| = \begin{aligned}\sigma_x^2\sigma_y^2 - \varrho^2\sigma_x^2\sigma_y^2 \\ = \sigma_x^2\sigma_y^2(1-\varrho^2),\end{aligned} \tag{2.9}$$

$$\gamma_{xx} = E[X \cdot X] = \sigma_x^2 \quad , \quad \gamma_{xy} = E[X \cdot Y] = \varrho\sigma_x\sigma_y$$

$$\gamma_{yy} = E[Y \cdot Y] = \sigma_y^2 \quad , \quad \gamma_{yx} = E[Y \cdot X] = \varrho\sigma_y\sigma_x. \tag{2.10}$$

$$\{\beta_{ij}\} = \begin{bmatrix}\beta_{xx} & \beta_{xy} \\ \beta_{yx} & \beta_{yy}\end{bmatrix} = \frac{1}{[\gamma]^{-1}} = \frac{1}{[\gamma]}\begin{bmatrix}\gamma_{yy} & -\gamma_{yx} \\ -\gamma_{xy} & \gamma_{xx}\end{bmatrix} = \frac{1}{\sigma_x^2\sigma_y^2(1-\varrho^2)}\begin{bmatrix}\sigma_y^2 & -\varrho\sigma_x\sigma_y \\ -\varrho\sigma_x\sigma_y & \sigma_x^2\end{bmatrix}.$$

$$\tag{2.11}$$

For n variables $X_1, X_2, \ldots \ldots X_n$,

$$p(x_1, x_2, \ldots \ldots x_n) = \frac{1}{(2\pi)^{n/2}\Delta^{1/2}} \exp\left[-\frac{1}{2}\sum_{i=1}^{n}\sum_{j=1}^{n}\sigma^{ij}(x_i-\mu_i)(x_j-\mu_j)\right], \tag{2.12}$$

where

$$\Delta = \left|\Sigma\right| = \det(\Sigma)$$

$$\Sigma = \{\sigma_{ij}\} \tag{2.13}$$

and σ^{ij} is an element of inverse matrix, so that

$$p(x_1, x_2, \ldots \ldots x_n) = \frac{1}{(2\pi)^{n/2}\Delta^{1/2}} \exp\left[-\frac{1}{2}\left\{(x-\mu)'\Sigma^{-1}(x-\mu)\right\}\right]. \tag{2.14}$$

2.2 PROPERTIES REQUIRED FOR ESTIMATOR

The following properties are required for the estimator of some statistical value.

2.2.1 Unbiasedness

As the number of samples n tends toward infinity, for the estimator $\hat{\theta}$ of real θ,

$$\text{bias}(\hat{\theta}) = \left\{E(\hat{\theta}) - \theta\right\} \to 0. \tag{2.15}$$

2.2.2 High Relative Efficiency

If we suppose that both estimators $\hat{\theta}_1, \hat{\theta}_2$ are unbiased, then the higher the

$$\text{rel. effic.} = \text{var.}(\hat{\theta}_1)/\text{var.}(\hat{\theta}_2) \tag{2.16}$$

is, the better estimator $\hat{\theta}_1$ is than $\hat{\theta}_2$.

2.2.3 Small Mean Square Error

Mean square error is defined as

$$
\begin{aligned}
M^2(\hat{\theta}) &= E[(\hat{\theta} - \theta)^2] \\
&= E\left[\left\{\hat{\theta} - E(\hat{\theta})\right\} + \left\{E(\hat{\theta}) - \theta\right\}\right]^2 \\
&= E\left[\left\{\hat{\theta} - E(\hat{\theta})\right\}^2\right] + \left\{E(\hat{\theta}) - \theta\right\}^2 + 2\left\{E(\hat{\theta}) - \theta\right\}E[\hat{\theta} - E(\hat{\theta})] \\
&= \text{var.}(\hat{\theta}) + b^2(\hat{\theta}), \tag{2.17}
\end{aligned}
$$

which should be small. When $M^2(\hat{\theta}_1) < M^2(\hat{\theta}_2)$, we adopt $\hat{\theta}_1$ as better than $\hat{\theta}_2$.

2.2.4 Consistency

As the number of the samples n tends toward infinity, var. $(\hat{\theta}) \rightarrow 0$, and bias $b^2(\hat{\theta}) \rightarrow 0$ must be satisfied. Then the mean square error $M^2(\hat{\theta}) \rightarrow 0$ also stands and is called the "mean square consistency."

2.2.5 Sufficiency

The estimator $\hat{\theta}$ must contain all the information $X_1, X_2, \ldots, X_n$ in the sample, relevant to the estimator of θ

$$\hat{\theta} = \hat{\theta}\ (X_1, X_2, \ldots, X_n).$$

2.3 AUTOCOVARIANCE FUNCTION AND ITS ESTIMATES

When the process $X(t)$ is stationary up to an order of 2, the covariance function

$$\text{cov.}\ [X(t)\ X(t+\tau)] = E\ [\{X(t)-\mu\}\{X(t+\tau)-\mu\}] \equiv R(\tau) \qquad (2.18)$$

is a function of τ only. Then, $\varrho(\tau) = R(\tau)/R(0)$ is called an autocovariance coefficient, and

$$R(0) = E\ [\{X(t)-\mu\}^2] = \text{var.}\ [X(t)] = \sigma^2. \qquad (2.19)$$

When the process is real valued, $R(-\tau) = R(\tau)$ as in Fig. 2.2, and when the process is complex valued, $R(-\tau) = R^*(\tau)$. This function $R(\tau)$ is a measure of similarity in a sense, and is also a measure of the memory of the process. $R(\tau)$ plays a big role later, in the parametric analysis in Part II, in identifying the statistical model that will fit the process. Mean μ, variance σ^2, $R(\tau)$, and $\varrho(\tau)$ are constant by t.
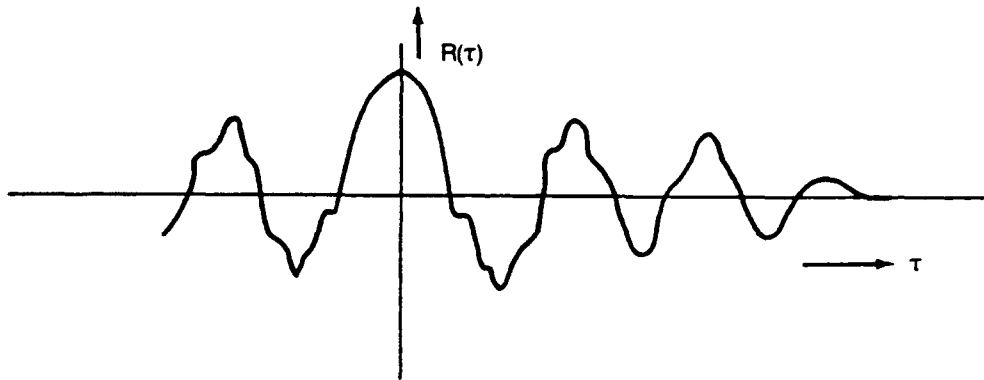
Fig. 2.2. Autocovariance function.

10

2.3.1 Estimates of R(r)

For the discrete parameter process x_t,

$$R(r) = E\ [(X_t - \mu)(X_{t+r} - \mu_{t+r})]$$
$$= E\ [X_t \cdot X_{t+r}], \tag{2.20}$$

when $\mu_t = \mu_{t+r} = E[X_t] = 0$.

2.3.2 Unbiased Estimate

Instead of averaging the ensemble, take the time average as

$$\hat{R}^o(r) = \frac{1}{N - |r|} \sum_{t=1}^{N-|r|} (X_t - \overline{X})\ (X_{t+r} - \overline{X}) \tag{2.21}$$

where $r = 0, \pm 1, \pm 2, \ldots\ldots \pm (N-1)$.

If we ignore the effect of estimating μ by $\overline{X}$, then $R^o(r)$ is an unbiased estimate of $R(r)$, because

$$E\ [\hat{R}^o(r)] = \frac{1}{N - |r|} \sum_{t=1}^{N-|r|} E[(X_t - \mu)(X_{t+r} - \mu)]$$

$$= \frac{1}{N - |r|} \sum_{t=1}^{N-|r|} R(r) = \frac{N - |r|}{N - |r|}\ R(r) = R(r). \tag{2.22}$$

2.3.3 Biased Estimate

On the contrary,

$$\hat{R}(r) = \frac{1}{N} \sum_{t=1}^{N-|r|} (X_t - \mu)(X_{t+|r|} - \mu) \tag{2.23}$$

is a biased estimate, because

$$E[\hat{R}(r)] = \frac{1}{N} \sum_{t=1}^{N-|r|} R(r) = \frac{1}{N}\ (N - |r|)\ R(r) = \left(1 - \frac{|r|}{N}\right) R(r)$$

$$= R(r) - \frac{|r|}{N}\ R(r), \tag{2.24}$$

11

biased by $(|r|/N)\ R(r)$. When $N \rightarrow \infty$, $E[R(r)] \rightarrow R(r)$, and is therefore asymptotically unbiased.

By statistical mathematics, we can get

$$\text{var. } [\hat{R}^o(r)] \rightarrow O(1/(N-|r|)) \qquad (2.25)$$

$$\text{var. } [\hat{R}(r)] \rightarrow O(1/N). \qquad (2.26)$$

1. When r is small relative to N, the difference between $\hat{R}^o(r)$ and $\hat{R}(r)$ is small, and the bias of $[\hat{R}(r)]$ is also small.

2. When r becomes large relative to N and approaches $N-1$, bias $[\hat{R}(r)] \rightarrow R(r)$. However, when $r \rightarrow \infty$, $\hat{R}(r) \rightarrow 0$. Therefore, when N is very large, the bias remains small at all r.

3. When $r \rightarrow (N-1)$,

$$\text{var. } [\hat{R}^o(r)] \sim O(1) \qquad (2.27)$$

$$\text{var. } [\hat{R}(r)] \sim O(1/N). \qquad (2.28)$$

Therefore, the tail of correlation $\hat{R}^o(r)$ shows a wild and erratic behavior. Also, from statistical mathematics, cov. $[\hat{R}(r)\ \hat{R}(r+s)]$ was computed and fairly high correlations between neighboring points were found when s is small. When r tends toward infinity, $R(r) \rightarrow 0$. It can be concluded here that $\hat{R}(r)$ will be less damped than $R(r)$ and will not decay as quickly as $R(r)$.

2.4 SPECTRUM ANALYSIS

The spectrum function decomposes a time varying quantity into a sum (or integral) of sine and cosine functions.

2.4.1 Spectrum for Various Processes

a. For Deterministic Periodic Functions—Fourier Series

For periodic functions with period T,

$$X(t) = \frac{1}{2} a_o + \sum_{n=1}^{\infty} \left[a_n \cos\left(\frac{\pi n t}{T}\right) + b_n \sin\left(\frac{\pi n t}{T}\right) \right] \qquad (2.29)$$

where

$$\begin{cases} a_n = \dfrac{1}{T} \displaystyle\int_{-\frac{T}{2}}^{\frac{T}{2}} X(t) \cos \dfrac{\pi n t}{T} \ dt \\[4mm] b_n = \dfrac{1}{T} \displaystyle\int_{-\frac{T}{2}}^{\frac{T}{2}} X(t) \sin \dfrac{\pi n t}{T} \ dt. \end{cases} \qquad (2.30)$$

The a_n and b_n functions are called Euler–Fourier coefficients. Equation 2.30 is based on the orthogonality of $\cos \dfrac{\pi n t}{T}$, $\sin \dfrac{\pi n t}{T}$.

For the existence of a_n, b_n, and for the convergence of the series, the conditions

$$\int_{-\frac{T}{2}}^{\frac{T}{2}} |X(t)| dt < \infty , \quad \int_{-\frac{T}{2}}^{\frac{T}{2}} |X(t)|^2 dt < \infty \qquad (2.31)$$

are sufficient.

Replacing a_n, b_n by $c_0 = a_o$, $c_n = \left[\dfrac{1}{2}\left(a_n^2 + b_n^2\right)\right]^{\frac{1}{2}}$, gives

the total energy $[-T/2$ to $T/2]$ as

$$\int_{-\frac{T}{2}}^{\frac{T}{2}} X^2(t) dt = \sum_{n=1}^{\infty} T\left[\frac{1}{4} a_o^2 + \frac{1}{2}\left(a_n^2 + b_n^2\right) \right] = T\left(\sum_{n=-\infty}^{\infty} c_n^2 \right) \qquad (2.32)$$

and the total power $[-T/2$ to $T/2]$ as

$$\sum_{n=-\infty}^{\infty} c_n^2, \tag{2.33}$$

c_n^2 is the contribution of the nth term to the total power, as in Fig. 2.3.
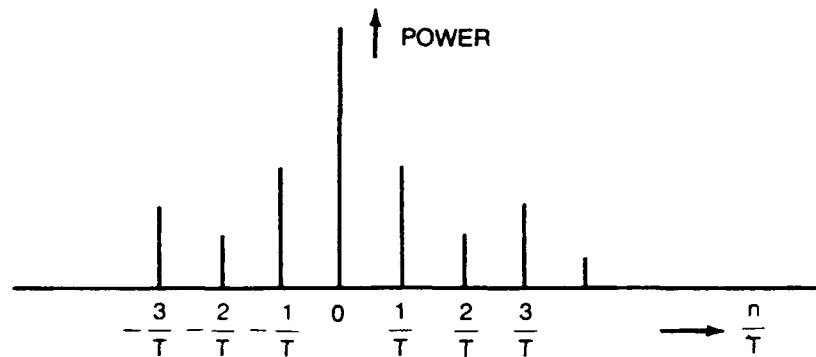
Fig. 2.3. Power spectrum of periodic function.

b. For Nonperiodic Deterministic Functions—Fourier Integral

For nonperiodic functions with finite energy as in Fig. 2.4,

$$X(t) = \int_{-\infty}^{\infty} X(\omega) \ e^{i\omega t} d\omega. \tag{2.34}$$

$$X(\omega) = \frac{1}{2\pi} \int_{-\infty}^{\infty} X(t) \ e^{-i\omega t} d\omega. \tag{2.35}$$
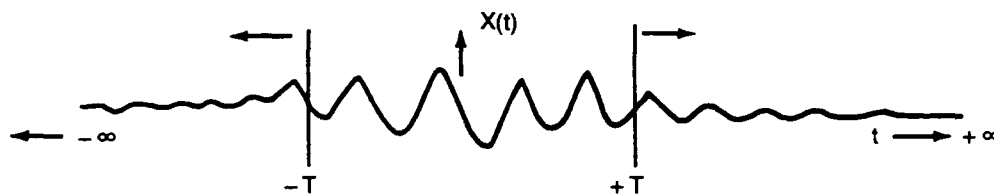
Fig. 2.4. Nonperiodic function with finite energy.

For the existence and convergence of this expansion, conditions

$$\int_{-\infty}^{\infty} |X(t)| \, dt < \infty, \qquad \int_{-\infty}^{\infty} |X(t)|^2 \, dt < \infty \qquad (2.36)$$

are necessary. In this case, Parseval's Relation is

$$\int_{-\infty}^{\infty} X^2(t) dt = 2\pi \int_{-\infty}^{\infty} X(\omega)^2 d\omega. \qquad (2.37)$$

Here, as in Fig. 2.5 $2\pi|X(\omega)|^2 d\omega$ is the contribution to the total energy of those components in $X(t)$ whose frequency lies between ω and $\omega + d\omega$. Accordingly, $2\pi|X(\omega)|^2$ denotes the energy density function. In this case determining the power makes no sense, because when $T \rightarrow \infty$, from Eq. 2.36, power tends to 0.
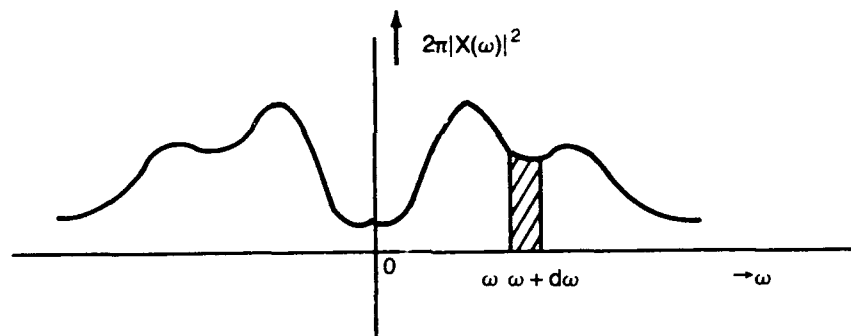
Fig. 2.5. Energy spectrum of nonperiodic function.

c. For Stationary Stochastic Processes

For a single realization $x(t)$ of $X(t)$, as in Fig. 2.6 assume $E[X(t)] = 0$; $X(t)$ is stochastically continuous. $[R(0) = \sigma_x^2, \varrho(0) = 1]$
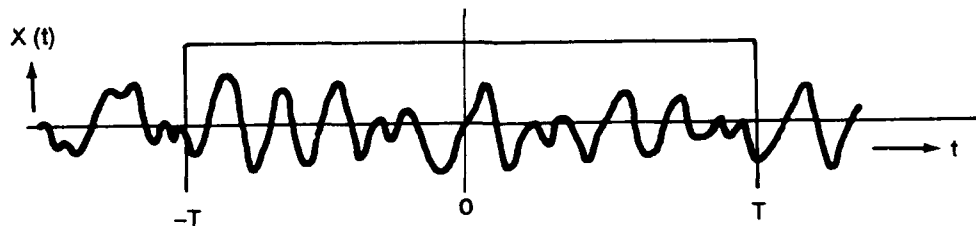
Fig. 2.6. Stationary stochastic process with finite power.

15

Since there is no periodicity, no Fourier series exists, and because of stational-

ity, $\int\limits_{-\infty}^{\infty} |X(t)| dt < \infty$ does not hold, so $X(t)$ does not possess a Fourier integral. Thus,

$2\pi \lim |X(\omega)|^2$ will not exist and may become infinity. So here

$$X_T(t) = \begin{cases} X(t) & -T < t < T \\ 0 & \text{otherwise} \end{cases} \qquad (2.38)$$

and the following process is introduced:

$$X_T(t) = \int\limits_{-\infty}^{\infty} X_T(\omega) e^{i\omega t} d\omega$$

$$X_T(\omega) = \frac{1}{2\pi} \int\limits_{-\infty}^{\infty} X_T(t) e^{-i\omega t} dt = \frac{1}{2\pi} \int\limits_{-T}^{T} X(t) e^{-i\omega t} dt. \qquad (2.39)$$

Then, since the power is $2\pi |X_T(\omega)|^2 / T$ instead of $2\pi |X_T(\omega)|^2$, which makes $T \to \infty$,

$\lim \dfrac{2\pi |X_T(\omega)|^2}{2T}$ is for the total process. The expected value of this power is

$$E\,[\text{Power}] = \lim E\left[\frac{2\pi |X_T(\omega)|^2}{2T}\right] \qquad (2.40)$$

and is defined as $s(\omega)$. By manipulation,

$$\frac{2\pi |X_T(\omega)|^2}{2T} = \frac{1}{2T}\,\frac{1}{2\pi}\,[2\pi X_T(\omega)]\,[2\pi X_T^*(\omega)]$$

$$= \frac{1}{2\pi}\,\frac{1}{2T} \int\limits_{-\infty}^{\infty} X_T(t) e^{-i\omega t} dt \int\limits_{-\infty}^{\infty} X_T(t-\tau) e^{i\omega(t-\tau)} dt$$

16

$$= \frac{1}{2\pi} \int_{-\infty}^{\infty} \left[\frac{1}{2T} \int_{-\infty}^{\infty} X_T(t) \ X_T(t-\tau)dt \right] e^{-i\omega\tau}d\tau$$

$$= \frac{1}{2\pi} \int_{-\infty}^{\infty} \hat{R}_T(\tau)e^{-i\omega\tau}d\tau , \tag{2.41}$$

*Denotes the complex conjugate.

Here,

$$\hat{R}_T(\tau) = \lim_{T \to \infty} \frac{1}{2T} \int_{-\infty}^{\infty} X_T(t)X_T(t-\tau)dt. \tag{2.42}$$

Accordingly, for the total

$$E \ [Power] = s(\omega) = \lim E \left[\frac{2\pi|X(\omega)|^2}{2T} \right]$$

$$= \lim_{T \to \infty} \frac{1}{2\pi} \int_{-\infty}^{\infty} e^{-i\omega t}E[\hat{R}_T(\tau)]dt. \tag{2.43}$$

Since $X_T(t)$ was defined as $X(t)$ for $-T < t < T$, and otherwise 0,

$$\hat{R}_T(\tau) = \begin{cases} \dfrac{1}{2T} \displaystyle\int_{-(T-|\tau|)}^{T} X(t) \ X(t-|\tau|)dt, & |\tau| < T \\ \\ 0 & |\tau| > T \end{cases} , \tag{2.44}$$

•

$$E[\hat{R}_T(\tau)] = \frac{1}{2T} \int\limits_{-(T-|\tau|)}^{T} E[X(t)\ X(t+\tau)]\ dt = \frac{1}{2T} \int\limits_{(T-|\tau|)}^{T} R(\tau)dt$$

$$= \begin{cases} R(\tau)\left[1 - \dfrac{|\tau|}{2T}\right] & |\tau| < T \\[3mm] 0 & |\tau| > T \end{cases} \tag{2.45}$$

As T approaches infinity,

$$s(\omega) = \lim_{T \to \infty} \left\{ \frac{1}{2\pi} \int\limits_{-T}^{T} \left[1 - \frac{|\tau|}{2T}\right] e^{-i\omega\tau} R(\tau)d\tau \right.$$

$$= \frac{1}{2\pi} \int\limits_{-\infty}^{\infty} e^{-i\omega\tau}\ R(\tau)d\tau . \tag{2.46}$$

For the existence of $s(\omega)$, $X(t)$ must have an autocovariance function $R(\tau)$ that is continuous everywhere, including at $\tau = 0$, and

$$R(\tau) = \int\limits_{-\infty}^{\infty} e^{i\omega\tau}\ dS(\omega) \tag{2.47}$$

$$\varrho(\tau) = \int\limits_{-\infty}^{\infty} e^{i\omega\tau}\ dF(\omega). \tag{2.48}$$

This relation is called Wiener–Khinchine's Theorem. Here, $F(\omega)$ is the normalized integrated spectrum $S(\omega)/\sigma_x^2$, where if $s(\omega)$ is continuous and smooth,

$$S(\omega) = \int\limits_{-\infty}^{\omega} s(\omega)d\omega\ , \quad \text{and } F(\omega) = \int\limits_{-\infty}^{\omega} f(\omega)d\omega, \tag{2.49}$$

where $f(\omega) = s(\omega)/\sigma_x^2$.

The properties of $F(\omega)$ and $f(\omega)$ correspond to those of the probability density and probability density distribution functions, $P(\omega)$ and $p(\omega)$, for continuous distribution.

2.4.2 Spectral Representation of the Stationary Random Process

Instead of using the Fourier integral, the stationary process is more generally expressed by the Fourier Stieltjes integral as

$$X(t) = \int_{-\infty}^{\infty} e^{i\omega t} \, dZ(\omega), \tag{2.50}$$

where $dZ(\omega)$ is in the order of $O(\sqrt{d\omega})$ and is larger than $d\omega$. $dZ(\omega)$ and $dZ(\omega')$ are uncorrelated, that is they are orthogonal to each other

$$E\left[|dZ(\omega)|^2\right] = dS(\omega). \tag{2.51}$$

When the process has a purely continuous spectrum, from Eq. 2.49, rewritten as

$$dS(\omega) = s(\omega) \, d\omega, \tag{2.49'}$$

$$E\left[|dZ(\omega)|^2\right] = s(\omega)d\omega = \Delta S(\omega). \tag{2.52}$$

For a real valued process,

$$R(-\tau) = R(\tau), \tag{2.53}$$

and

$$s(\omega) = \frac{1}{2\pi} \int_{-\infty}^{\infty} \cos\omega\tau \, R(\tau) \, d\tau = \frac{1}{\pi} \int_{0}^{\infty} \cos\omega\tau \, R(\tau) \, d\tau. \tag{2.54}$$

$s(\omega)$ is an even function, and

$$s(-\omega) = s(\omega). \tag{2.55}$$

Therefore,

$$R(\tau) = \int_{-\infty}^{\infty} \cos\omega\tau \, s(\omega) \, d\omega = 2\int_{0}^{\infty} \cos\omega\tau \, s(\omega) \, d\omega. \tag{2.56}$$

19

2.4.3 Spectrum of Discrete Parameter Process, Aliasing

For discrete process $\{X_t\}$,

1. $R(r)$ are defined only for integer values of r, $r = 0, \pm 1, \pm 2, \ldots$.

Therefore

$$
\begin{aligned}
s(\omega) &= \frac{1}{2\pi} \sum_{r=-\infty}^{\infty} e^{-i\omega r} R(r) \\
&= \frac{\sigma_x^2}{2\pi} + \frac{1}{\pi} \sum_{r=1}^{\infty} R(r) \cos r\omega.
\end{aligned}
\tag{2.57}
$$

Here Δt, the time interval of the discrete process, is assumed to be $\Delta t = 1$. If $\Delta t \neq 1$, change ω into $\omega' = \omega/\Delta t$; then

$$
s(\omega') = s(\omega) \; \Delta t.
\tag{2.58}
$$

From now on, in this lecture note, $\Delta t = 1$ is assumed.

2. $s(\omega)$ are continuous functions but are defined only for frequency $-\pi \leq \omega \leq \pi$, and are affected by aliasing.

$$
R(r) = \int_{-\infty}^{\infty} e^{i\omega r} \; dV(\omega) \qquad r = 0, \pm 1, \pm 2, \ldots.
$$

$$
= \sum_{n=-\infty}^{\infty} \int_{(2n-1)\pi}^{(2n+1)\pi} e^{i\omega r} dV(\omega) = \sum_{n=-\infty}^{\infty} \int_{-\pi}^{\pi} \exp\,[i(\omega + 2n\pi)r] \; dV(\omega + 2n\pi)
$$

$$
= \sum_{n=-\infty}^{\infty} \int_{-\pi}^{\pi} \exp\,(i\omega r) \; dV(\omega + 2n\pi) = \int_{-\pi}^{\pi} e^{i\omega r} \sum_{n=-\infty}^{\infty} dV(\omega + 2n\pi) = \int_{-\infty}^{\infty} e^{i\omega r} \; dS(\omega)
$$

$$
\tag{2.59}
$$

Thus

$$
S(\omega) = \sum_{n=-\infty}^{\infty} V(\omega + 2n\pi),
\tag{2.60}
$$

20

and

$$s(\omega) = \frac{dS(\omega)}{d\omega} = \sum_{n=-\infty}^{\infty} v(\omega + 2\pi n).$$ (2.61)

As is shown in Fig. 2.7, at frequency ω_0, the spectra not only of $v(\omega_0)$ but also of $v(\omega_0 \pm 2\pi), v(\omega_0 \pm 4\pi), v(\omega_0 \pm 6\pi) \dots$ are folded as the spectrum $s(\omega_0)$, as

$$s(\omega_0) = v(\omega_0) + v(\omega_0 \pm 2\pi) + v(\omega_0 \pm 4\pi) + v(\omega_0 \pm 6\pi) + \dots$$

$$= v(\omega_0) + v(2\pi \pm \omega_0) + v(4\pi \pm \omega_0) + v(6\pi \pm \omega_0) + \dots$$ (2.61')
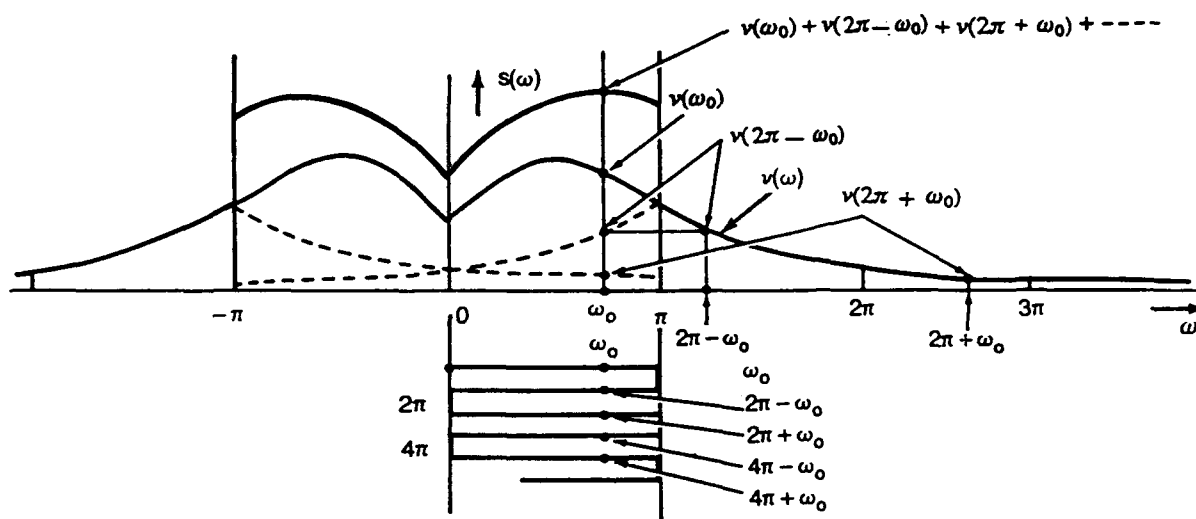
Fig. 2.7. Aliasing of the spectrum.

This is also illustrated in Fig. 2.8, where the harmonic functions of not only frequency 1/5, but also of 4/5, 6/5; 9/5, 11/5; 14/5, 16/5; .... can pass through the same sampling point O, as marked in the figure, at $\Delta t = 1$ sec intervals (see Table 2.1).

21
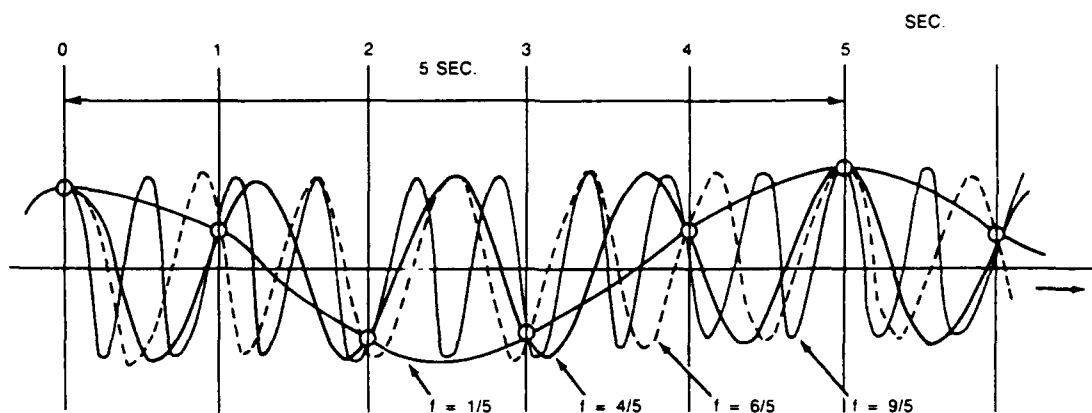
Fig. 2.8. Aliasing harmonic curves of frequency 1/5, 4/5, 6/5; 9/5, 11/5; . . . can pass through the same sampling points at $\Delta t = 1$.

Table 2.1. Aliasing frequencies.

ω	$\omega_0 = 2\pi \times \dfrac{1}{5}$	$\begin{cases} 2\pi - \omega_0 \\ 2\pi + \omega_0 \end{cases}$	$\begin{cases} 4\pi - \omega_0 \\ 4\pi + \omega_0 \end{cases}$	$\begin{cases} 6\pi - \omega_0 \\ 6\pi + \omega_0 \end{cases}$	. . .
f	$f_0 = \dfrac{\omega_0}{2\pi} = \dfrac{1}{5}$	$\begin{cases} 1 - f_0 = \dfrac{4}{5} \\ 1 + f_0 = \dfrac{6}{5} \end{cases}$	$\begin{cases} 2 - f_0 = \dfrac{9}{5} \\ 2 + f_0 = \dfrac{11}{5} \end{cases}$	$\begin{cases} 3 - f_0 = \dfrac{14}{5} \\ 3 + f_0 = \dfrac{16}{5} \end{cases}$	. . .

Equation 2.61 or 2.61' shows that, in cases of discrete process analysis of the spectrum ordinate at frequency ω_o, the power at higher frequencies $2\pi \pm \omega_o$,

$4\pi \pm \omega_o$ . . . . . . is spuriously folded on the real power at ω_o as in Fig. 2.7.

Accordingly, when a continuous process is to be transformed into a discrete process sampled at time intervals Δt, aliasing is the most important effect to be considered. The analyzed range of the frequency spectrum is between the Nyquist frequencies

$-\dfrac{\pi}{\Delta t}$ and $\dfrac{\pi}{\Delta t}$ (when $\Delta t = 1$, as in preceding sections $-\pi$ to π). Accordingly,

Δt should be small enough to avoid aliasing. Practically it is advisable to take $\dfrac{\pi}{\Delta t}$ as

large as $\dfrac{\pi}{\Delta t} > (1.2 \text{ to } 1.5)\omega_e$, where ω_e is the uppermost frequency of the interested frequency component of the spectrum. Then

$$\Delta t \leq \frac{\pi}{(1.2 \text{ to } 1.5)\omega_e}. \tag{2.62}$$

2.5 COMPUTATION OF THE SPECTRUM FOR A DISCRETE PROCESS

Here the procedure for calculating the spectrum for a discrete process is summarized. In many steps of the computations, the finiteness of the sample process, the discreteness of the data, and the choice of parameters will affect the results statistically and mathematically.

2.5.1 Spectrum Computation Through Periodogram

First, we take the periodogram $P_N(\omega)$ that is the square of the finite Fourier transform $F_x(\omega)$ of a single realization of this discrete process.

$$F_x(\omega) = \frac{1}{\sqrt{2\pi N}} \sum_{t=1}^{N} X_t \, e^{-i\omega t}, \tag{2.63}$$

$$P_N(\omega) = |F_x(\omega)|^2 = \frac{1}{2\pi N} \left| \sum_{t=1}^{N} x_t \, e^{-i\omega t} \right|^2$$

$$= \frac{1}{2\pi} \frac{1}{N} \sum_{t_1=1}^{N} \sum_{t_2=1}^{N} X_{t_1} X_{t_2}^* \cos (t_1 - t_2)\omega, \tag{2.64}$$

setting

$$t_1 \rightarrow t$$

$$t_2 \rightarrow t_1 + r$$

$$= \frac{1}{2\pi} \sum_{r=-(N-1)}^{N-1} \frac{1}{N} X_t X_{t+|r|} \cos r\omega. \tag{2.65}$$

From Eq. 2.24, we know that $\left(\dfrac{1}{N}\right) \cdot X_t X_{t+|r|}$ is the biased estimate of the autocorrelation $\hat{R}(r)$. Therefore,

$$P_N(\omega) = \frac{1}{2\pi} \sum_{r=-(N-1)}^{N-1} \hat{R}(r) \cos r\omega. \tag{2.66}$$

For the entire discrete process,

$$E\ [P_N(\omega)] = \frac{1}{2\pi} \sum_{r=-(N-1)}^{N-1} E\ [\hat{R}(r)]\ \cos\ r\omega,\qquad(2.67)$$

which, from Eq. 2.24

$$= \frac{1}{2\pi} \sum_{r=-(N-1)}^{N-1} \left\{1 - \frac{|r|}{N}\right\} R(r)\ \cos\ r\omega.\qquad(2.68)$$

From these relationships, the spectrum computation from the periodogram is the same as the spectrum estimation from auto correlation. The Fast Fourier Transform gives the periodogram directly through direct Fourier transfer and is statistically the same as this periodogram analysis. Accordingly, care should be taken in selecting the spectrum windows to be used in the F.F.T. as will be discussed later.

From Eq. 2.68 if N becomes ∞, surely

$$E\ [P_N(\omega)] \rightarrow s(\omega)\ .\qquad(2.69)$$

Then, from the periodogram, we can estimate the spectrum. $P_N(\omega)$ is an unbiased estimate of $s(\omega)$. Here, however, $R(r)$ is the theoretical auto correlation, and we think the spectrum is continuous and

$$R(r) = \int_{-\pi}^{\pi} s(\omega)\ \cos\ r\omega d\omega\ ,\qquad r = 0,\ \pm\ 1,\ \pm\ 2,\ .\ .\ .\qquad(2.70)$$

Thus

$$E\ [P_N(\omega)] = \frac{1}{2\pi} \sum_{r=-(N-1)}^{N-1} \left\{1 - \frac{|r|}{N}\right\} \int_{-\pi}^{\pi} s(\mu)\ \cos\ r\mu\ d\mu\ \cos\ r\omega$$

$$= \int_{-\pi}^{\pi} s(\mu) \frac{1}{N} \cdot \frac{1}{2\pi} \sum_{r=-(N-1)}^{N-1} \{N - |r|\} \frac{1}{2} \{\cos\ r(\mu+\omega) + \cos\ r(\mu-\omega)\}\ d\mu.\ (2.71)$$

Here we use the following relations on summations of digital quantities, which can easily be proved,

24

$$\sum_{r=-(N-1)}^{N-1} (N-|r|)\, f(r) = \sum_{u=0}^{N-1} \sum_{r=-u}^{u} f(r) \qquad (2.72)$$

$$\sum_{r=-u}^{u} \cos r\phi = \frac{\sin\left\{\left(u+\frac{1}{2}\right)\phi\right\}}{\sin\left(\frac{1}{2}\phi\right)} \qquad (2.73)$$

$$\sum_{u=0}^{N-1} \frac{\sin\left\{\left(u+\frac{1}{2}\right)\phi\right\}}{\sin\left(\frac{1}{2}\phi\right)} = \frac{\sin^2\left(\frac{N\phi}{2}\right)}{\sin^2\left(\frac{\phi}{2}\right)}. \qquad (2.74)$$

Then from these relations,

$$\frac{1}{2\pi} \sum_{r=-(N-1)}^{N-1} \left\{1-\frac{|r|}{N}\right\} \cos r\phi = \frac{1}{N}\frac{1}{2\pi} \sum_{r=-(N-1)}^{N-1} \{N-|r|\} \cos r\phi$$

$$= \frac{1}{2\pi}\frac{1}{N} \sum_{u=0}^{N-1} \sum_{r=-u}^{u} \cos r\phi = \frac{1}{2\pi N} \frac{\sin^2\left(\frac{N\phi}{2}\right)}{\sin^2\left(\frac{\phi}{2}\right)} \equiv F_{e_N}(\phi). \qquad (2.75)$$

This function is called the Fejer function $F_{e_N}(\theta)$ and has the form shown in Fig. 2.9.

When $\dfrac{N\theta}{2} \to \theta,$

$$F_{e_N}(\phi), \text{near } \phi = 0 \sim \frac{1}{2\pi N} \frac{\sin^2\theta}{\sin^2\left(\frac{\theta}{N}\right)} \sim \frac{N}{2\pi} \left(\frac{\sin\theta}{\theta}\right)^2.$$

25
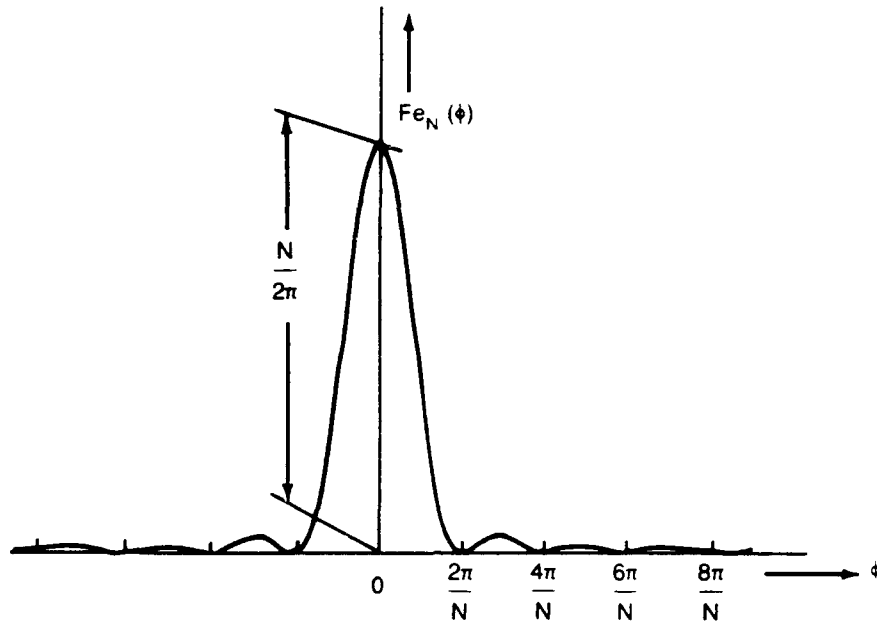
Fig. 2.9. Fejer Kernel Function $F_{eN}(\theta)$

Therefore,

$$\lim_{\phi \to 0} F_{e_N}(\phi) = \frac{N}{2\pi} \lim_{\theta \to 0} \left(\frac{\sin \theta}{\theta} \right)^2 \to \frac{N}{2\pi} . \qquad (2.76)$$

Putting this function $F_{e_N}(\theta)$ into Eq. 2.71 gives

$$E\ [P_N(\omega)] = \int_{-\pi}^{\pi} s(\phi) \frac{1}{2} \left\{ F_{e_N}(\phi + \omega) + F_{e_N}(\phi - \omega) \right\}\ d\phi . \qquad (2.77)$$

Taking into account the form of the Fejer kernel F_N gives

$$= \int_{-\pi}^{\pi} s(\phi) F_{e_N}(\phi - \omega)\ d\phi . \qquad (2.78)$$

When $N \to \infty$,

$$F_{e_N}(\phi) \to \delta(\phi) , \qquad (2.79)$$

F_{e_N} tends to Dirac's delta function, and

26

$$E \; [P_N(\omega)] = \int\limits_{-\pi}^{\pi} s(\phi) \; \delta(\phi - \omega) \; d\phi = s(\omega). \qquad (2.80)$$

When N is finite, $E[P_N(\omega)]$ is a kind of filtered spectrum, filtered by the Fejer kernel function F_{e_N}.

Though the details of manipulation by statistical mathematics are not shown here, we know that the variance of the periodogram can be calculated as

$$\text{var.} \; [P_N(\omega)] \; \text{is on the order of } s^2(\omega_p), \qquad (2.81)$$

$$\omega_p = \frac{2\pi p}{N} \left(\text{at } p \neq 0, \frac{N}{2} \right)$$

and also that $P_N(\omega)$ follow χ_2^2, χ^2 distribution with degree of freedom $\nu = 2$. As the mean and the variance of χ_ν^2 are ν and 2ν (here 2 and 4, respectively), then the signal to noise ratio S/N is

$$\frac{S}{N} \; \text{ratio} = \frac{\text{mean}}{\text{standard variation}} = \frac{2}{(2 \times 2)^{1/2}} = 1. \qquad (2.82)$$

Equations 2.80 and 2.81 can also be used to check Eq. 2.82. This S/N ratio of 1 means that this value of $P_N(\omega)$ is a very poor estimate of the spectrum. Further, the fact that var. $[P_N(\omega)]$ does not tend to 0, even when N tends to ∞, means this estimate of $E[P_N(\omega)]$ is not a consistent estimate of $s(\omega)$.

Furthermore, at two fixed neighboring frequencies ω_1 and ω_2, cov $[P_N(\omega_1), P_N(\omega_2)]$ can be calculated to decrease by the increase in N.

These facts are reflected in the erratic and widely fluctuating form of $P_N(\omega)$. $P_N(\omega)$ may produce a spurious peak in the region in which $P_N(\omega)$ is large, as shown in Fig. 2.10.

2.5.2 Consistent Estimation of the Spectrum

In the expression of the periodogram,
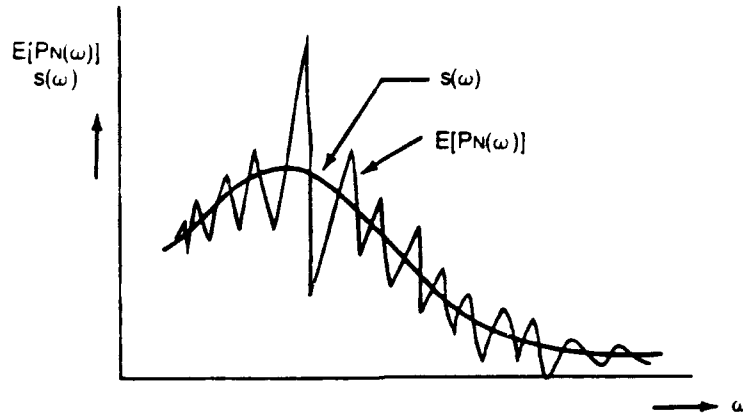
Fig. 2.10. Behavior of $E[P_N(\omega)]$.

$$P_N(\omega) = \frac{1}{2\pi} \sum_{r=-(N-1)}^{N-1} \hat{R}(r) \cos r\omega = \frac{1}{2\pi} \left\{ R(0) + 2 \sum_{r=1}^{N-1} \hat{R}(r) \cos r\omega \right\}, \quad (2.83)$$

var. $[\hat{R}(r)]$ is on the order of $O\!\left(\dfrac{1}{N}\right)$,

and var. $[P_N(\omega)]$ is on the order of $O(1)$ \hfill (2.84)

are known. The reason for the large var. $[P_N(\omega)]$ is, as shown in Eq. 2.83, that $P_N(\omega)$ adds too many terms in $\sum \hat{R}(r)$. These terms are slightly correlated, but the basic effect of too many terms of $\sum \hat{R}(r)$ in Eq. 2.83 remains the same.

Accordingly, the way to reduce this large variance in $P_N(\omega)$ is to reduce the number of additions from N to M and omit the term $N \gg M$ in Eq. 2.83,

$$E \left[\hat{s}_0(\omega)\right] = \frac{1}{2\pi} \sum_{r=-M}^{M} E \left[\hat{R}(r)\right] \cos r\omega . \qquad (2.85)$$

This reduction decreases the variance, and from Eq. 2.84 intuitively we find var. $[s_o(\omega)]$ is on the order of $O(M/N)$. This can be proved by statistical mathematics, although the manipulation is not shown here. Substituting Eq. 2.24 into Eq. 2.85 gives

$$E\left[\hat{s}_0(\omega)\right] = \frac{1}{2\pi} \sum_{r=-M}^{M} E\left[\hat{R}(r)\right] \cos r\omega$$

$$= \frac{1}{2\pi} \sum_{r=-M}^{M} \left(1 - \frac{|r|}{N}\right) R(r) \cos r\omega \rightarrow s(\omega), \quad (2.86)$$

as M tends to $\rightarrow \infty$, but more slowly than N tends to $\rightarrow \infty$. Namely, $N \rightarrow \infty$, $M \rightarrow \infty$ but $\frac{N}{M} \rightarrow \infty$ also, for example as M was on the order of $\sqrt{N}$.

When using the function $w_0(r)$, Eq. 2.85 is the same as,

$$\hat{s}_0(\omega) = \frac{1}{2\pi} \sum_{r=-(N-1)}^{(N-1)} w_0(r) \, \hat{R}(r) \cos r\omega \qquad (2.87)$$

where

$$w_0(r) = \begin{cases} 1 & -N < -M \leq r \leq M < N \\ 0 & \text{otherwise} \end{cases} \qquad (2.88)$$

More generally, many forms of functions $w(r)$ besides Eq. 2.88 are proposed as shown in Fig. 2.11. $R(r) \cos r\omega$ are even functions of r; therefore, if we take $w(r)$ as real even functions of r, then

$$\hat{s}(\omega) = \frac{1}{2\pi} \sum_{r=-(N-1)}^{N-1} w(r) \, \hat{R}(r) \, e^{-ir\omega}. \qquad (2.89)$$

29

Function $w(r)$ is referred to as the lag window.
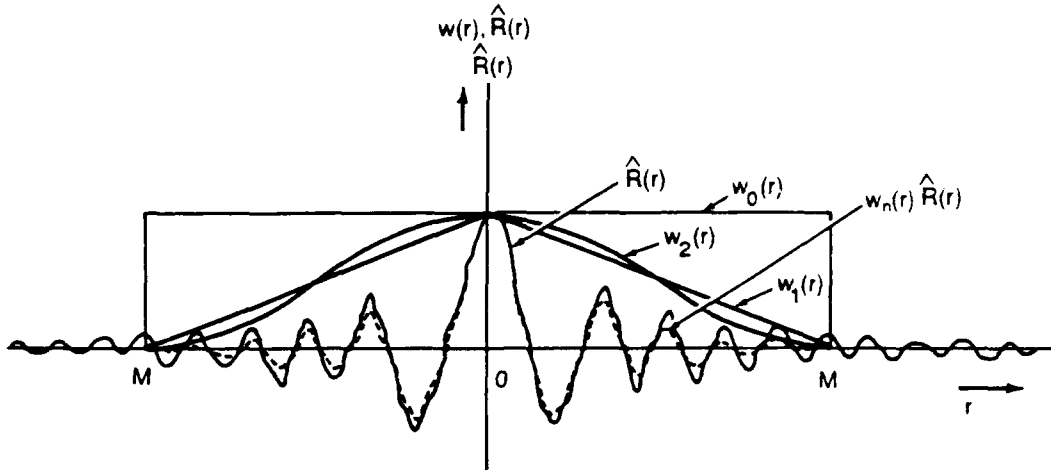
Fig. 2.11. Lag windows $w_n(r)$ with $R(r)$.

2.5.3 Spectral Windows

From Eq. 2.89,

$$\hat{s}(\omega) = \frac{1}{2\pi} \sum_{r=-(N-1)}^{N-1} w(r) \, \hat{R}(r) \, e^{-ir\omega}.$$

As Eq. 2.66 in Section 2.5.1 shows,

$$P_N(\omega) = \frac{1}{2\pi} \sum_{r=-(N-1)}^{N-1} \hat{R}(r) e^{-ir\omega}, \quad \hat{R}(r) = \int_{-\pi}^{\pi} P_N(\phi) e^{ir\phi} \, d\phi,$$

so inserting these relations into Eq. 2.89 gives

$$\hat{s}(\omega) = \int_{-\pi}^{\pi} P_N(\phi) \, W(\omega - \phi) \, d\phi, \tag{2.90}$$

where

$$W(\phi) = \frac{1}{2\pi} \sum_{r=-(N-1)}^{N-1} w(r) \, e^{-ir\phi}. \tag{2.91}$$

$\hat{s}(\omega)$ is obtained as a weighted integral of the periodogram, and weighting involves a smoothing operation in the neighborhood of ω. This operation reduces the contribution

30

from the "tail" of autocovariance $\hat{R}(r)$, which shows more erratic fluctuations than the real value of $R(r)$ and is statistically less reliable, as discussed at the end of Section 2.3.

As the inverse Fourier transfer of Eq. 2.91

$$w(r) = \int_{-\pi}^{\pi} e^{ir\phi} \ W(\phi) \ d\phi \qquad (2.92)$$

$r = 0, \pm 1, \pm 2, \ldots \pm (N-1)$; $[w(r) = 0 \text{ at } |r| > N-1]$.

Since $w(r)$ are real and even,

$$W(\phi) = \frac{1}{2\pi} \sum_{r=-(N-1)}^{N-1} w(r) \ \cos r\phi . \qquad (2.93)$$

$W(\phi)$, which is the Fourier pair with $w(r)$, is called the spectral window function, and $w(r)$ the lag window function.

$w_0(r)$, given by Eq. 2.88, is one of the lag windows and is called a "truncated window" or "do nothing window." Its Fourier transform $W_0(\phi)$ is from Eq. 2.73

$$W_0(\phi) = \frac{1}{2\pi} \sum_{-M}^{M} \cos r\phi = \frac{1}{2\pi} \frac{\sin\left[\left(M+\frac{1}{2}\right)\phi\right]}{\sin\left(\frac{\phi}{2}\right)}. \qquad (2.94)$$

This function, shown in Fig. 2.12, is also referred to as Dirichlet's kernel function $D_M(\phi)$. It has a high peak at $\phi = 0$ and rather deep valleys on both sides of the main lobe. This sometimes causes harm to the computation of the spectrum and results in some spurious negative values for the spectrum ordinates. Many studies have been made to obtain good windows, and many different windows with different characteristics have been proposed and claimed to be good from different points of view.

Several windows described by Priestley[23] are summarized in Fig. 2.13 and Fig. 2.14 in the form of pairs of lag window $w(r)$ and spectral window $W(\phi)$.

2.5.4 Effect of Windows

Some of the proposed window pairs are compared in Fig. 2.15. They were designed mostly under the following conditions:

1. $W_N(\phi) \geq 0$ is desirable to avoid the effect of large negative lobes.

31
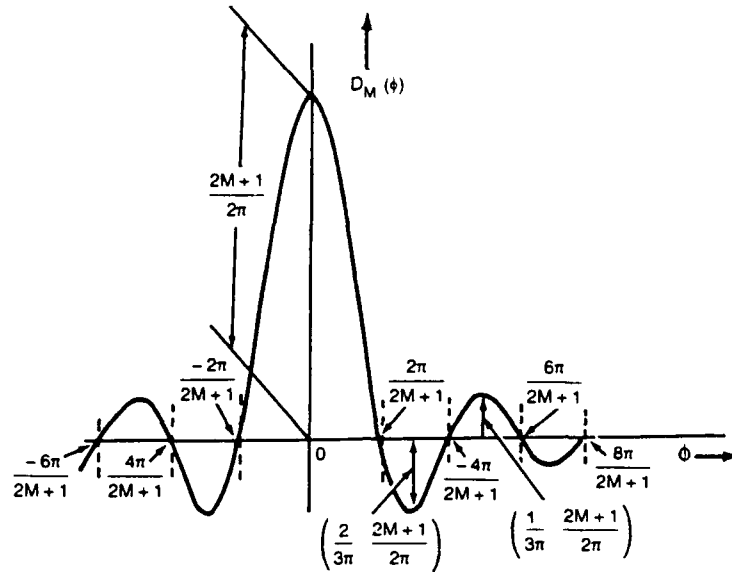
Fig. 2.12. The Dirichlet Kernel Function $[w_0(\phi) = D_M(\phi)]$.

2. $\displaystyle\int_{-R}^{R} W_N(\phi)\ d\phi = 1$, i.e., $w(0) = 1$ from Eq. 2.92, to keep $R(0)$ unchanged.

3. $\displaystyle\int_{-\pi}^{\pi} W_N^2(\phi)\ d\phi < \infty$, to make $\hat{s}(\omega)$ a consistent estimator.

4. $W_N(\phi) \underset{N \to \infty}{\longrightarrow} 0$, uniformly as $N \to \infty$.

5. $\displaystyle\frac{\sum \left(\frac{|r|}{N}\right) w^2(r)}{\sum w^2(r)} \to 0$ as $N \to \infty$, to ensure that $W_N(\phi)$ is not too narrow in relation

to $\left(\dfrac{1}{N}\right)$ and to have $\hat{s}(\omega)$ an asymptotically unbiased estimator of $s(\omega)$.

The effects of the spectral windows, most of them designed under the above conditions, can be summarized as follows:

1. Bias. that was 0 for the estimator "Periodogram $P_N(\omega)$," is now

32

TRUNCATED PERIODOGRAM

$$w(r) = \begin{cases} 1 \cdots |r| \leqslant M \\ 0 \cdots |r| > M \end{cases}$$

1.0

$-M$ 0   M $\rightarrow r$

$$W(\phi) = \frac{1}{2\pi}\left\{\frac{\sin[(M+\frac{1}{2})\phi]}{\sin(\phi/2)}\right\} = D_M(\phi)$$

$\frac{2M+1}{2\pi}$

$\frac{2\pi}{2M+1}$

BARTLETT'S

$$w(r) = \begin{cases} 1 - |r|/M \cdots |r| \leqslant M \\ 0 \quad\cdots\cdots |r| > M \end{cases}$$

1.0

$-M$ 0   M $\rightarrow r$

$$W(\phi) = \frac{1}{2\pi M}\left\{\frac{\sin(M\phi/2)}{\sin(\phi/2)}\right\}^2 = F_M(\phi)$$

$\frac{M}{2\pi}$

0   $\frac{\pi}{M}$ $\frac{2\pi}{M}$ $\rightarrow \phi$

DANIELL'S

$$w(r) = \frac{\sin(\pi r/M)}{(\pi r/M)} \qquad |r| \leqslant M$$

1.0

$\rightarrow r$

$$W(\phi) = \begin{cases} M/2\pi \cdots -\pi/M \leqslant \phi \leqslant \pi/M \\ 0 \cdots\cdots \text{OTHERWISE} \end{cases}$$

$\frac{M}{2\pi}$

$-\frac{\pi}{M}$ 0 $\frac{\pi}{M}$ $\rightarrow \phi$

GENERAL TUKEY

$$w(r) = \begin{cases} 1 - 2a + 2a\cos(\pi r/M) \\ \qquad\cdots |r| < M \\ 0 \qquad\cdots\cdots |r| > M \end{cases}$$

1.0

$1-4a$

$-M$ M $\rightarrow r$

$$W(\phi) = aD_M\left(\phi - \frac{\pi}{M}\right) + (1-2a)\,D_M(\phi) + aD_M\left(\phi + \frac{\pi}{\pi}\right)$$

$\frac{M}{2\pi}$

0   $\frac{2\pi}{M}$ $\rightarrow \phi$
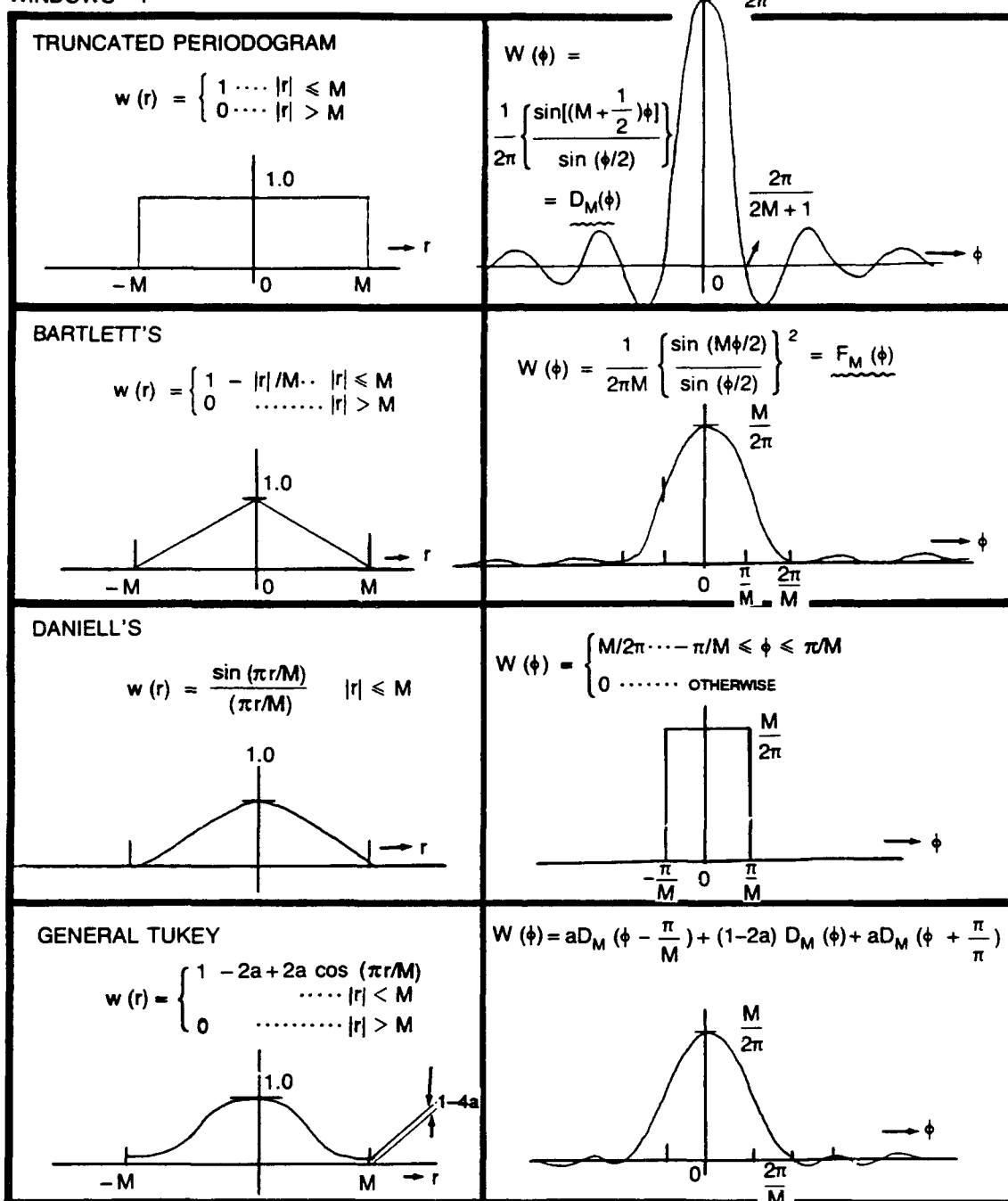
Fig. 2.13. Various window pairs (I).

33

TUKEY – HAMMING

$$w(r) = \begin{cases} 0.54 + 0.46 \cos(\pi r/M) \cdots |r| \leq M \\ 0 \qquad \cdots\cdots\cdots\cdots |r| > M \end{cases}$$

$$W(\phi) = 0.23\, D_M\left(\phi - \frac{\pi}{M}\right) + 0.54\, D_M(\phi) + 0.23\, D_M\left(\phi + \frac{\pi}{M}\right)$$

TUKEY — HANNING

$$w(r) = \begin{cases} 0.5\,\{\,1 + \cos(\pi r/M)\cdots |r| \leq M \\ 0 \qquad \cdots\cdots\cdots\cdots |r| > M \end{cases}$$

$$W(\phi) = 0.25\, D_M\left(\phi - \frac{\pi}{M}\right) + 0.5\, D_M(\phi) + 0.25\, D_M\left(\phi + \frac{\pi}{M}\right)$$

PARZEN

$$w(r) = \begin{cases} 1 - 6(r/M)^2 + 6(|r|/M)^3 & |r| \leq M/2 \\ 2\,(1 - |r|/M)^3 & \cdots\cdots\cdots M/2 \leq |r| \leq M \\ 0 & \cdots\cdots\cdots\cdots |r| > M \end{cases}$$

$$W(\phi) \sim \frac{3}{8\pi M^3} \left\{ \frac{\sin(M\phi/4)}{1/2\,\sin(\phi/2)} \right\}^4$$

BARTLETT - PRIESTLEY

$$w(r) = \frac{3M^2}{(\pi r)^2} \left\{ \frac{\sin(\pi r/M)}{\pi r/M} - \cos(\pi r/M) \right\}$$

$$W(\phi) = \begin{cases} \frac{3M}{4\pi} \left\{ 1 - \left(\frac{M\phi}{\pi}\right)^2 \right\} \cdots |\phi| \leq \pi/M \\ 0 \qquad \cdots\cdots\cdots\cdots |\phi| > \pi/M \end{cases}$$
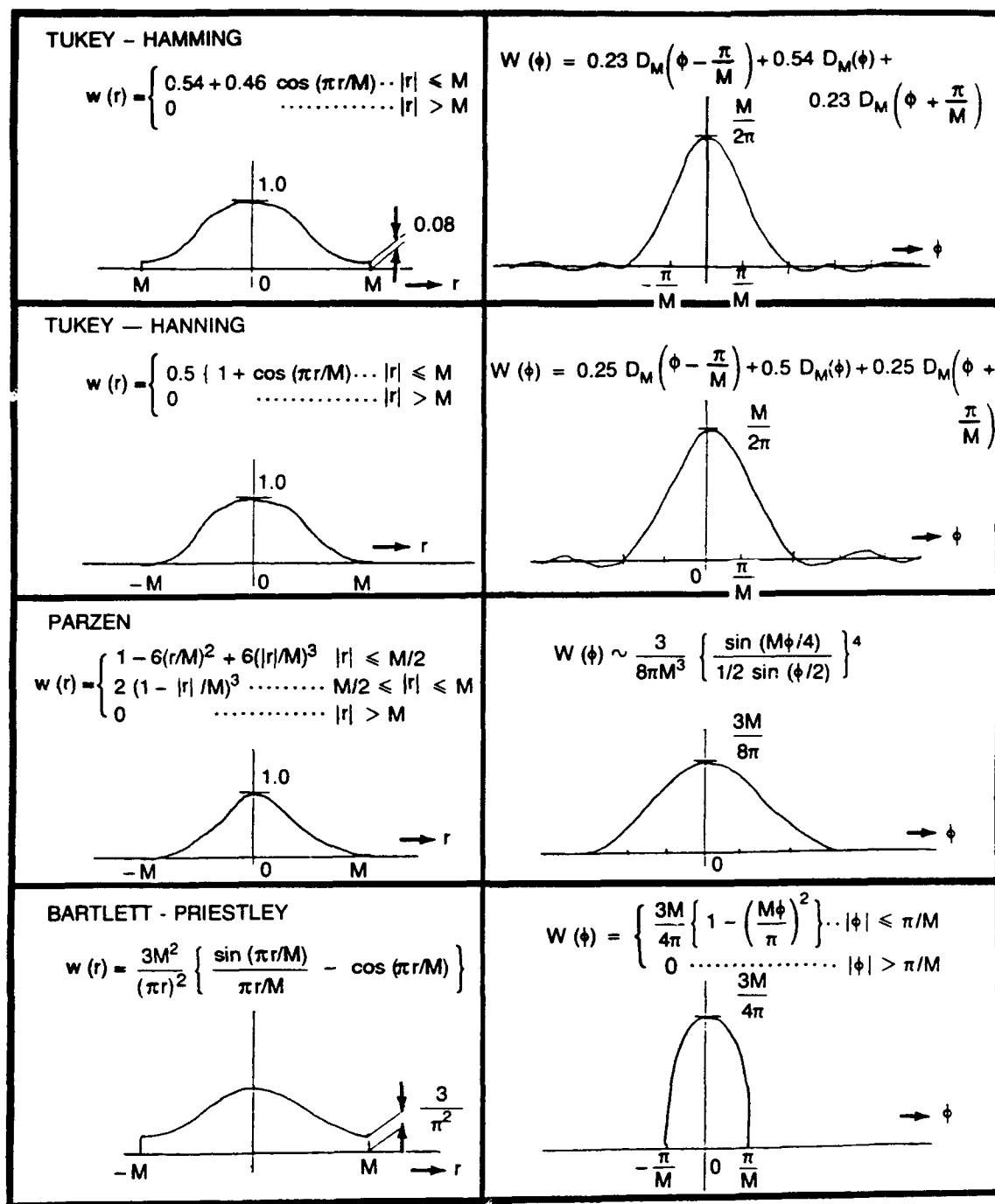
Fig. 2.14. Various window pairs (II).

34
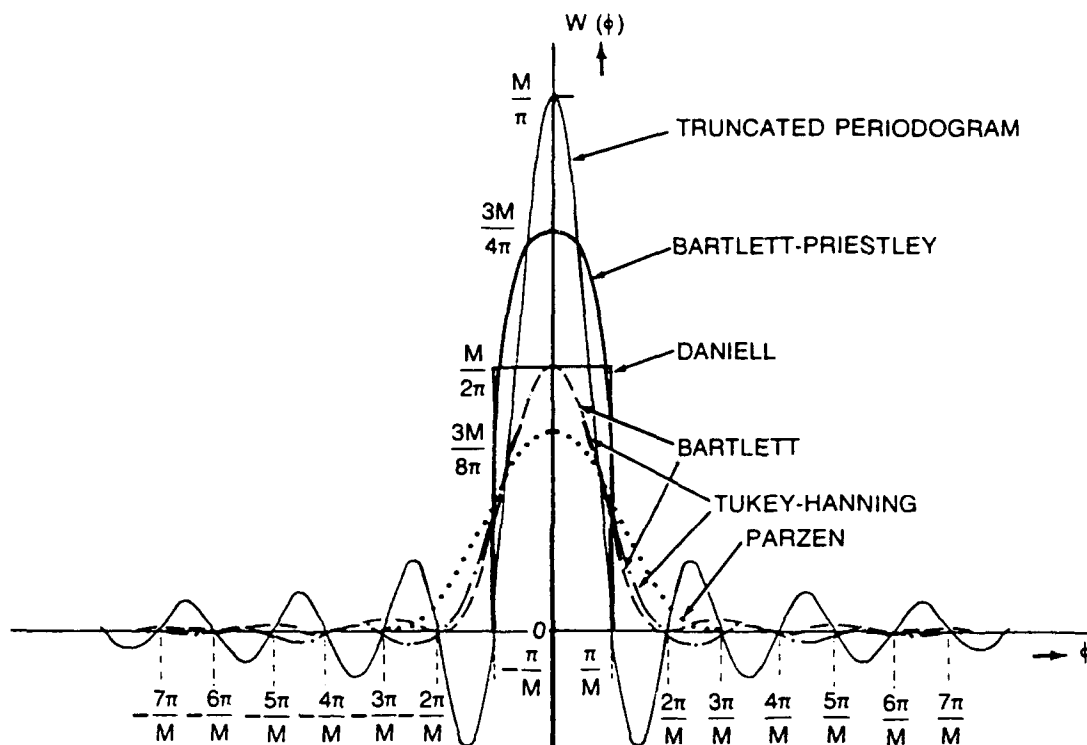
Fig. 2.15. Various spectral windows.

$$\text{bias } [\hat{s}(\omega)] = E\left\{\hat{s}(\omega) - s(\omega)\right\} \sim \frac{1}{2} s''(\omega) \int_{-\pi}^{\pi} \phi^2 W(\phi)\, d\alpha \qquad (2.95)$$

Here $s''(\omega)$ is the second derivative, and this is the bias at the peak of the spectrum when $s'(\omega) = 0$.

2. Variance, that was $s^2(\omega)$ for the estimator "Periodogram $P_N(\omega)$" as shown in Eq. 2.81, becomes

$$\text{var. } [\hat{s}(\omega)] \sim \frac{M}{N} s^2(\omega) \int_{-\infty}^{\infty} k^2(u)da = \frac{1}{N} s^2(\omega) \sum_{r=0}^{M} w^2(r), \qquad (2.96)$$

where

$$k(u) = k\left(\frac{r}{M}\right) = w(r), \quad u = \frac{r}{M}. \qquad (2.97)$$

35

When $w(r)$ can be expressed this way, the window is called a parameter window.

3. Equivalent degree of freedom v, as the χ^2 distribution that was $v = 2$ for the estimator $P_N(\omega)$, changes into

$$v = \frac{2N}{\left\{ \sum_r w_N^2(r) \right\}} \rightarrow \frac{2N}{\left\{ M \int_{-\infty}^{\infty} k^2(u)du \right\}}. \tag{2.98}$$

4. The spectrum window blurs the real spectrum, Fig. 2.16. Its extent depends on the window bandwidth (BW) which is defined in several different ways, although every definition tries to show the equivalent frequency range over which the smoothing is performed. For a single–peaked spectrum, this blur depends on the relative bandwidths of the spectrum and the spectrum window. Spectrum bandwidth is defined as the frequency range in which the spectrum shows half of the peak of the spectrum.
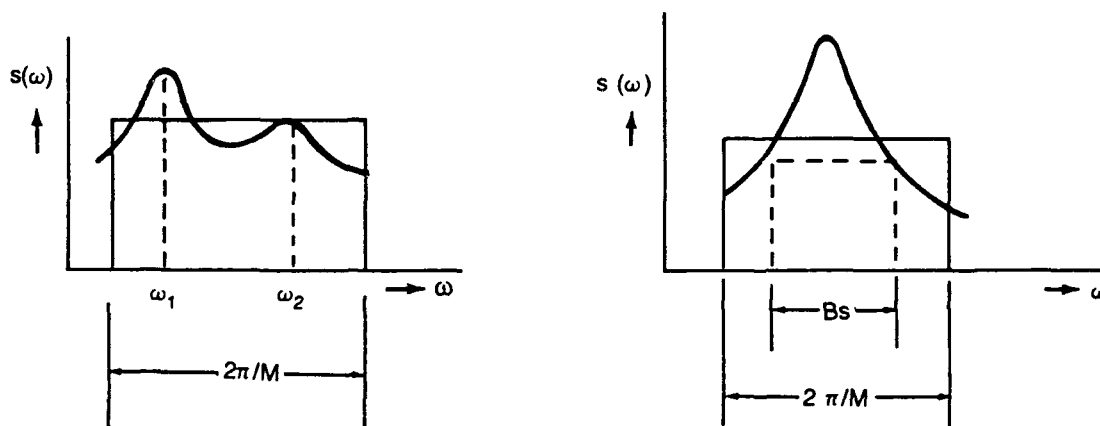
Fig. 2.16. Blur of the spectrum by Daniel's window, where the bandwidth is $2\pi/M$.

The resolution will be lower as the window bandwidth becomes narrower.

2.5.5 Expression of Confidence Interval and Precision of $\hat{s}(\omega)$

1. By χ_v^2 Approximation

36

As was mentioned in the preceding subsections, $\hat{s}(\omega)/s(\omega)$ can be approximated by χ_ν^2 distribution, with degree of freedom ν. Equivalent degree of freedom ν is expressed by Eq. 2.98 when the window is of the parameter type.

Accordingly, if $a_\nu(\alpha)$ and $b_\nu(\alpha)$ show the lower and upper $\left\{ 100\left(\dfrac{\alpha}{2}\right) \right\}$ percentage points of χ_ν^2 distribution, as shown in the key in Fig. 2.17,

$$\text{Prob. } [\chi_\nu^2 \le a_\nu(\alpha)] = \text{Prob. } [\chi_\nu^2 \ge b_\nu(\alpha)] = \frac{1-\alpha}{2}, \tag{2.99}$$

$$\text{Prob. } [a_\nu(\alpha) < \frac{\nu\hat{s}(\omega)}{s(\omega)} < b_\nu(\alpha)] = \alpha. \tag{2.100}$$

Therefore, α % confidence interval is

$$\left[\frac{\nu}{b_\nu(\alpha)} \hat{s}(\omega) \ , \ \frac{\nu}{a_\nu(\alpha)} \hat{s}(\omega) \right]. \tag{2.101}$$

This range is shown in Fig. 2.17 as a function of ν, with α, the confidence level, of 80%, 90%, or 95% as a parameter.

2. Approximation by Normal Distribution; see Fig. 2.18.

We know that when N tends to infinity, $R(r)$ follows the normal distribution, and as $\hat{s}(\omega)$ is a linear combination of $R(r), \hat{s}(\omega)$ also tends to follow the normal distribution. This relation can be assumed also from the fact that, when degrees of freedom $\nu \to \infty$, as $N \to \infty$, χ_ν^2–distribution tends to the normal distribution. Then, using the normal distribution, we can get the other expression for the confidence interval, as

$$\hat{s}(\omega) \pm c(x)\sqrt{\text{var. } \hat{s}(\omega)}. \tag{2.102}$$

Equations 2.100 and 2.101 give the confidence interval as,

$$\left[\frac{1}{1 + c(\alpha)\sqrt{\frac{2}{\nu}}} \hat{s}(\omega) \ , \ \frac{1}{1 - c(\alpha)\sqrt{\frac{2}{\nu}}} \hat{s}(\omega) \right]. \tag{2.102'}$$
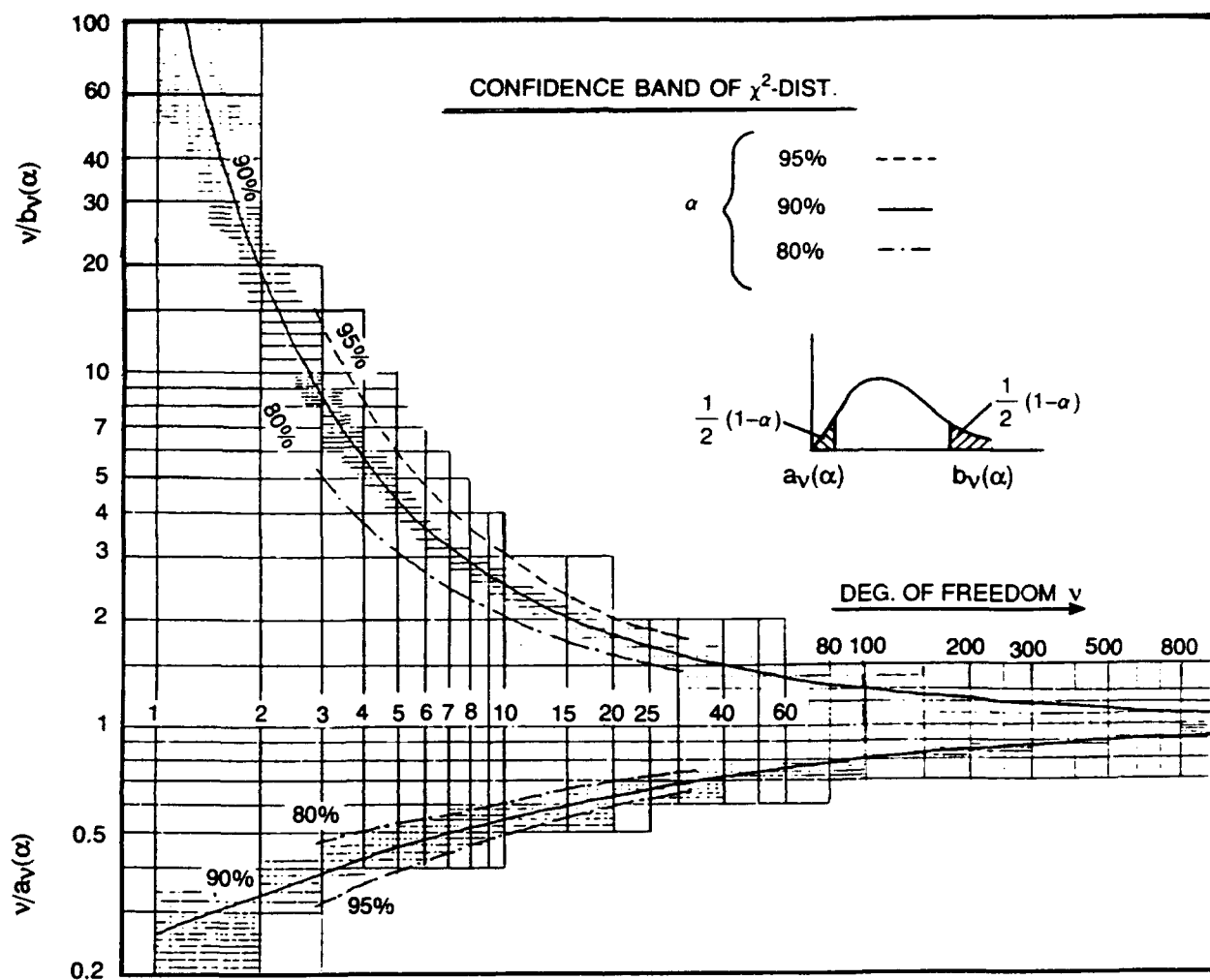
Fig. 2.17. Confidence band by χ^2–distribution.

This interval is shown in Fig. 2.19 at a confidence level of 90% (c = 1.64) as an example, with values of the χ^2–distribution at the 90% level. As ν increases, the confidence band shows almost the same level as the one from the χ^2–distribution.

3. Expressions of Precision of the Spectrum Estimation

There are several ways to express the measure of precision of the spectral estimates, and they are related to each other as shown in Priestly.[23]

$$\hat{s}(\omega) - C\,(\alpha)\sqrt{VAR.\ \hat{s}(\omega)} \qquad \hat{s}(\omega) \qquad \hat{s}(\omega) + C\,(\alpha)\sqrt{VAR.\ \hat{s}(\omega)}$$
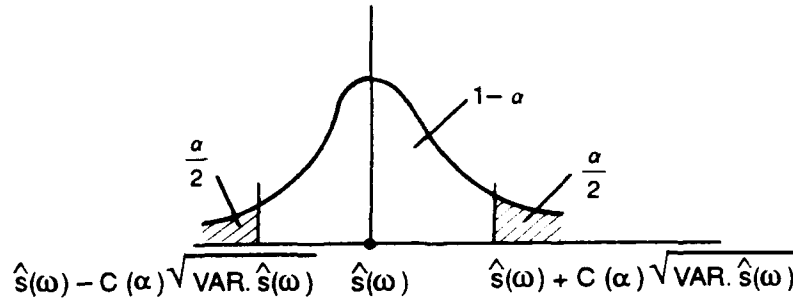
Fig. 2.18. Approximation by normal distribution.

i.) $p\%$ Gaussian range of percentage error $\delta(\omega)$

$$\delta(\omega) = c(p)\ \frac{v(\omega)}{s(\omega)} + \frac{|b(\omega)|}{s(\omega)}\ ,\qquad\qquad (2.103)$$

where $v(\omega) = \left[var.\ \{\hat{s}(\omega)\}\right]^{1/2}$: standard deviation

$b(\omega) = E\{\hat{s}(\omega)\} - s(\omega)$: bias

$c(p)$ is the two–sided $p\%$ point of the standardized normal distribution,

$$P\left[\frac{|\hat{s}(\omega) - s(\omega)|}{s(\omega)} \le \delta(\omega)\right] \ge \frac{p}{100}\ .\qquad\qquad (2.104)$$

ii.) The mean square percentage error $\eta(\omega)$

$$\eta^2(\omega) = \frac{\left[E\{\hat{s}(\omega) - s(\omega)\}^2\right]}{s^2(\omega)} = \frac{v^2(\omega) + b^2(\omega)}{s^2(\omega)}\ .\qquad\qquad (2.105)$$

By Chebycheff's inequality,
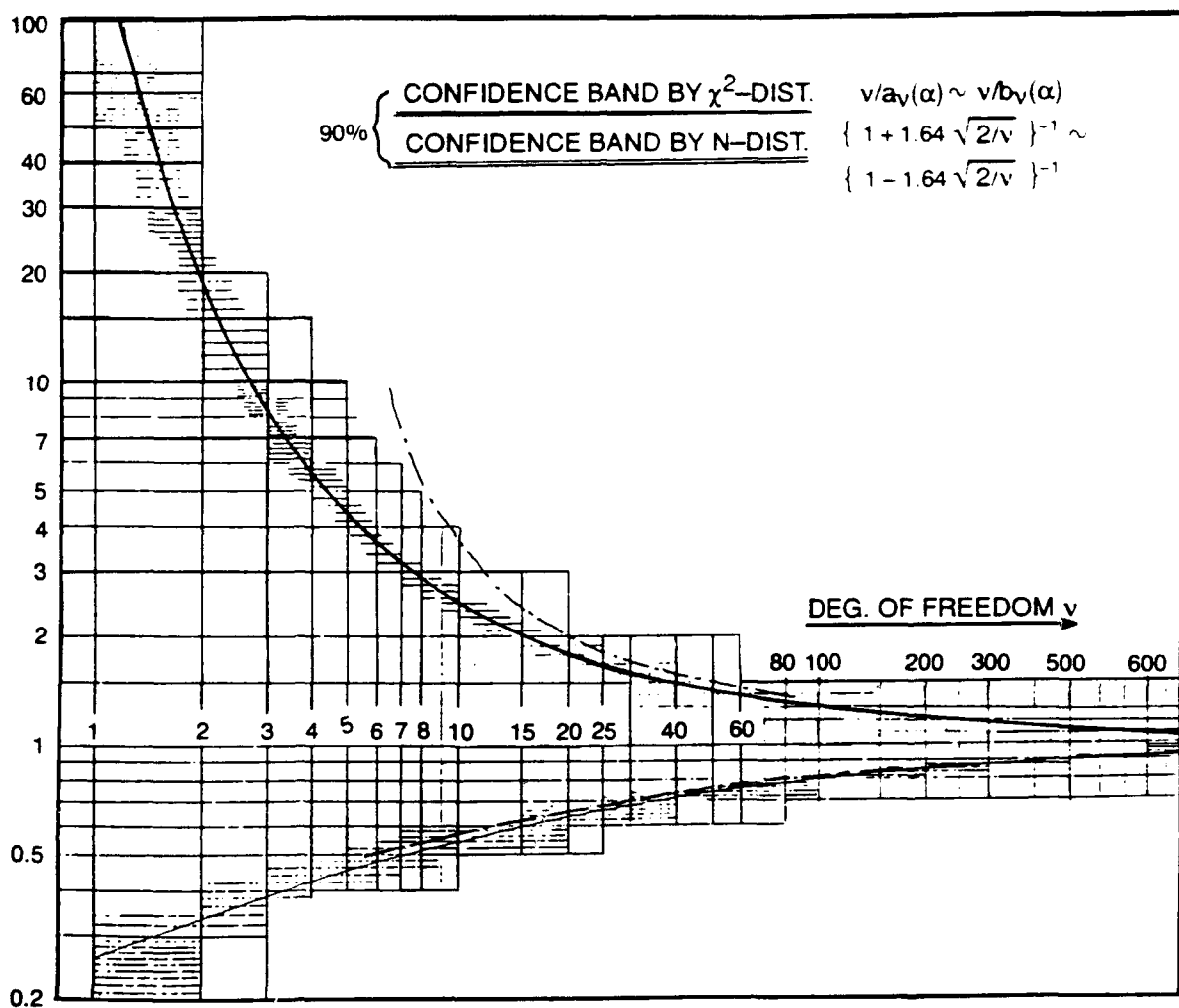
Fig. 2.19. Confidence band by χ^2–distribution, and Gaussian distribution (90% level).

$$p\left[\frac{|\hat{s}(\omega) - s(\omega)|}{s(\omega)} \leq \delta(\omega)\right] \geq 1 - \left\{\frac{\eta(\omega)}{\delta(\omega)s(\omega)}\right\}^2, \qquad (2.106)$$

in particular if we ignore the bias

$$b(\omega) = 0, \qquad \delta(\omega) = c(p)\eta(\omega). \qquad (2.107)$$

iii.) The signal to noise ratio introduced by Parzen[24] is

$$SNR\{\hat{s}(\omega)\} = \frac{E\{\hat{s}(\omega)\}}{\left[\text{var. } \{\hat{s}(\omega)\}\right]^{1/2}} \cdot \tag{2.108}$$

If we use the asymptotic normality of $\hat{s}(\omega)$, for large N

$$P\left[\left|\frac{\hat{s}(\omega) - E\{\hat{s}(\omega)\}}{E\{\hat{s}(\omega)\}}\right| \leq \delta\right] = \frac{p}{100} \cdot \tag{2.109}$$

So if we set

$$\delta(\omega) = c(p)\frac{\left[\text{var. } \{\hat{s}(\omega)\}\right]^{1/2}}{s(\omega)} , \tag{2.110}$$

and omit the bias $b(\omega)$ in Eq. 2.103, i.e., if $b(\omega) = 0$ or $E[\hat{s}(\omega)] \to \hat{s}(\omega)$, then

$$\delta(\omega) = c(p)\frac{1}{SNR\{\hat{s}(\omega)\}} \cdot \tag{2.111}$$

This relation shows that SNR $\left\{\hat{S}(\omega)\right\}$ is a simplified version of $\delta(\omega)$, when the bias of $\hat{s}(\omega)$ is ignored.

Also SNR can be expressed by equivalent degree of freedom ν, defined by Eq. 2.98 as $\nu = \dfrac{2N}{\displaystyle\sum_{r} w^2(r)}$, and as $\hat{s}(\omega)$ follows the χ^2–distribution with degree of freedom ν, where the mean and variance are ν and 2ν,

$$SNR\{\hat{s}(\omega)\} \doteqdot \frac{\nu}{\sqrt{2\nu}} = \left(\frac{\nu}{2}\right)^{1/2}$$

or

$$\nu = 2[SNR\{\hat{s}(\omega)\}]^2. \tag{2.112}$$

From Eqs. 2.111 and 2.112,

$$\delta(\omega) = c(p)\sqrt{2/\nu}. \tag{2.113}$$

41

The relationship shows that, if we assume the asymptotic normality of the spectrum estimate, then the proportional error $\delta(\omega)$ can be estimated from the equivalent number of degrees of freedom of the spectrum estimation ν, by Eq. 2.113, p and $c(p)$ being the level of confidence and $p/100$ the point of normal distribution as

$$\int_{-c(\alpha)}^{c(\alpha)} \frac{1}{\sqrt{2\pi}} e^{-\frac{x^2}{2}} \, dx = \frac{p}{100} \, . \tag{2.114}$$

From Eq. 2.98 or Table 2.2, we know that ν is proportional to N/M, and for most of the windows 2 to 3 times N/M. If, for example, $N/M \approx 10$ to 15, then ν is on the order of $\nu = 30$. If we adopt the confidence level of $p = 0.95$ (95%), then $c(p) = 1.96$. From the appropriate normal distribution

$$\delta(\omega) = 1.96 \sqrt{2/30} \doteq 0.506 \, .$$

This value means that the estimate of the spectrum ordinate has a proportional error in the order of 50% for this example.

2.5.6 Choice of the Spectral Window

It is now clear that, in order to get a consistent estimate of $s(\omega)$, we have to use a spectral window. Several spectral windows and their effects on the estimation are summarized in Table 2.2, from Priestley.[23]

Table 2.2. Effect of spectral windows.

	CHARACT. EXPONENT q	BIAS b (ω)	$\dfrac{\text{VAR}\{\hat{s}(\omega)\}}{s^2(\omega)}$	EQUIV. DEG. OF FREEDOM ν	WINDOW BANDWIDTH B_w
TRUNCATED PERIODOGRAM	∞	$0\ (M^{-\theta})$ θ: DECAY INDEX	$2\,\dfrac{M}{N}$	$\dfrac{N}{M}$	
BARTLETT	1	$-\dfrac{1}{M}\,s''(\omega)$	$1.5\,\dfrac{M}{N}$	$3\,\dfrac{N}{M}$	$1.56\,\dfrac{\pi}{M}$
DANIELL	2	$1.65\,\dfrac{\pi^2}{M^2}\,s''(\omega)$	$\dfrac{M}{N}$	$2\,\dfrac{N}{M}$	$2.0\,\dfrac{\pi}{M}$
TUKEY — GENERAL	2	$a\,\dfrac{\pi^2}{M^2}\,s''(\omega)$	$2(1-4a+6a^2)$ $\times\,\dfrac{M}{N}$	$(1-4a+6a^2)^{-1}$ $\times\,\dfrac{N}{M}$	$2\sqrt{6a}\,\dfrac{\pi}{M}$
TUKEY — HAMMING	2	$0.23\,\dfrac{\pi^2}{M^2}\,s''(\omega)$	$0.80\,\dfrac{M}{N}$	$2.52\,\dfrac{N}{M}$	$2.45\,\dfrac{\pi}{M}$
TUKEY — HANNING	2	$0.25\,\dfrac{\pi^2}{M^2}\,s''(\omega)$	$1.33\,\dfrac{M}{N}$	$2.67\,\dfrac{N}{M}$	$2.35\,\dfrac{\pi}{M}$
PARZEN	2	$0.01\,\dfrac{\pi^2}{M^2}\,s''(\omega)$	$0.54\,\dfrac{M}{N}$	$3.71\,\dfrac{N}{M}$	$3.82\,\dfrac{\pi}{M}$ $\vdots$ $(12/\pi)$
BARTLETT — PRIESTLY	2	$0.99\,\dfrac{\pi^2}{M^2}\,s''(\omega)$	$1.20\,\dfrac{M}{N}$	$1.4\,\dfrac{N}{M}$	$1.55\,\dfrac{\pi}{M}$

The spectral windows that make the spectral estimate consistent also affect the estimate in several other ways, as was summarized in Section 2.5.4. The most important parameter of this window is the size of M, which determines the window bandwidth (BW), that is by Priestley[23] expressed as,

$$B_w = \frac{2\sqrt{6}}{M}\left\{k^{(q)}\right\}^{\frac{1}{q}},\qquad(2.115)$$

where

$$k^{(q)} = \lim_{u\to 0}\left\{\frac{1-k(u)}{|u|q}\right\}.\qquad(2.116)$$

43

q is the largest integer that is a characteristic exponent of the function

$$k(u) \equiv k\left(\frac{r}{M}\right) = w_N(r), \text{ and the value of } q \text{ is listed in Table 2.2 for each representative}$$

spectrum window. When $q = 2$, as is the case for most of the listed spectral windows, there is a relationship

$$b(\omega) \text{ is on the order of } \frac{1}{2} s''(\omega) \int_{-\pi}^{\pi} \phi^2 W(\phi) d\phi$$

$$\text{is on the order of } \frac{1}{2M^2} s''(\omega) \int_{-\infty}^{\infty} \phi^2 K(\phi) d\omega, \tag{2.117}$$

where

$$K(\phi) = \frac{1}{2\pi} \int_{-\infty}^{\infty} k(u)e^{-i\omega u} du$$

or $k(u) = \int_{-\infty}^{\infty} K(\phi)e^{i\phi u} d\phi.$

To state the relative bandwidth of the spectral windows, we must define the bandwidth B_s of the spectrum itself. Usually, $B_s = \omega_2 - \omega_1$ where ω_2 and ω_1 are the frequency points at which the spectrum shows half the maximum power of the spectrum peak as in Fig. 2.20.
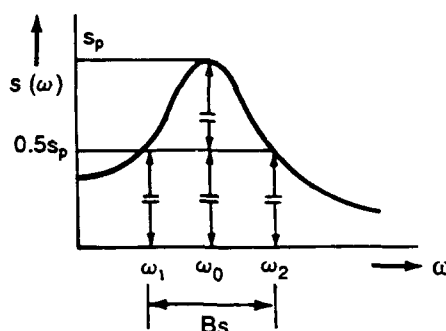
Fig. 2.20. Spectrum bandwidth.

To keep the blurring effect of the spectral window small, the bandwidth B_w of the window must be small compared with the spectrum bandwidth B_s. $B_w = \frac{1}{2}B_s$ is a popular guide.

As explained in Sections 2.5.2–2.5.5 the following tendencies, as shown in Table 2.3, are now clear.

Table 2.3. Statistical effects of the change of M.

M	VAR.	RELIABILITY	BIAS	WINDOW-BAND WIDTH	RESOLUTION
LARGE	LARGE	DOWN	SMALL	SMALL	UP
↕	↕	↕	↕	↕	↕
SMALL	SMALL	UP	LARGE	LARGE	DOWN

From sampling theorem it is known that, if $[\hat{s}(\omega)]$ is calculated from the frequency interval $\Delta\omega = \frac{\pi}{M}$, $\hat{s}(\omega)$ is completely determined, although since $\hat{s}(\omega)$ is a continuous function, it would be quite in order to evaluate it over a much finer set of points. It has been shown that we can generally use the value $\Delta\omega = \frac{1}{2}B_w$ for Daniel's window, where $B_w = \frac{2\pi}{M}$; accordingly $\Delta\omega = \frac{\pi}{M}$. When we use $\Delta\omega = \frac{\pi}{M}$, the spectrum window effect will be replaced by a weighted mean of the ordinates,

$$\hat{s}(\omega) = \sum_{i=-M}^{M} \alpha_i P_M\left(\omega + i\frac{\pi}{M}\right). \tag{2.118}$$

Values of α_i for several windows are shown in Table 2.4.

This table also gives values for the coefficient proposed by H. Akaike,[25] for minimizing the bias and variance of the estimate for the spectrum window. W_2 or its simplified form Q is generally used in most of our work, although W_3 would give a better spectrum with steeper peaks and deeper valleys. As a general procedure for choosing the best of W_1 to W_3, Akaike advises trying them all and, if no improvement in spectral form is recognized, adopting the window of the lower order.

45

Table 2.4. Coefficients α_i for various windows.

	α_{-3}	α_{-2}	α_{-1}	α_0	α_1	α_2	α_3	
TUKEY								
GENERAL			a	1-2a	a			
HAMMING			0.23	0.54	0.23			
HANNING			0.25	0.50	0.25			
PARZEN		0.008	0.164	0.657	0.164	0.008		
AKAIKE'S								WIDE
— W_1		0.	0.2434	0.5132	0.2432			↓
— W_2		−0.0600	0.2401	0.6398	0.2401	−0.0600		NARROW
— W_3	0.0149	−0.0891	0.2228	0.7029	0.2228	−0.0891	0.0149	
— Q		−0.06	0.24	0.64	0.24	−0.06		

2.5.7 Use of the Fast Fourier Transformation (F.F.T.) Method

There are misunderstandings sometimes that spectrum analysis by the Fast Fourier Transformation (F.F.T.) technique is completely different from getting the spectrum from analysis of auto correlation functions. However, Eq. 2.64 shows that this method is merely the one that gives the spectrum through a periodogram, and Eq. 2.66 shows that it is the same as calculating the spectrum from the Fourier transform of the auto correlation function.

Through the F.F.T. we get the spectrum ordinates at frequency $\dfrac{2\pi p}{N}$, or in the range

$-\pi \leq \omega \leq \pi$, at the frequency points $\dfrac{2\pi p}{N}$, $p = 0, \pm 1, \pm 2, \ldots \pm \dfrac{N}{2}$, in the dis-

crete case. This procedure corresponds to getting $\dfrac{N}{2} + 1$ ordinates in the frequency range

0 to π, or $N + 1$ ordinates in the frequency range $-\pi$ to π. It is the same as using

$M = \dfrac{N}{2}$ for a rectangular spectrum window and as a result, the individual spectrum ordi-

nates of $\dfrac{N}{2} + 1$ are so unreliable, statistically, and the variance so large that SNR = 100%,

equivalent to a degree of freedom $v = 2$. Accordingly, the same considerations on the use of the spectral window as were necessary for auto correlation methods are necessary for the F.F.T. method after getting the "raw" ordinates at $N + 1$ frequency points. Commercial programs or even a specialized spectrum analyzer through F.F.T. are now

available, but sometimes they do not say anything about "windows." We have to be careful in our choice of the window to be used in the analysis to obtain a reliable spectrum.

We can cut the number of computations from the order of N^2 for autocorrelation methods, N being the number of data, to $N(r_1 + r_2 + \ldots r_\phi)$ for the F.F.T. method when N is factored to $N = r_1 \cdot r_2 \cdot \ldots \cdot r_\phi$. Very commonly, $N = 2^P$ is used and then the number of computations is on the order of $2pN$ for F.F.T. For example, when $N = 1024 = 2^{10}$, the number of computations is reduced from the order of 1,000,000 to 20,000, or about 1/50.

The spectrum function is a powerful expression for showing the characteristics of a time series. However, we sometimes need the autocorrelation function to find the proper pair of lag and spectral windows, to decide the size of M compared with N, or to find an adequate statistical model from which we can go to the parametric analysis of the process, as will be mentioned in detail in Part II, Chapter 5.

The autocorrelation function $\hat{R}(s)$ can be obtained as the Fourier transform of $s(\omega)$ or as the periodogram $P_N(\omega)$ where, from Eq. 2.90,

$$s(\omega) = \int_{i-\infty}^{\infty} P_N(\phi) \ W_N(\omega - \phi) \ d\phi.$$

From Eqs. 2.64, 2.63, and 2.66,

$$P_N(\omega_p) = |F_x(\omega_p)|^2, \tag{2.64'}$$

$$F_x(\omega_p) = \frac{1}{\sqrt{2\pi N}} \sum_{t=1}^{N} X_r \ e^{-i\omega_p r}, p = 0, 1, \ \ldots \ \frac{N}{2} \tag{2.63'}$$

$$P_N(\omega_p) = \frac{1}{2\pi} \sum_{r=-(N-1)}^{N-1} \hat{R}(r) \ e^{-i\omega_p r}. \tag{2.66'}$$

Analogously, from Eq. 2.64' or from Eq. 2.66', we see that from $\dfrac{N}{2}$ ordinates of $P_N(\omega_p)$ it is impossible to get N values of $\hat{R}(r), r = 1, \ \ldots \ N$. We get only $\hat{R}(r)$ values at $r \leq \dfrac{N}{2}$.

In order to get $\hat{R}(r)$ values at $r = 0$ to N, we need N ordinates of the spectrum or the

periodogram $P_N(\omega_p)$. To make this possible we need N more data, and that can be realized by adding N 0's to the original data, as $\underbrace{\underbrace{x_0 \ldots \ldots x_{N-1}}_{N}, \underbrace{0,0,0, \ldots \ldots 0}_{N}}_{2N}$.

In this way the F.F.T. method can also be used for computing the correlation function from the spectrum ordinates at N frequency points as in Fig. 2.21.
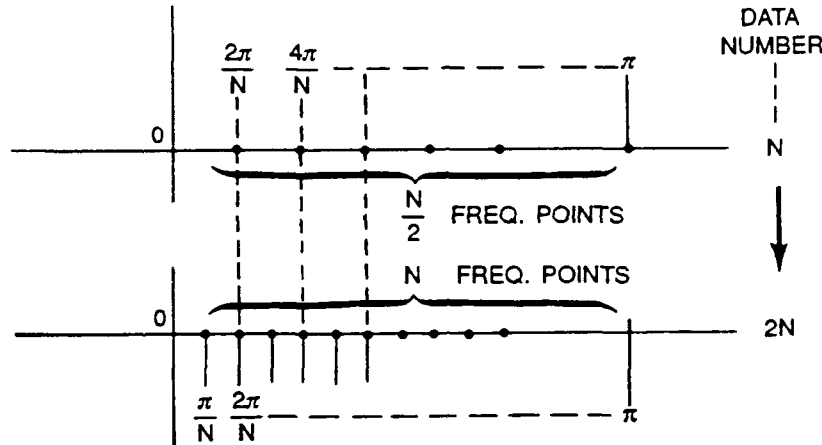
Fig. 2.21. Frequencies to calculate the spectrum.

2.5.8 Filtering

As was mentioned in Section 2.4.3, in sampling a continuous time series for computation of the spectrum, we have to pay attention to aliasing, and the sampling interval Δt should be small enough to avoid the aliasing. We must also be careful about the leakage of power or the blurring effect through the spectral window, especially when the spectrum has sharp peaks or steep valleys, because the spectral window acts as a smoothing filter. Besides, sometimes we are especially interested in the spectrum over a certain range of frequencies. Then the filtering technique is helpful in dividing the power of the spectrum by the frequencies or in modifying the shape of the spectrum to a shape more easily handled.

Generally, for a continuous process, the filtering effect can be expressed as

$$Y(t) = \int_{-\infty}^{\infty} g(\tau)X(t-\tau)d\tau, \qquad (2.119)$$

where $X(t), Y(t)$ are the original and filtered processes, respectively, and $g(\tau)$ shows the filtering effect in the time domain. For a physically realizable filter $g(\tau) = 0$, for $\tau < 0$, the range of integral can be from 0 to ∞. Then from the discussion in the preceding

48

subsections and assuming the existence of a spectrum of $X(t)$, $Y(t)$ and a Fourier transform of $g(u)$,

$$s_{YY}(\omega) = |G(\omega)|^2 s_{XX}(\omega), \tag{2.120}$$

$$G(\omega) = \int_{-\infty}^{\infty} g(\tau) e^{-i\omega\tau} d\tau. \tag{2.121}$$

A few samples of simple and ideal filters are given as follows:

1. Band–pass filter (Fig. 2.22)
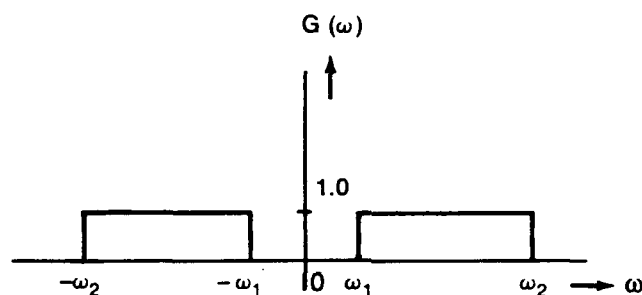
Fig. 2.22. Band–pass filter.

$$|G(\omega)|^2 = \begin{cases} 1 & ; \quad \text{for } \omega_1 \leq |\omega| \leq \omega_2 \\ 0 & \text{otherwise} \end{cases}. \tag{2.122}$$

Then

$$g(\tau) = \frac{1}{2\pi} \int_{-\infty}^{\infty} G(\omega) e^{i\omega t} d\omega = \frac{1}{2\pi} \int_{\omega_1}^{\omega_2} e^{i\omega t} d\omega$$

$$= \frac{\sin\omega_2\tau - \sin\omega_1\tau}{\pi\,\tau} \quad \text{for all } \tau \tag{2.123}$$

From the form of this function and Eq. 2.119, we need the input process $X(t)$ for $-\infty < t < \infty$, so theoretically this filter is physically unrealizable.

49

2. Low–pass filter (Fig. 2.23)
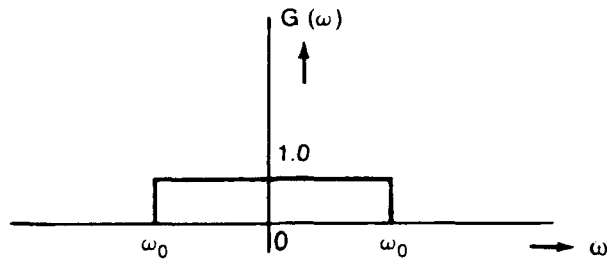
Fig. 2.23. Low–pass filter.

When $\omega_1 = 0$ for a band–pass filter,

$$|G(\omega)|^2 = \begin{cases} 1 & |\omega| \le \omega_0 \\ 0 & |\omega| > \omega_0 \end{cases}. \tag{2.124}$$

$$g(\tau) = \frac{\sin \omega_0 \tau}{\pi \tau} \tag{2.125}$$

3. High–pass filter (Fig. 2.24)
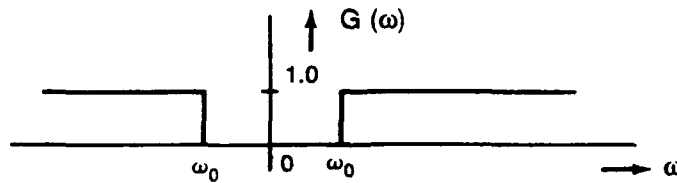
Fig. 2.24. High–pass filter.

When $\omega_2 \to \infty$ for a band–pass filter,

$$|G(\omega)|^2 = \begin{cases} 0 & |\omega| \le \omega_0 \\ 1 & |\omega| > \omega_0 \end{cases}. \tag{2.126}$$

Also for digital processes, we can express the digital filtering by

50

$$Y_t = \sum_{\tau=0}^{k} g_\tau X_{t-\tau}. \tag{2.127}$$

$$s_{YY}(\omega) = |G(\omega)|^2 s_{XX}(\omega) \tag{2.128}$$

$$G(\omega) = \sum_{\tau=0}^{k} g_\tau \, e^{-i\omega\tau}. \tag{2.129}$$

4. Low–pass digital filter (Fig. 2.25)
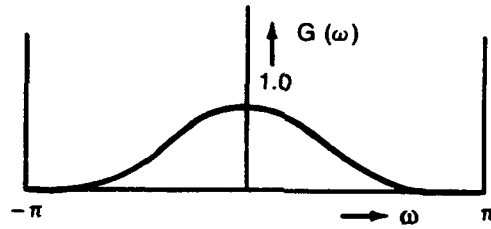
Fig. 2.25. Low–pass filter.

For example, the simplest equation for this type will be

$$Y_t = \frac{1}{2}(X_{t-1} + X_t). \tag{2.130}$$

Then

$$s_{YY}(\omega) = |G(\omega)|^2 s_{XX}(\omega)$$

$$= \left[\frac{1}{2}|1 + e^{-i\omega}|\right]^2 s_{XX}(\omega)$$

$$= \frac{1}{2}\{1 + \cos\omega\}s_{XX}(\omega). \tag{2.131}$$

5. High–pass digital filter (Fig. 2.26)

51
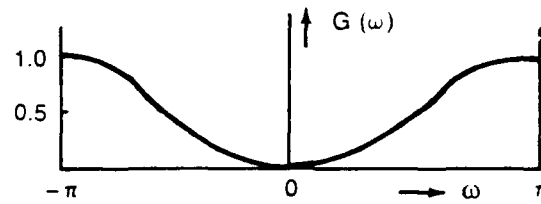
Fig. 2.26. High–pass filter.

The simplest equation for this type will be

$$Y_t = \frac{1}{2}(X_{t-1} - X_t) \tag{2.132}$$

Then

$$s_{YY} = \left[\frac{1}{2} |1 - e^{-i\omega}| \right]^2 s_{XX}(\omega)$$

$$= \frac{1}{2} \{1 - \cos \omega\} s_{XX}(\omega). \tag{2.133}$$

6. Pre–whitening digital filter (Fig. 2.27)
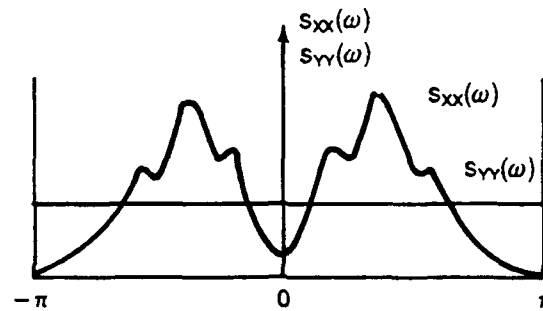
Fig. 2.27. Pre–whitening filter $|s_{YY}(\omega)/s_{XX}(\omega)|^{1/2}$.

If a digital filter such as

$$Y_t = a_0 X_t + a_1 X_{t-1} + a_2 X_{t-2} \ldots a_k X_{t-k} \ldots , \tag{2.134}$$

52

is used and the spectrum $s_{YY}(\omega)$ becomes a white spectrum $s_{YY}(\omega) = \sigma_Y^2$, then as will be shown in Section 5.4.2 of Part II,

$$s_{YY}(\omega) = \sigma_y^2 = |a_0 + a_1 e^{-i\omega} + a_2 e^{-2i\omega} + \ldots + a_k e^{-ki\omega}|^2 s_{XX}(\omega). \qquad (2.135)$$

Then

$$s_{XX}(\omega) = \frac{\sigma_y^2}{|a_0 + a_1 e^{-i\omega} + a_2 e^{-2i\omega} + \ldots + a_k e^{-ki\omega}|^2}. \qquad (2.136)$$

If we can find the filter that will make this spectrum completely white, that filter is called a complete pre–whitening filter. Then from Eq. 2.136, we can find $s_{XX}(\omega)$ from the variance σ_Y^2 of the filtered process (that is uniform), and the frequency function

$$|G(\omega)|^2 = |a_0 + a_1 e^{-i\omega} + a_2 e^{-2i\omega} + \ldots + a_k e^{-ki\omega}|^2. \qquad (2.137)$$

This tells us that finding the pre–whitening filter $G(\omega)$ is the same procedure as fitting a model to the X_t process expressed as

$$\epsilon_t = a_0 X_t + a_1 X_{t-1} + \ldots a_k X_{t-k} + \ldots, \qquad (2.138)$$

where ϵ_t is a completely random process with variance σ_Y^2. This is the problem of AR–model fitting to the process $X(t)$, which will be discussed in detail in Chapter 5, Part II of this paper.

2.6 MULTI–VARIATE SPECTRAL ANALYSIS; SPECTRAL ANALYSIS OF FREQUENCY RESPONSE

2.6.1 Two Variate Spectral Analysis

If there are two stochastic processes $\{X_{1,t}\}$ $\{X_{2,t}\}$ $t = 0, \pm 1, \pm 2, \ldots$, each weakly stationary, then Cov. $\{X_{1,t_1}\ X_{2,t_2}\}$ is a function of $(t_1 - t_2)$ only.

For this stationary bivariate process, the correlation matrix is defined as

$$R(r) = \begin{bmatrix} R_{11}(r) & R_{12}(r) \\ R_{21}(r) & R_{22}(r) \end{bmatrix}, \qquad (2.139)$$

where

53

$$\begin{cases} R_{11}(r) = E\Big[\{X_{1,t}-\mu_1\}^*\{X_{1,t+r}-\mu_1\}\Big] \\[2mm] R_{22}(r) = E\Big[\{X_{2,t}-\mu_2\}^*\{X_{2,t+r}-\mu_2\}\Big] \\[2mm] R_{21}(r) = E\Big[\{X_{1,t}-\mu_1\}^*\{X_{2,t+r}-\mu_2\}\Big] \;.\;.\;.\;.\;.\;. \; X_1 \text{ leading } X_2 \\[2mm] R_{12}(r) = E\Big[\{X_{2,t}-\mu_2\}^*\{X_{1,t+r}-\mu_1\}\Big] \;.\;.\;.\;.\;.\;. \; X_2 \text{ leading } X_1 \end{cases} \qquad (2.140)$$

$$R_{11}(-r) = R_{11}^*(r)$$

$$ (2.141)$$

$$R_{12}(r) = R_{21}^*(-r)$$

*Denotes the complex conjugate.

$$\varrho_{11}(r) = \frac{R_{11}(r)}{R_{11}(0)}$$

$$\varrho_{22}(r) = \frac{R_{22}(r)}{R_{22}(0)} \qquad (2.142)$$

$$\varrho_{21}(r) = \frac{R_{21}(r)}{\{R_{11}(0)\cdot R_{22}(0)\}^{1/2}} \;.$$

Then the spectrum matrix is

$$s(\omega) = \begin{vmatrix} s_{11}(\omega) & s_{12}(\omega) \\ s_{21}(\omega) & s_{22}(\omega) \end{vmatrix}, \qquad (2.143)$$

where

$$\begin{cases} s_{11}(\omega) = \dfrac{1}{2\pi} \sum_{r=-\infty}^{\infty} R_{11}(r)e^{-ir\omega} \\[2mm] s_{22}(\omega) = \dfrac{1}{2\pi} \sum_{r=-\infty}^{\infty} R_{22}(r)e^{-ir\omega} \\[2mm] s_{21}(\omega) = \dfrac{1}{2\pi} \sum_{r=-\infty}^{\infty} R_{21}(r)e^{-ir\omega} \ldots \ldots X_1 \text{ leading } X_2 \\[2mm] s_{12}(\omega) = \dfrac{1}{2\pi} \sum R_{12}(r)e^{-ir\omega} \ldots \ldots X_2 \text{ leading } X_1. \end{cases} \qquad (2.144)$$

For the spectrum to exist, the correlation function must be absolutely summable, for example,

$$\sum_{-\infty}^{\infty} |R_{21}(r)| < \infty. \qquad (2.145)$$

By spectral representation, using the Fourier–Stieltjes form,

$$X_{1,t} = \int_{-\pi}^{\pi} e^{it\omega} dZ_1(\omega) \qquad X_{2,t} = \int_{-\pi}^{\pi} e^{it\omega} dZ_2(\omega) \qquad (2.146)$$

$$E[dZ_1^*(\omega)\, dZ_1(\omega')] = \begin{cases} 0, & \omega \neq \omega' \\ s_{11}(\omega)d\omega, & \omega = \omega' \end{cases} \qquad (2.147)$$

$$E[dZ_2^*(\omega)\, dZ_2(\omega')] = \begin{cases} 0, & \omega \neq \omega' \\ s_{22}(\omega)d\omega, & \omega = \omega' \end{cases}. \qquad (2.148)$$

$dZ_1(\omega), dZ_1(\omega'); dZ_2(\omega), dZ_2(\omega')$ are orthogonal, respectively, and also cross orthogonal,

$$E[dZ_1^*(\omega)\, dZ_2(\omega')] = \begin{cases} 0, & \omega \neq \omega' \\ s_{21}(\omega)d\omega, & \omega = \omega' \end{cases} \qquad (2.149)$$

$$E[dZ_2^*(\omega)\ dZ_1(\omega')] = \begin{cases} 0, & \omega \neq \omega' \\ s_{12}(\omega)d\omega, & \omega = \omega' \end{cases}. \tag{2.150}$$

Inverting Eq. 2.144 gives for the two variate process

$$R_{21}(r) = \int\limits_{-\pi}^{\pi} e^{ir\omega} s_{21}(\omega)d\omega, \quad R_{12}(r) = \int\limits_{-\pi}^{\pi} e^{ir\omega} s_{12}(\omega)d\omega), \tag{2.151}$$

as was for the single variate process

$$R_{11}(r) = \int\limits_{-\pi}^{\pi} e^{ir\omega} s_{11}(\omega)d\omega, \quad R_{22}(r) = \int\limits_{-\pi}^{\pi} e^{ir\omega} s_{22}(\omega)d\omega). \tag{2.152}$$

When X_1 leads X_2, Eq. 2.144 gives

$$s_{21}(\omega) = \frac{1}{2\pi} \sum_{r=-\infty}^{\infty} R_{21}(r)e^{-ir\omega}.$$

Here, since $R_{21}(r)$ is not symmetrical on $r = 0$, the cross spectrum $s_{21}(\omega)$ is a complex function,

$$= Co_{21}(\omega) + iQu_{21}(\omega), \tag{2.153}$$

$$\begin{cases} Co_{21}(\omega) = \dfrac{1}{2\pi} \sum\limits_{r=-\infty}^{\infty} \dfrac{1}{2}\{R_{21}(r) + R_{21}(-r)\} \cos r\omega, & (2.154) \\[4mm] Qu_{21}(\omega) = \dfrac{1}{2\pi} \sum\limits_{r=-\infty}^{\infty} \dfrac{1}{2}\{-R_{21}(r) + R_{21}(-r)\} \sin r\omega. & (2.155) \end{cases}$$

$Co_{21}(\omega)$ and $Qu_{21}(\omega)$ are the co– and quadrature–spectra of $X_1(t)$ and $X_2(t)$ when $X_1(t)$ leads $X_2(t)$.

Thus the cross spectrum is expressed by its absolute value and argument as

$$|s_{21}(\omega)| = \left\{ Co_{21}^2(\omega) + Qu_{21}^2(\omega) \right\}^{1/2} \qquad (2.156)$$

$$\text{Arg } [s_{21}(\omega)] = \tan^{-1}\left[\frac{Co_{21}(\omega)}{Qu_{21}(\omega)} \right], \qquad (2.157)$$

and

$$d\omega |s_{21}(\omega)| \ e^{\text{Arg}[s_{21}(\omega)]} = s_{21}(\omega)d\omega$$

$$= E[dZ_1^*(\omega) \ dZ_2(\omega)]. \qquad (2.158)$$

In this case the coherency function $\gamma_{21}(\omega)$ is defined as

$$\gamma_{21}(\omega) = \frac{s_{21}(\omega)}{\{s_{11}(\omega)s_{22}(\omega)\}^{1/2}} = \frac{\text{cov}\left\{dZ_1^*(\omega) \ dZ_2(\omega)\right\}}{[\text{var}\{dZ_1(\omega)\} \ \text{var}\{dZ_2(\omega)\}]^{1/2}}. \qquad (2.159)$$

Thus $\gamma_{21}(\omega)$ is the correlation coefficient of $dZ_1^*(\omega)$ and $dZ_2(\omega)$. Here,

$$0 \le |\gamma_{21}(\omega)| \le 1 \quad \text{at all } \omega. \qquad (2.160)$$

Usually $|\gamma_{21}(\omega)|$ or $|\gamma_{21}(\omega)|^2$ is called the coherency function and shows the extent to which X_2, t and X_1, t are linearly related.

2.6.2 Linear Responses

Suppose there is a linear system, X_t being the input, Y_t the output as in Fig. 2.28. If

$$Y_t = \sum_{\tau=-\infty}^{\infty} g_t \ X_{t-\tau}, \qquad (2.161)$$

$\{g_t\}$ is called the impulse response function. If this is physically realizable,

$$g_t = 0 \quad \text{for} \quad \tau < 0.$$

INPUT   OUTPUT

X_t Y_t
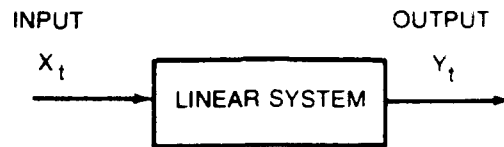
LINEAR SYSTEM

Fig. 2.28 Linear system.

However, we had better treat g_t for $-\infty \backsim +\infty$, because sometimes X_t itself does not express the real cause of Y_t, and g_t can even be non–zero at $\tau < 0$. We assume, for the impulse response,

$$\sum_{-\infty}^{\infty} |g_t| < \infty. \qquad (2.162)$$

Then

$$s_{YY}(\omega) = |G(\omega)|^2 \ s_{XX}(\omega), \qquad (2.163)$$

where

$$G(\omega) = \sum_{\tau = -\infty}^{\infty} g_t \ e^{-i\omega\tau}. \qquad (2.164)$$

$G(\omega)$ is called the transfer function or frequency response function of Y_t to X_t. For $s_{YY}(\omega)$ to be finite in total power $\int_{-\infty}^{\infty} s_{YY}(\omega)d\omega < \infty$, $s_{XX}(\omega)$ must be a bounded function of ω and $\int_{-\infty}^{\infty} |G(\omega)|^2 d\omega < \infty$. Accordingly, by Parseval's relation,

$$\sum_{-\infty}^{\infty} g_t^2 \ d\tau < \infty.$$

Using Eq. 2.161 gives

58

$$R_{YX}(r) = E\ [X_t^* Y_{t+r}] = \sum_{\tau = -\infty}^{\infty} g_\tau\ E[X_t^*\ X_{t+r-\tau}]$$

$$= \sum_{\tau = -\infty}^{\infty} g_\tau\ R_{XX}(r - \tau), \qquad (2.165)$$

and therefore

$$s_{YX}(\omega) = \frac{1}{2\pi} \sum_{r = -\infty}^{\infty} e^{-i\omega r} R_{YX}(r)$$

$$= \sum_{r = -\infty}^{\infty} g_t\ e^{-i\omega t} \frac{1}{2\pi} \sum_{r = -\infty}^{\infty} R_{XX}(r - t)\ e^{-i\omega(r-t)}$$

$$= G(\omega)\ s_{XX}(\omega). \qquad (2.166)$$

Accordingly,

$$G(\omega) = \frac{s_{YX}(\omega)}{s_{XX}(\omega)}. \qquad (2.167)$$

From Eq. 2.163

$$|G(\omega)|^2 = \frac{s_{YY}(\omega)}{s_{XX}(\omega)}. \qquad (2.163')$$

These equations show that, from the spectra of output and input, we get the $|G(\omega)|^2$, the response amplitude function, but if we need the complete response function including the phase relation, we have to use the cross spectrum $s_{YX}(\omega)$ as shown in Eq. 2.167.

In this ideal linear case

$$\gamma(\omega)^2 = \frac{s_{21}^2(\omega)}{\left\{s_{11}(\omega)\ s_{22}(\omega)\right\}} = \frac{\left[\frac{s_{YX}(\omega)}{s_{XX}(\omega)}\right]^2}{\left[\frac{s_{YY}(\omega)}{s_{XX}(\omega)}\right]} = \frac{|G(\omega)|^2}{|G(\omega)|^2} = 1. \qquad (2.168)$$

The coherency $|\gamma(\omega)|^2$ should be 1.

2.6.3 Linear Response in the Presence of Noise

When noise is added to the output Y_t, as in Fig. 2.29, where we assume N_t is real–valued, zero mean, uncorrelated with Y_t and with X_t.

$$Y'_t = Y_t + N_t = \sum_{-\infty}^{\infty} g_t \, X_{t-\tau} + N_t \,, \qquad (2.169)$$
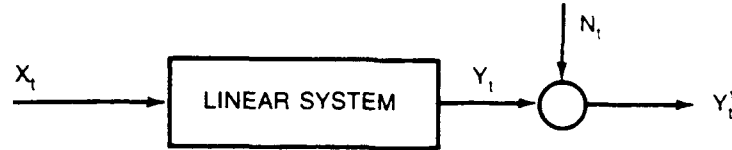
Fig. 2.29. Linear system in the presence of noise.

Then,

$$R_{Y'X}(r) = E[X_t^* \, Y'_{t+r}]$$

$$= \sum_{\tau=-\infty}^{\infty} g_\tau \, E[X_t^* \, X_{t+r-\tau}] + E[X_t^* \, N_{t+\tau}] \qquad (2.170)$$

$$= \sum_{\tau=-\infty}^{\infty} g_\tau \, R_{xx}(r-\tau),$$

because,

$$E[X_t^* \, N_{t+\tau}] = 0. \qquad (2.171)$$

Therefore

$$s_{Y'X}(\omega) = \frac{1}{2\pi} \sum_{r=-\infty}^{\infty} e^{-i\omega r} \left\{ \sum_{t=-\infty}^{\infty} g_t \, R_{xx}(r-\tau) \right\}$$

$$= G(\omega) s_{XX}(\omega) = s_{YX}(\omega) \qquad (2.172)$$

and

$$G(\omega) = \frac{s_{Y'X}(\omega)}{s_{XX}(\omega)} = \frac{s_{YX}(\omega)}{s_{XX}(\omega)} \qquad (2.173)$$

This shows that, if we take the cross spectrum of Y_t' with X_t, the frequency response function $G(\omega)$ can be obtained as the ratio of $s_{Y'X}(\omega)$ to the spectrum of input $s_{XX}(\omega)$ as was the ideal case in Eq. 2.167, because $s_{Y'X}(\omega)$ is not affected by the existence of noise N_t. However, taking the spectrum from Eq. 2.169 gives

$$s_{Y'Y'}(\omega) = |G(\omega)|^2 s_{XX}(\omega) + s_{NN}(\omega) = s_{YY}(\omega) + s_{NN}(\omega). \qquad (2.174)$$

Therefore, the coherency $\gamma^2(\omega)$ is

$$\gamma^2(\omega) = \frac{s_{Y'X}^2(\omega)}{s_{XX}(\omega)\ s_{Y'Y'}(\omega)} = \frac{\left\{\frac{s_{YX}(\omega)}{s_{XX}(\omega)}\right\}^2}{\frac{s_{Y'Y'}(\omega)}{s_{XX}(\omega)}}$$

$$= \frac{\{G(\omega)\}^2\{s_{Y'Y'}(\omega) - s_{NN}(\omega)\}}{\frac{\{s_{Y'Y'}(\omega) - s_{NN}(\omega)\}}{s_{XX}(\omega) \times s_{Y'Y'}(\omega)}}$$

$$= 1 - \frac{s_{NN}(\omega)}{s_{Y'Y'}(\omega)} = 1 - \eta^2(\omega). \qquad (2.175)$$

Here

$$\eta(\omega)^2 = \frac{s_{NN}(\omega)}{s_{Y'Y'}(\omega)} \qquad (2.176)$$

is called the residual error.

These results show that it is essential to calculate the cross spectrum to get a good estimate of the frequency response function.

2.6.4 Multiple Inputs Multiple Outputs Case

More generally for k multiple inputs and l multiple outputs, as in Fig. 2.30, the output is expressed by

$$Y_{i,t} = \sum_{\tau=-\infty}^{\infty} g_{i1,\tau} \, X_{i\cdot t-\tau} + \sum_{\tau=-\infty}^{\infty} g_{i2,\tau} \, X_{2\cdot t-\tau} + \ldots \sum_{\tau=-\infty}^{\infty} g_{ik,\tau} \, X_{k\cdot t-\tau} ,$$

$$+ \ldots \sum_{\tau=-\infty}^{\infty} g_{ik,\tau} \, X_{k\cdot t-\tau} , \qquad i = 1 \text{ to } l. \qquad (2.177)$$

or in vector form,

$$Y_t = \sum_{\tau=-\infty}^{\infty} g_t \, X_{t-\tau} . \qquad (2.178)$$

$$[l \times 1] \qquad [1 \times k] \, [k \times 1]$$
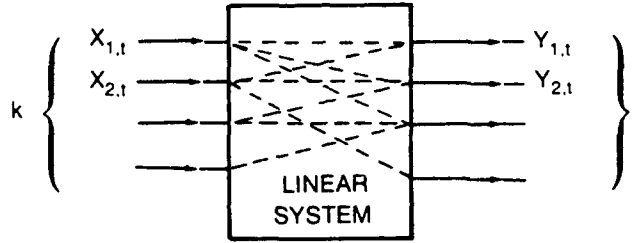
Fig. 2.30. Multiple inputs multiple outputs system.

If the output is expressed by spectral representation, then

$$Y_{i,t} = \int_{-\pi}^{\pi} e^{it\omega} \, dZ_i^{(y)}(\omega) \qquad i = 1 \text{ to } l, \qquad (2.179)$$

where

$$dZ_i^{(y)}(\omega) = G_{i\cdot 1}(\omega) dZ_1^{(x)}(\omega) + \ldots + G_{i\cdot k}(\omega) dZ_k^{(x)}(\omega) \qquad i = 1 \text{ to } l. \qquad (2.180)$$

2.6.5 Multiple Inputs Single Output Case, Multiple and Partial Coherencies

A multiple inputs, single output case, as in Fig. 2.31, is a special case of Eq. 2.177.
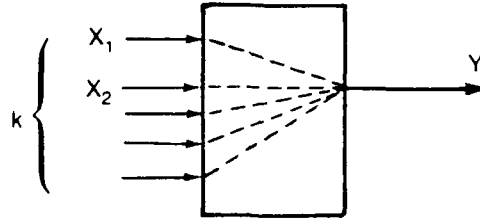
Fig. 2.31. Multiple inputs single output system.

$$Y_t = \sum_{\tau = -\infty}^{\infty} g_{1,\tau} X_{1,t-\tau} + \sum_{\tau = -\infty}^{\infty} g_{2,\tau} X_{2,t-\tau} + \ldots + \sum_{\tau = -\infty}^{\infty} g_{k,\tau} X_{k,t-\tau}. \quad (2.181)$$

Thus

$$R_{YY}(r) = \sum_{i=1}^{k} \sum_{j=1}^{k} \sum_{\alpha = -\infty}^{\infty} \sum_{\beta = -\infty}^{\infty} g_{i,\alpha} \; g_{j,\beta}^{*} \; R_{ij} \; (\alpha - \beta + r) \quad (2.182)$$

and

$$s_{YY}(\omega) = \sum_{i=1}^{k} \sum_{j=1}^{k} G_i(\omega) \; G_j^{*}(\omega) \; s_{ij}(\omega). \quad (2.183)$$

In the same way,

$$s_{Y_j}(\omega) = \sum_{i=1}^{k} G_i(\omega), \; s_{ij}(\omega), \quad (2.184)$$

where $R_{ij}(\tau) \equiv R_{X_iX_j}(\tau)$, $s_{ij}(\omega) \equiv s_{X_iX_j}(\omega)$, and $s_{Y_j}(\omega) \equiv s_{YX_j}(\omega)$.

The input is

$$X_t = [X_{1,t}, X_{2,t} \ldots X_{k,t}]. \quad (2.185)$$

Then setting

$$G(\omega) = [G_1(\omega), G_2(\omega) \ldots G_k(\omega)], \quad (2.186)$$

$$s_{XX}(\omega) = \begin{bmatrix} s_{11}(\omega) & s_{12}(\omega) & . & . & s_{1k}(\omega) \\ s_{21}(\omega) & s_{22}(\omega) & & & s_{2k}(\omega) \\ . & & . & & . \\ . & & . & & . \\ . & & . & & . \\ s_{k1} & & s_{k2}(\omega) & . & . & s_{kk}(\omega) \end{bmatrix}, \qquad (2.187)$$

$$s_{YY}(\omega) = [G_1(\omega)G_2(\omega) \ . \ . \ . \ G_k(\omega)] \begin{bmatrix} s_{11}(\omega) & s_{12}(\omega) & . & . & s_{1k}(\omega) \\ s_{21}(\omega) & . & & & s_{2k}(\omega) \\ . & & . & & . \\ . & & . & & . \\ . & & . & & . \\ s_{k1}(\omega) & s_{k2}(\omega) & . & . & s_{kk}(\omega) \end{bmatrix} \begin{bmatrix} G_1^*(\omega) \\ G_2^*(\omega) \\ . \\ . \\ . \\ G_k^*(\omega) \end{bmatrix}, \quad (2.188)$$

gives

$$s_{YY}(\omega) = G'(\omega) \ s_{XX}(\omega) \ G^*(\omega). \qquad (2.188\ ')$$

Here $G'(\omega)$ is the transpose of the vector $G(\omega)$.

Also

$$\begin{bmatrix} s_{Y1}(\omega) \\ s_{Y2} \\ . \\ . \\ . \\ s_{Yk}(\omega) \end{bmatrix} = \begin{bmatrix} s_{11}(\omega) & s_{12}(\omega) & . & . & . & . & s_{1k}(\omega) \\ s_{21}(\omega) & s_{22}(\omega) & & & & & s_{2k}(\omega) \\ . & & . & & & & . \\ . & & . & & & & . \\ . & & . & & & & . \\ s_{k1} & & s_{k2}(\omega) & . & . & . & . & s_{kk}(\omega) \end{bmatrix} \begin{bmatrix} G_1(\omega) \\ G_2(\omega) \\ . \\ . \\ . \\ G_k(\omega) \end{bmatrix}, \qquad (2.189)$$

gives

$$s_{YX}(\omega) = s_{XX}(\omega) \cdot G(\omega). \qquad (2.189')$$

Therefore

$$G(\omega) = s_{XX}^{-1}(\omega) \cdot s_{YX}(\omega), \qquad (2.190)$$

or

$$
\begin{bmatrix} G_1(\omega) \\ G_2(\omega) \\ . \\ . \\ . \\ G_k(\omega) \end{bmatrix} = \frac{1}{s_{XX}(\omega)} \begin{bmatrix} s_{Y1}(\omega) \\ s_{Y2}(\omega) \\ . \\ . \\ . \\ s_{Yk}(\omega) \end{bmatrix} .
\tag{2.190'}
$$

Thus the multiple coherency $\gamma^2_{YX}(\omega)$ is

$$
\gamma^2_{YX}(\omega) = \left| \frac{s_{YX}(\omega)}{s_{XX}(\omega)} \right|^2 \Bigg/ \frac{s_{YY}(\omega)}{s_{XX}(\omega)}
$$

$$
= \frac{s'_{YX}(\omega) \; s^*_{YX}(\omega)}{s_{XX}(\omega) \; s_{YY}(\omega)} = \frac{1}{s_{YY}(\omega)} \; G'(\omega), \; s^*_{YX}(\omega).
\tag{2.191}
$$

Here, as mentioned by L. Tick,[26] H. Akaike,[27] and Enochsen,[28] the conditional spectrum $S_{1\hat{2}.1}(\omega)$ is defined as

$$
s_{1\hat{2}.1}(\omega) = s_{11}(\omega) - s_{22}(\omega) \times \left| \frac{s_{12}(\omega)}{s_{22}(\omega)} \right|^2
$$

$$
= s_{11}(\omega) - \frac{|s_{12}(\omega)|^2}{s_{22}(\omega)} = s_{11}(\omega) \left\{ 1 - \frac{|s_{12}(\omega)|^2}{s_{11}(\omega), s_{22}(\omega)} \right\}
$$

$$
= s_{11}(\omega) \left\{ 1 - \gamma_{12}(\omega) \right\}.
\tag{2.192}
$$

This shows the spectrum of $X_1 X_1$ under the condition that X_2 has occurred, that is, the spectrum of $X_1 X_1$ masked the effect of X_2.

Generally, if the conditional spectrum of $s_{YX}(\omega)$, under the condition that x_j has occurred, is expressed by $s_{Y\hat{j}.12\ldots\hat{j}\ldots k}(\omega)$, then the partial coherency is defined as

$$
\gamma_{Y\hat{j}.12\ldots\hat{j}\ldots k}(\omega) = \frac{|s_{Y\hat{j}.12\ldots\hat{j}\ldots k}(\omega)|^2}{s_{\hat{jj}.12\ldots\hat{j}\ldots k}(\omega) s_{YY.12\ldots\hat{j}\ldots k}(\omega)}.
\tag{2.193}
$$

65

THIS PAGE INTENTIONALLY LEFT BLANK

CHAPTER 3

CONSIDERATIONS ON THE IMPROVEMENT OF COHERENCY FUNCTIONS

3.1 INTRODUCTION

Coherency functions $\gamma(\omega)$ can be considered good clues to finding the extent to which the system can be approximated as linear to the input X_t which can also be considered linear. If there is noise in the output Y_t, as was discussed in Section 2.6.3, the coherency function will be reduced, usually to coherencies of less than 1. It is difficult to find the real reason for this reduction, although Eqs. 2.175 and 2.176 tell us it is the effect of noise. Here not only noise in the output but also computational error, statistical bias, nonlinearity of the response characteristics, and the effect of feedback are all counted as noise in the result. All the effects that cannot be accounted for by linear, open relations are counted as noise. The author has made a few suggestions for improving the nonparametric spectrum analysis and the resulting computation of coherencies.

3.2 SHIFT OF THE OUTPUT IN CALCULATING THE CROSS SPECTRUM

$R_{ii}(r)$, the auto correlation function of a real process $i(t)$, is an even function and shows a maximum value at $r = 0$, the origin of the lag r. The lag window applied to this auto correlation to get consistent estimates of the spectrum ordinates is also usually an even function and has its peak at $r = 0$, and $w(0) = 1$, as in Fig 2.11. Accordingly, $R(0)$ remains unchanged and then gradually decreases toward $r = \pm M$. This procedure keeps the most reliable and important part of the correlation near $r = 0$ almost unchanged and reduces the contribution of the correlation at larger values of r near $\pm M$, where the correlation is less reliable, to nearly zero, preventing the formation of large negative lobes in the spectral window. This way is reasonable to get consistent estimates of the spectral ordinates and make the spectral window fulfill conditions 1–5 in Section 2.5.4.

However, in getting the cross correlation, if we use lag windows in the same way, sometimes important information is lost, and the result is an apparent reduction in coherencies. This was studied theoretically by N. Akaike and Y. Yamanouchi[29] (1962), but a more intuitive explanation by this author [Yamanouchi[30] (1961)] is given here.

In cross correlation $R_{ij}(r)$, if the phase relation of the output $j(t)$ lags or leads the input $i(t)$ considerably, the maximum value of the cross correlation, which is not the even function, will no longer lie at the origin $r = 0$ but will lie at a larger or minus value of r (distant from the origin). In applying lag windows, if we set the maximum of the lag window at $r = 0$, sometimes important information is lost at the peak of cross correlation. A small value of the lag window will be multiplied to the peak value of the cross correlation at a larger or minus value of r, and will keep the less important part of the cross correlation almost unchanged by the windows, as shown in the example in Fig. 3.1. This is not reasonable, so the author suggested shifting the origin of the cross correlation to its peak point and then applying the lag windows. The amount of the change of phase from this shift r_0 should, of course, be used later to modify the phase relation by $r_0\omega$.
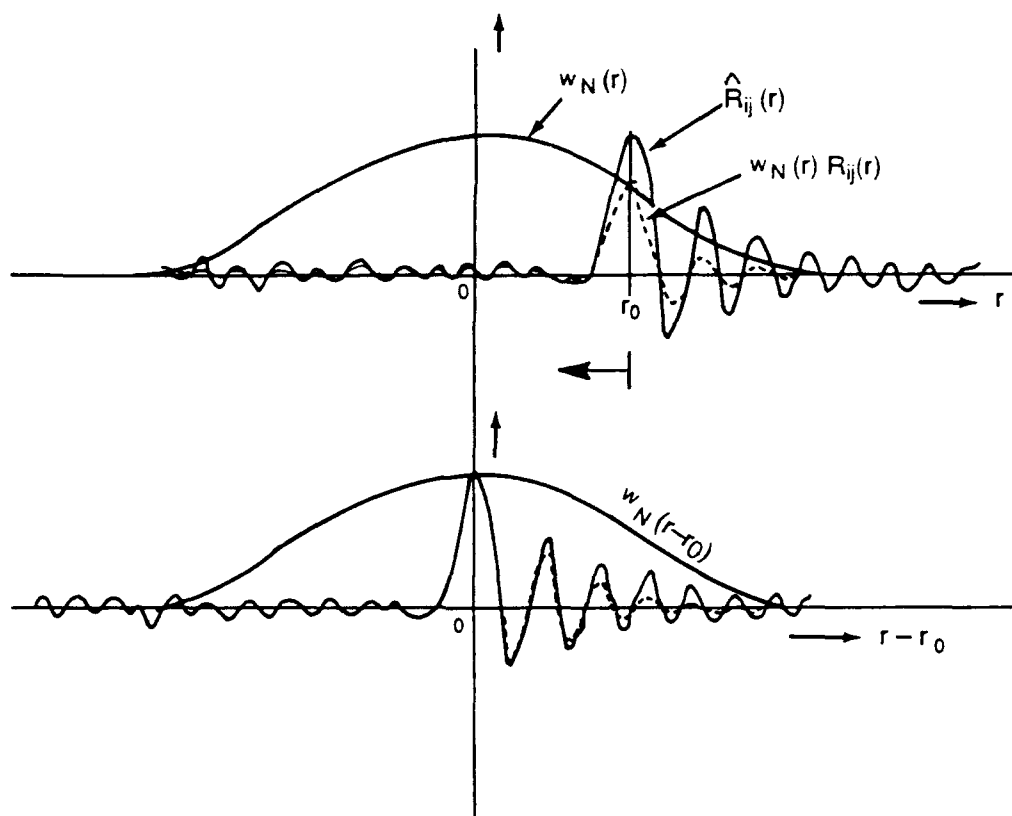
Fig. 3.1. Shift of cross correlation in applying the lag window.

This alignment technique can be expressed as a shift in lag windows as well as a shift in the origin of the correlation, or as a shift of the output time series relative to the input time series,

$$\hat{\hat{s}}_{ji}(\omega) = \frac{1}{2\pi} \sum_{r=-(N-1)-r_0}^{(N-1)-r_0} w(r-r_0)R_{ji}(r)e^{-i\omega r}, \qquad (3.1)$$

where $w(r)$ is the standard type of lag window for estimation of the auto–spectra.

Thus

$$\hat{\hat{s}}_{ji}(\omega) = \frac{1}{2\pi} \sum_{r=-(N-1)}^{(N-1)} w(r)R_{ji}(r+r_0)e^{-i\omega(r+r_0)}. \qquad (3.2)$$

So if we set

$$\hat{s}_{ji}'(\omega) = \frac{1}{2\pi} \sum w(r)R_{ji}(r + r_0)e^{-i\omega r}, \qquad (3.3)$$

then

$$\hat{s}_{ji}(\omega) = \hat{s}_{ji}(\omega) \times e^{-i\omega r_0}. \qquad (3.4)$$

The phase is shifted by ωr_0 by this shift in the origin. Accordingly the phase of the output should be modified by $-r_0\omega$ after the cross spectrum analysis. Figure 3.2 shows an example of this shift in the analysis of a 5-ft model ship rolling in tank waves[31] (beam sea, without advance speed). From this figure, we find the amount of shift on cross correlation should be $r_0 = 9$. The results of the analysis are shown in Figs. 3.3 and 3.4. The improvement in the coherencies due to the shift is clearly shown in the upper part of Fig. 3.4. The improvements in phase relation and in gain are also apparent, although these improvements are partly due to the large $m(= 60 > 40)$.
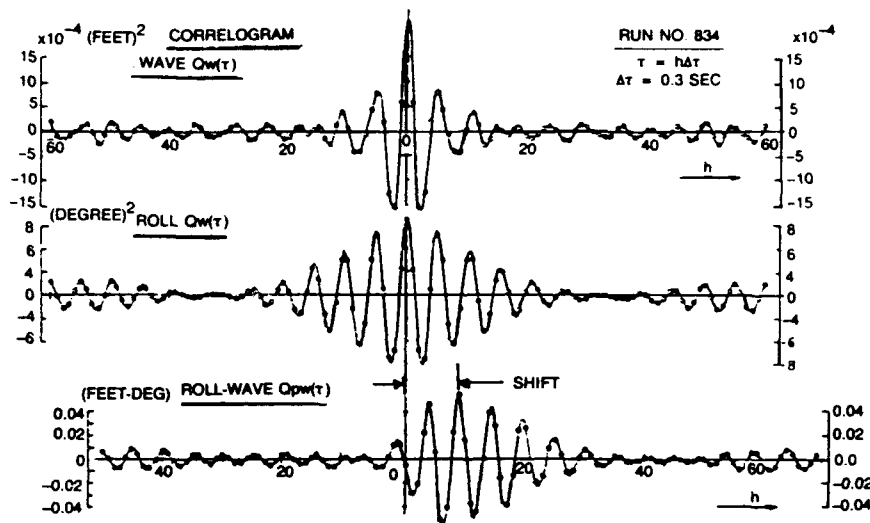
Fig. 3.2. Auto and cross correlations of wave, roll, roll–wave
for a model ship in tank (run 834).
(From Yamanouchi.[31])

Of special interest to us is that the improvement in coherencies is also reflected in the change of bandwidth of the cross spectrum. Before the shift in origin, the co- and quad–spectra in Fig. 3.3 had a narrower bandwidth than after the shi^ showing that the blurring effect of the spectral window is smaller for the cross spectra with broader bandwidth than for those with narrower bandwidth. Thus this shift improved the estimate of the cross spectra by reducing the leakage of power. Although we refer to improvement, we do not have experimental data in regular waves for comparison in this run. However, in Figs. 3.5–3.7, which show the same kind of result for run 832 and the data in regular waves (Fig. 3.7), we notice the same tendency and conclude that the results obtained by

this shift are best in this analysis and closest to the experimental data obtained in regular waves.
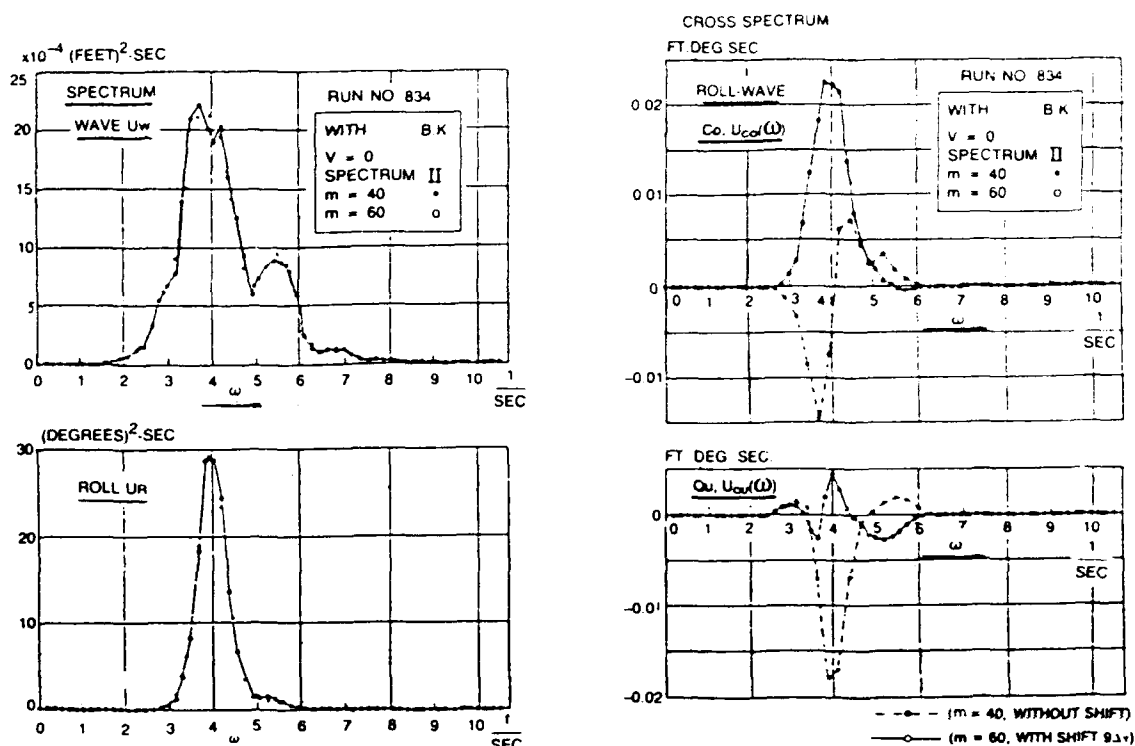
Fig. 3.3. Auto and cross spectra of wave, roll, roll–wave (run 834) (max. lag no. m=60 with shift and m=40 without shift).

(From Yamanouchi.[31])

3.3 IMPULSE RESPONSE FUNCTIONS FROM THE CROSS AND AUTO CORRELATIONS

By Eq. 2.169 for a linear system,

$$y_t = \sum_{u=-\infty}^{\infty} g_u \, X_{t-u} + N_t, \tag{3.5}$$

where g_u is the linear impulse response function of the linear system, X_t and Y_t are the input and output, respectively, and N_t is the noise, uncorrelated with X_t and Y_t. By Eq. 2.164

$$G(\omega) = \sum_{u = -\infty}^{\infty} g_u \, e^{-i\omega u} \qquad (3.6)$$

where $G(\omega)$ is the frequency response function of this system. Then as already shown by Eqs. 2.165, 2.170; 2.166, 2.172,

$$R_{YX}(r) = \sum_{u} g_u \, R_{XX}(r - u) \qquad (3.7)$$
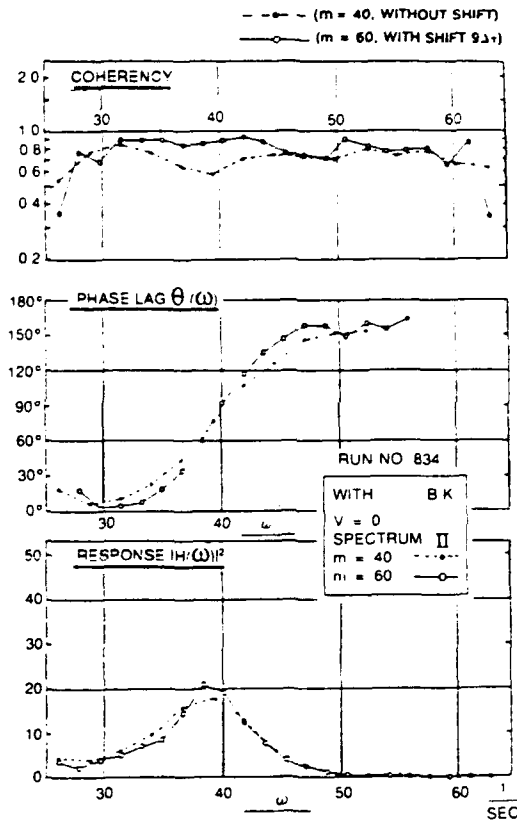
Fig. 3.4. Frequency responses of roll-wave (run 834)
(m=60 with shift and m=40 without shift).

(From Yamanouchi.[31])

$$s_{YX}(\omega) = G(\omega) \, s_{XX}(\omega) \qquad (3.8)$$

If we assume that g_u (with $-\infty < u < \infty$) can be approximated by finite terms of g_u (with $-n < u < n$), then Eq. 3.7 gives the matrix of Eq. 3.9,

71
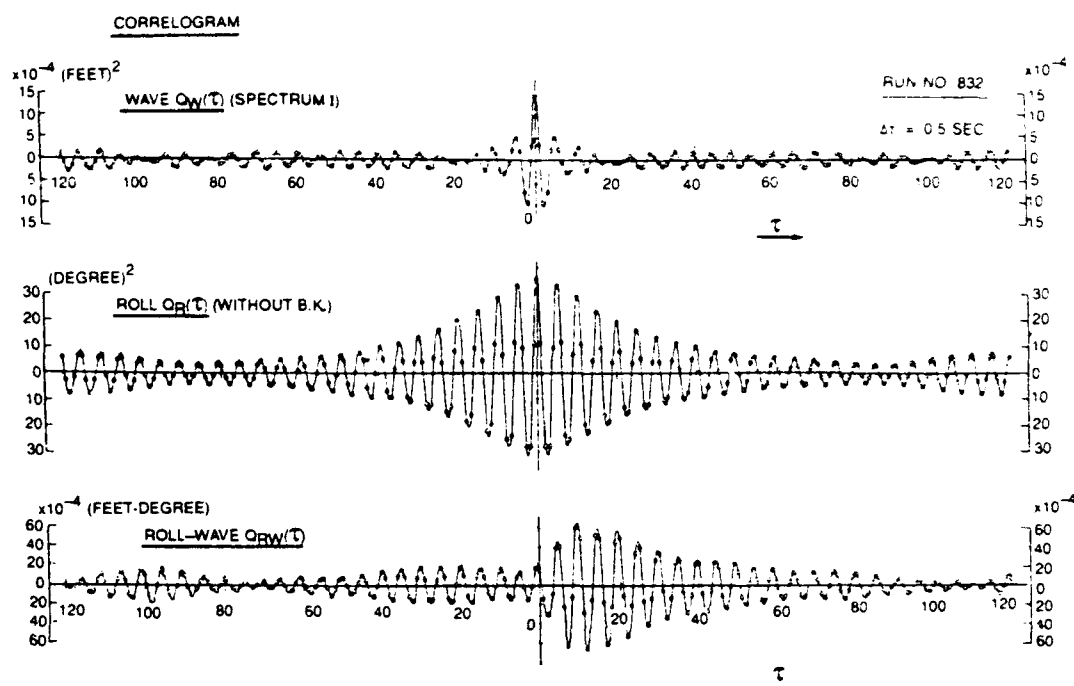
Fig. 3.5. Auto and cross correlation of wave, roll, roll-wave of a
model ship (run 832).
(From Yamanouchi.[31])

$$
\begin{bmatrix}
R_{YX}(-n) \\
R_{YX}(-n+1) \\
\cdot \\
\cdot \\
\cdot \\
\cdot \\
R_{YX}(0) \\
\cdot \\
\cdot \\
\cdot \\
R_{YX}(n-1) \\
R_{YX}(n)
\end{bmatrix}
=
\begin{bmatrix}
R_{XX}(0) & R_{XX}(1) \dots \dots R_{XX}(n) \dots \dots R_{XX}(2n) \\
R_{XX}(1) & R_{XX}(0) \dots \dots R_{XX}(n-1) \dots R_{XX}(2n-1) \\
\cdot & \cdot & \cdot & \cdot \\
\cdot & \cdot & \cdot & \cdot \\
\cdot & \cdot & \cdot & \cdot \\
\cdot & \cdot & \cdot & \cdot \\
R_{XX}(n) & R_{XX}(n-1) \dots R_{XX}(0) \dots \dots R_{XX}(n) \\
\cdot & \cdot & \cdot & \cdot \\
\cdot & \cdot & \cdot & \cdot \\
\cdot & \cdot & \cdot & \cdot \\
R_{XX}(2n-1) & R_{XX}(2n-2) \dots R_{XX}(n-1) \dots R_{XX}(1) \\
R_{XX}(2n) & R_{XX}(2n-1) \dots R_{XX}(n) \dots \dots R_{XX}(0)
\end{bmatrix}
\begin{bmatrix}
g_{-n} \\
g_{-n+1} \\
\cdot \\
\cdot \\
\cdot \\
\cdot \\
g_0 \\
\cdot \\
\cdot \\
\cdot \\
g_{n-1} \\
g_n
\end{bmatrix}
, (3.9)
$$

using the relation $R(-r) = R(r)$. Here for the cross correlations, we use the shifted version
of $R_{YX}(r)$, as $R_{YX}(0)$ is to be the maxima over the range $r = -n$ to n, and for the auto cor-
relation, the range 0 to $2n$. The matrix on the right hand side of Eq. 3.9 is large on the
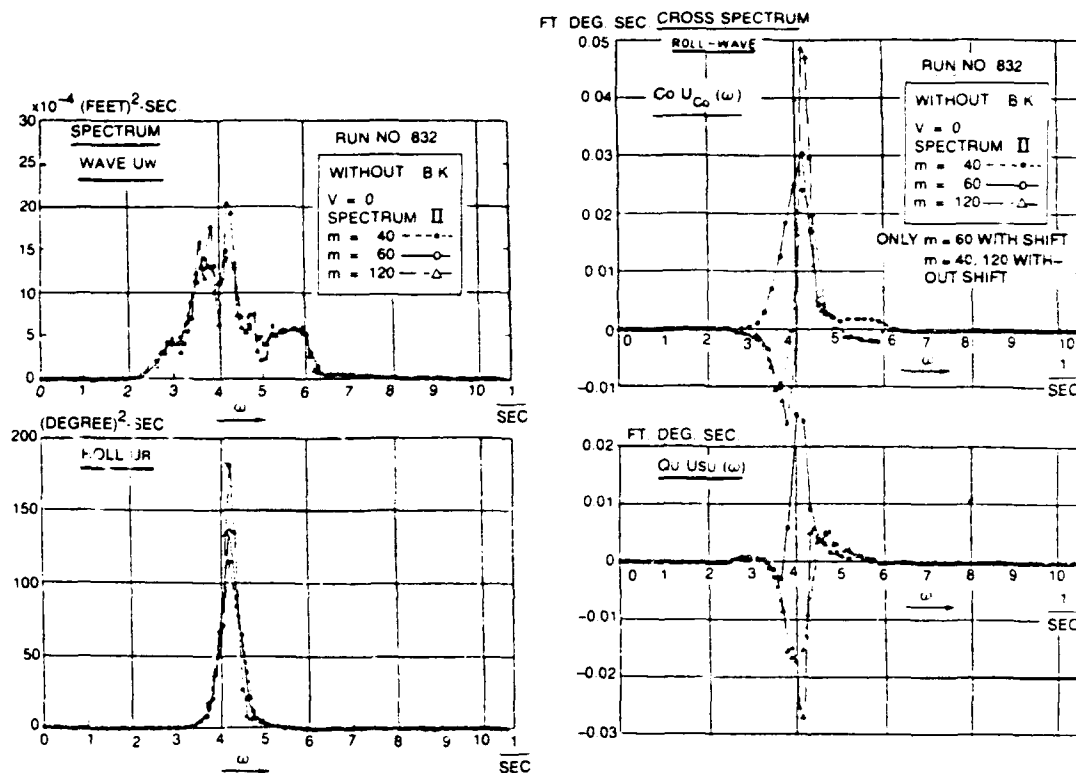
Fig. 3.6. Auto and cross spectra of wave, roll, roll–wave (run 832)
(m=60 with shift, and m=40 and 120 without shift).
(From Yamanouchi.[31])

diagonal and is symmetrical around the diagonal. The solution of Eq. 3.9 gives g_u over

the range $u = -n$ to n. This author [Yamanouchi[32]] believes this method provides the lag window free estimate of the impulse response function, or the spectral window free estimate of the frequency response function from Eq. 3.6. The choice of the lag window or the spectrum window is a serious problem in getting a good estimation of the spectra and the frequency response relations of the output to the input, as was discussed in Sections 2.5.2–2.5.6. This method eliminates the problem of windows and frees the calculation from their blurring effect. The use of Eq. 3.9 might eliminate also some of the uncertainties and errors in the algorithm for the correlation.

Figures 3.8–3.11 show the analysis of the rolling of model ships afloat in irregular beam seas. g_u for -90 to 90 was analyzed using $R_{YX}(\omega)$ of -90 to 90 and R_{XX} of 0 to 180. The correlations in Fig. 3.8, where the cross correlations are already shifted by 9, are shown in normalized form and the calculated g_u are shown at the top of Fig. 3.9 for u of -30 to $+30$ only, though the g_u were computed for u of -90 to $+90$. For comparison, the impulse response function obtained as the Fourier inverse transform of the frequency response function calculated by cross and auto spectrum analysis is shown at the bottom of Fig. 3.9. They look very similar.

The frequency response function obtained as the Fourier transform of the impulse response function g_u calculated by this method is shown in Fig. 3.10 together with the results of cross and auto spectral analysis. Again, the frequency response function

73
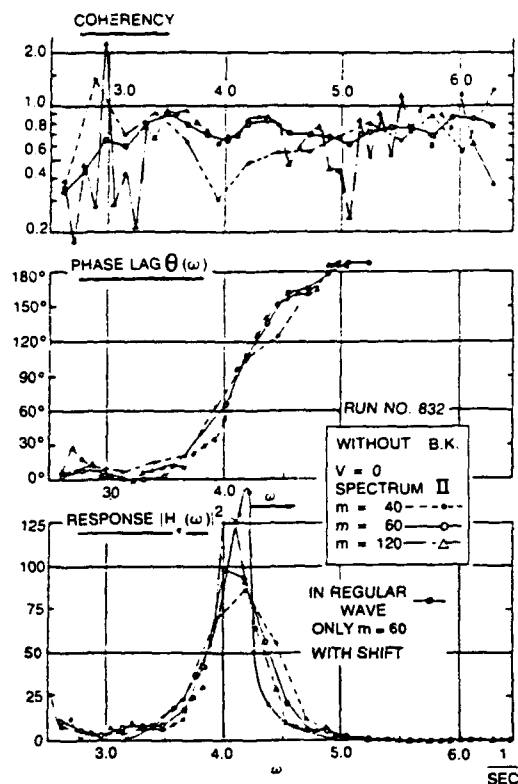
Fig. 3.7. Frequency responses of roll–waves (run 832).
(From Yamanouchi.[31])

$|G(\omega)|$, i.e., the amplitude gain, from these different methods is very similar. From the time history of inputs X_t of the waves, and the use of Eq. 3.5 which neglects the noise N_t, the output Y_t was synthesized, using values of g_u, $u = -90$ to 90, as shown in Fig. 3.11. These results show that this method gives reasonably good results.

This example is for the roll of a model ship where, because of the small damping of the motion, the impulse response function g_u is slow to decay. We need a larger number of terms, i.e., g_u for a longer range of u. With much larger damping, as with the heave or pitch response of a real ship, this author believes we will get better results.

Here the more statistical, stricter estimation of reliability or confidence in the results is lacking. This author found later that the procedure was the same as that to solve the Yule–Walker equations used for the AR–model fitting, that will be mentioned in Part II. Accordingly, the above mentioned belief was more strictly examined statistically as the choice of order in AR–model fitting, as mentioned in Section 5.5.

3.4 EXAMPLE OF MULTIPLE INPUT ANALYSIS, A TRIAL FOR NONLINEAR ANALYSIS OF SHIP'S RESPONSE

Here a multiple input analysis of a ship's behavior at sea, performed by this author [Yamanouchi[33]], will be shown to demonstrate the usefulness of the method. Often, one
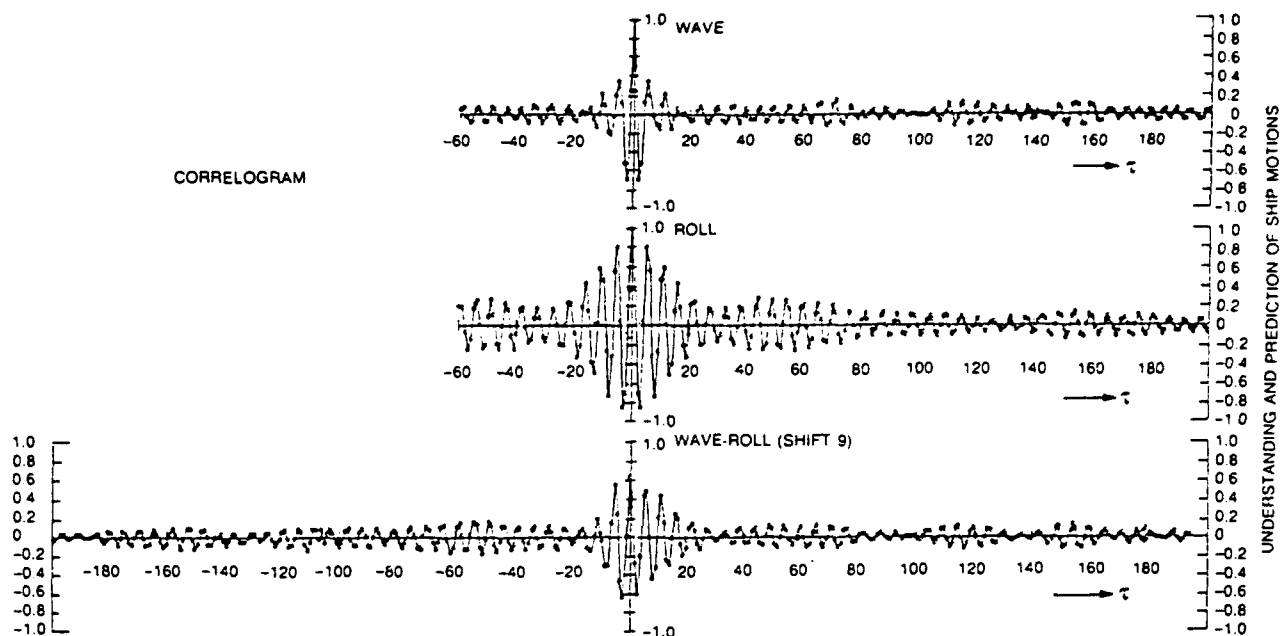
Fig. 3.8. Auto correlation of waves, roll, and cross correlation of wave–roll of a model ship (shift $r_o = 9$).
(From Yamanouchi.[32])
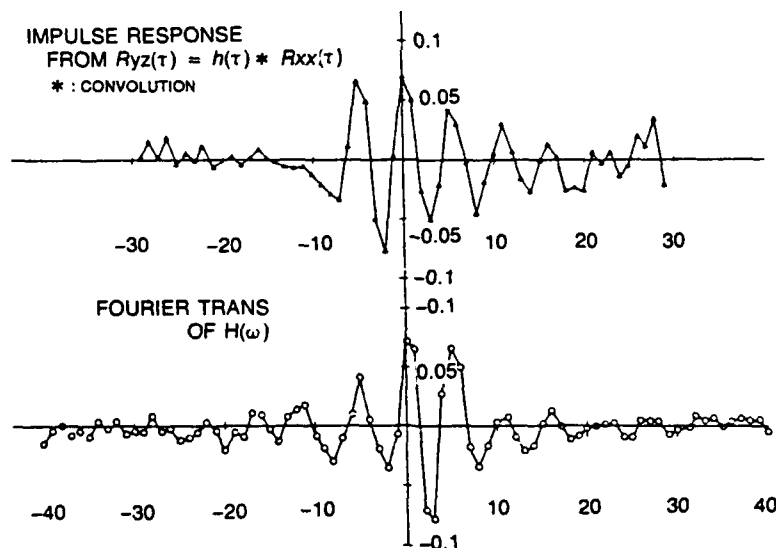
Fig. 3.9. Impulse response of roll to wave height (without advance speed).
(From Yamanouchi.[32])

output is analyzed as the response to a single definite input. This approach is reasonable when the real source of excitation for the system is actually single and no other source need be considered, even if several outputs are correlated or combined. For example, even though the sway, roll and yaw, or pitch, heave and surge motions of a ship are

75
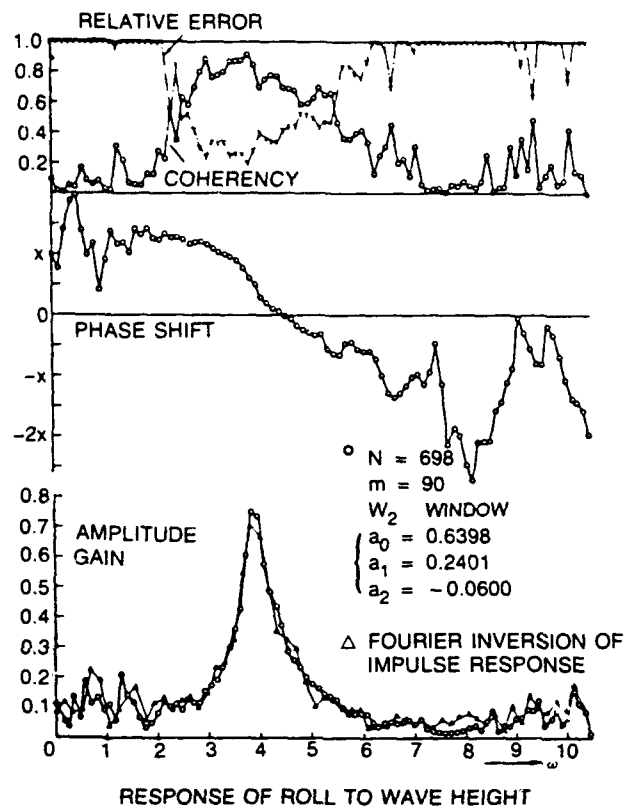
Fig. 3.10. Frequency response of roll to wave height.
(From Yamanouchi.[32])
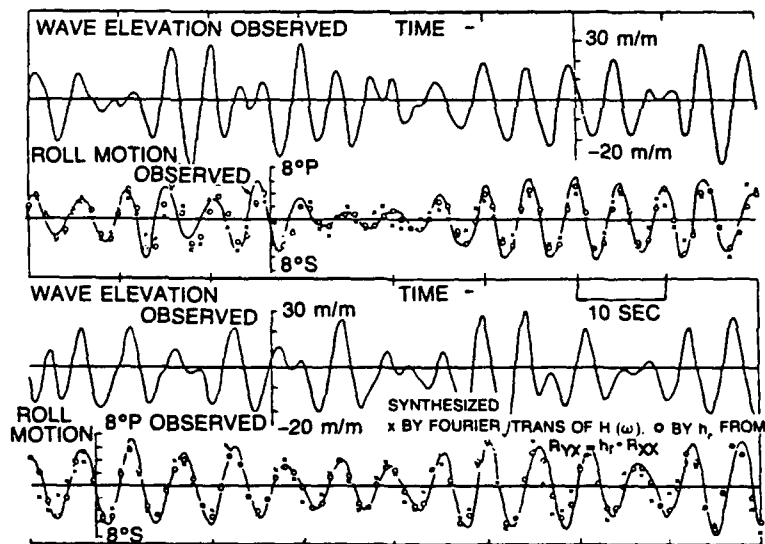
Fig. 3.11. Comparison of synthesized and observed output of roll.
(From Yamanouchi.[32])

correlated and combined with each other, we can get the response of a single roll, sway, or yaw and so on, to the wave (either slope or height), as frequency response functions by solving the simultaneous equations of motion of the necessary degree of freedom, considering the waves as only one source of excitation.

This is not the case, however, when one output must be considered as the response to many related inputs. Shown here is an example that this author encountered in the analysis of a ship's motion and stress. The ship was a cargo liner on the New York line, under service in winter on the North Pacific Ocean.[34] The relative wave heights of encountering waves were measured by an on-board ultrasonic sensor located on the side of the hull near midship. Because of the poor position of the measuring device, no attempt was made to convert the readings to absolute encountering wave heights. However, the real encountering waves are only one input to the stresses and the motions of the ship. In analyzing the transverse stresses induced on the web frame near midship, this author tried to express the effect of real waves by the relative wave heights measured at the side of the ship and by supplementing with other inputs like rolling, pitching, and vertical acceleration measured at the same time. These additional inputs were correlated with each other, as shown in Fig. 3.12, and multiple input analysis techniques were adopted to analyze the response.
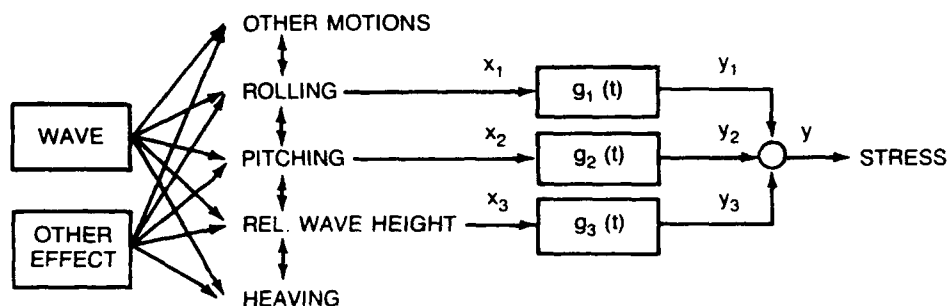
Fig. 3.12. Multiple inputs interpretation.
(From Yamanouchi.[33])

With stress as the output and such inputs as relative wave height, rolling, pitching, and vertical acceleration, and with various numbers of inputs, the effects of some particular inputs were investigated by checking the multiple and partial coherencies that show the effects of a particular input in the presence of one or more other inputs.

Another trial investigation was the analysis of nonlinearity of output to input. Considerations on nonlinearity that provide another reason for getting a poor coherency function are generally treated in Part III of this lecture, but for convenience one trial is described here in relation to multiple input analysis. Figure 3.13 is an example of a record of simultaneous measurement of many responses of this ship such as roll, relative wave height, vertical accelerations at four points, stress on the web frame, revolution and torque of the propeller, helm angle, yaw, encounter time of waves to the stern, and so on. Some of the responses were picked up, sampled, digitized, and punched on a tape after the test. (At that time data were processed using punched tapes.)

Fig. 3.13. Examples of record on visi-corder (test no. 220).

(From Yamanouchi.[33])

Table 3.1 summarizes the measurements of the responses and shows that these thirteen representative runs cover a good variety of sea conditions, wave heights, and directions. This is reflected in the variation of normalized correlations and spectra, for example in the rolling, pitching, stress, and relative wave heights in Fig. 3.14 and Fig. 3.15.

If we assume a variety of environmental conditions, it is possible that various sea conditions might appear ideally by the same chance, and the average of all normalized wave spectra might give us a nearly white spectrum, or the spectrum of white noise. Then the averaged response might show the characteristics of the response to the white noise, i.e., the characteristics of the response functions themselves, as was discussed by Yamanouchi, et al.[35] The average normalized correlation diagram or correlogram and averaged spectra are shown in Fig. 3.16.

These averaged rolled and pitch spectra are not the ideal ones, but quite reasonably show the smooth peak at its natural frequency. Moreover, the correlation functions of roll, pitch and stress show the beautiful forms of damped oscillation. The averaged spectrum of stress has a smooth peak at twice the frequency of the roll natural frequency. The natural frequency of the stress response should be in a higher frequency range, but must have been cut off by the filters and should not appear in the averaged spectra. The peak that does appear at the double frequency of the roll natural frequency might indicate that the transverse stress induced at the web frame is quadratic nonlinear to the rolling motion.

To check this possibility, an artificial process of rolling square was made as shown in Fig. 3.17. This naturally has a biased mean as shown in its variational form in the time series and also in the spectrum in Fig. 3.18, where the power value near $\omega = 0$ is large. In the next step, a digital high pass filter, shown by Eq. 2.132, was applied to this roll squared process as $X_n(t) = \dfrac{1}{2} \left\{ x_n^2 - x_{n-1}^2 \right\}$. The filtered roll squared process appears at the bottom of Fig. 3.17 and its spectrum in Fig. 3.18. In Fig. 3.18, we find the shape of the spectrum of the filtered roll squared process is similar to that of the averaged spectrum of the stress, which validates the assumption that the stress is a quadratic and nonlinear response to rolling motion.

The lower two graphs in Fig. 3.19 show the results of single input–output spectrum analysis, with the stress as output and relative wave height or rolling as a single input. Coherencies γ^2 values are so low that the stress cannot be the output of only the relative wave height nor only of rolling. The top of Fig. 3.19 shows on the contrary that relative wave height is fairly well explained just by rolling; the coherency, especially in the frequency range in which rolling has reasonable power, has a value pretty near 1.

Since we found that the stress was quite possibly quadratic and nonlinear to the rolling, the next step was to find the response of stress to the single roll squared process, (roll)^2. To eliminate the effect of large bias on (roll)^2, the response of stress to the single (roll)^2 filtered process was also obtained. The results are shown in Fig. 3.20, and the coherency is again rather low.

To check the coexistence of many other inputs, multiple input analysis was introduced. Stress was considered as the output of rolling, pitching, relative wave height, and

Table 3.1. Summary of seaways and particulars of measurement and analysis for test runs. (From Yamanouchi.[33])

RUN NO.	DATE TIME	WIND SCALE	WIND DIR. (DEG) / VEL. (M/S)	SEA STATE SKETCH (SWELL ⇨ / SEA →)	OBSERVED WAVES SCALE	SWELL/SEA HT. (M)	SWELL/SEA PERIOD (SEC.)	1	2	3	4	Δt (SEC.)	TOTAL / MAX. LAG (N/m)
204	JAN. 15 1335~1345	3	-70 / 13		5	4.8 / 1.2	8.5 / 5.3	R	P	S	W	1.5	630 / 60
205	JAN. 16 0910~0920	3	-127 / 6		4	2.2 / 0.7	9.0 / 4.0	R	P	S	W	1.5	600 / 60
206	JAN. 17 0900~0910	3	-80 / 8		3	3.5 / 0.7	11.3 / 3.7	R	P	S	W	1.5	600 / 60
207	JAN. 18 0900~0910	4	-70 / 11.5		4	2.9 / 1.0	9.7 / 6.2	R	P	S	W	1.5	600 / 60
208	JAN. 19 0900~0910	2	10 / 5.5		3	3.0 / 0.5	10.6 / 3.5	R	P	S	W	1.5	600 / 60
209	JAN. 20 0900~0910	2	-120 / 7		3	1.5 / 1.0	8.7 / 5.8	R	P	S	W	1.5	400 / 60
211	JAN. 22 0900~0910	6	0 / 12.5		5	3.9 / 1.5	9.3 / 5.6	R	P	A	W	1.5	550 / 60
214	JAN. 23 0805~0820	5	-10 / 12		8	7.8 / 3.2	13.5 / 6.0	R	P	S		1.125	800 / 80
215	JAN. 23 1400~1415	6	35 / 16		7	6.4 / 2.1	11.4 / 6.2	R	P	S		1.125	800 / 80
216	JAN. 25 1317~1330	4	40 / 8.5		8	6.2 / 1.6	11.0 / 5.5	R	P	S		1.125	720 / 80
218	JAN. 26 1330~1350	7	75 / 20		8	5.4 / 2.0	8.7 / 6.8	R	P	S		1.125	800 / 80
219	JAN. 26 1530~1545	7	35 / 17		7	6.2 / 1.8	8.5 / 5.7	R	P	S		1.125	800 / 80
220	JAN. 27 0900~0918	2	30 / 5		4	1.5 / 1.5	9.0 / 8.0	R	A	S	W	1.5	800 / 60

R: ROLLING   S: STRESS   A: VERT. ACC.
P: PITCHING   W: REL. WAVE HT.
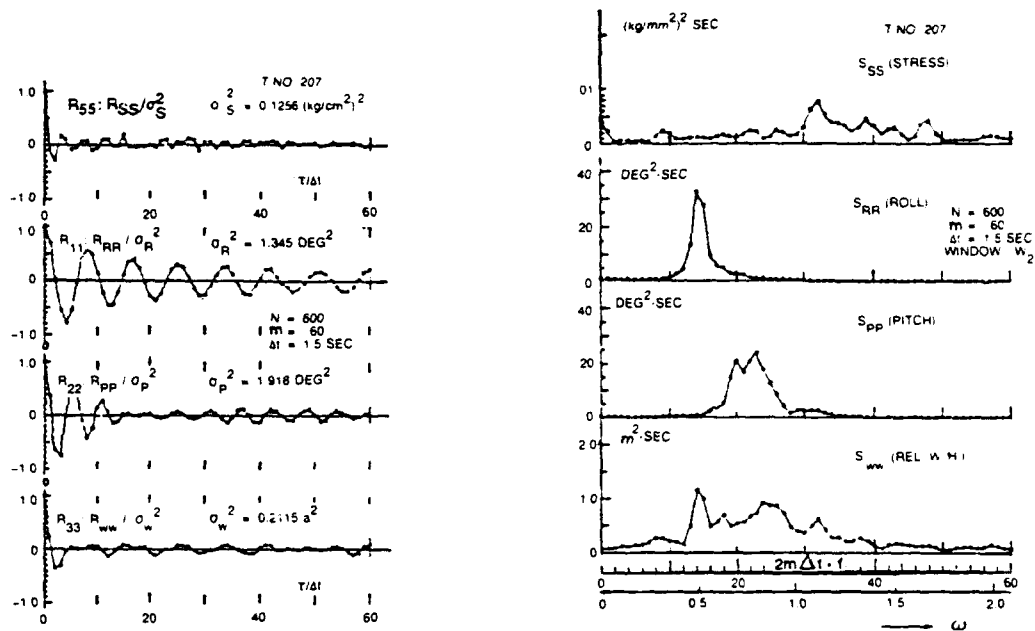
Fig. 3.14. Example of auto correlations (normalized) and the spectra (run 207).
(From Yamanouchi.[33])
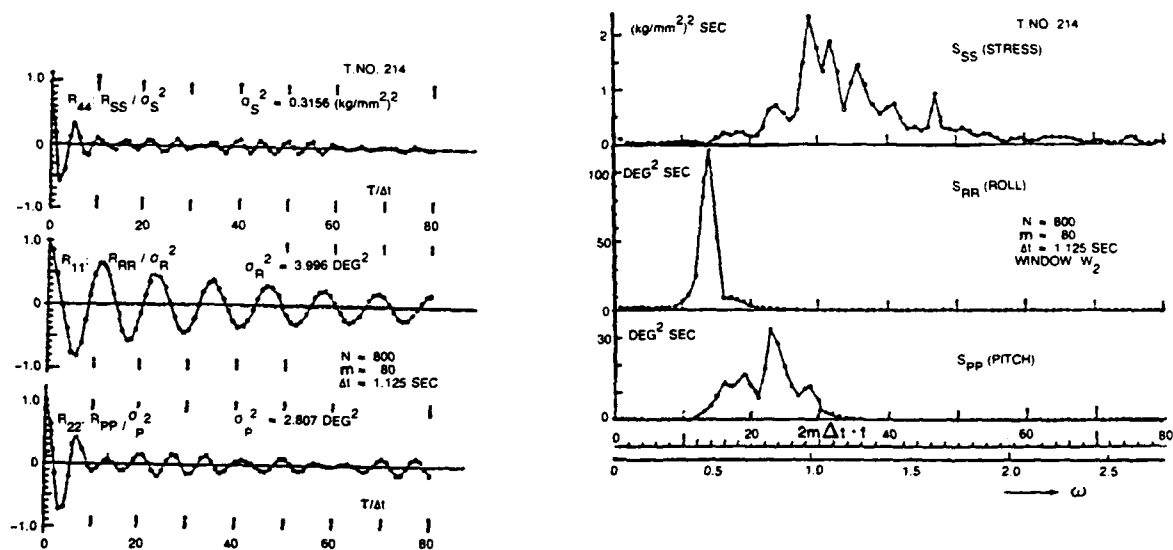
Fig. 3.15. Example of auto correlations (normalized) and the spectra (run 214).
(From Yamanouchi.[33])
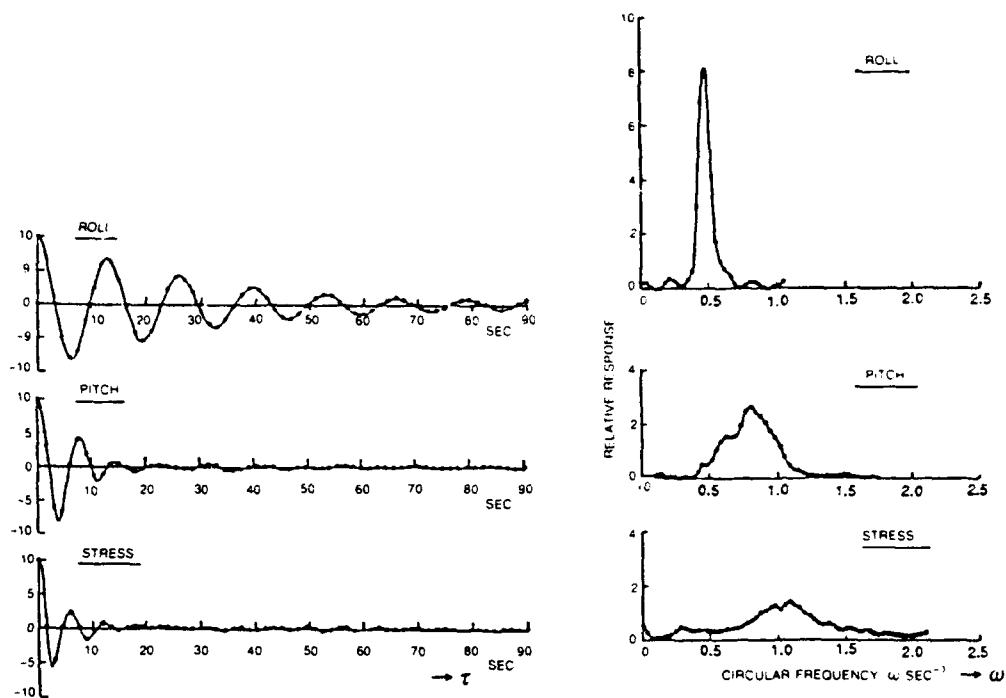
Fig. 3.16. Averaged correlograms and spectra (normalized).
(From Yamanouchi.[33])
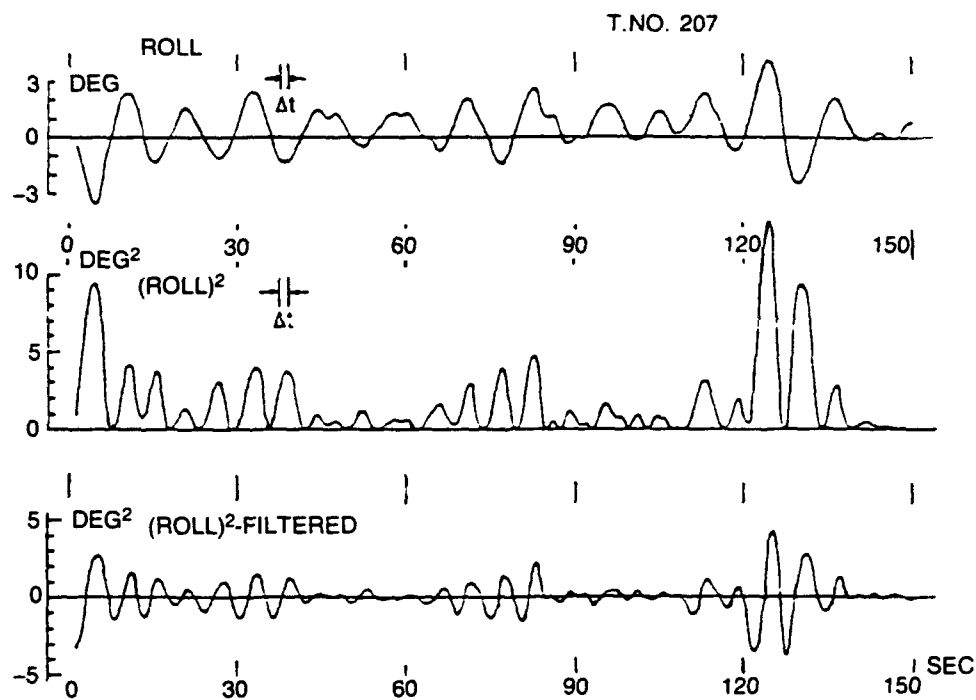
Fig. 3.17. Roll, $(roll)^2$, $1/2\{(roll)_n{}^2 - (roll)_{n+1}{}^2\}$ processes.
(From Yamanouchi.[33])

82
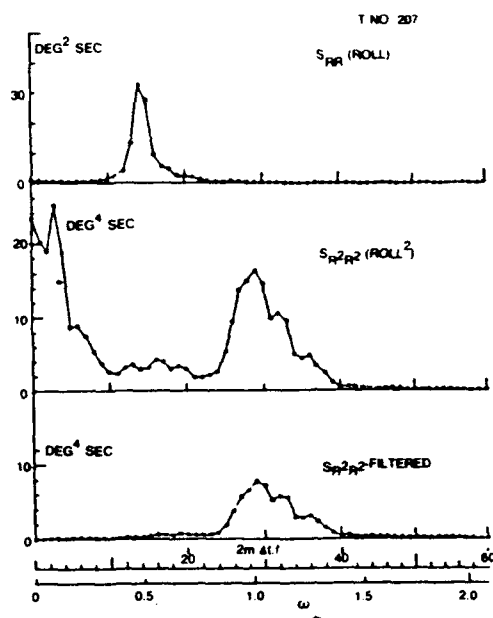
Fig. 3.18. Spectra of roll, (roll)^2, (roll)^2–filtered.
(From Yamanouchi.[33])

heaving. Heaving itself was not measured, but its effect was assumed to be included in the vertical acceleration of a representative point and also to be combined in pitching, rolling, and relative wave height. Examples of four–input analysis are shown in Figs. 3.21 and 3.22, in which stress as the output is given on channel 5 and the inputs of rolling on channel 1, pitching on channel 2, relative wave height on channel 3, and (roll)^2 filtered on channel 4. Figure 3.21 shows five auto correlations of output and input R_{55}, R_{11}, R_{22}, R_{33}, R_{44}; ten cross correlations of combinations of the one output with four inputs R_{51}, R_{52}, R_{53}, R_{54}; R_{21}; R_{41}, R_{42}, R_{43}; R_{31}, R_{32}; and five auto spectra of stress S_{55}, rolling S_{11}, pitching S_{22}, relative wave height S_{33}, and roll squared. Figure 3.22 shows conditional (partial) gains and phase relations as H_{SR-PWR^2}, H_{SP-PWR^2}, H_{SW-RPR^2}, and H_{SR^2-RPW} in the form of absolute values and arguments. The notation follows the convention already explained in Section 2.6.5 on partial coherencies. For example,

$$H_{SP-RWR^2}(\omega) = \frac{S_{SP-RWR^2}(\omega)}{S_{PP-RWR^2}(\omega)}$$

shows the frequency response of stress to R: rolling, W: relative wave height, and R^2: squared roll filtered processes under the condition that the effect of pitch has been masked. In the same way, multiple and partial cross spectral analysis was tried with stress as one output (4), and roll R (1), pitch P (2), and (roll)^2 filtered R^2 (3) as three inputs. In another one output/three input cases, pitching P was replaced by vertical acceleration A.

83
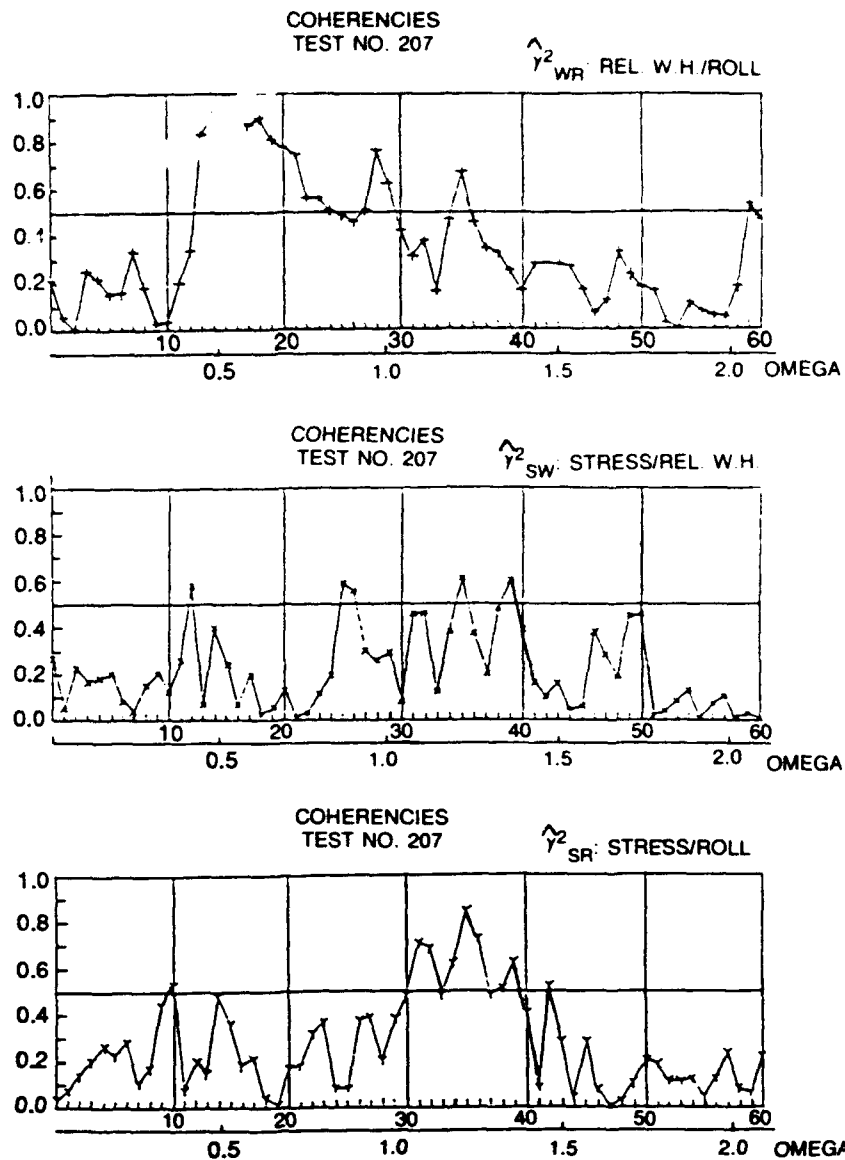
Fig. 3.19. Coherencies for single input–output relations.
(From Yamanouchi.[33])

The results of spectrum analysis of the first three–input case are shown in Fig. 3.23 and Fig. 3.24.

Auto correlations R_{44}, R_{33}, R_{22}, R_{11}, and all combinations of cross correlation R_{41}, R_{42}, R_{43}, R_{31}, R_{32}, R_{21} and auto spectra S_{44}, S_{11}, S_{33} are shown in Fig. 3.23. Partial gains and phase relations H_{SR-PR^2}, H_{SP-RR^2}, and H_{SR^2-RP} are shown in Fig. 3.24. The effects of the increase in probable inputs are more clearly shown in the multiple coherencies, and the effects of several inputs when the effect of a certain input was masked are shown on

COHERENCIES
TEST NO. 207

$\hat{\gamma}^2_{SR^2}$; STR./(ROLL)^2

1.0
0.8
0.6
0.4
0.2
0.0

10   20   30   40   50   60
0.5   1.0   1.5   2.0   OMEGA

COHERENCIES
TEST NO. 207

$\hat{\gamma}^2_{SR^2-filt.}$; STR./(ROLL)^2-filt.

1.0
0.8
0.6
0.4
0.2
0.0

10   20   30   40   50   60
0.5   1.0   1.5   2.0   OMEGA
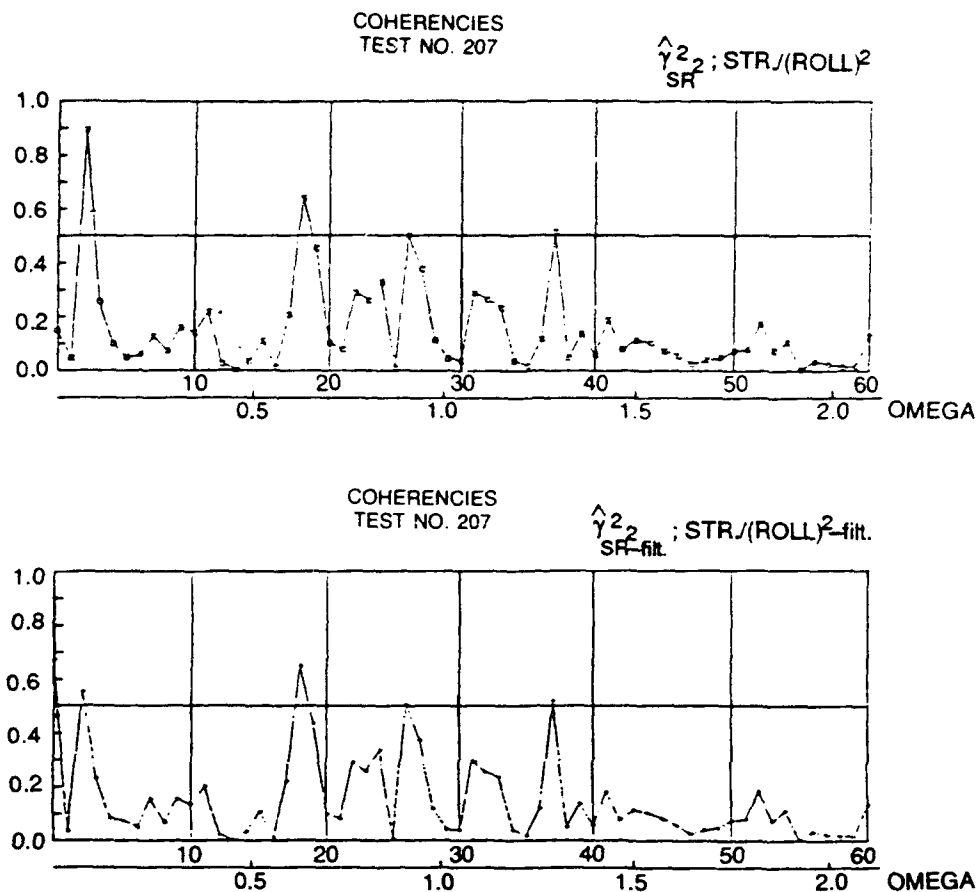
Fig. 3.20. Coherency of squared rolling process and filtered squared
rolling process to the stress.
(From Yamanouchi.[33])

the partial coherencies. The results for two–input, three–input and four–input cases are compared in Fig. 3.25.

This figure indicates that the multiple coherency shows higher levels as more inputs are taken into account. Moreover, examining the partial coherencies, $\gamma^2_{SR-PWR^2}$,

γ_{SR^2-RPW} and others, at the bottom figure of Fig. 3.25, we find that the contributions of rolling and of (roll)^2–filters are large compared with the other inputs. This finding supports the assumption of quadratic nonlinearity of transverse stress to the rolling motion.

Figure 3.26 shows the multiple and partial coherencies for the two–inputs and three–inputs cases, and here again we find the coherency improves with increasing number of inputs, including the (roll)^2–filtered process. Also the contributions of rolling and (roll)^2–filtered are large, compared with the contribution of pitching. The multiple coherency is very close to 1 around the frequency range in which the output, here the stress, has important response to input.
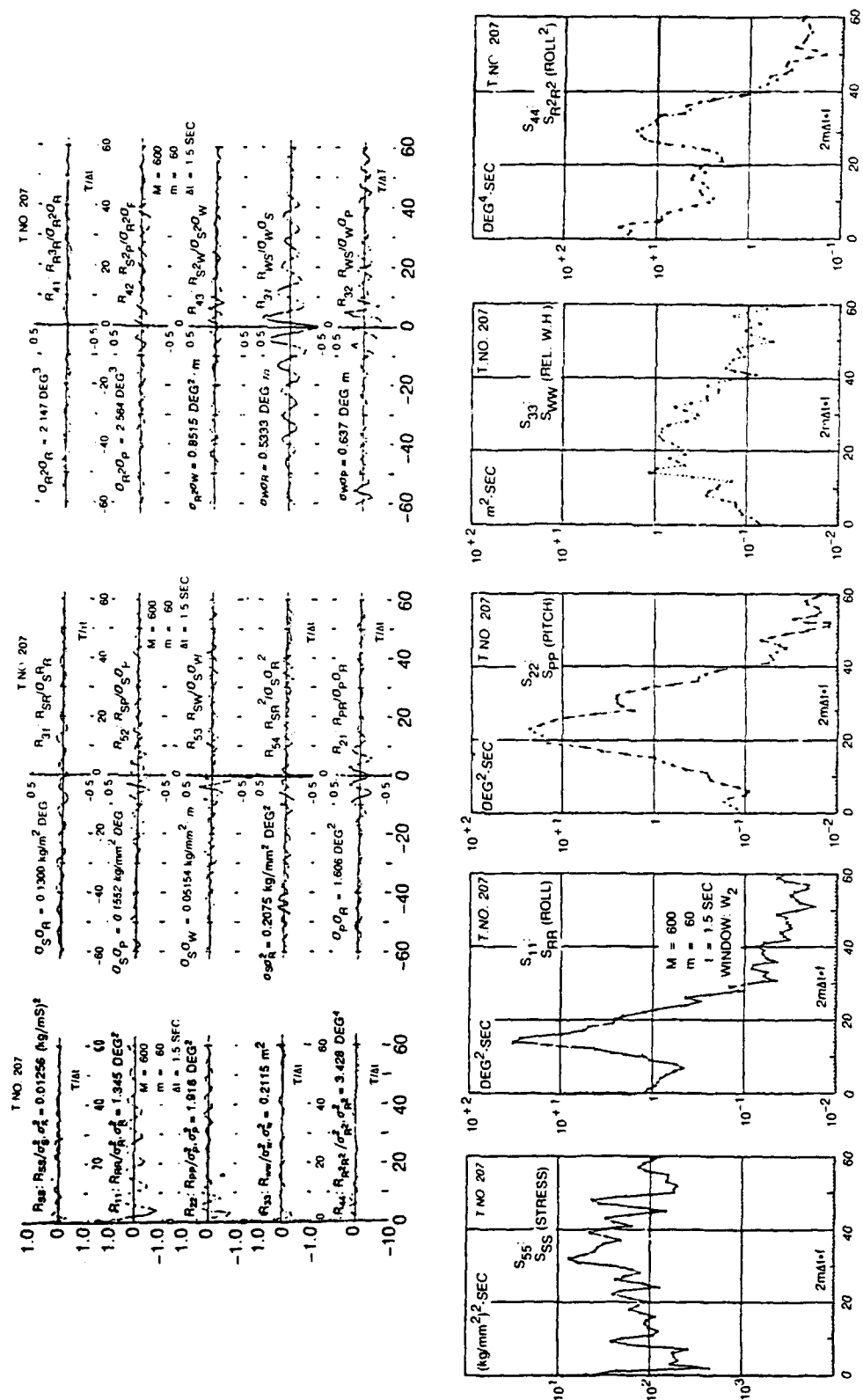
Fig. 3.21. Example of four-inputs analysis – (I); correlations and spectra. (From Yamanouchi.[33])
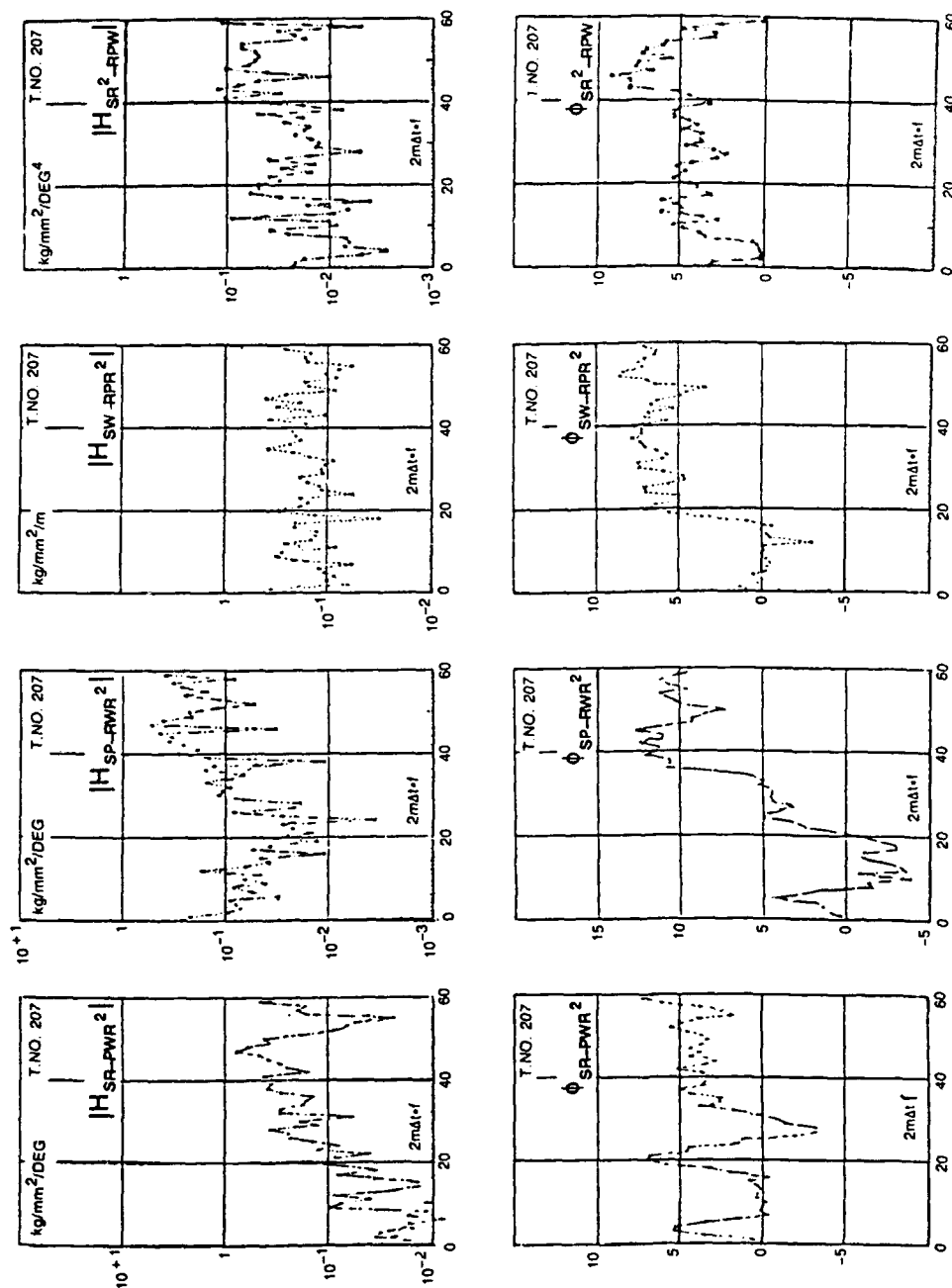
Fig. 3.22. Example of four-inputs analysis — (I); partial amplitude gains and phase shifts. (From Yamanouchi.[33])
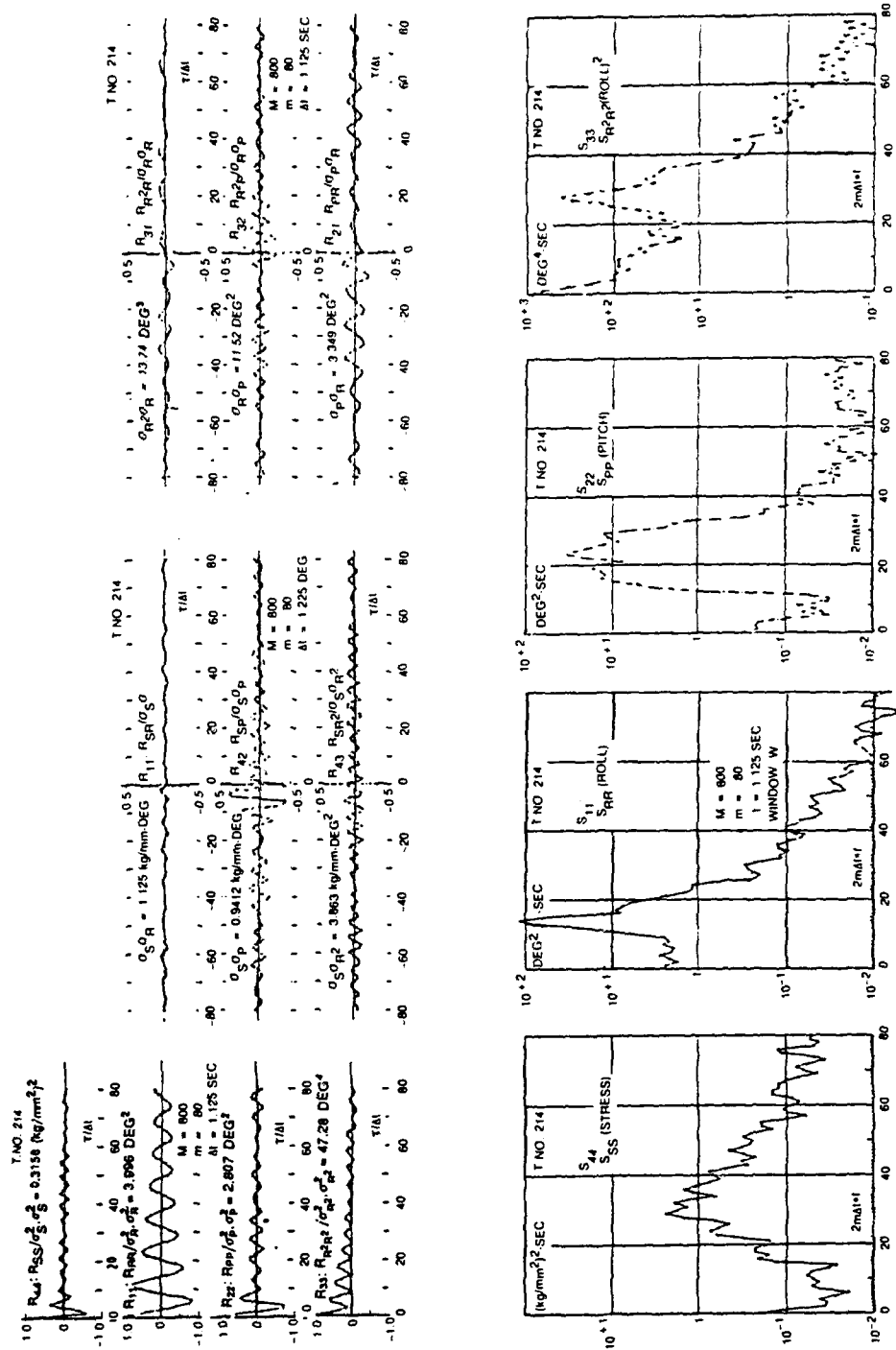
Fig. 3.23 Example of three-inputs analysis; correlations and spectra.
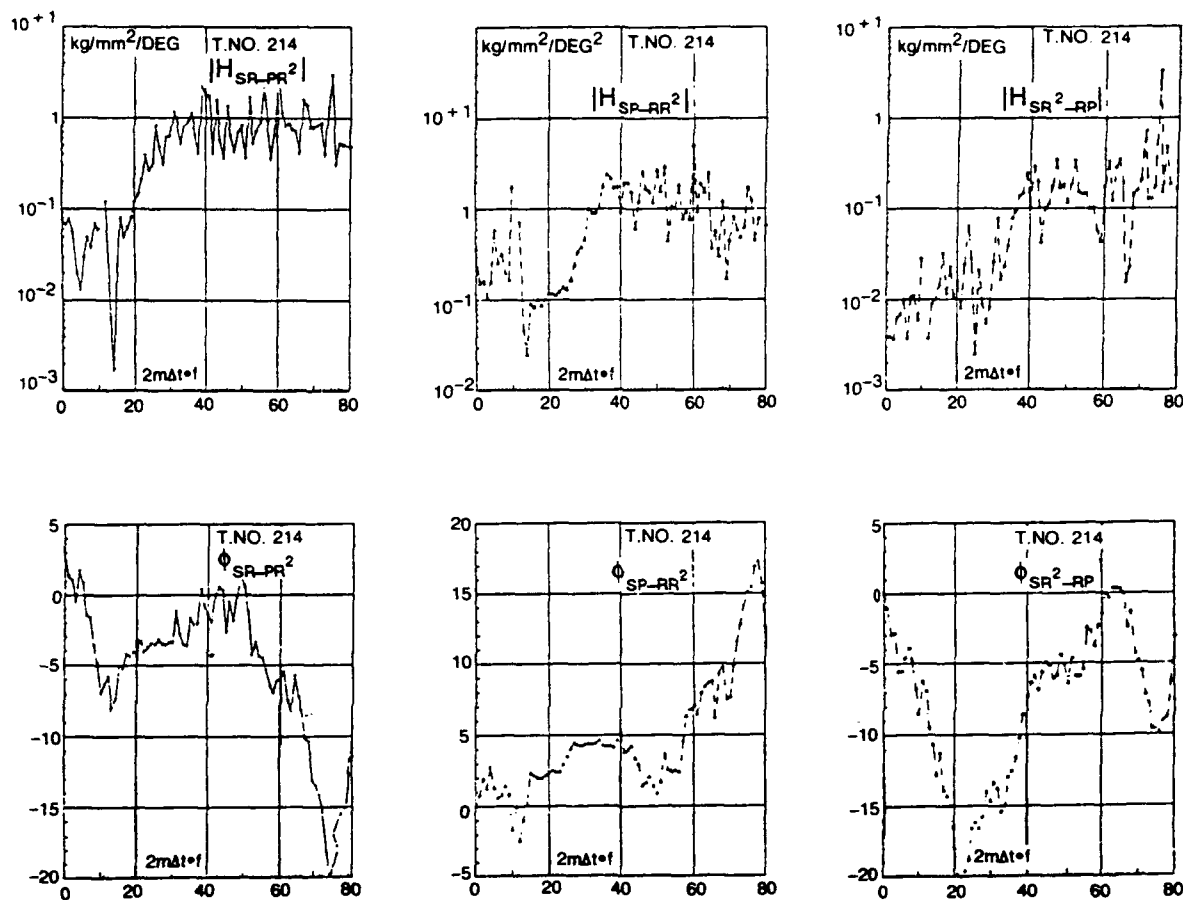
(From Yamanouchi.[33])

Fig. 3.24. Example of three–inputs analysis; amplitude gain and phase shift.
(From Yamanouchi.[33])

To show more clearly the usefulness of multi input analysis, apart from the nonlinearity of responses, another example used the vertical acceleration as a linear output and rolling, pitching, and relative wave height as inputs. The multiple and partial coherencies are given in Fig. 3.27, in which the multiple coherency is almost 1 at the important range of frequencies and the contribution of rolling is large for this vertical acceleration, as we expected.

Figure 3.28 is another example of two–input and three–input analysis for stress which does not take into account the nonlinearity of rolling. Comparison with Figs. 3.25 and 3.26 at the important range of frequencies for stress shows lower coherencies when the nonlinear response of rolling is not taken into account.

Later, the author found that taking the input process squared as an input is very reasonable in discussing the quadratic response character of the output as shown in Section 11.4, in Part III.

89
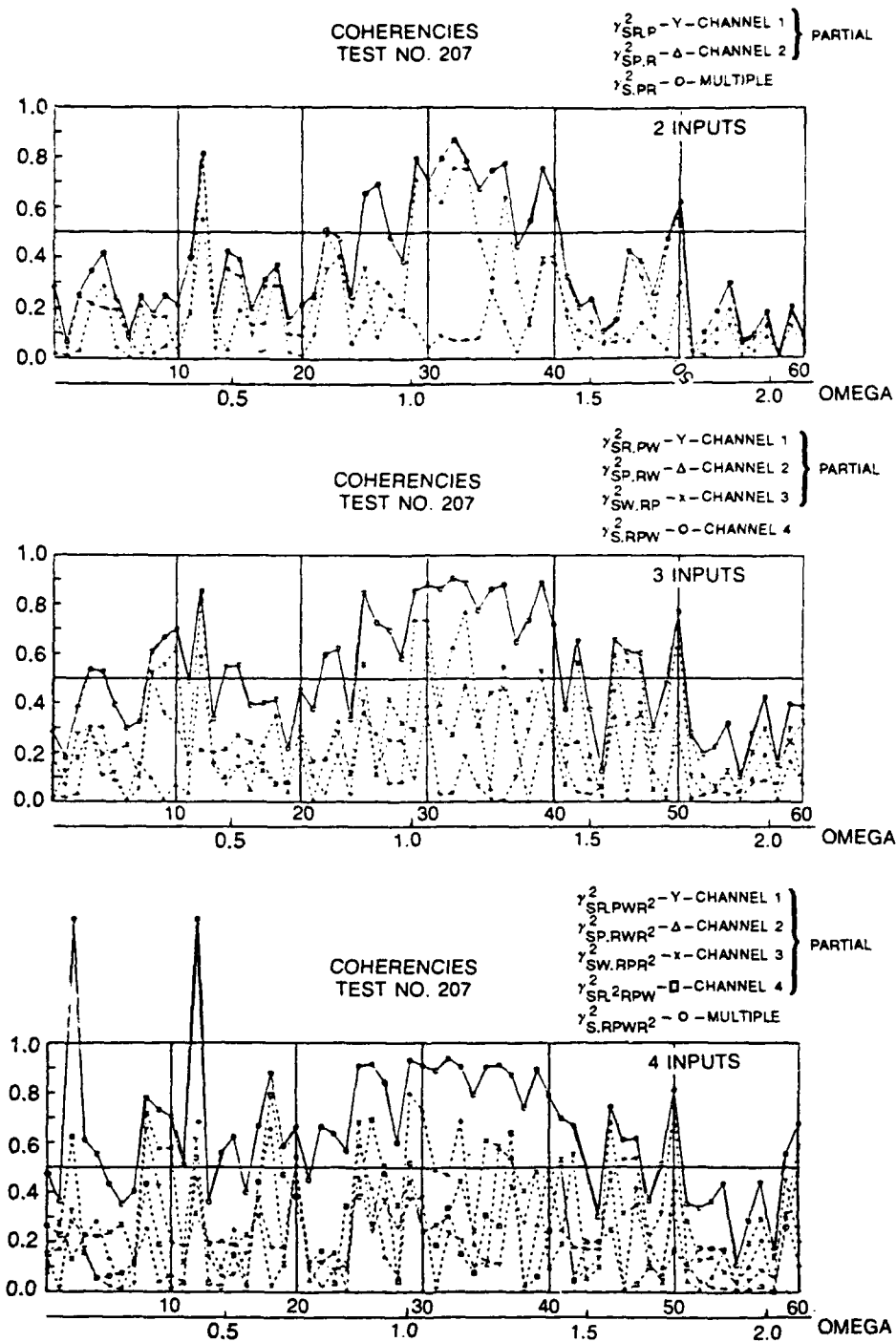
Fig. 3.25. Examples of multiple and partial coherencies – (l); stress–roll, pitch, relative wave height, and (roll)^2; comparison of two–, three–, and four–inputs cases.

(From Yamanouchi.[33])
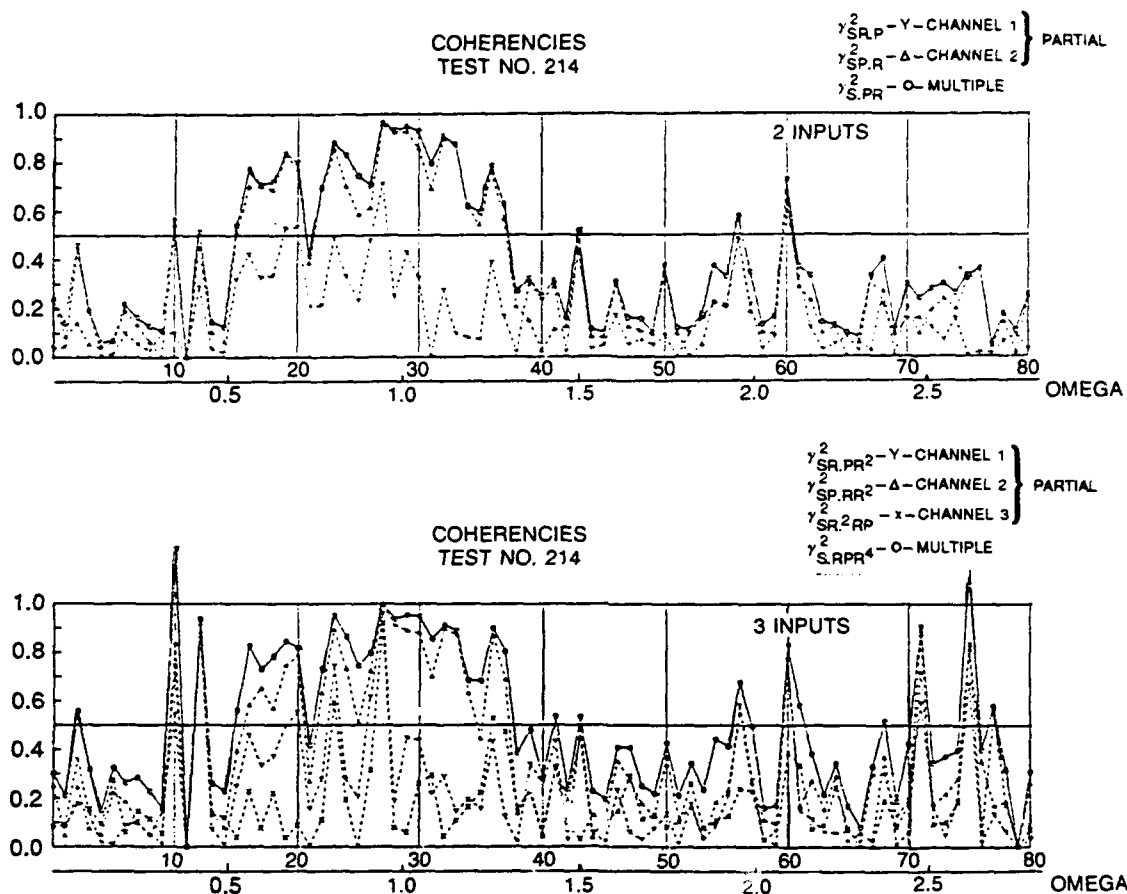
Fig. 3.26. Examples of multiple and partial coherencies – (II); stress–roll, pitch, and (roll)^2; comparison of two– and three–inputs cases.

(From Yamanouchi.[33])

COHERENCIES
TEST NO. 211

$\gamma^2_{AR.P}$ – Y – CHANNEL 1
$\gamma^2_{AP.R}$ – Δ – CHANNEL 2 } PARTIAL
$\gamma^2_{A.RP}$ – O – CHANNEL 3

2 INPUTS

OMEGA

COHERENCIES
TEST NO. 211

$\gamma^2_{AR.PW}$ – Y – CHANNEL 1
$\gamma^2_{AP.RW}$ – Δ – CHANNEL 2 } PARTIAL
$\gamma^2_{AW.RP}$ – x – CHANNEL 3
$\gamma^2_{A.RPW}$ – O – MULTIPLE

3 INPUTS

OMEGA
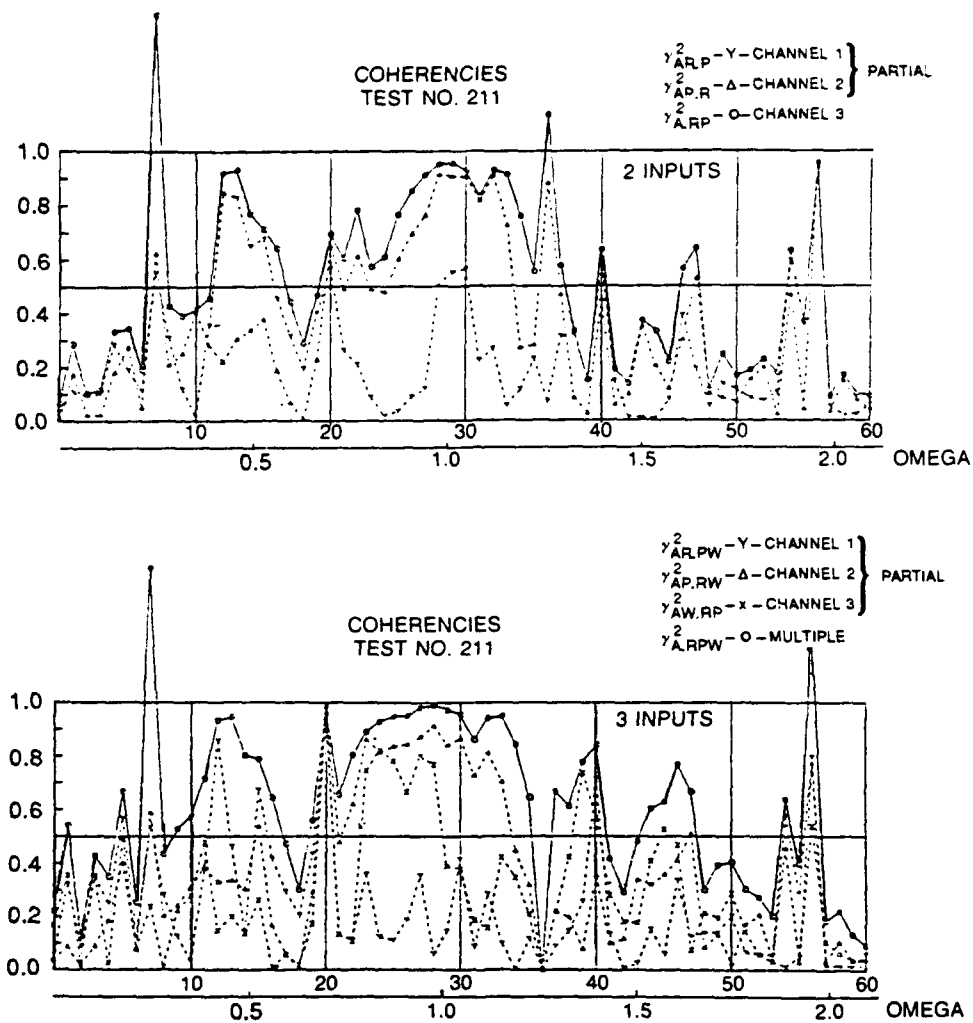
Fig. 3.27. Example of multiple and partial coherencies – (III); vertical acceleration–
roll, pitch, and relative wave height; comparison of two– an
three–inputs cases.
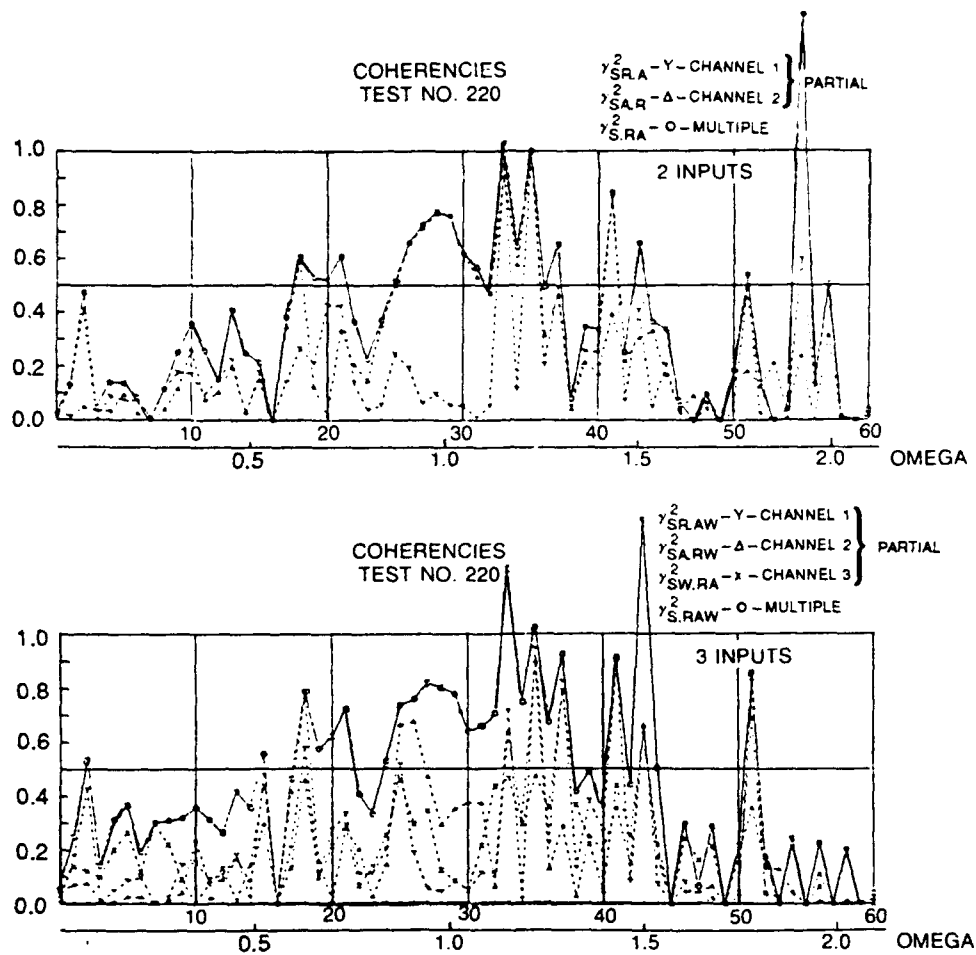
(From Yamanouchi.[33])

Fig. 3.28. Example of multiple and partial coherencies – (IV); stress–roll, vertical acceleration and relative wave height; comparison of two– and three–inputs cases, when the (roll)^2 is not taken into consideration.

(From Yamanouchi.[33])

THIS PAGE INTENTIONALLY LEFT BLANK

CHAPTER 4

CONCLUSION FOR PART I

In Part I, the nonparametric procedure for analyzing the irregular time series was discussed. At the beginning of Chapter 2 the basic procedure for obtaining the spectrum through periodograms was summarized and then a few considerations for improving this method were introduced in Chapter 3. The conclusions derived from the discussion are as follows:

1. The spectral analysis technique with the use of periodograms is well established and affords us a powerful approach for analyzing irregular phenomena.

2. In sample computations of the correlation function as well as of the spectra, however, care is necessary in sampling the data. The sampling time interval, the length of record, maximum length of lag, and proper windows must be chosen to get consistent estimates and avoid aliasing, blurring by the windows, or loss of reliability.

3. Spectral–lag window pairs have been proposed by many scholars, and were shown that we must be careful of the effect of windows on the reliability, variability, and resolution of the results.

4. Computation of the spectrum through periodograms by use of the Finite Fourier Transform is the same as that computed through the correlation function.

5. The Fast Fourier Transform (F.F.T.) method is a convenient algorithm for reducing the number of operations in the computation, but the considerations of the windows are also necessary and important in applying this method.

6. The correlation functions can also be conveniently calculated by the F.F.T. method if proper precautions are taken.

7. In connection with the choice of windows, the use of filters before applying the window is worth considering.

8. Not only the spectrum functions but also the correlation functions (correlograms) should be investigated carefully in estimating the character of the process.

9. In applying the spectral window in cross spectral analysis or in response analysis, the shift of the origin of the cross correlation (shift of the output record) should be considered to minimize the leakage of power through the use of spectral windows in computing cross spectrum.

10. Cross spectral analysis is essential in the analysis of the response process of a dynamic system to get full information on the frequency response functions of the system. Cross spectral analysis is effective in reducing the effect of noise that contaminates the output.

11. The coherency function is a good index to the extent to which the response can be expressed by linear relations. To make the coherency function useful the computations of all spectra must be done properly according to the preceding items 4–10 in getting the coherencies.

12. The impulse response function may be obtained from the cross and auto correlations of output and input, without the trouble of choosing a window. This procedure

was found later to be closely related to the AR–model fitting technique discussed in Section 5.5.

13. In the analysis of seakeeping data, multiple input analysis is helpful. Partial coherencies and the multiple coherency give a good clue to the extent of contributions from each input.

14. In connection with consideration of the filtration of the stochastic process, the model fitting techniques that try to express the stochastic process by a finite number of parameters are found to look promising to supplement the nonparametric method. The model fitting technique or parametric method will be reviewed in detail in Part II.

PART II

MODEL FITTING TECHNIQUES
(PARAMETRIC SPECTRAL ANALYSIS)

CHAPTER 5

DISCRETE MODEL, MODEL FITTING,
CORRELATION AND SPECTRUM FUNCTIONS

5.1. INTRODUCTION

In Part I, the procedures for estimating the spectrum nonparametrically through autovariance from a sample observation were summarized and discussed. We noted that the statistical consideration of each step of the computations are important in getting reliable results, and the author suggested several ways to improve reliability. In Part II, another approach to getting reliable results from a single or a short observation of a process will be discussed. The method introduced here is called a parametric approach, because some type of model is fitted to the sample observation, and then the parameters of the model are estimated statistically. In looking for the models, we can use the knowledge that we already have about the process, such as the degrees of freedom, and the physical characteristics of the equations of motion that govern the behavior of the system or about the inputs. A few methods which use the parametric approach, such as the maximum likelihood method (MLM) and the maximum entropy method (MEM) are essentially the same with the one mentioned here, and will be explained later.

In this analysis, the criteria for deciding the fitness of the model are very important. The method introduced here, called the "MAIC Method," was introduced by Dr. H. Akaike of Japan and provides a powerful guide in finding the properly fitted model, proper from a statistical point of view. In this analysis, the time domain expression of this process, the time histories themselves, and the correlation of the processes play a big role as was pointed out in Sections 1.3 and 2.5.8 and in the conclusion to Part I.

This parametric approach is not yet well known in the field of naval architecture, although a few books by Priestley,[23] Pandit and Wu,[36] Box and Jenkins,[37] and others[38] deal with it in part or in depth. For this reason Sections 5.2.1 to 5.2.5 give several statistical models of stationary time series in some detail with simulated examples by this author. Then criteria for choosing the model, estimating the parameters, and deriving the spectrum will be given at the end of Chapter 5.

Chapter 6 discusses the application of this method to a two–variate process, an input/output system, and the usefulness of this method for the analysis of a response system with feedback is shown.

In Chapter 7, examples of the application of this method to the analysis of seakeeping data and a comparison with analysis by the nonparametric method are shown. Finally, Chapter 8 provides conclusions and summaries for Part II.

5.2. DISCRETE PARAMETRIC MODELS

There are many statistical models for expressing time series. Among them the auto-regressive (AR) model, the moving average (MA) model, and the mixed autoregressive moving average (ARMA) model are the most representative linear models that we encounter in the analysis of irregular records of observations. In Part II, only the linear models are introduced. Some types of nonlinear models will be referred to later in Part III. The order of the AR, MA, and ARMA models indicates the degree of simplicity or complexity of the models.

Here in Part II, the discrete time process sampled from the continuous time process, with an interval Δt is expressed by $\{X_t\}$ and its realization by X_t. Except as otherwise indicated, Δt is taken as 1. If $\Delta t \neq 1$, each function is easily transformed to proper form, as was already mentioned in Section 2.4.3. The explanation of the character of the elementary models is based largely on the work of Priestly[23] and Pandit and Wu.[36]

5.2.1 Pure Random Process

$\{X_t\}$ is called a pure random process if it is the sequence of uncorrelated random variables that are stationary up to order 2, and is written

$$X_t = \epsilon_t . \tag{5.1}$$

The mean is

$$E\{X_t\} = \mu , \tag{5.2}$$

the variance is

$$E\left\{(X_t - \mu)^2\right\} = \sigma_t^2 = \sigma_\epsilon^2 \tag{5.3}$$

and the covariance function is

$$R(r) = \text{cov.}\left\{X_t, X_{t+r}\right\} = \begin{cases} 0 & r \neq 0 \\ \sigma^2 & r = 0 \end{cases} . \tag{5.4}$$

$R(r)$ is a function of r only and is normalized by σ^2 as

$$\varrho(r) = \begin{cases} 0 & r \neq 0 \\ 1 & r = 1 \end{cases} . \tag{5.5}$$

Its spectrum is then

$$s(\omega) = \frac{1}{2\pi} \sum_{r=\infty}^{\infty} R(r) e^{-i\omega r} = \frac{\sigma^2}{2\pi} = \text{const. (for} -\pi \geq \omega \geq \pi). \tag{5.6}$$

In this case

1. When this process is also Gaussian, then X_t is not only uncorrelated, but also $X_t, X_{t-1}, \cdots X_{t-r}$, are independent of each other.

2. The spectrum $s(\omega)$ is flat for the interval of frequency ω for $-\pi$ to π, and is referred to as white noise.

3. The process is also referred to as a memoryless process.
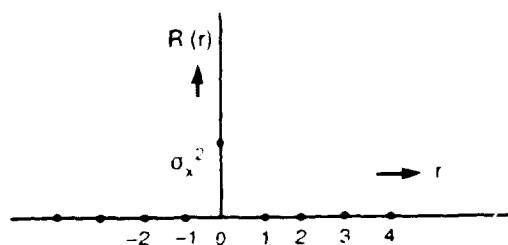
Fig. 5.1. Theoretical autocovariance of a pure random process.
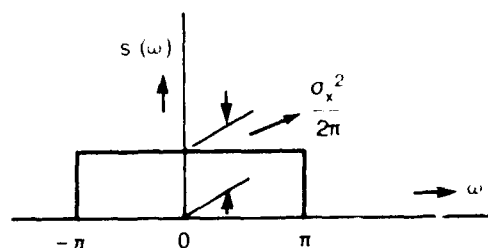
Fig. 5.2. Theoretical spectrum of a pure random process.

5.2.1.1 Example of a Pure Random Process. Figure 5.3 shows an example of a pure random Gaussian process generated for $t = 1 \sim 600$, with average 0 and variance 1.0. At the bottom, a part ($t = 100 \sim 250$) of the record is shown expanded on the time axis. Its readings are listed in Appendix A1 as Table A1.1; pp. 251, 252, and 253, for reference. This process was generated by the method of "Random number generation and testing," generally popular as "multiplication type residual method."

It was found that by this method it is hard to get a really white process with precisely designed variance of $\sigma_\epsilon^2 = 1.0$ from this short record ($N = 600$), and the sample variance appeared as $\hat{\sigma}_\epsilon^2 = 1.046490$. Figure 5.4a shows the theoretical autocorrelation coefficient $\varrho(0) = R(0)/R(0) = 1$, $\varrho(r) = R(r)/R(0) = 0$, $r \neq 0$ by Eq. 5.5. Figure 5.4b shows the estimated $\hat{\varrho}(r) = \hat{R}(r)/\hat{R}(0)$ from the generated process. From the model fitting technique and order determination that will be mentioned in Section 5.5, the order appeared to be 0, and AR(0) appeared to be the most appropriate model to fit this process. The estimated autocorrelation of this model fitted by Eq. 5.4 is just the same with the theoretical $\varrho(r)$ shown as Fig. 5.4a because the difference is only in σ_ϵ values, that its drawing was omitted. Figure 5.5a shows the theoretical spectrum function of this process designed by Eq. 5.6, that is, the white noise. Figure 5.5b shows the estimated spectrum of the model fitted by Eq. 5.6. This is also the white noise and looks very similar to the

99
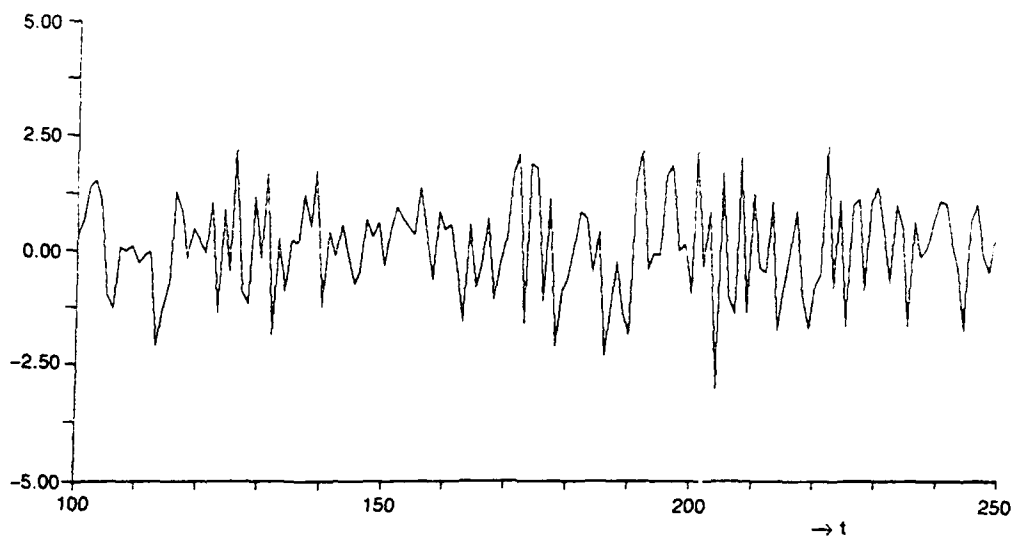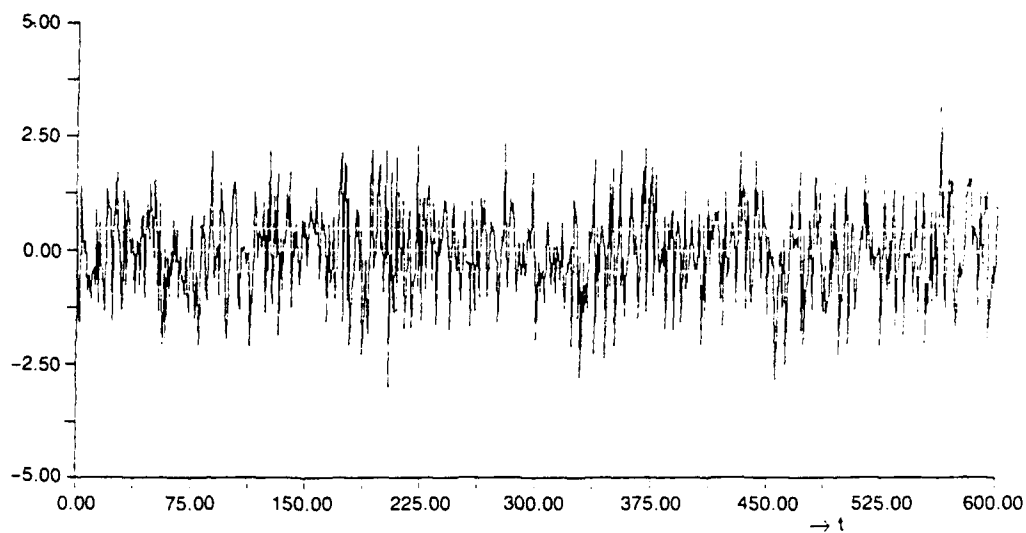
Fig. 5.3. Simulated pure random process AR(0)

$$X_t = \epsilon_t, \quad \epsilon_t : N[0, 1].$$

theoretical spectrum except that the variance was a little larger, $\hat{\sigma}_\epsilon^2 = 1.046490$, as mentioned above.

In Fig. 5.5c, for comparison, the estimated spectrum, calculated by the nonparametric or correlation method, and the Fourier transform of the calculated $\hat{R}(r)$ in Fig. 5.4b are
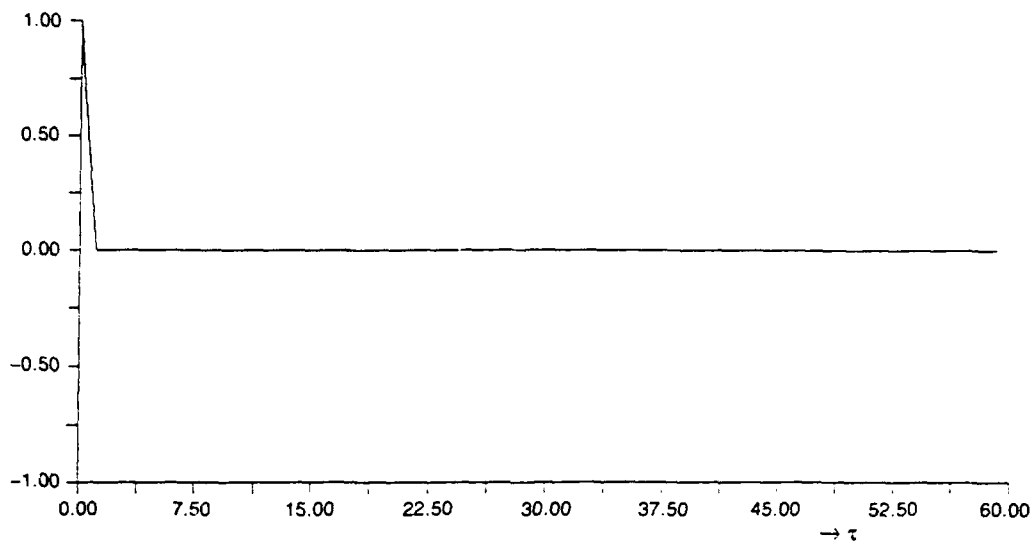
Fig. 5.4a. Theoretical AR(0).
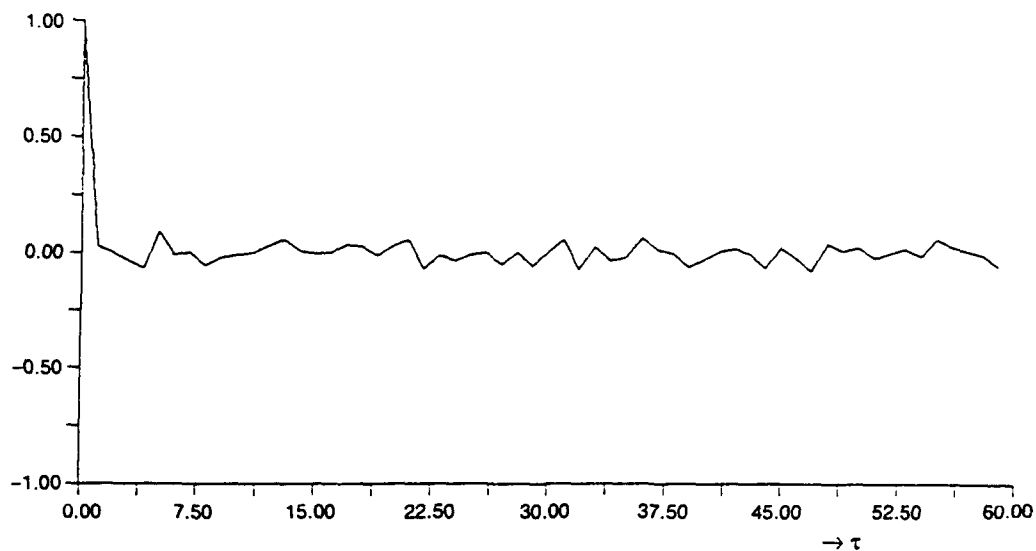
Fig. 5.4b. Estimated.

Fig. 5.4. Autocorrelation coefficient for pure random process AR(0)
$$X_t = \epsilon_t, \qquad \epsilon_t : N[0, 1].$$

shown. The maximum lag number $M = 60$ and the so–called Hanning Type spectral win
dow was used to calculate this spectrum. It looks very different from the white spectrum
and has many sizable peaks and valleys. In the figures, the 90% level of confidence inter-
val of this estimate, based on the χ^2–distribution of the equivalent degree of freedom

101

(here approximately equal to 27), as is explained in Section 2.5.5 is shown as vertical lines for reference.
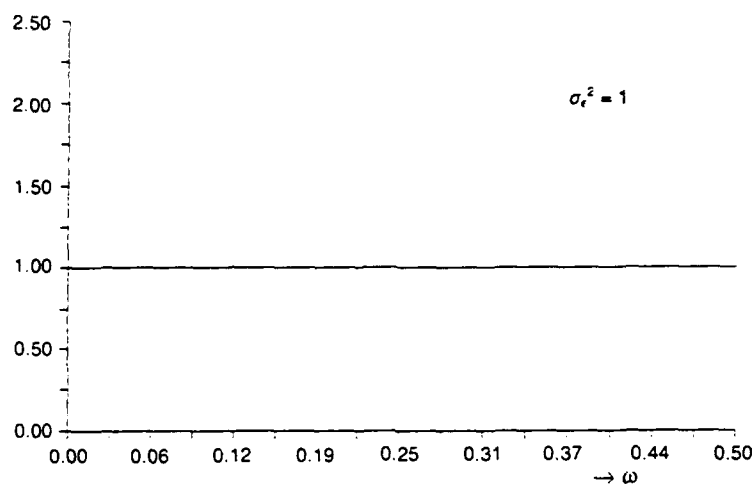
Fig. 5.5a. Theoretical AR(0).
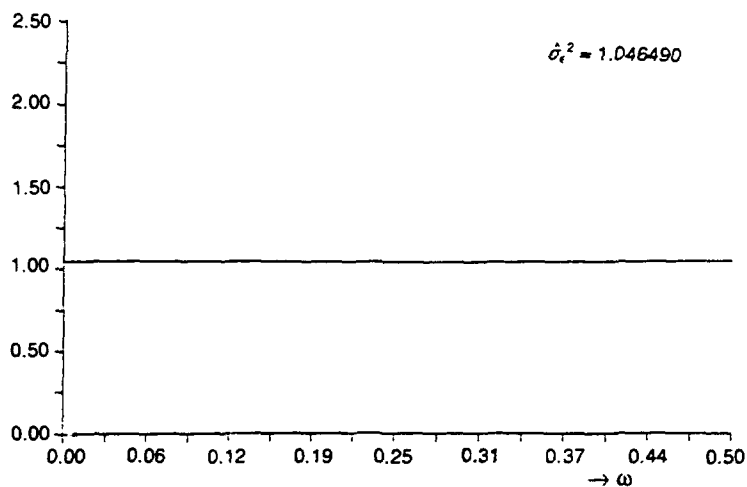
Fig. 5.5b. Estimated by model fitting as optimum AR(0).

Fig. 5.5. Spectrum for pure random process AR(0)
$$X_t = \epsilon_t, \quad \epsilon_t : N[0, 1].$$

This difference tells us that the process might not actually be white in this short period of 600 and also that it is hard to get the 'real' character of the spectrum by the nonparametric method from this short record. It is interesting to note, however, that by the model fitting method, even from this short record, the fluctuations disappeared and the spectrum appeared to be white.
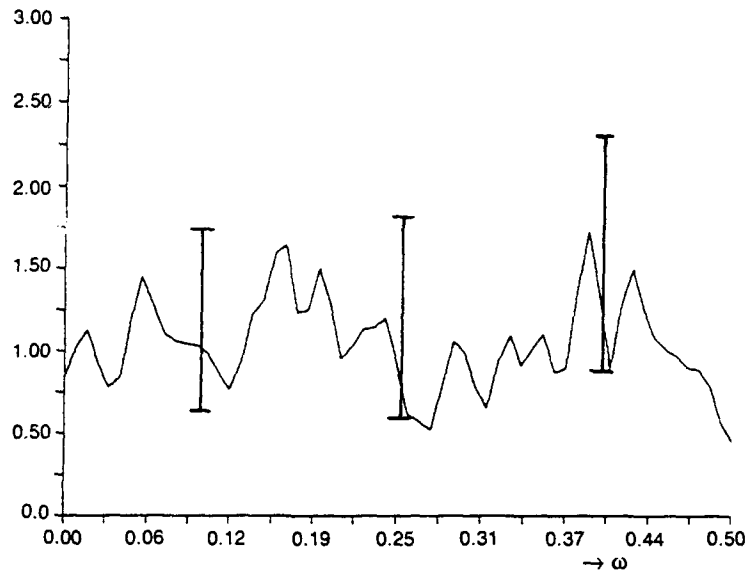
Fig. 5.5c. Estimated by nonparametric method.

Fig. 5.5. (Continued)

5.2.2 Autoregressive Process of the First Order, AR(1).

When X_t follows the relation

$$X_t = aX_{t-1} + \epsilon_t ,\qquad (5.7)$$

where a is a constant and $\{\epsilon_t\}$ is a stationary pure random process,

then
$$E[\epsilon_t \cdot \epsilon_{t-r}] = \begin{cases} \sigma_\epsilon^2 & \text{when} \quad r = 0 \\ 0 & \text{otherwise.} \end{cases} \qquad \text{(Fig. 5.7)} \qquad (5.8)$$

$\{X_t\}$ is called an autoregressive process of the first order AR(1). Equation 5.7 means that

1. X_t has a linear regression on X_{t-1} as in Fig. 5.6

2. ϵ_t plays the role of error in the above relations of regression

3. X_t is dependent on one step back value of the same process X_{t-1}.

103
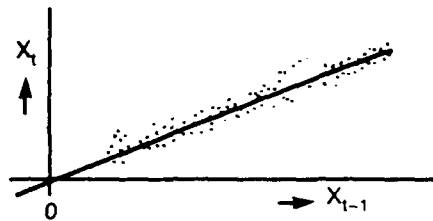
Fig. 5.6. X_t vs. X_{t-1}.

Besides, when $\{X_t\}$ is Gaussian, this process is called a "Linear Markov Process" as will be explained in Part III.
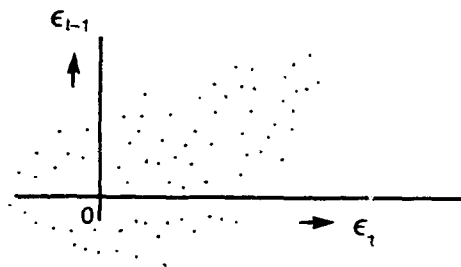
Fig. 5.7. ϵ_t vs. ϵ_{t-1}.

5.2.2.1 Green's Function of AR(1).

$$X_t = \epsilon_t + aX_{t-1}$$

$$= \epsilon_t + a(\epsilon_{t-1} + aX_{t-2})$$

$$= \cdots$$

$$= \epsilon_t + a\ \epsilon_{t-1} + -a^2\ \epsilon_{t-2} + \cdots + a^{t-1}\{\epsilon_1 + aX_0\}$$

$$= \sum_{r=0}^{t-1} a^r\ \epsilon_{t-r} + a^t\ X_0. \tag{5.9}$$

If initially $X_0 = 0$, or $X_r = 0$ when $r \leq 0$,

then
$$X_t = \sum_{r=0}^{t-1} a^r \epsilon_{t-r}, \tag{5.10}$$

or, considering the stationarity of X_t and assuming that $X_{-\infty}$ exist,

$$X_t = \sum_{u=-(N-1)}^{t} a^{t-u} \epsilon_u + a^{t+N} X_{-N}. \text{ If } X_{-N} \text{ is } 0, \text{ when } N \text{ tends to } \infty$$

$$X_t = \sum_{u=-\infty}^{t} a^{t-u} \epsilon_u \rightarrow \sum_{j=0}^{\infty} a^j \epsilon_{t-j}, \tag{5.11}$$

which is the same form as Eq. 5.10. Setting

$$G_j = a^j \tag{5.12}$$

gives

$$X_t = \sum_{j=0}^{\infty} G_j \, \epsilon_{t-j} = \sum_{j=-\infty}^{t} G_{t-j} \, \epsilon_j. \tag{5.13}$$

G_j is called Green's function for AR(1).

Green's function G_j shows the weight given in the present response of X_t to the disturbance ϵ_{t-j}, which entered the system j time units back. It also indicates how well the system remembers the disturbance ϵ_{t-j} or how slowly or quickly the dynamic response of the system to any particular ϵ_{t-j} decays. Equation 5.13 is called Wold's decomposition and gives the decomposition of X_t into an infinite number of orthogonal variables $G_j \, \epsilon_{t-j}$. Equation 5.13 also implies that the AR(1) process can be inverted into an infinite order moving average process MA (∞) as

$$X_t = G_o \, \epsilon_t + G_1 \, \epsilon_{t-1} + G_2 \, \epsilon_{t-2} + \cdots + G_j \, \epsilon_{t-j} + \cdots. \tag{5.13'}$$

5.2.2.2 Solution of the Difference Equation. Equation 5.7 is a difference equation and can be written

$$X_t - aX_{x-1} = \epsilon_t. \tag{5.7'}$$

The general solution of the difference equation is the sum of the solution of its homogeneous equation plus a particular solution of Eq. 5.7'. The homogeneous equation of Eq. 5.7' is

$$X_t - aX_{t-1} = 0, \tag{5.14}$$

its solution being

$$X_t = A\mu^t, \tag{5.15}$$

where μ is the root of its characteristic equation, equated to zero.

$$f(Z) = Z - a = 0, \tag{5.16}$$

namely

$$\mu = a. \tag{5.17}$$

A is an arbitrary constant and is determined by the initial conditions. From Eqs. 5.15 and 5.17,

$$X_t = Aa^t. \tag{5.18}$$

One particular solution of Eq. 5.7 is obtained as follows using the backward shifting operator B. Equation 5.7 is

$$(1 - aB) \ X_t = \epsilon_t, \tag{5.19}$$

$$X_t = (1 - aB)^{-1}\epsilon_t = \sum_{j=0}^{\infty} (a^j B^j)\epsilon_t = \sum_{j=0}^{\infty} a^j \epsilon_{t-j}. \tag{5.20}$$

This equation is the same as Eq. 5.10 or 5.13 expressed by Green's function. Therefore, the general solution of Eq. 5.7 is

$$X_t = Aa^t + \sum_{j=0}^{\infty} a^j \epsilon_{t-j} \tag{5.21}$$

The first term that is the solution of the homogenous equation is the free oscillation of this system. When $|a| < 1$, this free oscillation decays, and only the second term remains as a stationary oscillation as in Eq. 5.20. Equation 5.19 is, more generally,

$$\alpha(B)X_t = \epsilon_t, \tag{5.22}$$

$$X_t = \alpha^{-1}(B)\epsilon_t, \tag{5.23}$$

where

$$\alpha(Z) = 1 - aZ. \tag{5.24}$$

In order to have the free oscillation damp out, $|a| < 1$ is necessary and, with the characteristic Eq. 5.16 equated to zero, $f(Z) = 0$ must have its root inside the unit circle. Then from the equation

$$\alpha(Z) = 0, \tag{5.25}$$

or $1 - aZ = 0$, its root is the reverse of the root of the equation $Z - a = 0$, or $f(Z) = 0$. We find $\alpha(Z) = 0$ must have its root outside the unit circle.

5.2.2.3 Inverse Function of AR(1). Green's function can be considered as an indication of how X_t can be expressed by the MA (∞) process, because X_t is expressed as the summation of infinite ϵ_t at preceding time points.

$$X_t = \sum_{j=0}^{\infty} G_j \, \epsilon_{t-j}$$

$$= G_0\epsilon_t + G_1\epsilon_{t-1} + G_2\epsilon_{t-2} + \cdots + G_j \, \epsilon_{t-j} + \cdots$$

$$= (G_0 B^0 + G_1 B + G_2 B^2 + \cdots + G_j \, B^j + \cdots) \, \epsilon_t$$

$$= \sum_{j=0}^{\infty} (G_j \, B^j) \, \epsilon_t.$$

Usually $G_0 = 1$. As the inverse relation to this Green's function, if

$$\epsilon_t = \sum_{j=0}^{\infty} (-I_j B^j) \, X_t$$

$$= (-I_0 - I_1 B - I_2 B^2 \cdots - I_j B^j + \cdots) X_t$$

$$= -I_0 X_t - I_1 \, X_{t-1} - I_2 \, X_{t-2} - \cdots - I_j \, X_{t-j} - \cdots, \tag{5.26}$$

functions $I_0, I_1, \cdots I_j$ are called inverse functions, and usually $-I_0 = 1$.

Therefore

$$\epsilon_t = X_t - I_1 X_{t-1} - I_2 X_{t-2} - \cdots - I_j \, X_{t-j} \cdots. \tag{5.27}$$

This inverse function shows how X_t can be expressed by AR (∞). Therefore the inverse function of a pure autoregressive process AR(n) actually has no meaning. For example, for AR(1) as in Eq. 5.7;

$$I_0 = -1, \qquad I_1 = +a, \qquad I_j = 0 \text{ for } j \geq 2. \tag{5.28}$$

5.2.2.4 Stationality of AR(1). From Eq. 5.10

$$X_t = \lim_{t \to \infty} \sum_{j=0}^{t-1} a^j \epsilon_{t-j} = \epsilon_t + a\epsilon_{t-1} + a^2\epsilon_{t-2} + \cdots a^{t-1}\epsilon_1.$$

Then if

$$E[\epsilon_t] = \mu_\epsilon \text{ for all } t, \tag{5.29}$$

and as ϵ_t represents white noise,

$$E[\epsilon_t \cdot \epsilon_u] = \begin{cases} \sigma_\epsilon^2, & t = u \\ 0, & t \neq u \end{cases}, \tag{5.30}$$

we can get

107

$$E[X_t] = \lim_{t \to \infty} \mu_\epsilon \left\{ 1 + a + a^2 + \cdots + a^{t-1} \right\} = \lim_{t \to \infty} \begin{cases} \dfrac{1-a^t}{1-a} \mu_\epsilon & a \neq 1 \\ \\ \mu_\epsilon\, t & a = 1 \end{cases}, \quad (5.31)$$

$$\text{cov. } [X_t \cdot X_{t+r}] = \lim_{t \to \infty} \left[\left(\sum_{i=0}^{t-1} a^i \epsilon_{t-i} \right) \left(\sum_{j=0}^{t-1} a^j \epsilon_{t+r-j} \right) \right]$$

$$= \lim_{t \to \infty} \sigma_\epsilon^2 \left\{ a^r + a^{r+2} + \cdots + a^{r+2(t-1)} \right\}.$$

Therefore
$$R(r) = \lim_{t \to \infty} \begin{cases} \sigma_\epsilon^2 a^r \left(\dfrac{1-a^{2t}}{1-a^2} \right), & a \neq 1 \\ \\ \sigma_\epsilon^2 t, & a = 1 \end{cases} \qquad (5.32)$$

If $\mu_\epsilon = 0$,

$$\text{var. } [X_t] = R(0) = \lim_{t \to \infty} \begin{cases} \sigma_\epsilon^2 \dfrac{1-a^{2t}}{1-a^2}, & a \neq 1 \\ \\ \sigma_\epsilon^2 t, & a = 1 \end{cases} \qquad (5.33)$$

From these results:

[a.] When $\mu_\epsilon \neq 0$

$E[X_t]$ is, from Eq. 5.31, a function of time and therefore $\{X_t\}$ is not stationary, even to order 1.

(1.) When $|a| < 1$, and when t tends to a large value

$$E[X_t] = \frac{\mu_\epsilon}{1-a} = \text{const. by } t. \qquad (5.34)$$

Therefore $\{X_t\}$ is asymptotically stationary to order 1.

(2.) When $a = 1$

$$E[X_t] = \mu_\epsilon t \qquad (5.35)$$

$E[X]$ increases by time t. Therefore, $\{X_t\}$ is not stationary, even up to order 1. This is the case of Random Walk.

[b.] When $\mu_\epsilon = 0$

$$E[X_t] = 0.$$

$$\text{cov. } [X_t \cdot X_{t+r}] = R(r) = \sigma_\epsilon^2 a^r \left(\frac{1-a^{2t}}{1-a^2} \right).$$

108

(1.) When $|a| < 1$, i.e., when $f(Z) = Z - a = 0$ has its root inside the unit circle or when $\alpha(Z) = 1 - aZ = 0$ has its root outside the unit circle, from Eq. 5.32, even $E\{X_t\} = 0$ holds, the cov. $[X_t, X_{t+r}]$ is a function of time. Accordingly, $\{X_t\}$ is not stationary even up to order 2. However, when $t \to \infty$,

$$\text{cov. } [X_t \cdot X_{t+r}] = R(r) = \frac{\sigma_\epsilon^2}{1-a^2} a^r \quad \text{const. by } t, \tag{5.36}$$

$$\text{var. } [X_t] = E[X_t \; X_t] = R(0) = \frac{\sigma_\epsilon^2}{1-a^2} \quad \text{const. by } t. \tag{5.37}$$

Therefore, $\{X_t\}$ is asymptotically stationary up to order 2. The form of $R(r)$ will be different by the sign of a, although it gradually decays as r increases as in Fig. 5.8.

(a) $0 < a < 1$ (b) $-1 < a < 0$
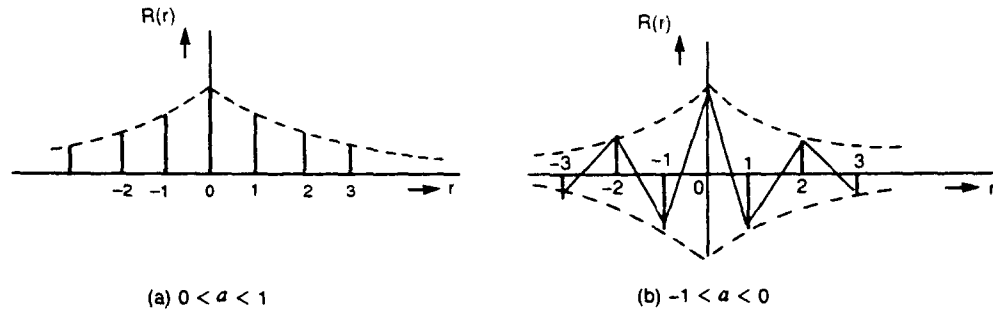
Fig. 5.8. $R(r)$ of AR(1).

(2.) When $|a| > 1$, i.e., when $f(Z) = Z - a$ has its root outside the unit circle, or when $\alpha(Z) = 1 - aZ$ has its root inside the unit circle,

$$\text{cov. } [X_t \cdot X_{t+r}] = R(r) = \frac{\sigma_\epsilon^2}{a^2 - 1} a^r (a^{2t} - 1) \tag{5.38}$$

$$\text{var. } [X_t] = \frac{\sigma_\epsilon^2}{a^2 - 1} (a^{2t} - 1). \tag{5.39}$$

In this case, $E[X] = 0$, but not only does $R(r)$ not converge to a small value as r increases, but both $R(r)$ and $R(0)$ change by the time t and are not stationary. As time passes, these values continue to increase. Accordingly, this process is not stationary up to order 2, even asymptotically.

5.2.2.5 Autocovariance and Spectrum of AR(1). The general solution of $R(r)$ can also be obtained more simply as the solution of a first order homogenous difference equation, because in this case, from Eq. 5.7,

$$X_t = aX_{t-1} + \epsilon_t, \tag{5.7}$$

assuming $\mu_\epsilon = 0$ and $E[X_t] = 0$. Multiplying both sides of Eq. 5.7 by X_{t-r} and taking the expected values gives

$$R(r) = a \ R(r-1) \qquad \text{when } r \neq 0 \qquad (5.40)$$

$$R(0) = a^2 R(0) + \sigma_\epsilon^2 \qquad \text{when } r = 0, \qquad (5.41)$$

because

$$E[X_i \cdot \epsilon_j] = \begin{cases} 0 & i \neq j \\ E[\epsilon_j^2] = \sigma_\epsilon^2 & i = j, \end{cases} \qquad (5.42)$$

Equation 5.40 is the same type of homogeneous difference equation as that of the original process $\{X_t\}$ shown in Eq. 5.14.

$$R(r) - aR(r-1) = 0. \qquad (5.43)$$

Using the backward shift operator B gives

$$(1 - aB)R(r) = 0. \qquad (5.44)$$

Thus
$$R(r) = (1 - aB)^{-1}R(r) = 0 \qquad (5.45)$$

and
$$R(r) = A\mu^r. \qquad (5.46)$$

Here μ is the root of $f(Z) = Z - a = 0$ when $\mu = a$

and thus
$$R(r) = Aa^r. \qquad (5.47)$$

In order to be asymptotically stationary, $R(r) \to 0$ as $(r) \to \infty$ when $|a| < 1$ and $f(Z) = 0$ must have its roots inside the unit circle.

From Eq. 5.41

$$R(0) = \sigma_x^2 = A = \frac{\sigma_\epsilon^2}{1 - a^2}. \qquad (5.48)$$

Therefore, the general solution is, from Eq. 5.43,

$$R(r) = \frac{\sigma_\epsilon^2}{1 - a^2} a^r = R(0)a^r = \sigma_x^2 a^r. \qquad (5.49)$$

This equation is the same as Eq. 5.36.

5.2.2.6 $s(\omega)$ of AR(1). Here we assume $\mu_\epsilon \equiv 0$, $|a| < 1$.

Then the spectrum $s(\omega)$ is obtained as the Fourier transform of $R(r)$

$$s(\omega) = \frac{1}{2\pi} \sum_{r=-\infty}^{\infty} R(r) \cdot e^{-i\omega r}$$

$$= \frac{1}{2\pi} \left\{ R(0) + 2 \sum_{r=1}^{\infty} R(r) \cos r\omega \right\}.$$

Substituting the values of $R(0)$ and $R(r)$ in Eqs. 5.48 and 5.49 gives

$$= \frac{1}{2\pi} \sigma_x^2 \left\{ 1 + 2 \sum_{r=1}^{\infty} a^r \cos r\omega \right\}$$

$$= \frac{\sigma_x^2}{2\pi} \left[1 + 2 \sum_{r=1}^{\infty} \Re e \left\{ a^r e^{+ir\omega} \right\} \right]$$

$$= \frac{\sigma_x^2}{2\pi} \left[1 + 2 \Re e \left\{ a e^{i\omega} + (a e^{i\omega})^2 + (a e^{i\omega})^3 + \cdots \right\} \right]$$

$$= \frac{\sigma_x^2}{2\pi} \left[1 + 2 \Re e \left\{ \frac{a e^{+i\omega}}{1 - a e^{+i\omega}} \right\} \right]$$

$$= \frac{1}{2\pi} \sigma_x^2 \left[1 + 2 \Re e \left\{ \frac{a \cos \omega + ia \sin \omega}{(1 - a \cos \omega) - i\, a \sin \omega} \right\} \right]$$

$$= \frac{\sigma_x^2}{2\pi} \left\{ 1 + 2 \frac{a \cos \omega (1 - a \cos \omega) - a^2 \sin^2 \omega}{(1 - a \cos \omega)^2 + a^2 \sin \omega} \right\} = \frac{\sigma_x^2}{2\pi} \frac{1 - a^2}{1 - 2a \cos \omega + a^2},$$

here $\Re e \{\cdot\}$ indicates to take the real part of a function $\{\cdot\}$.

Inserting Eq. 5.37, that is $\sigma_x^2 = \dfrac{\sigma_\epsilon^2}{1 - a^2}$, gives

$$s(\omega) = \frac{\sigma_\epsilon^2}{2\pi} \frac{1}{(1 - 2a \cos \omega + a^2)}$$

$$= \frac{\sigma_\epsilon^2}{2\pi \left| 1 - a e^{-i\omega} \right|^2} = \frac{\sigma_\epsilon^2}{2\pi \left| \alpha(e^{-i\omega}) \right|^2}. \tag{5.50}$$

Therefore,

$$s(0) = \frac{\sigma_x^2}{2\pi} \frac{1 - a^2}{(1 - a)^2} = \frac{\sigma_x^2}{2\pi} \frac{1 + a}{1 - a}$$

$$= \frac{\sigma_\epsilon^2}{2\pi} \frac{1}{(1 - a)^2}, \tag{5.51}$$

111

$$s(\pi) = s(-\pi) = \frac{1-a}{1+a} \frac{\sigma_x^2}{2\pi} = \frac{\sigma_\epsilon^2}{2\pi} \frac{1}{(1+a)^2}. \qquad (5.52)$$

Its shape will then be as shown in Fig. 5.9.
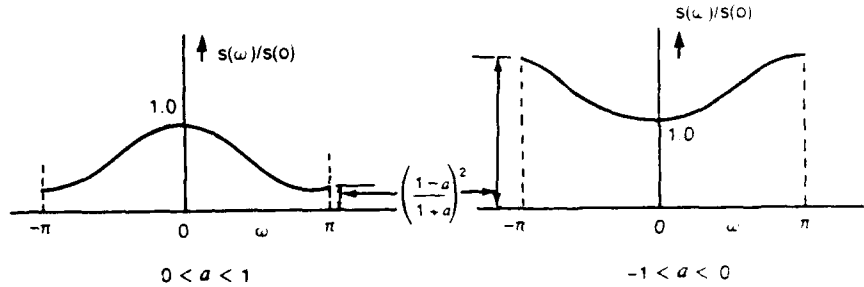
Fig. 5.9. $s(\omega)$ of AR(1).

5.2.2.7 Estimation of a and σ_ϵ^2. When we are given a set of data, $X_1 \cdots X_N$, with numbers N, and the AR(1) model is to be fitted (the determination of order will be discussed later in Section 5.5), we can easily estimate the values of a and σ_ϵ^2 by the minimum least squares method as

$$\hat{a} = \frac{\displaystyle\sum_{t=2}^{N} X_t X_{t-1}}{\displaystyle\sum_{t=2}^{N} X_{t-1}^2} \qquad (5.53)$$

and the minimized residual sum is

$$\hat{\sigma}_\epsilon^2 = \frac{1}{N-1} \sum_{t=2}^{N} (X_t - \hat{a} X_{t-1})^2. \qquad (5.54)$$

The same results can also be derived from Eq. 5.40 and Eq. 5.41 as

$$\hat{a} = \frac{\hat{R}(1)}{\hat{R}(0)} \qquad (5.55)$$

$$\text{and} \quad \hat{\sigma}_\epsilon^2 = (1 - \hat{a}^2)\hat{R}(0). \qquad (5.56)$$

Equations 5.53 and 5.55 have the same content as if the sample correlation were replaced with $\hat{R}(0)$ and $\hat{R}(1)$. Obtaining $\hat{a}$ by the linear minimum least squares method from Eq. 5.53 is actually done by Eq. 5.55. Then, the variance σ_ϵ^2 of ϵ_t is estimated by Eq. 5.56.

5.2.2.8 Example of AR(1). Figure 5.10 is an example of the AR(1) process simulated by an AR(1) model $X_t - 0.5 X_{t-1} = \epsilon_t$, where $a = -0.5$ in Eq. 5.7. In order to look at the pattern of variations, at the bottom of this figure, a part ($t = 100$ to 250) of this process is shown expanded on the time axis. Its readings are listed in Appendix A1 as Table

112
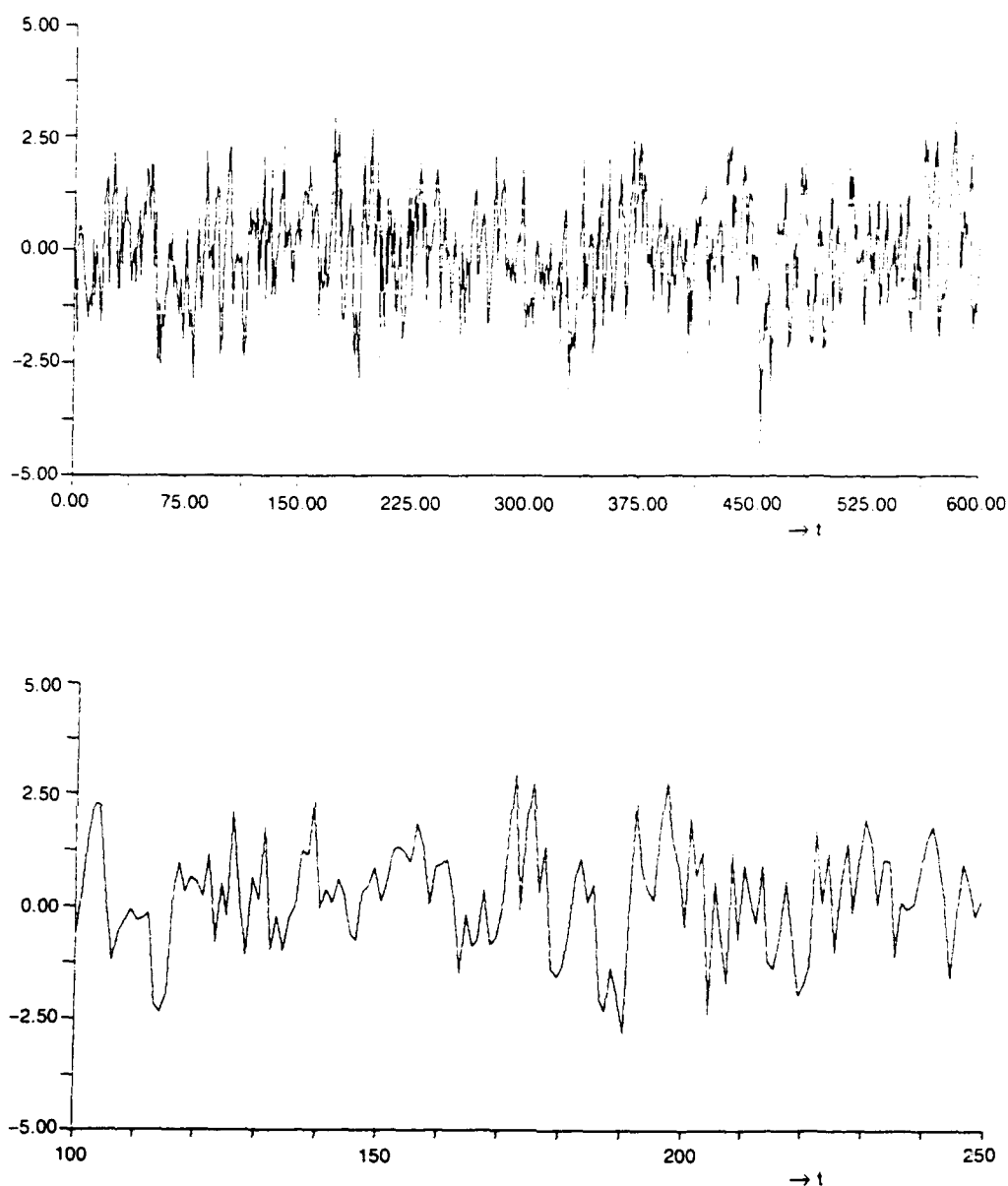
Fig. 5.10. Simulated AR(1) process

$$X_t - 0.5 \ X_{t-1} = \epsilon_t, \qquad \epsilon_t: \ N[0, 1].$$

A1.2; pp. 251, 252, and 253. Here ϵ_t is a pure random Gaussian process N[0, 1], and the same process, which was generated as a pure random process AR(0) in Fig. 5.3, was used. Figure 5.11a shows the theoretical autocorrelation coefficient $\varrho(r) = R(r)/R(0)$, from Eqs. 5.36 and 5.37 using the designed value of $\sigma_\epsilon^2 = 1$ and $a = -0.5$. Figure 5.11b is the estimated autocorrelation function $\hat{\varrho}(r) = \hat{R}(r)/\hat{R}(0)$ from the simulated process in Fig. 5.10. An AR model was fitted to this process, and the order actually obtained was 1 by
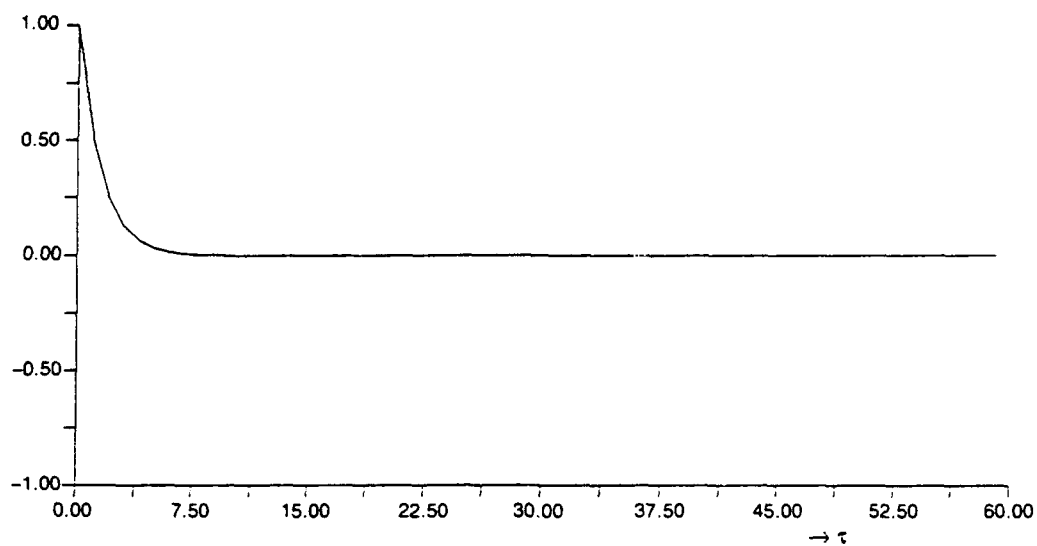
Fig. 5.11a. Theoretical.
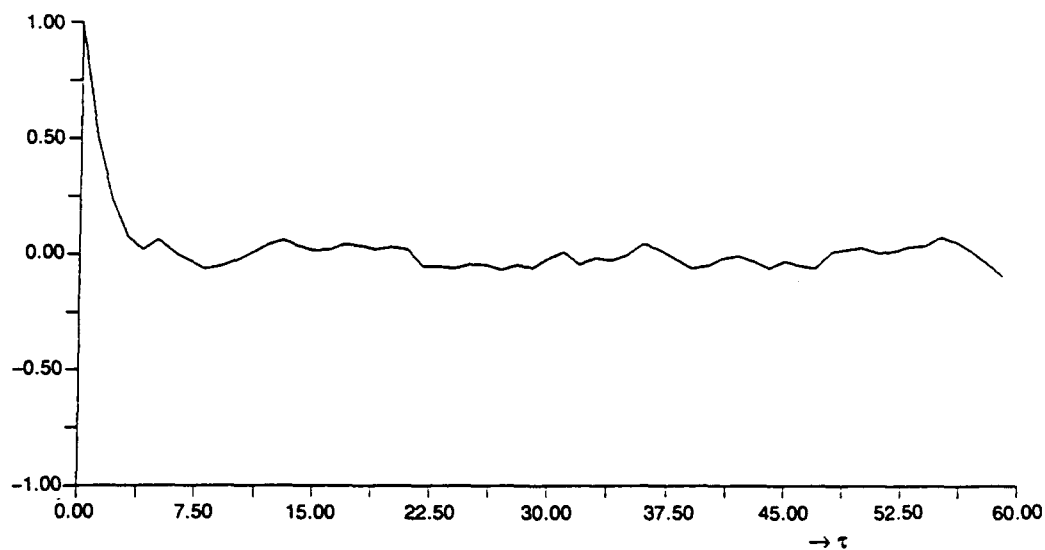
Fig. 5.11b. Estimated.

Fig. 5.11. Autocorrelation coefficient for AR(1) process
$$X_t - 0.5 \ X_{t-1} = \epsilon_t, \quad \epsilon_t : N[0, 1].$$

114

the method of order determination that will be mentioned later in Section 5.5. Now with the order as 1, a and σ_ϵ^2 were calculated from Eqs. 5.55 and 5.56, as $\hat{a} = -0.50933$ and $\hat{\sigma}_\epsilon^2 = 1.04646$, which are close to the $a = -0.5$ and $\sigma_\epsilon^2 = 1.0$ used to generate the process. We also estimated the correlation coefficient $\hat{\varrho}(r) = \hat{R}(r)/\hat{R}(0)$ from Eqs. 5.36 and 5.37, using these $\hat{a}$ and $\hat{\sigma}_\epsilon^2$. These values are so close to the theoretical $R(r)$, or just the same in $\varrho(r) = R(r)/R(0)$ in Fig. 5.11a that their drawing was omitted. Figure 5.12a is the theoretical spectrum from Eq. 5.50, using the design values of $a = -0.5$ and $\sigma_\epsilon^2 = 1$.

$$\alpha = -0.5$$
$$\sigma_\epsilon^2 = 1.0$$
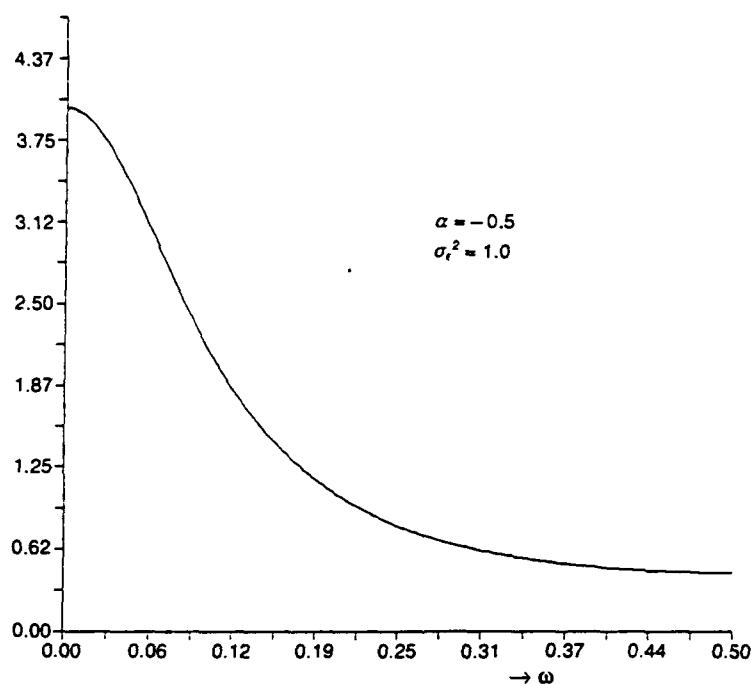
Fig. 5.12a. Theoretical AR(1).

Fig. 5.12. Spectrum for AR(1) process $X_t - 0.5\ X_{t-1} = \epsilon_t,\quad \epsilon_t: N[0, 1]$.

The estimated spectrum $\hat{s}(\omega)$, with $\hat{a} = -0.50933$ and $\hat{\sigma}_\epsilon^2 = 1.04646$ obtained by model fitting and also by Eq. 5.50, is given as b in Fig. 5.12. For comparison, as c in Fig. 5.12, the spectrum $\hat{s}(\omega)$ was also estimated by the nonparametric method as the Fourier transform of $\hat{R}(r)$ in Fig. 5.11b, using the Hanning window and maximum lag $M = 60$. It is interesting that the spectrum estimated by model fitting is very similar to the theoretical spectrum, Fig. 5.12a, of this generated process. On the other hand, the spectrum estimated by the nonparametric method Fig. 5.12c is more wavy than the theoretical one, although the fundamental shape is similar. The wavy fluctuations were found to come mostly from the wavy fluctuation of the input white noise $\{\epsilon_t\}$ that is shown in Fig. 5.5c, as the incomplete whiteness of the pure random process $\{\epsilon_t\}$ generated. In the figures,
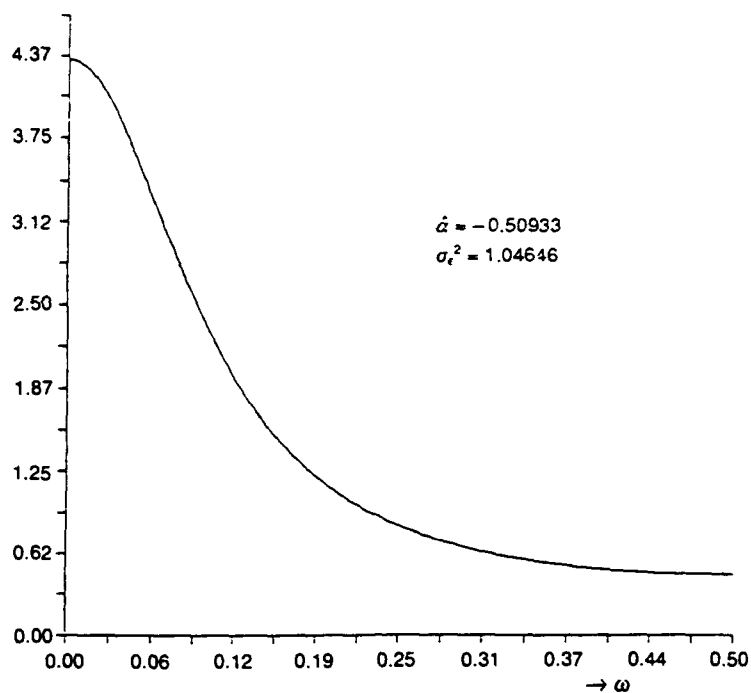
Fig. 5.12b. Estimated by AR model fitting as optimum AR(1).
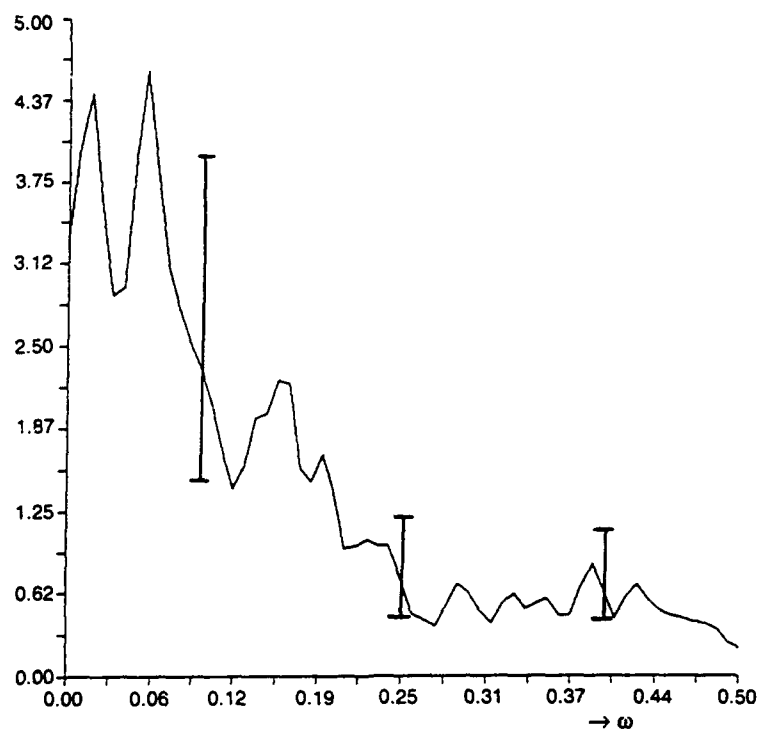
Fig. 5.12c. Estimated by nonparametric method.

Fig. 5.12. (Continued)

116

the 90% level of confidence interval of this estimate, based on the χ^2-distribution of the equivalent degree of freedom (here approximately equal to 27) as is explained in Section 2.5.5 is shown as vertical lines for reference.

5.2.3 Autoregressive Process of the Second Order, AR(2)

As was shown in the last section for the AR(1) process, the residual part ϵ_t of X_t, obtained by subtracting the linearly dependent part aX_{t-1} from X_{t-1},

$$\epsilon_t = X_t - aX_{t-1} \tag{5.7'}$$

was a purely random process uncorrelated with ϵ_{t-1}, $\epsilon_{t-2}\cdots$ as in Fig. 5.13a and uncorrelated with X_{t-2}, $X_{t-3}\cdots$ as in Fig. 5.13b.

Fig. 5.13a. ϵ_t vs. ϵ_{t-1} for AR(1).
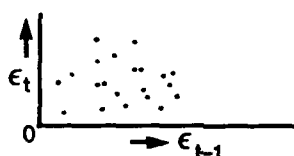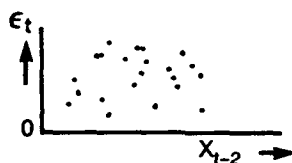
Fig. 5.13b. ϵ_t vs. X_{t-2} for AR(1).

Fig. 5.13. Characters of ϵ_t for AR(1).

$$E[\epsilon_t \cdot \epsilon_{t-r}] = \begin{cases} \sigma_\epsilon^2 & r = 0 \\ 0 & r \neq 0 \end{cases} \quad E[\epsilon_t \cdot X_{t-2}] \equiv 0.$$

If this relation does not exist and the residual ϵ_t', that is,

$$\epsilon_t' = X_t - a'X_{t-1}, \tag{5.57}$$

was linearly correlated with X_{t-2} as in Fig. 5.14, then

117

$$\epsilon_t' = a_2' \, X_{t-2} + \epsilon_t. \tag{5.58}$$

The residual part $\epsilon_t = \epsilon_t' - a_2' \, X_{t-2}$ is now a purely random process. Then inserting Eq. 5.57 into Eq. 5.58 gives $X_t - a' X_{t-1} - a_2' \, X_{t-2} = \epsilon_t$.
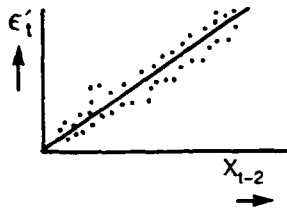
Fig. 5.14. ϵ_t' vs. X_{t-2} for AR(2).

Here changing $-a' = a_1$, $-a_2' \rightarrow a_2$,

$$X_t + a_1 X_{t-1} + a_2 X_{t-2} = \epsilon_t. \tag{5.59}$$

The process, which satisfies Eq. 5.59, is called the autoregressive process of the second order. Here, a_1 and a_2 are constant, $\{\epsilon_t\}$ is a stationary pure random process, and we assume $E[\epsilon_t] = 0$.

5.2.3.1 Solution of AR(2), Green's Function for AR(2). Starting from Eq. 5.59

$$X_t + a_1 X_{t-1} + a_2 X_{t-2} = \epsilon_t,$$

we can solve X_t as the general solution of a second order difference equation, i.e., a general solution equals a complementary function plus a particular solution. A complementary function is the solution of the homogeneous equation

$$X_t + a_1 X_{t-1} + a_2 X_{t-2} = 0. \tag{5.60}$$

The solution of this homogeneous equation is in the shape of

$$A_1 \, \mu_1^t + A_2 \, \mu_2^t. \tag{5.61}$$

μ_1, μ_2, being the roots of the characterisitc equation $f(Z) = 0$. The particular solution can be obtained, using the backward shifting operator B, as

$$(1 + a_1 B + a_2 B^2) X_t = \epsilon_t. \tag{5.62}$$

Setting

$$\alpha(Z) = 1 + a_1 Z + a_2 Z^2, \tag{5.63}$$

$$\alpha(B) X_t = \epsilon_t. \tag{5.64}$$

If the quadrant $\qquad f(Z) = Z^2 + a_1 Z + a_2 Z^2 = 0 \tag{5.65}$

has two roots μ_1, μ_2,

$$\left\{1 - (\mu_1 + \mu_2)B + \mu_1\mu_2 B^2\right\}X_t = \epsilon_t, \qquad (5.66)$$

$$\begin{cases} \mu_1 + \mu_2 = -a_1 \\ \mu_1\mu_2 = a_2, \end{cases} \qquad (5.67)$$

$$(1 - \mu_1 B)(1 - \mu_2 B)X_t = \epsilon_t, \qquad (5.66')$$

then

$$X_t = \frac{\epsilon_t}{\alpha(B)} = \frac{\epsilon_t}{(1 + a_1 B + a_2 B^2)} = \frac{1}{(1 - \mu_1 B)(1 - \mu_2 B)}\epsilon_t$$

$$= \frac{1}{\mu_1 - \mu_2}\left\{\frac{\mu_1}{(1 - \mu_1 B)} - \frac{\mu_2}{(1 - \mu_2 B)}\right\}\epsilon_t$$

$$= \frac{1}{\mu_1 - \mu_2}\left\{\sum_{j=0}^{\infty}(\mu_1^{j+1} - \mu_2^{j+1})B^j\right\}\epsilon_t$$

$$= \sum_{j=0}^{\infty}\left\{\frac{\mu_1^{j+1} - \mu_2^{j+1}}{\mu_1 - \mu_2}\right\}\epsilon_{t-j}. \qquad (5.68)$$

X_t is a particular solution. Therefore, if the expression of Green's function G_j is used,

$$X_t = \sum_{j=0}^{\infty} G_j \; \epsilon_{t-j}. \qquad (5.69)$$

Thus

$$G_j = \frac{\mu_1^{j+1} - \mu_2^{j+1}}{\mu_1 - \mu_2} = \frac{\mu_1}{\mu_1 - \mu_2}\mu_1^j + \frac{\mu_2}{\mu_2 - \mu_1}\mu_2^j$$

$$= g_1 \mu_1^j + g_2 \mu_2^j, \qquad (5.70)$$

where $g_1 = \dfrac{\mu_1}{\mu_1 - \mu_2}$

$\qquad\quad g_2 = \dfrac{\mu_2}{\mu_2 - \mu_1}.$

This solution X_t can also be written as

$$X_t = \sum_{j=0}^{\infty} G_j\, \epsilon_{t-j} = G_0\epsilon_t + G_1\epsilon_{t-1} + G_2\epsilon_{t-2} + \cdots . \qquad (5.71)$$

Equation 5.71 shows the AR(2) process is expressed by MA(∞), as was the case for AR(1).

5.2.3.2 Inverse Function for AR(2). To say the inverse function for the autoregressive process has little meaning was pointed out for AR(1). Formally, however, for AR(2), from

$$X_t + a_1 X_{t-1} + a_2 X_{t-2} = \epsilon_t,$$

$$(1 + a_1 B + a_2 B^2)X_t = \sum_{j=0}^{\infty} (-I_j)X_{t-j}$$

$$= (-I_0 - I_1 B - I_2 B^2 \cdots I_j B^j)X_t . \quad (j \rightarrow \infty)$$

Therefore

$$I_0 = -1$$
$$I_1 = -a_1$$
$$I_2 = -a_2$$
$$I_j = 0 \quad \text{for} \quad j \geq 3. \qquad (5.72)$$

5.2.3.3 Stationality of AR(2). Returning to the general solution of X_t, we must consider the behavior of the complementary function or the solution of the homogeneous Eq. 5.60 that is in the shape of

$$A_1\, \mu_1^t + A_2\, \mu_2^t.$$

This complementary function represents the free oscillation of a forced oscillation system which should die out over time t and become asymptotically stationary. For this condition it is necessary that

$$|\mu_1| < 1, \quad |\mu_2| < 1.$$

This means that the quadrant, as expressed by Eq. 5.65 equated to zero,

$$f(Z) = Z^2 + a_1 Z + a_2 = 0 \qquad (5.73)$$

should have roots less than 1 in their absolute values. Therefore, $f(Z) = 0$ must have roots inside the unit circle. These roots of $f(Z)$ are the reciprocals of the roots of

$$\alpha(Z) = 1 + a_1 Z + a_2 Z^2. \qquad (5.74)$$

Accordingly, $\alpha(Z)$ must have roots outside the unit circle in order for AR(2) to be asymptotically stationary.

$f(Z) = 0$, i.e.,

$$Z^2 + a_1 Z + a_2 = 0$$

has two roots

$$\mu_1, \mu_2 = \frac{-a_1 \pm \sqrt{a_1^2 - 4a_2}}{2}, \tag{5.75}$$

and these two roots μ_1, μ_2 satisfy Eq. 5.67. Therefore, from the condition $|\mu_1| < 1$, $|\mu_2| < 1$,

$$1 > a_2 > -1 \tag{5.76}$$

and, as $\mu_1 < \mu_2 < 1$,

$$\mu_1(1 - \mu_2) < 1 - \mu_2.$$

Thus

$$\mu_1 + \mu_2 - \mu_1 \mu_2 < 1$$

and

$$-a_1 - a_2 < 1$$
$$a_1 + a_2 > -1, \quad (a_2 > -a_1 - 1) \tag{5.77}$$

and as $\mu_1 > -1$, $-\mu_1 < 1$, $-1 < \mu_2 < 1$

$$-(1 + \mu_2)\mu_1 < (1 + \mu_2).$$

Thus

$$-(\mu_1 + \mu_2) - \mu_1\mu_2 < 1$$

and

$$a_1 - a_2 < 1, \quad (a_2 > a_1 - 1). \tag{5.78}$$

Therefore, as shown in Fig. 5.15, on a $0 - a_1$, a_2 plane, the region inside of $\triangle$ ABC is the stable zone for a_1 and a_2. This stable zone is divided into two subzones.

1. When Eq. 5.73 has two real roots or coincident equal roots,

$$a_1^2 \geq 4a_2 \quad \text{or} \quad a_2 \leq \frac{1}{4}a_1^2. \tag{5.79}$$

This is subzone [I] in Fig. 5.16.

2. When Eq. 5.73 has unequal complex roots,

$$a_1^2 < 4a_2, \quad \text{or} \quad a_2 > \frac{1}{4}a_1^2. \tag{5.80}$$

This is subzone [II] in Fig. 5.16.

121
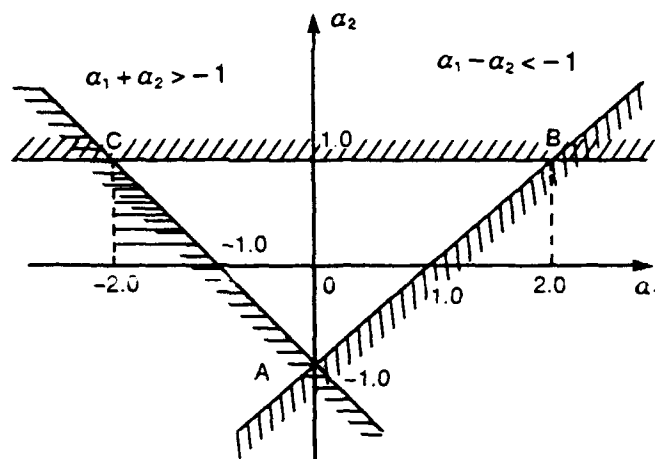
Fig. 5.15. $0 - a_1$, a_2 plane.
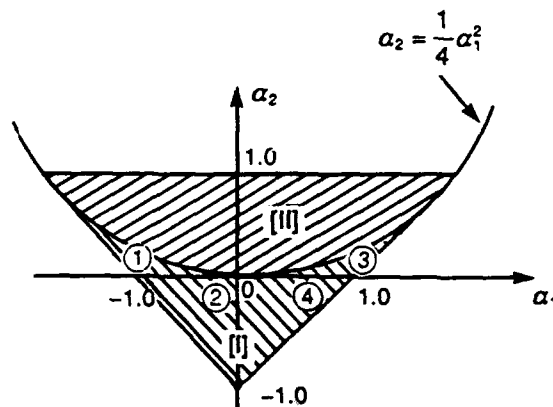
Fig. 5.16. Stable Subzones [I], [II]; ①, ②, ③, ④.

5.2.3.4 Autocovariance of AR(2). From Eq. 5.59

$$X_t + a_1 X_{t-1} + a_2 X_{t-2} = \epsilon_t$$

assuming $E[X_t] = 0$,

$$\left\{ E[\epsilon_t \cdot \epsilon_{t-r}] = \delta(r)\sigma_\epsilon^2 = \begin{cases} 0 & r \neq 0 \\ \sigma_\epsilon^2 & r = 0 \end{cases} \right.$$

$\delta(r)$ is Kronecker's delta function.

From Eq. 5.59

$$E[X_{t-r} \cdot \epsilon_t] = \begin{cases} 0 & r \neq 0 \\ E[\epsilon_t^2] = \sigma_\epsilon^2 & r = 0 \end{cases} \tag{5.81}$$

$$E[X_t \, X_{t-r}] + a_1 E[X_{t-1} \, X_{t-r}] + a_2 \, E[X_{t-2} \cdot X_{t-r}] = E[\epsilon_t \cdot X_{t-r}].$$

122

Therefore, when

$$r = 0 \quad : \quad R(0) + a_1 R(1) + a_2 R(2) = \sigma_\epsilon^2 \tag{5.82}$$

$$r = 1 \quad : \quad R(1) + a_1 R(0) + a_2 R(1) = 0 \tag{5.83}$$

$$r = 2 \quad : \quad R(2) + a_1 R(1) + a_2 R(0) = 0 \tag{5.84}$$

$$r \geq 2 \quad \text{generally} \quad R(r) + a_1 R(r-1) + a_2 R(r-2) = 0. \tag{5.85}$$

From Eq. 5.83

$$R(1)(1 + a_2) = -a_1 R(0) = -a_1 \sigma_x^2,$$

$$R(0) = \sigma_x^2,$$

and therefore

$$R(1) = \left(\frac{-a_1}{1 + a_2} \right) \sigma_x^2. \tag{5.86}$$

Inserting this value into Eq. 5.84 gives

$$R(2) = \left\{ \frac{a_1^2}{1 + a_2} - a_2 \right\} \sigma_x^2. \tag{5.87}$$

Substituting $R(1)$, $R(2)$ into Eq. 5.82, gives

$$\sigma_x^2 = \frac{(1 + a_2)\sigma_\epsilon^2}{(1 - a_2)(1 - a_1 + a_2)(1 + a_1 + a_2)}. \tag{5.88}$$

This equation connects σ_x^2 with σ_ϵ^2. From Eq. 5.86

$$R(1) = \frac{-a_1}{(1 - a_2)(1 - a_1 + a_2)(1 + a_1 + a_2)} \sigma_\epsilon^2. \tag{5.89}$$

From Eq. 5.87

$$R(2) = \frac{+a_1^2 - a_2(1 + a_2)}{1 + a_2} \sigma_x^2$$

$$= \frac{+a_1^2 - a_2^2 - a_2}{(1 - a_2)(1 - a_1 + a_2)(1 - a_1 + a_2)} \sigma_\epsilon^2. \tag{5.90}$$

Equation 5.85 is a homogeneous equation with the same coefficient as the homogeneous Eq. 5.60. Its solution is in the shape of

$$R(r) = B_1 \mu_1^{\,r} + B_2 \mu_2^{\,r}, \tag{5.91}$$

μ_1, μ_2 being the roots of Eq. 5.73, $f(Z) = Z^2 + a_1 Z + a_2 = 0$. B_1, B_2 are constants and are determined by the boundary conditions, as

$$R(0) = \sigma_x^2, \quad R(1) = \left(-\frac{a_1}{1} + a_2\right)\sigma_x^2.$$

Thus $\qquad B_1 + B_2 = \sigma_x^2 \quad \text{and} \quad B_1\mu_1 + B_2\mu_2 = \dfrac{-a_1}{1 + a_2}\sigma_x^2.$

Therefore $\qquad B_1 = \dfrac{\mu_1(1 - \mu_2^2)}{(\mu_1 - \mu_2)(1 + \mu_1\mu_2)}\sigma_x^2 \tag{5.92}$

$$B_2 = \dfrac{\mu_2(1 - \mu_1^2)}{(\mu_2 - \mu_1)(1 + \mu_1\mu_2)}\sigma_x^2. \tag{5.93}$$

Then $\quad R(r) = \left[\dfrac{(1 - \mu_2^2)\mu_1}{(\mu_1 - \mu_2)(1 + \mu_1\mu_2)}\mu_1^{\,r} - \dfrac{(1 - \mu_1^2)\mu_2}{(\mu_1 - \mu_2)(1 + \mu_1\mu_2)}\mu_2^{\,r}\right]\sigma_x^2. \tag{5.94}$

If we need the expression σ_ϵ^2 from Eq. 5.88

$$\sigma_x^2 = \dfrac{1 + a_2}{(1 - a_2)(1 - a_1 + a_2)(1 + a_1 + a_2)}\sigma_\epsilon^2$$

$$= \dfrac{1 + \mu_1\mu_2}{(1 - \mu_1\mu_2)(1 - \mu_1^2)(1 - \mu_2^2)}\sigma_\epsilon^2, \tag{5.95}$$

then

$$R(r) = \left[\dfrac{\mu_1}{(\mu_1 - \mu_2)(1 - \mu_1^2)(1 - \mu_1\mu_2)}\mu_1^{\,r} - \dfrac{\mu_2}{(\mu_1 - \mu_2)(1 - \mu_2^2)(1 - \mu_1\mu_2)}\mu_2^{\,r}\right]\sigma_\epsilon^2. \tag{5.96}$$

This equation is in the form of $R(r) = B_1\,\mu_1^{\,r} + B_2\,\mu_2^{\,r}$.

There are a variety of cases in which, depending on the sign of μ_1, μ_2, the autocovariance function appears different in its tendency.

1. When $a_2 \le a_1^2/4$ (subzone [I] in Fig. 5.16), μ_1, μ_2 are real, and

   a. if $a_1 < 0$, $a_2 > 0$ (region ① in Fig. 5.16), $\mu_1 > 0$, $\mu_2 > 0$
   and $R(r)$ stays positive as in Fig. 5.17(A),

   b. if $a_1 < 0$, $a_2 < 0$ (region ② in Fig. 5.16), then μ_1, μ_2 have opposite signs,

c. if $a_1 > 0$, $a_2 > 0$ (region ③ in Fig. 5.16), then $\mu_1 < 0$, $\mu_2 < 0$ and in this case $R(r)$ alternate signs by r as in Fig. 5.17(B), and

d. if $a_1 > 0$, $a_2 < 0$ (region ④ in Fig. 5.16), then μ_1, μ_2 have opposite signs.

Therefore, for a and c, the autocovariance function shows the patterns (A) and (B) in Fig. 5.17, respectively. For b and d, the shape will be (A) or (B), depending on the size of μ_1, μ_2.

$R(\gamma)$ of AR(2); $a_2 \geq \dfrac{a_1^2}{4}$

(A) : a, $(a_1 < 0, a_2 > 0)$ (B) : c, $(a_1 > 0, a_2 > 0)$
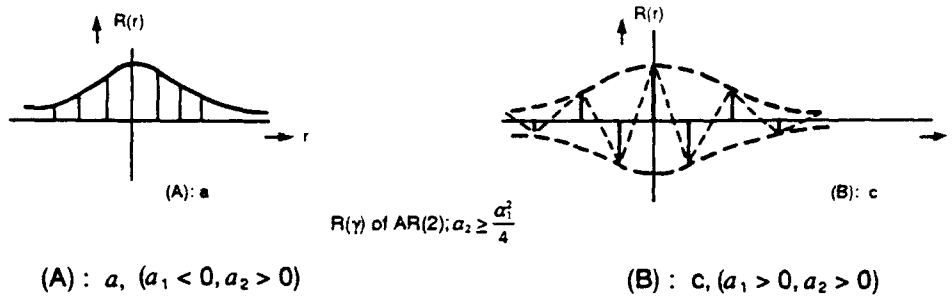
Fig. 5.17. $R(r)$ of AR(2); $a_2 \leq a_1^2/4$.

2. When $a_2 > a_1^2/4$, (subzone [II] in Fig. 5.16), μ_1, μ_2 are complex and conjugate to each other, and from Eqs. 5.67 and 5.75

$$\mu_1 \mu_2 = a_2, \qquad \mu_1 = \sqrt{a_2}\, e^{i\sigma} \qquad \mu_2 = \sqrt{a_2}\, e^{-i\sigma} \qquad (5.97)$$

and $-a_1 = \mu_1 + \mu_2$, which satisfies

$$-a_1 = 2\sqrt{a_2}\cos\sigma. \qquad (5.98)$$

Thus

$$\cos\sigma = -a_1/2\sqrt{a_2} \qquad (5.98')$$

and

$$\mu_1 - \mu_2 = 2\sqrt{a_2}\, i \sin\sigma. \qquad (5.99)$$

Using the relations of Eqs. 5.97 to 5.99 in Eq. 5.94 gives

$$R(r) = a_2^{r/2} \frac{\left\{ \sin(r+1)\,\sigma - a_2 \sin(r-1)\sigma \right\}}{(1 + a_2)\sin\sigma} \sigma_x^2.$$

Here again setting

$$\tan\theta = \left(\frac{1 + a_2}{1 - a_2} \right) \tan\sigma, \qquad (5.100)$$

gives

$$R(r) = a_2^{r/2} \left\{ \frac{\sin(r\sigma + \theta)}{\sin\theta} \right\} \sigma_x^2. \tag{5.101}$$

Equation 5.101 shows that $R(r)$ has the form of a damping periodic function with period $2\pi/\sigma$ and damping a_2.

From Eq. 5.98'

$$\sigma = \cos^{-1}\left(-a_1/2\sqrt{a_2}\right) \tag{5.98''}$$

so a_2 determines the damping and $a_1/\sqrt{a_2}$ determines the period (see Fig. 5.18).
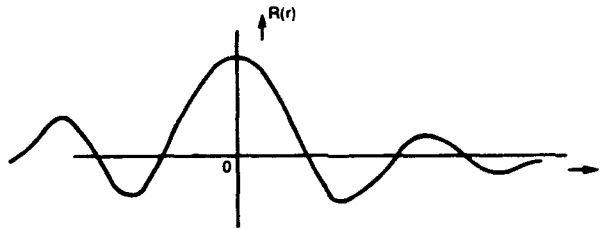
Fig. 5.18. $R(r)$ of AR(2); $a_2 > a_1^2/4$.

As an extreme case of stationality, when $a_2 = 1$, from Eq. 5.100 $\theta = \pi/2$. Therefore from Eq. 5.101

$$R(r) \rightarrow \cos r\sigma \quad \sigma_x^2. \tag{5.102}$$

This is an undamped cosine curve and shows that $R(r)$ does not decay with increasing r but continues to oscillate in this case.

5.2.3.5 Estimation of a_1, a_2. From Eqs. 5.83 and 5.84

$$\begin{cases} a_1 R(0) + a_2 R(1) = -R(1) \\ a_1 R(1) + a_2 R(0) = -R(2) \end{cases}$$

Thus
$$\hat{a}_1 = \frac{- \begin{vmatrix} R(1) & R(1) \\ R(2) & R(0) \end{vmatrix}}{\begin{vmatrix} R(0) & R(1) \\ R(1) & R(0) \end{vmatrix}}, \qquad \hat{a}_2 = \frac{- \begin{vmatrix} R(0) & R(1) \\ R(1) & R(2) \end{vmatrix}}{\begin{vmatrix} R(0) & R(1) \\ R(1) & R(0) \end{vmatrix}}, \tag{5.103}$$

or

$$\hat{a}_1 = \frac{R(1)\,R(2) - R(0)\,R(1)}{R^2(0) - R^2(1)},$$

$$\hat{a}_2 = \frac{R^2(1) - R(0)R(2)}{R^2(0) - R^2(1)}. \tag{5.103'}$$

By solving the linear equation on $\hat{a}_1$, $\hat{a}_2$, we can easily determine the $\hat{a}_1$, $\hat{a}_2$ from the autocorrelation $R(0)$, $R(1)$, and $R(2)$. Equations 5.83 and 5.84 can be written in vector form as

$$R_2 \cdot \hat{a} = -r, \tag{5.104}$$

where

$$R_2 = \begin{bmatrix} R(0) & R(0) \\ R(1) & R(0) \end{bmatrix} \tag{5.105}$$

$$a = [\hat{a}_1, \hat{a}_2]', \qquad r = [R(1), R(2)]'. \tag{5.106}$$

therefore

$$\hat{a} = -\frac{r}{R_2}. \tag{5.107}$$

Thus $\hat{a} = [\hat{a}_1, \hat{a}_2]'$ can be determined from $r = [R(1), R(2)]'$ and

$$R_2 = \begin{bmatrix} R(0) & R(0) \\ R(1) & R(0) \end{bmatrix},$$

namely, from $R(0), R(1)$ and $R(2)$.

After $\hat{a}_1$, $\hat{a}_2$ are obtained, σ_ϵ^2 can be estimated from Eq. 5.82,

$$\hat{\sigma}_\epsilon^2 = R(0) + \hat{a}_1 R(1) - \hat{a}_2 R(2). \tag{5.108}$$

5.2.3.6 Spectrum of AR(2). From Eq. 5.59 for AR(2)

$$X_t + a_1 X_{t-1} + a_2 X_{t-2} = \epsilon_t,$$

$$X_{t-r} + a_1 X_{t-r-1} + a_2 X_{t-r-2} = \epsilon_{t-r}. \tag{5.109}$$

Taking the product of both sides of these two equations, respectively, and then taking expectation of each term,

$$E[X_t \cdot X_{t-r}] + a_1^2\, E[X_{t-1} \cdot X_{t-r-1}] + a_2^2\, E[X_{t-2} \cdot X_{t-r-2}]$$

$$+ a_1\, E[X_t \cdot X_{t-r-1}] + a_1 a_2\, E[X_{t-1} \cdot X_{t-r-2}] + a_2\, E[X_t\, X_{t-r-2}]$$

$$+ a_1\, E[X_{t-r}\, X_{t-1}] + a_1 a_2\, E[X_{t-r-1} X_{t-2}] + a_2\, E[X_{t-r} X_{t-2}] = E[\epsilon_t \cdot \epsilon_{t-r}]. \tag{5.110}$$

Therefore, for $r \neq 0$,

127

$$R_x(r)\left\{1 + a_1^2 + a_2^2\right\} + a_1[R_x(r+1) + R_x(r-1)] + a_1a_2[R_x(r+1) + R_x(r-1)]$$
$$+ a_2[R_x(r+2) + R_x(r-2)] = R_\epsilon \ (r) \tag{5.110'}$$

According to the relation between autocovariance and the spectrum,

$$\frac{-1}{2\pi}\sum_{-\pi}^{\pi} R_x(r \mp 1)e^{-i\omega r} = \frac{1}{2\pi}\sum_{-\pi}^{\pi} R_x(r \mp 1)e^{-i\omega(r \mp 1)} \cdot e^{\mp i\omega} \tag{5.111}$$
$$= s_x(\omega) \cdot e^{\mp i\omega}.$$

Then, transforming both sides of Eq. 5.110' by Fourier transformation and, taking into account Eq. 5.111,

$$s_x(\omega)\left\{1 + a_1^2 + a_2^2 + (a_1 + a_1a_2)(e^{-i\omega} + e^{i\omega}) + a_2(e^{-2i\omega} + e^{2i\omega})\right\}$$
$$= s_\epsilon(\omega) = \frac{1}{2\pi}\sigma_\epsilon^2, \tag{5.112}$$

$$s_x(\omega)\left|1 + a_1e^{-i\omega} + a_2e^{-2i\omega}\right|^2 = \frac{1}{2\pi}\sigma_\epsilon^2. \tag{5.112'}$$

Thus
$$s_x(\omega) = \frac{\sigma_\epsilon^2}{2\pi \left|1 + a_1e^{-i\omega} + a_2e^{-2i\omega}\right|^2}, \tag{5.113}$$

from the function $\alpha(Z)$ of Eq. 5.74

$$s_x(\omega) = \frac{\sigma_\epsilon^2}{2\pi \left|\alpha(e^{-i\omega})\right|^2}, \tag{5.114}$$

or

$$s_x(\omega) = \frac{\sigma_\epsilon^2}{2\pi \left\{(1 + a_1^2a_2^2 + 2(a_1 + a_1a_2)\cos\omega + 2a_2\cos 2\omega)\right\}}$$
$$= \frac{\sigma_\epsilon^2}{2\pi \ (1-a_2)^2 + a_1^2 + 2a_1(1+a_2)\cos\omega + 4a_2\cos\omega}. \tag{5.115}$$

Substituting σ_x^2 for σ_ϵ^2 in Eq. 5.88 gives

$$S_x(\omega) = \frac{(1-a_2)[(1+a_2)^2 - a_1^2]\sigma_x^2}{2\pi(1+a_2)\left\{(1-a_2)^2 + a_1^2 + 2a_1(1+a_2)\cos\omega + 4a_2\cos^2\omega\right\}}. \tag{5.115'}$$

From this expression, and setting $\dfrac{ds(\omega)}{d\omega} = 0$,

128

when $a_2 > 0$ and $\left| \dfrac{a_1(1 + a_2)}{4a_2} \right| < 1$, the spectrum has a peak at

$$\omega_0 = \cos^{-1}\left\{ -\frac{a_1(1 + a_2)}{4a_2} \right\}. \qquad (5.116)$$

When $a_2 < 0$ and $\left| \dfrac{a_1(1 + a_2)}{4a_2} \right| < 1$, the spectrum has a trough at the same ω_0 as shown in Fig. 5.19.
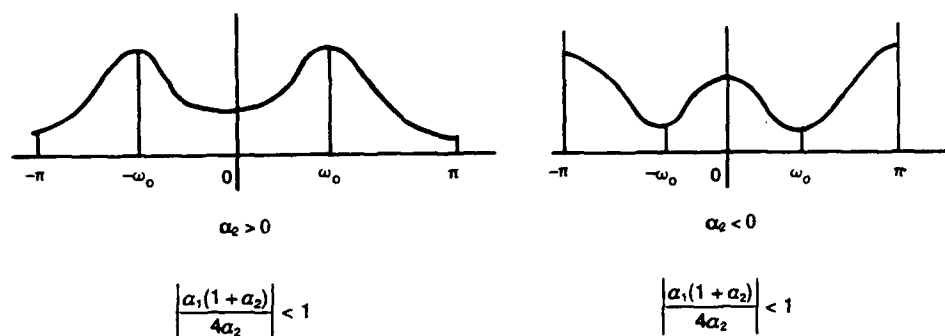
Fig. 5.19. $s(\omega)$ of AR(2).

5.2.3.7 Example of AR(2). In Fig. 5.20, an example of the AR(2) process for $a_1 = -0.5$, $a_2 = 0.8$, $\sigma_\epsilon^2 = 1.0$, expressed as $X_t - 0.5\,X_{t-1} + 0.8\,X_{t-2} = \epsilon_t$, was generated over $t = 1$ to 600, using the same pure random process ϵ_t as was generated in Fig. 5.4. A part of this process ($t = 100$ to 250) is also shown with the time axis extended. Its readings are listed in Appendix A1 as Table A1.3; pp. 251, 254, and 255.

129
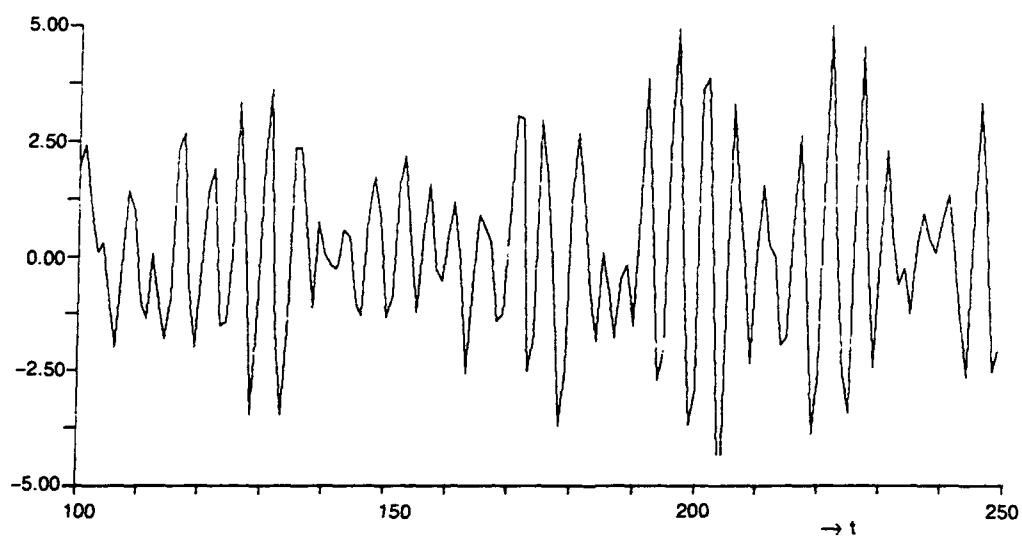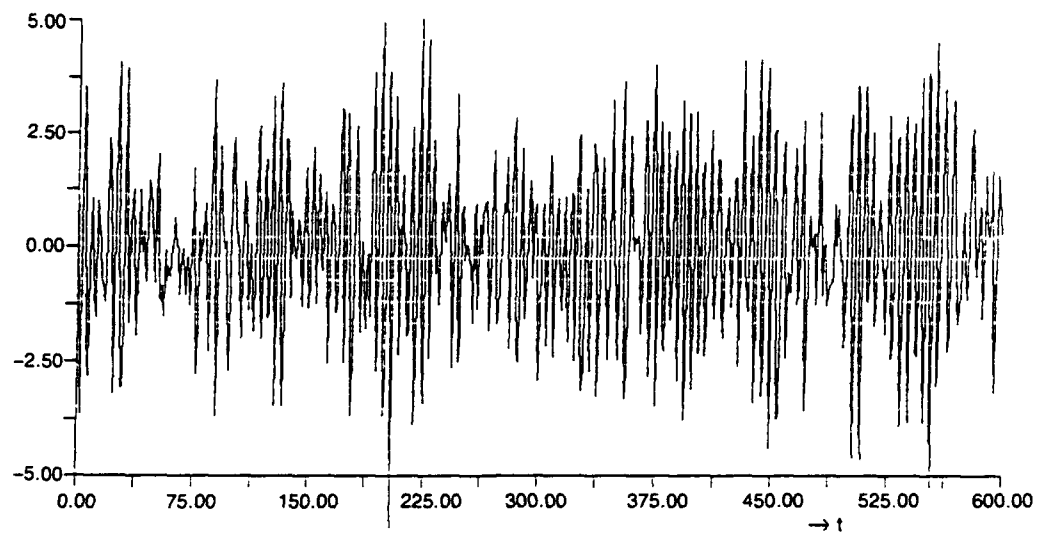
Fig. 5.20. Simulated AR(2) process $X_t - 0.5\ X_{t-1} + 0.8\ X_{t-2} = \epsilon_t,\quad \epsilon_t: N[0,1]$.

130

Figure 5.21a shows the theoretical autocorrelation coefficient $\rho(r) = R(r)/R(0)$ of this generated AR(2) process, calculated by Eq. 5.90, using the values of coefficients $a_1 = -0.5$, $a_2 = 0.8$, and the variance $\sigma_\epsilon^2 = 1.0$. Part b of the same figure shows the estimated $\hat{\varrho}(r) = \hat{R}(r)/\hat{R}(0)$, actually calculated from the generated process. An AR(n) model was fitted and its order was searched by AIC criteria and found to be $n = 2$. Then parameters were estimated by the method described in this section by Eqs. 5.103' and 5.108. The results were

$$\hat{a}_1 = -0.54156, \quad \hat{a}_2 = 0.81838, \quad \text{and} \, \hat{\sigma}_\epsilon^2 = 1.04702,$$

which are close to the values actually used in generating the process. The autocorrelation coefficients were estimated from Eq. 5.90 using these values just as were the theoretical values. The results were quite similar and very close to the theoretical values in Fig. 5.21a, so again the drawings were omitted.
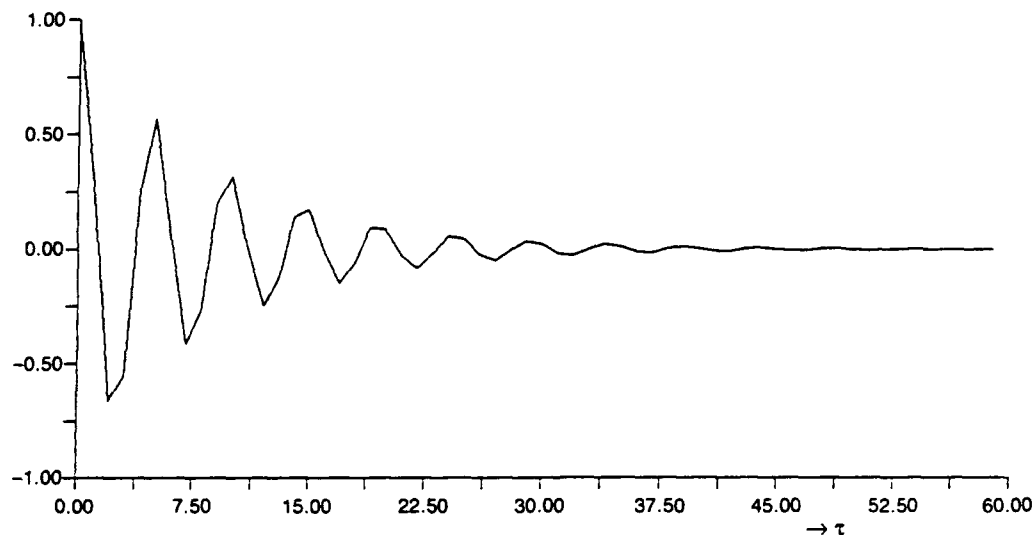
Fig. 5.21a. Theoretical.

Fig. 5.21. Autocorrelation coefficient for AR(2) process
$X_t - 0.5 \, X_{t-1} + 0.8 \, X_{t-2} = \epsilon_t, \quad \epsilon_t : \mathrm{N}[0, 1]$.
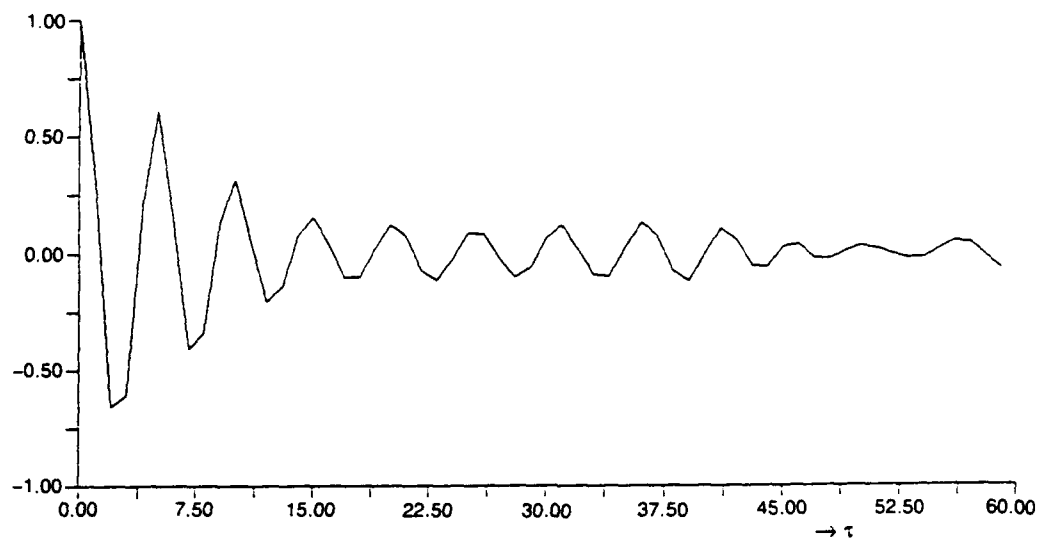
Fig. 5.21b. Estimated.

Fig. 5.21. (Continued)

Figure 5.22 shows the spectra, Fig. 5.22a the theoretical one given by Eq. 5.115, Fig. 5.22b the estimated one from the fitted model AR(2), and Fig. 5.22c the one estimated by the nonparametric method from the generated process (Fig. 5.20), using the same maximum lag number (60) and Hanning window as for Fig. 5.5c and Fig. 5.12c. The a and b spectra look very similar to each other and in this case c also looks similar to a and b. In Fig. 5.22c, the 90% level of confidence interval of this estimate based on the χ^2-distribution of the equivalent degree of freedom (here approximately equal to 27) as is explained in Section 2.5.5 is shown by vertical lines for reference.
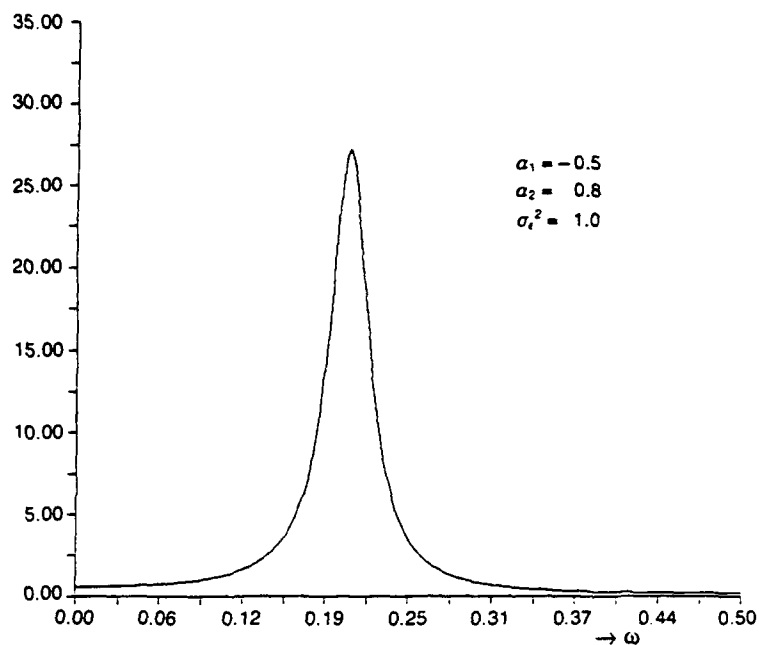
Fig. 5.22a. Theoretical AR(2).
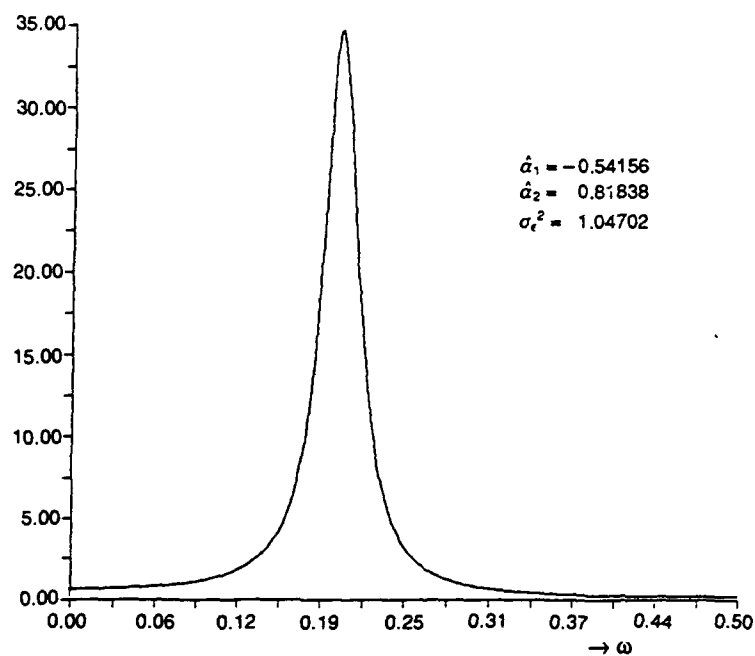
Fig. 5.22b. Estimated by AR model fitting as optimum AR(2).

Fig. 5.22. Spectrum for AR(2) process $X_t - 0.5\ X_{t-1} + 0.8\ X_{t-2} = \epsilon_t$, $\quad \epsilon_t$: N[0, 1].
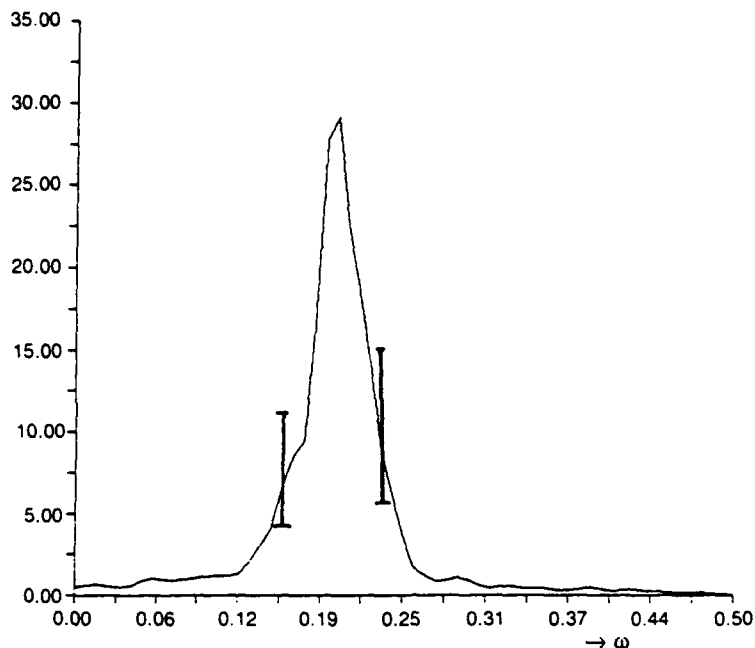
Fig. 5.22c. Estimated by nonparametric method.

Fig. 5.22. (Continued)

5.2.4 Second Order Autoregressive First Order Moving Average Process, ARMA(2.1)

More generally for AR(2), when the residual series ϵ_t' of X_t, obtained by subtracting the part which is linearly dependent on X_{t-1},

$$\epsilon_t' = X_t - a_1' X_{t-1} \tag{5.117}$$

was correlated not only with X_{t-2} as for AR(2) but also with ϵ_{t-1} as shown in Fig. 5.23.

(a) ϵ_t' vs. X_{t-2}.   (b) ϵ_t' vs. ϵ_{t-1}
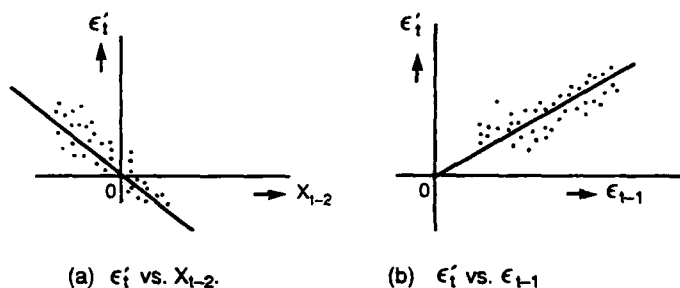
Fig. 5.23. Characters of ϵ_t' for ARMA(2.1).

Then

$$\epsilon_t' = a_2' X_{t-2} + b_1 \epsilon_{t-1} + \epsilon_t . \tag{5.118}$$

134

ϵ_t is now a purely uncorrelated random process,

$$E[\epsilon_t \cdot \epsilon_{t-r}] = \begin{cases} \sigma_\epsilon^2 & r = 0 \\ 0 & r \neq 0 \end{cases}. \tag{5.119}$$

From Eqs. 5.117 and 5.118

$$X_t - a_1' X_{t-1} - a_2' X_{t-2} = b_1 \epsilon_{t-1} + \epsilon_t$$

this equation is expressed generally, changing $-a_1'$ to a_1 and $-a_2'$ to a_2, as

$$X_t + a_1 X_{t-1} + a_2 X_{t-2} = b_1 \epsilon_{t-1} + \epsilon_t. \tag{5.120}$$

When the process X_t is expressed by Eq. 5.120, where a_1, a_2, and b_1 are constants and ϵ_t is a random variable, this process X_t is called a second order autoregressive first order moving average process, ARMA(2.1).

Equation 5.120 can be written as

$$\epsilon_t = X_t + a_1 X_{t-1} + a_2 X_{t-2} - b_1 \epsilon_{t-1}. \tag{5.120'}$$

This expression shows that, in order to compute the present value of ϵ_t, we need ϵ_{t-1}, and when we compute ϵ_t recursively, we need the preceding values of ϵ_{t-1} starting from the beginning ϵ_{t-2}, $\epsilon_{t-3} \cdots$. This situation is different from AR(1) and AR(2) as shown by Eq. 5.7 and Eq. 5.59 for which we do not need any preceding values of ϵ_{t-1}. This makes the estimation of the ARMA(2.1) model much more difficult than that of the AR(1) and AR(2) models. This difficulty can also be shown as follows.

From Eq. 5.120'

$$\epsilon_{t-1} = X_{t-1} + a_1 X_{t-2} + a_2 X_{t-3} - b_1 \epsilon_{t-2}. \tag{5.121}$$

Inserting this into Eq. 5.120 gives

$$X_t = -a_1 X_{t-1} - a_2 X_{t-2} + b_1 \left\{ X_{t-1} + a_1 X_{t-2} + a_2 X_{t-3} - b_1 \epsilon_{t-2} \right\} + \epsilon_t$$

$$X_t = (-a_1 + b_1) X_{t-1} + (-a_2 + a_1 b_1) X_{t-2} + a_2 b_1 X_{t-3} - b_1^2 \epsilon_{t-2} + \epsilon_t. \tag{5.122}$$

Here ϵ_{t-2} is still included, so it should be expressed in the same way as Eq. 5.121 by X_{t-2}, $X_{t-3} \cdots$ and ϵ_{t-3}, and so on. However, even with Eq. 5.122, when the dependence of X_t is expressed in terms of past X_t, the equation is nonlinear in the unknown parameters a_1, a_2, and b_1. As a result, the regression becomes nonlinear and requires a nonlinear least squares method for estimation, which is different from the case of AR(1), AR(2) or the general AR model as will be shown in Section 5.4, where all coefficients can be obtained by the linear least squares method. The estimation of a_1, a_2, b_1 for ARMA(2.1) will be shown later.

5.2.4.1 Green's Function for ARMA(2.1). Equation 5.120 is expressed, using the backward shift operator B, as

$$(1 + a_1 B + a_2 B^2) X_t = (1 + b_1 B) \epsilon_t. \tag{5.123}$$

Then

$$X_t = \frac{(1 + b_1 B)}{(1 + a_1 B + a_2 B^2)} \epsilon_t$$

$$= \frac{(1 + b_1 B)}{(1 - \mu_1 B)(1 - \mu_2 B)} \epsilon_t$$

$$= \left\{ \frac{\left(1 + \frac{b_1}{\mu_1}\right)}{\left(1 - \frac{\mu_2}{\mu_1}\right)} \frac{1}{(1 - \mu_1 B)} + \frac{\left(1 + \frac{b_1}{\mu_2}\right)}{\left(1 - \frac{\mu_1}{\mu_2}\right)} \frac{1}{1 - \mu_2 B} \right\} \epsilon_t$$

$$= \sum_{j=0}^{\infty} \left\{ \left(\frac{\mu_1 + b_1}{\mu_1 - \mu_2}\right) \mu_1^j + \left(\frac{\mu_2 + b_1}{\mu_2 - \mu_1}\right) \mu_2^j \right\} \epsilon_{t-j}$$

$$= \sum_{j=0}^{\infty} G_j \, \epsilon_{t-j}. \qquad (5.124)$$

Green's function is

$$G_j = \left(\frac{\mu_1 + b_1}{\mu_1 - \mu_2}\right) \mu_1^j + \left(\frac{\mu_2 + b_1}{\mu_2 - \mu_1}\right) \mu_2^j. \qquad (5.125)$$

When $b_1 = 0$, then Green's function will be that of the AR(2) already given as Eq. 5.70. Green's function can also be easily derived as a solution of the homogeneous equation, Eq. 5.120,

$$(1 + a_1 B + a_2 B^2) X_t = 0 \qquad (5.126)$$

with the initial conditions as follows.

Substituting

$$X_t = \sum_{j=0}^{\infty} G_j \, \epsilon_{t-j} = \left[\sum_{j=0}^{\infty} G_j \, B^j \right] \epsilon_t$$

into Eq. 5.123 gives

$$(1 + a_1 B + a_2 B^2) \left[\sum_{j=0}^{\infty} G_j \, B^j \right] \epsilon_t = (1 + b_1 B) \epsilon_t$$

$$(1 + a_1 B + a_2 B^2)(G_0 + G_1 B + G_2 B^2 + G_3 B^3 + \cdots) \epsilon_t = (1 + b_1 B) \epsilon_t. \qquad (5.127)$$

Comparing the coefficients of B on both sides of Eq. 5.127 shows

$$G_0 = 1 \qquad\qquad G_0 = 1 \tag{5.128}$$

$$G_0 a_1 + G_1 = b_1 \qquad \text{or} \qquad G_1 = b_1 - a_1 \tag{5.129}$$

$$G_0 a_2 + a_1 G_1 + G_2 = 0 \qquad G_2 = -a_1(b_1 - a_1) - a_2 \tag{5.130}$$

$$\cdots \qquad\qquad G_j = -a_1 G_{j-1} - a_2 G_{j-2}, \quad j \geq 2. \tag{5.131}$$

Eqs. 5.128 – 5.130 are the initial conditions.

The solution of the homogeneous Eq. 5.126 is the solution of an nth order differential equation, that is, a linear combination of exponential functions, μ^j, μ being the characteristic roots, i.e., the roots of the characteristic equation $f(Z)$. Equation 5.73 in this case is of second order.

Therefore for this case,

$$G_j = g_1 \, \mu_1^j + g_2 \, \mu_2^j. \tag{5.132}$$

Using the initial conditions given by Eqs. 5.128 and 5.129,

$$g_1 + g_2 = 1 \tag{5.133}$$

$$g_1 \mu_1 + g_2 \mu_2 = \mu_1 + \mu_2 + b_1, \tag{5.134}$$

where

$$(\mu_1 + \mu_2 = -a_1).$$

Solving gives

$$g_1 = \frac{\mu_1 + b_1}{\mu_1 - \mu_2} \tag{5.135}$$

$$g_2 = \frac{\mu_2 + b_1}{\mu_2 - \mu_1}. \tag{5.136}$$

Inserting these values into Eq. 5.132, gives the same expression of Green's function Eq. 5.125 for ARMA(2.1). As will be discussed in some detail in the next section, in order that the original process X_t, which can be considered as an output of the input ϵ_t, be stationary, $\mu_1 \, \mu_2$ should be less than 1 in absolute value, $|\mu_1| < 1$, $|\mu_2| < 1$, where μ_1, μ_2 are the roots of the characteristic Eq. 5.73.

$$f(Z) = Z^2 + a_1 Z + a_2 = 0$$

$$\mu_1, \ \mu_2 = \frac{-a_1}{2} \pm \frac{\sqrt{a_1^2 - 4a_2}}{2} \tag{5.137}$$

for $\mu_1 + \mu_2 = -a_1$ and $\mu_1 \mu_2 = a_2$. When $a_1^2 - 4a_2 < 0$, then μ_1, μ_2 are complex and conjugate to each other as

$$\mu_1, \mu_2 = \frac{-a_1}{2} \pm i \frac{\sqrt{4a_2 - a_1^2}}{2}. \tag{5.137'}$$

When this was expressed as

$$= \gamma e^{\pm i\omega}, \tag{5.138}$$

$$\gamma = |\mu_1| = |\mu_2| = \left\{ \left(\frac{a_1}{2}\right)^2 + \left[\frac{\sqrt{4a_2 - a_1^2}}{2}\right]^2 \right\}^{1/2} = \sqrt{a_2} \tag{5.139}$$

$$\omega = \tan^{-1} \frac{\sqrt{4a_2 - a_1}}{-a_1} = \cos^{-1} \frac{-a_1}{2\sqrt{a_2}} = \cos^{-1} \frac{\mu_1 + \mu_2}{\sqrt{\mu_1 \mu_2}}. \tag{5.140}$$

Then inserting Eq. 5.138 into Eq. 5.125 gives

$$G_j = \left(\frac{\mu_1 + b_1}{\mu_1 - \mu_2}\right)\left(\gamma \ e^{i\omega}\right)^j + \left(\frac{\mu_2 + b_1}{\mu_2 - \mu_1}\right)\left(\gamma \ e^{-i\omega}\right)^j$$

$$= \frac{\gamma^j}{(\mu_1 - \mu_2)} \left\{ (\mu_1 + b_1)e^{j(i\omega)} - (\mu_2 + b_1)e^{-j(i\omega)} \right\}$$

$$= \gamma^j \left\{ \cos j\omega - \frac{a_1 - 2b_1}{\sqrt{4a_2 - a_1^2}} \sin \ j\omega \right\}. \tag{5.141}$$

Therefore, if putting

$$\frac{-a_1 - 2b_1}{\sqrt{4a_2 - a_1^2}} = U, \tag{5.142}$$

$$G_j = \gamma^j \sqrt{1 + U^2} \cos(j\omega + \delta) \tag{5.143}$$

where

$$\delta = \tan^{-1} \left\{ \frac{a_1 - 2b_1}{\sqrt{4a_2 - a_1^2}} \right\}. \tag{5.144}$$

Now let $\sqrt{1 + U^2} = V$ again,

$$G_j = \gamma^j V \cos(j\omega + \delta)$$

$$= V e^{ji\omega} \cdot e^{i\delta} \gamma^j + V e^{ji\omega} e^{-i\delta} \gamma^j$$

$$= g_1 \gamma^j + g_2 \gamma^j. \tag{5.145}$$

Then

$$g_1, g_2 = V e^{\pm ji\omega} e^{\pm i\delta} = |g| e^{\pm i(j\omega + \delta)}. \tag{5.146}$$

138

Therefore
$$|g| = V,$$ (5.147)

$$\text{Arg}[g] = j\omega + \delta.$$ (5.148)

From Eq. 5.143 G_j can be expressed as a damping cosine curve with damping $\gamma = \sqrt{a_2}$ determined by a_2 and the period by

$$\frac{2\pi}{\omega} = \frac{2\pi}{\cos^{-1}\dfrac{-a_1}{2\sqrt{a_2}}}.$$

After a_2 was fixed, period is decided by a_1 and phase that is δ different from that of μ_1, μ_2 by $\delta = \tan^{-1}\dfrac{a_1 - 2b_1}{\sqrt{4a_2 - a_1^2}}$, as is shown in Fig. 5.24.
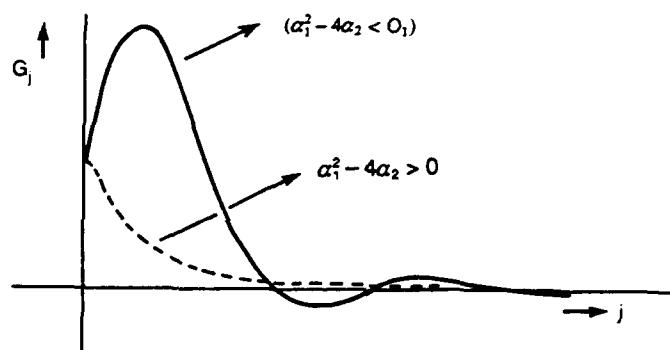
Fig. 5.24. G_j for ARMA(2.1).

Green's function and the autocovariance function are closely related as expected, because using Green's function,

$$R(r) = E[X_1\ X_{t-r}]$$

$$= E\left[\left(\sum_{i=0}^{\infty} G_i \epsilon_{t-i}\right)\left(\sum_{j=0}^{\infty} G_i \epsilon_{t-r-j}\right)\right]$$

$$= \sigma_\epsilon^2 \sum_{j=0}^{\infty} G_j\ G_{j+r}.$$ (5.149)

5.2.4.2 Inverse Function of ARMA(2.1). In Eq. 5.123

$$(1 + a_1 B + a_2 B^2)X_t = (1 + b_1 B)\epsilon_t.$$

If we express ϵ_t by an inverse function as

$$\epsilon_t = \sum_{j=0}^{\infty} -I_j \, X_{t-j} = (-I_0 - I_1 B - I_2 B^2 - \cdots \; I_j \, B^j \cdots)X_t,$$

then Eq. 5.123 becomes $(1 + a_1 B + a_2 B^2)X_t = (1 + b_1 B)(-I_1 B - I_2 B^2 - \cdots I_j \, B^j \cdots)X_t$.

Comparing the coefficients of the powers of B gives

$$-I_0 = 1 \qquad\qquad\qquad (5.150)$$

$$a_1 = b_1 - I_1$$

$$a_2 = -b_1 I_1 - I_2$$

$$0 = -I_3 - b_1 I_2 \qquad\qquad\qquad (5.151)$$

$$0 = -I_j - b_1 I_{j-1}, j \geq 3$$

or

$$I_1 = b_1 - a_1$$

$$I_2 = -a_2 - b_1(b_1 - a_1) \qquad\qquad (5.151')$$

$$I_j = -b_1 I_{j-1}, j \geq 3.$$

The last equation of Eq. 5.151' is $(1 + b_1 B)\, I_j = 0$ for $j \geq 3$.

Therefore $\qquad\qquad\qquad I_j = -b_1 \, I_{j-1}. \qquad\qquad (5.152)$

This Eq. 5.152 is the recursive equation for I_j.

5.2.4.3 Stationality and Invertibility of ARMA(2.1). The stationality of ARMA(2.1) depends on the convergence of the free oscillation that comes from the complementary function or the solution of the homogeneous equation. The homogeneous equation of ARMA(2.1) is the same as the homogeneous equation of AR(2), Eq. 5.60, which is

$$X_t + a_1 X_{t-1} + a_2 X_{t-2} = 0.$$

Accordingly, the relations required of the coefficients a_1 and a_2 for the ARMA(2.1) process to be stationary are the same as for AR(2), as has already been shown in Section 5.2.3 and in Figs. 5.15 and 5.16.

On the other hand, the invertibility of ARMA(2.1) depends on the boundedness

of ϵ_t, $\epsilon_t = \sum_{j=0}^{\infty} -I_j \, \epsilon_{t-j}$, when $j \to \infty$ and from the relation derived as Eq. 5.152,

$I_j = -b_1 I_{j-1}$, $|b|$ should be less than 1. This requirement corresponds to the character required for a_1 of AR(1), $|a_1| < 1$, so that the process AR(1) is stationary when $G_j = a_1 G_{j-1}$.

5.2.4.4 Autocovariance Function for ARMA(2.1). From Eq. 5.120

$$X_t = -a_1 X_{t-1} - a_2 X_{t-2} + \epsilon_t + b_1 \epsilon_{t-1}.$$

Therefore, multiplying both sides by X_{t-r} and taking the expected values,

$$E[X_t \cdot X_{t-r}] = -a_1 E[X_{t-1} \cdot X_{t-r}] - a_2 \ E[\ X_{t-2} \cdot X_{t-r}]$$
$$+ E[\epsilon_t \cdot X_{t-r}] + b_1 E[\epsilon_{t-1} X_{t-r}]. \tag{5.153}$$

Another way, by Green's function,

$$X_t = \sum_{j=0}^{\infty} G_j \ \epsilon_{t-j} = G_0 \ \epsilon_t + G_1 \ \epsilon_{t-1} + G_2 \ \epsilon_{t-2} + \cdots G_j \ \epsilon_{t-j} + \cdots$$

where G_j is expressed by Eqs. 5.128 to 5.131. Accordingly,

$$X_{t-r} = \quad G_0 \ \epsilon_{t-r} + G_1 \epsilon_{t-r-1} + G_2 \epsilon_{t-r-2} + \cdots G_j \ \epsilon_{t-r-j} + \cdots$$
$$= \epsilon_{t-r} + (b_1 - a_1)\epsilon_{t-r-1} + \left\{ -a_2 - a_1(b_1 - a_1) \right\} \ \epsilon_{t-r-2} + \cdots$$
$$+ \left\{ -a_2 G_{j-2} - a_1 G_{j-1} \right\} \ \epsilon_{t-r-j} + \cdots . \tag{5.154}$$

Using these relations from Eq. 5.153 gives

$$r = 0 \ \text{when} \ R(0) = -a_1 R(1) - a_2 R(2) + \sigma_\epsilon^2 + (b_1 - a_1) \ b_1 \sigma_\epsilon^2 \tag{5.155}$$

$$r = 1 \ \text{when} \ R(1) = -a_1 R(0) - a_2 R(1) + b_1 \sigma_\epsilon^2 \tag{5.156}$$

$$r \geq 2 \ \text{when} \ R(r) = -a_1 R(r-1) - a_2 R(r-2). \tag{5.157}$$

In order to express the values of $R(r)$ recursively, we have to solve for $R(0)$ and $R(1)$, using Eqs. 5.155 and 5.156 after substituting $R(2)$ from Eq. 5.157. Then Eqs. 5.155 and 5.156 will be

$$(1 - a_2^2) \ R(0) + a_1(1 - a_2)R(1) = (1 - a_1 b_1 + b_1^2) \ \sigma_\epsilon^2 \tag{5.158}$$

$$a_1 R(0) + (1 + a_2)R(1) = b_1 \sigma_\epsilon^2. \tag{5.159}$$

Therefore

$$R(0) = \frac{\begin{vmatrix} (1 - a_1 b_1 + b_1^2) & a_1(1 - a_2) \\ b_1 & (1 + a_2) \end{vmatrix}}{\begin{vmatrix} (1 - a_2^2) & a_1(1 - a_2) \\ a_1 & (1 + a_2) \end{vmatrix}} \ \sigma_\epsilon^2, \tag{5.160}$$

$$R(1) = \frac{\begin{vmatrix} (1 - a_2^2) & (1 - a_1 b_1 + b_1^2) \\ a_1 & b_1 \end{vmatrix}}{\begin{vmatrix} (1 - a_2^2) & a_1(1 - a_2) \\ a_1 & (1 + a_2) \end{vmatrix}} \ \sigma_\epsilon^2, \tag{5.161}$$

$$R(r) = -a_1 R(r-1) - a_2 R(r-2) \quad r \geq 2, \tag{5.162}$$

141

$$\varrho(0) = 1 \qquad (5.163)$$

$$\varrho(1) = \frac{\begin{vmatrix} (1 - a_2^2) & (1 - a_1 b_1 + b_1^2) \\ (a_1) & (B_1) \end{vmatrix}}{\begin{vmatrix} (1 - a_1 b_1 + b_1^2) & a_1(1 - a_2) \\ (b_1) & (1 + a_2) \end{vmatrix}} \qquad (5.164)$$

$$\varrho(r) = -a_1 \varrho(r - 1) - a_2 \varrho(r - 2) \qquad r \geq 2. \qquad (5.165)$$

These are the autocovariance functions of ARMA(2.1). As was done for AR(2) in Section 5.2.3, we can get the same results as the solution of the homogeneous equation because Eq. 5.157 is the homogeneous equation with the same coefficient as the homogeneous Eq. 5.126 or Eq. 5.60 of AR(2) expressed by Eq. 5.59.

Its solution is in the shape of

$$R(r) = B_1 \, \mu_1^r + B_2 \, \mu_2^r, \qquad (5.166)$$

μ_1, μ_2 being the roots of characteristic equation

$$f(Z) = Z^2 + a_1 Z + a_2 = 0 \qquad (5.167)$$

or

$$\mu_1 + \mu_2 = -a_1$$
$$\mu_1 \mu_2 = a_2.$$

B_1 and B_2 are constants and are determined by the boundary conditions

$$B_1 + B_2 = R(0)$$
$$B_1 \mu_1 + B_2 \mu_2 = R(1).$$

After algebraic manipulation,

$$B_1 = \sigma_\epsilon^2 g_1 \left\{ \frac{g_1}{(1 - \mu_1^2)} + \frac{g_2}{(1 - \mu_1 \mu_2)} \right\}$$

$$\qquad (5.167)$$

$$B_2 = \sigma_\epsilon^2 g_2 \left\{ \frac{g_2}{(1 - \mu_1^2)} + \frac{g_1}{(1 - \mu_1 \mu_2)} \right\}$$

or, using the relations of Eqs. 5.135 and 5.136,

$$B_1 = \sigma_\epsilon^2 \frac{(\mu_1 + b_1)}{(\mu_1 - \mu_2)^2} \left\{ \frac{(\mu_1 + b_1)}{(1 - \mu_1^2)} - \frac{\mu_2 + b_1}{1 - \mu_1 \mu_2} \right\} \qquad (5.168)$$

$$B_2 = \sigma_\epsilon^2 \frac{\mu_2 + b_1}{(\mu_1 - \mu_2)^2} \left\{ \frac{\mu_2 + b_1}{1 - \mu_2^2} - \frac{\mu_1 + b_1}{1 - \mu_1 \mu_2} \right\} \tag{5.169}$$

and

$$R(0) = \sigma_\epsilon^2 \left\{ \frac{g_1^2}{1 - \mu_1^2} + \frac{g_2^2}{1 - \mu_2^2} + \frac{2 g_1 \, g_2}{1 - \mu_1 \mu_2} \right\}$$

$$= \sigma_\epsilon^2 \frac{1}{(\mu_1 - \mu_2)^2} \left\{ \frac{(\mu_1 + b_1)^2}{(1 - \mu_1^2)} + \frac{(\mu_2 + b_1^2)}{(1 - \mu_1^2)} + \frac{2(\mu_1 + b_1)(\mu_2 + b_1)}{1 - \mu_1 \mu_2} \right\} \tag{5.170}$$

$$R(1) = \sigma_\epsilon^2 \frac{\mu_1}{(\mu_1 - \mu_2)^2} \left\{ \frac{(\mu_1 + b_1)^2}{(1 - \mu_1^2)} - \frac{(\mu_1 + b_1)(\mu_2 + b_1)}{1 - \mu_1 \mu_2} \right\}$$

$$+ \sigma_\epsilon^2 \frac{\mu_2}{(\mu_1 - \mu_2)^2} \left\{ \frac{(\mu_2 + b_1)^2}{(1 - \mu_2^2)} - \frac{(\mu_1 + b_1)(\mu_2 + b_1)}{1 - \mu_1 \mu_2} \right\}. \tag{5.171}$$

Using the B_1, B_2 in Eq. 5.166, we get the general expression for $R(r)$.

The autocovariance function can be expressed using Green's function as Eq. 5.149. Then, starting from the expression of Green's function

$$G_j = g_1 \, \mu_1^j + g_2 \, \mu_2^j,$$

the same results can be derived for $R(r)$, although the manipulations will not be shown here.

5.2.4.5 Estimations of a_1, a_2, b_1, and σ_ϵ^2 of ARMA(2.1). From Eq. 5.157

$$R(r) = -a_1 R(r-1) - a_2 R(r-2) \qquad r \geq 2.$$

Therefore, for estimation, with the sample values of autocovariances,

$$\hat{R}(2) = -\hat{a}_1 \hat{R}(1) - \hat{a}_2 \hat{R}(0) \tag{5.172}$$

$$\hat{R}(3) = -\hat{a}_1 \hat{R}(2) - \hat{a}_2 \hat{R}(1). \tag{5.173}$$

Solving these linear equations gives

$$\hat{a}_1 = \frac{\begin{vmatrix} \hat{R}(2) & -\hat{R}(0) \\ \hat{R}(3) & -\hat{R}(1) \end{vmatrix}}{\begin{vmatrix} -\hat{R}(1) & -\hat{R}(0) \\ -\hat{R}(2) & -\hat{R}(1) \end{vmatrix}} = \frac{\hat{R}(3)\hat{R}(0) - \hat{R}(1)\hat{R}(2)}{\hat{R}^2(1) - \hat{R}(0)\hat{R}(2)} = \frac{\hat{\varrho}(3) - \hat{\varrho}(1)\hat{\varrho}(2)}{\hat{\varrho}^2(1) - \hat{\varrho}(2)} \qquad (5.174)$$

$$\hat{a}_2 = \frac{\begin{vmatrix} -\hat{R}(1) & \hat{R}(2) \\ -\hat{R}(2) & \hat{R}(3) \end{vmatrix}}{\begin{vmatrix} -\hat{R}(1) & -\hat{R}(0) \\ -\hat{R}(2) & -\hat{R}(1) \end{vmatrix}} = \frac{\hat{R}^2(2) - \hat{R}(1)\hat{R}(3)}{\hat{R}^2(1) - \hat{R}(0)\hat{R}(2)} = \frac{\hat{\varrho}^2(2) - \hat{\varrho}(1)\hat{\varrho}(3)}{\hat{\varrho}^2(1) - \hat{\varrho}(2)}. \qquad (5.175)$$

After $\hat{a}_1$ and $\hat{a}_2$ have been determined $\hat{b}_1$ and $\hat{\sigma}_\epsilon^2$ can be obtained by solving Eqs. 5.155 and 5.156. From them, Pandit and Wu[36] showed that b_1 can be obtained as the solution of a quadratic equation

$$b_1^2 + Cb_1 + 1 = 0 \qquad (5.176)$$

where

$$C = -a_1 + \frac{1 + \hat{a}_1\hat{\varrho}_1 + \hat{a}_2\hat{\varrho}_2}{-\hat{a}_1 - (\hat{a}_2 - 1)\hat{\varrho}_1}, \qquad (5.177)$$

although this is quadratic in terms of b_1 and is not a linear relation.

5.2.4.6 Spectrum of ARMA(2.1). The expression of ARMA(2.1) is, by Eq. 5.120,

$$X_t + a_1 X_{t-1} + a_2 X_{t-2} = \epsilon_t + b_1 \epsilon_{t-1}$$

or, using the backward shift operator B, by Eq. 5.123,

$$\alpha(B)X_t = \beta(B)\epsilon_t \qquad (5.120')$$

$$\begin{cases} \alpha(Z) = 1 + a_1 Z + a_2 Z \\ \beta(Z) = 1 + b_1 Z. \end{cases}$$

Therefore

$$X_{t-r} + a_1 X_{t-r-1} + a_2 X_{t-r-2} = \epsilon_{t-r} + b_1 \epsilon_{t-r-1}. \qquad (5.178)$$

Taking the product of Eqs. 5.120 and 5.178 and then taking expected values of each term gives

144

$$E[X_t \cdot X_{t-r}] + a_1^2 E[X_{t-1} \cdot X_{t-r-1}] + a_2^2 E[X_{t-2} \cdot X_{t-r-2}]$$
$$+ a_1 E[X_t \cdot X_{t-r-1}] + a_1 a_2 E[X_{t-1} X_{t-r-2}] + a_2 [X_t \cdot X_{t-r-2}]$$
$$+ a_1 E[X_{t-r} X_{t-1}] + a_1 a_2 E[X_{t-r-1} \cdot X_{t-2}] + a_2 E[X_{t-r} \cdot X_{t-2}]$$
$$= E[\epsilon_t \cdot \epsilon_{t-r}] + b_1^2 E[\epsilon_{t-1} \cdot \epsilon_{t-r-1}] + b_1 E[\epsilon_{t-r-1} \cdot \epsilon_t]$$
$$+ b_1 E[\epsilon_{t-1} \cdot \epsilon_{t-r}],$$
$$R_x(r)\{1 + a_1^2 + a_2^2\} + a_1[R_x(r+1) + R_x(r-1)] + a_1 a_2[R_x(r+1) + R_x(r-1)]$$
$$+ a_2[R_x(r+2) + R_x(r-2)]$$
$$= R_\epsilon(r)\{1 + b_1^2\} + b_1[R_\epsilon(r+1) + R_\epsilon(r-1)]. \qquad (5.179)$$

Here we use the relation shown by Eq. 5.111

$$\frac{1}{2\pi}\sum_{-\pi}^{\pi} R(r \mp 1)e^{-i\omega r} = \frac{1}{2\pi}\sum_{-\pi}^{\pi} R(r \mp 1)e^{-i\omega(r \mp 1)}e^{\mp i\omega}$$

$$= s(\omega) \cdot e^{\mp i\omega}.$$

Taking the Fourier transform of both sides of Eq. 5.179 gives

$$s_x(\omega)\left\{1 + a_1^2 + a_2^2 + (a_1 + a_1 a_2)(e^{-i\omega} + e^{i\omega}) + a_2(e^{-2i\omega} + e^{2i\omega})\right\}$$
$$= s_\epsilon(\omega)\left\{1 + b_1^2 + b_1(e^{i\omega} + e^{-i\omega})\right\}$$
$$= \frac{1}{2\pi}\sigma_\epsilon^2\left\{1 + b_1^2 + b_1(e^{i\omega} + e^{-i\omega})\right\}, \qquad (5.180)$$

$$s_x(\omega)\left|1 + a_1 e^{-i\omega} + a_2 e^{-2\omega}\right|^2 = \frac{1}{2\pi}\sigma_\epsilon^2\left|1 + b_1 e^{-i\omega}\right|^2. \qquad (5.181)$$

Therefore
$$s_x(\omega) = \frac{\sigma_\epsilon^2 \left|\beta(e^{-i\omega})\right|^2}{2\pi \left|\alpha(e^{-i\omega})\right|^2} \qquad (5.182)$$

$$= \frac{\sigma_\epsilon^2}{2\pi} \frac{\left|1 + b_1 e^{-i\omega}\right|^2}{\left|1 + a_1 e^{-i\omega} + a_2 e^{-2i\omega}\right|^2} \qquad (5.182')$$

$$= \frac{\sigma_\epsilon^2}{2\pi} \frac{\left\{1 + b_1^2 + 2b_1(e^{-i\omega} + e^{i\omega})\right\}}{\left\{1 + a_1^2 + a_2^2 + (a_1 + a_1 a_2)(e^{-i\omega} + e^{i\omega}) + a_2(e^{-2i\omega} + e^{2i\omega})\right\}}$$

$$= \frac{\sigma_\epsilon^2}{2\pi} \frac{1 + b_1^2 + 2b_1 \cos\omega}{[1 + a_1^2 + a_2^2 + 2a_1(1 + a_2)\cos\omega + 2a_2 \cos 2\omega]}. \qquad (5.182'')$$

145

Here Δt is assumed to be 1, as was mentioned at the beginning of Part II. As a result, $S_x(\omega)$ are obtained in the range $-\pi < \omega < \pi$. However, if $\Delta t \neq 1$ and the spectrum is calculated for $-\pi/\Delta t < \omega < \pi/\Delta t$, then the spectrum is easily inverted into

$$ s_x(\omega) = \Delta t \cdot \frac{\sigma_\epsilon^2}{2\pi} \frac{|\beta(e^{-i\omega})|^2}{|\alpha(e^{-i\omega})|^2}. \qquad (5.183) $$

5.2.4.7 Example of ARMA(2.1) Simulated. Figure 5.25 is an example of a generated ARMA(2.1) process over $t = 1$ to 600, when $a = -0.3$, $a_2 = +0.4$, $b_1 = -0.7$, and $\sigma_\epsilon^2 = 1.0$, namely by

$$ X_t - 0.3 \, X_{t-1} + 0.4 \, X_{t-2} = \epsilon_t - 0.7 \, \epsilon_{t-1}. $$

Here ϵ_t is the pure random process we generated as AR(0) in Fig. 5.3. Its readings are listed in Appendix A1 as Table A1.4; pp. 251, 254, and 255. The correlations and spectra of this example are shown in Figs. 5.26 and 5.27. Figure 5.26a shows the theoretical autocorrelation coefficient $\varrho(r) = R(r)/R(0)$ of this generated ARMA(2.1), calculated by Eqs. 5.160, 5.161, 5.162, or 5.163, 5.164, 5.165, using the design values of $a_1 = -0.3$, $a_2 = 0.4$, $b_1 = -0.7$ and $\sigma_\epsilon^2 = 1.0$. Figure 5.26b shows the estimated

$\hat{\varrho}(r) = \hat{R}(r)/\hat{R}(0)$, calculated from the generated process.

We can see in Fig. 5.26b that the autocorrelation coefficient at higher lag r continues to fluctuate, even after the theoretical coefficient, shown in Fig. 5.26a, has died down and converged to zero. On the other hand, the values at low lag numbers look very similar to the theoretical values. An ARMA(n,m) process was fitted and its optimum orders n and m were searched by AIC criteria as explained in Section 5.5.4, using these autocorrelations b, and actually were found to be $n = 2$, $m = 1$. Then the parameters were estimated by the method described in this section as Eqs. 5.174, 5.175, 5.155, and 5.156. The values thus obtained are

$$ \hat{a}_1 = -0.37842, \quad \hat{a}_2 = 0.40130, \quad \hat{b}_1 = -0.73968, \quad \hat{\sigma}_\epsilon^2 = 1.0400 $$

which are not very close, but pretty close to the values actually used to generate this process. The autocorrelation coefficients $\hat{\varrho}(r) = \hat{R}(r)/\hat{R}(0)$ were then estimated using these estimated parameters by Eqs. 5.160, 5.161, and 5.162, just as for the theoretical values. The results are similar and very close to the theoretical values shown in Fig. 5.26a, so that drawings were again omitted.

146
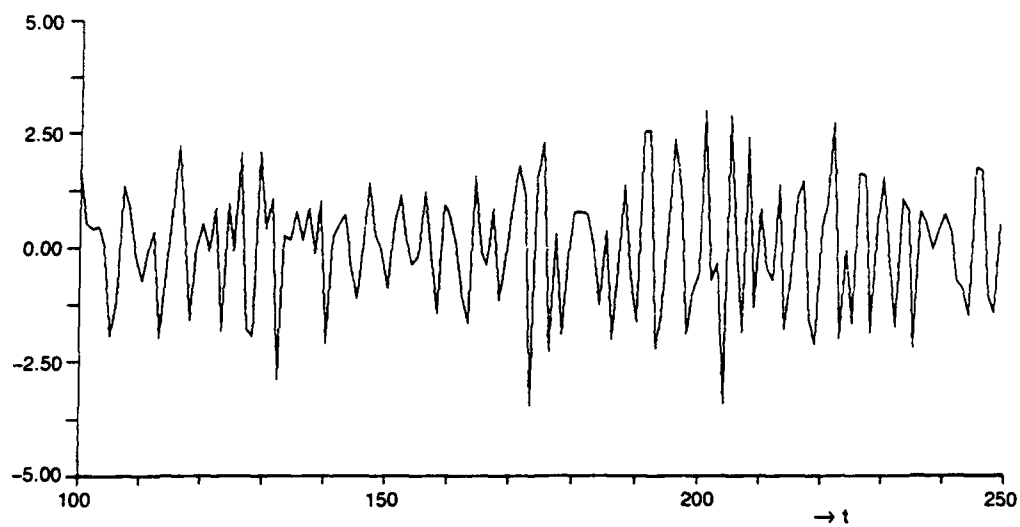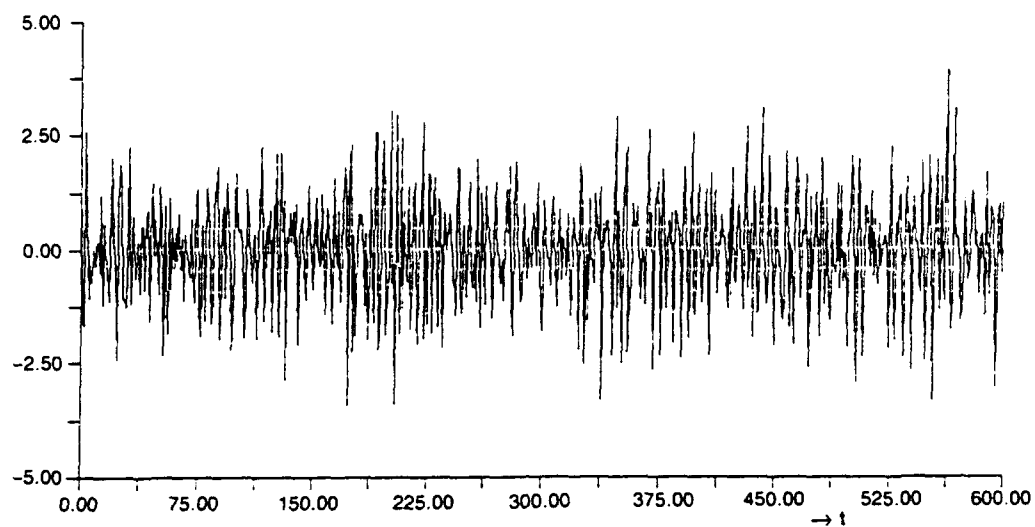
Fig. 5.25. Simulated ARMA(2.1) process (1) $X_t - 0.3\ X_{t-1} + 0.4\ X_{t-2} = \epsilon_t - 0.7\epsilon_{t-1}$, ϵ_t: N[0, 1].

147
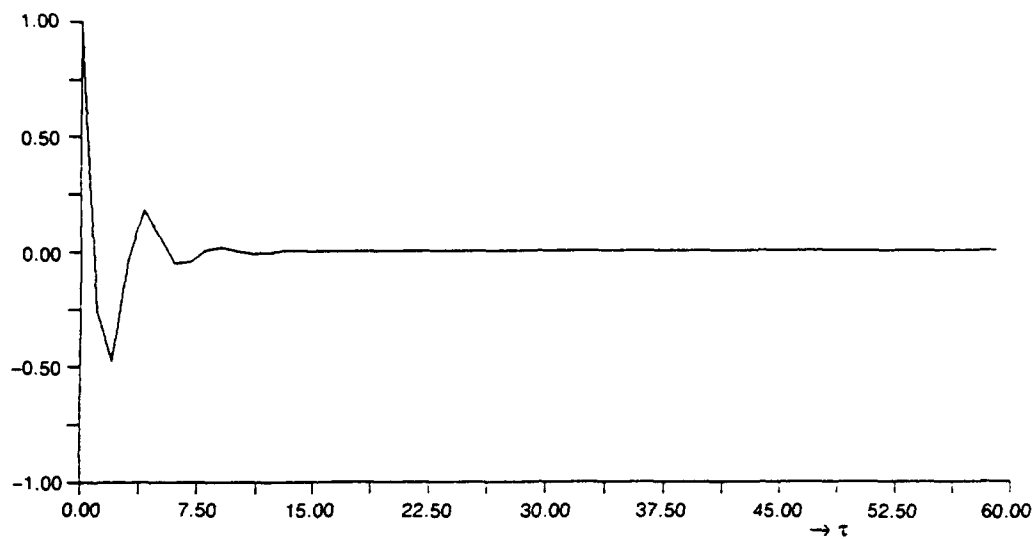
Fig. 5.26a. Theoretical.
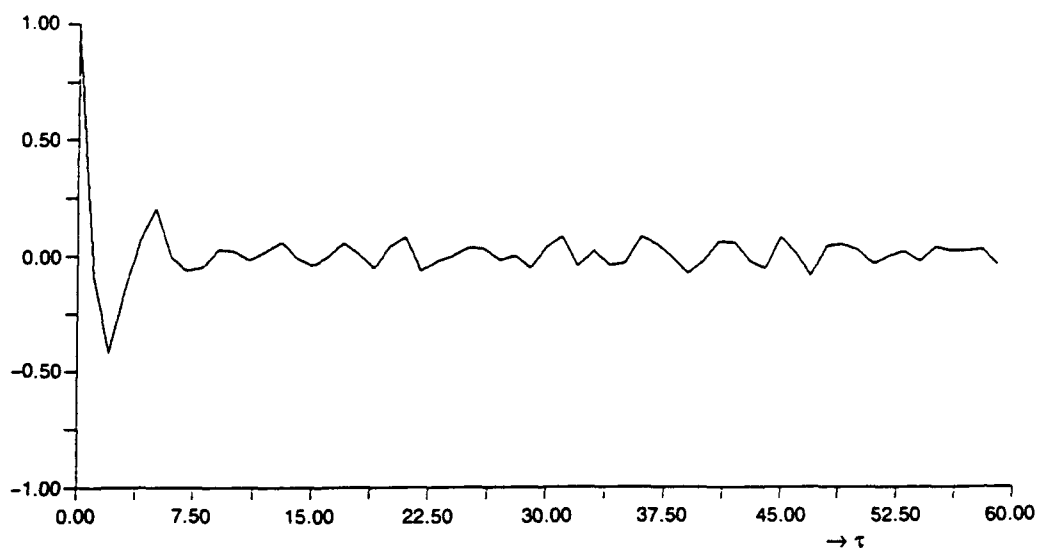
Fig. 5.26b. Estimated.

Fig. 5.26. Autocorrelation coefficient for ARMA(2.1) process (1)

$$X_t - 0.3 \ X_{t-1} + 0.4 \ X_{t-2} = \epsilon_t - 0.7\epsilon_{t-1}, \quad \epsilon_t : N[0, 1].$$

Figure 5.27 shows the spectra, the theoretical one from Eq. 5.182" in Fig. 5.27a, the one estimated from the fitted model ARMA(2.1), using the estimated parameters in Fig. 5.27b, and the one estimated by the nonparametric method from the generated process of Fig. 5.25 in Fig. 5.27c, with a maximum lag number of 60 and Hanning window. Spectra a and b are similar and close to each other, and c fluctuated as expected. In another trial, instead of the ARMA (n,m) model, an AR model was fitted to this generated ARMA(2.1) process. The optimum order n was searched by AIC criteria as AR(n), and was found to be $n = 6$. Its parameters $\hat{a}_1$ to $\hat{a}_6$ and $\hat{\sigma}_\epsilon^2$ were estimated by the method described in Sections 5.4.3 and 5.4.4 as

$$\hat{a}_1 = -0.35801, \quad \hat{a}_2 = -0.64448, \quad \hat{a}_3 = -0.45424,$$

$$\hat{a}_4 = -0.34915, \quad \hat{a}_5 = -0.10554, \quad \hat{a}_6 = -0.11502,$$

$$\hat{\sigma}_\epsilon^2 = 1.03499.$$

These values are listed in Table 5.1.

The value of $\hat{\sigma}_\epsilon^2$ is very close to the theoretical value of $\sigma_\epsilon^2 = 1.0$. The spectrum of this fitted AR(6) is shown as Fig. 5.27d. It is interesting to find that this spectrum Fig. 5.27d is very smooth, but its shape looks like the smoother shape of spectrum Fig. 5.27c, the one estimated by the nonparametric method. In Fig. 5.27c, by vertical lines, the 90% level of confidence interval of this estimate, based on the χ^2-distribution of the equivalent degree of freedom (here approximately equal to 27) as is explained in Section 2.5.5 is shown for reference.

As another example of the ARMA(2.1) process, the sign of the parameter b_1 in the previous example was changed, and another ARMA(2.1) process was generated, keeping a_1, a_2, and σ_ϵ^2 the same,

$$a_1 = -0.3, \quad a_2 = +0.4, \quad b_1 = +0.7, \quad \sigma_\epsilon^2 = 1.0.$$

As for the previous example, its time history (readings are listed in Appendix A1 as Table A1.5; pp. 251, 256, and 257), autocorrelation, and spectra are shown as Figs. 5.28, 5.29, and 5.30.

In this example, the AIC criteria gave ARMA(3.1) as the optimum model to be fitted, instead of ARMA(2.1), though the difference in AIC is not so large. The estimated spectrum of this optimum ARMA(3.1) is shown as Fig. 5.30b, and for reference the spectrum of the fitted ARMA(2.1) model is shown as Fig. 5.30e. ARMA(3.1) gave the minimum value of AIC and ARMA(2.1) did not. However, the ARMA(2.1) spectrum Fig. 5.30e looks more like the theoretical spectrum Fig. 5.30a than does that of ARMA(3.1), spectrum Fig. 5.30b. Spectrum Fig. 5.30d shows the spectrum of the fitted optimum AR(n) model, where n appeared to be 8 by AIC criteria. It is interesting to find that this spectrum Fig. 5.30d shows again the same pattern of variation as spectrum Fig. 5.30c obtained by the nonparametric method. The estimated values of parameters $\hat{a}_1, \hat{a}_2, \cdots \hat{a}_8$ and $\hat{\sigma}_\epsilon^2$ are listed in Table 5.1, and $\hat{\sigma}_\epsilon^2 = 1.04911$ is very close to the theoretical value $\hat{\sigma}_\epsilon^2 = 1.0$.
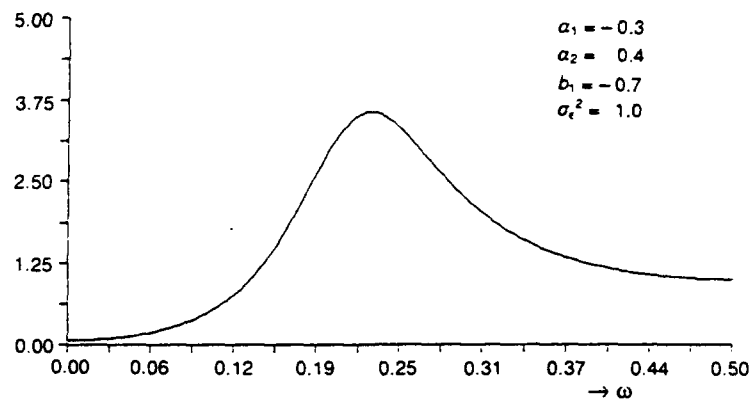
Fig. 5.27a. Theoretical ARMA process ARMA(2.1).
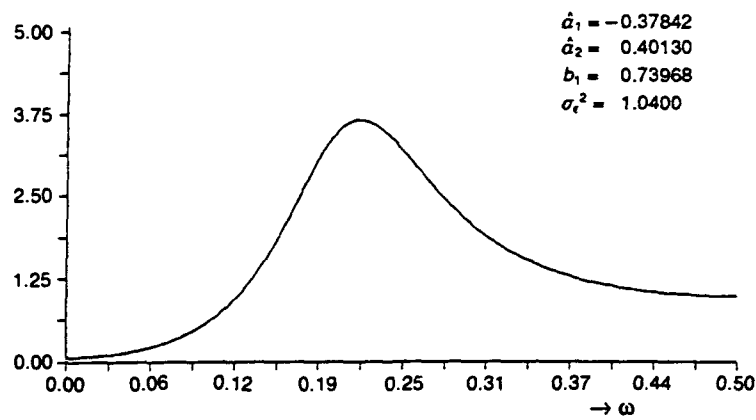
Fig. 5.27b. Estimated by ARMA model fitting as optimum ARMA(2.1).

Fig. 5.27. Spectrum for ARMA(2.1) process (1)

$$X_t - 0.3\ X_{t-1} + 0.4\ X_{t-2} = \epsilon_t - 0.7\epsilon_{t-1}, \quad \epsilon_t : \text{N}[0, 1].$$
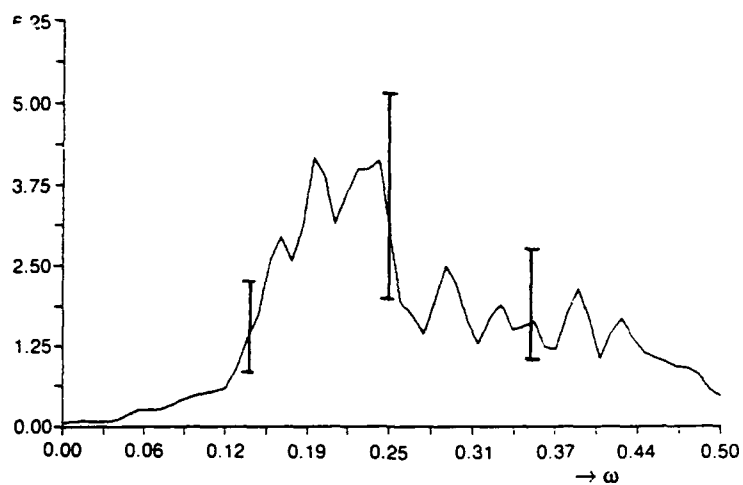
Fig. 5.27c. Estimated by nonparametric method.
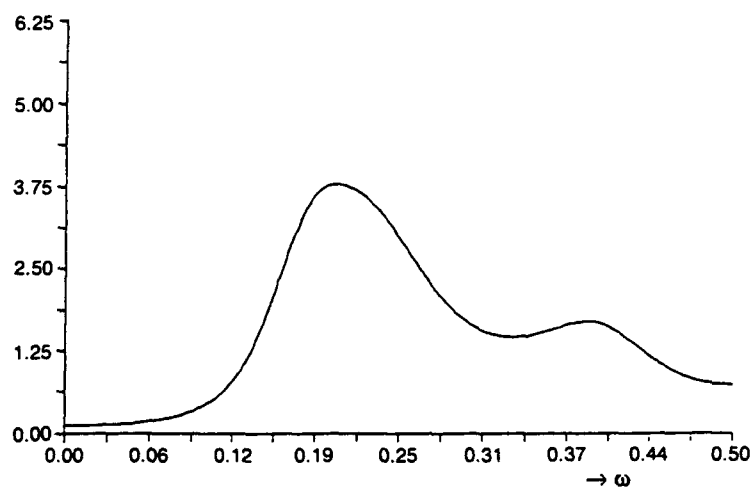
Fig. 5.27d. Estimated by AR model fitting, AR(6).

Fig. 5.27. (Continued)

151
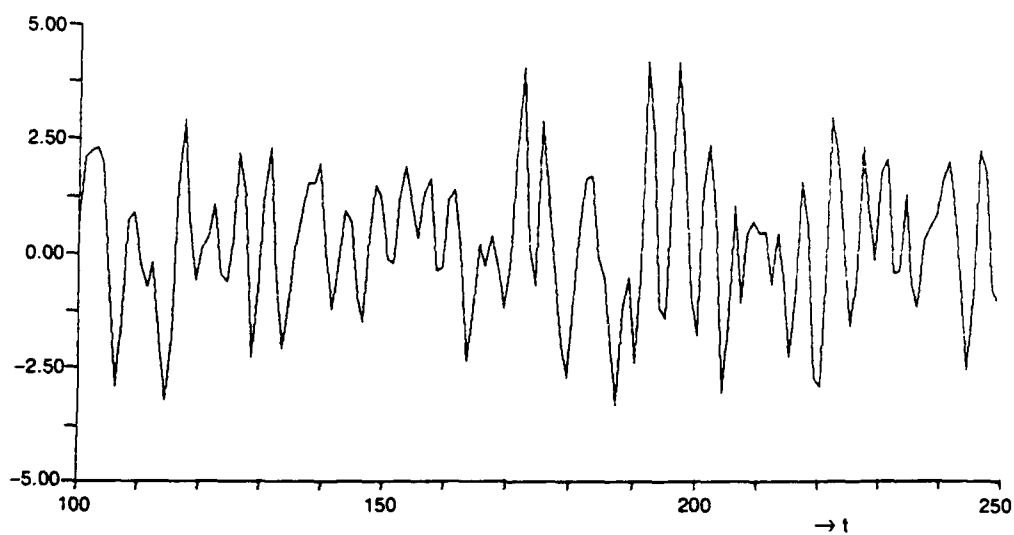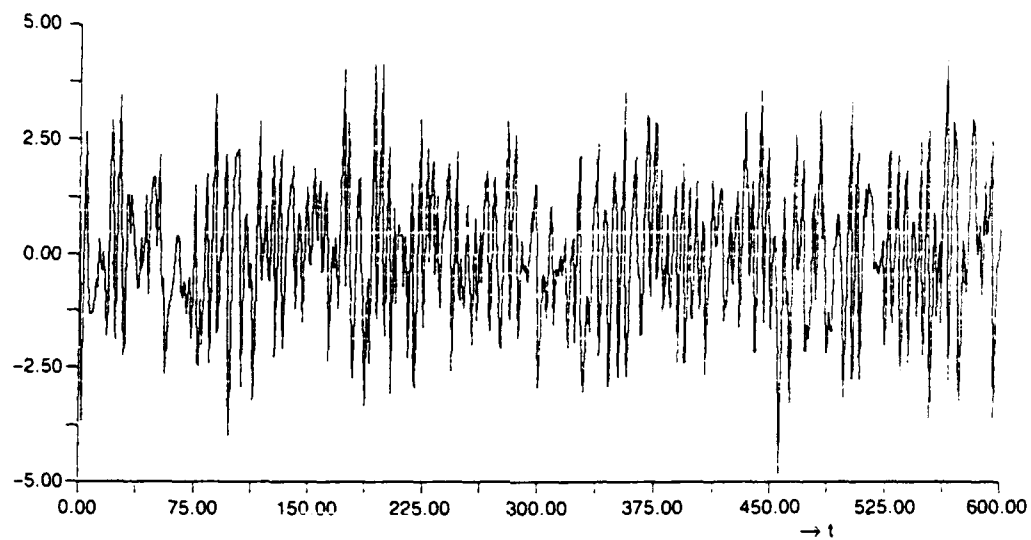
Fig. 5.28. Simulated ARMA(2.1) process (2)

$$X_t - 0.3\ X_{t-1} + 0.4\ X_{t-2} = \epsilon_t + 0.7\epsilon_{t-1}, \quad \epsilon_t\colon\ N[0,1].$$
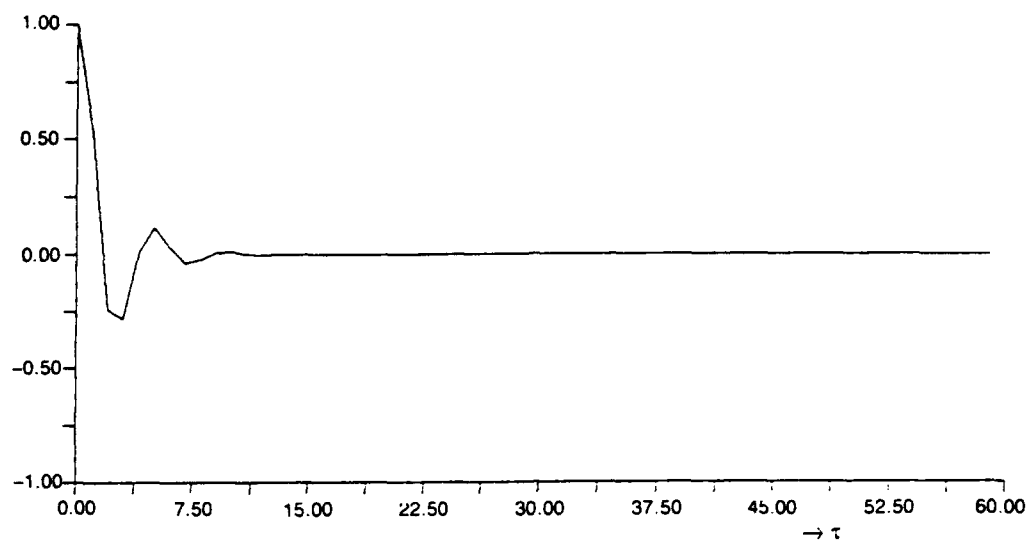
Fig. 5.29a. Theoretical.
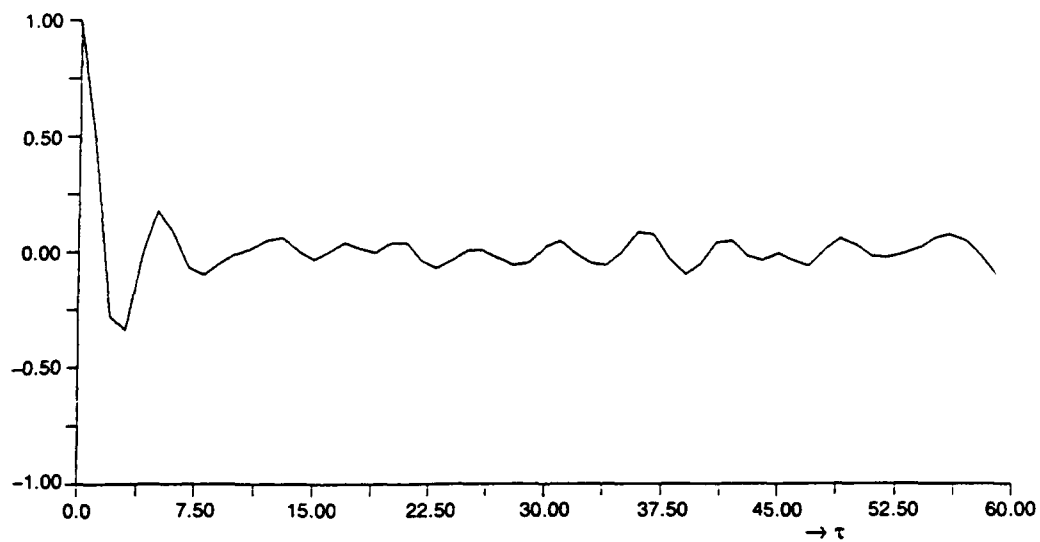
Fig. 5.29b. Estimated.

Fig. 5.29. Autocorrelation coefficient for ARMA(2.1) process (2)

$$X_t - 0.3 \ X_{t-1} + 0.4 \ X_{t-2} = \epsilon_t + 0.7\epsilon_{t-1}, \quad \epsilon_t : N[0, 1].$$
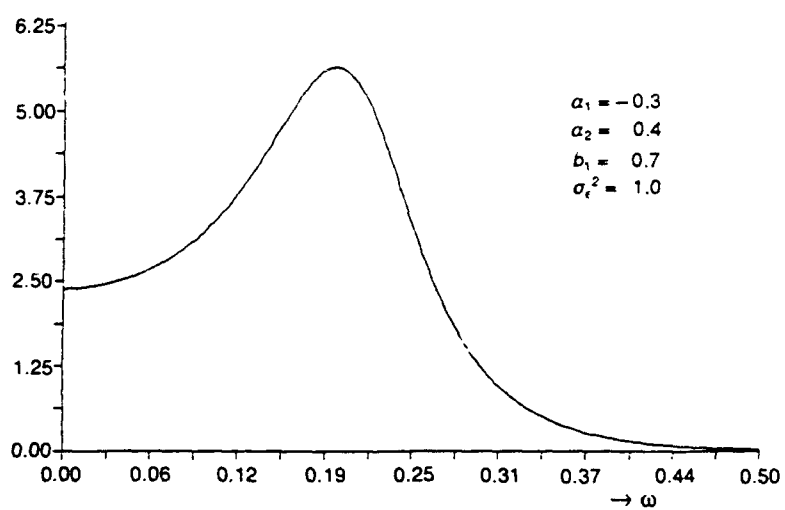
Fig. 5.30a. Theoretical ARMA process ARMA(2.1).

Fig. 5.30. Spectrum for ARMA(2.1) process (2)

$$X_t - 0.3 \ X_{t-1} + 0.4 \ X_{t-2} = \epsilon_t + 0.7\epsilon_{t-1}, \quad \epsilon_t: \ N[0, 1].$$
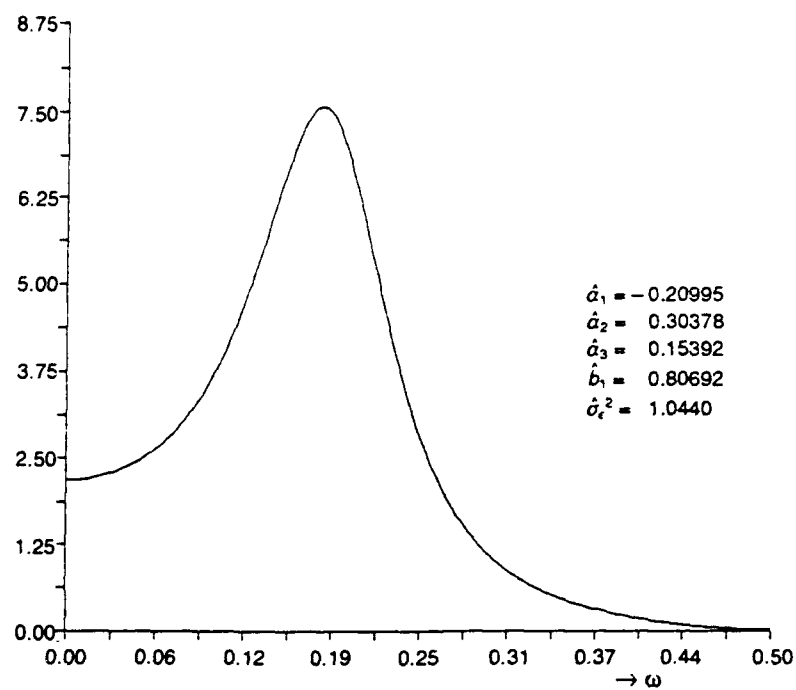
Fig. 5.30b. Estimated by ARMA model fitting as optimum, ARMA(3.1).

Fig. 5.30. (Continued)
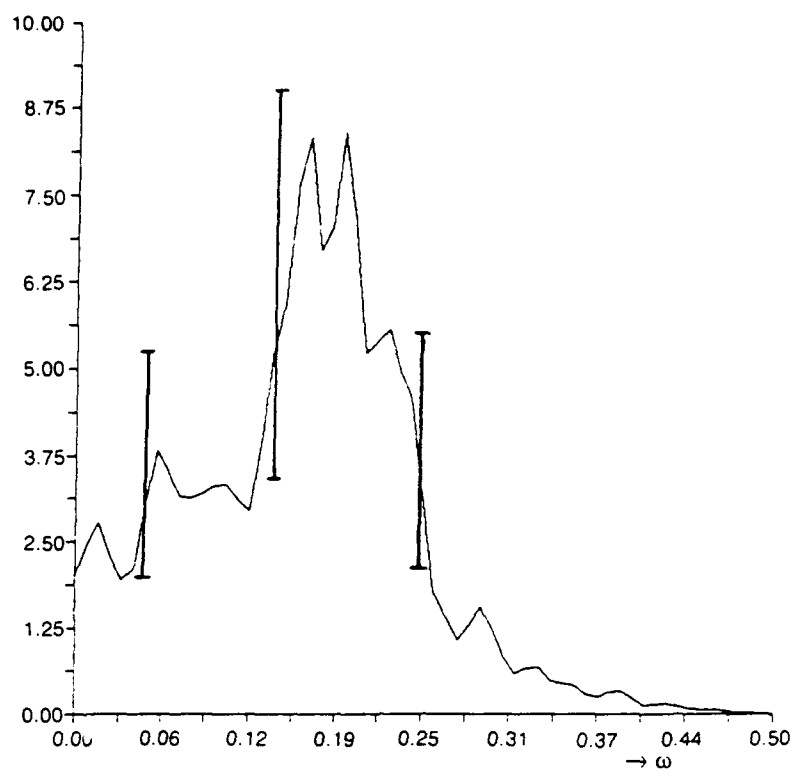
Fig. 5.30c. Estimated by nonparametric method.
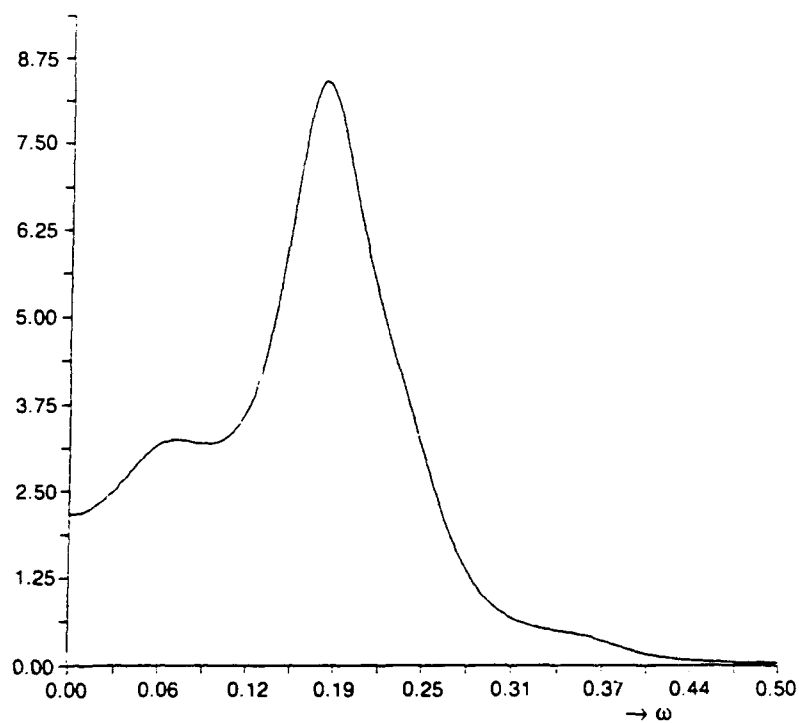
Fig. 5.30d. Estimated by AR model fitting, AR(8).

Fig. 5.30. (Continued)

$\acute{a}_1 = -0.34559$
$\acute{a}_2 = 0.41494$
$b_1 = 0$
$\sigma_\epsilon^2 = 1.0558$
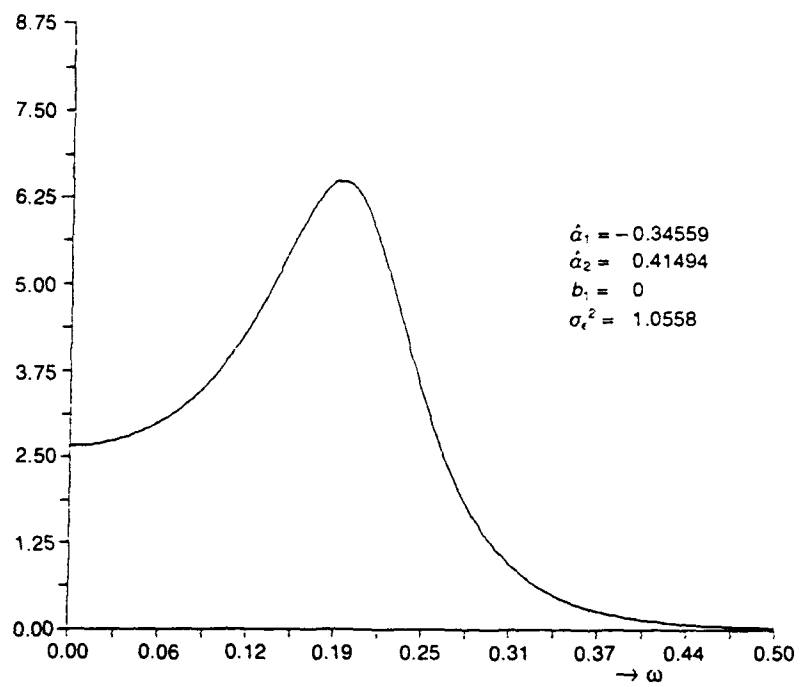
Fig. 5.30e. Estimated as ARMA(2.1) [not optimum].

Fig. 5.30. (Continued)

157

Table 5.1. Results of estimation by model fitting —— [I].

Fig. No.	Process ARMA (n,m)		Generated	Readings in	Estimated as Optimum	Estimated Equivalent AR (N)
5.3	AR (0)	n	0		0	
.		m	0	A1.1	0	
5.5	ARMA (0,0)	σ_ϵ^2	1.0		1.04649	—
5.10	AR (1)	n	1		1	
.		a	− 0.5	A1.2	− 0.50933	—
5.12	ARMA (0,1)	σ_ϵ^2	1.0		1.04646	
5.20	AR (2)	n	2		2	
.		a_1	− 0.5		− 0.54156	
.		a_2	+ 0.8	A1.3	+ 0.81838	—
5.22	ARMA (0,2)	σ_ϵ^2	1.0		1.04702	
5.25	ARMA (2,1)	n	2		2	6
.		m	1		1	0
.	[Process (1)]					
.		a_1	− 0.3		− 0.37842	a_1 − 0.35801
.						a_2 − 0.64448
.		a_2	+ 0.4	A1.4	+ 0.40130	a_3 − 0.45424
.						a_4 − 0.34915
.		b_1	− 0.7		− 0.73968	a_5 − 0.10554
.						a_6 − 0.11502
5.27	ARMA (2,1)	σ_ϵ^2	1.0		1.0400	σ_ϵ^2 : 1.03419
5.28	ARMA (2,1)	n	2		2 (NOT OPTIMUM)	8
.		m	1		1	0
.	[Process (2)]					
.		a_1	− 0.3		− 0.34559	a_1 1.00947
.		a_2	+ 0.4		+ 0.41494	a_2 − 1.08338
.		b_1	+ 0.7		+ 0.69856	a_3 0.09614
.		σ_ϵ^2	1.0	A1.5	1.0558	a_4 − 0.50333
.		n	2		3 (OPTIMUM)	a_5 0.40894
.		m	1		1	a_6 − 0.30626
.		a_1	− 0.3		− 0.20995	a_7 0.17930
.		a_2	+ 0.4		+ 0.30378	a_8 − 0.09768
.		a_3	0		+ 0.15392	
.		b_1	+ 0.7		+ 0.80692	
5.30	ARMA (2,1)	σ_ϵ^2	1.0		1.0440	σ_ϵ^2 : 1.04911

158

5.2.5 ARMA(1.1), MA(2) ARMA(1.2) MA(1), and ARMA(2.2)

5.2.5.1 ARMA(1.1). In ARMA(2.1), expressed by Eq. 5.120

$$X_t + a_1 X_{t-1} + a_2 X_{t-2} = \epsilon_t + b_1 \epsilon_{t-1},$$

when $a_2 = 0$, the process is called ARMA(1.1). We can easily get Green's function, the inverse function, the autocovariance, and the spectrum function of ARMA(1.1) by modifying those functions for ARMA(2.1) by setting $a_2 = 0$.

5.2.5.2 MA(2). When $a_1 = a_2 = 0$ in Eq. 5.120 and there exist b_2 in addition to b_1,

$$X_t = \epsilon_t + b_1 \epsilon_{t-1} + b_2 \epsilon_{t-2}. \tag{5.184}$$

This process is called MA(2).

In this case Green's function is the function for expressing X_t by MA (∞), so to speak of Green's function for a pure moving average process has no meaning. However, formally,

$$X_t = \sum_{j=0}^{\infty} G_j \epsilon_{t-j}$$

and

$$
\begin{aligned}
G_0 &= 1 \\
G_1 &= b_1 \\
G_2 &= b_2 \\
G_j &= 0 \qquad j \geq 3.
\end{aligned}
$$

In this case the inverse function for expressing X_t by AR (∞) is meaningful. From Eq. 5.184,

$$
\begin{aligned}
X_t &= (1 + b_1 B + b_2 B^2) \epsilon_t \\
&= \beta(B)\epsilon_t, \tag{5.184'}
\end{aligned}
$$

here

$$\beta(Z) = 1 + b_1 Z + b_2 Z^2. \tag{5.185}$$

Now supposing the quadrant

$$f_2(Z) = Z^2 + b_1 Z + b_2 = 0 \tag{5.186}$$

has two roots v_1 and v_2, $f_2(Z) = (Z - v_1)(Z - v_2)$

$$v_1, v_2 = \frac{1}{2}\left(-b_1 \pm \sqrt{b_1^2 - 4b_2}\right). \tag{5.187}$$

Then
$$\left\{1 - (\nu_1 + \nu_2)B + \nu_1\nu_2 B^2\right\}\epsilon_t = X_t$$

$$\nu_1 + \nu_2 = -b_1$$

$$\nu_1\,\nu_2 = b_2$$

$$(1 - \nu_1 B)(1 - \nu_2 B)\,\epsilon_t = X_t.$$

$$\epsilon_t = \frac{X_t}{\beta(B)} = \frac{X_t}{(1 + b_1 B + b_2 B^2)} = \frac{1}{(1 - \nu_1 B)(1 - \nu_2 B)}X_t$$

$$= \frac{1}{\nu_1 - \nu_2}\left\{\frac{\nu_1}{1 - \nu_1 B} - \frac{\nu_2}{1 - \nu_2 B}\right\}\,X_t$$

$$= \frac{1}{\nu_1 - \nu_2}\left\{\sum_{j=0}^{\infty}(\nu_1^{j+1} - \nu_2^{j+1})B^j\right\}X_t$$

$$= \sum_{j=0}^{\infty}\left\{\frac{\nu_1^{j+1} - \nu_2^{j+1}}{\nu_1 - \nu_2}\right\}X_{t-j}. \tag{5.188}$$

Therefore, if the expression of the inverse function I_j is used here as

$$\epsilon_t = \sum_{i=0}^{\infty}(-I_j)\,X_{t-j}\;,$$

$$I_j = -\frac{\nu_1^{j+1} - \nu_2^{j+1}}{\nu_1 - \nu_2} = \frac{\nu_1}{\nu_2 - \nu_1}\nu_1{}^j + \frac{\nu_2}{\nu_1 - \nu_2}\nu_2{}^j. \tag{5.189}$$

This relation, as well as the way to derive it, is the same as that used for the derivation of Green's function for AR(2), already shown in Section 5.2.3. For invertibility of MA(2), ϵ_t must be bounded by $t \to t-j$, $j \to \infty$. Then by the same logic as was used for AR(2), $|\nu_1| < 1$, $|\nu_2| < 1$ should stand for MA(2), and the conditions that must be satisfied by b_1, b_2 are the same as the conditions that had to be satisfied by a_1, a_2 of AR(2). This condition is shown in Fig. 5.31, which is similar to Figs. 5.15 and 5.16, where a_1, a_2 are replaced by b_1, b_2. This triangular zone is again subdivided into subzones [I] and [II], depending on

$$b_1^2 \geq 4b_2[\text{I}] \text{ and } b_1^2 < 4b_2[\text{II}].$$

Subzone [I] is divided into four regions:

$$\text{①} \quad b_1 < 0, b_2 > 0$$
$$\text{②} \quad b_1 < 0, b_2 < 0$$
$$\text{③} \quad b_1 > 0, b_2 > 0$$
$$\text{④} \quad b_1 > 0, b_2 < 0$$

as shown in Fig. 5.31, just similar to Fig. 5.16.
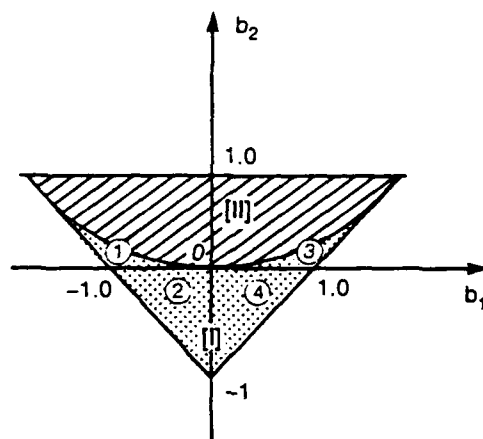
Fig. 5.31. Invertible Subzones [I] and [II]; ①, ②, ③, ④ for b_1, b_2.

$$X_t = \epsilon_t + b_1 \epsilon_{t-1} + b_2 \epsilon_{t-2}$$

$$X_{t-r} = \epsilon_{t-r} + b_1 \epsilon_{t-r-1} + b_2 \epsilon_{t-r-2}.$$

Therefore, multiplying both sides of these two equations respectively and taking the expected values of each term,

$$E[X_t \cdot X_{t-r}] = E[\epsilon_t \cdot \epsilon_{t-r}] + b_1^2 E[\epsilon_{t-1} \cdot \epsilon_{t-r-1}] + b_2^2 E[\epsilon_{t-2} \epsilon_{t-r-2}]$$
$$+ b_1 \Big\{ E[\epsilon_{t-1} \epsilon_{t-r}] + E[\epsilon_t \cdot \epsilon_{t-r-1}] \Big\} + b_2 \Big\{ E[\epsilon_{t-2} \epsilon_{t-r}] + E[\epsilon_t \cdot \epsilon_{t-r-2}] \Big\}$$
$$+ b_1 b_2 \Big\{ E[\epsilon_{t-1} \cdot \epsilon_{t-r-2}] + E[\epsilon_{t-2} \cdot \epsilon_{t-r-1}] \Big\}.$$

Thus

$$R_x(0) = (1 + b_1^2 + b_2^2) \, R_\epsilon(0) \qquad (5.190)$$

$$R_x(1) = R_x(-1) = (b_1 b_2 + b_1) R_\epsilon(0) \qquad (5.191)$$

$$R_x(2) = R_x(-2) = b_2 \cdot R_\epsilon(0) \qquad (5.192)$$

$$R_x(r) = 0 \qquad r \geq 3 \qquad (5.193)$$

because

$$E[\epsilon_t \; \epsilon_{t-r}] = \delta_r \cdot \sigma_\epsilon^2 = \begin{cases} \sigma_\epsilon^2, & r = 0 \\ 0, & r \neq 0 \end{cases} ; \quad \delta_r \text{ is Kronecker's delta function.}$$

$R_x(r) = 0$ for $r \geq 3$. This is an interesting characteristic of MA(2). Generally, for MA(n), $R_x(r) = 0$ for $r \geq n + 1$. In the same way as for ARMA(2.1)

$$s(\omega) = \frac{\sigma_\epsilon^2}{2\pi} \; \left| 1 + b_1 e^{-i\omega} + b_2 e^{-2i\omega} \right|^2 . \qquad (5.194)$$

Estimation of b_1, b_2, and σ_ϵ^2 is possible by solving the quadratic Eqs. 5.190, 5.191, and 5.192 for b_1, b_2, and σ_ϵ^2.

5.2.5.3 Example of MA(2), MA(1), and ARMA(2.2). As was done for AR(0), AR(1), AR(2), and ARMA(2.1) in the preceding sections, an MA(2) model was generated over $t = 1$ to 600 by $X_t = \epsilon_t + 0.2\epsilon_{t-1} + 0.8\epsilon_{t-2}$ as in Fig. 5.32. For ϵ_t, the same pure random process N[0, 1] as was generated in Fig. 5.3 in Section 5.2.1 for AR(0) is used. Its readings are listed in Appendix A1 as Table A1.6; pp. 251, 256, and 257. Figure 5.33a shows the theoretical $R(r)$ using the design values $b_1 = +0.2$, $b_2 = +0.8$, and $\sigma_\epsilon^2 = 1.0$, and Fig. 5.33b the estimated sample autocorrelation $R(r)$. It is interesting to note that theoretically $R(r) = 0$ for $r \geq 3$.

Figure 5.34a shows the theoretical spectrum given by Eq. 5.194 where $b_1 = +0.2$, $b_2 = +0.8$, and $\sigma_\epsilon^2 = 1.0$, which are all design values, and Fig. 5.34b the spectrum of the fitted model given by Eq. 5.194 where $b_1 = 0.18662$, $b_2 = 0.78000$, and $\sigma_\epsilon^2 = 1.0816$ calculated by the method described in Section 5.3.3. Of course again in this example, order determination by AIC, to be explained in Section 5.5, gave the proper value of $m = 2$. Figure 5.34c is the spectrum calculated by the nonparametric method. Here again the 90% level confidence interval is shown by vertical lines for reference. This was originally generated as MA(2). However, as will be discussed in Section 5.4, often an AR model is fitted generally to the processes taking advantage of the fact that the determination of parameters is much easier than for ARMA.

Figure 5.34d shows the spectrum of the AR model fitted to this process. The order of this AR process is $n = 13$ and is naturally higher than 2 for m as MA(m). This result shows that, if this MA(2) is to be approximated by AR(n), AR(13) is the closest model to be adopted. Again, it is interesting to note that the spectrum Fig. 5.34d of AR(13) looks very similar to the spectrum Fig. 5.34c estimated by the nonparametric method.
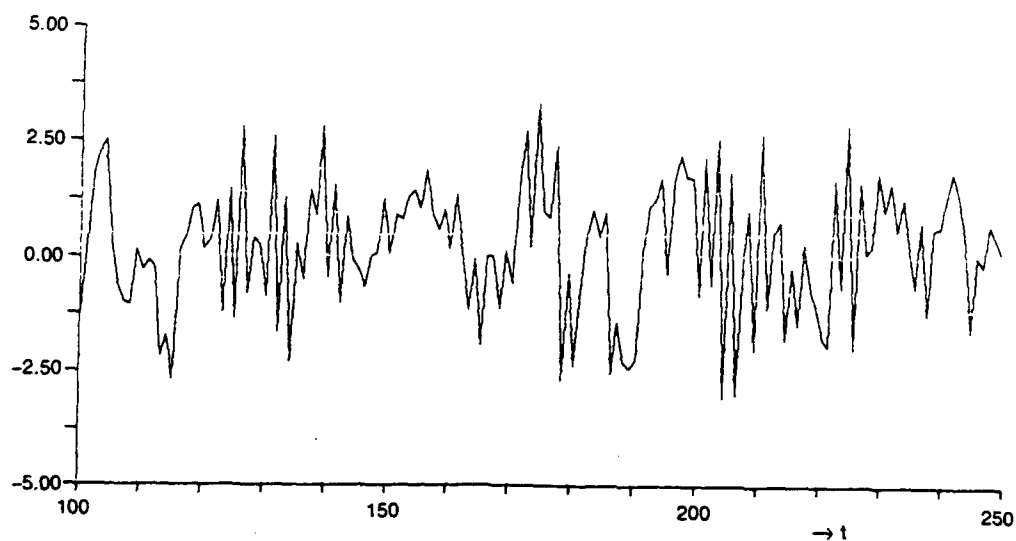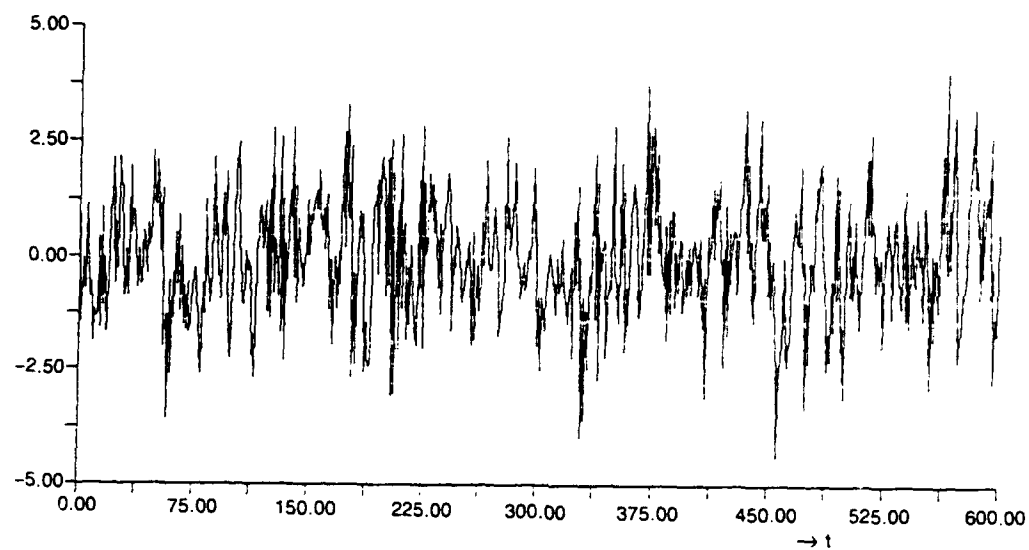
Fig. 5.32. Simulated MA(2) process $X_t = \epsilon_t + 0.2\,\epsilon_{t-1} + 0.8\,\epsilon_{t-2}$, $\quad \epsilon_t$: N[0, 1].

163
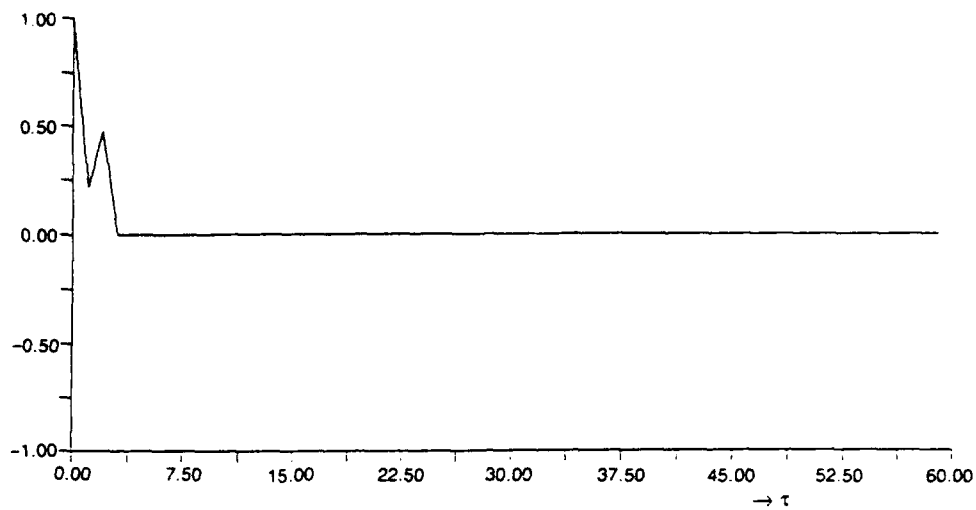
Fig. 5.33a. Theoretical.
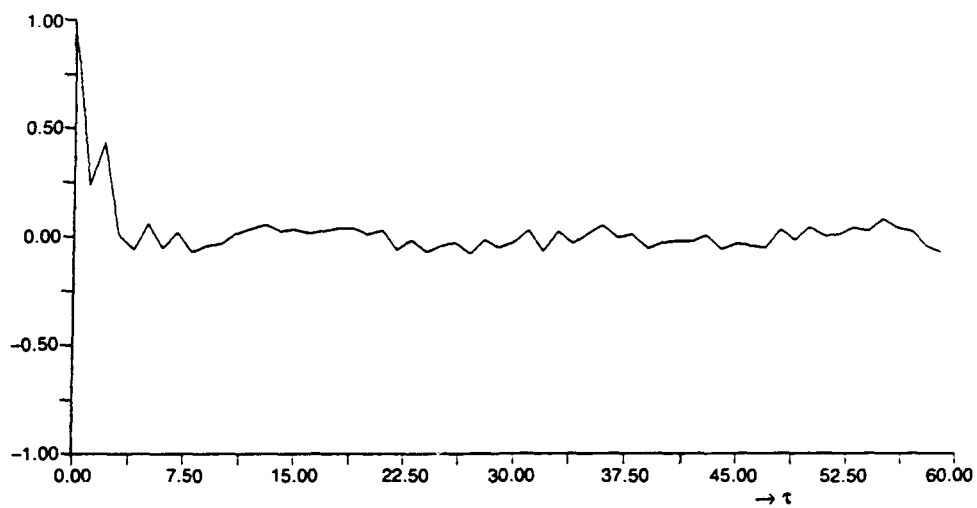
Fig. 5.33b. Estimated.

Fig. 5.33. Autocorrelation coefficient for MA(2) process
$$X_t = \epsilon_t + 0.2\,\epsilon_{t-1} + 0.8\,\epsilon_{t-2}, \quad \epsilon_t: N[0, 1].$$

164
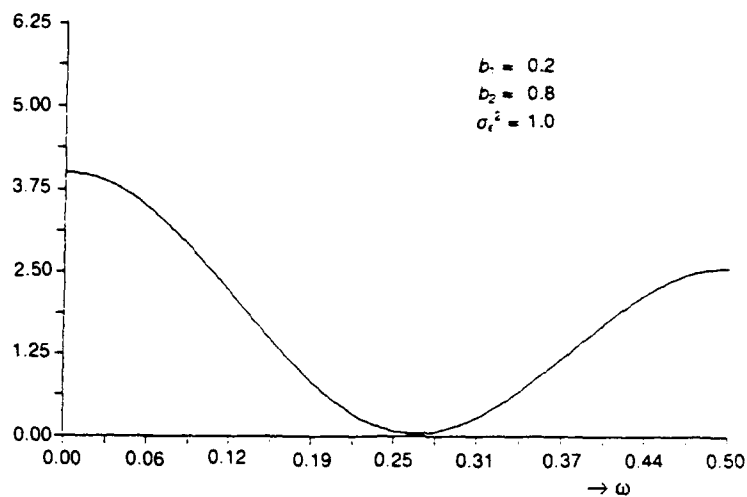
Fig. 5.34a. Theoretical MA(2).
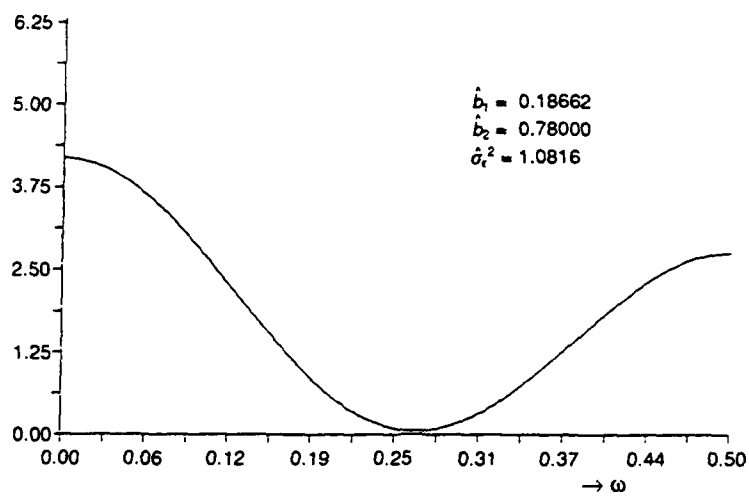
Fig. 5.34b. Estimated by MA model fitting as optimum, MA(2).

Fig. 5.34. Spectrum for MA(2) process $X_t = \epsilon_t + 0.2\,\epsilon_{t-1} + 0.8\,\epsilon_{t-2}$, ϵ_t: N[0, 1].

165
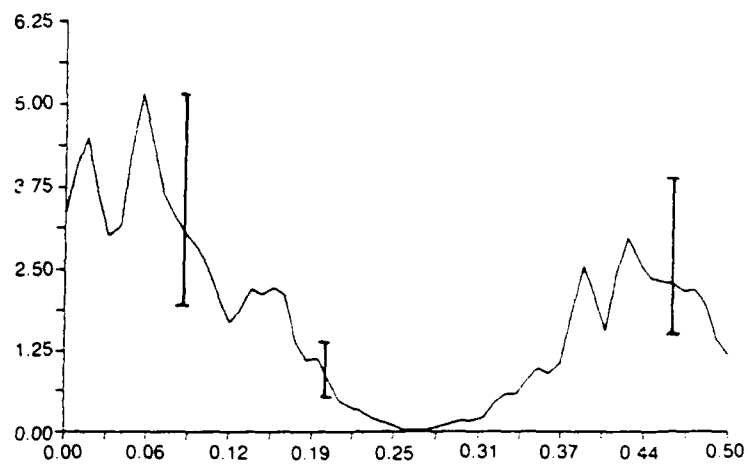
Fig. 5.34c. Estimated by nonparametric method.
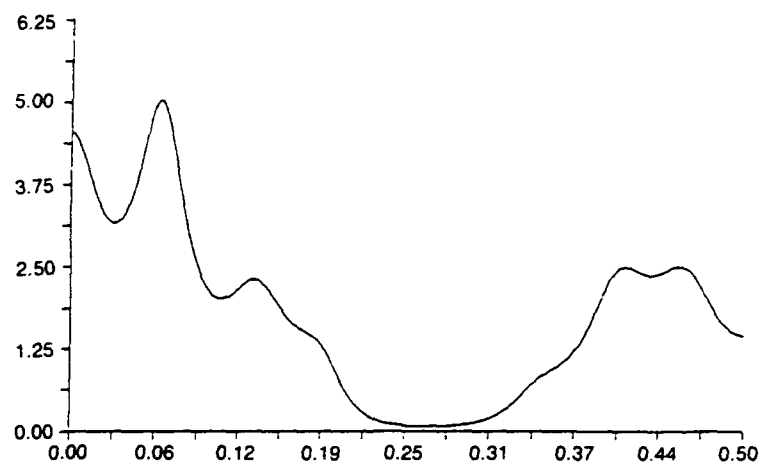
Fig. 5.34d. Estimated by AR model fitting, AR(13).

Fig. 5.34. (Continued)

166

Figures 5.35, 5.36, and 5.37 show the same kind of results for a generated MA(1) process, $X_t = \epsilon_t - 0.7\epsilon_{t-1}$, for ϵ_t: $N[0, 1]$, i.e., for $b_1 = -0.7$, $\sigma_\epsilon^2 = 1.0$. Figures 5.38, 5.39, and 5.40 are also for an MA(1) process, $X_t = \epsilon_t + 0.7\epsilon_{t-1}$, i.e., for $b_1 = +0.7$, $\sigma_\epsilon^2 = 1.0$, just changing the sign of b_1 from -0.7 to $+0.7$.

Figures 5.35 and 5.38 show the time history over $t = 1$ to 600. Their readings are listed in Appendix A1 as Tables A1.7 and A1.8; pp. 251, 258, and 259. Figures 5.36 and 5.39 show the autocorrelation. Theoretically, $R(r) = 0$ for $r \geq 2$.
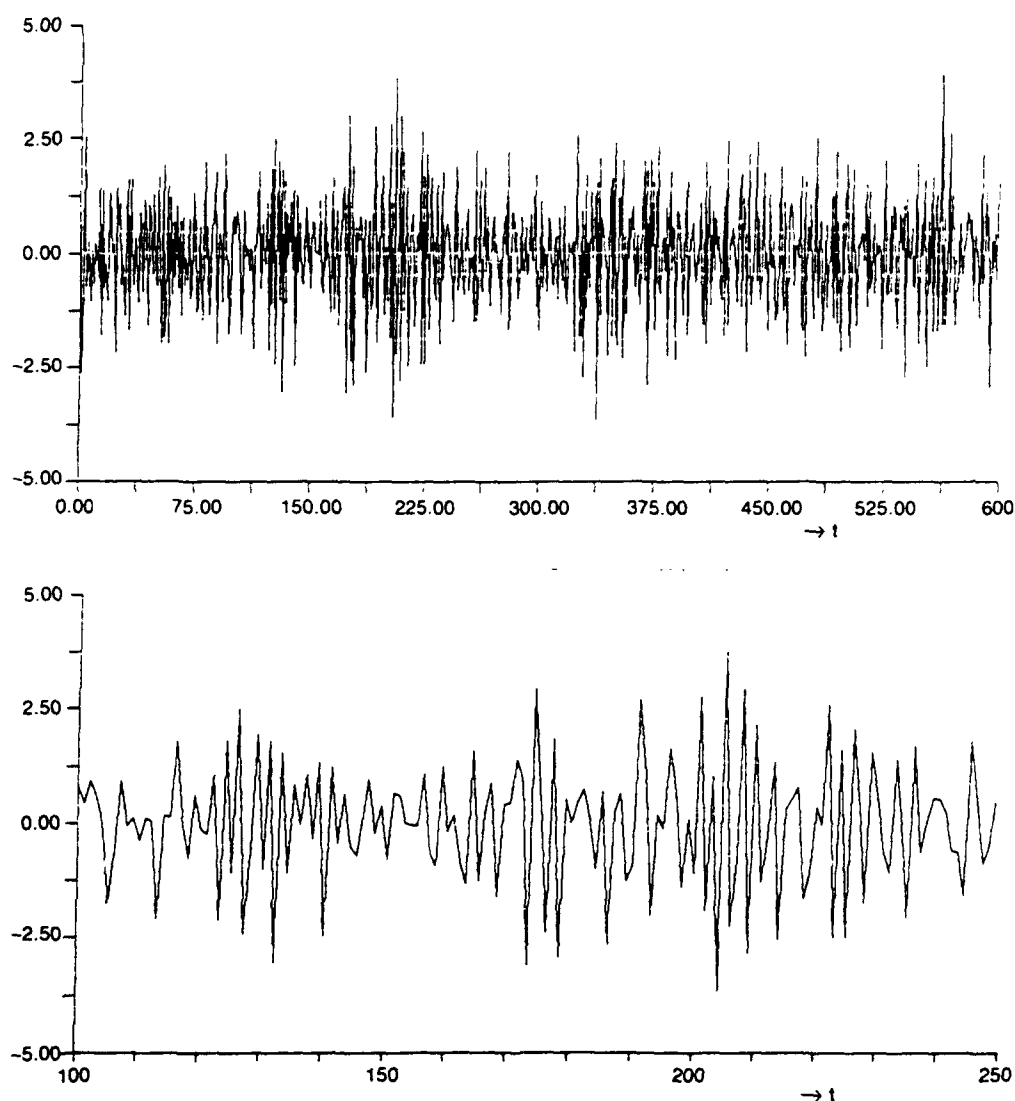
Fig. 5.35. Simulated MA(1) process (1)

$$X_t = \epsilon_t - 0.7\epsilon_{t-1}, \quad \epsilon_t: N[0, 1].$$

167
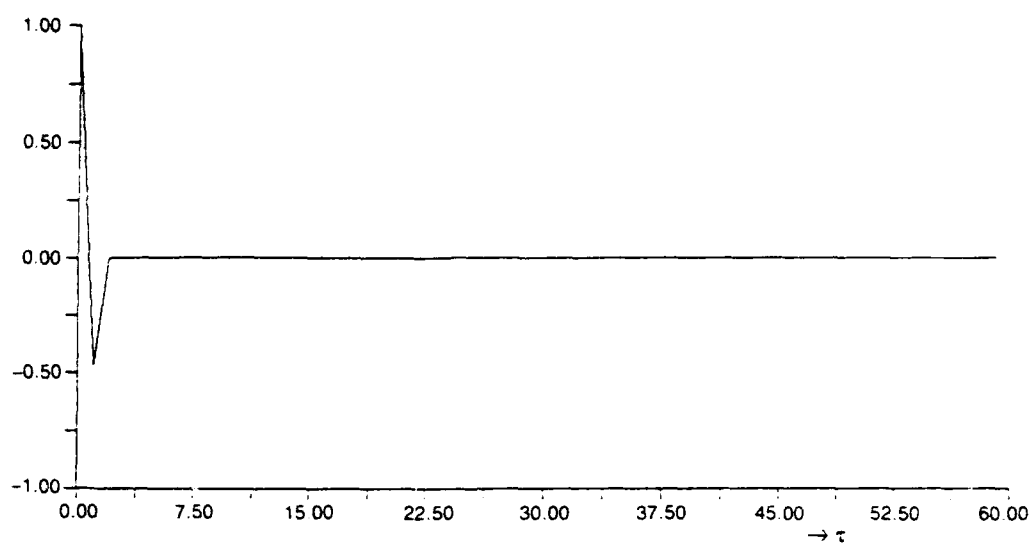
Fig. 5.36a. Theoretical.
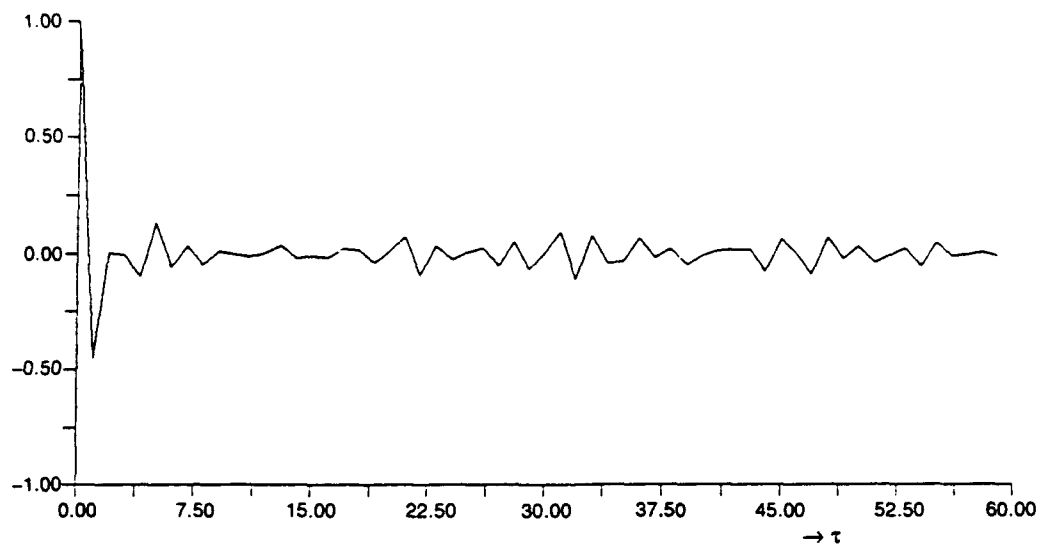
Fig. 5.36b. Estimated.

Fig. 5.36. Autocorrelation coefficient for MA(1) process (1)

$$X_t = \epsilon_t - 0.7\epsilon_{t-1}, \quad \epsilon_t : N[0, 1].$$

168

Figures 5.37 and 5.40 are the spectra: a the theoretical, b that estimated by model fitting as optimum, c that estimated by the nonparametric method, and d the spectrum of the fitted AR(n) model. The n appeared to be 4 and 8 for Fig. 5.37 and Fig. 5.40, respectively.

$b_1 = -0.7$

$\sigma_\epsilon^2 = 1.0$
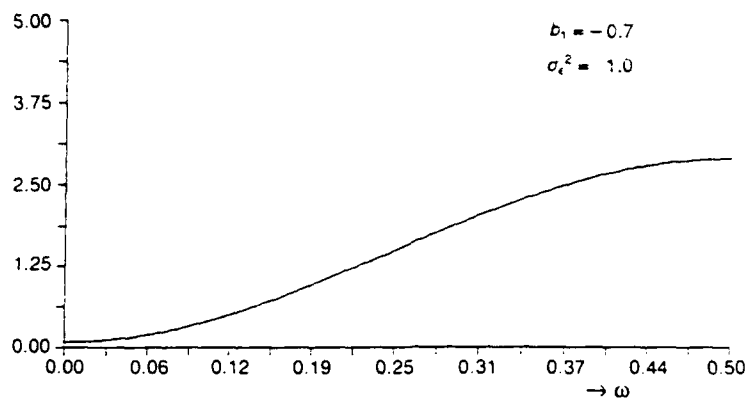
Fig. 5.37a. Theoretical MA(1).

$\hat{b}_1 = -0.70294$

$\hat{\sigma}_\epsilon^2 = 1.0478$
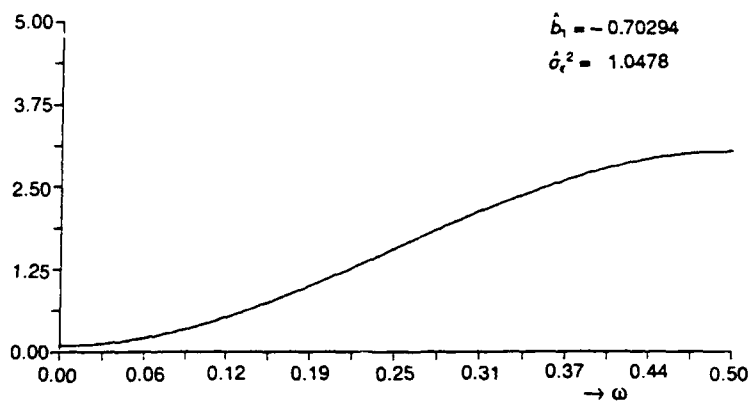
Fig. 5.37b. Estimated by MA model fitting as optimum, MA(1).

Fig. 5.37. Spectrum of MA(1) process (1)

$$X_t = \epsilon_t - 0.7\epsilon_{t-1}, \qquad \epsilon_t : N[0, 1].$$
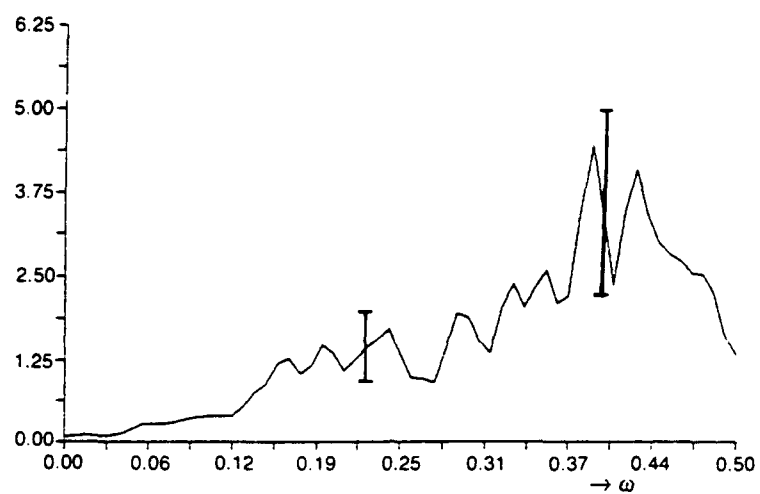
Fig. 5.37c. Estimated by nonparametric method.
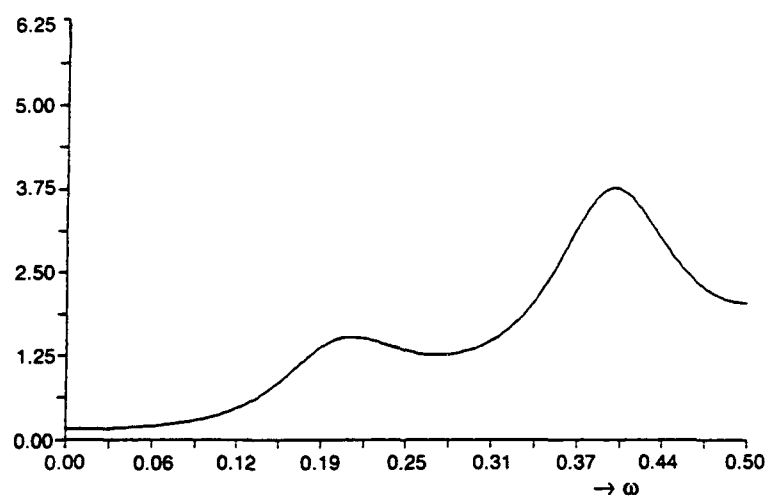
Fig. 5.37d. Estimated by AR model fitting, AR(4).

Fig. 5.37. (Continued)
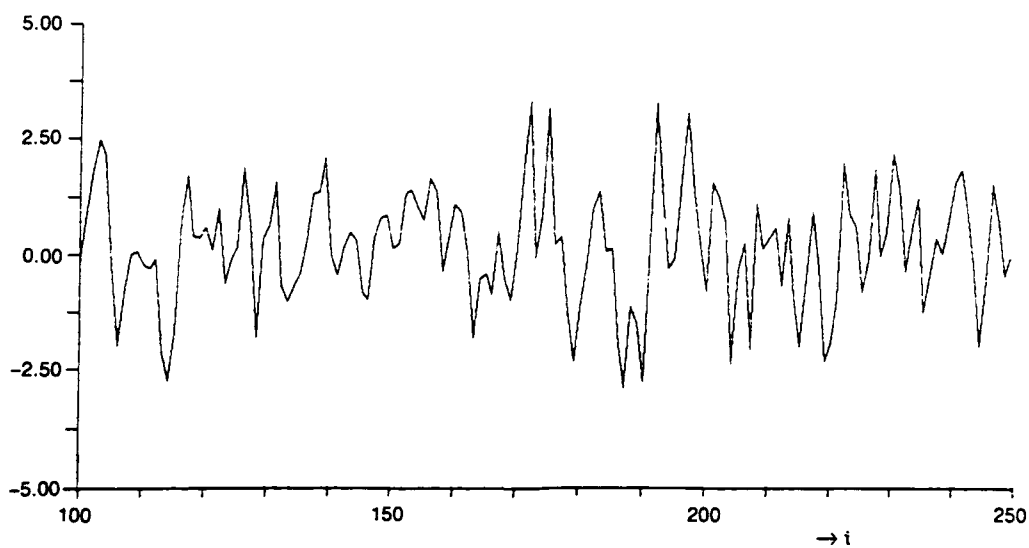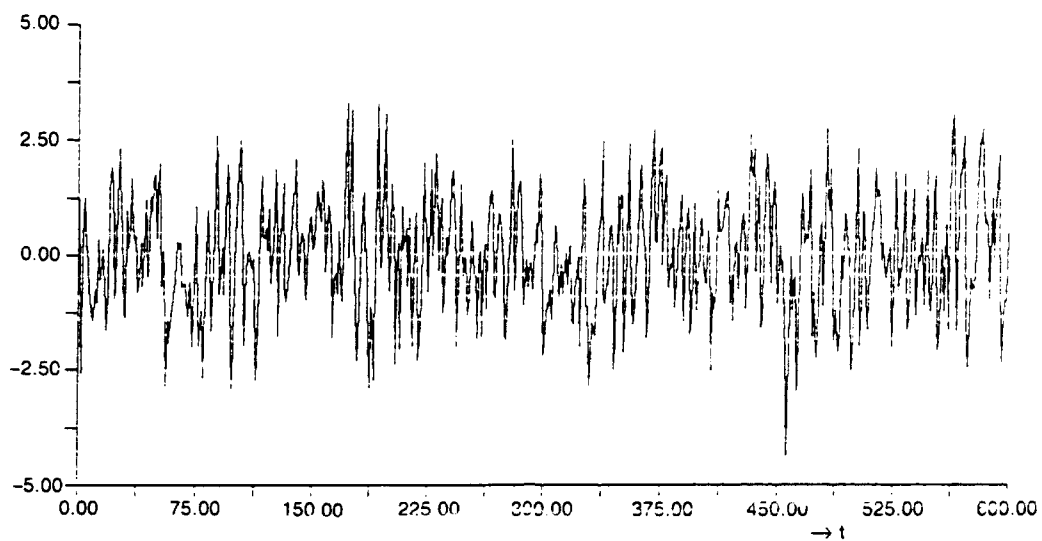
Fig. 5.38. Simulated MA(1) process (2) $X_t = \epsilon_t + 0.7\epsilon_{t-1}$, ϵ_t: N[0, 1].

171
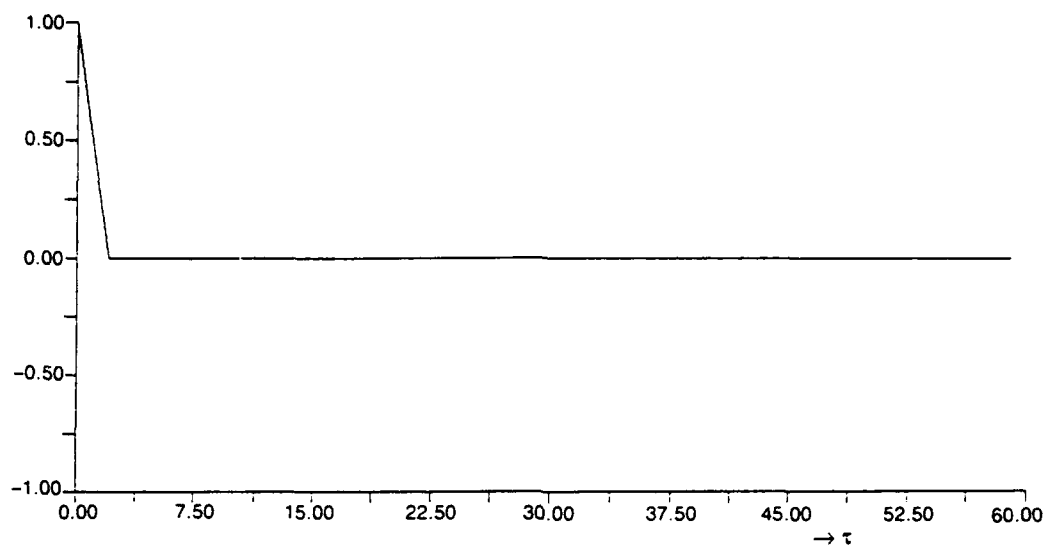
Fig. 5.39a. Theoretical.
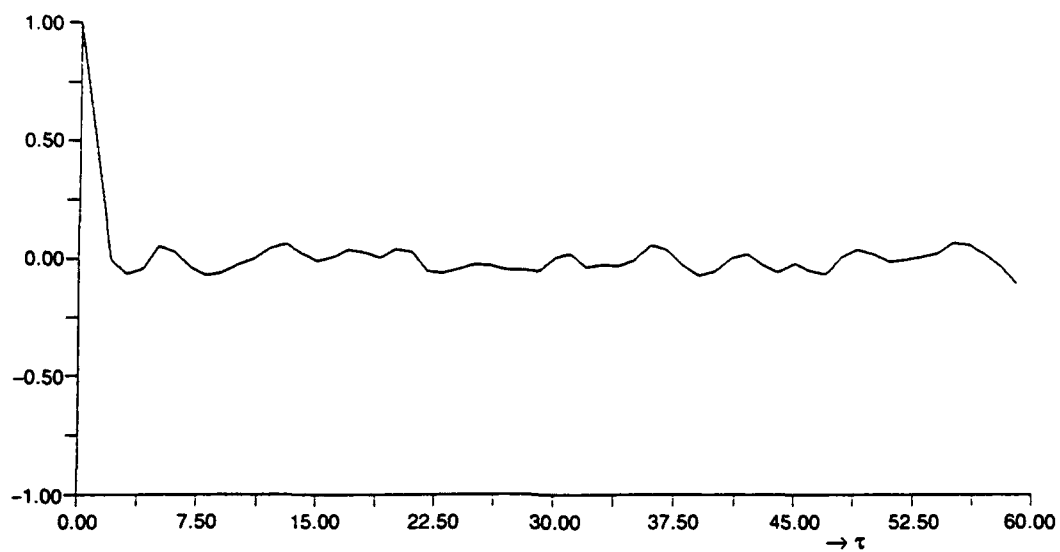
Fig. 5.39b. Estimated.

Fig. 5.39. Autocorrelation coefficient for MA(1) process (2)
$$X_t = \epsilon_t + 0.7\epsilon_{t-1}, \qquad \epsilon_t: N[0, 1].$$

172
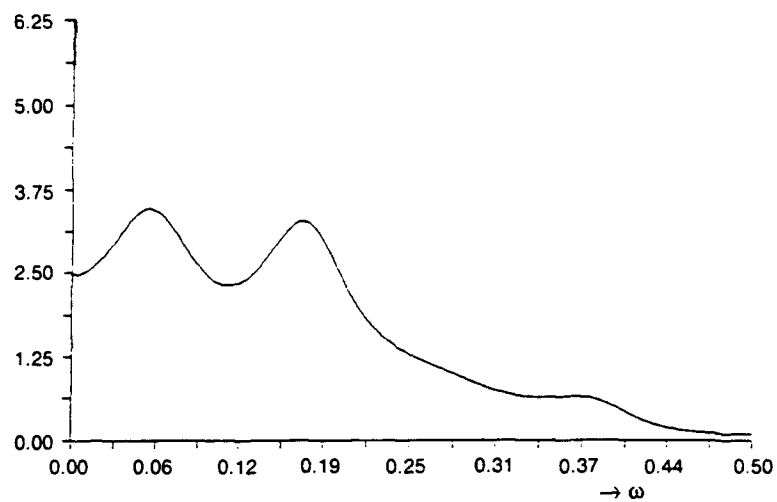
Fig. 5.40d. Estimated by AR model fitting, AR(8).

$\hat{b}_1 = 0.74320$

$\hat{\sigma}_\epsilon^2 = 1.0442$
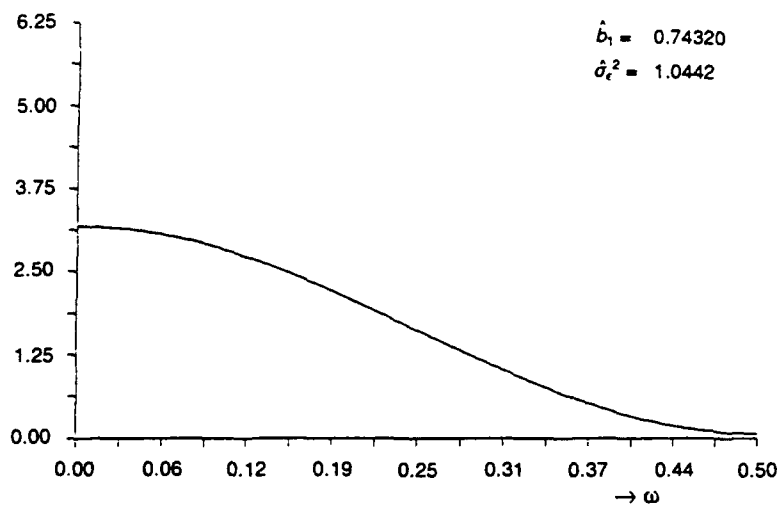
Fig. 5.40e. Estimate as MA(1) [not optimum].

Fig. 5.40. (Continued)

175

The values of parameters $\hat{b}_1$ (and b_2, a_1 if any) and of $\hat{\sigma}_\epsilon^2$ estimated, and also of estimated $\hat{a}_1 \cdots \hat{a}_n$ of AR(n) models are listed in Table 5.2. By comparing Fig. 5.37 and Fig. 5.40, we can find the difference of the pattern of the spectra by the difference of the sign of parameter b_1. The same tendency appears in the difference between Fig. 5.27 and Fig. 5.30. We can recognize this difference also in comparing the original form of the generated processes in Fig. 5.35 and Fig. 5.38, and Fig. 5.25 and Fig. 5.28.

Figures 5.41, 5.42, and 5.43 show the results for a generated ARMA(2.2) model. Its time history readings are listed in Appendix A1 as Table A1.9; pp. 251 and 260. The figures are the same as for the other examples, so no explanation will be given here. The estimated values of parameters $\hat{a}_n$, $\hat{b}_n$, and $\hat{\sigma}_\epsilon^2$ are listed in Table 5.2. The optimum m, n for a fitted ARMA(n,m) model appeared to be $n = 2$, $m = 2$ by AIC criteria for this case too. In this case $\hat{\sigma}_\epsilon^2$ appeared to be 0.84312, quite different from $\sigma_\epsilon^2 = 1.0$, but we could not find the reason or the error for their poor estimation.
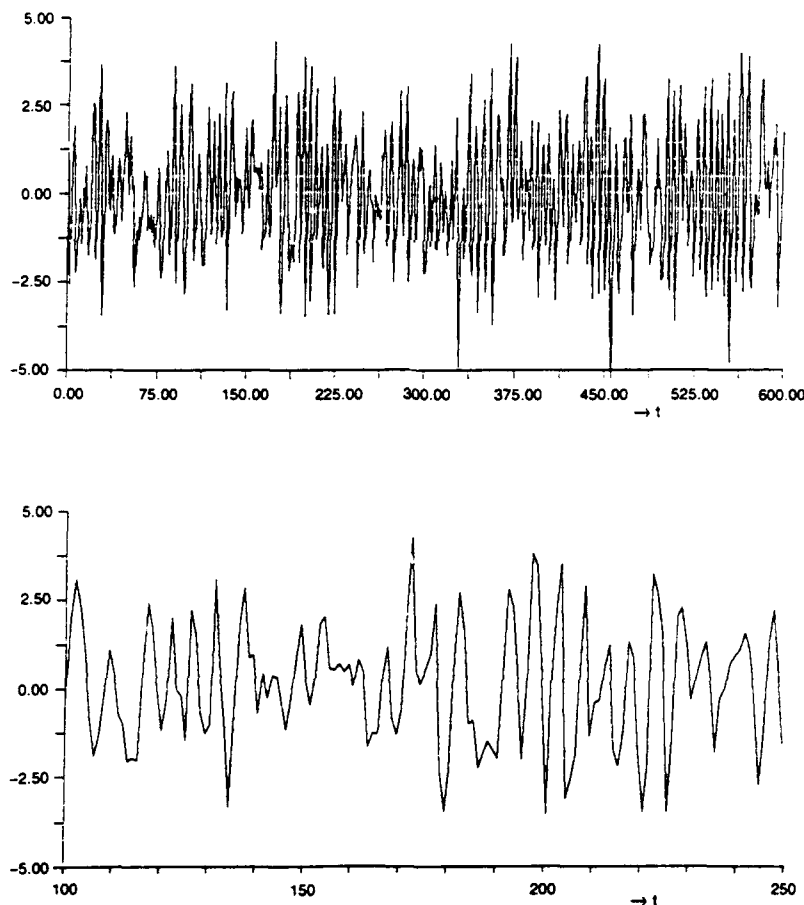
Fig. 5.41. Simulated ARMA(2.2) process

$$X_t - 0.5X_{t-1} + 0.8X_{t-2} = \epsilon_t + 0.2\epsilon_{t-1} + 0.8\epsilon_{t-2}, \quad \epsilon_t : N[0, 1].$$

176
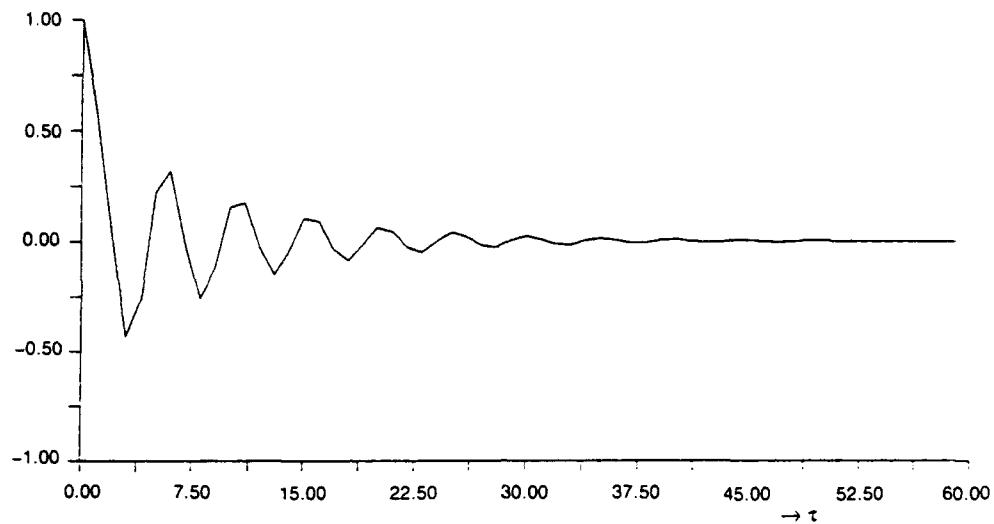
Fig. 5.42a. Theoretical.
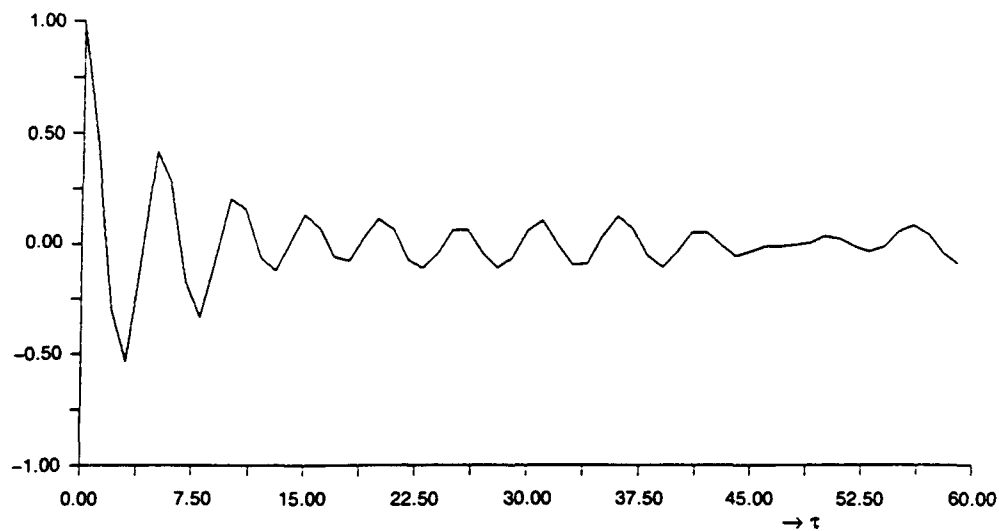
Fig. 5.42b. Estimated.

Fig. 5.42. Autocorrelation coefficient for ARMA(2.2) process
$$X_t - 0.5X_{t-1} + 0.8X_{t-2} = \epsilon_t + 0.2\epsilon_{t-1} + 0.8\epsilon_{t-2}, \quad \epsilon_t : N[0, 1].$$
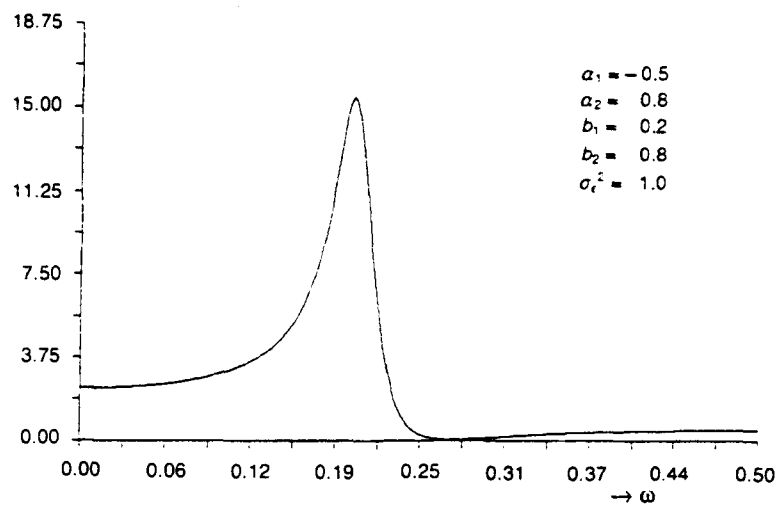
Fig. 5.43a. Theoretical ARMA(2.2).
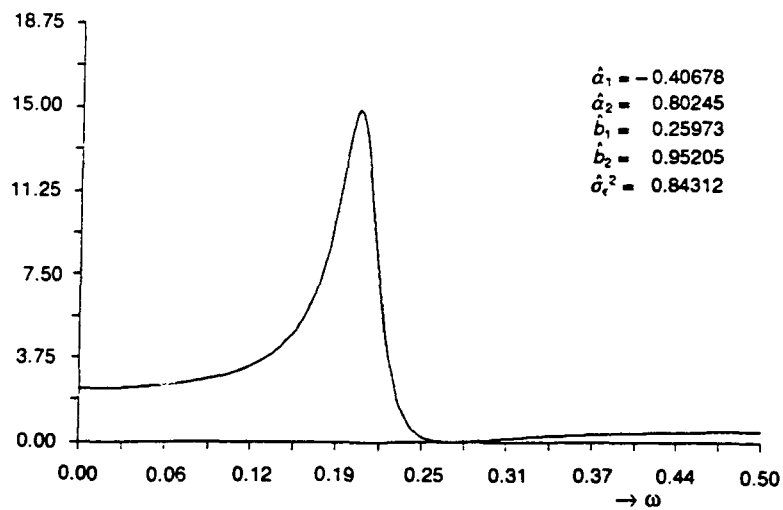
Fig. 5.43b. Estimated by ARMA model fitting as optimum, ARMA(2.2).

Fig. 5.43. Spectrum for ARMA(2.2) process

$$X_t - 0.5X_{t-1} + 0.8X_{t-2} = \epsilon_t + 0.2\epsilon_{t-1} + 0.8\epsilon_{t-2}, \quad \epsilon_t: N[0, 1].$$
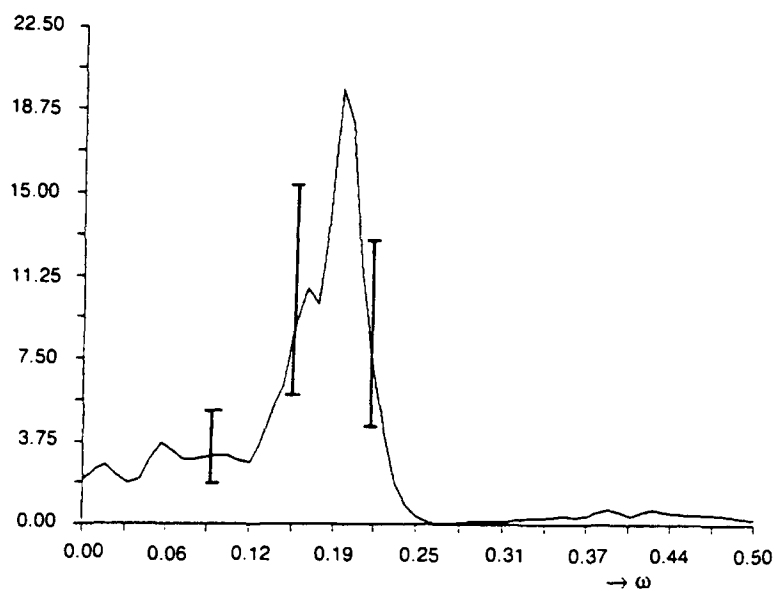
Fig. 5.43c. Estimated by nonparametric method.
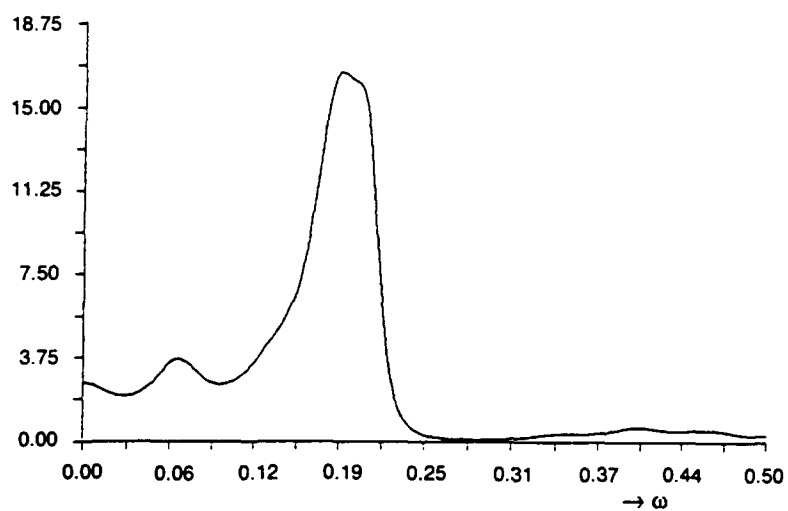
Fig. 5.43d. Estimated by AR model fitting, AR(15).

Fig. 5.43. (Continued)

179

Table 5.2. Results of estimation by model fitting —— [II].

Fig. No.	Process ARMA (n,m)		Generated	Readings in	Estimated as Optimum	Estimated Equivalent AR (N)
5.32	MA (2)	n	0		0	13
		m	2		2	0
		b_1	+ 0.2		0.18662	a_1 − 0.223 $\quad$ a_7 + 0.374 a_2 − 0.719 $\quad$ a_8 − 0.201 a_v − 0.278
		b_2	+ 0.8	A1.6	0.78000	a_3 + 0.334 $\quad$ a_{10} − 0.064 a_4 + 0.551 $\quad$ a_{11} + 0.167
						a_5 − 0.449 $\quad$ a_{12} + 0.001 a_6 − 0.301 $\quad$ a_{13} − 0.113
5.34	ARMA (0,2)	σ_ϵ^2	1.0		1.0816	σ_ϵ^2 : 1.05489
5.35	MA (1)	n	0		0	4
		m	1		1	0
	[Process (1)]			A1.7		
		b_1	− 0.7		− 0.70294	a_1 + 0.646 $\quad$ a_3 + 0.299 a_2 + 0.423 $\quad$ a_4 + 0.234
5.37	ARMA (0,1)	σ_ϵ^2	1.0		1.0478	σ_ϵ^2 : 1.04127
	MA (1)	n	0		0 $\left(\begin{array}{c}\text{NOT}\\\text{OPTIMUM}\end{array}\right)$	8
5.38		m	1		1	0
	[Process (2)]					
		b_1	+ 0.7		+ 0.74320	a_1 − 0.71964 a_2 + 0.49117
		σ_ϵ^2	1.0		1.0442	a_3 − 0.30087 a_4 + 0.26673
		n	0	A1.8	1	a_5 − 0.26548 a_6 − 0.18590
		m	1		2 $\;$ (OPTIMUM)	a_7 − 0.09790 a_8 + 0.08703
		(a_1)	0		+ 0.80208	
		b_1	+ 0.7		+ 1.5161	
		(b_2)	0		+ 0.55205	
5.40	ARMA (0,1)	σ_ϵ^2	1.0		1.0359	σ_ϵ^2 : 1.03356
		n	2		2	15
5.41	ARMA (2,2)	m	2		2	10
		a_1	− 0.5		− 0.40878	a_1 − 0.721 $\quad$ a_9 + 0.091 a_2 + 0.192 $\quad$ a_{10} − 0.252
		a_2	+ 0.8	A1.9	+ 0.80245	a_3 + 0.515 $\quad$ a_{11} − 0.015 a_4 − 0.190 $\quad$ a_{12} − 0.158
		b_1	+ 0.2		+ 0.25973	a_5 − 0.456 $\quad$ a_{13} + 0.015 a_6 + 0.361 $\quad$ a_{14} + 0.098
		b_2	+ 0.8		+ 0.95205	a_7 + 0.177 $\quad$ a_{15} + 0.105 a_8 − 0.237
5.43	ARMA (2,2)	σ_ϵ^2	1.0		0.84312	σ_ϵ^2 : 1.06480

5.2.5.4 ARMA(1,2) Process. The equation for the ARMA(1,2) process is

$$X_t + a_1 X_{t-1} = \epsilon_t + b_1 \ \epsilon_{t-1} + b_2 \ \epsilon_{t-2}, \tag{5.195}$$

or, using the backward shift operator,

$$(1 + a_1 B)X_t = (1 + b_1 B + b_2 B^2)\epsilon_t. \tag{5.195'}$$

Analogous to ARMA(2.1), the stationality is determined by the left-hand side of this equation, i.e., by the autoregression part. On the other hand, the invertibility is determined by the character of the right-hand side of Eq. 5.195'. Accordingly, the stationality is the same as for AR(1) and the invertibility is the same as for MA(2). Green's function, the inverse function, the autocovariance function, and the spectrum function can be obtained in the same way as for ARMA(2.1).

5.3 GENERAL ARMA(n,m) PROCESS

5.3.1 General ARMA(n,m) Process, Its Stationality and Invertibility

Analogous to the preceding section, when

$$X_t + a_1 X_{t-1} + a_2 X_{t-2} + \cdots + a_n X_{t-n} = \epsilon_t + b_1 \ \epsilon_{t-1} + b_2 \ \epsilon_{t-2} + \cdots + b_m \epsilon_{t-m},$$

$$\tag{5.196}$$

the process X_t is referred to as the nth order autoregressive, mth order moving average process, ARMA(n,m). When the backward shift operator B is used,

$$(1 + a_1 B + a_2 B^2 + \cdots + a_n \ B^n)X_t = (1 + b_1 B + b_2 \ B^2 + \cdots + b_m B^m)\epsilon_t \tag{5.196'}$$

$$\alpha(B)X_t = \beta(B)\epsilon_t, \tag{5.196''}$$

where

$$\alpha(Z) = 1 + a_1 Z + a_2 Z^2 + \cdots + a_n Z^n$$

$$\beta(Z) = 1 + b_1 Z + b_2 Z^2 + \cdots + b_m Z^m. \tag{5.197}$$

Green's function is derived from

$$X_t = \sum_{j=0}^{\infty} G_j \ \epsilon_{t-j} = \frac{\beta(B)}{\alpha(B)}\epsilon_t, \tag{5.198}$$

and the inverse function is derived as

$$\epsilon_t = \sum_{j=0}^{\infty} -I_j \ X_{t-j} = \frac{\alpha(B)}{\beta(B)}X_t. \tag{5.199}$$

By the same logic as we had for ARMA(2.1), for this process to be stable, the characteristic function

$$f_1(Z) = Z^n + a_1 Z^{n-1} + a_2 Z^{n-2} + \cdots + a_n \tag{5.200}$$

equated to 0, i.e., $f_1(Z) = 0$ must have all its roots $\mu_1, \mu_2, \cdots \mu_n$ inside the unit circle,

or $\alpha(Z) = 1 + a_1 Z + a_2 Z^2 + \cdots + a_n = 0$ must have all its roots outside the unit circle.

Conversely, for this process to be invertible, the characteristic function

181

$$f_2(Z) = Z^m + b_1 Z^{m-1} + b_2 Z^{m-2} + \cdots + b_m = 0 \qquad (5.201)$$

must have all its roots $\nu_1, \nu_2 \cdots \nu_m$ inside the unit circle or

$$\beta(Z) = 1 + b_1 Z + b_2 Z^2 + \cdots + b_m Z^m$$

must have all its roots outside the unit circle.

5.3.2 Green's Function for ARMA(n,m)

Green's function G_j is defined as

$$X_t = \sum_{j=0}^{\infty} G_j \, \epsilon_{t-j} = G_0 \, \epsilon_t + G_1 \, \epsilon_{t-1} + \cdots + G_j \, \epsilon_{t-j} + \cdots$$

$$= (G_0 + G_1 B + G_2 B^2 + \cdots + G_j \, B^j + \cdots) \epsilon_t.$$

Then Eq. 5.196' is

$$(1 + a_1 B + a_2 B^2 + \cdots + a_n B^n)(G_0 + G_1 B + G_2 B^2 + \cdots + G_j \, B^j + \cdots) \epsilon_t$$

$$= (1 + b_1 B + b_2 B^2 + \cdots + b_m \, B^m) \epsilon_t. \qquad (5.202)$$

Equating the same order of backward shifting operator B for both sides of Eq. 5.202,

$$G_0 = 1$$
$$a_1 G_0 + G_1 = b_1$$
$$a_2 G_0 + G_1 a_1 + G_2 = b_2$$
$$\cdots$$
$$a_m G_0 + G_1 a_{m-1} + G_2 a_{m-2} + \cdots + G = b_m.$$
$$a_k G_0 + G_1 a_{k-1} + G_2 a_{k-2} \cdots + G_k = 0 \qquad \text{for } k > m, \qquad (5.203)$$

or

$$G_0 = 1$$
$$G_1 = b_1 - a_1$$
$$G_2 = b_2 - (b_1 - a_1)a_1 - a_2$$
$$\cdots$$
$$G_m = b_m \cdots - a_m. \qquad (5.204)$$

Explicitly Green's function can be obtained through the solution of the homogeneous equation

$$X_t + a_1 X_{t-1} + a_2 X_{t-2} + \cdots a_n \, X_{t-n} = 0 \qquad (5.205)$$

with initial conditions given by Eq. 5.204, that is, in the form

$$G_j = g_1 \, \mu_1^j + g_2 \, \mu_2^j + \cdots + g_n \, \mu_n^j \qquad (5.206)$$

where $\mu_1, \mu_2 \cdots \mu_n$ are the eigenvalues or the roots of the characterization equation

$$f_1(Z) = Z^n + a_1 Z^{n-1} + a_2 Z^{n-2} + \cdots a_n = 0.$$

Especially when $m = n - 1$, namely for ARMA$(n, n - 1)$, by Pandit and Wu[36]

$$g_i = \frac{(\mu_i^{n-1} + b_1\mu_i^{n-2} + \cdots + b_{n-1})}{(\mu_i - \mu_1)(\mu_i - \mu_2) \cdots (\mu_i - \mu_{i-1})(\mu_i - \mu_{i+1}) \cdots \mu_i - \mu_n)}$$

$$i = 1, 2, \cdots n \qquad (5.207)$$

where the denominator is the product of all terms $(\mu_i - \mu_j)$ for $j = 1, 2, \cdots n$, excluding the zero term $(\mu_i - \mu_i)$. Equations 5.135 and 5.136 are the special cases $j = 1$ and 2 for $n = 2$. Each real root μ_j in Eq. 5.206 provides an exponentially dynamic mode like an AR(1) model, whereas a complex conjugate pair of roots as in Eq. 5.137' gives an exponentially decaying sinusoidal mode, whose frequency and decay rate can be obtained as Eqs. 5.140 and 5.139 illustrated in Fig. 5.24 in Section 5.2.4.

5.3.3 Autocovariance and Spectrum Function of ARMA(n,m)

For the ARMA(n,m) process,

$$X_t = -a_1 X_{t-1} - a_2 X_{t-2} - \cdots a_n X_{t-n} + \epsilon_t + b_1 \epsilon_{t-1} + b_2 \epsilon_{t-2} + \cdots + b_m \epsilon_{t-m}.$$

Here, taking into account the relations

$$X_t = \sum G_j \epsilon_{t-j} = G_0 \epsilon_t + G_1 \epsilon_{t-1} + G_2 \epsilon_{t-2} + \cdots + G_j \epsilon_{t-j} + \cdots$$

$$X_{t-r} = \sum G_j \epsilon_{t-r-j} = G_0 \epsilon_{t-r} + G_1 \epsilon_{t-r-1} + G_2 \epsilon_{t-r-2} + \cdots + G_j \epsilon_{t-r-j} + \cdots$$

$$E[\epsilon_t \cdot \epsilon_{t-r}] = \delta_r \sigma_\epsilon^2 ,$$

multiplying both sides of these upper two equations term by term, respectively, and taking the expected values gives,
when $r = 0$,

$$R(0) = -a_1 R(1) - a_2(R)(2) - \cdots - a_n R(n) + (G + b_1 G_1 + b_2 G_2 + \cdots b_m G_m)\sigma_\epsilon^2$$

when $r = 1$,

$$R(1) = -a_1 R(0) - a_2 R(1) - a_3 R(2) - \cdots - a_n R(n-1)$$
$$+ (b_1 G_0 + b_2 G_1 + b_3 G_2 + \cdots + b_m G_{m-1})\sigma_\epsilon^2$$

$$R(2) = \cdots \cdots \cdots$$

when $r = m$,

$$R(m) = -a_1 R(m-1) - a_2 R(m-2) + \cdots a_n R(m-n)$$
$$+ b_m G_0 \sigma_\epsilon^2$$

and

$$R(k) = -a_1 R(k-1) - a_2 R(k-2) + \cdots + a_n R(k-n), \quad k \geq m + 1. \qquad (5.208)$$

Analogous to the case of ARMA(2.1), $R(0)$ to $R(k), k \leq n + 1$, can be obtained by solving these simultaneous equations. Also, if necessary, we can get the general expression for $R(r), k \geq m + 1$, by generalizing the case of ARMA(2.1). By the same procedure we used for ARMA(2.1), the spectrum $s(\omega)$ for the ARMA(n,m) process is naturally

183

obtained as

$$s(\omega) = \frac{\sigma_\epsilon^2 \left| \beta(e^{-i\omega}) \right|^2}{2\pi \left| \alpha(e^{-i\omega}) \right|^2} \tag{5.209}$$

$$= \frac{\sigma_\epsilon^2}{2\pi} \frac{\left| 1 + b_1 e^{-i\omega} + b_2 e^{-2i\omega} + \cdots + b_m e^{-m i \omega} \right|^2}{\left| 1 + a_1 e^{-i\omega} + a_2 e^{-2i\omega} + \cdots + a_{i,2}^{-n i \omega} \right|^2}. \tag{5.209'}$$

5.3.4 Estimation of $a_1 \ldots a_n$, $b_1 \ldots b_n$ of ARMA(n,m)

For starting values of $a_1 \cdots a_n$, $b_1 \cdots b_n$, we can get a first approximation of the estimates from Eq. 5.208. Namely, with the use of n simultaneous equations on

$$R(m+1), \quad R(m+2) \cdots R(m+n) \quad \text{for } k \geq m+1$$

autoregressive parameters $a_1, a_2, \cdots a_n$ can be estimated, although the less reliable values of autocorrelation at larger $m + n$ must be used. Then, inserting these values in the first $(m + 1)$ equations in Eq. 5.208 on $R(0), R(1) \cdots R(m)$, $m + 1$ unknown parameters $b_1 \cdots b_m$ and σ_ϵ^2 can be estimated theoretically by solving the nonlinear equations on these parameters.

The necessity for solving nonlinear equations can be shown as follows: In the expression for ARMA(n,m)

$$X_t + a_1 X_{t-1} + a_2 X_{t-2} + \cdots + a_n X_{t-n} = \epsilon_t + b_1 \epsilon_{t-1} + \cdots + b_m \epsilon_{t-m},$$

using recursively

$$\epsilon_{t-1} = X_{t-1} + a_1 X_{t-2} + a_2 X_{t-3} + \cdots + a_{n-1} X_{t-n} + a_n X_{t-n-1}$$

$$- b_1 \epsilon_{t-2} - b_2 \epsilon_{t-3} - \cdots - b_m \epsilon_{t-m-1}$$

in

$$X_t = -a_1 X_{t-1} - a_2 X_{t-2} \cdots - a_n X_{t-n}$$
$$+ b_1 \epsilon_{t-1} + b_2 \epsilon_{t-2} \cdots + b_m \epsilon_{t-m} + \epsilon_t,$$

$$X_t = (-a_1 + b_1) X_{t-1} + (-a_2 - a_1 b_1) X_{t-2} + \cdots + (-a_n - a_{n-1} b_1) X_{t-n} - a_n b_1 X_{t-n-1}$$

$$+ (b_1^2 - b_2) \epsilon_{t-2} + (b_1 b_2 - b_3) \epsilon_{t-3} + \cdots + b_1 b_m \epsilon_{t-m-1} + \epsilon_t. \tag{5.210}$$

We still have the terms $\epsilon_{t-2}, \epsilon_{t-3} \cdots$ that should be expressed by X_{t-2}, $X_{t-3} \cdots$ and also $\epsilon_{t-2}, \epsilon_{t-3}$. When the dependence of X_t is expressed in terms of past X_t, the equation will be nonlinear in the unknown parameters $a_1, a_2 \cdots$ and $b_1, b_2, \cdots$, because their products and squares are involved. Thus, the regression becomes nonlinear and requires a nonlinear least squares method for estimation.

Actually, however, it is troublesome to solve the nonlinear equations, and other approximation methods are used. An approximation method introduced by Pandit and Wu[36] is to use the inverse function, taking advantage of the linearity between the unknown coefficient and the inverse function as shown in Eq. 5.150 for ARMA(2.1). In this method, we first fit the pure autoregressive model of an appropriate large order AR(k) to this ARMA(n,m) process and then use the coefficients of this AR(k) model as an approximation for inverse functions at larger values of k. Then from the equation that connects b_j and I_j, we can gradually improve the approximation of b_j and a_j and finally adjust the results from the viewpoint of invertibility. The procedure is rather complicated, and care is necessary to get good estimates. In any case estimation of the coefficients for ARMA (n,m) is not necessarily easy.

Estimation of the parameters for the pure autoregressive process AR(n) is more straightforward, as we saw for AR(2) in Section 5.2.3 or as will be shown in Section 5.4, since it can be done through linear regression.

In practical applications of the model fitting technique, the pure autoregressive process AR(k) is frequently used as the model to be fitted, although the order k sometimes becomes a little larger than n of ARMA(n,m), which should be the actual model to be fitted to the process under consideration. We saw this tendency in examples of ARMA(2.1), MA(2), MA(1), and ARMA(2. 2) shown in Figs. 5.27, 5.30, 5.34, 5.37, 5.40, and 5.43.

5.3.5 Adoption of ARMA(n, n − 1), ARMA(2n, 2n −1)

As was mentioned in Sections 5.2.2 and 5.2.4, Green's functions and the autocovariance functions are in the form for AR(1): $G_j = a^j = \mu^i$; $R(r) = B\mu^j$ and for ARMA(2.1):

$G_j = g_1 \mu_i^j + g_2 \mu_2^j$; $R(r) = B\mu_1^j + B_2 \mu_2^j$, and show increasing complexity as the order increases. For AR(2), as derived in Section 5.2.3, G_j and $R(r)$ were of the same type as those for ARMA(2.1). However, as was mentioned in Section 5.2.4, ARMA(2.1) is recommended by Pandit and Wu[36] as a more general process that is made up of two exponentials. The other reason for preferring ARMA(2.1) over AR(2) is the fact that the ARMA(2.1) process is more closely related to the system that is governed by the second order differential equation, as will be explained in Section 6.3.2. In the same way, for a more complex process made up of three exponentials, AR(3.2) is the most general process. Extending this relation, ARMA(n, $n-1$) is recommended by Pandit and Wu[36] as the most general process when the process is represented by nth order dynamics as

$$G_j = g_1 \mu_1^j + g_2 \mu_2^j + \cdots + g_n \mu_n^j \; ; \quad R(r) = B_1 \mu_j^j + B_2 \mu_2^j + \cdots B_n \mu_n^j.$$

The reason that $n - 1$ should be the order of the moving average part is also shown in Pandit and Wu.[36] Furthermore, as they pointed out, empirical experience indicates that it is better to increase n in steps of two and fit ARMA($2n$, $2n - 1$) models for $n = 1, 2, 3$.

Also, if a complex root appears among μ_j, and $a_1, a_2 \cdots$ are to be real, complex roots must appear as conjugate pairs as was shown for ARMA(2.1) in Section 5.2.4. Therefore to fit an ARMA($2n$, $2n - 1$) model is more practical than to fit an odd order model.

185

5.4 GENERAL AUTOREGRESSIVE PROCESS AR(n)

5.4.1 Adoption of AR(n) Model

The general autoregressive model

$$X_t + a_1 X_{t-1} + a_2 X_{t-2} + \cdots + a_n = \epsilon_t \qquad (5.211)$$

is considered to be a special case of the general autoregressive moving average model ARMA(n,m) when $m = 0$. If invertibility is satisfied for the ARMA(n,m) model,

$$\epsilon_t = \left(\sum_{j=0}^{\infty} -I_j B^j \right) X_t$$

$$= X_t - I_1 X_{t-1} - I_2 X_{t-2} - \cdots - I_j X_t - \cdots.$$

This expression means that ARMA(n,m) is transformed into an autoregressive model of infinite order AR(∞). Practically, if a large enough n is taken, almost all of the ARMA (n,m) process can be approximated by an AR(n') process if we assume invertibility.

The general character of the AR(n) process will be summarized here, as AR(n) is the most common model used in the practical application of model fitting techniques as was already mentioned in Section 5.3.4. The estimation of parameters is much easier for the AR(n) process than for the MA(m) or AR(n,m) processes.

5.4.2 Green's Function of AR(n)

The AR(n) process is expressed as

$$X_t + a_1 X_{t-1} + a_2 X_{t-2} + \cdots + a_n = \epsilon_t \qquad (5.211)$$

$$(1 + a_1 B + a_2 B^2 + \cdots + a_n B^n) X_t = \epsilon_t \qquad (5.211')$$

$$\alpha(B) X_t = \epsilon_t. \qquad (5.211'')$$

Here

$$\alpha(Z) = 1 + a_1 Z + a_2 Z^2 + \cdots a_n Z^n. \qquad (5.212)$$

Using Green's function G_j gives

$$X_t = \sum_{j=0}^{\infty} G_j \epsilon_{t-j} = \left(\sum_{j=0}^{\infty} G_j B^j \right) \epsilon_t = G_o + G_1 \epsilon_{t-1} + G_2 \epsilon_{t-2} + \cdots + G_j \epsilon_{t-j}$$

$$= (G_o + G_1 B + G_2 B^2 + \cdots + G_j B^j + \cdots) \epsilon_t \qquad (5.213)$$

$$= \frac{\epsilon_t}{(1 + a_1 B + a_2 B^2 + \cdots + a_n B^n)}. \qquad (5.213')$$

Equating the same power of B on both sides,

$$G_o = 1$$

$$G_o a_1 + G_1 = 0$$

$$a_2 G_o + a_1 G_1 + G_2 = 0$$

$$a_3 G_o + a_2 G_1 + a_1 G_2 + G_3 = 0 \qquad (5.214)$$

$$\cdots \cdots$$

$$a_n G_o + a_{n-1} G_1 + \cdots + G_n = 0,$$

or

$$G_1 = -a_1$$

$$G_2 = -a_2 + a_1^2$$

$$G_3 = -a_3 + a_2 a_1 + a_1(a_2 - a_1^2) = -a_3 + 2a_1 a_2 - a_1^3. \qquad (5.215)$$

$$\cdots \cdots \cdots \cdots$$

Generally

$$(a_n B^n + \cdots + 1) G_n = 0.$$

Explicitly as shown in Section 5.3.2

$$G_j = g_1 \mu_1^j + g_2 \mu_2^j + \cdots + g_n \mu_n^j \qquad (5.216)$$

where $\mu_1 \cdots \mu_n$ are the eigenvalues or the roots of the characteristic equation equated to zero as

$$f_1(z) = z^n + a_1 z^{n-1} + \cdots + a_n = 0 \qquad (5.217)$$

and

$$g_i = \frac{\mu_i^{n-1}}{(\mu_i - \mu_1)(\mu_1 - \mu_2) \cdots (\mu_i - \mu_{i-1})(\mu_i - \mu_{i+1}) \cdots (\mu_i - \mu_n)} \qquad (5.218)$$

where the denominator is the product of all terms $\mu_i \cdots \mu_j$ for $j = 1, 2 \cdots n$, excluding the zero term $\mu_i - \mu_i$, as the special case where $b_1 \equiv b_2 \equiv b_3 \equiv \cdots \equiv b_m \equiv 0$ in Eq. 5.207.

5.4.3 Autocorrelation and Spectrum Function for AR(n)

For AR(n)

$$X_t = -a_1 X_{t-1} - a_2 X_{t-2} \cdots - a_n X_{t-n} + \epsilon_t.$$

Therefore

$$X_{t-r} = -a_1 X_{t-r-1} - a_2 X_{t-r-2} - \cdots - a_n X_{t-r-n} + \epsilon_{t-r}. \qquad (5.219)$$

Multiplying both sides of these two equations, respectively, taking the expected values gives

$$R(0) = -a_1 R(1) - a_2 R(2) \cdots - a_n \ R(n) + \sigma_\epsilon^2$$

$$R(1) = -a_1 R(0) - a_2 R(1) \cdots - a_n R(n-1) \cdot$$

$$\cdot$$

$$\cdot \qquad\qquad\qquad\qquad\qquad (5.220)$$

$$\cdot$$

$$R(k) = -a_1 R(k-1) - a_2 R(k-2) \cdots - a_n R(k-n)$$

$$k = 1 \cdots n.$$

Using the backward shift operator B gives

$$B^j R(k) = R(k-j). \qquad\qquad (5.221)$$

Then the last equation in Eq. 5.220 is

$$R(k) = \left(\sum_{j=1}^{n} -a_j \ B^j \right) R(k) \qquad\qquad (5.222)$$

or

$$\sum_{j=0}^{n} (a_j \ B^j) R(k) = 0. \qquad\qquad (5.222')$$

Equation 5.222 is very similar to the expression of the homogeneous equation of the process itself in Eqs. 5.211', 5.211'' when $\epsilon_t = 0$ as

$$\alpha(B) R(k) = 0. \qquad\qquad (5.222'')$$

Therefore, as was Eq. 5.166 for AR(2), the general form of $R(k)$ is

$$R(k) = B_1 \ \mu_1^k + B_2 \ \mu_2^k + \cdots + B_n \ \mu_n^k. \qquad\qquad (5.223)$$

Here $\mu_1, \mu_2 \cdots \mu_n$ are the eigenvalues, and $B_1, B_2, \cdots B_n$ are constants that can be obtained theoretically from the boundary conditions

$$R(0) = B_1 + B_2 + \cdots + B_n$$

$$R(1) = B_1 \ \mu_1 + B_2 \ \mu_2 + \cdots + B_n \ \mu_n$$

$$\cdot$$

$$\qquad\qquad\qquad\qquad\qquad (5.224)$$

$$\cdot$$

$$\cdot$$

The spectrum is, as given by Eq. 5.209,

$$s(\omega) = \frac{\sigma_\epsilon^2}{2\pi \ \left| \alpha(e^{-i\omega}) \right|^2} = \frac{\sigma_\epsilon^2}{2\pi \ \left| 1 + a_1 e^{-i\omega} + a_2 e^{-2i\omega} + \cdots + a_n e^{-ni\omega} \right|^2}. \qquad (5.225)$$

5.4.4 Estimation of Parameter $a_1 \ldots a_n$ and μ

In this section, we assume that the order n of the autoregressive process $AR(n)$ is already known. Determination of the order n is discussed in the next section. Here the statistical considerations for the estimation are treated in some detail, compared with the case for $AR(2)$ in Section 5.2.3. As the most general type of $AR(n)$ process, we assume the nonzero mean process to be

$$(X_t - \mu) + a_1(X_{t-1} - \mu) + a_2(X_{t-2} - \mu) + \cdots + a_n(X_{t-n} - \mu) = \epsilon_t. \tag{5.226}$$

By analogy with the multivariate regression of X_t with $X_{t-1} \cdots X_{t-n}$, with regressive coefficients $a_1, a_2 \cdots a_n$ and residual error ϵ_t, we can use the least squares method to estimate $a_1 \cdots a_n$, μ, and ϵ_t, that is, to minimize

$$Q(\mu_1, a_1 \cdots a_n) = \sum_{t=n+1}^{N} \epsilon_t^2$$

$$= \sum_{t=n+1}^{N} \left\{ (X_t - \mu) + a_1(X_{t-1} - \mu) + \cdots + a_n(X_{t-n} - \mu) \right\}^2. \tag{5.227}$$

The reason for this lower limit $n + 1$ is that we do not have observations X_0, $X_{-1}, \cdots X_{-(n-1)}$ from which to derive $\epsilon_o, \cdots \epsilon_n$. N is the total number of observations of X_t. The residual error ϵ_t is assumed to be Gaussian and independent of each other. Accordingly, the joint probability distribution of $\epsilon_{n+1} \cdots \epsilon_n$ is

$$p(\epsilon_{n+1}, \epsilon_{n+2} \cdots \epsilon_N) = \left(\frac{1}{\sqrt{2\pi}\sigma_\epsilon} \right)^{N-n} \prod_{t=n+1}^{n} e^{-\frac{\epsilon_t}{2\sigma_\epsilon^2}}$$

$$= \left(\frac{1}{\sqrt{2\pi}\sigma_\epsilon} \right)^{N-n} \exp\left[\frac{-1}{2\sigma_\epsilon^2} \sum_{t=n+1}^{N} \epsilon_t^2 \right] \tag{5.228}$$

$$= \left(\frac{1}{\sqrt{2\pi}\sigma_\epsilon} \right)^{N-n} \exp\left[\frac{-1}{2\sigma_\epsilon^2} Q(\mu, a_1, a_2 \cdots a_n) \right]. \tag{5.229}$$

Here the variables are transformed from $(\epsilon_{n+1}, \epsilon_{n+2} \cdots \epsilon_n)$ to $(X_{n+1}, X_{n+2}, \cdots X_N)$ using

$$
\begin{bmatrix}
\epsilon_{n+1} = (X_{n+1}-\mu)+a_1(X_n-\mu)+a_2(X_{n-1}-\mu)\cdot\ \cdot\ \cdot+a_n(X_1-\mu) \\
\epsilon_{n+2} = (X_{n+2}-\mu)+a_1(X_{n+1}-\mu)+a_2(X_n-\mu)+\cdot\ \cdot\ \cdot+a_n(X_2-\mu) \\
\cdot \\
\cdot \\
\cdot \\
\epsilon_N = (X_N-\mu)+a_1(X_{N-1}-\mu)+a_2(X_{N-2}-\mu)+\cdot\ \cdot\ \cdot+a_n(X_{N-n}-\mu).
\end{bmatrix}
\quad (5.230)
$$

From Eq. 5.230 the Jacobian to transform $p(\epsilon_{n+1},\epsilon_{n+2}\cdot\ \cdot\ \cdot\epsilon_N)$ to $p(X_{n+1},X_{n+2}\cdot\ \cdot\ \cdot X_N)$ is

$$
J = \frac{\partial(\epsilon_{n+1}\,\epsilon_{n+2}\cdot\ \cdot\ \cdot\ \epsilon_N)}{\partial(X_{n+1}\ X_{n+2}\cdot\ \cdot\ \cdot X_N)} = 1.
\quad (5.231)
$$

Therefore from Eq. 5.229,

$$
p(X_{n+1}, X_{n+2},\cdot\ \cdot\ \cdot X_N) = \left(\frac{1}{\sqrt{2\pi}\,\sigma_\epsilon}\right)^{N-n} \times
$$

$$
\exp-\frac{1}{2\sigma_\epsilon^2}\sum_{t=n+1}^{N}\left\{(X_t-\mu)+a_1(X_{t-1}-\mu)+\cdot\ \cdot\ \cdot+a_n(X_{t-n}-\mu)\right\}^2
$$

$$
= \left(\frac{1}{\sqrt{2\pi}\,\sigma_\epsilon}\right)^{N-n}\exp\left[\frac{-1}{2\sigma_\epsilon^2}\left\{Q(\mu_1,a_1,a_2\cdot\ \cdot\ \cdot a_n)\right\}\right].
\quad (5.232)
$$

This is actually the conditional joint distribution, given that the initial observations $X_1\cdot\ \cdot\ \cdot X_n$ remain fixed at their realization $X_1\cdot\ \cdot\ \cdot X_n$. Here n is assumed to be relatively small compared with the number of observations N. We can then use this $p(X_{n+1},\cdot\ \cdot\ \cdot X_N)$ as the adequate approximation of likelihood function of $\mu_1,a_1,a_2\cdot\ \cdot\ \cdot a_n$, given the observations $X_1, X_2\cdot\ \cdot\ \cdot\ X_N$. Then the log–likelihood function L is

$$
L(\mu_1,a_1,a_2,\cdot\ \cdot\ \cdot a_n) = \log\ p(X_{n+1},X_{n+2},\cdot\ \cdot\ \cdot X_N)
$$

$$
= \frac{-(N-n)}{2}\log(2\pi\ \sigma_\epsilon^2)-\frac{1}{2\sigma_\epsilon^2}\sum_{t=n+1}^{N}\left\{(X_t-\mu)+a_1(X_{t-1}-\mu)+\cdot\ \cdot\ \cdot+a_n(X_{t-n}-\mu)\right\}^2.
$$
$$
(5.233)
$$

Therefore the maximum likelihood estimate for $\mu_1 a_1\cdot\ \cdot\ \cdot a_n$ is to maximize L, i.e., to minimize

$$
Q(\mu_1,a_1,a_2\cdot\ \cdot\ \cdot a_n) = \sum_{t=n+1}^{N}\left\{(X_t-\mu)+a_1(X_{t-1}-\mu)+\cdot\ \cdot\ \cdot+a_n(X_{t-n}-\mu)\right\}^2.
\quad (5.234)
$$

190

This is the same as adopting the least squares estimate as already mentioned. That is obtained from

$$\frac{\partial Q}{\partial \mu} = 0$$

and

$$\frac{\partial Q}{\partial a_j} = 0 \qquad j = 1, \cdots n$$

as

$$\sum_{t = n+1}^{N} \left\{ (X_t - \mu) + a_1(X_{t-1} - \mu) + \cdots + a_n(X_{t-n} - \mu) \right\} = 0 \qquad (5.235)$$

and

$$\sum_{t = n+1}^{N} \left\{ (X_t - \mu) + a_1(X_{t-1} - \mu) + \cdots + a_j(X_{t-j} - \mu) \cdots + a_n(X_{t-n} - \mu) \right\}(X_{t-j} - \mu) = 0. \qquad (5.236)$$

From Eq. 5.235

$$\hat{\mu} = \frac{\overline{X}_o + \hat{a}_1 \overline{X}_1 + \hat{a}_2 \overline{X}_2 \cdots + a_n \overline{X}_n}{1 + \hat{a}_1 + \hat{a}_2 + \cdots + \hat{a}_n}, \qquad (5.237)$$

where

$$\overline{X}_j = \frac{1}{N-n} \sum_{t = n+1}^{N} X_{t-j} \quad j = o, \cdots n.$$

When n is small compared to N_1, $\overline{X}_j$ will be close to $\overline{X} = \frac{1}{N}\sum_{t-1}^{N} X_t$ and Eq. 5.237 will be

$$\hat{\mu} = \overline{X}. \qquad (5.238)$$

From Eq. 5.236

$$\sum_{t = n+1}^{N} \left\{ (X_t - \overline{X}) + \hat{a}_1(X_{t-1} - \overline{X}) + \cdots + \hat{a}_j(X_{t-j} - \overline{X}) \cdots + \hat{a}_n(X_{t-n} - \overline{X}) \right\} \times$$

$$\left\{ (X_{t-j} - \overline{X}) \right\} = 0, \qquad j = 1, \cdots n.$$

Here, if we approximate further, under the assumption that k is also small in relation to N, then

$$\sum_{t = n+1}^{N} (X_{t-k} - \overline{X})(X_{t-j} - \overline{X}) = N\hat{R}(j - k),$$

and Eq. 5.236 becomes

191

$$\hat{R}(j) + a_1\hat{R}(j-1) + \cdots a_j\hat{R}(0) \cdots + a_n\hat{R}(j-n) = 0 \qquad (5.239)$$
$$j = 1 \cdots n.$$

From this relation $\hat{a}_1, \hat{a}_2, \cdots \hat{a}_j \cdots \hat{a}_n$ can be estimated by solving the simultaneous equations

$$\begin{cases} a_1\hat{R}(0) + a_2\hat{R}(1) + \cdots a_n\hat{R}(n-1) = -\hat{R}(1) \\ a_1\hat{R}(1) + a_2\hat{R}(0) + \cdots + a_n\hat{R}(n-2) = -\hat{R}(2) \\ \cdot \\ \cdot \\ \cdot \\ a_1\hat{R}(n-1) + a_2\hat{R}(n-2) + \cdots + a_n\hat{R}(0) = -\hat{R}(n). \end{cases} \qquad (5.240)$$

This can be transformed, using the vector expression, to

$$(a_1, a_2, \cdots a_n)' = \hat{a} \qquad (5.241)$$

$$\left\{ \hat{R}(1)\hat{R}(2) \cdots \hat{R}(n) \right\}' = r \qquad (5.242)$$

$$\hat{R}_n = \begin{bmatrix} \hat{R}(0) & \hat{R}(1) \cdots \hat{R}(n-1) \\ \hat{R}(1) & \hat{R}(0) \cdots \hat{R}(n-2) \\ \cdot & \cdot \\ \cdot & \cdot \\ \cdot & \cdot \\ \hat{R}(n-1) & \hat{R}(n-2) \quad \hat{R}(0) \end{bmatrix} \qquad (5.243)$$

$$\hat{R}_n \cdot \hat{a} = -r. \qquad (5.244)$$

Therefore

$$\hat{a} = \frac{-r}{\hat{R}_n}. \qquad (5.245)$$

Equation 5.239 or 5.240 is identical with the Yule–Walker equations.

All these relations mean that, if the approximations as given here are introduced, the maximum likelihood method can be replaced by the least squares method, and the least squares method is reduced to get the solution of the Yule–Walker equations. Priestley[23] describes in more detail the precise estimation through a rigorous likelihood function.

5.4.5 Estimation of σ_ϵ^2 for AR(n)

σ_ϵ^2 is estimated as the variance of the residual error ϵ_t from $Q = \sum_{t=n+1}^{N} \epsilon_t^2$.

Because $(N - n)$ observations are summed and $n + 1$ parameters (μ and na_j's) have been estimated, the unbiased estimation is

$$\hat{\sigma}_\epsilon^2 = \frac{1}{(N-n)-(n+1)} Q(\hat{\mu}, \hat{a}_1, \hat{a}_2, \cdots \hat{a}_n)$$

$$= \frac{1}{N-2n+1} \sum_{t=n+1}^{N} \left\{ (X_t - \bar{X}) + \hat{a}_1(X_{t-1} - \bar{X}) + \cdots + \hat{a}_n(X_{t-n} - \bar{X}) \right\}^2$$

$$= \frac{N-n}{N-2n+1} \left[R(0) + a_1 R(1) + \cdots + a_n R(n) \right] . \tag{5.246}$$

When $n \ll N$,

$$\hat{\sigma}_\epsilon^2 = R(0) + a_1 R(1) + \cdots + a_n R(n) \tag{5.246'}$$

This result is the same as we obtained from the first equation of Eq. 5.220.

5.5 DETERMINATION OF THE ORDER OF THE FITTED MODEL

As was explained in the preceding sections, the process becomes more complicated as the order increases. Thus AR(2) is more complicated than AR(1) and ARMA(3.2) is more complicated than ARMA(2.1). Estimation of parameters has been discussed in each section, so here only the determination of the order will be discussed. Several different methods have been described by Priestley.[23] The MAIC method developed by H. Akaike is now considered to be the most reasonable from the point of view of statistical considerations and of information theory and is explained and recommended in the following section.

5.5.1 Residual Error Method

The change of residual error, expressed for example by Eq. 5.246' for AR(n), is investigated. If the order is far smaller than the true order, σ_ϵ^2, the residual error, will decrease considerably as the order increases from j to n. From there on, the decrease in residual error may not be significant but will remain at the same level. Point n is adopted as the proper order of the model.
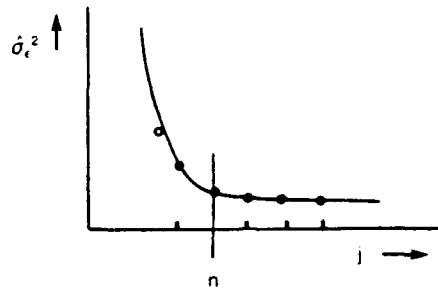
Fig. 5.44. Residual error.

Sometimes, however, it is not easy to determine the order because the rate of change does not show clearly by this method.

5.5.2 Partial Autocorrelation Method

If a_{n_i} denotes the ith autoregressive parameter of an $AR(n)$ process, then the auto–correlation coefficient ϱ_i is from Eq. 5.220,

$$\varrho_i = -a_{n1}\varrho_{i-1} - a_{n2}\varrho_{i-2} \cdots - a_{nn}\varrho_{i-n}$$
$$i = 1, 2, \cdots n \tag{5.247}$$

which gives the Yule–Walker equations,

$$\begin{cases} \varrho_1 = -a_{n1}\varrho_o - a_{n2}\varrho_1 \cdots - a_{nn}\varrho_{n-1} \\ \varrho_2 = -a_{n1}\varrho_1 - a_{n2}\varrho_o \cdots - a_{nn}\varrho_{n-2} \\ \cdots \\ \varrho_n = -a_{n1}\varrho_{n-1} - a_{n_2}\varrho_{n-2} \cdots - a_{nn}\varrho_o. \end{cases} \tag{5.248}$$

Then, the last coefficient a_{nn} of the fitted $AR(n)$ model is called the partial autocorrelation ϱ_n', for $n = 1, 2 \cdots$, and will be used[37] to suggest the order of the AR model.

Since $\varrho_o = 1$, from Eq. 5.248,

$$-a_{11} = \varrho_1 \rightarrow \varrho_1'$$

$$-a_{22} = \frac{\begin{vmatrix} 1 & \varrho_1 \\ \varrho_1 & \varrho_2 \end{vmatrix}}{\begin{vmatrix} 1 & \varrho_1 \\ \varrho_1 & 1 \end{vmatrix}} = \frac{\varrho_1^2 - \varrho_2}{1 - \varrho_1^2} \rightarrow \varrho_2' \tag{5.249}$$

194

$$-a_{nn} = \cfrac{\begin{vmatrix} 1 & \varrho_1 & \varrho_2 & \cdots & \varrho_{n-2} & \varrho_1 \\ \varrho_1 & 1 & \varrho_1 & \cdots & \varrho_{n-3} & \varrho_2 \\ \cdot & & \cdot & & \cdot & \cdot \\ \cdot & \cdot & \cdot & & \cdot & \cdot \\ \cdot & \cdot & \cdot & & \cdot & \cdot \\ \cdot & & \cdot & & 1 & \varrho_{n-1} \\ \varrho_{n-1} & \varrho_{n-2} & \varrho_{n-3} & \cdots & \varrho_1 & \varrho_n \end{vmatrix}}{\begin{vmatrix} 1 & \varrho_1 & \varrho_2 & \cdots & \varrho_{n-2} & \varrho_{n-1} \\ \varrho_1 & 1 & \varrho_1 & \cdots & \varrho_{n-3} & \varrho_{n-2} \\ \cdot & & & & & \cdot \\ \cdot & & & & & \\ \cdot & & & & 1 & \varrho_1 \\ \varrho_{n-1} & \varrho_{n-2} & \varrho_{n-3} & \cdots & \varrho_1 & 1 \end{vmatrix}} \rightarrow \varrho_n' \qquad (5.249')$$

A plot of $\varrho_1' \varrho_2' \cdots \varrho_n'$ against n is called the partial autocorrelation function diagram. If the true order was n, ϱ_k' or $-a_{k\,k}$ should vanish for $k > n$ and the plot of the partial autocorrelation should show the real order n.

For this purpose, a recursive method for calculating ϱ_n' when $-a_{nn}$ are estimated from Yule–Walker equations has been given by Durbin[39] as

$$\hat{a}_{n+1,j} = \hat{a}_{n,j} - \hat{a}_{n+1,n+1} \hat{a}_{n,n-j+1}, \qquad j = 1, \cdots n \qquad (5.250)$$

$$\hat{a}_{m+1,n+1} = \frac{\hat{\varrho}(m+1) - \sum_{j=1}^{n} \hat{a}_{n,j} \hat{\varrho}(n+1-j)}{1 - \sum_{j=1}^{n} \hat{a}_{n,j} \varrho(j)}. \qquad (5.251)$$

5.5.3 Visual Inspection of the Autocorrelation

As has been shown in the preceding sections, the types of models and their orders are well reflected in the pattern of the curve of the autocorrelation function. For example, for the MA(m) model, the correlation cut down to 0 after the lag m, and for the AR(m) model, the correlation has the form of damping oscillations. Box and Jenkins[37] have developed this method and showed many examples of estimating the order from these patterns. However, it requires skill and long experience to be able to estimate the actual order correctly by this inspection.

5.5.4 Akaike's FPE, AIC, and BIC Criteria

FPE. Akaike[40] first proposed computing the final prediction error (FPE) in determining the order n of $AR(n)$ as

$$\text{FPE}(q) = \frac{N+q}{N-q}\hat{\sigma}_\epsilon^2 \tag{5.252}$$

where N = number of observations to which the model is fitted, q = the order of the AR model

$$\hat{\sigma}_\epsilon^2 = \left\{\hat{R}(0) + a_1\hat{R}(1) + \cdots + a_q\hat{R}(q)\right\}$$

and adopting as n the value of q that minimize the FPE, as in Fig. 5.45.
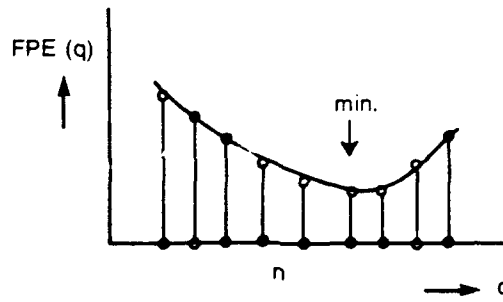
Fig. 5.45. FPE vs. q.

AIC. Later Akaike[41-45] proposed a more refined method of minimum AIC (Akaike's Information Criteria) based on information entropy theory. This is a very general concept available for general statistics problems, as an example of curve fitting, that is shown in Appendix A-2.[46] AIC is defined as

$$\text{AIC}(q) = (-2)\log_e[\text{Max. Likelihood}] + 2q \tag{5.253}$$

where q is the number of parameters. Including $\hat{\sigma}_\epsilon^2$, $n+1$ parameters have to be estimated, so

$$q = n + 1. \tag{5.254}$$

The $\log_e$ [maximized likelihood] is L in Eq. 5.233 or, omitting the constant,

$$L = -\frac{N-n}{2}\log\sigma_\epsilon^2 - \frac{1}{2\sigma_\epsilon^2}Q.$$

Here Q is defined as the sum of squares and from Eq. 5.246

$$\hat{\sigma}_\epsilon^2 = \frac{1}{N}Q.$$

Thus

$$L = -\frac{N-n}{2}\log\hat{\sigma}_\epsilon^2 - \frac{N}{2}Q. \tag{5.255}$$

Ignoring the second term, which is constant, and inserting it in Eq. 5.253

196

$$AIC(q) = (-2)\left(-\frac{N-n}{2}\log\hat{\sigma}_\epsilon^2\right) + 2q$$

$$= (N-n)\log\hat{\sigma}_\epsilon^2 + 2(n+1). \tag{5.256}$$
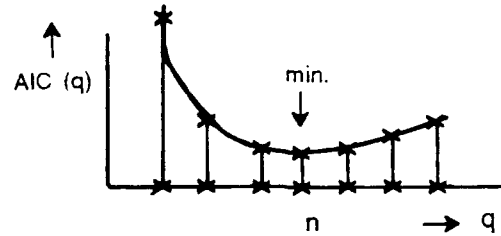
Fig. 5.46. AIC(q) vs. q.

The AIC (q) is plotted against n as in Fig. 5.46, which shows where the AIC (n) has a minimum value. This minimum value is called MAIC, the minimum AIC, and this method for obtaining that MAIC is called the MAIC method. Akaike[41,42] made clear that, based on information theory, AIC is a measure of close fitness of approximation = a measure of minimum difference: (statistical model–true model).

So if we express the statistical distribution of the occurrence of the data for the model as $p(x)$ and the statistical distribution of the true data derived from the true structure of the data, as $q(x)$, to minimize AIC is to minimize

$$I = \int p(x)\log\frac{p(x)}{q(x)},$$

the so–called Kulback's[47] information criterion. Also the so–called information entropy $S(q,p)$ is defined as $S(q,p) \approx -I$. So to minimize AIC is to maximize the entropy $S(q,p)$. Accordingly, the minimum AIC criteria are also called the maximum entropy criteria.

FPE was introduced to find the order of the AR model. AIC is, however, a very general criterion and can be used for ARMA or MA(m) models too. For the ARMA (n,m) model, we can use this criterion setting

$$AIC(n,m) = (N-m-n)\log\hat{\sigma}_\epsilon^2 + 2(n+m+1). \tag{5.257}$$

Plotting AIC(n,m) over an appropriate grid of n, m we can adopt (n,m) that minimize AIC(n,m).

197

Akaike also made it clear that, for large N, FPE, and AIC are equivalent, because

$$\log FPE(q) = \log\left[\frac{1 + q/N}{1 - q/N} \cdot \hat{\sigma}_\epsilon^2\right]$$

$$= \log(1 + q/N) - \log(1 - q/N) + \log \hat{\sigma}_\epsilon^2$$

$$= \log \hat{\sigma}_\epsilon^2 + 2q/N \quad \text{(for large } N\text{)}. \tag{5.258}$$

Therefore $\qquad AIC(q) = N \log[FPE(q)]$.

When N, the number of observations, is large enough, the FPE criterion is the same as the AIC(q) criterion.

BIC(q). Akaike[48,49] also proposed the BIC(q) criterion, based on the Baysian concept, as a new criterion for determining the order. That is,

$$BIC(q) = N \log \hat{\sigma}_\epsilon^2 - (N - q) \log(1 - q/N) + q \log N$$

$$+ q \log\left\{q^{-1}\left[\frac{\hat{\sigma}_x^2}{\hat{\sigma}_\epsilon^2} - 1\right]\right\}. \tag{5.259}$$

This equation can be modified as follows if we approximate

$$\{(-N - q) \log(1 - q/N)\} = \{-(N - q)(-q/N)\} = q - q^2/N \doteqdot q$$

for N >> q. Then

$$BIC(q) = AIC(q) + q(\log N - 1) + q \log\left\{q^{-1}\left[\frac{\hat{\sigma}_x^2}{\sigma_\epsilon^2} - 1\right]\right\}$$

$$= [N \log \hat{\sigma}_\epsilon^2 + 2\underline{q}] + q(\log N) - \underline{q} + q \log\left\{q^{-1}\left(\frac{\hat{\sigma}_x^2}{\hat{\sigma}_\epsilon^2} - 1\right)\right\}. \tag{5.260}$$

This relation shows that the difference between BIC(q) and AIC(q) is approximately one q of AIC(q) and is replaced with $q \log N$. This replacement has the effect of increasing the weight attached to the penalty term which takes account of the number of parameters in the model. Shibata[50] tells us that AIC(q) slightly overestimates and BIC(q) slightly underestimates the real q value.

5.5.5 Examples of Order Determination through MAIC

In Sections 5.2.1 to 5.2.5, examples of the synthesized processes AR(0), AR(1), AR(2), ARMA(2.1), MA(2), MA(1), and ARMA(2.2) generated by mathematical models were shown. When these processes were given as observed data, the orders N and M of each process were estimated by the MAIC method and then parameters $a_1 \cdots a_n$; $b_1 \cdots b_m$ were estimated by the method described at each subsection. The results are

summarized in Tables 5.1 and 5.2. From these results, we can find the criteria of MAIC that give us the correct values of the order except in a few cases. Estimation of parameters $a_1 \cdots a_n$; $b_1 \cdots b_n$, and σ_ϵ^2 is rather reasonable in these examples. Tables 5.1 and 5.2 list the AR(n) model fitted to the original ARMA or MA models. It is interesting that the values of N obtained by the MAIC method are somewhat larger than n or m of the original processes. These models are the AR models which approximate most closely the original ARMA or MA models. We can say these examples gives us good proof that the model fitting method, supported by order determination through AIC criteria, is a very reasonable and powerful method for analyzing the linear stochastic processes.

THIS PAGE INTENTIONALLY LEFT BLANK

CHAPTER 6

MODEL FITTING TO THE RESPONSE OF THE LINEAR DYNAMIC SYSTEM TO IRREGULAR INPUT

6.1 INTRODUCTION

In Chapter 5, the characteristics, stability, and invertibility of a single linear stochastic process X_t were discussed and it was concluded that AR, MA, or ARMA models of appropriate order can usually be fitted to most of the linear stationary time series to represent their statistical properties.

The characteristics of the model fitting techniques is, the author believes, that all of these AR, MA, and ARMA models relate the process X_t to the pure random process ϵ_t, although the relations that connect ϵ_t to X_t are different for the different models.

For

$$\text{AR}: \quad X_t + a_1 X_{t-1} + a_2 X_{t-2} + \ldots + a_n X_{t-n} = \epsilon_t;$$

$$\text{MA}: \quad X_t = \epsilon_t + b_1 \epsilon_{t-1} + b_2 \epsilon_{t-2} \ldots + b_m \epsilon_{t-m}; \quad \text{and} \qquad (6.1)$$

$$\text{ARMA}: \quad X_t + a_1 X_{t-1} + a_2 X_{t-2} \ldots + a_n X_{t-n} = \epsilon_t + b_1 \epsilon_{t-1}$$

$$+ b_2 \epsilon_{t-2} + \ldots + b_m \epsilon_{t-m}.$$

In all of these models, ϵ_t was supposed to be the input to an imaginary system, and X_t was treated as the output of the same system. All the characteristics of X_t are expressed in relation to those of the pure random (white) process.

6.2 RESPONSE SYSTEM WITH FEEDBACK

6.2.1 One Input / One Output System

Here we consider the output Y of a real linear system with input X_t, usually expressed as

$$Y_t = \sum_{u=0}^{\infty} g_u X_{t-u} + \epsilon_t'. \qquad (6.2)$$

Here g_u is the so-called impulse response function of Y_t to X_t or the weighting function of this linear system to X_t. Now suppose we have N observations of the input/output pair $[X_t, Y_t]$, $t = 1$ to N.

If ϵ_t' is a pure random (white) noise, then we can estimate the coefficient g_u to minimize

$$\sum_{n=1}^{N}\left\{ Y_t - \sum_{u=0}^{\infty} g_u X_{t-u} \right\}^2. \tag{6.3}$$

However, ϵ_t' is not necessarily white, and moreover it may sometimes have some feedback effect on the input.

As already discussed in Section 2.6.3, even when noise exists in the output Y_t of input X_t, if there is no feedback effect as in Fig. 6.1, we can get rid of the effect of noise in computing the real spectrum of the output by finding the real response function of this system from the cross spectrum of the output to the input.
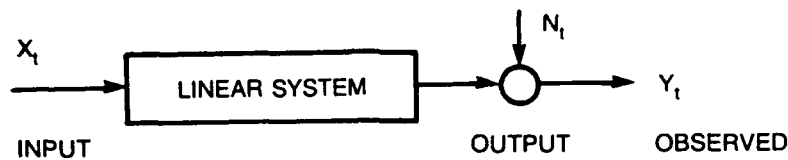
Fig. 6.1. Linear system without feedback.

However, if somehow this output is fed back to the input, as in Fig. 6.2, the input X_t is no longer uncorrelated with N_t, and N_t is included in X_t as a part of the input. Accordingly, taking the cross correlation does not help in getting the real response characteristic of this system.
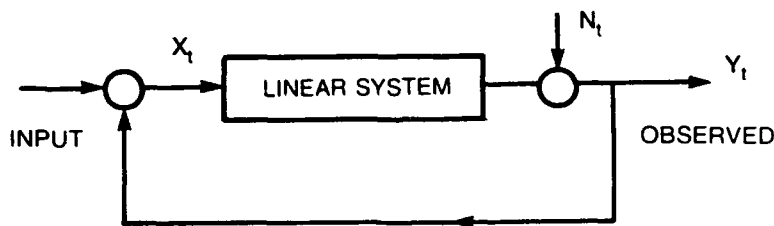
Fig. 6.2. Linear system with feedback.

By a parametric method different from the nonparametric method referred to above, we can obtain the real relation by fitting an appropriate model to this system, getting rid of the effect of noise by following Akaike.[51]

Under these circumstances, we first transform the noise ϵ_t' into pure white noise. Generally ϵ_t' can be expressed by an AR model of arbitrary order l,

$$\epsilon_t' + C_1\epsilon_{t-1}' + C_2\epsilon_{t-2}' \ldots + C_l\epsilon_{t-l}' = \epsilon_t, \tag{6.4}$$

ϵ_t being a pure random process.

From Eq. 6.2

$$\epsilon_t' = Y_t - \sum_{u=0}^{\infty} g_u X_{t-u}, \tag{6.2'}$$

$$\epsilon_{t-l}' = Y_{t-l} - \sum_{u=0}^{\infty} g_u X_{t-l-u}. \tag{6.5}$$

Inserting these values into Eq. 6.4 gives, where $l \rightarrow \infty$

$$\left\{ Y_t - \sum_{u=0}^{\infty} g_u X_{t-u} \right\} + C_1 \left\{ Y_{t-1} - \sum_{u=0}^{\infty} g_u X_{t-1-u} \right\} + C_2 \left\{ Y_{t-2} - \sum_{u=0}^{\infty} g_u X_{t-2-u} \right\}$$

$$+ \ldots + C_l \left\{ Y_{t-l} - \sum_{u=0}^{\infty} g_u X_{t-l-u} \right\} + \ldots = \epsilon_t, \tag{6.6}$$

or

$$Y_t + C_1 Y_{t-1} + C_2 Y_{t-2} + \ldots + C_l Y_{t-l} + \ldots$$

$$- \sum_{u=0}^{\infty} \left\{ g_u X_{t-u} + C_1 g_u X_{t-1-u} + C_2 g_u X_{t-2-u} + \ldots \right.$$

$$\left. + C_l g_u X_{t-l-u} + \ldots \right\} = \epsilon_t, \tag{6.7}$$

or

$$\sum_{l=0}^{\infty} C_l Y_{t-l} = \sum_{u=0}^{\infty} g_u \sum_{l=0}^{\infty} C_l X_{t-u-l} + \epsilon_t$$

$$= \sum_{u=0}^{\infty} \sum_{l=0}^{\infty} g_{u'-l} C_l X_{t-u'} + \epsilon_t. \tag{6.8}$$

203

where $(u' = l + u)$ and $u' > l$. Accordingly, if we set

$$\sum_{l=0}^{\infty} g_{u'-l} C_l = h_{u'},$$

Eq. 6.8 will be

$$\sum_{l=0}^{\infty} C_l Y_{t-l} = \sum_{u'=0}^{\infty} h_{u'} X_{t-u'} + \epsilon_t. \qquad (6.9)$$

Since ϵ_t is a pure random process, C_l and $h_{u'}$ can be estimated by the least squares method.

From Eq. 6.9

$$\epsilon_t^* = \sum_{l=0}^{\infty} C_l^* Y_{t-l} - \sum_{u'=0}^{\infty} h_{u'}^* X_{t-u'}, \qquad (6.10)$$

$$(* = \text{conjugate})$$

and

$$\epsilon_{t+s} = \sum_{l=0}^{\infty} C_l Y_{t+s-l} - \sum_{u'=0}^{\infty} h_{u'} X_{t+s-u'}. \qquad (6.11)$$

Taking the products of both sides of Eqs. 6.10 and 6.11, and then taking the statistical expectation of each term

$$R_{\epsilon\epsilon}(s) = \sum_{l=0}^{\infty} C_l^* \sum_{l=0}^{\infty} C_l R_{yy}(s) - \sum_{l=0}^{\infty} C_l^* \sum_{u'=0}^{\infty} h_{u'} R_{xy}(s - u' + l)$$

$$- \sum_{l=0}^{\infty} C_l \sum_{u'=0}^{\infty} h_{u'}^* R_{yx}(s - l + u')$$

$$+ \sum_{u'=0}^{\infty} h_{u'}^* \sum_{u'=0}^{\infty} h_{u'} R_{xx}(s). \qquad (6.12)$$

Then, by the Fourier transform,

$$\frac{1}{2\pi} \int\limits_{-\infty}^{\infty} R_{\epsilon\epsilon}(s) \ e^{-i\omega s} d\omega = \sum_{l=0}^{\infty} C_l^* \ e^{+il\omega} \sum C_l \ e^{-il\omega} \frac{1}{2\pi} \int\limits_{-\infty}^{\infty} R_{yy}(s) \ e^{-i\omega s} d\omega$$

$$- \sum_{l=0}^{\infty} C_l^* \ e^{+il\omega} \sum_{u'=1}^{\infty} h_{u'} \ e^{-iu'\omega} \frac{1}{2\pi} \int R_{xy}(s - u' + l') \ e^{-i(s-u'+l)\omega} \ d\omega$$

$$- \sum_{l=0}^{\infty} C_l \ e^{-il\omega} \sum_{u'=0}^{\infty} h_{u'}^* \ e^{+iu'\omega} \frac{1}{2\pi} \int R_{yx} \ e^{-i(s-l+u')\omega} \ d\omega$$

$$+ \sum_{u'=0}^{\infty} h_{u'}^* \ e^{+iu'\omega} \sum_{u'=0}^{\infty} h_{u'} \ e^{-iu'\omega} \frac{1}{2\pi} \int R_{xx}(s) \ e^{-i\omega s}. \qquad (6.13)$$

If we set

$$\sum_{l=0}^{\infty} C_l \ e^{-il\omega} = C_l(\omega) \qquad , \qquad \sum C_l^* \ e^{+il\omega} = C_l^*(\omega) \quad ,$$

$$\sum_{u'=0}^{\infty} h_{u'} \ e^{-iu'\omega} = H_{u'}(\omega) \ , \qquad \sum h_{u'}^* \ e^{+iu'\omega} = H_{u'}^*(\omega) \ , \qquad (6.14)$$

Eq. 6.13 becomes

$$\frac{1}{2\pi}\sigma_{\epsilon\epsilon}^2 = C_l(\omega)C_l^*(\omega)s_{yy}(\omega) - C_l^*(\omega)H_{u'}(\omega)s_{xy}(\omega)$$

$$- C_l(\omega)H_{u'}^*(\omega)s_{yx}(\omega)$$

$$+ H_{u'}(\omega)H_{u'}^*(\omega) \cdot s_{yx}(\omega). \qquad (6.15)$$

From this relation, we can get $s_{xx}(\omega)$, $s_{yy}(\omega)$, and s_{xy} (s_{yx}), and Eq. 6.15 can be written

$$\frac{\sigma_{\epsilon\epsilon}^2}{2\pi} = [C_l(\omega), H_{u'}(\omega)] \begin{bmatrix} S_{yy}(\omega) - S_{xy}(\omega) \\ -S_{yx}(\omega) \quad S_{xx}(\omega) \end{bmatrix} \begin{bmatrix} C_l^*(\omega) \\ H_{u'}^*(\omega) \end{bmatrix}. \qquad (6.16)$$

Equation 6.16 shows the relation of the power of the white noise to the spectra of input and output and also of the cross spectra of input to output and the frequency response functions.

205

6.2.2 General Two–Dimensional, P–Dimensional Case

More generally, as the expansion of Eq. 6.8, we can think of a system, diagrammed in Fig. 6.3, in which the output $X_{1,t}$ is fed back to the input $X_{2,t}$ as well as the input $X_{2,t}$ being fed to the output $X_{1,t}$,

$$X_{1,t} = \sum_{l=1}^{\infty} C_{1.1,l}\, X_{1,t-l} + \sum_{u=1}^{\infty} C_{1.2,u}\, X_{2,t-u} + \epsilon_{1,t},$$

$$X_{2,t} = \sum_{l=1}^{\infty} C_{2.1,l}\, X_{1,t-l} + \sum_{u=1}^{\infty} C_{2.2,u}\, X_{2,t-u} + \epsilon_{2,t}.$$

(6.17)
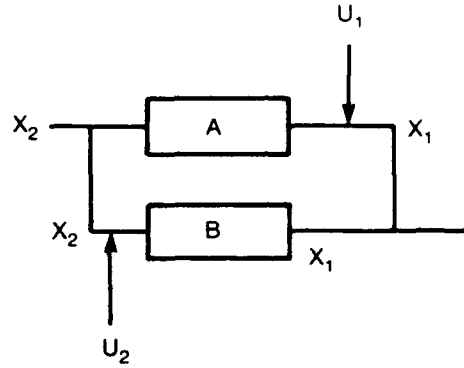
Fig. 6.3. Two–dimensional feedback system.

This equation can be written in vector form as

$$\begin{bmatrix} X_{1,t} \\ X_{2,t} \end{bmatrix} = \begin{bmatrix} C_{11.1} & C_{12.1} \\ C_{21.1} & C_{22.1} \end{bmatrix} \begin{bmatrix} X_{1,t-1} \\ X_{2,t-1} \end{bmatrix} + \begin{bmatrix} C_{11.2} & C_{12.2} \\ C_{21.2} & C_{22.2} \end{bmatrix} \begin{bmatrix} X_{1,t-2} \\ X_{2,t-2} \end{bmatrix}$$

$$+ \ldots + \begin{bmatrix} C_{11,k} & C_{12,k} \\ C_{21,k} & C_{22,k} \end{bmatrix} \begin{bmatrix} X_{1,t-k} \\ X_{2,t-k} \end{bmatrix} + \ldots + \begin{bmatrix} \epsilon_{1,t} \\ \epsilon_{2,t} \end{bmatrix}. \qquad (6.18)$$

Cutting off the terms at appropriate k by some criterion gives

$$X_t = a_1 X_{t-1} + a_2 X_{t-2} + \ldots + a_k X_{t-k} + \epsilon_t$$

$$= \sum_{u=1}^{k} a_u X_{t-u} + \epsilon_t, \qquad (6.19)$$

where $X_t = \begin{bmatrix} X_{1,t} \\ X_{2,t} \end{bmatrix}$ $a_m = \begin{bmatrix} C_{11,m} & C_{1,2,m} \\ C_{2,1,m} & C_{22,m} \end{bmatrix}$ $\epsilon_t = \begin{bmatrix} \epsilon_{1,t} \\ \epsilon_{2,t} \end{bmatrix}$.

More generally, in the P–dimensional process the dimensions $X_{1,t}$, $X_{2,t}$, $X_{p,t}$ are connected by feedback systems to each other. This process can be reduced to the P–dimensional AR(k) model, with k as an appropriate order,

$$X_t = a_1 X_{t-1} + a_2 X_{t-2} + \ldots + a_k X_{t-k} + \epsilon_t, \qquad (6.20)$$

where $X_t = \begin{bmatrix} X_1 \\ X_2 \\ \cdot \\ \cdot \\ \cdot \\ X_P \end{bmatrix}$ $a_m = \begin{bmatrix} C_{11,m} & \ldots & C_{1p,m} \\ C_{21,m} & \ldots & C_{2p,m} \\ \cdot & & \cdot \\ \cdot & & \cdot \\ \cdot & & \cdot \\ C_{p1,m} & \ldots & C_{pp,m} \end{bmatrix}$ $\epsilon_t = \begin{bmatrix} \epsilon_1 \\ \epsilon_2 \\ \cdot \\ \cdot \\ \cdot \\ \epsilon_P \end{bmatrix}$.

Eq. 6.20 can then be written

$$X_t = \sum_{m=1}^{k} a_m X_{t-m} + \epsilon_t, \qquad (6.20')$$

or

$$\left\{ 1 - \sum_{m=1}^{k} a_m (B^m) \right\} X_t = \epsilon_t, \qquad (6.20'')$$

or $\qquad \alpha(B) X_t = \epsilon_t,$

here

$$\alpha(Z) = \left[1 - \left\{ a_1 Z + a_2 Z^2 + \ldots + a_k Z^k \right\} \right]. \qquad (6.21)$$

207

Then the spectrum is

$$s_x(\omega) = \frac{s_\epsilon(\omega)}{\left|\alpha(e^{-i\omega})\right|^2} \tag{6.22}$$

$$= \frac{1}{2\pi} \frac{\sum_\epsilon}{\left|1 - a_1\, e^{-i\omega} - a_2\, e^{-2i\omega} - \ldots - a_k\, e^{-ki\omega}\right|^2}, \tag{6.22'}$$

where

$$E[\epsilon_t\, \epsilon_u'] = \begin{cases} 0 & t \neq u \\ \sum_\epsilon & t = 0 \end{cases} \tag{6.23}$$

The order k can be obtained from Akaike's minimum AIC criterion in this case too; i.e., we can find k that minimizes

$$\text{AIC}\ (p, k) = N\log\left|\sum_\epsilon(k)\right| + 2p^2 k, \tag{6.24}$$

where

$$\sum_\epsilon(k) = \sum_{m=0}^{k} \hat{a}_m R_x(m), \tag{6.25}$$

as it was for the scalar case.

Through these procedures, after fixing the order k, we get the coefficient $a_1 \ldots a_k$, as for the scalar case. Then we can get the spectrum matrix from Eq. 6.22.

$$\begin{bmatrix} S_{x_1 x_1} & S_{x_1 x_2} & \ldots & S_{x_1 x_p} \\ S_{x_2 x_1} & S_{x_2 x_2} & \ldots & S_{x_2 x_p} \\ \cdot & & & \cdot \\ \cdot & & & \cdot \\ \cdot & & & \cdot \\ S_{x_p x_1} & & & S_{x_p x_p} \end{bmatrix} \tag{6.26}$$

The cross spectrum, for example $S_{x_1 x_2}(\omega)$, is obtained in complex form

$$S_{x_1 x_2}(\omega) = Co_{x_1 x_2}(\omega) + iQx_1 x_2(\omega) \tag{6.27}$$

as an element of the spectrum matrix, Eq. 6.26.

Then the frequency response function of x_1 to x_2 is

$$\left|G_{x_1x_2}(\omega)\right| = \frac{\sqrt{\left[Co_{x_1x_2}(\omega)\right] + \left[Qu_{x_1x_2}(\omega)\right]^2}}{S_{x_2x_2}(\omega)}. \tag{6.28}$$

The phase relation is

$$\phi_{x_1x_2}(\omega) = \text{Arg}[G_{x_1x_2}(\omega)] = \tan^{-1}\left\{\frac{Qu_{x_1x_2}(\omega)}{Co_{x_1x_2}(\omega)}\right\} \tag{6.29}$$

and the coherency function is

$$\gamma_{x_1x_2}(\omega) = \frac{\left|S_{x_1x_2}(\omega)\right|^2}{S_{x_1x_1}(\omega)S_{x_2x_2}(\omega)}. \tag{6.30}$$

6.3 AUTOREGRESSIVE CONTINUOUS PROCESS

So far only discrete processes have been dealt with in which difference equations have been used to formulate the processes. When we study the response of some dynamic systems, however, the processes are in many cases substantially continuous. Usually, however, for computational analysis these processes are sampled at a certain time interval Δt, and then the readings are digitized and are treated as discrete processes. The analysis technique for a discrete process has been shown in detail in the preceding sections.

Sometimes, however, it is helpful in understanding the response dynamics of a system to treat the process directly as the continuous process.

Although difference equations have been used to formulate discrete processes, differential equations are used to formulate continuous processes. We are more accustomed to dealing with differential equations to express the physical characteristics of the response of the dynamic systems than with difference equations.

In this section, the differential equations that formulate the continuous process will be introduced. Then, following the derivation of Pandit and Wu,[36] the relation of these differential equations to the difference equations which formulate the digitized processes will be summarized, since in practical applications, we might want to determine the characteristics of the differential equations from the digitized data of responses and inputs.

6.3.1 The First Order Continuous Autoregressive Process A(1)

For the first order continuous autoregressive process, referred to as A(1), the first order differential equation

$$\frac{d}{dt}X(t) + \alpha_o X(t) = Z(t) \tag{6.31}$$

can be formulated. Here $Z(t)$ is the forcing function or the white noise, expressed as

209

$$E\{Z(t)\} = 0$$

$$E[Z(t)Z(t-u)] = \delta(u)\sigma_Z^2 \tag{6.32}$$

$$= E[Z(t)]^2 = \delta(0)\sigma_Z^2,$$

$\delta(0)$ is Dirac's delta function,

$$\delta(u) = \begin{cases} \infty & \text{when } u = 0 \\ 0 & \text{when } u \neq 0, \end{cases}$$

$$\text{and } \int_{-\infty}^{\infty} \delta(u)du = 1. \tag{6.33}$$

Accordingly, $E[Z(t)]^2 \Rightarrow \infty$, which means that the white noise $Z(t)$ is physically unrealizable. The output $X(t)$ is a stochastic process with zero mean. Using the differential operator $D = d/dt$, $D = (d/dt)^n$,

$$X(t) = (D + \alpha_0)^{-1}Z(t). \tag{6.34}$$

When we express Green's function as $G(v)$,

$$X(t) = \int_0^\infty G(v) \cdot Z(t-v)dv = \int_{-\infty}^t G(t-v)Z(v)dv. \tag{6.35}$$

This equation is the orthogonal decomposition of $X(t)$, since the $Z(t)$'s are uncorrelated, or independent at different times. From Eq. 6.34 and Eq. 6.35, it is also clear that, when the forcing function is Dirac's delta function, $X(t)$ is the Green's function,

$$(D + \alpha_0)G(t) = \delta(t)$$

$$G(t) = \int_0^\infty G(v)\delta(t-v)dv. \tag{6.36}$$

Here, since the solution of the homogeneous equation

$$(D + \alpha_0)^{-1}X(t) = 0 \tag{6.37}$$

is

$$X(t) = C \ e^{\lambda t}, \tag{6.38}$$

210

where λ is the root of the characteristic equation

$$\lambda + \alpha_0 = 0, \quad \text{or} \quad \lambda = -\alpha_0, \tag{6.39}$$

$$X(t) = C\; e^{-\alpha_0 t}. \tag{6.40}$$

This coefficient C is determined from the initial conditions given by the characteristics of Dirac's delta function as $G(t) = 0$, $t < 0$, $G(0) = 1$; therefore $C = 1$. Green's function is obtained as

$$G(t) = \begin{cases} e^{-\alpha_0 t} & t \geq 0 \\ 0 & t < 0 \end{cases} \tag{6.41}$$

$$= u(t)\; e^{-\alpha_0 t} \tag{6.41'}$$

here $u(t)$ is the unit step function.

The autocorrelation function is $R(s) = E[X(t)\; X(t-s)]$.

$$\text{Using } X(t) = \int_0^\infty G(v')\; Z(t-v')\; dv'$$

$$\text{and } X(t-s) = \int_0^\infty G(v)\; Z(t-s-v)\; dv$$

gives

$$R(s) = \int_0^\infty \int_0^\infty G(v')G(v)E[Z(t-v')Z(t-s-v)]dv\,dv'$$

$$= \int_0^\infty \int_0^\infty \sigma_Z^2 \delta(s+v-v')G(v)G(v')dv\,dv'$$

$$= \sigma_Z^2 \int_0^\infty G(v)G(v+s)dv = \sigma_Z^2 \int_0^\infty e^{-\alpha_0 v}\; e^{-\alpha_0(v+s)}dv = \frac{\sigma_Z^2}{2\alpha_0}e^{-\alpha_0 s}$$

$$R(-s) = R(s), \tag{6.42}$$

thus

211

$$R(s) = \frac{\alpha_Z^2}{2\alpha_0} e^{-\alpha_0 |s|}. \tag{6.43}$$

Now suppose we have the sampled discrete data from a continuous process with sampling interval Δt, and the data show an autoregressive process as shown by Eq. 5.7'

$$X_t - a_1 X_{t-1} = \epsilon_1.$$

The covariance function is, from Eq. 5.49, $R(r) = \dfrac{\sigma_\epsilon^2}{1-a^2} a^r$. $R(r) = (\sigma_\epsilon^2/1 - a^2)a^r$.

Relation of A(1) to AR(1) by Covariance Equivalence. When $s = r\Delta t$, the autocovariance function for a continuous process must be equivalent to that of the discrete process at $t = r\Delta t$. Setting $s = r\Delta t$ in Eq. 6.42 gives

$$R(r\Delta t) = \frac{\sigma_Z^2}{2\alpha_0} e^{-\alpha_0 r\Delta t} = \frac{\sigma_Z^2}{2\alpha_0} \left(e^{-\alpha_0 \Delta t} \right)^r. \tag{6.44}$$

For discrete computation this is equivalent to $R(r) = \dfrac{\sigma_\epsilon^2}{1-a^2} a^r$.

Therefore

$$e^{-\alpha_0 \Delta t} = a \tag{6.45}$$

$$\frac{\sigma_Z^2}{2\alpha_0} = \frac{\sigma_\epsilon^2}{1-a^2} \tag{6.46}$$

or

$$-\alpha_0 \Delta t = \ln a \quad or \quad \alpha_0 = -\frac{\ln a}{\Delta t} \tag{6.45'}$$

and

$$\sigma_Z^2 = \frac{2\alpha_0 \sigma_\epsilon^2}{1-a^2}. \tag{6.46'}$$

From these relations, we can convert the continuous process A(1) into a sampled process AR(1), or vice versa, by inverting the coefficients from Eqs. 6.45' and 6.46'. From Eq. 6.43, the variance is

$$R(0) = \frac{\sigma_Z^2}{2\alpha_0}. \tag{6.47}$$

The spectrum is given by the Fourier transform of $R(s)$ as

$$s(\omega) = \frac{1}{2\pi} \int\limits_{-\infty}^{\infty} \Re e \left\{ \frac{\sigma_Z^2}{2\alpha_0} e^{-\alpha_0 |s|} e^{-i\omega s} \right\} ds$$

$$= \frac{\sigma_Z^2}{2\pi} \frac{1}{|\alpha_0 + i\omega|^2} = \frac{\sigma_Z^2}{2\pi} \frac{1}{\alpha_0^2 + \omega^2}, \tag{6.48}$$

$\Re e \{ \cdot \}$ showing to take the real part of a function $\{ \cdot \}$.

If we express

$$(D + \alpha_0) = \alpha(D),$$

then

$$s(\omega) = \frac{\sigma_Z^2}{2\pi} \frac{1}{|\alpha(i\omega)|^2}, \tag{6.49}$$

which is again a form similar to Eq. 5.50 for the discrete process.

6.3.2 Correspondence of A(2) to ARMA(2.1)

Generally for a damped mass spring linear vibrating system, the second order differential equation as

$$M\ddot{X}(t) + B\dot{X}(t) + KX(t) = f(t) \tag{6.50}$$

stands as its fundamental formulation, where $f(t)$ represents the forcing function.
Here

M = mass

B = damping coefficient (linear to the velocity)

K = restoring coefficient (linear to the displacement).

Transforming Eq. 6.50 by conventional expressions as

$$\frac{B}{M} = 2\kappa\omega_n \qquad \kappa = \frac{1}{2} \frac{\frac{B}{M}}{\omega_n} = \frac{B}{2\sqrt{KM}}$$

$$\text{or} \tag{6.51}$$

$$\frac{K}{M} = \omega_n^2 \qquad \omega_n = \sqrt{\frac{K}{M}}$$

gives

$$\frac{d^2}{dt} X(t) + 2\kappa\omega_n \frac{d}{dt} X(t) + \omega_n^2 X(t) = \frac{1}{M} f(t). \tag{6.52}$$

213

Using the differential operator $D = d/dt$ gives

$$(D^2 + 2\kappa\omega_n D + \omega_n^2)X(t) = \frac{1}{M}f(t), \qquad (6.53)$$

or

$$(D^2 + a_1 D + a_0)X(t) = \frac{1}{M}f(t), \qquad (6.53')$$

where $a_1 = 2\kappa\omega_n$, $a_0 = \omega_n^2$.

Eq. 6.53' is analogous to the AR model of the discrete process AR(2) as given by Eq. 5.59 or Eq. 5.62,

$$X_t + a_1 X_{t-1} + a_2 X_{t-2} = \epsilon_t \quad \text{or} \quad (1 + a_1 B + a_2 B^2)X_t = \epsilon_t.$$

If we assume $(1/M)f(t)$ is a continuous pure random process $Z(t)$, then we can say that $X(t)$ is an autoregressive process of continuous time of order 2 and express this process as A(2) as did Pandit and Wu.[36]

Then A(2) can be expressed as

$$(D^2 + 2\kappa\omega_n D + \omega_n^2)X(t) = Z(t) \qquad (6.54)$$

where $E[Z(t)Z(t')] = \sigma_Z^2 \cdot \delta(t - t') = \begin{cases} \sigma_Z^2 & \text{when } t = t' \\ 0 & \text{when } t \neq t' \end{cases}$

which corresponds to Eq. 5.62 for AR (2), and

$$X(t) = (D^2 + 2\kappa\omega_n D + \omega_n^2)^{-1}Z(t) = (D^2 + a_1 D + a_0)^{-1}Z(t). \qquad (6.55)$$

Then using the Green's function $G(t)$,

$$X(t) = (D^2 + 2\kappa\omega_n D + \omega_n^2)^{-1}Z(t)$$

$$= \int_0^\infty G(\nu)Z(t - \nu)d\nu, \qquad (6.56)$$

and

$$(D^2 + a_1 D + a_0)G(t) = \delta(t) \qquad (6.57)$$

214

$$G(t) = \int_0^\infty G(v)\delta(t-v)\,dv. \qquad (6.58)$$

Then thinking the characters of derivatives in Eq. 6.57, at $t = 0$, $G''(t)$ that is $D^2 G(t)$ contains the same discontinuity as does $\delta(t)$. Therefore, $G'(t)$ must contain the same discontinuity as does the unit step function, and similarly $G(t)$, which is the integral of $G'(t)$, behaves like the integral of the unit step function, which is a ramp function.

Therefore, $G(t)$ is continuous at $t = 0$, and the initial conditions are

$$G'(t) = G(t) = 0, \quad t < 0$$

$$G'(0) = 1, \qquad G(0) = 0. \qquad (6.59)$$

From these initial conditions (Eq. 6.59), the coefficients C_1, C_2 of the solution of the homogeneous equation

$$(D^2 + \alpha_1 D + \alpha_0)G(t) = 0, \qquad (6.60)$$

that is, of

$$G(t) = C_1 e^{\lambda_1 t} + C_2 e^{\lambda_2 t}, \qquad (6.61)$$

are determined as

$$C_1 = \frac{1}{\lambda_1 - \lambda_2}, \quad C_2 = \frac{-1}{\lambda_1 - \lambda_2}. \qquad (6.62)$$

Therefore

$$G(t) = \begin{cases} \dfrac{e^{\lambda_1 t} - e^{\lambda_2 t}}{\lambda_1 - \lambda_2} & \text{for } t > 0 \\[2mm] 0 & \text{otherwise.} \end{cases} \qquad (6.63)$$

Here λ_1, λ_2 are the eigenvalues or the roots of the characteristic equation equated to zero, as

$$f_2(z) = Z^2 + \alpha_1 Z + \alpha_0 \equiv 0, \qquad (6.64)$$

or

$$Z^2 + 2\kappa\omega_n Z + \omega_n^2 \equiv (Z - \lambda_1)(Z - \lambda_2) = 0. \qquad (6.64')$$

Then

$$\lambda_1, \lambda_2 = \frac{1}{2}\left(-\alpha_1 \pm \sqrt{\alpha_1^2 - 4\alpha_0}\right)$$

or

$$= \omega_n\left(-\kappa \pm \sqrt{\kappa^2 - 1}\right). \tag{6.65}$$

This Green's function is the so-called unit impulse response function that shows the response of this physical system to the unit impulse.

$$G(t) = \frac{e^{\lambda_1 t}}{\lambda_1 - \lambda_2} - \frac{e^{\lambda_2 t}}{\lambda_1 - \lambda_2}. \tag{6.66}$$

This impulse response function shows different forms as follows, depending on $\kappa \gtreqless 1$.

a. When $\kappa \geq 1$ ($\alpha_1^2 \geq 4\alpha_0$), $\lambda_1 \lambda_2$ are real. Therefore $G(t)$ is a linear combination of two exponentials, as is shown in Fig. 6.4.

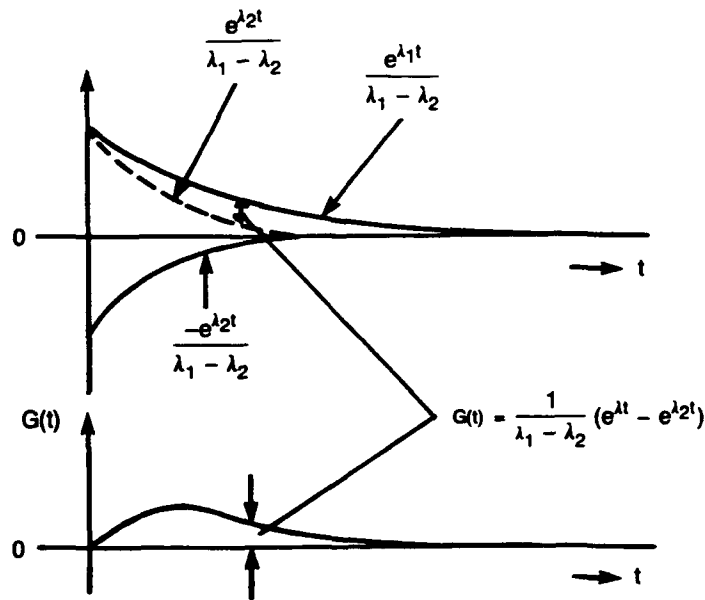**Fig. 6.4.** $G(t)$ for $\kappa \geq 1$.

Then

$$G(t) = \frac{e^{-\kappa\omega_n t}}{2\omega_n\sqrt{\kappa^2-1}} \left(e^{\omega_n\sqrt{\kappa^2-1}\,t} - e^{-\omega_n\sqrt{\kappa^2-1}\,t} \right)$$

$$= \frac{e^{-\kappa\omega_n t}}{\omega_n\sqrt{\kappa^2-1}} \sinh\left(\omega_n\sqrt{\kappa^2-1}\;t\right). \tag{6.67}$$

b. When $\kappa < 1$ $(\alpha_1^2 < 4\alpha_0)$, $\lambda_1\lambda_2$ are complex. $G(t)$ is a damped sine wave because

$$G(t) = \frac{e^{-\kappa\omega_n t}}{2\omega_n\sqrt{\kappa^2-1}} \left(e^{i\omega_n\sqrt{1-\kappa^2}\,t} - e^{-i\omega_n\sqrt{1-\kappa^2}\,t} \right) \tag{6.68}$$

$$= \frac{e^{-\kappa\omega_n t}}{\omega_n\sqrt{1-\kappa^2}} \sin\left(\omega_n\sqrt{1-\kappa^2}\;t\right). \tag{6.68'}$$

This equation is in the form of the impulse response function when $\kappa < 1$, as in Fig. 6.5.

c. When $\kappa = 0$, $G(t)$ shows an undamped sine curve as is also shown in Fig. 6.5.
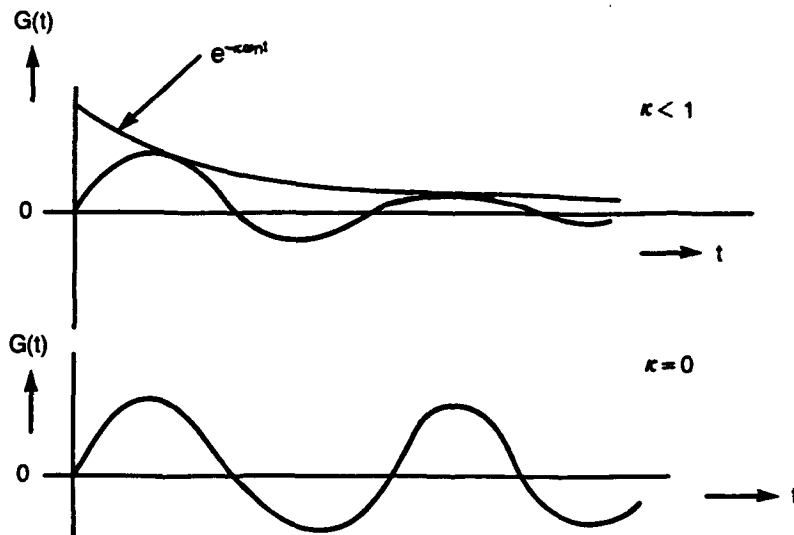

Fig. 6.5. $G(t)$ for $\kappa < 1$, $\kappa = 0$.

217

Using $G(t)$ in Eq. 6.56 gives

$$X(t) = \int_0^\infty \frac{e^{\lambda_1 v} - e^{\lambda_2 v}}{\lambda_1 - \lambda_2} Z(t - v)dv$$

$$= \int_{-\infty}^t \frac{e^{\lambda_1(t-v)} - e^{\lambda_2(t-v)}}{\lambda_1 - \lambda_2} Z(v)dv. \tag{6.69}$$

Equation 6.69 is the orthogonal decomposition of $X(t)$ and also shows the general solution of the nonhomogeneous Eq. 6.54.

The autocovariance function is then, by Eq. 6.56,

$$R(s) = E[X(t)\ X(t-s)]$$

$$= E\left[\int_0^\infty G(v')Z(t-v')dv' \int_0^\infty G(v)Z(t-s-v)dv\right]$$

$$= \int_0^\infty \int_0^\infty G(v')G(v)E[Z(t-v')Z(t-s-v)]dvdv'$$

$$= \sigma_Z^2 \int_0^\infty \left[\int_0^\infty G(v')G(v)\delta(v+s-v')dv'\right]dv$$

$$= \sigma_Z^2 \int_0^\infty G(v)G(v+s)dv. \tag{6.70}$$

Inserting in Eq. 6.70 the expression $G(v) = \dfrac{e^{\lambda_1 t} - e^{\lambda_2 t}}{\lambda_1 - \lambda_2}$ and manipulating gives

$$R(s) = \frac{\sigma_Z^2}{2\lambda_1\lambda_2(\lambda_1^2 - \lambda_2^2)}(\lambda_2 e^{\lambda_1 s} - \lambda_1 e^{\lambda_2 s}) = \frac{\sigma_Z^2}{2\lambda_1(\lambda_1^2 - \lambda_2^2)}e^{\lambda_1 s} - \frac{\sigma_Z^2}{2\lambda_2(\lambda_1^2 - \lambda_2^2)}e^{\lambda_2 s}. \tag{6.71}$$

Then the variance is

$$R(0) = \frac{-\sigma_Z^2}{2\lambda_1\lambda_2(\lambda_1 + \lambda_2)} = \frac{\sigma_Z^2}{4\kappa\omega_n^3}. \tag{6.72}$$

The autocovariance coefficient $\varrho(s)$ is

$$\varrho(s) = \frac{\lambda_2 e^{\lambda_1 s} - \lambda_1 e^{\lambda_2 s}}{\lambda_2 - \lambda_1}. \tag{6.72'}$$

If this is a real process, then $R(-s) = R(s)$ and

$$R(s) = \frac{\sigma_2^2}{2\lambda_1\lambda_2(\lambda_1^2 - \lambda_2^2)} (\lambda_2 e^{\lambda_1|s|} - \lambda_1 e^{\lambda_2|s|}). \tag{6.71'}$$

Therefore, from the Fourier transform, the spectrum is, after manipulation,

$$s(\omega) = \frac{1}{2\pi} \int_{-\infty}^{\infty} R(s) e^{-i\omega s} ds$$

$$= \frac{\sigma_Z^2}{2\pi} \int_{-\infty}^{\infty} \frac{(\lambda_2 e^{\lambda_1|s|} - \lambda_1 e^{\lambda_2|s|})}{2\lambda_1\lambda_2(\lambda_1^2 - \lambda_2^2)} e^{-i\omega s} ds$$

$$= \frac{\sigma_Z^2}{2\pi} \frac{1}{\left| (i\omega)^2 + \alpha_1(i\omega) + \alpha_0 \right|^2}$$

$$= \frac{\sigma_Z^2}{2\pi} \frac{1}{(\omega^2 - \omega_n^2) + 4\kappa^2\omega_n^2\omega^2}. \tag{6.73}$$

If we use Eq. 6.54,

$$(D^2 + D\alpha_1 + \alpha_0)X(t) = Z(t)$$

$$\alpha(D)X(t) = Z(t).$$

Here $\alpha(Z) = Z^2 + \alpha_1 D + \alpha_0$.

Then from Eq. 6.73

$$s(\omega) = \frac{\sigma_Z^2}{2\pi} \frac{1}{|\alpha(i\omega)|^2}. \tag{6.73'}$$

This form is similar to Eq. 5.114, which is the expression for the discrete process AR(2).

Relation of A(2) to ARMA(2.1) by Covariance Equivalence. As was discussed in Section 5.3.5, ARMA(2.1) is more general and more flexible than AR(2). The Green's function for AR(2) is composed of two exponentials as $G_j = g_1\mu_1^j + g_2\mu_2^j$, that is one step extension or complication of AR(1) process where the Green's function is $G_j = \mu^j$ that is one exponential. By the same token, we can say that ARMA(2.1) corresponds more closely or more generally and uniquely with A(2) than AR(2) does with A(2).

Now let us express the ARMA(2.1) that corresponds with A(2) as Eq. 5.120

$$X_t + a_1 X_{t-1} + a_2 X_{t-2} = \epsilon_t + b_1 \epsilon_{t-1},$$

or as Eq. 5.123,

$$(1 + a_1 B + a_2 B^2)X_t = (1 + b_1 B)\epsilon_t.$$

The autocovariance function for this ARMA(2.1) is from Eq. 5.166,

$$R(r) = B_1\mu_1^r + B_2\mu_2^r,$$

where μ_1, μ_2 are the roots of the characteristic equation equated to zero for ARMA(2.1). Here

$$f(Z) = Z^2 + a_1 Z + a_2 = 0.$$

From Eqs. 5.67 and 5.75

$$\mu_1 + \mu_2 = -a_1$$

$$\mu_1\mu_2 = a_2,$$

$$\mu_{1,2} = \frac{1}{2}\left(-a_1 \pm \sqrt{a_1^2 - 4a_2}\right),$$

and from Eqs. 5.168 and 5.169

$$B_1 = \frac{\sigma_\epsilon^2(\mu_1 + b_1)}{(\mu_1 - \mu_2)^2}\left[\frac{\mu_1 + b_1}{1 - \mu_1^2} - \frac{\mu_2 + b_1}{1 - \mu_1\mu_2}\right]$$

$$B_2 = \frac{\sigma_\epsilon^2(\mu_2 + b_1)}{(\mu_1 - \mu_2)^2}\left[\frac{\mu_2 + b_1}{1 - \mu_2^2} - \frac{\mu_1 + b_1}{1 - \mu_1\mu_2}\right].$$

On the other hand, for A(2), when $s = r\Delta t$, from Eq. 6.71,

$$R(r\Delta t) = \frac{\sigma_Z^2}{2\lambda_1\lambda_2(\lambda_1^2 - \lambda_2^2)}(\lambda_2 e^{\lambda_1 r\Delta t} - \lambda_1 e^{\lambda_2 r\Delta t}).$$

Therefore, if we put this in the form

$$= d_1\mu_1^r + d_2\mu_2^r, \tag{6.74}$$

then

$$d_1 = \frac{\sigma_Z^2}{2\lambda_1(\lambda_1^2 - \lambda_2^2)}$$

$$\tag{6.75}$$

$$d_2 = \frac{-\sigma_Z^2}{2\lambda_2(\lambda_1^2 - \lambda_2^2)}.$$

Here λ_1, λ_2 are the characteristic roots or eigenvalues of Eq. 6.64. Then

$$\lambda_1 + \lambda_2 = -\alpha_1$$

$$\tag{6.76}$$

$$\lambda_1\lambda_2 = \alpha_0.$$

Then, as we did in Section 6.3.1, from the rule of covariance equivalence

$$e^{\lambda_1\Delta t} = \mu_1 \qquad \text{therefore } \frac{\ln\mu_1}{\Delta} = \lambda_1 \tag{6.77}$$

$$e^{\lambda_2\Delta t} = \mu_2 \qquad \text{therefore } \frac{\ln\mu_2}{\Delta} = \lambda_2, \tag{6.78}$$

and also

$$e^{\lambda_1\Delta t} + e^{\lambda_2\Delta t} = \mu_1 + \mu_2 = -a_1 \tag{6.79}$$

$$e^{-\alpha_1\Delta t} = e^{(\lambda_1+\lambda_2)\Delta t} = \mu_1\mu_2 = a_2 \quad \text{therefore } \ln a_2 = (\lambda_1 + \lambda_2)\Delta t = -\alpha_1\Delta t \tag{6.80}$$

$$\alpha_1 = \frac{\ln a_2}{\Delta t}. \tag{6.81}$$

Equating the values of d_1, d_2 for A(2) as in Eq. 6.75 and B_1, B_2 for ARMA(2.1), expressed by Eqs. 5.168 and 5.169, gives

$$\frac{\sigma_Z^2}{2\lambda_1(\lambda_1^2 - \lambda_2^2)} = \frac{\sigma_\epsilon^2(\mu_1 + b_1)}{(\mu_1 - \mu_2)^2}\left[\frac{\mu_1 + b_1}{1 - \mu_1^2} - \frac{\mu_2 + b_1}{1 - \mu_1\mu_2}\right]$$

$$-\frac{\sigma_Z^2}{2\lambda_2(\lambda_1^2 - \lambda_2^2)} = \frac{\sigma_\epsilon^2(\mu_2 + b_2)}{(\mu_1 - \mu_2)^2}\left[\frac{\mu_2 + b_1}{1 - \mu_2^2} - \frac{\mu_1 + b_1}{1 - \mu_1\mu_2}\right].$$

(6.82)

Taking the ratio on both sides of the two equations in Eq. 6.82 gives

$$-\frac{\lambda_2}{\lambda_1} = \frac{(\mu_1 + b_1)\left[\dfrac{\mu_1 + b_1}{1 - \mu_1^2} - \dfrac{\mu_2 + b_1}{1 - \mu_1\mu_2}\right]}{(\mu_2 + b_1)\left[\dfrac{\mu_2 + b_1}{1 - \mu_2^2} - \dfrac{\mu_1 + b_1}{1 - \mu_1\mu_2}\right]}.$$

(6.83)

This is a quadratic equation in b_1 and has the form

$$b_1^2 + 2Pb_1 + 1 = 0.$$

(6.84)

Thus

$$2P = -\left(b_1 + \frac{1}{b_1}\right).$$

(6.85)

After manipulation, we get .

$$2P = \frac{\lambda_1(1 + \mu_1^2)(1 - \mu_2^2) - \lambda_2(1 + \mu_2^2)(1 - \mu_1^2)}{\lambda_1\mu_1(1 - \mu_2^2) - \lambda_2\mu_2(1 - \mu_1^2)}$$

(6.86)

and also

$$b_1 = -P \pm \sqrt{P^2 - 1}.$$

(6.87)

The homogeneous equations of Eqs. 6.53 or 6.54 is

$$(D^2 + a_1 D + a_0)X(t) = 0$$

$$(D^2 + 2\kappa\omega_n + \omega_n^2)X(t) = 0,$$

and its eigenvalues λ_1, λ_2 are, according to Eq. 6.65,

222

$$\lambda_{1,2} = \frac{1}{2}\left(-\alpha_1 \pm \sqrt{\alpha_1^2 - 4\alpha_0}\right) = -\omega_n\left(\kappa \pm \sqrt{\kappa^2 - 1}\right).$$

We can transform Eq. 6.86 into the equation expressed by a_1, a_2, and b_1 of the corresponding ARMA(2.1) model by the relation of the so-called covariance equivalence.

a. When $\alpha_1^2 < 4\alpha_0$ ($\kappa^2 < 1$):

Further, for simplicity of expression, we set

$$\begin{aligned} \lambda_1 &= -u + iv \\ \lambda_2 &= -u - iv. \end{aligned} \tag{6.88}$$

Then

$$v = \frac{1}{2}\sqrt{4\alpha_0 - \alpha_1^2} = \frac{1}{2}\omega_n\sqrt{1 - \kappa^2}$$

$$u = \frac{1}{2}\alpha_1 \tag{6.89}$$

$$\begin{aligned} \alpha_1 &= 2u \\ \alpha_0 &= u^2 + v^2. \end{aligned} \tag{6.90}$$

From the covariance equivalence relations between AR(2) and ARMA(2.1) we have Eqs. 6.77, 6.78, 6.79, and 6.80. Further use of Eq. 6.88 gives

$$-a_1 = \mu_1 + \mu_2 = e^{(-u+iv)\Delta t} + e^{(-u-iv)\Delta t} = e^{-u\Delta t} \cdot 2\cos(v\Delta t)$$

$$\mu_1 - \mu_2 = e^{-u\Delta t} \cdot 2i \sin(v\Delta t)$$

$$1 - a_2 = 1 - \mu_1\mu_2 = e^{-u\Delta t} \cdot 2 \sinh(u\Delta t)$$

$$1 + a_2 = 1 + \mu_1\mu_2 = e^{-u\Delta t} \cdot 2 \cosh(u\Delta t) \tag{6.91}$$

$$\mu_1^2 - \mu_2^2 = 2e^{-2u\Delta t} \cdot i \sin(2v\Delta t)$$

$$1 - a_2^2 = 1 - \mu_1^2\mu_2^2 = 2e^{-2v\Delta t} \cdot \sinh(2u\Delta t).$$

Inserting these expressions into Eq. 6.86 gives

223

$$P = \frac{v \, \sinh \, (2u\Delta t) - u \, \sin \, (2v\Delta t)}{2u \, \sin \, (v\Delta t) \, \cosh \, (u\Delta t) - 2v \, \sinh \, (u\Delta t) \, \cos \, (v\Delta t)}. \quad (6.92)$$

Then,

$$v = \frac{u \, [2P \, \sin \, (v\Delta t) \, \cosh \, (u\Delta t) + \sin \, (2v\Delta t)]}{2P \, \sinh \, (u\Delta t) \, \cos \, (v\Delta t) + \sinh \, (2u\Delta t)}. \quad (6.93)$$

From Eqs. 6.90 and 6.81

$$u = \frac{-\ln \, (a_2)}{2\Delta t}, \quad e^{-u\Delta t} = \sqrt{a_2}. \quad (6.94)$$

Therefore, from Eqs. 6.91 and 6.94

$$\cos \, (v\Delta t) = \frac{-a_1}{2\sqrt{a_2}}$$

$$\sin \, (v\Delta t) = \frac{\sqrt{-(a_1^2 - 4a_2)}}{2\sqrt{a_2}}$$

$$\cosh \, (u\Delta t) = \frac{1 + a_2}{2\sqrt{a_2}} \quad\quad (6.95)$$

$$\sinh \, (u\Delta t) = \frac{1 - a_2}{2\sqrt{a_2}}.$$

With Eqs. 6.95 and 6.85, Eq. 6.93 can be transformed into an equation with a_1, a_2, and b_1,

$$v = \frac{-\ln \, (a_2)}{2\Delta t} \, \sqrt{-(a_1^2 - 4a_2)} \left[\frac{-2a_1 + (1 + a_2)\left(b_1 + \frac{1}{b_1}\right)}{2(1 - a_2^2) - a_1(1 - a_2)\left(b_1 + \frac{1}{b_1}\right)} \right]. \quad (6.96)$$

If we look at the first equation of Eq. 6.95, v is derived as

$$v = \frac{1}{\Delta t} \, \cos^{-1} \left(\frac{-a_1}{2\sqrt{a_2}} \right). \quad (6.97)$$

That value is not unique, since it does not include the MA parameter b_1. However, Eq. 6.96 shows that v is uniquely determined from a_1, a_2, and b_1, since it includes the MA parameter b_1 as well as a_1 and a_2. This is another reason why generally we prefer ARMA(2.1) over AR(2) as the discrete process corresponding to A(2) and u is expressed by Eq. 6.91.

224

After u, v are determined, α_1, α_0, or R, ω_n can be easily derived from u, v by Eq. 6.90

b. When $\alpha_1^2 \geq 4\alpha_0$ $(\kappa^2 > 1)$:

We can set

$$\lambda_1 = -u + v$$
$$\lambda_2 = -u - v. \tag{6.98}$$

Then computing the necessary elements for P in Eq. 6.86 in a similar way, we get

$$\mu_1 + \mu_2 = e^{\lambda_1 \Delta t} + e^{\lambda_2 \Delta t} = e^{-u\Delta t} \cdot 2 \cosh (v\Delta t)$$

$$\mu_1 - \mu_2 = e^{-u\Delta t} \cdot 2 \sinh (v\Delta t)$$

$$1 - \mu_1 \mu_2 = e^{-u\Delta t} \cdot 2 \sinh (u\Delta t)$$

$$1 + \mu_1 \mu_2 = e^{-u\Delta t} \cdot 2 \cosh (u\Delta t) \tag{6.99}$$

$$(\mu_1 + \mu_2)(\mu_1 - \mu_2) = 2 \ e^{-2u\Delta t} \sinh (2v\Delta t)$$

$$(1 - \mu_1^2 \mu_2^2) = 2 \ e^{-2u\Delta t} \sinh (2u\Delta t).$$

Inserting these values in Eq. 6.86 for P gives, after manipulation,

$$P = \frac{u \ \sinh (2v\Delta t) - v \ \sin (2u\Delta t)}{2u \ \sinh (v\Delta t) \cosh (u\Delta t) - 2v \ \cosh (v\Delta t) \sinh (u\Delta t)}. \tag{6.100}$$

Then

$$v = \frac{u \ [2P \ \sinh (v\Delta t) \cosh (u\Delta t) - \sinh (2v\Delta t)]}{2P \ \cosh (v\Delta t) \sinh (u\Delta t) - \sinh (2u\Delta t)}. \tag{6.101}$$

As were for $\alpha_1^2 < 4\alpha_0$, the sin, cos, sinh, cosh functions are expressed by a_1, a_2 for this case. Therefore, after v and u have been determined, α_1, α_2 or κ, ω_n can be determined from u, v easily. Their derivations are omitted here because we are usually less concerned with the case when $\kappa^2 > 1$.

For this case, the coefficients α_1, α_0 or κ, ω_n of the differential equation are derived from a_1, a_2, and b_1 uniquely. The differential equation which expresses the continuous autoregressive process can be obtained from the parameters a_1, a_2, and b_1 of the

difference equation that formulates the discrete autoregressive and moving average process ARMA(2.1).

The above mentioned is for the simple case of ARMA(2.1) versus AR(2). For the more complicated cases of ARMA(4.3), ARMA(6.5) . . . , theoretically A(4), A(6), . . . , should correspond, and the parameters of differential equations that formulate these A(4), A(6) . . . should be derived from the parameters of the difference equations that formulate ARMA(4.3), ARMA(6.5) . . . , although their relations might be much more complicated than for A(2) from ARMA(2.1). The differential equations that formulate the continuous autoregressive process give us good clues to finding the physical characteristics of their response processes.

The second order linear differential equation is the basic equation of a linear dynamic system with one degree of freedom. Accordingly, the above discussion indicates that the ARMA(2.1) process represents the dynamic behavior of a linear system with one degree of freedom under the excitement of white noise.

CHAPTER 7

EXAMPLES OF MODEL FITTING TECHNIQUE APPLIED TO THE ANALYSIS OF SEAKEEPING DATA

In this chapter, examples of application of the model fitting technique to seakeeping data will be presented to demonstrate the applicability of this technique to the analysis of these data.

7.1 EXAMPLES OF AR(n) MODEL FITTING FOR THE PREDICTION OF SEAKEEPING DATA

Figure 7.1[46] shows examples of fitting of AR(n) models to observed seakeeping data. After the appropriate order number n was determined by the MAIC method, as described in Section 5.5.4, the parameters $a_1 \ldots a_n$ were calculated from 800 observed data points for the respective processes. Here for rolling $n=7$ and for swaying $n=19$ were found to be the optimum. Figure 7.1 shows the values predicted for each process by

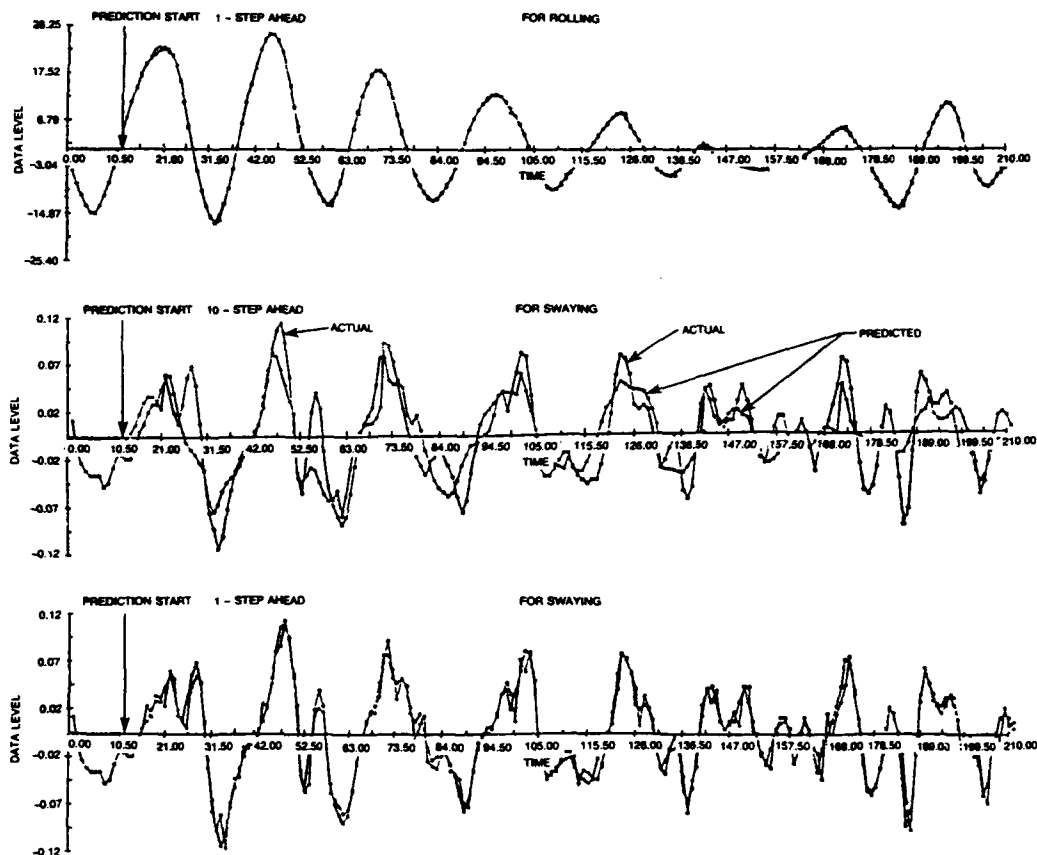$$X_t = -a_1 X_{t-1} - a_2 x_{t-2} - - - - a_n X_{t-n} \tag{7.1}$$

Fig. 7.1. Comparison between the predicted values of seakeeping data and the observed values.

(From Yamanouchi, et al.[46])

227

using these $a_1 \ldots a_n$. One–step–ahead predictions for rolling and swaying and a 10– steps–ahead prediction for swaying are shown here.

7.2 EXAMPLES OF MODEL FITTING TECHNIQUE APPLIED TO THE SEAKEEPING DATA

Figure 7.2[46] shows examples of spectra of model seakeeping data obtained in a model basin for a model of a ship. On the left–hand side (a), the spectra calculated by the nonparametric method, the so–called Blackman–Tukey method, are shown and on the right–hand side (b), the same spectra calculated by the parametric method, i.e., the AR(n) model fitting technique. The spectra for wave height, heaving, and relative wave height are shown on a logarithmic scale, and the Nyquist frequency of 2.50 shows

$\Delta t = (1/2.50 \times 2) = 0.2$ sec. The total number of observations is $N = 225$, which is rather small, and the maximum lag number for the B–T method is 50, which is large compared to N. We can find the spectrum from the AR model, the order of each process being shown by the AR number in each figure. The spectra are very smooth and the peaks of the spectra are sharply defined even from these short records (small number of observations).

Figure 7.3[46] shows the behavior of AIC values that were used to find the order n of the AR models fitted to each set of these seakeeping data. From this figure, we found n to be 11, 9, and 10 for wave height, heave, and relative wave height, respectively. These values give the minimum AIC.

Figure 7.4 shows the time series of an AR(2) model simulated by the difference equation,

$$X_t - 0.5X_{t-1} + 0.7X_{t-2} = \epsilon_t$$

when $a_1 = -0.5$, $a_2 = 0.7$ in Eq. 5.59 for a general AR(2) model. There, ϵ_t is white noise with Gaussian distribution $N(0, 1)$, i.e., with 0 mean and a variance 1. The time series are also shown in the same figure. The number of observations is $N = 1,000$ for both time series ϵ_t and X_t. The theoretical spectrum of this AR(2) model is shown at the top of Fig. 7.5.[52] An AR(n) model was fitted to the simulated process, and from AIC criteria, the optimum n was estimated as $n=2$. The coefficients a_1, a_2, and the variance σ_ϵ^2 of ϵ_t were estimated by the method described in Section 5.2.3, and the spectrum $s(\omega)$ was calculated using these parameters, as shown at the bottom of Fig. 7.5. Independent of this order $n=2$ by minimum AIC criteria, spectra were also estimated for higher n; A(10) and AR(20) models were fitted and their spectra were obtained as shown in the same Fig. 7.5.
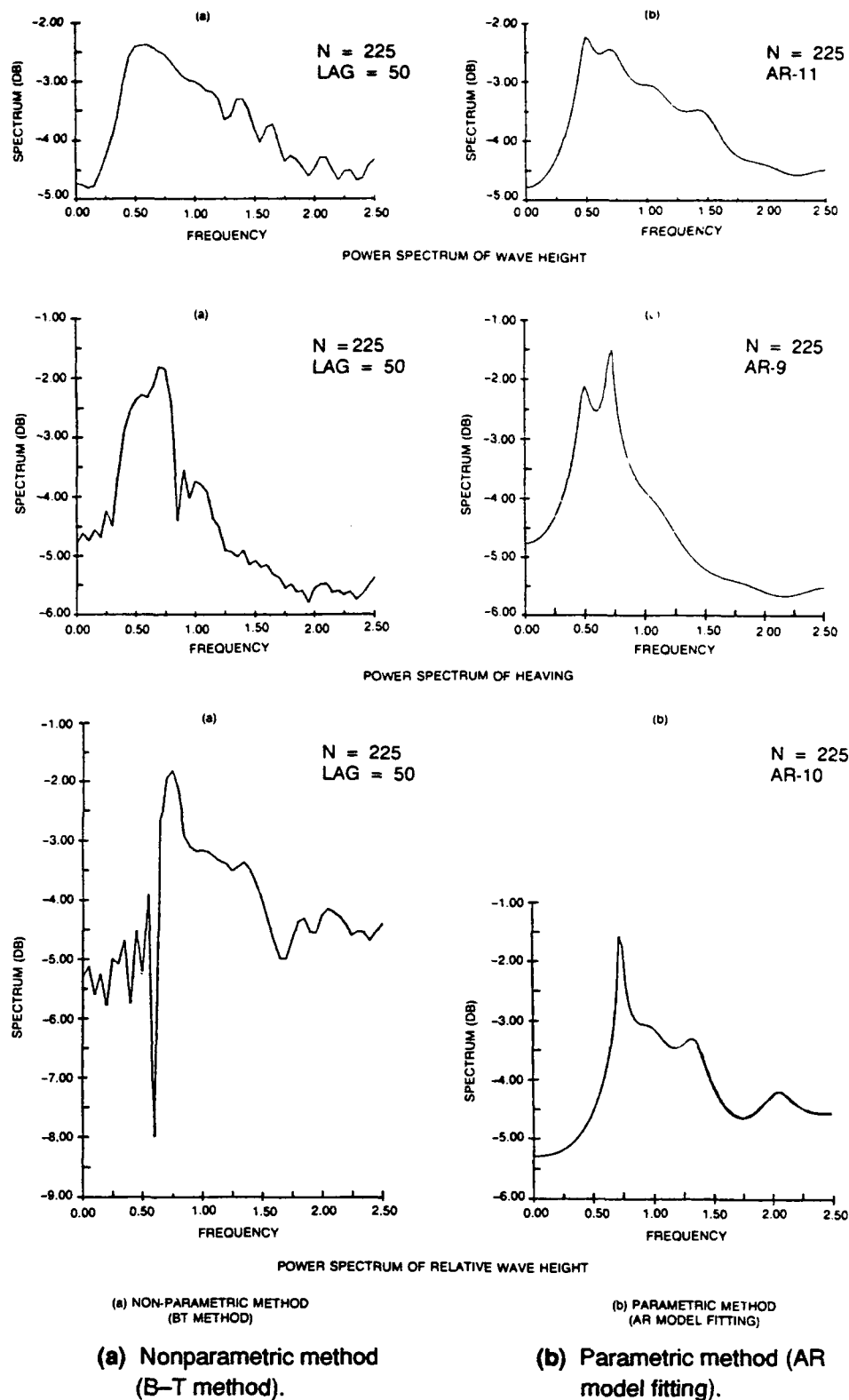
(a) Nonparametric method (B–T method).

(b) Parametric method (AR model fitting).

Fig. 7.2. Examples of spectra of model seakeeping data. (From Yamanouchi, et al.[46])
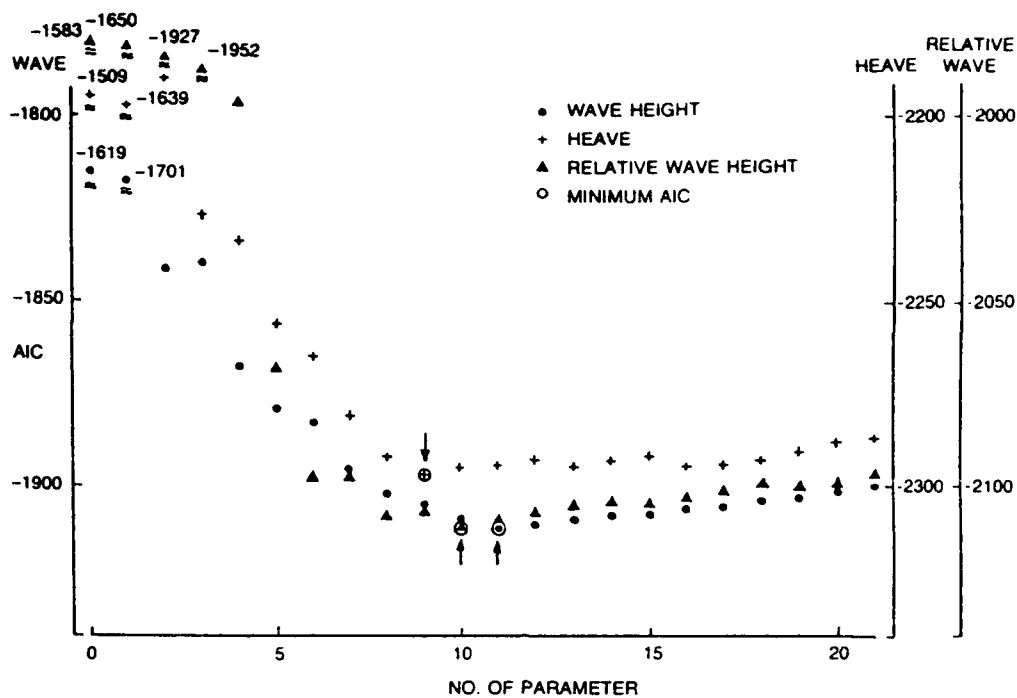
229

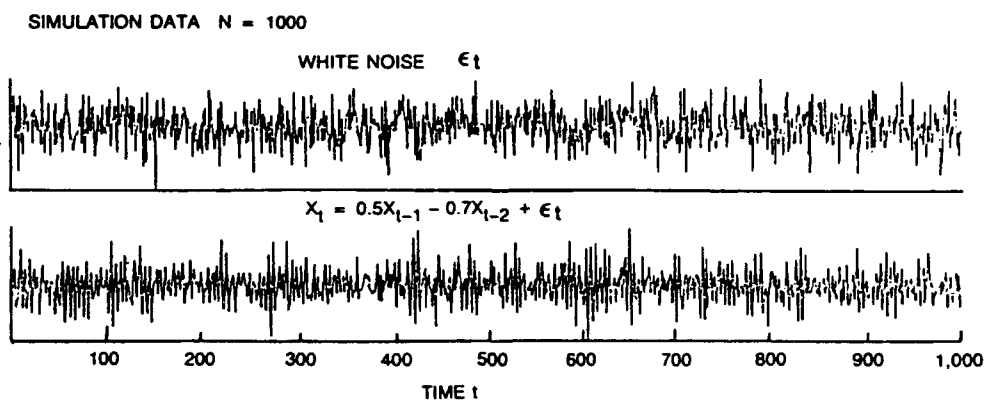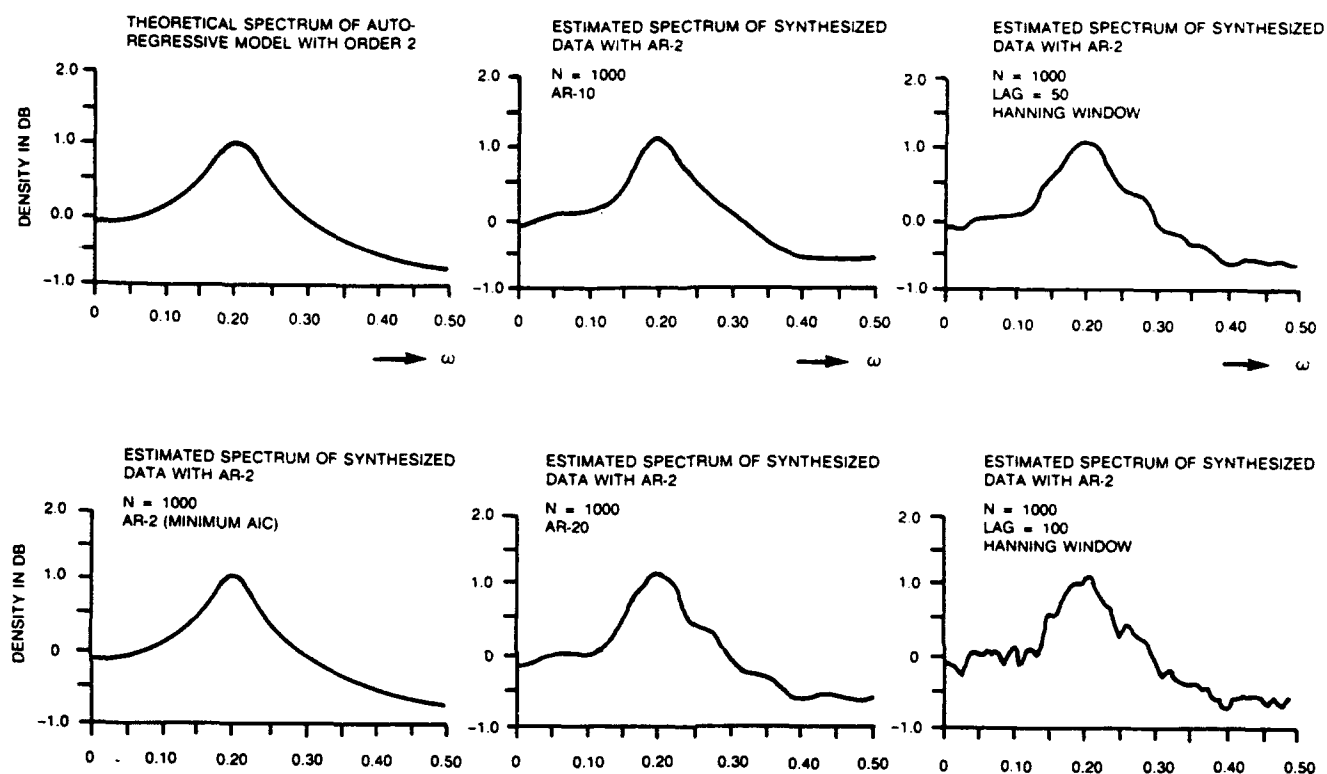**Fig. 7.3.** Behavior of AIC for seakeeping data in getting the spectra (b) in Fig. 7.2. (From Yamanouchi, et al.[46])

Fig. 7.4. Simulated AR(2) process $X_t = 0.5\ X_{t-1} - 0.7\ X_{t-2} + \epsilon_t$, ϵ_t is a white noise $N(0,1)$.

(From Yamanouchi, et al.[52])

230

THEORETICAL SPECTRUM OF AUTO-REGRESSIVE MODEL WITH ORDER 2

ESTIMATED SPECTRUM OF SYNTHESIZED DATA WITH AR-2
N = 1000
AR-10

ESTIMATED SPECTRUM OF SYNTHESIZED DATA WITH AR-2
N = 1000
LAG = 50
HANNING WINDOW

ESTIMATED SPECTRUM OF SYNTHESIZED DATA WITH AR-2
N = 1000
AR-2 (MINIMUM AIC)

ESTIMATED SPECTRUM OF SYNTHESIZED DATA WITH AR-2
N = 1000
AR-20

ESTIMATED SPECTRUM OF SYNTHESIZED DATA WITH AR-2
N = 1000
LAG = 100
HANNING WINDOW

(a) AR method (optimum).   (b) AR method (not optimum).   (c) B–T method.

Fig. 7.5 Comparison of AR–model fitting method and B–T method and the effect of changing orders of AR–model fitted to the simulated AR–2 process.
(From Yamanouchi, et al.[52])

231

For comparison, the spectra calculated by the nonparametric method (Blackman–Tukey method) are also shown in this figure. The maximum lag numbers are 50 and 100, which give a fairly high confident estimate since these numbers are 1/20 and 1/10 of the total number of observations $N=1,000$. It is interesting to note that the result for lag=50 looks much like the one for AR(20). The impressive point here is, of course, that the estimate from the model fitting technique, which determines the order from the minimum AIC criteria, gives a result that checks the theoretical process very well.

Figure 7.6 compares the estimates from AR model fitting and the B–T method for the same simulated process (Fig. 7.4) for a wider range of order (AR 1–16) and maximum lag numbers of 20–500, for reference.

Figure 7.7[52] shows a few examples of the analysis of actual at-sea ship performance data. Rolling, wave height measured by buoy, and the horizontal acceleration of the engine bed (as of different frequency characteristics, because the engine bed is mostly excited by the prime movers of the ship) were analyzed by three different methods: the AR model fitting method, the F.F.T. method, and the Blackman–Tukey method. The sampling time interval was $\Delta t=1$ sec for roll and wave height, $\Delta t=0.02$ sec, much smaller for acceleration. The spectrum of the horizontal acceleration of the engine bed estimated by the AR model fitting method gives very reasonable results, compared with the ones obtained by other methods, the former clearly showing the existence of multiple natural frequencies.

Figure 7.8[53] shows other examples of the spectra of the horizontal acceleration of the engine bed estimated by the AR model fitting method at orders n of 5, 10, 15, 20, 30, and 55. The result at $n=10$, where the AIC shows minimum values, looks most reasonable and clearly shows the existence of multiple natural frequencies in horizontal vibration.

7.3 EXAMPLES OF PARAMETRIC ANALYSIS OF RESPONSE CHARACTERS OF MARINE VEHICLES AND STRUCTURES

Figure 7.9[52] shows an example of simple response, the case of yaw angle versus rudder angle of a seagoing ship. The results for the spectra of input and output and the frequency responses from two methods, the AR model fitting and nonparametric methods, are compared. When the spectrum and response characteristics do not show any abrupt changes with frequency, as in the example, most of the results from the two methods look similar. However, when we look at the Nyquist diagram or the mode diagram of the frequency response characteristics, the results from the AR model fitting are much better and smoother and more reasonable, physically, than those from the nonparametric method.

Figures 7.10 and 7.11[46] show the results of seakeeping data for a model ship in waves produced in the towing tank, also analyzed by two different methods.

From these figures we see that the AR–model fitting techniques give smoother curves for the spectra and for the frequency responses. Also, in the important range of frequencies, the coherency values are closer to 1, showing that the response characteristics are more reliable when estimated by this method.

In both figures, the cross spectra are shown by their real and imaginary parts, i.e., by co– and quadrature–spectra. The shape of these spectra, which show very sharp peaks,
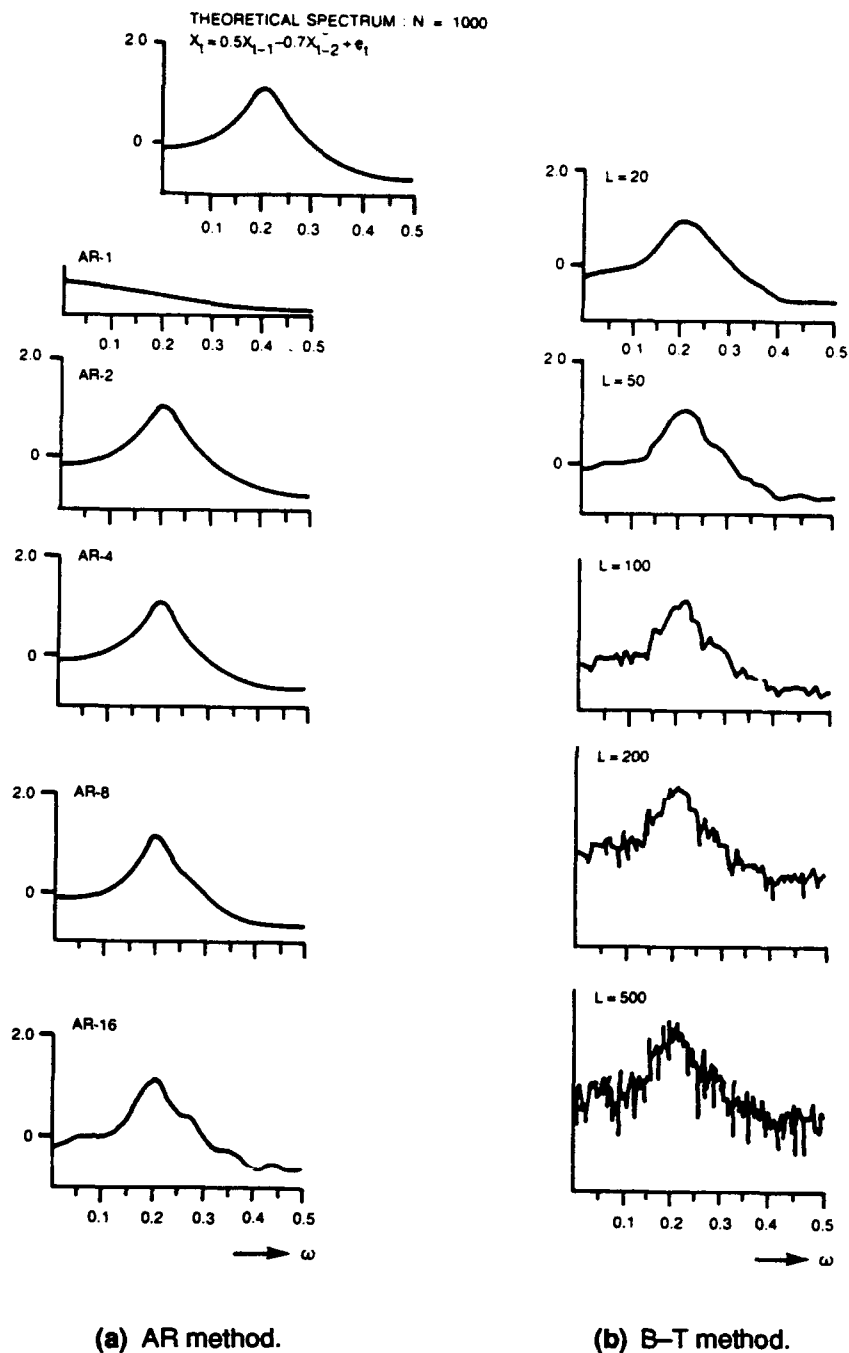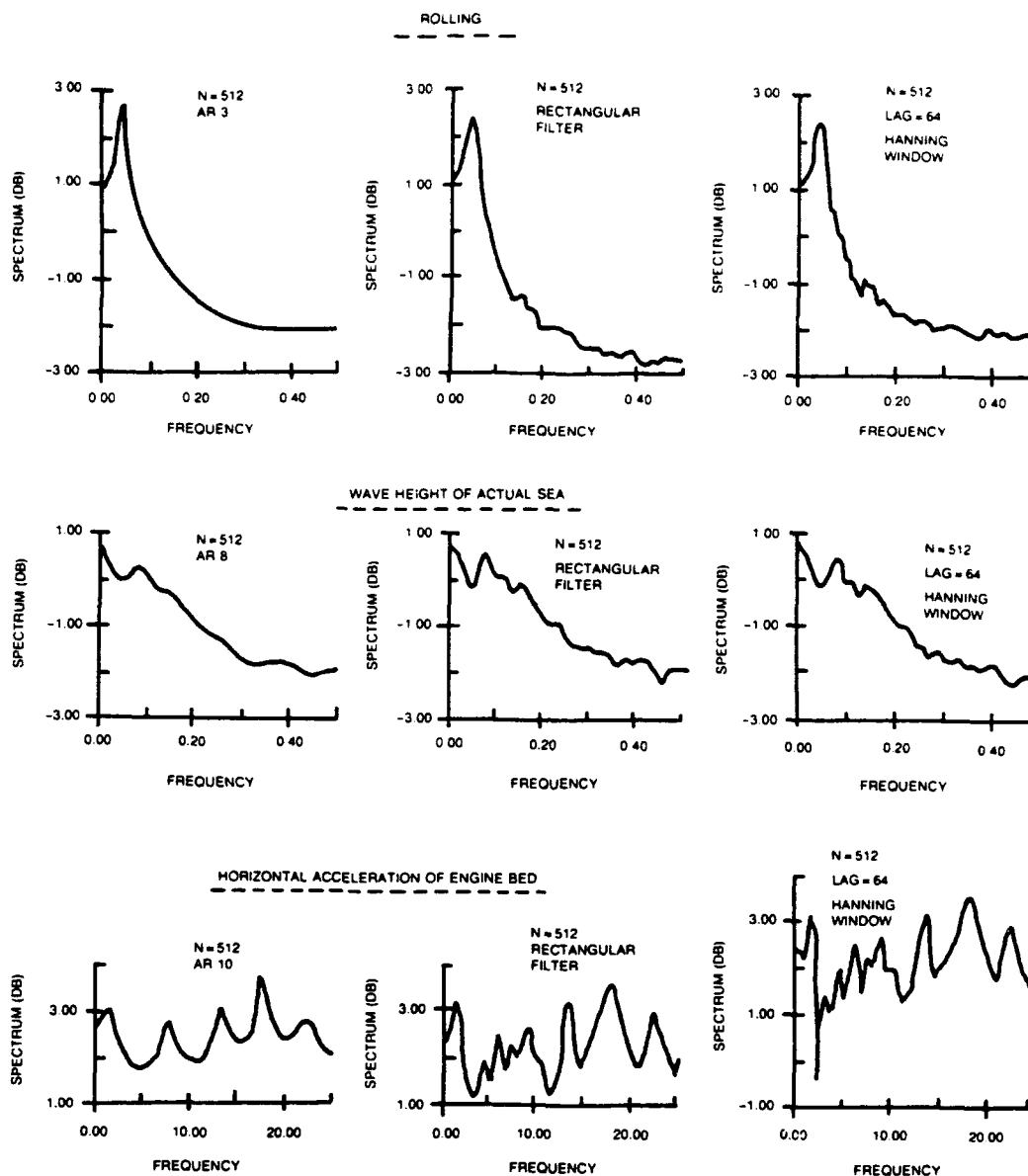
Fig. 7.6. Effect of changing orders in AR–model fitting to the simulated AR(2) process (Fig. 7.4) [MAIC shows order is AR–2] and the comparison with spectrum obtained by B–T method.

(From Yamanouchi, et al.[52])

233

ROLLING

WAVE HEIGHT OF ACTUAL SEA

HORIZONTAL ACCELERATION OF ENGINE BED

(a) AR model fitting.   (b) F.F.T. method.   (c) B–T method.

Fig. 7.7. Comparison of the spectrum through AR–model fitting and conventional methods.
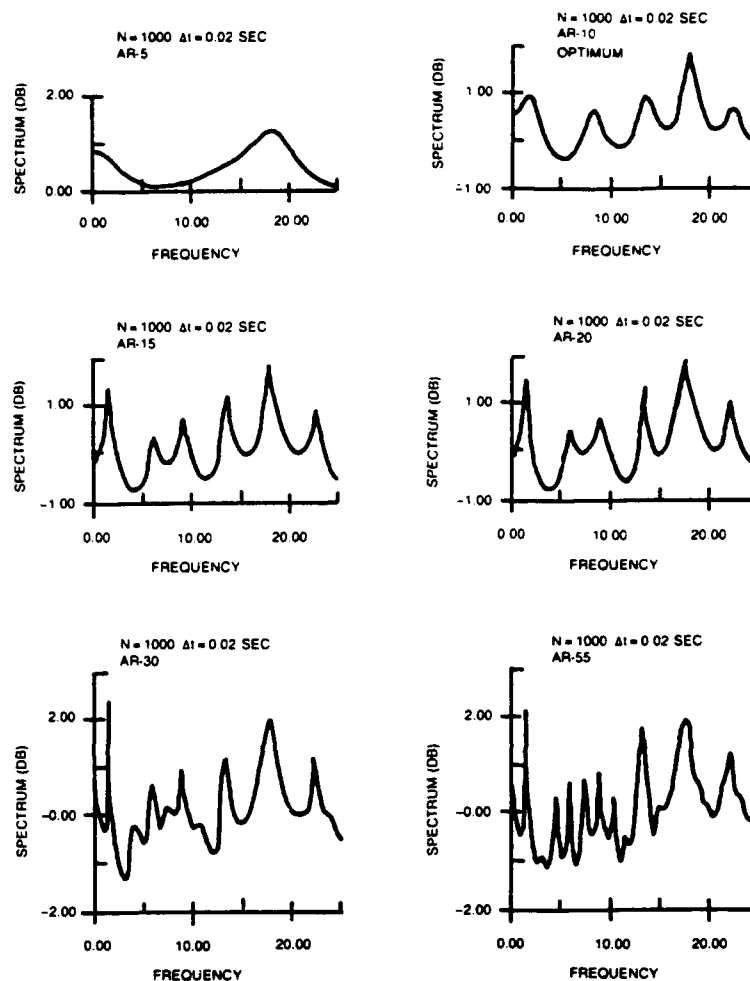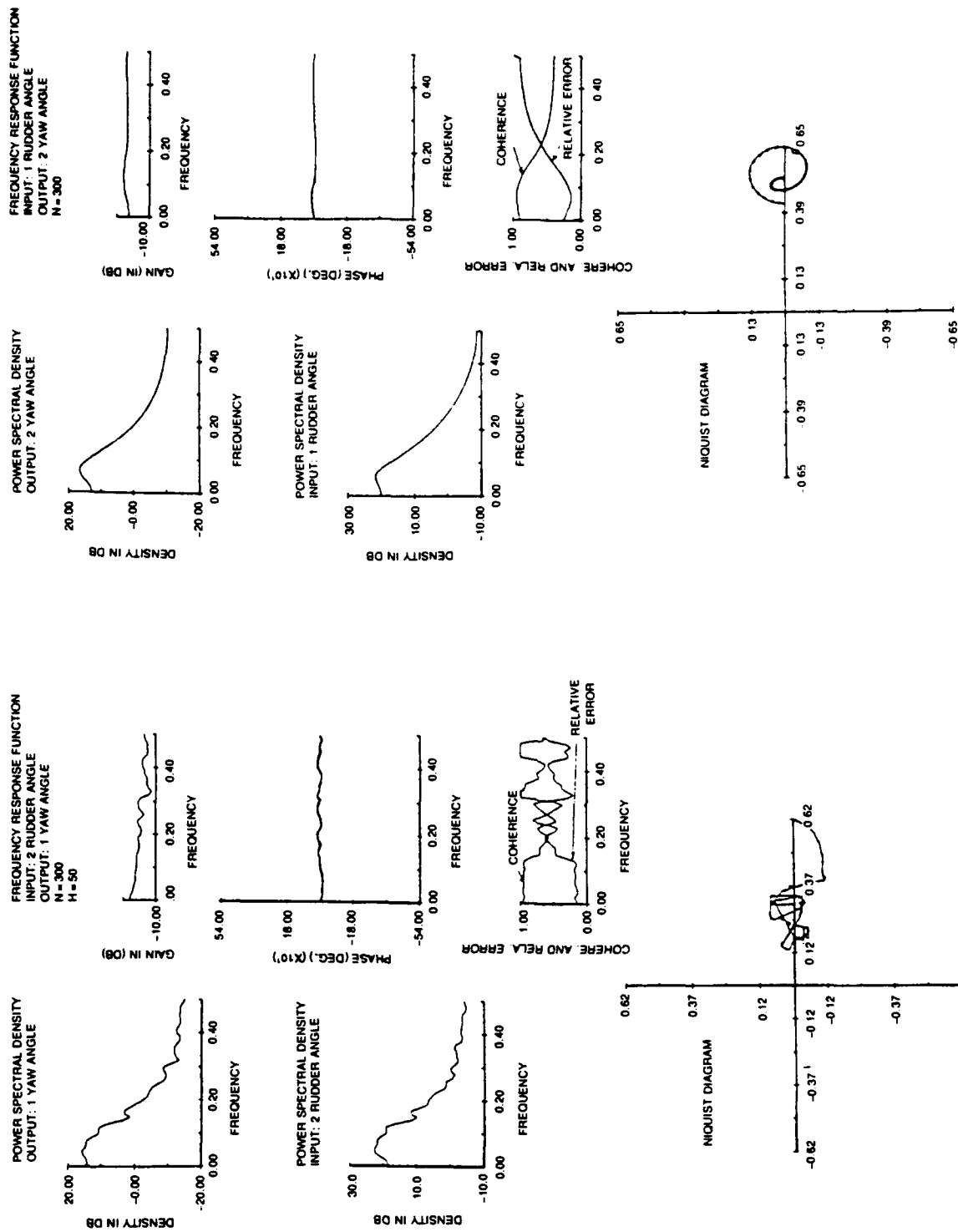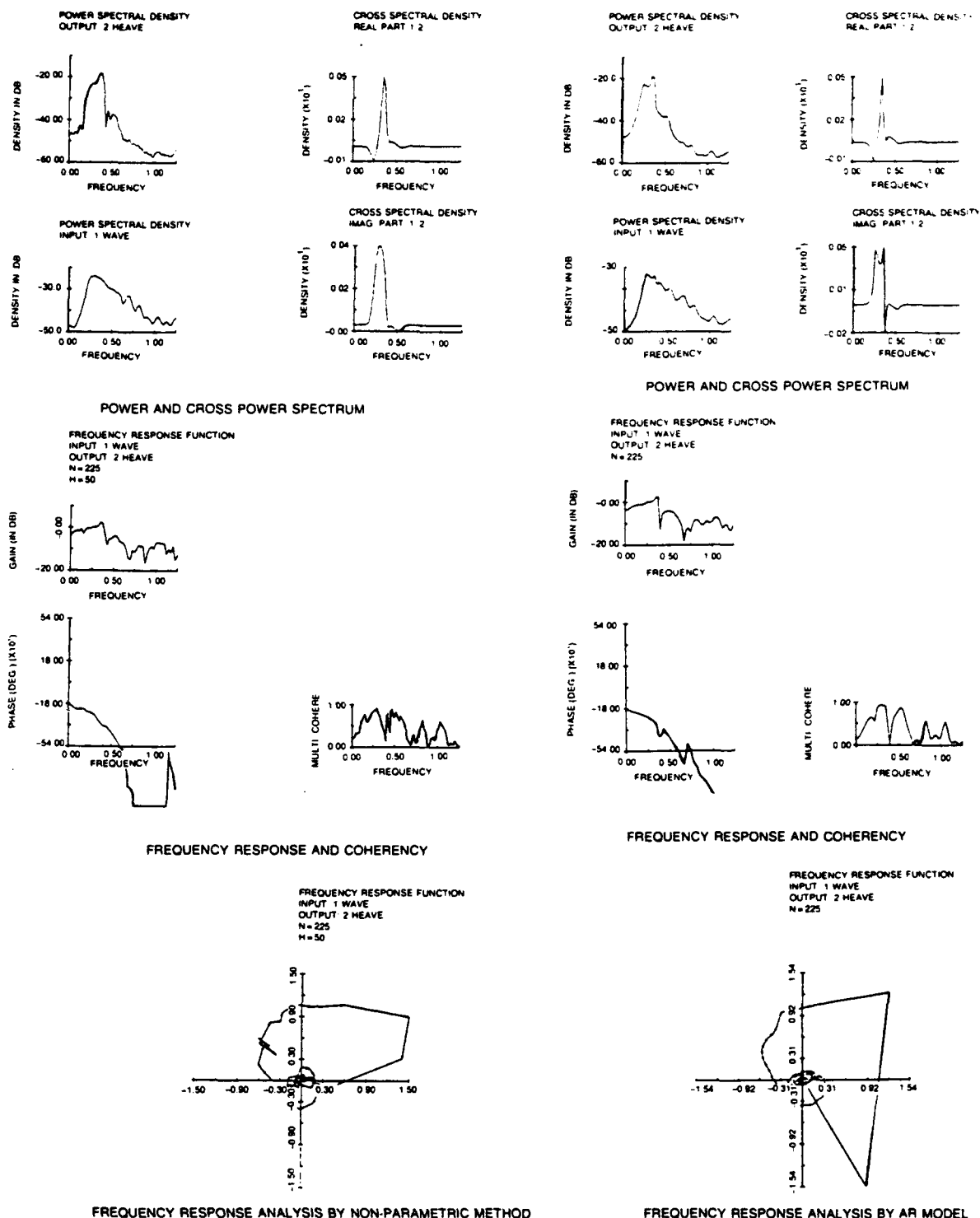
(From Yamanouchi, et al.[52])

234

Fig. 7.8. Effect of changing the orders in AR–model fitting (by MAIC; AR=10).
(From Oda, Yamanouchi, et al.[53])

indicates that the AR method gives better results than the B–T method and more precisely follows the rapid changes in the curves.

By the way, the time shift techniques that this author proposed in Section 3.2 might have given even greater improvement in the results if it were properly applied. The rapid change in phase response with frequency shows this fact and indicates that there is still room for improvement by the proper shift of responses even in the case of using model fitting techniques. Figure 7.12[54] is an example of the same kind of comparison of two analysis methods used on the pitch motion of a model of an offshore semisubmersible as shown by Fig. 7.13 on irregular waves in the model tank.

235

(a) Nonparametric method.

(b) AR-model fitting method.

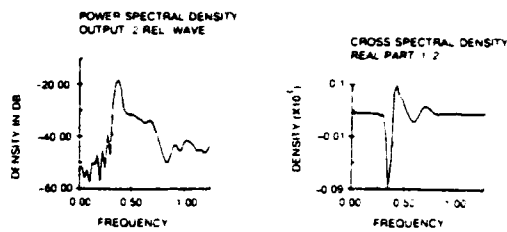Fig. 7.9. Comparison of methods to analyze the frequency response characters of a ship on the sea. (From Yamanouchi, et al.[52])

236

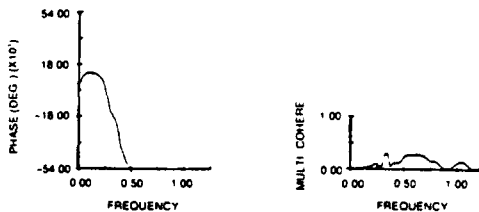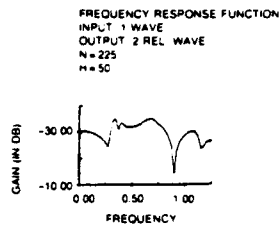**(a)** Nonparametric method (max. lag = 50).

(b) AR–model fitting method (order *n*=11).

Fig. 7.10. Comparison of methods to analyze the frequency response characters of a model ship in the tank – sample 1.
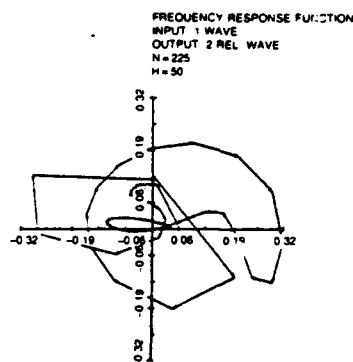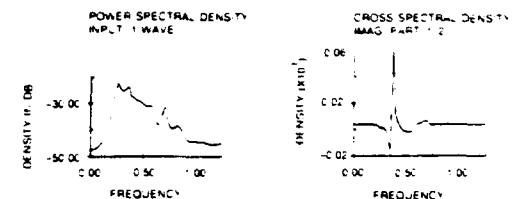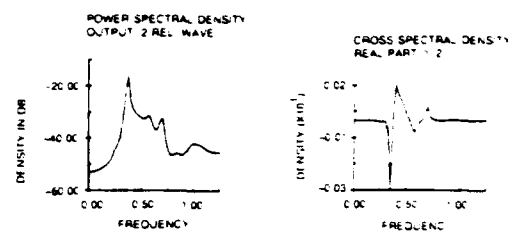
(From Yamanouchi, et al.[46])
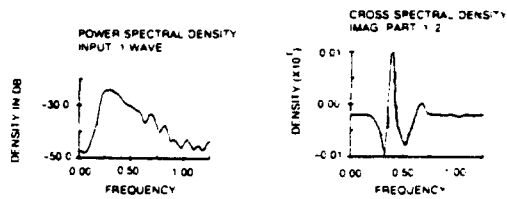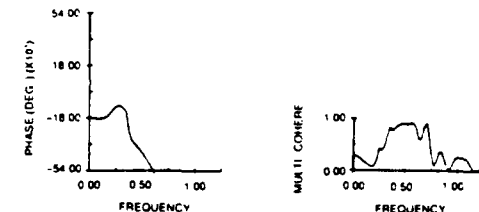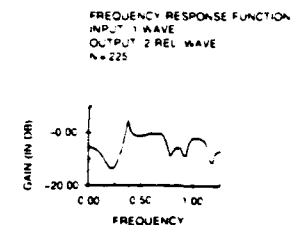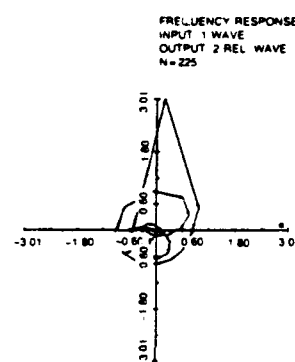
(a) Nonparametric method (max. lag = 50).　　**(b)** AR–model fitting method (order n=14).

Fig. 7.11. Comparison of methods to analyze the frequency response characters of a model ship in the tank – sample 2.

(From Yamanouchi, et al.[46])
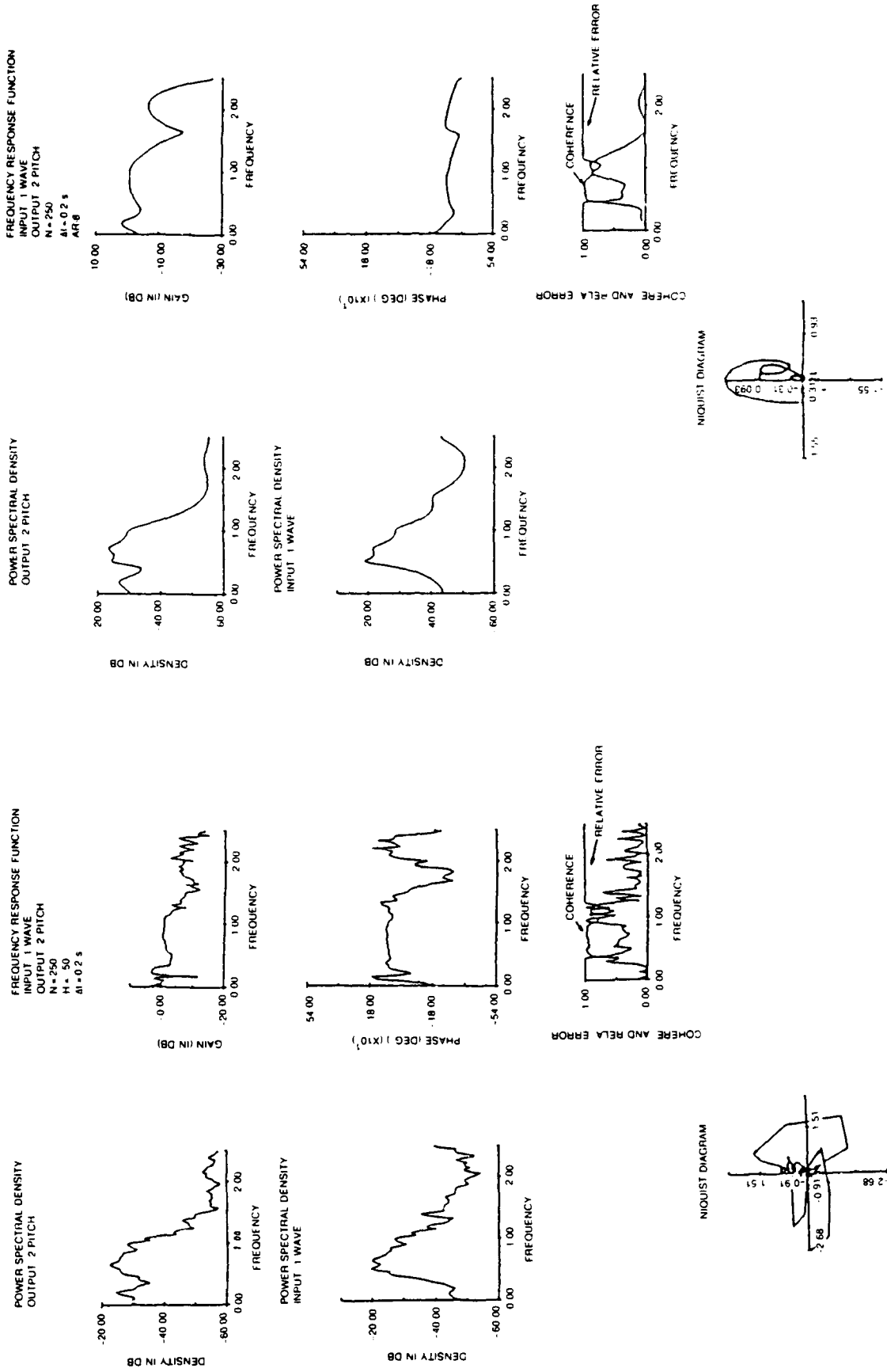
(b) AR-model fitting method (order $n=8$).

Fig. 7.12. Comparison of methods to analyze the frequency response characters of a model offshore structure. (From Yamanouchi, et al.[54])
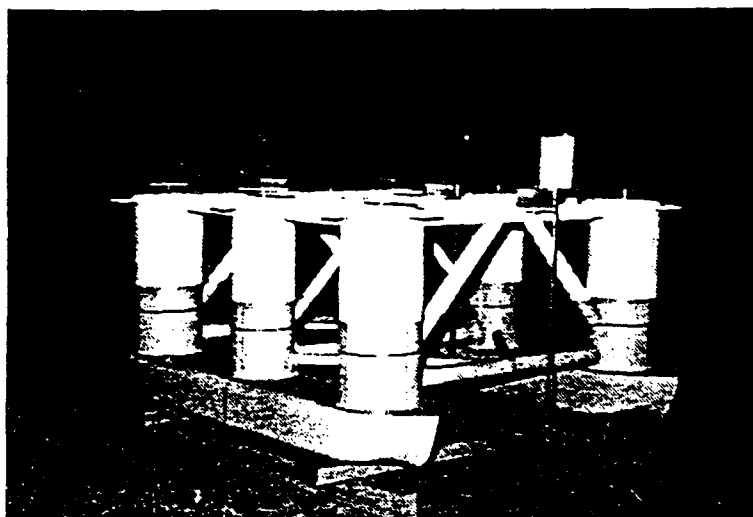
(a) Nonparametric method (max. log = 50).

239

Fig. 7.13. Photograph of a semisubmersible model (scale 1/90).
(From Oda, Yamanouchi, et al.[53])

Figures 7.14–7.17[53] show the results of frequency response analysis of the model seakeeping data as heave, relative wave height, pitch, and surge in irregular waves determined by the AR model fitting technique for the same offshore semisubmersible. These data were analyzed as a one–input/one–output vector process, although, if we like, we can analyze them as a one–input/multiple–output vector AR process. The orders of AR models fitted to these systems are marked on each of the figures.

Figure 7.16 is concerned with the same response under the same conditions as Fig. 7.12. From these results, we can find the same characteristics of AR–model fitting techniques. All the spectra and the frequency responses are much smoother and follow well the rapid changes with the frequency. These tendencies are more clearly indicated by Fig. 7.18.

In Fig. 7.18 the response characteristics of heave, relative wave height, pitch, and surge are shown expanded in the important range of response frequencies for 6–24 second periods for a full–scale structure. The results obt⌐ined by the AR model fitting and B–T methods are shown with results of experiments in regular waves in the tank. The figures show rather surprisingly how well the results from the AR model fitting technique follow the minor changes of the response in amplitude as well as in phase relations obtained in experiments with the regular harmonic waves of several frequencies.

POWER SPECTRAL DENSITY
INPUT 1 WAVE

POWER SPECTRAL DENSITY
OUTPUT 2 HEAVE

CROSS SPECTRAL DENSITY
REAL PART 1 2

CROSS SPECTRAL DENSITY
IMAG PART 1 2
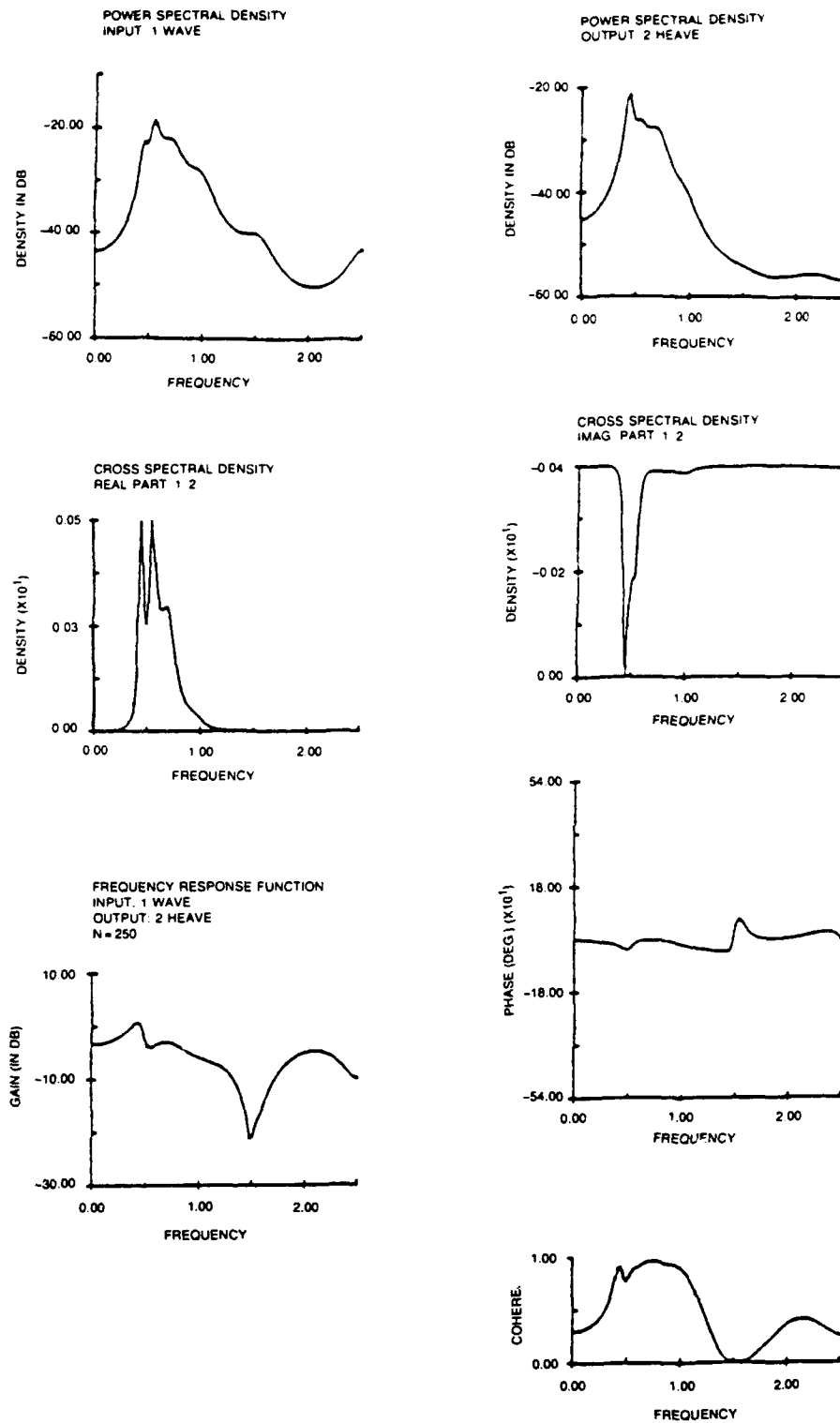
FREQUENCY RESPONSE FUNCTION
INPUT: 1 WAVE
OUTPUT: 2 HEAVE
N = 250

Fig. 7.14. Frequency response analysis for heave by AR–model fitting
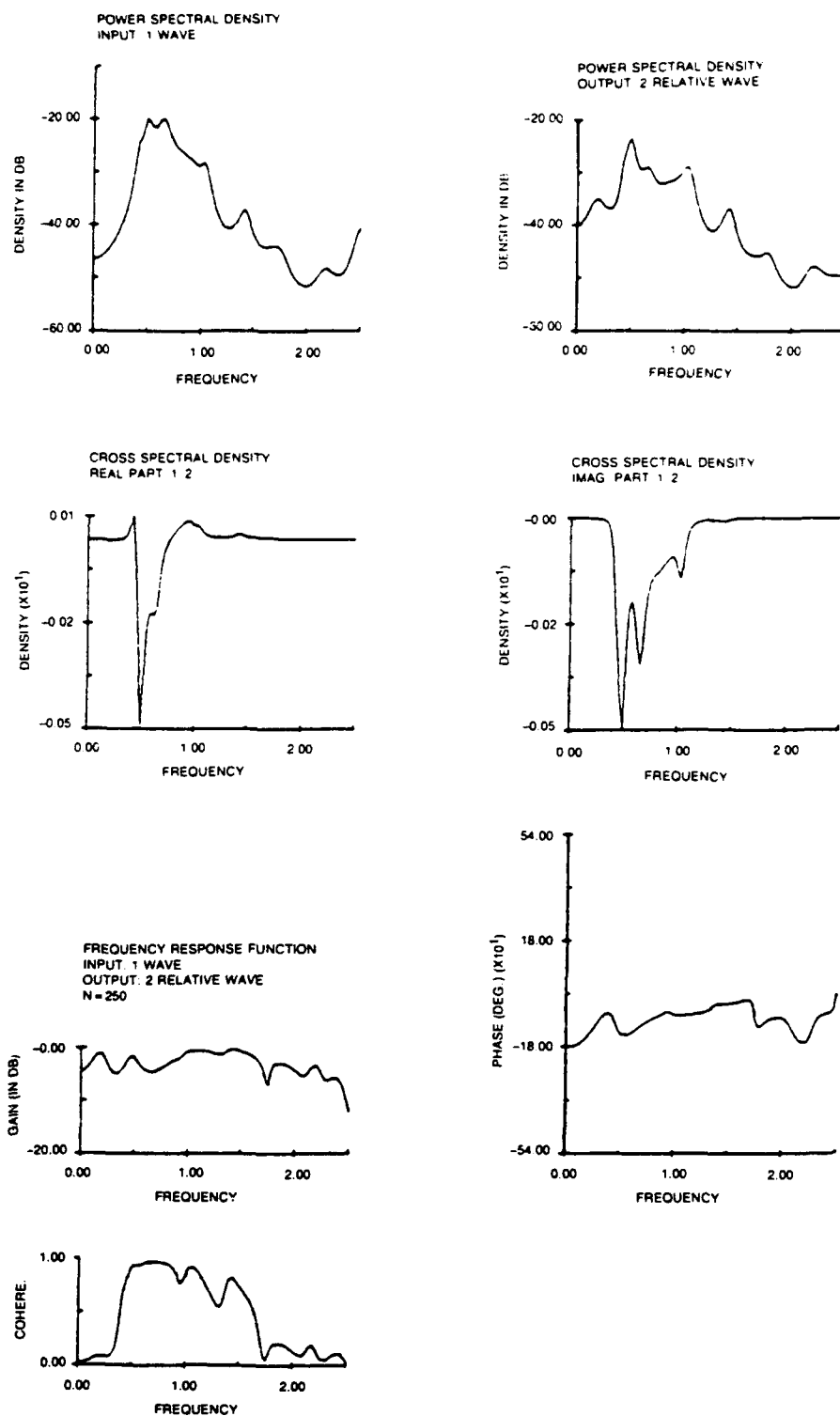(N=250, Δt=0.2 sec, AR–8).
(From Oda, Yamanouchi, et al.[53])

241

Fig. 7.15. Frequency response analysis for relative wave height by
AR–model fitting (N=250, Δt=0.2 sec, AR–15).

(From Oda, Yamanouchi, et al.[53])

242
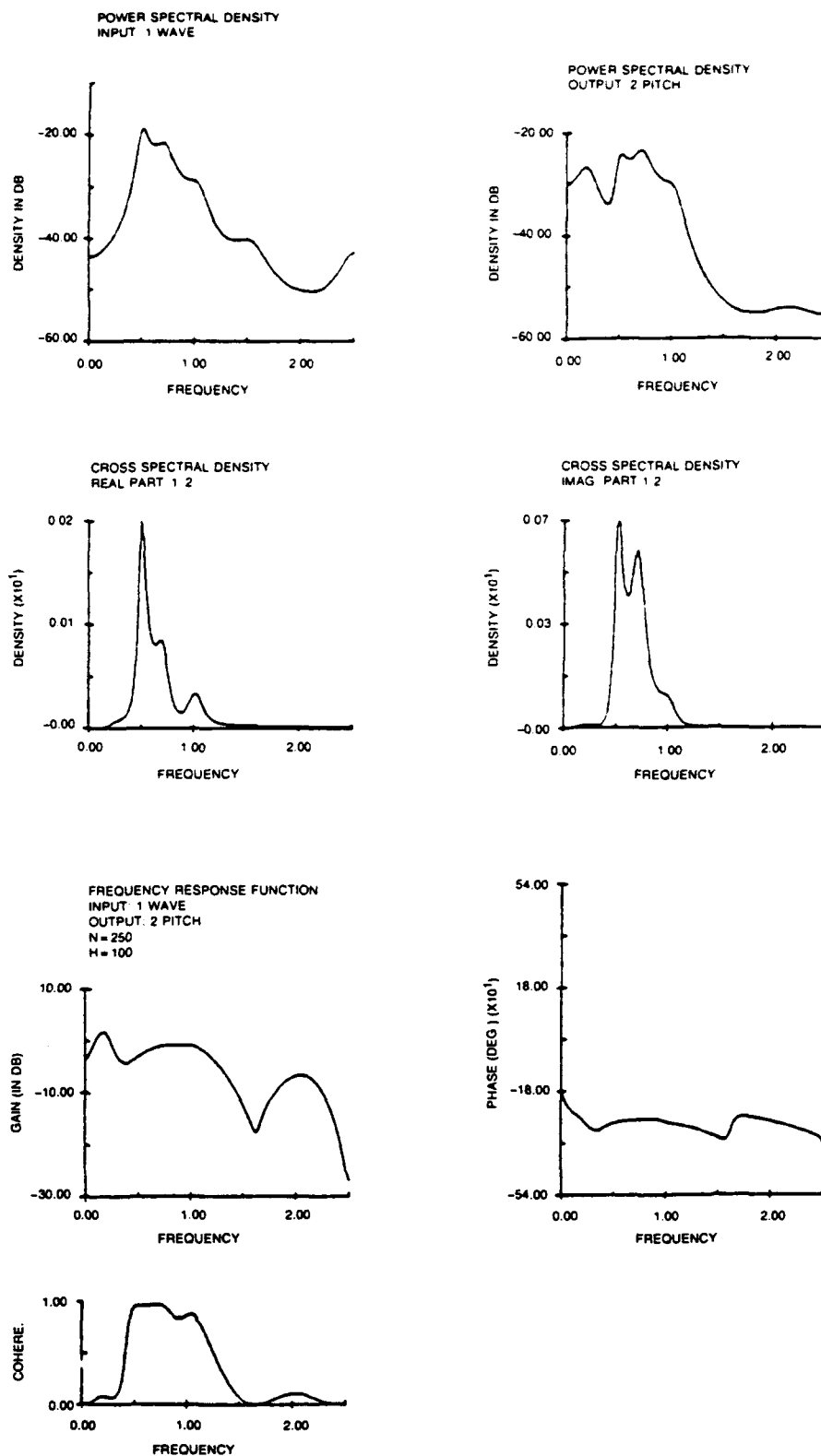
Fig. 7.16. Frequency response analysis for pitch by AR–model fitting (N=250, Δt=0.2 sec, AR–8).

(From Oda, Yamanouchi, et al.[53])

243

Fig. 7.17. Frequency response analysis for surge by AR–model fitting (N=250, $\Delta t \approx 0.2$ sec, AR–11). (From Oda, Yamanouchi, et al.[53])
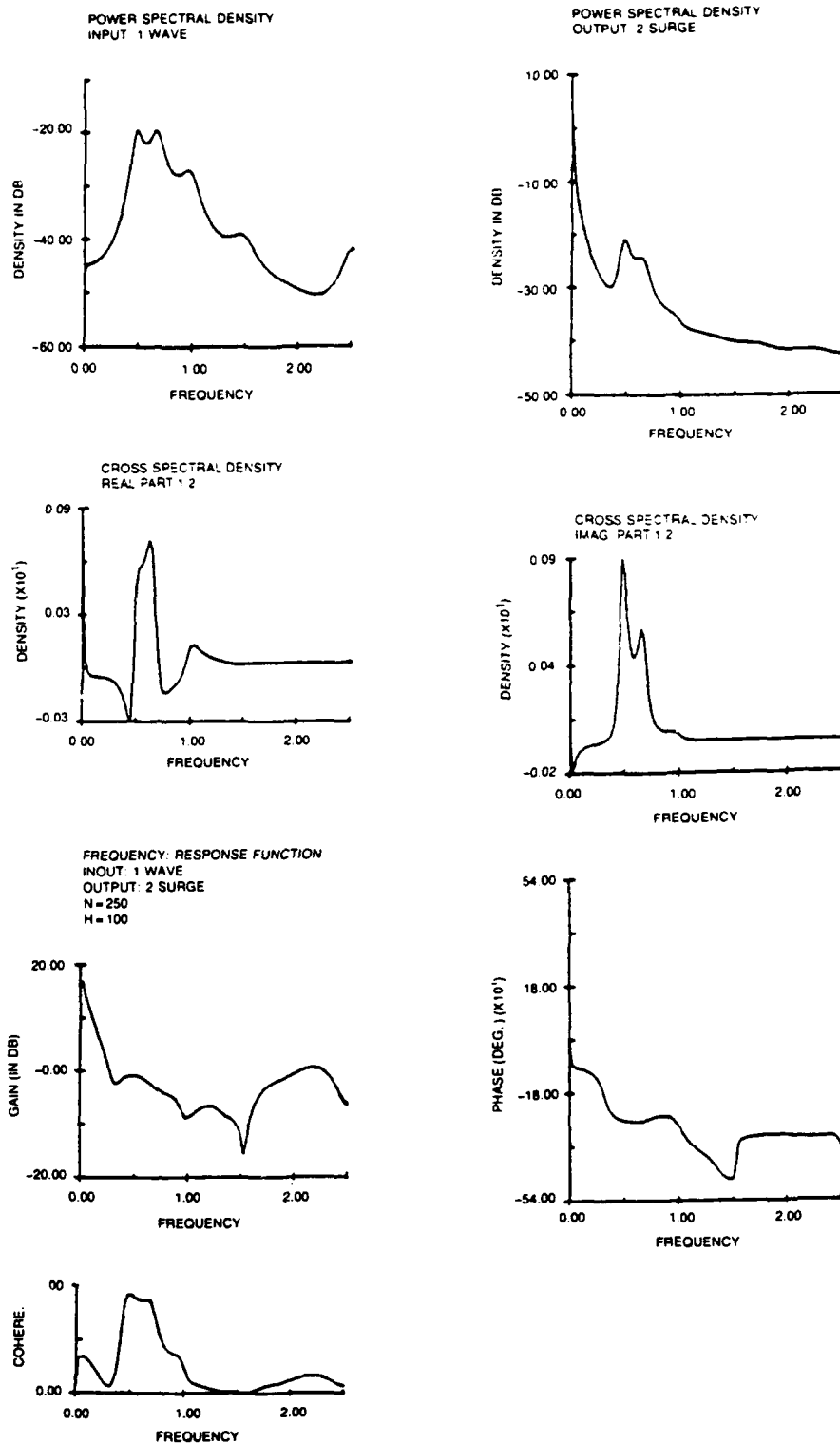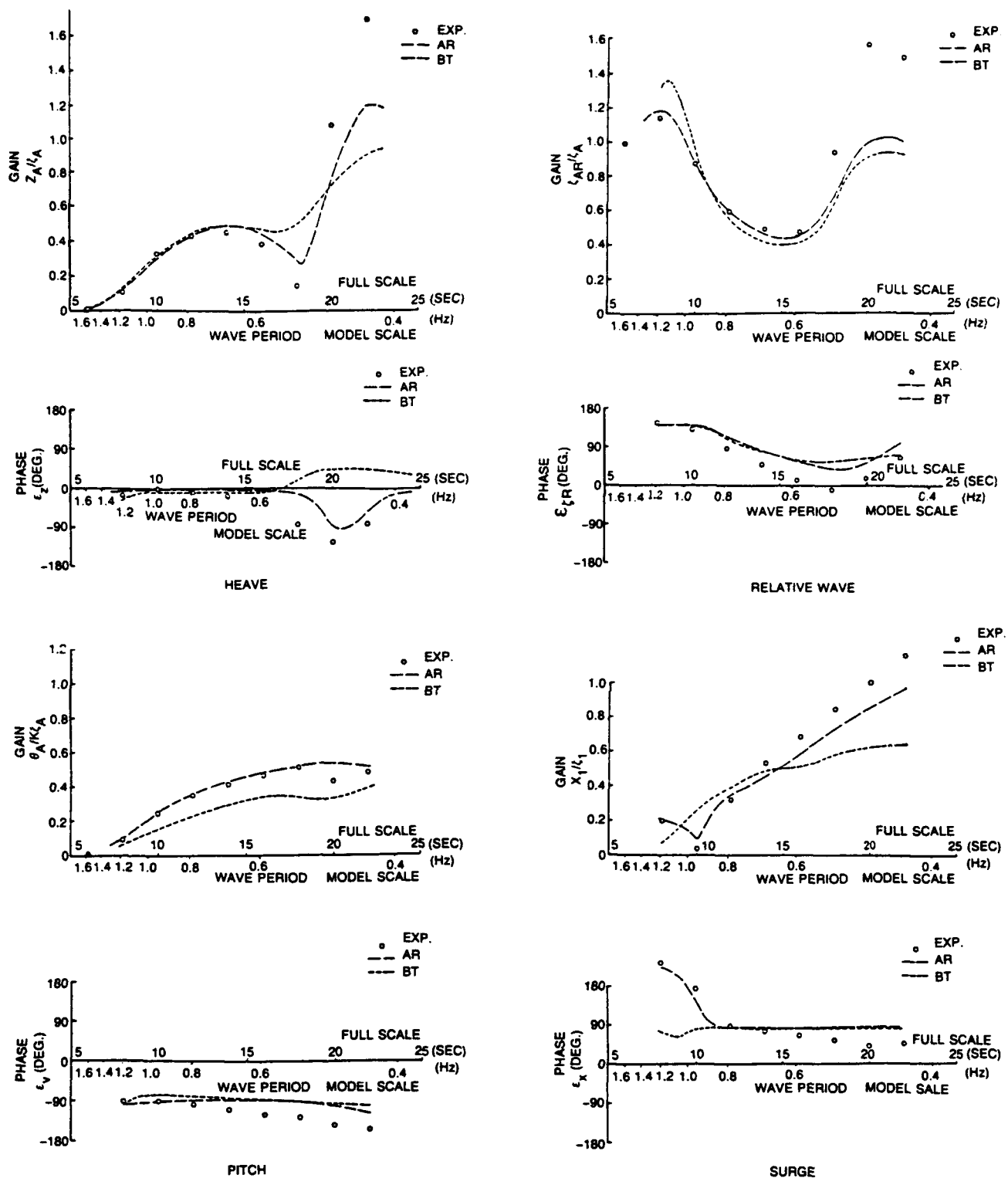
244

Fig. 7.18. Frequency response characters by different methods and
through experiments in regular waves.

(From Oda, Yamanouchi, et al.[53])

245

THIS PAGE INTENTIONALLY LEFT BLANK

CHAPTER 8

CONCLUSION FOR PART II

In Part II, we have discussed the model fitting technique or parametric analysis method for a random process. Comparing this method with those discussed in Part I for nonparametric analysis, we can conclude as follows:

1. The examples in Sections 5.2.1 to 5.2.5 show that the autoregressive (AR), moving average (MA), or autoregressive moving average (ARMA) model of rather low order can represent pretty complicated looking processes with various frequency characteristics.

2. For a given process, generally we can fit an autoregressive (AR), moving average (MA), or autoregressive moving average mixture type (ARMA) model of certain finite order. From the sample autocovariance functions at rather low lag numbers, we can estimate the finite number of parameters of the model and the variance of the residual errors, once the order of the model has been determined.

3. The characteristics of the discrete parameter model are closely related to those of the correlations of that model. To find the finite number of parameters to express the process, the correlation function until the finite order is sufficient, as mentioned in item (2). Sample correlations at low lag numbers are more reliable than those at higher lag numbers, and there is no need to be concerned about the lag windows as there is in the nonparametric analysis (the so-called Blackman–Tukey method), where, ideally, we need the correlation function over

   $-\infty$ to $+\infty$ of the lag numbers. This concern about lag windows and consistent estimates, resulted in many efforts to find good windows. Not using the lag window is also one reason why we can get better results by the model fitting technique then from rather short records.

4. The order of the AR(k), MA(l), or ARMA(k, l) models that are to be fitted to a sample process, as the best from a statistical point of view, can be determined by Akaike's information criteria (AIC) as the combination of the parameters (k, l) which minimizes AIC.

5. Evaluation of the parameters of the AR(k) model is easily performed by solving the Yule Walker equation, which is a linear relation of parameters. The solution by Yule Walker's equation is a good approximation of the solution by the maximum likelihood and least squares method. On the contrary, for the MA and ARMA models, estimation of parameters is more troublesome and difficult and involves solving the nonlinear least squares equations.

6. As far as stability and invertibility are fulfilled, the AR and ARMA processes of finite order can be inverted to the MA process of infinite order and, conversely, the MA and ARMA processes of finite order can be inverted to an AR model of infinite order. Usually, however, in this approximation, the order increases from the original MA or ARMA order. The order of the AR model that best approximates the original MA or ARMA is obtained through the AIC criteria. In this approximation, estimation of parameters becomes much easier than for the original MA or ARMA process as mentioned in item (5). Accordingly, AR model fitting is usually used practically for general processes.

7. After an appropriate AR, MA, or ARMA model has been fitted, it is easy to calculate its spectrum. The spectrum function can be estimated analytically from only a few parameters that characterize the fitted model. The spectrum thus obtained is smooth compared to the spectrum computed by the nonparametric method, or by the Fourier transform of the estimated autocorrelation. A sharp-peaked spectrum can be obtained by this method, free from the smoothing or blurring effects of the spectrum window that are inevitably applied in the nonparametric method.

8. From the characteristics of the model fitting technique, we can get a fairly reliable and sharp spectrum even from rather short records of observation, when reliable autocorrelation functions at large lag numbers are difficult to estimate.

9. The AR model is effective in finding the peak frequency and in estimating the peak value of the spectrum. Usually the second order of an autoregressive model is necessary to identify one peak of the spectrum.

10. When the purpose of the analysis is to estimate the characteristics of responses, the AR model that estimates the peak effectively is an appropriate approximation of the ARMA model. The ARMA model, however, is more reasonable for expressing the response of a linear dynamic process to random excitations, as will be mentioned later.

11. To express the flat valley of a spectrum, however, a large order becomes necessary if an AR model is to be fitted. A flat valley is more easily expressed by an MA model of low order. This tendency comes from the character of the transform function of the spectrum.

12. The ARMA model that expresses peaks by an AR model and flat valleys by an MA will be the most appropriate in general cases.

13. The model fitting technique relates all linear stationary processes to appropriate AR, MA, or ARMA models. All of these models assume that the process is the output of a pure random process or of white noise. The linear relations of this process to white noise can be derived as the Green's function of these models.

14. When a process is the linear output of some input that is not necessarily white but colored, we can get the response of this process to the real white noise if we assume that the colored input is the output of the real white noise. In this way we can relate all the colored input to a random process.

15. Even when the linear response system has some feedback effects, we can fit a vector autoregressive process, inverting the input into a pure random process by applying an autoregressive process technique to the input, as mentioned in item (14). We can get the linear response characteristics of the system from the elements of the spectrum matrix of the vector process. In observations of sea-keeping data, sometimes the feedback effect is concealed, so this method can be applied effectively in the analysis of such data. With the conventional nonparametric method, the kind of system that has feedback effects is hard to handle.

16. A second order autoregressive continuous process A(2), formulated by a second order linear differential equation of the damped mass spring vibration type, can be transformed into a discrete ARMA(2.1) process formulated by a difference equation and by the equivalent correlation theory, the coefficient of the

differential equation can be expressed by the coefficient of difference equation and visa versa. The second order autoregressive continuous process A(2) is then the basic process, as the response of a linear vibration system to the white noise with one degree of freedom. Conversely, when a dynamic process with one degree of freedom is excited by white noise, the digitized response can be expressed by an ARMA(2.1) model. When the input is colored and not white, we can invert this system to a pure random process (white noise as mentioned in item 14) although the order increases. Thus the ARMA model is the most general process for expressing the oscillatory response of a linear system.

17. An advantage of the parametric analysis is that, by fitting a certain discrete model to the response process, theoretically we can estimate the characteristics of the differential equation that governs the response of a continuous process by inverting the difference equation that expresses the discrete model into the equivalent differential equation that formulates the continuous process.

18. The confidence limit of each parameter of a fitted discrete model can be evaluated. The remaining statistical considerations are taken care of by adopting the most adequate order of the model based on Akaike's information criteria. However, if we could express the overall reliability by some simple expression, say, for example by a confidence band at some level of probability, it would be easier to give us more confidence in the parametric method, directly comparing with the result by the nonparametric method.

19. The AR model was adopted here first and was applied to the seakeeping data of ships and offshore structures, both for models in the tank and for the actual ships and structures at sea. From the results, we found this model fitting technique was practical to apply and was a promising method of analysis, sometimes giving us better results than the conventional nonparametric method. At least this model fitting or parametric analysis technique supplements the nonparametric method.

20. The ARMA model is the most general and is directly connected with the continuous AR model or its formulating differential equations that govern the behavior of the system. It seems to be the most desirable for estimating the physical characteristics of the process, although its handling in the estimation of parameters is more complicated than for a pure AR model. Accumulation of experience with this application is now very much needed, this author believes.

THIS PAGE INTENTIONALLY LEFT BLANK

APPENDIX A1

DATA FOR THE GENERATION OF THE PROCESSES

Data for the generation of a pure random process AR(1), AR(2), ARMA(2.1), MA(2), MA(1), and ARMA(2.2), given in Chapter 5, Figs. 5.3, 5.10, 5.20, 5.25, 5.28, 5.32, 5.35, 5.38, and 5.41, and Tables 5.1 and 5.2 are listed on the following pages.

Table A1.1

600 observations from a pure random process $X_t = \epsilon_t$.

Table A1.2

600 observations from an AR(1) process $X_t - 0.5\, X_{t-1} = \epsilon_t$.

Table A1.2

600 observations from an AR(1) process $X_t - 0.5\, X_{t-1} = \epsilon_t$.
(Continued)

61	-1.87887	-1.16703	1.50359	-1.25088	-1.04649
62	-1.64978	-0.83944	0.21097	0.05472	-0.71092
63	-0.77196	-0.30054	-1.06274	-0.42397	-0.28300
64	-0.78236	-0.70531	-0.11766	-1.33351	-1.30207
65	-0.97344	0.93733	0.24305	-2.19487	-3.07886
66	0.97710	-2.23748	1.00754	-0.60585	-0.64272
67	-1.76609	-2.23748	1.82612	-2.19681	-0.05162
68	-0.12402	0.58989	2.28999	1.11775	-0.00076
69	-1.03248	-0.46890	0.30156	-0.40793	1.66339
70	-2.36036	-1.45221	0.73160	-0.41560	2.06949
71	0.75606	-1.68369	1.06910	-0.27821	-0.72801
72	0.27633	-0.01102	-1.42960	-0.94655	-0.75540
73	0.16958	1.42613	-1.70400	-0.77706	1.22847
74	-0.12686	-1.51855	-1.13856	1.17339	2.41212
75	2.96775	1.13944	1.41516	1.07053	0.24523
76	2.22439	-0.14235	1.73790	1.43802	0.40946
77	0.29042	-0.01031	0.26957	0.57984	-1.11190
78	-0.11156	-0.02011	0.55274	1.19117	-1.53230
79	-0.81576	0.24371	0.04900	-0.24256	0.44513
80	1.10821	0.77611	0.44449	-0.68653	-0.62684
81	0.45755	0.53552	0.14346	-0.39155	-1.16108
82	0.49695	0.44006	2.27241	-0.57707	0.49478
83	-0.55587	0.65660	0.11177	0.75378	-0.53660
84	1.10002	-1.20340	1.51711	-0.71501	-0.99659
85	0.08314	-1.67478	1.46345	-0.41616	2.37400
86	-0.20295	0.72273	0.72273	0.26171	-0.62625
87	-0.10350	1.27744	1.46360	2.19492	0.92625
88	-0.08723	1.25256	1.20910	2.04974	1.40238
89	-1.02200	1.56432	1.49246	2.09385	-0.85961
90	-0.11701	1.30340	1.26072	1.10139	-1.78034
91	-0.00142	0.05662	0.56660	-1.10139	-0.35862
92	-2.92943	-0.35076	2.42510	2.51367	-2.16417
93	-0.02725	0.36910	2.97677	0.47578	-1.18392
94	0.05130	0.66267	-0.54153	0.27602	2.00921
95	1.93961	1.49651	1.26180	-2.2229	2.05885
96	-1.92351	1.14606	-0.04712	-1.92026	2.04829
97	0.21014	1.24452	1.19608	0.97277	-2.12668
98	1.96645	-0.34574	1.65745	1.65745	
99	0.41255	0.26022	2.26022		
100	0.11285	1.54471	0.62351	1.61406	-0.37460
101	0.43519	0.60566	0.49625	-1.21694	0.98595
102	0.29610	0.39685	-0.44955	1.91330	0.98678
103	1.86863	1.13445	0.26409	0.58076	-0.27162
104	-0.27022	-0.22657	0.02504	0.05074	-2.03531
105	-0.41051	1.17437	0.63857	-0.51672	-0.01426
106	-0.70157	-0.10793	1.47591	1.34427	-1.27035
107	-0.08713	-0.15425	0.19562	1.34215	-1.16849
108	-0.63597	-0.34656	0.31962	0.29641	-0.12153
109	-0.98546	0.34025	0.30660	-0.05892	1.36259
110	-0.56240	-1.17425	1.28649	-1.35894	-1.36259
111	-1.81521	-0.01526	1.02855	1.02936	0.46808
112	2.54009	-1.32662	2.99819	2.05144	2.35146
113	-0.93152	0.74647	0.84724	1.08859	-1.44806
114	2.12774	-1.05916	2.96985	1.62637	1.02634
115	1.01217	2.46454	0.37751	0.07664	1.35733
116	0.11281	1.27676	0.30014	2.28407	-0.76057
117	-1.40820	-1.74102	-2.03310	-1.36107	0.31416

Table A1.1

600 observations from a pure random process $X_t = \epsilon_t$.
(Continued)

61	-1.94013	-0.22760	-0.92007	0.50703	-0.41708
62	-1.12653	-0.00555	0.62519	-0.05277	-0.73728
63	-0.41650	0.08544	-0.94247	0.12240	-0.07102
64	-0.64086	0.56951	-0.22182	-1.27468	-0.63532
65	-0.32240	-0.21050	0.10900	-2.07304	1.12629
66	0.86267	-0.64478	-1.47421	-0.10208	-2.77613
67	-0.22656	-1.32444	-0.72238	-1.27375	0.45068
68	-0.19734	0.65090	1.09555	-2.26275	0.50726
69	-1.00667	0.04734	0.53601	0.20473	-0.20473
70	-2.35998	-0.27205	1.45792	-0.78150	1.87119
71	-0.07564	2.06172	-0.22725	0.25634	2.20859
72	-0.75841	-0.14919	-1.42409	-0.23175	-0.25473
73	-0.53358	1.40134	0.39094	-0.07494	0.34687
74	-0.49456	-1.47513	-0.36928	1.74267	0.64178
75	2.25351	-1.26523	1.14384	0.46395	1.87605
76	1.01933	0.06964	-0.66681	0.56903	0.47378
77	-0.41304	0.05538	-0.32470	0.76452	-1.69938
78	-0.59317	0.52667	0.57330	0.91175	-1.70746
79	-0.25901	0.65154	0.57723	-0.28198	1.56058
80	-0.33854	1.33021	0.83254	-0.64629	-0.01086
81	-0.66011	0.30715	-0.41142	-0.31962	-0.43117
82	0.81037	0.70853	2.04278	0.55933	-1.57374
83	-0.37527	1.14673	0.91521	0.69740	-0.11789
84	-0.85263	0.65379	-0.04354	-0.04354	-1.03738
85	-0.06535	1.63321	1.30134	0.64814	-0.32852
86	-0.60183	0.61395	0.46049	-0.09965	-1.12745
87	-1.27468	2.17545	0.34999	1.45312	1.27744
88	-0.40532	1.26662	-0.71730	-0.71730	-1.10470
89	-0.40532	1.39532	0.58206	1.30454	-1.36541
90	-0.58013	1.36107	-0.31799	0.45899	-1.40804
91	-0.32782	0.34931	-0.31058	0.37436	-1.22964
92	-2.19324	0.83846	-0.07468	0.01120	0.39733
93	-0.26202	-0.67236	-2.48376	-1.02399	0.10103
94	1.09119	0.05750	-0.16743	0.29502	2.02616
95	1.77015	0.37714	0.69744	0.36488	-1.27306
96	-0.84143	0.52736	-0.14722	0.20184	1.29811
97	-1.65276	1.31152	-0.28522	0.82226	-1.14870
98	-0.78547	-0.01349	-0.96680	-1.37652	-3.43809
99	-0.37320	-0.17656	-2.27714	1.54960	-1.09674
100	-0.37320		-2.27714	-0.63000	
101	1.17629	1.48220	-0.05115	-2.02581	0.43243
102	0.62269	1.36539	-1.29373	-0.72191	-0.37748
103	0.19687	0.54440	0.25091	1.68863	0.03013
104	1.37617	0.19097	-0.30323	0.44871	0.56200
105	-0.13441	0.09146	0.13833	0.03822	-2.06068
106	0.60714	1.37963	0.05138	-0.83600	0.24410
107	0.69444	0.54871	1.37605	-0.00324	-1.63748
108	-0.25196	0.27732	-0.27874	1.24384	-1.83956
109	-0.05173	-0.22457	-0.14619	0.45622	-0.26974
110	-0.23657	1.17270	0.38657	-1.34927	-0.29988
111	-1.13392	1.45550	0.69336	-2.00168	0.69312
112	-5.07815	2.06235	-1.08092	-0.48509	0.98275
113	0.20206	-1.22760	1.81230	0.75240	1.32571
114	1.47155	-0.12744	-1.16242	-1.34927	1.59279
115	-0.20704	-0.52150	-0.31766	0.25080	-0.43302
116	1.61357	-0.53440	1.72743	0.14145	1.11475
117	0.32851	0.16672	-1.18957	1.36947	0.55414
118	-0.27505	1.30172	-0.95355	1.48760	0.28740
119	-0.27505	1.22236	-0.29538	-0.79813	-1.90260
120	-1.02792	-1.23502			1.00470

253

Table A1.3

600 observations from an AR(2) process

$$X_t - 0.5\,X_{t-1} + 0.8\,X_{t-2} = \epsilon_t.$$

1	1.69914	-1.41601	-3.63645	0.73994
2	1.12792	-2.06655	-2.81734	-0.30542
3	-0.24443	-1.09501	-1.51197	1.01053
4	0.08138	-0.88881	-0.80881	0.16721
5	2.38649	2.03588	-3.18262	1.21211
6	2.83909	4.09772	3.05978	-3.06189
7	0.46816	3.97685	-0.86161	-0.59158
8	0.07845	2.96966	-1.92601	-0.76515
9	1.25985	0.47670	0.02359	-0.26651
10	-0.20927	1.47878	-0.13272	-0.20811
11	-0.77736	0.98824	1.21505	-1.18216
12	-0.83256	-1.52869	2.04661	0.00493
13	-0.06451	0.01986	-0.07440	-0.74410
14	-0.02666	-0.05456	-0.00759	0.63021
15	0.05555	-0.23372	-0.45254	-0.04015
16	-1.74309	0.21175	-0.21230	-1.25881
17	-0.30390	-0.14500	-2.76466	-2.00669
18	-2.26488	-0.03738	0.00757	0.31487
19	-0.02034	-1.03998	2.05509	-0.20898
20	-1.96401	0.13526	2.23317	0.43424
21	-0.91006	-1.37686	1.45527	3.72556
22	-0.95107	-1.36759	-0.20831	1.44696
23	-0.90130	2.27755	1.04696	-0.96342
24	-0.23932	3.40262	1.4423H	-0.65785
25	-0.05347	3.35716	2.59957	-1.41702
26	2.02132	3.64233	2.76014	-3.47499
27	2.35552	2.35927	-1.54616	-3.46465
28	-1.01037	0.51281	0.51281	-1.11753
29	-1.32041	-0.12094	-0.22636467	0.58645
30	-1.22774	-1.27645	-0.85936	1.74687
31	0.30003	0.83777	-0.00081	2.18826
32	-0.92188	-0.51475	1.59672	-0.23837
33	0.82799	1.09460	-0.09068	-2.55275
34	2.16920	0.67875	0.33048	-1.42090
35	-0.10813	3.07644	3.00671	-2.51307
36	-1.51411	1.20609	-0.51484	-3.67140
37	-2.08764	2.06356	-1.23295	-0.74063
38	-1.24665	-0.74455	-1.77170	-0.43274
39	-0.07903	0.59265	3.59285	0.83849
40	-1.74475	2.72463	4.47184	0.27196
41	-2.51578	3.64606	3.37318	-0.10407
42	0.92500	3.32364	1.22921	-0.04579
43	1.90636	1.53355	2.55016	-0.01196
44	-0.90636	0.69950	5.03208	-0.16936
45	0.38683	1.37135	4.56733	0.64616
46	-0.55835	1.35905	0.52224	0.35256
47	-0.06251	2.10119	0.99236	-0.58268
48	-0.70232	0.10538	0.95287	0.40911
49		-0.90636	-1.00605	-1.35200
50		-2.19694	-2.51549	-0.58594
51		-2.28965	-1.26491	0.01452
52		-1.56254	-1.26268	0.62471
53		-0.70232	0.67271	-0.19137

Table A1.3

600 observations from an AR(2) process

$$X_t - 0.5 X_{t-1} + 0.8 X_{t-2} = \epsilon_t.$$ (Continued)

61	-2.91095	-1.34731	0.75504	0.93833	-0.53594
62	-2.14517	-0.64938	2.01763	1.47555	-1.61361
63	-2.40374	0.17444	1.06775	0.51671	-0.66687
64	-1.38766	0.43917	1.10789	-1.07207	-2.05767
65	-0.49358	1.19075	1.09424	-2.47052	-0.98436
66	-2.34691	2.45572	-2.12387	-3.12859	-2.64133
67	0.95565	1.26645	-2.05308	-2.71375	-0.22325
68	2.25671	1.95786	-0.85308	-3.24448	-0.05027
69	0.56378	1.96944	1.06911	-0.78355	-1.45227
70	-2.45927	-0.33987	3.25540	-1.11810	-0.17408
71	-1.05716	-2.45103	-0.60704	1.91365	3.65104
72	-0.46381	-3.30103	-2.70401	1.05779	2.43737
73	0.90604	-0.09554	0.09566	2.77985	2.79767
74	-0.44908	-1.35490	-0.95746	2.01500	4.01115
75	1.42847	1.41281	-1.40850	2.74772	1.85017
76	1.41190	2.31313	1.19312	2.52455	-0.34455
77	1.68153	3.47281	-0.11567	2.11130	-1.93483
78	-1.59878	-0.27235	1.50378	3.29090	3.77510
79	-0.37503	-0.47709	1.51704	0.74041	3.10144
80	0.40280	0.74122	2.65034	-0.50393	-2.20871
81	-0.29024	2.97411	2.44097	-1.55277	-2.20871
82	-1.41281	1.45513	4.13067	-2.30973	-0.34875
83	-1.78625	1.93534	-2.36815	-2.09301	1.99536
84	-2.45693	2.57072	-0.38672	-1.55204	-1.39489
85	-2.08153	-0.15059	2.56907	0.23051	1.30496
86	1.91988	0.19273	1.07661	-0.50631	2.59423
87	-0.37503	1.45643	1.91704	-0.50393	3.10144
88	-2.81844	-1.62773	-0.82712	2.65034	-0.64701
89	-0.37161	-0.55810	1.22081	0.44097	0.50149
90	1.55380	-0.62230	-0.36815	-0.86925	-0.20825
91	1.60802	0.13194	3.55681	-2.05508	-1.24062
92	1.91988	-0.01151	0.13284	0.27749	1.66691
93	0.37503	0.27266	0.97718	-1.06727	-0.79672
94	-0.40280	-1.27662	-0.06740	-0.84389	-0.04247
95	-0.66029	0.92072	0.01980	0.82292	0.82292
96	-0.36037	0.26077	-2.17923	-1.78540	-0.24606
101	2.48158	2.52562	0.47115	-4.60212	-1.49171
102	3.55833	3.34186	2.45945	-4.04105	-0.73044
103	2.90449	2.90150	-1.13393	-1.19953	0.33751
104	2.50455	1.18214	-1.71580	-1.35490	0.13319
105	1.01610	0.31004	-0.21953	-0.46958	-1.87984
106	0.04288	2.35023	1.46955	-2.42518	-2.14413
107	0.17364	2.57283	2.41255	-0.67763	-3.90633
108	-1.66302	1.80359	2.89560	0.63334	-3.83937
109	-2.47808	1.94563	2.73806	0.38239	-2.69000
110	-2.36510	3.35890	3.76146	-1.04104	-3.82937
111	-1.32052	4.15347	3.68422	-3.24069	-5.25384
112	-1.15349	0.93460	2.10671	-3.04267	-2.22394
113	0.34402	-1.17146	3.48458	1.69901	-0.61245
114	2.26749	-1.57356	2.69056	3.26010	1.07039
115	-0.60133	-1.14830	-1.54063	-1.05525	0.27186
116	0.77309	-0.42434	0.17657	-0.01612	2.04145
117	2.62140	1.09951	-1.56255	-0.64757	-0.08670
118	0.88902	0.67732	0.04619	1.56077
119	0.46838	0.22793	0.68281	1.66266	-1.61752
120	-3.16681	-1.32631	1.57691	1.05037	0.26996

Table A1.4

600 observations from an ARMA(2.1) process (1)

$$X_t - 0.3 X_{t-1} + 0.4 X_{t-2} = \epsilon_t - 0.7\epsilon_{t-1}.$$ (Continued)

61	-1.80937	1.04339	0.27601	-0.19753	-0.25182
62	-0.92511	0.62822	1.14858	-0.39782	-1.27912
63	-0.12501	0.35113	0.60693	0.23260	0.19185
64	-0.62663	0.79332	-1.47950	-1.47950	-0.12457
65	0.67675	0.25694	-2.22353	-2.23253	1.87906
66	1.53126	-0.40167	-2.55357	-0.32447	-1.58591
67	1.11117	-0.19813	-0.29918	-0.77858	1.22840
68	0.55182	0.19995	1.37218	-3.32396	0.54513
69	-0.13137	0.57337	0.02243	-0.16070	0.68188
70	-2.35695	0.94560	2.87481	-1.31784	0.87296
71	-0.59645	2.53689	0.69346	1.63821	2.24323
72	-2.28674	1.20161	-0.76545	1.10612	0.51851
73	0.46049	0.95673	0.08322	1.10612	0.06420
74	-0.28466	1.22602	0.40877	2.61500	0.04290
75	0.77111	1.85251	0.94450	1.01001	1.47729
76	-0.25628	2.35047	1.74307	0.56537	-1.30972
77	0.62046	2.62277	1.15119	0.78807	-2.05660
78	0.84993	0.62627	0.42162	0.30099	2.40604
79	0.06921	1.51653	0.58842	-1.20117	-1.95491
80	0.64664	2.54476	1.25891	-1.45909	0.50738
81	1.42356	2.65519	1.17929	-0.40749	-0.14203
82	1.31779	-0.93725	2.55510	-1.41518	-0.52594
83	-0.55605	1.29123	-0.10713	1.05765	0.00166
84	0.74575	-0.25801	0.23606	-0.71577	-1.31606
85	0.87446	1.87554	1.07854	-0.01113	-0.77378
86	-0.30643	-1.22421	-1.20443	-0.75296	-1.36535
87	1.26262	2.65510	0.60055	-0.12001	1.93377
88	1.95007	-0.25796	-0.24799	0.39933	0.31025
89	-0.30560	-0.57175	-1.43594	-1.41518	-1.37432
90	-0.70719	-0.04250	-0.19780	-0.42249	-1.21696
91	-0.91156	0.22551	0.56020	-0.02259	-1.14760
92	1.54908	2.39611	0.23606	-0.15811	-1.74162
93	0.11965	2.16325	1.78754	0.35314	1.93377
94	1.35603	2.05571	2.05571	-1.17055	-0.55175
95	1.63517	2.61314	1.23994	1.37984	-0.74787
96	-0.15538	1.21445	1.05735	1.07455	0.44397
101	2.04525	1.10087	1.47849	-2.94551	1.55824
102	1.96540	-0.06004	-2.37648	-0.49713	-0.92924
103	0.93873	-0.31701	-3.41091	-1.26291	-0.60867
104	0.66731	-0.31679	-0.80600	-0.54709	-0.38957
105	-0.07672	-0.13544	-0.27367	-0.03069	-2.20611
106	1.40006	2.25709	-0.79726	-2.01398	0.54401
107	0.10348	0.84826	1.20504	-0.94627	-2.40051
108	0.55183	1.58144	0.33692	0.51722	2.69985
109	0.22212	1.14901	0.13015	0.13763	-0.59986
110	-0.97098	1.92897	0.92052	-2.46529	0.46318
111	0.81851	2.05332	-0.03189	-3.32143	-0.20561
112	0.50315	1.97028	-1.35174	-0.92208	1.58639
113	-0.82133	-1.15281	3.91477	0.10421	-0.75561
114	-1.79243	-1.04972	3.07373	0.49105	0.21826
115	0.22566	1.26010	-1.37896	-0.58526	1.08243
116	0.65491	-0.66497	-0.36973	-0.63623	1.27795
117	0.96214	0.04863	0.36858	-0.98475	0.01227
118	0.33819	0.16631	1.48556	0.68918	0.42975
119	-1.02298	0.93610	0.78792	0.68205	-3.05447
120	-0.88526	0.63883	0.97622	-0.55403	1.00669

Table A1.5
600 observations from an ARMA(2.1) process (2)

$$X_t - 0.3 X_{t-1} + 0.4 X_{t-2} = \epsilon_t + 0.7\epsilon_{t-1}.$$

1	1.69914	-1.41601	-0.20606	2.67355
2	1.01914	-0.55241	-1.32624	-1.30114
3	-1.11959	-0.55789	-0.35048	-0.11834
4	-1.37266	0.05691	-1.20500	-1.20500
5	1.76115	2.93763	1.73395	1.86657
6	1.22402	3.45966	-0.27620	2.23428
7	-1.92011	1.29683	2.25360	1.29948
8	0.81021	-0.32857	1.31008	-0.69673
9	0.35963	0.04942	-0.78581	-0.05300
10	-0.91770	-0.30493	1.29331	1.62543
11	0.14593	0.90712	1.70575	-0.90492
12	-0.55104	2.64485	2.20142	-1.13651
13	-0.87381	-2.54063	-1.98984	0.39964
14	0.22172	-0.54068	-0.36038	-0.79437
15	1.34730	-0.79819	1.00065	-0.93806
16	1.51316	-0.67519	-0.51354	0.99343
17	-2.00387	0.64712	-2.39569	1.76427
18	-2.41783	-1.10153	1.14725	1.77105
19	-1.74853	-1.50415	0.95152	3.49234
20	-0.55104	-1.61447	0.35245	0.62919
21	2.21625	1.55475	1.48268	-2.66854
22	0.58083	2.00559	2.23396	1.95640
23	-0.56204	2.91657	1.492/1	0.89608
24	-0.23869	-0.73069	-1.86666	-0.82413
25	-0.11962	1.46575	0.68044	0.82412
26	0.58083	0.34495	-0.45919	-1.11636
27	0.14249	2.15121	-2.28625	1.95162
28	1.31456	2.30035	-2.09181	-1.14992
29	-0.17539	0.78944	1.50906	1.14992
30	-0.00051	-1.26020	0.20683	-0.72197
31	-0.40424	2.34375	0.51251	-2.74799
32	-0.12239	0.47686	1.27399	-0.07055
33	2.87189	0.36074	1.88123	0.54279
34	2.21183	-0.12	-1.26365	1.19903
35	-0.55595	2.19579	2.52666	0.89873
36	-2.41205	-0.26705	1.93025	3.07524
37	-1.44717	1.65515	0.81301	0.66134
38	-1.83197	1.35520	0.36860	0.49921
39	-0.00051	1.02299	0.41350	2.76807
40	-0.40424	0.42802	0.56499	0.03818
41	2.20459	-1.00819	2.04621	0.18070
42	-2.93890	-0.74203	0.91292	1.28070
43	-1.62145	-0.61246	-0.41818	3.74618
44	-1.76995	2.51173	0.56342	-2.59336
45	1.50752	-1.19977	-0.72975	-1.04519
46	-1.04215	2.33951	-0.85912	
47	-0.10341	-0.73635	1.20417	1.07669
48	-0.42481	-1.64142	-2.00189	0.78016
49	-6.68284	-1.01773	0.49302	0.06882
50	1.51453	1.81961	0.91546	-1.72196
51	0.45009	1.69468	1.14409	0.89830
52	-1.95248	-2.08118	-0.09863	2.89263
53	2.04563	-1.35072	1.19597	2.60750
54	1.76967	-0.10560	-1.87022	0.31630
55	-0.21590	-0.59623	-0.23807	0.01254
56	0.91608	0.48772	1.50957	-0.47026

Table A1.6
600 observations from an MA(2) process

$$X_t = \epsilon_t + 0.2\epsilon_{t-1} + 0.8\epsilon_{t-2}.$$

1	1.69914	-1.41501	-0.43502	-0.02127	-0.69853
2	1.13900	0.41640	-0.36413	-0.55822	1.86166
3	-1.17660	-1.31581	-1.26546	0.43806	-1.58378
4	1.08880	-1.09669	-0.02142	-1.65058	-0.55779
5	-0.31540	1.29806	2.15563	-0.58925	0.75500
6	-0.26401	2.18039	1.57051	1.54352	-0.87965
7	-0.64932	-0.16170	-0.65261	1.97649	0.54351
8	1.00602	1.01587	0.65261	-0.67551	0.17488
9	-0.60699	-0.56963	0.56413	0.28379	-0.36935
10	0.74427	0.25791	0.70903	2.31469	1.22032
11	1.13467	2.11011	1.09420	0.10606	1.47978
12	-1.97594	-1.47964	-3.57158	-0.51477
13	2.58302	-0.54750	1.34172	0.51957	-0.60652
14	0.93010	-1.10240	0.22602	-1.67682	-0.64278
15	1.59853	0.55115	-1.66141	-1.47787	-0.62702
16	-0.23794	-0.24963	0.99919	1.33132	-2.16535
17	-2.60936	0.57921	1.25166	1.27260	-0.41893
18	-0.62992	-1.01851	-0.35989	2.17660	0.45949
19	1.08125	0.43177	-0.92799	-0.92799	1.39326
20	0.44675	1.67265	1.80604	-3.57158	-2.23641
21	1.37969	0.12216	1.75710	2.33198	2.50298
22	0.45187	-0.60323	-1.04910	-1.34238	-0.13927
23	-0.34252	-0.07213	-0.25259	2.17036	1.70761
24	-0.18258	0.85252	-0.67348	1.00601	-1.11982
25	2.69293	2.05350	1.21883	-1.21180	1.46212
26	-1.36669	-1.83360	-1.55065	0.56314	-3.24370
27	-0.27370	0.51214	1.43191	1.12950	-2.30506
28	-0.46311	1.55250	0.00327	-1.12950	2.82257
29	0.31277	0.74461	0.20378	0.20950	-0.07744
30	-0.03159	1.88623	-0.31721	-0.26923	1.25536
31	1.03193	1.25797	1.92101	1.01951	1.44821
32	-0.14772	-2.65767	-0.12380	2.27944	1.02387
33	1.05026	-0.10410	-0.02835	1.26675	-0.03758
34	1.86120	1.52345	2.71358	1.72759	0.11100
35	1.42120	-0.83552	-2.42595	2.50096	3.31726
36	0.91542	0.67637	-0.49057	1.01403	-0.34926
37	-1.90261	-2.54505	-1.91562	-1.57524	-0.42746
38	-1.66658	-0.54574	2.279/4	0.72477	-1.12860
39	-1.26365	-2.23839	-1.07558	-0.67085	2.86275
40	2.52666	-0.77274	1.72759	0.20581	1.52864
41	1.93025	-1.63016	-1.63016	1.23931	0.15775
42	0.81301	2.15032	-3.01121	0.57320	0.62028
43	0.36860	3.00867	-3.17650	0.51642	-1.65299
44	0.41350	-1.13540	0.50994	0.37707	0.09466
45	0.56499	-1.47562	-1.57592		
46	2.04621	-1.54244	-1.62032	0.07671	-0.19971
47	0.91292	-1.01265	0.55357	-0.54106	-1.82471
48	-0.41818	1.59002	-1.18232	0.54112	-0.76258
49	0.56342	1.25757	-1.23335	-0.08943	-0.28990
50	0.01635	1.22112	1.68314	-0.35942	0.09914
51	-0.60921	-0.99212	-0.64082	-0.55543	2.62139
52	-0.34465	-0.51660	-1.45569	-0.26905	1.27328
53	-0.58540	-0.17035	-0.54112	-0.18103	-0.94286
54	-0.16750	2.12503	-0.75454	-0.73837	-0.12948
55	-0.24811	0.36507	1.06608	1.46886	1.02634
56	-1.75128	-1.29295	-1.11764		
57	-0.09863	1.07622	-0.15428		
58	2.05991	0.54476	-0.18103		
59	-0.47765	-0.11599	-0.73837		
60	-0.05017	0.47961	1.46886		

256

600 observations from an MA(2) process

$$X_t = \epsilon_t + 0.2\epsilon_{t-1} + 0.8\epsilon_{t-2}.$$

(Continued)

Table A1.5

600 observations from an ARMA(2,1) process (2)

$$X_t - 0.3\,X_{t-1} + 0.4\,X_{t-2} = \epsilon_t + 0.7\epsilon_{t-1}.$$

(Continued)

Table A1.7

600 observations from an MA(1) process (1)

$$X_t = \epsilon_t + 0.7\epsilon_{t-1}$$

Table A1.8

600 observations from an MA(1) process (2)

$$X_t = \epsilon_t - 0.7\epsilon_{t-1}$$

Table A1.7

600 observations from an MA(1) process (1)

$X_t = \epsilon_t + 0.7\epsilon_{t-1}$. (Continued)

Table A1.8

600 observations from a MA(1) process (2)

$X_t = \epsilon_t - 0.7\epsilon_{t-1}$. (Continued)

APPENDIX A2

POLYNOMIAL MODEL FITTING TO OBSERVED DATA[46]

Given pairs of data $\{X_i, Y_i\}$, $i = 1 \cdots N$, we often want to express Y_i as a polynomial of X_i.

If we fit $\hat{y}_{M \cdot i}$, a polynomial of x_i of order M, as

$$\hat{y}_{M \cdot i} = a_0 + a_1 x_i + a_2 x_i^2 + \cdots + a_M x_i^M \tag{A2.1}$$
$$i = 1, \cdots N,$$

we can estimate the coefficients $a_0, a_1 \cdots a_m$ by the least squares method. Namely, computing the mean square of the difference

$$\sigma_M^2 = \frac{1}{N} \sum_{i=1}^{N} (y_i - \hat{y}_{M,i})^2, \tag{A2.2}$$

and find the $a_0, a_1 \cdots a_m$ that make σ_M^2 minimum. Then from

$$\left.\begin{array}{l} \dfrac{\partial \sigma_M^2}{\partial a_0} = 0, \quad a_0 + \left(\sum x_i\right) a_1 + \cdots + \left(\sum x_i^M\right) a_M = \sum y_i \\[4mm] \dfrac{\partial \sigma_M^2}{\partial a_1} = 0, \quad \left(\sum x_i\right) a_0 + \left(\sum x_i^2\right) a_1 + \cdots + \left(\sum x_i^{M+1}\right) a_M = \sum x_i\, y_i \\[2mm] \qquad \vdots \\[2mm] \dfrac{\partial \sigma_M^2}{\partial a_M} = 0, \quad \left(\sum x_i^M\right) a_0 + \left(\sum x_i^{M+1}\right) a_1 + \cdots + \left(\sum x_i^{2M}\right) a_M = \sum x^M \cdot y_i \end{array}\right\} \tag{A2.3}$$

The $a_0 \cdots a_M$ are calculated as the solution of the simultaneous Eq. A2.3.

Here, the most serious problem is determining the order. We can make $\hat{y}_{M i}$ as close as we wish to y_i by making the order M very large. However, if M is too large, $\hat{y}_{M i}$ follows, even to the random error of the observations. Of course, if M is too small, $\hat{y}_{M i}$ sometimes neglects the variations in the data that really exist, as shown in Fig. A2.1. Order 1 is too small, but order 5 seems too large.
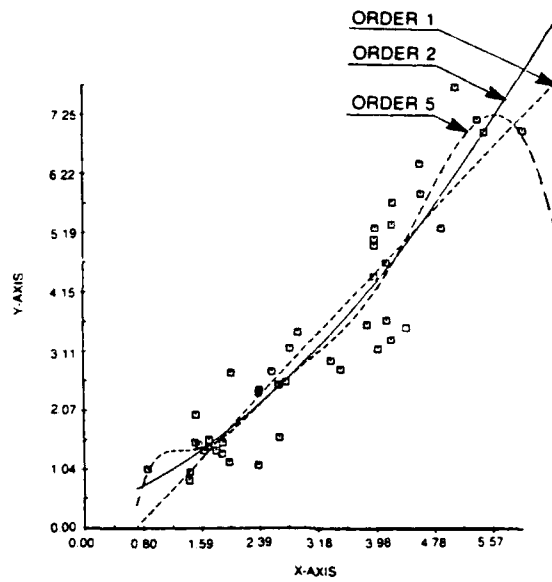
Fig. A2.1. Fitting of polynomials to the observed data.
(From Yamanouchi, et al.[46])

All observed data include the statistical error. Accordingly, when x_i are given, instead of Eq. A2.1, y_i should be represented by a regressive polynomial,

$$y_i = a_o + a_1 x_i + a_2 x_i^2 + \cdots + a_M x_i^M + \epsilon_i. \tag{A2.4}$$

Here ϵ_i is a probability variable that follows the normal distribution with 0 mean and variance σ_ϵ^2. Here, we can define that model fitting is the statistical selection of a model to fit best to data in statistical meaning. When we use Eq. A2.4 as the model, we can use the minimum AIC criteria or the MAIC method to determine the order M. When y_i is approximated by a polynomial of order M as in Eq. A2.1, the coefficient $\hat{a}_j$'s has the values determined by the least squares method,

$$-L = \min(1/N) \sum_{i=1}^{N} (y_i - y_{M,i})^2. \tag{A2.5}$$

Then let us investigate the behavior of this mean square of the residual error

$$\frac{1}{N} \sum_{i=1}^{N} (y_i - y_{M,i})^2 = \sigma_\epsilon^2$$

or N times the logarithm of Eq. A2.5

$$N \log \sum (y_i - \hat{y}_{M,i})^2 = N \log \sigma^2. \tag{A2.6}$$

This value A2.6 is shown in Fig. A2.2 by the mark O and tells us that the larger the value of M, the smaller this value A2.6 is, or the larger the order M, the smaller the residual error σ_ϵ^2.
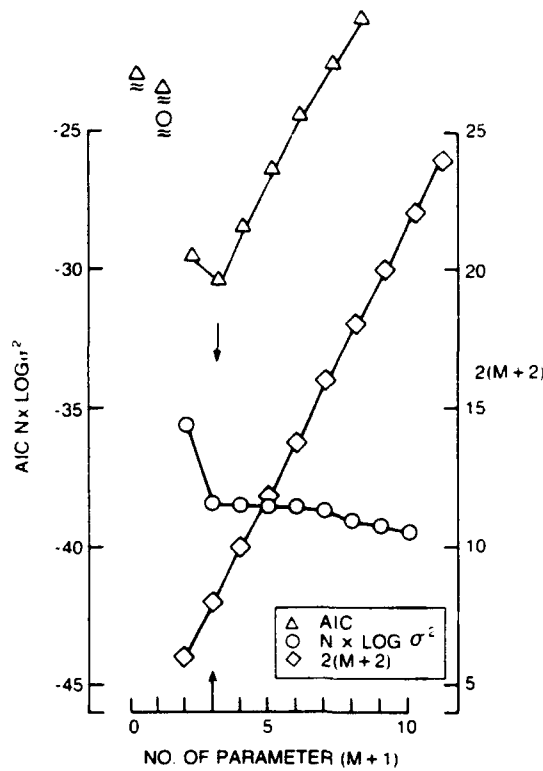
Fig. A2.2. Behavior of AIC for Fig. A2.1.
(From Yamanouchi, et al.[46])

However, this procedure of guiding M from Eq. A2.6 does not give us the best values of the order, because Eq. A2.6 does not include the goodness of fit to the real structure of the data or the decrease in reliability with the increase in the number of parameters to be estimated. So, to show the penalty for this increase in the order, if we add the term

$$2 \times (\text{no. of parameters}) = 2(M + 2) \qquad (A2.7)$$

to Eq. A2.6, that gives us the AIC,

$$\text{AIC}(M) = N \log \sum_{i=1}^{N} (y_i - \hat{y}_{M,i})^2 + 2(M + 2). \qquad (A2.8)$$

The number of parameters $M + 2$ comes from $(M + 1)$ $\hat{a}_j$'s for $a_o, a_1 \cdots a_M$ plus 1 for σ^2 that we must also estimate. The behavior of $2(M + 2)$ is shown in Fig. A2.2 by the mark ◊ as a straight curve that increases linearly by M. Then AIC, expressed as the sum of $N \log \sigma^2$ and 2 $(M + 2)$, behaves like the △ in Fig. A2.2 and shows a minimum at a certain M, here $M + 1 = 3$ for the data shown in Fig. A2.1. Thus the order of the polynomial is determined as $M = 2$ by AIC criteria.

263

From the discussions in Section 5.4.3, we know that Eq. A2.5, the estimation that minimizes $(1/N) \sum_{i=1}^{N} (y_i - y_{M,i})^2$, is the estimate that maximizes the likelihood function L, or the logarithmic likelihood function $\log L$. Accordingly, Eq. A2.8 can be written as

$$\text{AIC} = -2\log(\text{max likelihood}) + 2(\text{no. of parameters}). \qquad (A2.9)$$

Eq. A2.9 supplements the characteristics of AIC, this author believes. As another example of polynomial fitting, Fig. A2.3 shows the plot of the observed data for a maneuverability test of a ship.

By the same procedure, from the behavior of AIC in Fig. A2.4, the order was determined as $M = 5$, and the fifth order polynomial was estimated as the best fit to these data.
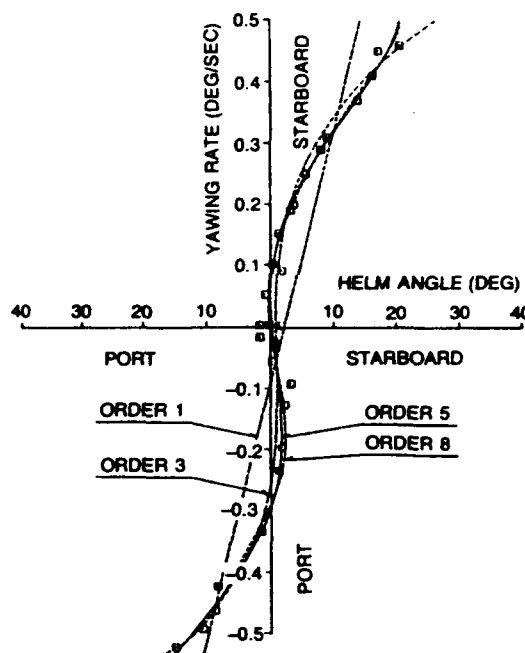
Fig. A2.3. Fitting of polynomials to the data of maneuvering test of ship. (From Yamanouchi, et al.[46])

264

On Fig. A2.4, the behavior of AIC is shown for this fitting.
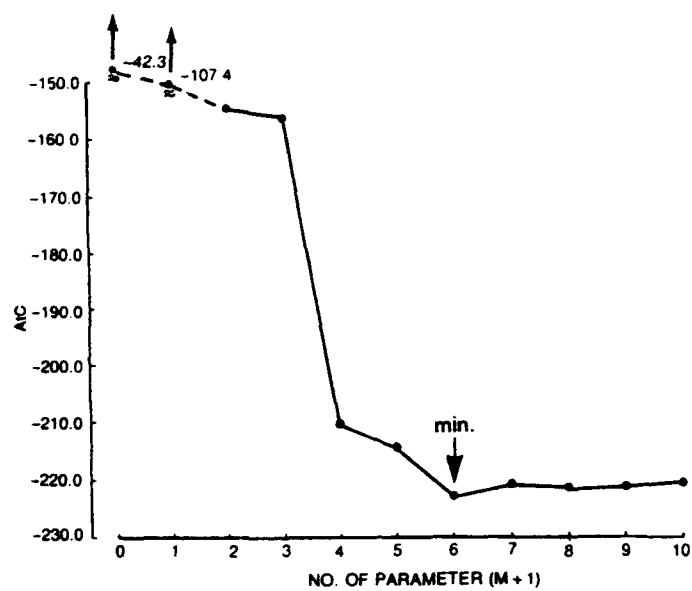
Fig. A2.4. Behavior of AIC for Fig. A2.3.
(From Yamanouchi, et al.[46])

265

THIS PAGE INTENTIONALLY LEFT BLANK

PART III

TREATMENT OF NONLINEARITIES

CHAPTER 9

INTRODUCTION

9.1 INTRODUCTION FOR PART III

In the preceding sections, Part I and Part II, the processes were assumed to be almost linear, and in so far as the process is linear, the periodogram analysis shown in Part I and the model fitting method in Part II are effective methods of analysis. For example, a Fourier–Stieltjes expression for the process assumed to exist in Part I is originally a linear expression, and the AR, MA, or ARMA models treated in Part II are based on the idea of decomposing the processes into independent or orthogonal processes, i.e., assuming their linearity. However, if the process is nonlinear, these methods can no longer be applied directly. We need some special considerations for their treatment.

In most engineering fields, many phenomena can be approximated as linear. However, no phenomena are purely linear but include some elements of nonlinearity. Today in nonlinear phenomena such as the effect of viscosity, the secondary potential forces that include the interaction of two frequency components of excitations have come to be considered important in treating the behavior of ocean vehicles and structures, although useful information has been derived even under the limitations of linear approximation.

Here in Part III, the nonlinearity of waves themselves that are the source of excitation to systems of ocean vehicles and structures is first investigated. According to a few works already published, their nonlinearity is usually not large.

The approximation methods that have been used to treat nonlinear response processes, such as the linearization method and the perturbation method, are summarized. As more advanced approximations, the Voltera or functional expansion of the nonlinear process and the application of polyspectra are then introduced.

As an extension of these approximation method, a slightly different aspect of the analysis of the probability characteristics of the process, the probability distribution function of the extremes, is summarized. As extensive work has been published recently on the analysis of nonlinearity response including these probability characteristics by J. F. Dalzell,[12,13,55-58] only the derivation of general characteristics of several functions and the results of these applications are reviewed.

Next in Part III, the treatment of stochastic processes as Markov processes is introduced, and then the application of the Fokker–Planck equation, also recently introduced by J. B. Roberts[59-61] in the analysis of seakeeping data, is reviewed.

Finally, as a slightly different approach, or as the extension of the model fitting techniques discussed in Part II, a few examples of this extension to the nonlinear process are briefly reviewed.

267

9.2 NONLINEARITY OF OCEAN WAVES

Wave theory has developed remarkably in recent decades with the assumption of a wave as a stochastic process. In most cases, however, the assumption is based on infinitesimal amplitudes and is valid only when the wave height is small compared with the wave length, and wave length is small compared with the water depth. All the quadratic terms of the derivatives were assumed to be small and were neglected, and the fundamental equations of motion were linearized and the linearized potential function was derived.

In this section, the results of only a few works on the investigation of the effect of this neglect will be reviewed to show that the effects are indeed small.

9.2.1 Second Order Spectrum of Waves by L. J. Tick and Others

To take account of quadratic terms, L. J. Tick[62,63] expanded the potential function of a wave $\phi(x, z, t)$ around the mean position of the wave $z = 0$ by Taylor expansion,

$$\phi(x, z, t) = \phi(x, z, t)\Big|_{z=0} + \frac{\partial \phi(x, z, t)}{\partial z}\Big|_{z=0} z + \ldots , \qquad (9.1)$$

and carried it to the second term. Using this expression in the fundamental equations for waves, through the perturbation method he expressed this velocity potential as the sum of the linear part $\phi_1(t)$ and the quadratic term $\phi_2(t)$ as

$$\phi(t) = \phi_1(t) + \phi_2(t). \qquad (9.2)$$

As a result, the wave height is supposed to be composed of two parts, linear and quadratic, corresponding to these two potentials, as

$$\eta(t) = \eta^{(1)}(t) + \eta^{(2)}(t), \qquad (9.3)$$

and expressed

$$\eta^{(1)}(t) = \int_{-\infty}^{\infty} e^{-j\omega t} d\xi(\omega). \qquad (9.4)$$

Here

$$E[|d\xi|^2] = s^{(1)}(\omega) d\omega, \qquad (9.5)$$

$$\eta^{(2)}(t) = \int\limits_{-\infty}^{\infty} \int\limits_{-\infty}^{\infty} e^{-j(\omega+\omega')t} \, Q(\omega,\omega')d\xi(\omega)d\xi(\omega'), \qquad (9.6)$$

and

$$Q(\omega,\omega') = -\left[sgn(\omega), sgn(\omega')\right]\frac{|\omega|\omega + |\omega'|\omega'}{2}. \qquad (9.7)$$

Then the spectrum of $\eta(t)$ was derived as

$$s(\omega) = s^{(1)}(\omega) + \frac{1}{g^2} \int\limits_{-\infty}^{\infty} \frac{[|\omega - \lambda|(\omega - \lambda) + |\lambda|\lambda]^2}{2} \, s^{(1)}(\omega - \lambda)s^{(1)}(\lambda)d\lambda$$

$$= s^{(1)}(\omega) + \frac{1}{g^2}s^{(2)}(\omega). \qquad (9.8)$$

As an example, Tick took the simplified Neumann–Pierson type spectrum as $s^{(1)}(\omega) = 1.8 \times 1.0^4\omega^{-6}|\omega| > \omega_0$ and computed this $s^{(2)}(\omega)$ for $\omega_0 = 2,3,6$ rad/sec.

Figure 9.1 shows the results and $(1/g^2)s^{(2)}(\omega)$ is as small as several hundredths of $s^{(1)}(\omega)$ at the most.

L. Tick[63] considered also a shallow water depth and derived the type of $Q_h(\omega,\omega')$ for this case that corresponds to $Q(\omega,\omega')$ in Eq. 9.6, as

$$Q_h(\omega,\omega') = \frac{1}{2}\frac{|k\ k'|k\ k'}{\omega\ \omega'} - \frac{\omega\ \omega'}{2} - \frac{(\omega + \omega')^2}{2}$$

$$+ \frac{(\omega + \omega')^2\left[\frac{|k\ k'|k\ k'}{\omega\ \omega'} + \frac{1}{2}\ \omega\ \omega' + \frac{\omega\ k'^4 + \omega'\ k^4}{2\omega\ \omega'(\omega+\omega')} - \frac{(\omega+\omega')^2}{2}\right]}{(|k|\ k + |k'|\ k)\ \tanh\ [d^2(|k|\ k + |k|\ k')] - (\omega + \omega')^2}. \qquad (9.9)$$

Here $d^2 = (h/g)$, $k = k(\omega)$, $k' = k(\omega')$ are the solutions of $\omega^2 = k^2\ \tanh\ d^2k^2$. As an example, he showed $s^{(2)}(\omega)$ of $s(\omega) = s^{(1)}(\omega) + s^{(2)}(\omega)$, for the following type spectrum,

269
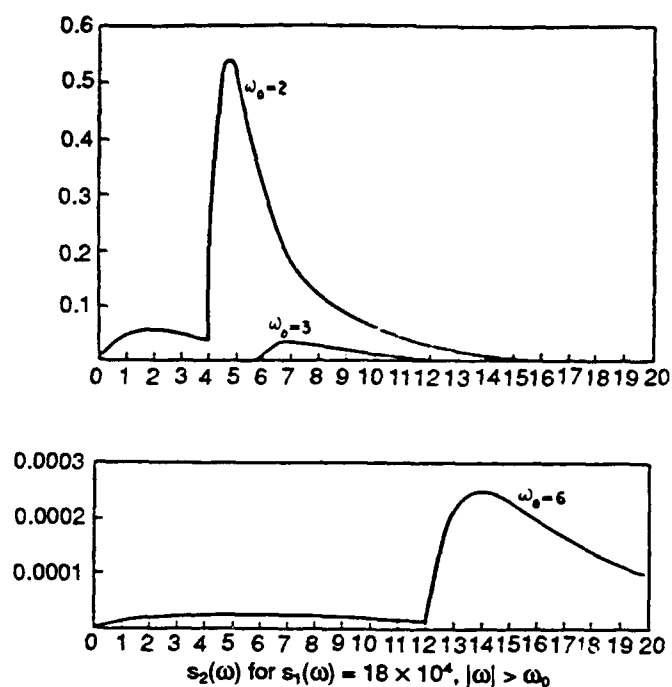
Fig. 9.1. The second order spectra.
(From Tick.[62])

$$s^{(1)}(\omega) = C\ \omega^{-4}\ e^{-6\omega}, \quad \omega < 2$$

and showed $s^{(2)}(\omega)$ as in Fig. 9.2. In this case, even when the water depth $h = 32.2$ ft, the effect of nonlinearity is small.

He pointed out the necessity for computing the bispectrum to show clearly the quadratic effect of the waves as will be discussed in Section 9.2.2.

On the nonlinearity of the waves M. S. Longuet–Higgins[64, 65] and D. M. Phillips[66] discussed work along the same lines, and M. Hineno[67] referred these works and showed clearly the quadratic effect, as in Fig. 9.3, that was calculated for a modified Moskowitz–Pierson type spectrum. In Fig. 9.4, the quadratic and linear parts of the spectrum produced in the experimental water tank are shown.

Hineno[67] also showed the quadratic kernel functions $g_2(\tau_1, \tau_2)$ as Fig. 9.5, that is, the Fourier transform of quadratic frequency responses $G_2(\omega_1, \omega_2)$, equivalent to the $Q(\omega, \omega')$ by L. Tick, as

270
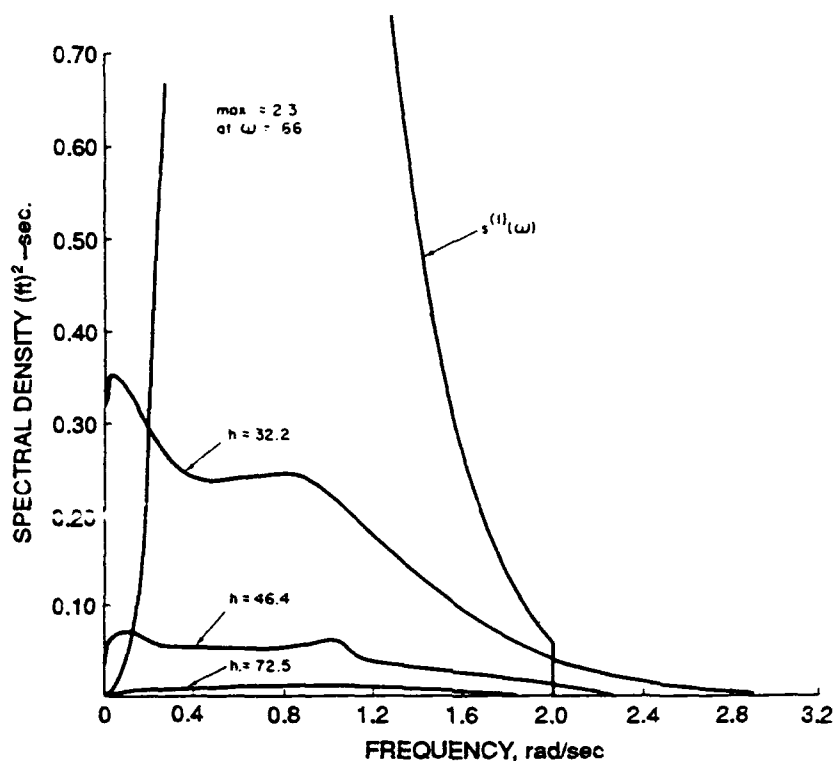
Fig. 9.2. The second order spectra $s^{(2)}(\omega)$ for varying depth h = 32.2, 46.4, and 72.5 ft. (From Tick.[63])

$$G_2(\omega_1, \omega_2) = \frac{1}{2g}(\omega_1^2 + \omega_2^2) \qquad \text{for the sum } (\omega_1 + \omega_2) \text{ frequency component}$$

$$= -\frac{1}{2g} |\omega_1^2 - \omega_2^2| \qquad \text{for the difference frequency component.} \qquad (9.10)$$

Figures 9.3 and 9.4 indicate that the quadratic effect on the spectrum computations is very small for ordinary cases. M. Hineno[67] extended this result and calculated the probability distribution of the maximum and minimum of the waves. The results are introduced in Section 12.7, and from the results we find that the effect of the nonlinearity is not large.

9.2.2 Bispectrum of Waves

L. Tick[62] suggested the need for bispectrum analysis for ocean waves. Such an analysis was performed by K. Hasselman et al.[68] as shown in Fig. 9.6. The exposition on the bispectrum is given in Section 11.3. Here, one bispectrum for shallow waves is given as an example, and it indicates that the nonlinearity is not large in this analysis either.

271
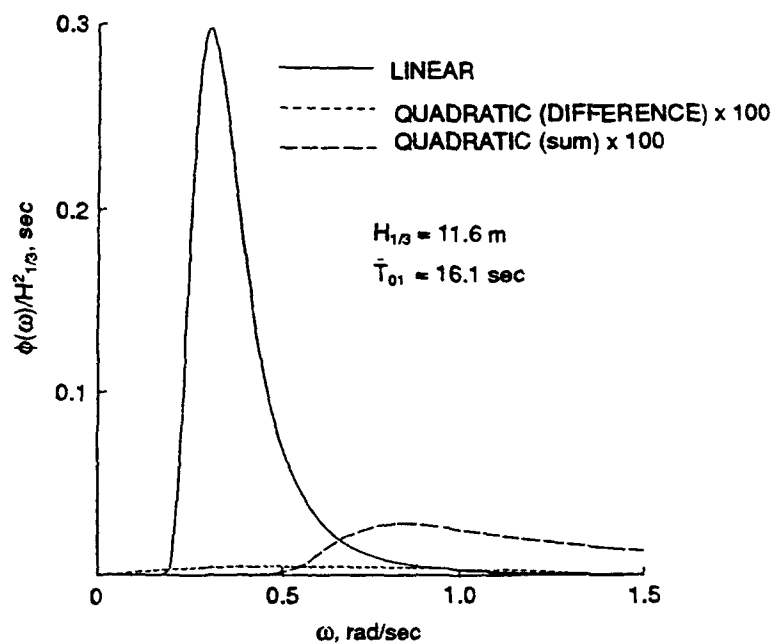
Fig. 9.3. Linear and quadratic component of wave spectrum of Pierson–Moskowitz.
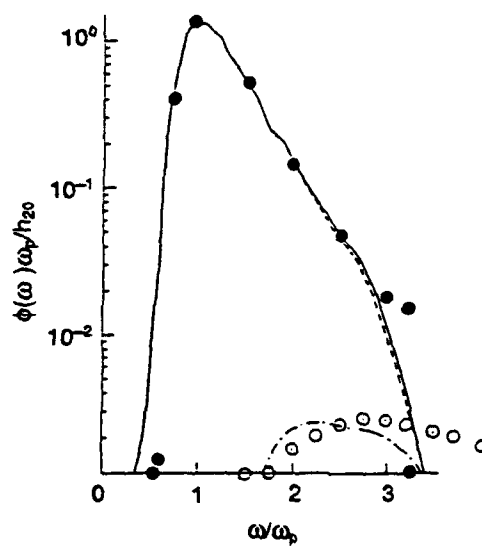
Fig. 9.4. Linear and quadratic component of wave spectrum of
waves produced in a towing tank.

(From Hineno.[67])

272
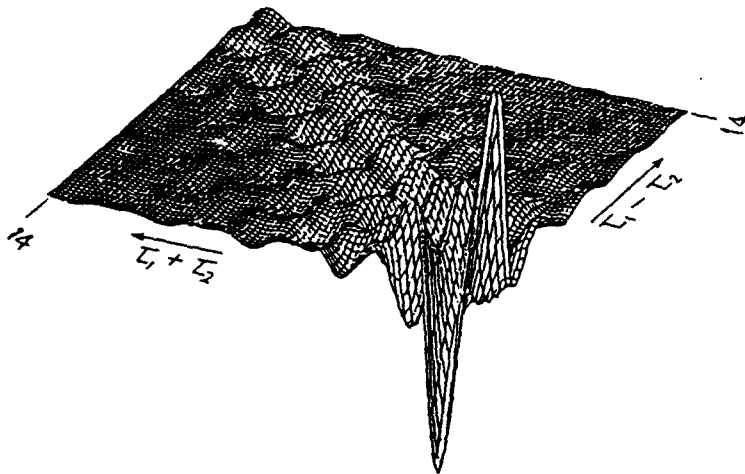
Fig. 9.5. Quadratic kernel function $g_2(\tau_1, \tau_2)$ of wave. (From Hineno.[67])
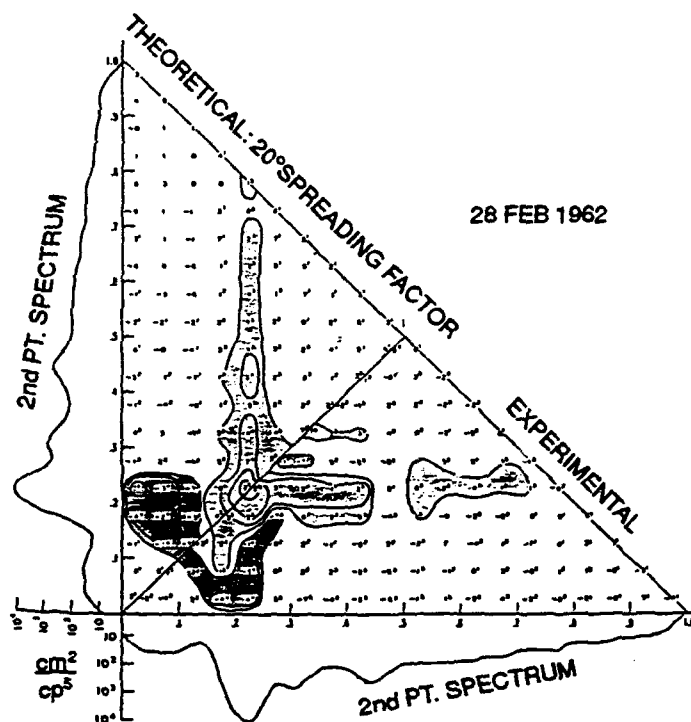
Fig. 9.6. Bispectrum of ocean wave.

[The number -7^4 denotes -7×10^4 cm^3 sec^2. Contours are drawn for -10^3, -10^4, -10^5, and -10^6.] (From Hasselman, et al.[68])

9.3 RESPONSE OF THE BEHAVIOR OF A MARINE VEHICLE ON WAVES

When the amplitude of oscillation in six degrees of freedom is small, the behavior of a marine vehicle in waves can be expressed approximately by linear equations.

Here, for simplicity, if we assume that a floating body in a regular wave train $\zeta(t) = Z(\omega)e^{j\omega t}$ is subjected to a force $b\zeta(t)$ that is linear with wave height $\zeta(t)$, the equation of motion is well approximated[69] by

$$a_1\ddot{x}(t) + a_2\dot{x}(t) + a_3 x(t) = b\zeta(t). \tag{9.11}$$

The response $x(t)$ will be in the form $X(\omega)e^{j\omega t}$,

where

$$X(\omega)e^{j\omega t} = |X(\omega)|e^{j\left(\omega t + \delta_\zeta(\omega) + \sigma_x(\omega)\right)}. \tag{9.12}$$

$\delta_\zeta(\omega), \sigma_x(\omega)$ are the phase relations of the exciting force to the wave height, and the response to the exciting force, respectively.

Generally, for a body floating on the surface of water, the coefficients a_1, a_2, b of the inertia term $a_1\ddot{x}(t)$, the damping term, and the compulsory term, respectively, are generally functions of the frequency and so we find $a_1 = A_1(\omega), a_2 = A_2(\omega)$, and $a_3 = A_3(\omega), b = B(\omega)$.

The equation of motion, Eq. 9.11, will be

$$-\omega^2 A_1(\omega)X(\omega)e^{j\omega t} + j\omega A_2(\omega)X(\omega)e^{j\omega t} + A_3(\omega)X(\omega)e^{j\omega t} = B(\omega)Z(\omega)e^{i\omega t}. \tag{9.13}$$

Therefore, the frequency response function $H_{x\zeta}(\omega)$ of the behavior $X(\omega)$ to wave height $Z(\omega)$ is

$$H_{x\zeta}(\omega) = \frac{X(\omega)}{Z(\omega)} = \frac{B(\omega)}{-\omega^2 A_1(\omega) + j\omega A_2(\omega) + A_3(\omega)}. \tag{9.14}$$

From this, expressing $H_{x\zeta}(\omega)$ just as $H(\omega)$,

$$X(\omega) = H(\omega)Z(\omega). \qquad (9.15)$$

Taking the Fourier transform gives

$$x(t) = \int\limits_{-\infty}^{\infty} h(\tau)\zeta(t-\tau)d\tau. \qquad (9.16)$$

Here

$$h(\tau) = \int\limits_{-\infty}^{\infty} H(\omega)e^{j\omega\tau}d\omega, \qquad (9.17)$$

is the impulse response function.

When the waves are expressed by a Fourier integral,

$$\zeta(t) = \frac{1}{2\pi} \int\limits_{-\infty}^{\infty} Z(\omega)e^{j\omega t}d\omega, \qquad (9.18)$$

the linear response $x(t)$ will be

$$x(t) = \frac{1}{2\pi} \int\limits_{-\infty}^{\infty} X(\omega)e^{j\omega t}d\omega. \qquad (9.19)$$

Strictly speaking, these integrals (Eqs. 9.18 and 9.19) should be Fourier–Stieltjes integrals in the form of

$$\frac{1}{2\pi} \int\limits_{-\infty}^{\infty} e^{j\omega t}dZ(\omega), \quad \frac{1}{2\pi} \int\limits_{-\infty}^{\infty} e^{j\omega t}dX(\omega), \qquad (9.20)$$

where

$$dZ(\omega) \ dZ(\omega') \ = \ s_z(\omega)\delta(\omega + \omega')$$

$$dX(\omega) \ dX(\omega') \ = \ s_x(\omega)\delta(\omega + \omega') \qquad , \qquad (9.21)$$

$s_z(\omega)$, $s_x(\omega)$ being the spectrum of wave height $\zeta(t)$ and response $x(t)$, respectively. Here, however, for simplicity we use the ordinary Fourier integral form.

From Eqs. 9.18, 9.19, and 9.13, Eq. 9.11 will be

$$\frac{1}{2\pi}\left[\int_{-\infty}^{\infty} \left\{ -\omega^2 A_1(\omega) \right\} X(\omega)e^{j\omega t} d\omega + \int_{-\infty}^{\infty} \left\{ j\omega A_2(\omega) \right\} X(\omega)e^{j\omega t} d\omega + \int_{-\infty}^{\infty} A_3(\omega) X(\omega)e^{j\omega t} d\omega \right]$$

$$= \frac{1}{2\pi} \int_{-\infty}^{\infty} B(\omega) Z(\omega) e^{j\omega t} d\omega. \qquad (9.22)$$

From Eq. 9.19

$$x(t - \tau) = \frac{1}{2\pi} \int_{-\infty}^{\infty} X(\omega)e^{j\omega t}e^{-i\omega\tau} d\omega. \qquad (9.23)$$

Then setting

$$\int_{-\infty}^{\infty} A_i(\omega)e^{j\omega\tau} d\omega = k_i(\tau)$$

$$\int B(\omega)e^{j\omega\tau} d\omega = l(\tau), \qquad (9.24)$$

Eq. 9.22 will be in the form of a Fourier convolution,

$$\int\limits_{-\infty}^{\infty} k_1(\tau)\ddot{x}(t-\tau)d\tau + \int\limits_{-\infty}^{\infty} k_2(\tau)\dot{x}(t-\tau)d\tau + \int k_3(\tau)x(t-\tau)d\tau$$

$$= \int\limits_{-\infty}^{\infty} l(\tau)\ z(t-\tau). \qquad (9.25)$$

Actually, however, taking into account the Kramer–Kronig's theory that connects the added mass and the damping for floating and oscillating bodies and also the fact that the restoring term $a_3 x(t)$ is not a function of frequency, the equation of motion is, as T. F. Ogilvie[70] pointed out, in the form of

$$\{M + m(\infty)\}\ \ddot{x}(t) + \int\limits_{-\infty}^{\infty} K(t-\tau)\ \dot{x}(t)d\tau + C\ x(t) = f_e(t). \qquad (9.26)$$

Here $m(\infty)$ is the added mass at frequency $\omega = \infty$.

9.4 NONLINEARITY OF THE BEHAVIOR OF MARINE VEHICLES

When the waves are moderate and the amplitudes of the motions are mild, the response of marine vehicles is well expressed by linear equations, as was shown in the preceding sections.

The nonlinearity of ocean waves was found to be not as large as was shown in Section 9.2. Even when the wave itself is linear, sometimes the exciting force exerted by the wave can be nonlinear with respect to wave height. For example, for drifting vehicles or for the slowly varying behavior of moored offshore structures, the exciting force is not linear with the wave height because of the effects of the secondary potentials of waves. For rolling near the synchronous frequency, the vehicle might oscillate with such a large amplitude that the damping and the restoring force are not linear with the velocity or the displacement. For oscillatory motions, in many cases viscous resistance that is not linear to the velocity of motion sometimes plays a big role in addition to that of wave making resistance that is linear, and results as nonlinear damping.

Usually, however, even in cases of this kind, the effect of nonlinearity is assumed to be small or weak in the succeeding discussions, as will be mentioned again in Chapter 11. Generally, under certain restrictions (as the sum of the absolute values of all kernel functions is not infinite), the nonlinear response can be expressed by

$$x(t) = h_0 + \int\limits_{-\infty}^{\infty} h_1(\tau)\zeta(t-\tau)d\tau + \int\limits_{-\infty}^{\infty}\int\limits_{-\infty}^{\infty} h_2(\tau_1,\tau_2)\zeta(t-\tau_1)\zeta(t-\tau_2)d\tau_1 d\tau_2$$

$$+ \int\limits_{-\infty}^{\infty}\int\limits_{-\infty}^{\infty}\int\limits_{-\infty}^{\infty} h_3(\tau_1,\tau_2\tau_3)\zeta(t-\tau_1)\zeta(t-\tau_2)\zeta(t-\tau_3)d\tau_1 d\tau_2 d\tau_3$$

$$+ \ldots \ldots$$

$$+ \int\limits_{-\infty}^{\infty}\int\limits_{-\infty}^{\infty} \ldots \int\limits_{-\infty}^{\infty} h_i(\tau_1,\tau_2 \ldots \tau_i)\ \zeta(t-\tau_1)\zeta(t-\tau_2) \ldots \zeta(t-\tau_i)d\tau_1 d\tau_2 \ldots d\tau_i$$

$$+ \ldots \ldots$$

$$= \sum_{n=0}^{\infty} \int\limits_{-\infty}^{\infty}\int\limits_{-\infty}^{\infty} \ldots \int\limits_{-\infty}^{\infty} h_n(\tau_1,\tau_2, \ldots \tau_n)\zeta(t-\tau_1)\zeta(t-\tau_2) \ldots \zeta(t-\tau_n)$$

$$d\tau_1 d\tau_2 \ldots d\tau_n, \tag{9.27}$$

instead of by Eq. 9.16 for the linear case as,

$$x(t) = h_0 + \int\limits_{-\infty}^{\infty} h(\tau)\zeta(t-\tau)d\tau. \tag{9.28}$$

Here in Eq. 9.27

$$h_n(\tau_1,\tau_2 \ldots \tau_n) = \left(\frac{1}{2\pi}\right)^n \int\limits_{-\infty}^{\infty}\int \ldots \int H_n(\omega_1,\omega_2 \ldots \omega_n)$$

$$\times \exp(i\omega_1\tau_1 + i\omega_2\tau_2 + \ldots + i\omega_n\tau_n)d\omega_1 d\omega_2 \ldots d\omega_n$$

$$n = 0 \frown \infty. \tag{9.29}$$

278

$h_n(\tau_1, \tau_2 \ldots \tau_n)$ is called the n th order impulse response function and

$H_n(\omega_1, \omega_2 \ldots \omega_n)$ the n th order frequency response function. The expansion of $x(t)$ in Eq. 9.29 is called the functional expression or the Voltera–Wiener expression. The treatment of nonlinear processes from this stand point and the application of polyspectra in the analysis of the nonlinear response system is dealt with in Chapter 11.

When the nonlinearities are expressed explicitly in the form of the equation of motion as

$$M\ddot{x} + B(\dot{x}) + K(x) = F(t),$$

with the nonlinearity in the damping and restoring terms, there have been a few efforts to overcome the difficulties. In Chapter 10, these efforts will be summarized.

Hasselman[71] formulated the equations of motion for a quadratic nonlinear ship's motion, expressing the wave field by surface displacement $\zeta(x, t) = \zeta_1$ and its normal surface velocity $(d\zeta/\partial t)$ $(x, t) \equiv \zeta_2$, where $x = (x_1, x_2)$ is the horizontal Cartesian coordinate vector. He derived a generalized nonlinear equation expressed in functional form and made it clear that, through cross–spectrum and cross–bispectrum analysis, it is possible to get the linear and quadratic frequency responses from the data obtained from irregular waves on the ocean. For his formulation, the frequency components that are the sum and difference of two component frequencies appear to be important. His expression is, however, in generalized form and is not necessarily adequate for practical applications. Almost the same content will be explained later in scalar form in Section 11.3, for a general dynamic system with quadratic nonlinear characteristics.

THIS PAGE INTENTIONALLY LEFT BLANK

CHAPTER 10

APPROXIMATION METHODS FOR THE ANALYSIS OF NONLINEAR SYSTEM IN RANDOM EXCITEMENT

10.1 INTRODUCTION

Nonlinear vibration systems have been studied for a long time. The equivalent linearization is the most popular method for handling the weakly nonlinear system, and the perturbation method has been used to obtain the equivalent linear expressions. However, most of the studies have been concerned with systems under deterministic excitation. In this chapter, systems under random or stochastic excitation are treated. The equivalent linearization method and the perturbation method are treated independently for convenience of explanation.

10.2 EQUIVALENT LINEARIZATION METHOD

Suppose there is a weakly damped, slightly nonlinear oscillation expressed as

$$\ddot{x} + \alpha\dot{x} + \beta|\dot{x}|\dot{x} + \omega_0^2 x + kx^3 = F(t). \tag{10.1}$$

When, for example in case of rolling with moderate amplitude, the damping term includes the quadratic term $\beta|\dot{x}|\dot{x}$ for viscous damping in addition to the linear damping $\alpha\dot{x}$, the restoring term includes the cubic term kx^3 that comes from the shape of the righting arm curve (stability curve). Generally when $k \gtrless 0$, this system is called a hard or soft spring oscillation system.

In the deterministic case, or when this system is exposed to a harmonic excitation $F(t)$, this nonlinear damping can be linearized with the equivalent linear damping

$$\alpha_e = \alpha + \alpha_e{}' = \alpha + \left(\frac{8\omega_0}{3\pi}\right)\beta x_0 \tag{10.2}$$

using the amplitude of oscillation x_0.

This relation was derived by Jacobson (1930),[72] equating the energy dissipation by the damping term $\alpha\dot{x} + \beta|\dot{x}|\dot{x}$ and by $\alpha_e\dot{x}$ during one period of oscillation at amplitude x_0. In the same way, equating the work done by the restoring term at amplitude x_0, the equivalent linear restoring coefficient ω_{eq}^2 is as shown in Fig. 10.1,

$$\omega_{eq}^2 = \omega_0^2 + \frac{1}{2}kx_0^2. \tag{10.3}$$
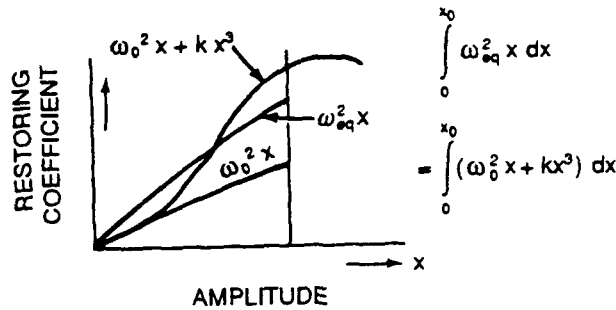
Fig. 10.1. Restoring coefficient.

However, for the stochastic case, when the exciting term is stochastic in character, we cannot use Eqs. 10.3 and 10.2 directly. T. K. Caughey[73] formulated this case as follows. Nonlinear oscillation can be expressed as

$$\ddot{x} + \alpha \dot{x} + \omega_0^2 x + \eta \cdot g(x, \dot{x}, t) = f(t), \tag{10.4}$$

where η is small, $g(x, \dot{x}, t)$ includes all nonlinear effects, and $f(t)$ is a random excitation. When the equivalent linearized damping coefficient α_{eq} and the linearized restoring coefficient ω_{eq}^2 are obtained,

$$\ddot{x} + \alpha_e \dot{x} + \omega_{eq}^2 x = f(t), \tag{10.5}$$

and the error $e(x, \dot{x}, t)$ is expressed by

$$e(x, \dot{x}, t) = (\alpha - \alpha_{eq})\dot{x} + (\omega_0^2 - \omega_{eq})x + \eta \cdot g(x, \dot{x}, t). \tag{10.6}$$

Namely, $\alpha_{eq}, \omega_{eq}^2$ are to be set to minimize the time average

$$|\overline{e^2}| = \lim_{t \to \infty} \frac{1}{2T} \int_{-T}^{T} e^2(x, \dot{x}, t) dt. \tag{10.7}$$

282

Therefore from

$$\frac{\partial |\overline{e^2}|}{\partial \alpha_{eq}} = 0, \quad \overline{2[(\alpha - \alpha_{eq})\dot{x}^2 + (\omega_0^2 - \omega_{eq}^2)x\dot{x} + \eta x g(x, \dot{x}, t)]^2} = 0 \quad (10.8)$$

and

$$\frac{\partial |\overline{e^2}|}{\partial \omega_{eq}^2} = 0, \quad \overline{2[(\alpha - \alpha_{eq})x, \dot{x} + (\omega_0^2 - \omega_{eq}^2)x^2 - \eta x g(x, \dot{x}, t)]^2} = 0. \quad (10.9)$$

If this process $x(t)$ is stationary,

$$[\overline{x\dot{x}}] = 0. \quad (10.10)$$

Therefore from Eqs. 10.8 and 10.9

$$\alpha_{eq} = \alpha + \overline{\eta[xg(x, \dot{x}, t)]}/[\overline{\dot{x}^2}], \quad (10.11)$$

$$\omega_{eq}^2 = \omega_0^2 + \overline{\eta[x, g(x, \dot{x}, t)]}/[\overline{x^2}]. \quad (10.12)$$

If we assume ergodicity, the time average can be replaced with the ensemble average, and therefore

$$\alpha_{eq} = \alpha + \eta \cdot E[\dot{x}g(x, \dot{x})]/E[\dot{x}^2], \quad (10.11')$$

$$\omega_{eq}^2 = \omega_0^2 + \eta \cdot E[x, g(x, \dot{x})]/E[x^2]. \quad (10.12')$$

This shows how α_{eq}, ω_{eq}^2 can be estimated from the original expression Eq. 10.4. When the form of $\eta \cdot g[x, \dot{x}, t]$ is given, the equivalent linearized values α_{eq}, ω_{eq}^2 can easily be obtained by Eqs. 10.11' and 10.12'.

For example, for a Duffing type oscillation,

$$\ddot{x} + \alpha\dot{x} + \omega_0^2\left\{x + \epsilon x^3\right\} = f(t), \quad (10.13)$$

283

$g\{x\} = x^3$, $\eta = \epsilon \omega_0^2$. When $\epsilon > 0$, we call it a hard spring system, and when $\epsilon < 0$, a soft spring system.

From Eq. 10.12'

$$\omega_{eq}^2 = \omega_0^2 \left[1 + \epsilon E[x^4]/E[x^2] \right]. \tag{10.14}$$

When nonlinearity is weak, x can be approximated as Gaussian, and then

$$E[x^4] = 3 \left(E[x^2] \right)^2 \tag{10.15}$$

and thus

$$\omega_{eq}^2 = \omega_0^2 [1 + 3\epsilon \sigma_x^2]. \tag{10.16}$$

When every coefficient is linearized, the response can be obtained. If $f(t)$ is almost white in the important range, $E[x^2]$ for this case can be computed as

$$E[x^2] \approx \sigma_{x_0}^2 - 3\epsilon \sigma_{x_0}^4. \tag{10.17}$$

Here $\sigma_{x_0}^2$ is the variance for linear oscillation. Eq. 10.17 shows that, when $\epsilon > 0$, $E[x^2]$ is smaller than $\sigma_{x_0}^2$ by nearly $3\epsilon \sigma_{x_0}{}^4$.

Applying these general results (Eqs. 10.11 and 10.12), L. A. Vassilopoulos[74] obtained α_{eq} and ω_{eq}^2 for ship's rolling, expressed as

$$\ddot{x} + \alpha \dot{x} + \beta |\dot{x}|\dot{x} + \omega_0^2 \, x + \epsilon \cdot k \cdot x^3 = f(t), \tag{10.18}$$

as

$$\alpha_{eq} = \alpha + \alpha_e = \alpha + \sqrt{8/\pi} \cdot \beta \, \sigma_{\dot{x}} \tag{10.19}$$

$$\omega_{eq}^2 = \omega_0^2 + [3\sigma_x^2] \cdot k. \tag{10.20}$$

Further, assuming that the damping is small and the spectrum of the wave slopes is flat in the important range for rolling, i.e., $\sigma_{\dot{x}} \approx \omega_0 \sigma_x$, he derived

284

$$\alpha + \alpha_e = \alpha + \sqrt{8/\pi} \cdot \beta \cdot \omega_0 \sigma_x. \qquad (10.21)$$

Comparing this expression with Eq. 10.2 for the deterministic case gives

$$x_0 = \left[\frac{\sqrt{\frac{8}{\pi}}}{\left(\frac{8}{3\pi}\right)} \right] \sigma_x = \frac{1.6}{0.85} \sigma_x \approx 2 \, \sigma_x, \qquad (10.22)$$

namely for our interest, x_0 appeared almost equal to the significant amplitude for the stochastic case.

P. Kaplan[75] used this general result and calculated the ship's rolling for the same example that this author solved by the perturbation method as shown in the next section. Kaplan found that the result checked very well with this author's result.

10.3 PERTURBATION METHOD

10.3.1 Trial for Ship's Rolling

This author showed[32] the results of the computation of nonlinear rolling using the perturbation method. The effect of nonlinear damping was investigated first. One degree of freedom rolling is expressed as

$$I\ddot{\phi} + N_1\dot{\phi} \pm N_2(\dot{\phi})^2 + K_1\phi = M, \qquad (10.23)$$

$$\ddot{\phi} + 2\alpha\dot{\phi} + \beta|\dot{\phi}|\dot{\phi} + \omega_0^2\phi = m(t). \qquad (10.24)$$

Starting with a 0 order approximation ϕ_0 (when $\beta = 0$), that is linear,

$$\ddot{\phi}_0 + 2\alpha\dot{\phi}_0 + \omega_0^2\phi_0 = m(t), \qquad (10.25)$$

$$\phi_0 = \int_{-\infty}^{\infty} h_{\phi_0 m}(t - \tau) \, m(t)d\tau = \int_{-\infty}^{\infty} h_{\phi_0 m}(\tau) \, m(t - \tau)d\tau. \qquad (10.26)$$

Here $h_{\phi_0 m}(\tau)$ is the impulse response of the 0 order, namely linear approximation ϕ_0 to the exciting moment $m(t)$,

$$h_{\phi_0 m}(\tau) = \frac{1}{2\pi} \int_{-\infty}^{\infty} H_{\phi_0 m}(\omega)\ e^{j\omega\tau}\ d\tau.$$ (10.27)

Frequency response $H_{\phi_0 m}(\omega)$ is easily obtained by Eq. 10.25.

Then, when the nonlinear damping term is shifted to the right–hand side of Eq. 10.24 and $\dot{\phi}_0$ is used in the nonlinear term, the first approximation ϕ_1 is expressed by

$$\ddot{\phi}_1 + 2\alpha\dot{\phi}_1 + \omega_0^2\phi_1 = m(t) - \beta|\dot{\phi}_0|\dot{\phi}_0.$$ (10.28)

As the left–hand side of Eq. 10.28 is in the same form with that of Eq. 10.25, using $h_{\phi_0 m}(\tau)$ as the impulse response function gives

$$\phi_1 = \int_{-\infty}^{\infty} h_{\phi_0 m}(t-\mu)\{m(\mu) - \beta|\dot{\phi}_0(\mu)|\dot{\phi}_0(\mu)\}\ d\mu,$$ (10.29)

$$\equiv \phi_0(t) - \phi_1'(t).$$ (10.29')

Since α and β are small, the convergence of this approximation is assumed. Then, the correlation function is

$$R_{\phi_1\phi_1}(\tau) = E\big[\{\phi_0(t+\tau) - \phi_1'(t+\tau)\}\{\phi_0(t) - \phi_1'(t)\}^*\big]$$

(* Shows the conjugate)

$$= E[\phi_0(t+\tau)\phi_0^*(t)] - 2\ \Re e\left\{E[\phi_1(t+\tau)\phi_1'(t)]\right\} + E[\phi_1'(t+\tau)\phi_1'^*(t)],$$ (10.30)

here $\Re e\{\cdot\}$ indicates to take the real part of a function $\{\cdot\}$.

The spectrum is manipulated by taking the Fourier transformation of $R_{\phi_1\phi_1}(\tau)$,

$$S_{\phi_1\phi_1}(\omega) = S_{\phi_0\phi_0}(\omega) - 2\sqrt{\frac{2}{\pi}}\ \sigma_{\dot\phi_0}\beta\ S_{\phi_0\phi_0}(\omega)\cdot\omega\cdot Im\left\{H_{\phi_o m}(\omega)\right\}$$

$$+ \beta^2|H_{\phi_o m}(\omega)|^2\left[\frac{8}{\pi}\sigma_{\dot\phi_0}^2\,\omega^2 S_{\phi_0\phi_0}(\omega) + \frac{4}{3\pi\sigma_{\phi_0}^2}\ S_{\dot\phi_0\dot\phi_0}(\omega)\right], (10.31)$$

where $Im\{\cdot\}$ indicates the imaginary part of a function $\{\cdot\}$.

Here

$$S_{\dot\phi_0\dot\phi_0}(\omega) = \int\limits_{-\infty}^{\infty}\int\limits_{-\infty}^{\infty} S_{\dot\phi_0\dot\phi_0}(\omega_1)\ S_{\dot\phi_0\dot\phi_0}(\omega_2)\ S_{\dot\phi_0\dot\phi_0}(\omega - \omega_1 - \omega_2)d\omega_1 d\omega_2.\quad (10.32)$$

In the computation of these values, the expected values $E[\xi\cdot\eta\cdot|\eta|]$ and $E[\xi,|\xi|\cdot\eta\cdot|\eta|]$, that include the absolute values $|\xi|,|\eta|$ must be calculated. Here ξ and η follow the two variables' Gaussian distribution,

$$p(\xi,\eta) = \frac{1}{2\pi\sigma_\xi\sigma_\eta\sqrt{1-\varrho^2}}\exp\left[\frac{\sigma_\eta^2\xi^2 - 2\varrho\sigma_\xi\sigma_\eta\xi\eta + \sigma_\xi^2\eta^2}{2\sigma_\xi^2\sigma_\eta^2(1-\varrho^2)}\right]\qquad (10.33)$$

(ϱ is the correlation).

The expected values of the two variables such as $E[\xi,\eta^3]$ $E[\xi^2,\eta^2]$ have been computed by Isserlis,[76] a long time ago, but no reference was found on the expected values of the products of variance that include the absolute values as $E[\xi,\eta,|\eta|], E[\xi\cdot|\xi|\cdot\eta\cdot|\eta|]$. These were calculated by this author and were found as

$$E[\xi\cdot\eta\cdot|\eta|] = \sqrt{\frac{2}{\pi}}\ \varrho\cdot\sigma_\xi\sigma_\eta^2,\qquad (10.34)$$

$$E[\xi\cdot|\xi|\eta\cdot|\eta|] = \frac{2\sigma_\xi^4\sigma_\eta^2}{\pi}\left[\sqrt{1-\varrho}\cdot 3\varrho + 2(1+2\varrho^2)\times\tan^1\left\{\frac{\sqrt{1+\varrho}-\sqrt{1-\varrho}}{\sqrt{1+\varrho}+\sqrt{1-\varrho}}\right\}\right].$$

$$(10.35)$$

287

A numerical example for a ship model, with $\omega_0 = 3.85$, $(\alpha/\omega_0) = 0.06705$, $\beta = 0.08$, and waves with a Neumann type spectrum and a peak at ω_0, is shown in Figs. 10.2 – 10.5. Figure 10.5 shows the overall effect of nonlinear damping, and Fig. 10.4 shows the effects of nonlinearity on the term of Eq. 10.31, especially the double convolution $S_{\phi\dot\phi}(\omega)$ of the spectrum $S_{\dot\phi\dot\phi}(\omega)$, shown by Eq. 10.32.

In the same way, the author also calculated the effect of a nonlinear restoring force expressed as

$$I\ddot\phi + N\dot\phi + (K_1\phi + K_3\phi^3) = M, \tag{10.36}$$

$$\ddot\phi + 2\alpha\dot\phi + \omega_0^2\phi + k_3\phi^3 = m(t). \tag{10.37}$$

Starting with a 0 approximation ϕ_0, for $k_3 \approx 0$, the spectrum of the first order approximation ϕ_1 when $k_3 \neq 0$, is

$$S_{\phi_1\phi_1}(\omega) = S_{\phi_0\phi_0}(\omega) - k_3 \cdot 2\Re e[H_{\phi_0 m}(\omega) \cdot 3\sigma_{\phi_0}^3 S_{\phi_0\phi_0}(\omega)]$$

$$+ k^3|H_{\phi_0 m}(\omega)|^2 \left\{ 9\sigma_{\phi_0}^4 S_{\phi_0\phi_0}(\omega) + 6\sigma S_{\phi_0\phi_0}^{(2)}(\omega) \right\}. \tag{10.38}$$

Here

$$S_{\phi_0\phi_0}^{(2)}(\omega) = \int\limits_{-\infty}^{\infty} \int\limits_{-\infty}^{\infty} S_{\phi_0\phi_0}(\omega_1) S_{\phi_0\phi_0}(\omega_2) S_{\phi_0\phi_0}(\omega - \omega_1 - \omega_2) d\omega_1 d\omega_2. \tag{10.39}$$

10.3.2 General Formulation of the Perturbation Method

S. H. Crandall[77] formulated a general approach to the case with a nonlinear restoring term by the perturbation method, as follows.

The equation of motion is expressed as

$$\ddot X + 2\alpha\dot X + \omega_0^2[X + \epsilon g(X)] = f(t) \tag{10.40}$$

where ϵ has a small value. Then X can be expanded in terms of powers of ϵ

288

Fig. 10.3. Linear response of roll to the exciting moment. (From Yamanouchi.[32])

Fig. 10.2. Spectra of wave, roll, and roll angular velocity. (From Yamanouchi.[32])

289
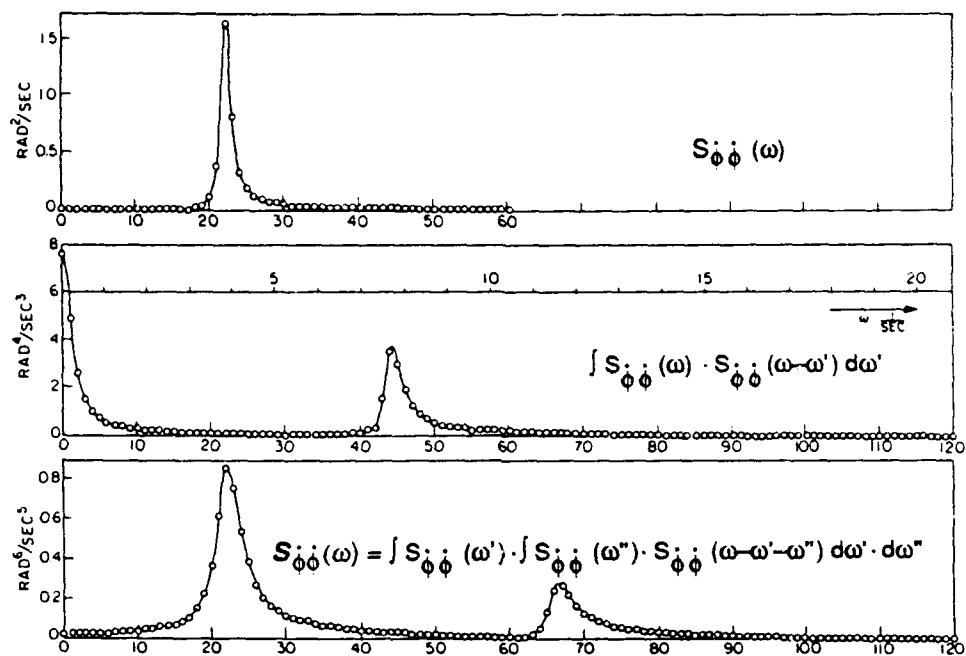
Fig. 10.4. Convolution of spectrum $S_{\dot\phi\dot\phi}$.
(From Yamanouchi.[32])
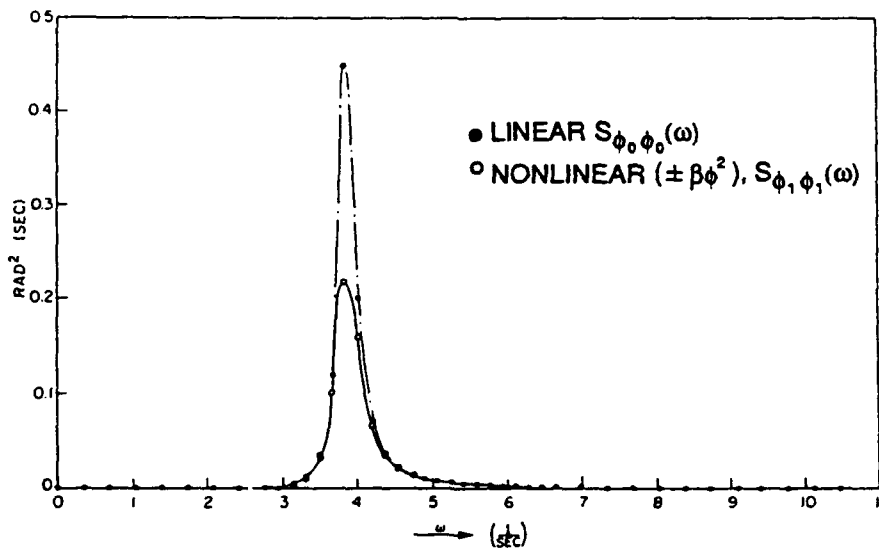
Fig. 10.5. Computed nonlinear spectrum of rolling.
(From Yamanouchi.[32])

$$X = X_0 + \epsilon X_1 + \epsilon^2 X_2 + \ldots \ . \tag{10.41}$$

Substituting Eq. 10.41 in Eq. 10.40, gives

$$[\ddot{X}_0 + 2\alpha\dot{X}_0 + \omega_0^2 X_0 - f(t)] + \epsilon[\ddot{X}_1 + 2\alpha\dot{X}_1 + \omega_0^2 X_1 + \omega_0^2 g(X_0)]$$

$$+ \epsilon^2[\ddot{X}_2 + 2\alpha\dot{X}_2 + \omega_0^2 X_2 + \omega_0^2 g(X_1)] + \ldots \equiv 0. \tag{10.42}$$

This equation is independent of ϵ, so each term with powers of ϵ should independently be equal to zero,

$$\ddot{X}_0 + 2\alpha\dot{X}_0 + \omega_0^2 X_0 = f(t)$$

$$\ddot{X}_1 + 2\alpha\dot{X}_1 + \omega_0^2 X_1 = -\omega_0^2 g(X_0) \tag{10.43}$$

$$\ddot{X}_2 + 2\alpha\dot{X}_2 + \omega_0^2 X_2 = -\omega_0^2 g(X_1) = -\omega_0^2 X_1 g'(X_0).$$

Usually the first approximation $X = X_0 + \epsilon X_1$ is used. From Eq. 9.16

$X_0 = \displaystyle\int_{-\infty}^{\infty} h(\tau)f(t-\tau)d\tau$. Here X_0 is the linear response. Accordingly, from the first equation of Eq. 10.43

$$h(\tau) = \frac{e^{-\alpha\tau}}{\sqrt{(\omega_0^2 - \alpha^2)}}\sin\left\{\left(\omega_0^2 - \alpha^2\right)^{\frac{1}{2}}\tau\right\}. \tag{10.44}$$

Then from the second equation of Eq. 10.43

$$X_1(t) = -\omega_0^2 \int_{-\infty}^{\infty} h(\tau)gX_0(t-\tau)d\tau, \tag{10.45}$$

which is the expression for the first order approximation.

Here some expectations are

$$X_1 = X_0 + \epsilon X_1,$$

$$E[X_1^2] = E[X_0^2] + 2\epsilon E[X_0 X_1]$$

and $$E[X_0^2] = \int\limits_{-\infty}^{\infty} \int\limits_{-\infty}^{\infty} h(\tau_1) \ h(\tau_2) E\big[f(t-\tau_1)f(t-\tau_2)\big] d\tau_1 \ d\tau_2. \qquad (10.46)$$

When $f(t)$ is stationary,

$$R_f(\tau) = E[f(t) \ f(t+\tau)].$$

For example, for Duffing type oscillations as

$$\ddot{X} + 2\alpha\dot{X} + \omega_0^2[X + \epsilon X^3] = f(t), \qquad (10.47)$$

in Eq. 10.40,

$$g(X) = X^3. \qquad (10.48)$$

Therefore from Eq. 10.45,

$$E[X_0 X_1] = -\omega_0^2 \int\limits_{-\infty}^{\infty} h(\tau) E[X_0(t) X_0^3(t-\tau)] d\tau$$

$$= -\omega_0^2 \int\limits_{-\infty}^{\infty} h(\tau) d\tau \int\limits_{-\infty}^{\infty} h(\tau_1) d\tau_1 \int\limits_{-\infty}^{\infty} h(\tau_2) d\tau_2 \int\limits_{-\infty}^{\infty} h(\tau_3) d\tau_3 \int\limits_{-\infty}^{\infty} h(\tau_4) d\tau_4$$

$$X \ E[f(t-\tau_1)f(t-\tau-\tau_2)f(t-\tau-\tau_3)f(t-\tau-\tau_4)].$$

When $Z(t)$ is a zero mean stationary random process, the following relations apply:

$$E[Z(t_1)] = 0, \quad E[Z(t_1)Z(t_2)] = R_2(t_2 - t_1),$$

$$E[Z(t_1)Z(t_2)Z(t_3)] = 0,$$

$$E[Z(t_1)Z(t_2)Z(t_3)Z(t_4)] = R_2(t_1 - t_2)R_2(t_3 - t_4) \tag{10.49}$$

$$+ R_2(t_1 - t_3)R_2(t_2 - t_4) + R_2(t_1 - t_4)R_2(t_2 - t_3).$$

From these relations and the assumption that the external force is white in the important range of frequency in which the response shows a peak,

$$R_f(\tau) \approx \frac{1}{2}W_0\delta(\tau)$$

($\delta(\tau)$ is Dirac's function.) Using these relations in the second equation of Eq. 10.46 gives

$$E[X_1^2] \approx \sigma_x^2 - 3\epsilon\sigma_x^4. \tag{10.50}$$

It is interesting that the same result was derived by the equivalent linearization method, Eq. 10.17.

THIS PAGE INTENTIONALLY LEFT BLANK

CHAPTER 11

VOLTERA EXPANSION AND APPLICATION OF POLYSPECTRA

11.1 VOLTERA–WIENER EXPRESSION

Suppose there is a weakly nonlinear response process $Y(t)$ which is an output of a linear input process $X(t)$. Both $Y(t)$ and $X(t)$ are stationary up to an appropriate order. Then when the sum of the absolute values of all kernel functions is not infinite, $Y(t)$ can be expressed as

$$Y(t) = \int\limits_{-\infty}^{\infty} h(\tau)\ X(t-\tau)\ d\tau + \int\limits_{-\infty}^{\infty}\int\limits_{-\infty}^{\infty} h_2(\tau_1,\tau_2)\ X(t-\tau_1)\ X(t-\tau_2)\ d\tau_1 d\tau_2$$

$$+ \int\limits_{-\infty}^{\infty}\int\int h_3(\tau_1,\tau_2,\tau_3,)\ X(t-\tau_1)\ X(t-\tau_2)\ X(t-\tau_3)\ d\tau_1 d\tau_2\ d\tau_3 \cdots \quad (11.1)$$

$$= \sum_{n=0}^{\infty} \underbrace{\int\limits_{-\infty}^{\infty}\int\limits_{-\infty}^{\infty} \cdots \int\limits_{-\infty}^{\infty}}_{n} h_n(\tau_1,\tau_2,\cdots\tau_n)\ X(t-\tau_1)\ X(t-\tau_2)\cdots X(t-\tau_n)$$

$$d\tau_1 d\tau_2 \cdots d\tau_n. \quad (11.1')$$

Here $h_n(\tau_1\tau_2\cdots\tau_n)$ is a real function of n variables $-\infty < \tau_i < +\infty$, $i = 1,2,\cdots n$ and is called nth kernel function. All kernels are assumed to be smooth, absolutely integratable, and to possess Fourier transforms. Besides, all these are supposed to be time invariant. When, for any $\tau_i < 0$, $h_n(\tau_1,\tau_2,\cdots\tau_n) = 0$, then the lower limit of these integrals can be 0. For $n = 0$, h_o is the value of $Y(t)$ when $X(t) \equiv 0$. So we can include $n = 0$, generally; otherwise we assume $h_o \equiv 0$. When $n = 1$, $Y(t)$ will be the linear system that has been treated in Part I and II and as Eq. 9.16

$$Y(t) = \int\limits_{-\infty}^{\infty} h(\tau)\ X(t-\tau)\ d\tau. \quad (11.2)$$

Equation 11.1 is assumed to be a kind of Taylor expansion of $Y(t)$ around the linear process expressed by Eq. 11.2. Accordingly, the terms for $n \geq 2$ are regarded as modifying small terms.

If we change the variables,

$$Y(t) = \sum_{n=1}^{\infty} \int\limits_{-\infty}^{\infty}\int\limits_{-\infty}^{\infty} \cdots \int\limits_{-\infty}^{\infty} h_n(t-\tau_1,t-\tau_2,\cdots t-\tau_n)\ X(\tau_1)\ X(\tau_2)\cdots X(\tau_n)$$

$$d\tau_1 d\tau_2 \cdots d\tau_n\ . \quad (11.3)$$

Equation 11.1 or 11.3 is called the Voltera–Wiener or functional expression.

11.2 HIGHER ORDER RESPONSE FUNCTION,

$$h_n(\tau_1, \tau_2, \cdot \cdot \cdot \tau_n); H_n(\omega_1, \omega_2, \cdot \cdot \cdot \omega_n)$$

When $h_n(\tau_1, \tau_2, \cdot \cdot \cdot \tau_n)$ are smooth and absolutely integratable, the nth order Fourier pair exists as was stated at the beginning,

$$h_n(\tau_1, \tau_2, \cdot \cdot \cdot \tau_n) = \frac{1}{(2\pi)^n} \int_{-\infty}^{\infty} \cdot \cdot \cdot \int_{-\infty}^{\infty} \exp i\{\omega\tau_1 + \omega_2\ \tau_2 + \cdot \cdot \cdot + \omega_n\ \tau_n\}\ H_n(\omega_1, \omega_2, \cdot \cdot \cdot \omega_n)$$

$$d\omega_1\ a\omega_2 \cdot \cdot \cdot d\omega_n, \quad (11.4)$$

$$H_n(\omega_1, \omega_2, \cdot \cdot \cdot \omega_n) = \int_{-\infty}^{\infty} \cdot \cdot \cdot \int_{-\infty}^{\infty} \exp[-i(\omega_1\ \tau_1 + \omega_2\ \tau_2 + \cdot \cdot \cdot + \omega_n\tau_n)]$$

$$h_n(\tau_1, \tau_2, \cdot \cdot \cdot \tau_n)\ d\tau_1 d\tau_2 \cdot \cdot \cdot d\tau_n, \quad (11.5)$$

$h_n(\tau_1, \tau_2, \cdot \cdot \cdot \tau_n)$ are real functions and are symmetrical for $\tau_1, \tau_2 \cdot \cdot \cdot \tau_n$,

thus

$$h_n(\tau_1, \tau_2, \cdot \cdot \cdot \tau_n) = h_n(\tau_2, \tau_1, \cdot \cdot \cdot \tau_n) = \cdot \cdot \cdot = h_n(\tau_2, \tau_3, \cdot \cdot \cdot \tau_n, \tau_1) \quad (11.6)$$

$$H_n(\omega_1, \omega_2, \cdot \cdot \cdot \omega_n) = H_n(\omega_2, \omega_1, \cdot \cdot \cdot \omega_n) = \cdot \cdot \cdot = H_n(\omega_2, \omega_3, \cdot \cdot \cdot \omega_n, \omega_1). \quad (11.7)$$

If we regard $Y(t)$ as the output and $X(t)$ as the input process, $h_n(\tau_1, \tau_2, \cdot \cdot \cdot \tau_n)$ is called the nth order impulse response function and $H_n(\omega_1, \omega_2, \cdot \cdot \cdot \omega_n)$ is the nth order frequency response function.

When the processes are not continuous but discrete, then the Voltera–Wiener expression for the nonlinear response Y_t and linear input X_t is

$$Y_t = \sum_{u=o}^{\infty} g_u\ X_{t-u} + \sum_{u=o}^{\infty} \sum_{v=o}^{\infty} g_{nv}\ X_{t-u}\ X_{t-v}$$

$$+ \sum_{u=o}^{\infty} \sum_{v=o}^{\infty} \sum_{\omega=o}^{\infty} g_{uvw}\ X_{t-u}\ X_{t-v}\ X_{t-w} + \cdot \cdot \cdot \quad (11.8)$$

$$= \sum_{n=1}^{\infty} \underbrace{\sum \sum \cdot \cdot \cdot \sum}_{n} g_{u_1 u_2} \cdot \cdot \cdot {}_{u_n}\ X_{t-u_1}\ X_{t-u_2} \cdot \cdot \cdot X_{t-u_n}, \quad (11.8')$$

and the following discrete Fourier pair is assumed to exist:

$$G(\omega_1, \omega_2, \cdots \omega_n) = \sum_{u_1=0}^{\infty} \sum_{u_2=0}^{\infty} \cdots \sum_{u_n=0}^{\infty} g_{u_1 u_2 \cdots u_n} \ e^{-i(\omega_1 u_1 + \omega_2 u_2 + \cdots + \omega_n u_n)}$$

(11.9)

$$g_{u_1 u_2 \cdots u_n} = \frac{1}{(2\pi)^n} \int_{-\pi}^{\pi} \cdots \int_{-\pi}^{\pi} G(\omega_1, \omega_2, \cdots \omega_n) \ e^{i(\omega_1 u_1 + \omega_2 u_2 + \cdots + \omega_n u_n)}$$

$$d\omega_1 d\omega_2 \cdots \cdots d\omega_n. \quad (11.10)$$

For convenience the expressions for a continuous process will be used in this chapter unless otherwise stated.

11.3 SECOND ORDER NONLINEAR PROCESS BISPECTRUM, CROSS BISPECTRUM

For example in Eq. 11.1, the quadratic nonlinear characteristics of $Y(t)$ is expressed by $n = 2$, and the terms $n > 3$ can be neglected. Then Eq. 11.1 becomes

$$Y(t) = \int_{-\infty}^{\infty} h_1(\tau) X(t-\tau) d\tau + \int_{-\infty}^{\infty} \int_{-\infty}^{\infty} h_2(\tau_1, \tau_2) \ X(t-\tau_1) \ X(t-\tau_2) \ d\tau_1 d\tau_2, \quad (11.11)$$

which corresponds to Eq. 11.2 for a linear process. As the expected values of the second moment, the auto or cross covariance functions $R_{XX}(\tau)$, $R_{YY}(\tau)$, and $R_{YX}(\tau)$, and their Fourier transforms, the auto or cross spectra $s_{XX}(\omega)$, $s_{YY}(\omega)$, and $s_{YX}(\omega)$ played big roles in the analysis of the responses of linear systems, the expected values of the third moments $R_{XXX}(\tau_1, \tau_2)$, $R_{YYY}(\tau_1, \tau_2)$, $R_{YXX}(\tau_1, \tau_2)$, and their double Fourier transforms $s_{XXX}(\omega_1, \omega_2)$, $s_{YYY}(\omega_1, \omega_2)$, $s_{YXX}(\omega_1, \omega_2)$, are important in the analysis of second order nonlinear processes. The third moment correlation functions are, for example,

$$R_{YYY}(\tau_1, \tau_2) = E[\{Y(t+\tau_1) - m_Y\}\{Y(t+\tau_2) - m_Y\}\{Y(t) - m_Y\}] \quad (11.12)$$

$$R_{XXY}(\tau_1, \tau_2) = E[X(t+\tau_1) \ X(t+\tau_2)\{Y(t) - m_Y\}]. \quad (11.13)$$

Here $E[X(t)] = 0$ is assumed. Their double Fourier transforms are called the bispectrum $s_{YYY}(\omega_1, \omega_2)$ or the cross bispectrum $s_{XXY}(\omega_1, \omega_2)$,

$$s_{YYY}(\omega_1, \omega_2) = \frac{1}{(2\pi)^2} \int_{-\infty}^{\infty} \int_{-\infty}^{\infty} R_{YYY}(\tau_1, \tau_2) \exp[-i(\omega_1 \tau_1 + \omega_2 \tau_2)] d\tau_1 d\tau_2 \quad (11.14)$$

$$s_{XXY}(\omega_1, \omega_2) = \frac{1}{(2\pi)^2} \int_{-\infty}^{\infty} \int_{-\infty}^{\infty} R_{XXY}(\tau_1, \tau_2) \exp[-i(\omega_1 \tau_1 + \omega_2 \tau_2)] \ d\tau_1 d\tau_2. \quad (11.15)$$

The inverse transforms are

$$R_{YYY}(\tau_1\tau_2) = \int\limits_{-\infty}^{\infty}\int\limits_{-\infty}^{\infty} s_{YYY}(\omega_1,\omega_2)\exp[i(\omega_1\tau_1 + \omega_2\tau_2)]\ d\omega_1 d\omega_2 \qquad (11.16)$$

$$R_{YYY}(\tau_1,\tau_2) = \int\limits_{-\infty}^{\infty}\int\limits_{-\infty}^{\infty} s_{XXY}(\omega_1,\omega_2)\exp[i(\omega_1\tau_1 + \omega_2\tau_2)]\ d\omega_1 d\omega_2. \qquad (11.17)$$

When the input process $X(t)$ is a Gaussian process, then

$$R_{XXX}(\tau_1,\tau_2) = E[X(t+\tau_1)\ X(t+\tau_2)\ X(t)] \equiv 0. \qquad (11.18)$$

Therefore

$$s_{XXX}(\omega_1,\omega_2) \equiv 0, \qquad (11.19)$$

The bispectrum does not exist for a linear Gaussian process.

For a quadratic (second order nonlinear) process $Y(t)$, $R_{YYY}(\tau_1,\tau_2) \neq 0$, $R_{XXY}(\tau_1,\tau_2) \neq 0$ and the bispectrum exists as shown by Eq. 11.14 and Eq. 11.15.

Now, assuming $Y(t)$ is a stationary process and its Fourier–Stieltjes integral is

$$\{Y(t) - m_Y\} = \int\limits_{-\infty}^{\infty} dZ(\omega)\exp(i\omega\ t), \qquad (11.20)$$

then
$$\{Y(t+\tau_1) - m_Y\} = \int\limits_{-\infty}^{\infty} dZ(\omega_1)\exp(i\omega_1 t + i\omega_1,\tau_1),$$

$$\{Y(t+\tau_2) - m_Y\} = \int\limits_{-\infty}^{\infty} dZ(\omega_2)\exp(i\omega_2 t + i\omega_2\tau_2).$$

Therefore

$$R_{YYY}(\tau_1,\tau_2) = E[\{(Y(t+\tau_1) - m_Y\}\{Y(t+\tau_2) - m_Y\}\{Y(t) - m_Y\}]$$

$$= \int\int\limits_{-\infty}^{\infty}\int \exp[i(\omega_1 + \omega_2 + \omega_3)t] \cdot \exp[i(\omega_1\tau_1 + \omega_2\tau_2)$$

$$E[dZ(\omega_1)dZ(\omega_2)dz(\omega_3)] \qquad (11.21)$$

[ω is expressed as ω_3].

Because of its stationarity, $R_{YYY}(\tau_1,\tau_2)$ is a function only of τ_1,τ_2; it is not a function of t but is independent of t. Accordingly, the integral has a value only when

$$\omega_1 + \omega_2 + \omega_3 = 0 \text{ or } \omega_3 = -\omega_1 - \omega_2 \qquad (11.22)$$

298

comparing Eq. 11.21 with Eq. 11.16, and taking into account the relation

$$\frac{1}{2\pi} \int_{-\infty}^{\infty} \exp[i(\omega_1 + \omega_2 + \omega_3)t dt = \delta(\omega_1 + \omega_2 + \omega_3)],$$

$$\int_{-\infty}^{\infty} E[dZ(\omega_1) \ dZ(\omega_2) \ dZ(\omega_3)] \ \delta(\omega_1 + \omega_2 + \omega_3)d\omega_3 = s_{YYY}(\omega_1, \omega_2)$$
$$d\omega_1 d\omega_2. \quad (11.23)$$

This shows that $E[dZ(\omega_1) \ dZ(\omega_2) \ dZ(\omega_3)]$ must be 0 except along the line $\omega_1 + \omega_2 + \omega_3 = 0$. This corresponds to the fact that, for the linear case,

$$R_{XX}(\tau) = \int_{-\infty}^{\infty} \int_{-\infty}^{\infty} \exp i(\omega + \omega')t \exp i\omega\tau \cdot E[dZ(\omega) \cdot dZ\omega']$$

$$= \int_{-\infty}^{\infty} \exp i\omega \ \tau \cdot s_{XX}(\omega) \ d\omega, \quad (11.24)$$

and $\int_{-\infty}^{\infty} E[dZ(\omega)dZ(\omega')]\delta(\omega + \omega')d\omega' = s_{XX}(\omega)d(\omega)$.

By the same logic that because of stationarity, $R_{XX}(\tau)$ should be independent of t, therefore $E[dZ(\omega) \ dZ(\omega')]$ must be zero except when $\omega + \omega' = 0$, i.e., only along the line $\omega + \omega' = 0$ and $\omega' = -\omega$.

Because of the symmetry of $R_{XXX}(\tau_1, \tau_2)$,

$$R_{XXX}(\tau_1, \tau_2) = R_{XXX}(\tau_2, \tau_1) = R_{XXX}(-\tau_1, \tau_2 - \tau_1) = R_{XXX}(\tau_2 - \tau_1, -\tau_1)$$

$$= R_{XXX}(-\tau_2, \tau_1 - \tau_2) = R_{XXX}(\tau_1 - \tau_2, -\tau_2) \quad (11.25)$$

the spectra also have symmetry,

$$s_{XXX}(\omega_1, \omega_2) = s_{XXX}(\omega_2, \omega_1) = s_{XXX}(\omega_1, -\omega_1 - \omega_2) = s_{XXX}(-\omega_1 - \omega_2, \omega_1)$$

$$= s_{XXX}(\omega_2, -\omega_1 - \omega_2) = s_{XXX}(-\omega_1 - \omega_2, \omega_2) \quad (11.26)$$

and $$s_{XXX}(\omega_1, \omega_2) = s * (-\omega_1, -\omega_2). \quad (11.27)$$

Accordingly, when we think of the bispectrum $s_{XXX}(\omega_1, \omega_2)$ we must consider the third frequency ω_3, besides ω_1 and ω_2, that makes

$$\omega_1 + \omega_2 + \omega_3 = 0, \qquad \omega_3 = -\omega_1 - \omega_2.$$

From Eq. 11.26, the bispectrum is found[78] to be the same for six permutations for two of the three frequencies ω_1, ω_2, and ω_3. Twelve bispectra, including the conjugate bispectra

show the same modulus as is shown in Fig. 11.1 for ① to ⑫. These bispectra are repre-sented by a bispectrum in the first octant ① where $|\omega_3| \geq \omega_1 \geq \omega_2$. The bispectrum is shown by the modulus and the phase angle.
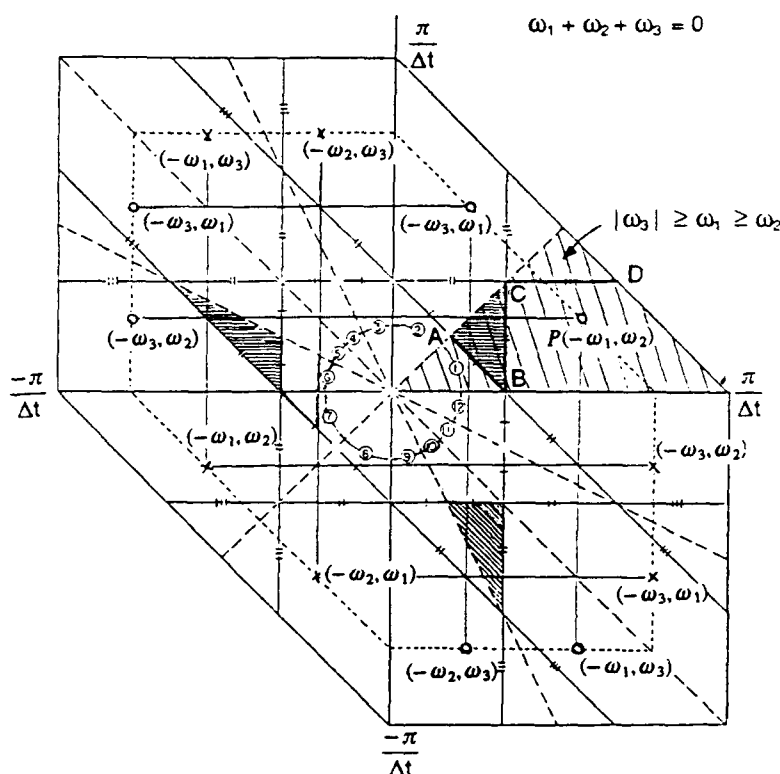
Fig. 11.1. Symmetric character of bispectrum.
(From Yamanouchi and Ohtsu.[78])

The points marked O in sub-octants ②, ⑤, ⑥, ⑨, and ⑩ show the same bispectra, equal to $s_{XXX}(\omega_1, \omega_2)$ at mark O in octant ①, and the bispectra at points x in the six sub-octants ③, ④, ⑦, ⑧, ⑪, and ⑫ show its conjugate. Also in Fig. 11.1, the segments of line in each sub-octant are shown marked by short lines +, ++, +++ that correspond to the segmented line AB +, BC ++, CD +++ in octant ① that shows the same bispectrum. At a fixed frequency ω_B in Fig. 11.1, the bispectrum along the segment BA ($\omega_B = \omega_3$) shows interference with the two components at the smaller frequencies ω_1 and ω_2, that makes $\omega_1 + \omega_2 = \omega_B = \omega_3$; the spectrum along the segment BC ($\omega_B = \omega_1$) shows interference with one smaller frequency component ω_2 and one higher frequency component $\omega_3(\omega_3 = \omega_2 + \omega_1)$; and the bispectrum along the segment CD ($\omega_B = \omega_2$) shows interference with the components at two higher frequencies $\omega_3(\omega_3 = \omega_1 + \omega_2)$ and ω_1. The hexagonal boundary shape in Fig. 11.1 shows the

300

boundary of the frequency region in which the bispectrum can be calculated for the data sampled by interval Δt .

Figure 11.2 is an example of the bispectrum of the rolling of an actual ship on the sea, reported by Y. Yamanouchi and K. Ohtsu.[78],[79] The bispectrum in Fig. 11.2 shows higher values along a similarly shaped segment ABCD in Fig. 11.1 with ω_B at the frequency at which the linear spectrum, drawn down the side of the ω_1 axis, shows the peak value, that implies the nonlinear interference is higher along these shaped segment lines, as ABCD.

ROLLING BISPECTRUM
SEIUN MARU (modulus)

DATA NO. 751
SKEWNESS   0.22185
PEAKEDNESS   2.79025

LOG SCALE
DEG³/(CPS)²

THE NUMBERS GIVE THE CONTRIBUTION TO THE
MEAN CUBED RECORD IN DEG³ PER (CPS)²

ROLLING BISPECTRUM SEIUN MARU (modulus)

EXAMPLE: 45¹ = 0.45 X 10¹ RAD

ROLLING BISPECTRUM
SEIUN MARU

(ARGUMENT)

ROLLING BISPECTRUM SEIUN MARU (Argument)
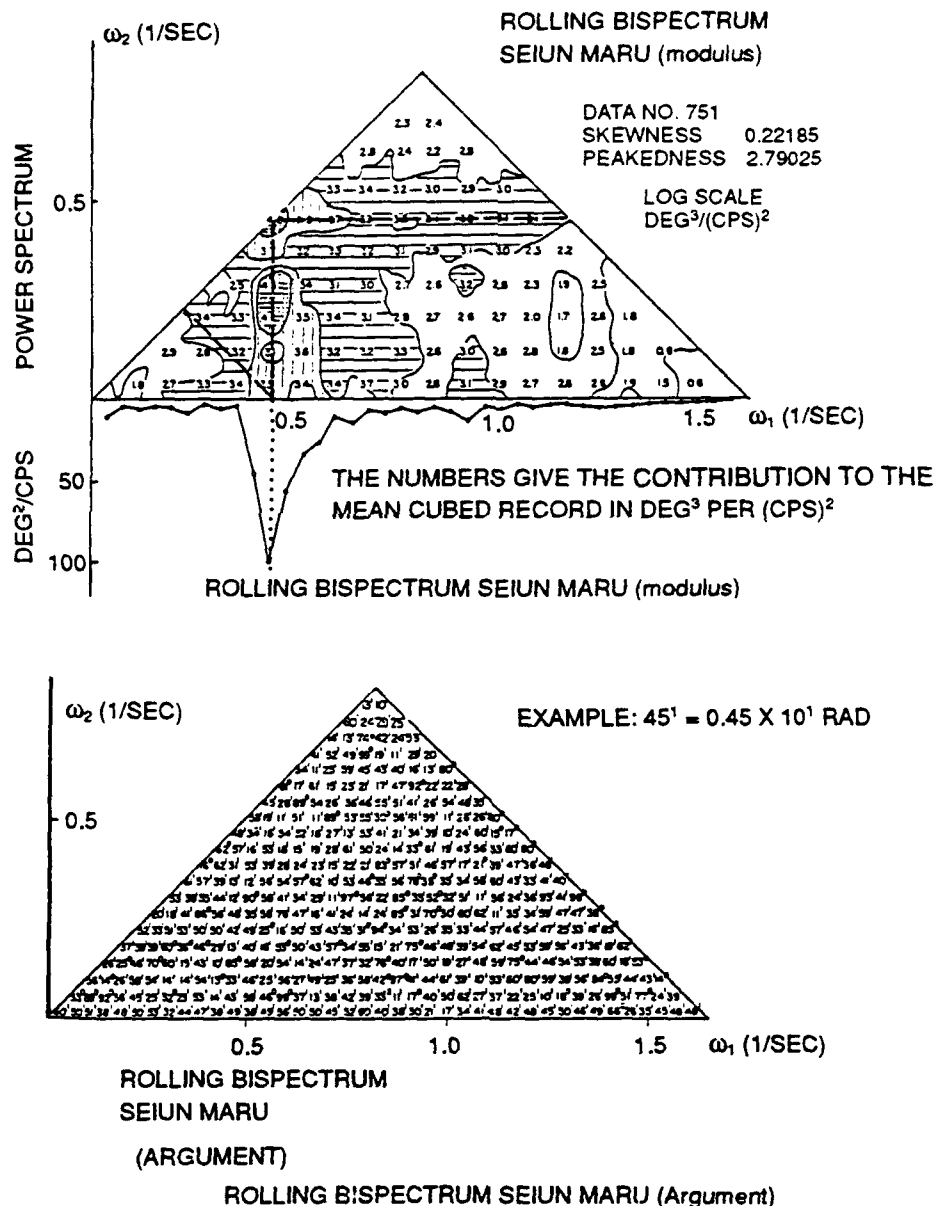
Fig. 11.2. An example of bispectrum of rolling of a ship on the sea.
(From Yamanouchi and Ohtsu,[78],[79] (1972).)

301

As has been formulated in Eqs. 11.12 and 11.6

$$E[\{Y(t) - m_Y\}\{Y(t + \tau_1) - m_Y\}\{Y(t_1 + \tau_2) - m_Y\}] = R_{YYY}(\tau_1, \tau_2)$$

$$= \int_{-\infty}^{\infty} \int_{-\infty}^{\infty} s(\omega_1, \omega_2) \exp[+i(\omega_1\tau_1 + \omega_2\tau_2)] \, d\omega_1 d\omega_2$$

thus

$$E\left[\{Y(t) - m_Y\}^3\right] = R_{YYY}(0, 0) = \int_{-\infty}^{\infty} \int_{-\infty}^{\infty} s(\omega_1, \omega_2) d\omega_1 d\omega_2. \qquad (11.28)$$

The bispectrum shows the contribution of the third moment of frequency components at three frequencies $\omega_1, \omega_2,$ and ω_3, where $\omega_1 + \omega_2 + \omega_3 = 0$ are satisfied. When square mean, cubic mean, and fourth power mean are expressed as

$$E\left[\{y(t) - my\}^2\right] = \sigma^2, \quad E\left[\{y(t) - my\}^3\right] = \mu^3, \quad E\left[\{y(t) - my\}^4\right] = \mu^4,$$

the statistical values called skewness s, and peakedness p are defined as

$$s = \frac{\mu^3}{(\sigma^2)^{3/2}} \qquad (11.29)$$

$$p = \frac{\mu^4}{(\sigma^2)^2}. \qquad (11.30)$$

When $Y(t)$ is a Gaussian (not nonlinear) process, $\mu^3 = 0$, $\mu^4 = 3\sigma^4$. Therefore,

$s = 0$, $p = 3$. By the values of s and p, we can show the extent of nonlinearity of the process.[79]

11.4 CHARACTERS OF QUADRATIC RESPONSE TO GAUSSIAN INPUT PROCESS

As already was shown in Eq. 11.2, when $X(t)$, the input process is a Gaussian linear process with $E[X(t)] = 0$,

$$R_{XXX}(\tau_1, \tau_2) = E\left[(X(t + \tau_1) \, X(t + \tau_2) \, X(t)\right] = 0 \qquad (11.31)$$

$$s_{XXX}(\omega_1, \omega_2) = 0. \qquad (11.32)$$

Several statistical relations of the quadratic nonlinear output $Y(t)$ to input $X(t)$ and their derivations will be summarized as follows:

1. Mean of $Y(t)$, $E[Y(t)] \equiv m_Y$.

From Eq. 11.11, and as $E[X(t-\tau)] = 0$,

$$m_Y \equiv E[Y(t)] = \int\limits_{-\infty}^{\infty} \int\limits_{-\infty}^{\infty} h_2(\tau_1, \tau_2)\ E[X(t-\tau_1) \cdot X(t-\tau_2)]\ d\tau \cdot d\tau_2$$

$$= \int\limits_{-\infty}^{\infty} \int\limits_{-\infty}^{\infty} h_2(\tau_1, \tau_2)\ R_{XX}(\tau_2 - \tau_1)\ d\tau_1 d\tau_2 \qquad (11.33)$$

$$= \int\limits_{-\infty}^{\infty} \int\limits_{-\infty}^{\infty} h_2(\tau_1, \tau_2) \left\{ \int\limits_{-\infty}^{\infty} s_{XX}(\omega) \exp i\omega(\tau_2 - \tau_1)\ d\omega \right\}\ d\tau_1 d\tau_2$$

$$= \int\limits_{-\infty}^{\infty} \int\limits_{-\infty}^{\infty} h_2(\tau_1, \tau_2) \exp i(\omega\tau_2 - \omega\tau_1)\ d\tau_1 d\tau_2 \int\limits_{\infty}^{-\infty} s_{XX}(\omega)\ d\omega$$

$$= \int\limits_{-\infty}^{\infty} H_2(\omega, -\omega) s_{XX}(\omega)\ d\omega \qquad (11.33')$$

because $\displaystyle\int\limits_{-\infty}^{\infty} \int\limits_{-\infty}^{\infty} h_2(\tau_1, \tau_2) \exp i(\omega\tau_2 - \omega\tau_1) d\tau_1, d\tau_2 = H_2(\omega, -\omega)$

2. Cross correlation $R_{YX}(\tau)$; cross spectrum $s_{YX}(\omega)$.

For $R_{YX}(\tau) = E[\{Y(t) - m_Y\} \cdot X(t-\tau)] = E\{Y(t) \cdot X(t-\tau)\} - m_Y\ E[X(t-\tau)]$,

inserting Eq. 11.11 and $E[X(t-\tau)] = 0$, yields

$$= \int\limits_{-\infty}^{\infty} h_1(\tau_1) E[X(t-\tau_1) X(t-\tau)] d\tau_1 = \int\limits_{-\infty}^{\infty} h_1(\tau_1) R(\tau - t_1) d\tau\ . \qquad (11.34)$$

Therefore

$$s_{YX}(\omega) = \frac{1}{2\pi} \int\limits_{-\infty}^{\infty} R_{YX}(\tau) \cdot e^{-i\omega\tau} \, d\tau = \frac{1}{2\pi} \int\limits_{-\infty}^{\infty} \int\limits_{-\infty}^{\infty} h_1(\tau_1) R(\tau - \tau_1) \, e^{-i\omega\tau} d\tau_1 d\tau$$

$$= \frac{1}{2\pi} \int\limits_{-\infty}^{\infty} h_1(\tau) \cdot e^{i\omega\tau_1} \, d\tau_1 \cdot \int\limits_{\infty}^{-\infty} R(\tau - \tau_1) \, e^{-i\omega(\tau - \tau_1)} d\tau$$

$$= H_1(\omega) s_{XX}(\omega) \tag{11.35}$$

and $\quad H_1(\omega) = s_{YX}(\omega)/s_{XX}(\omega).$ \hfill (11.36)

Eq. 11.36 shows even when $Y(t)$ includes the nonlinear component, if the input $X(t)$ was a Gaussian process, the linear response frequency function $H_1(\omega)$ is expressed by the ratio of $s_{YX}(\omega)$ and $s_{XX}(\omega)$ as in the purely linear case.

3. Autocovariance $R_{YY}(\tau)$; linear spectrum $s_{YY}(\omega)$.

As in the linear process, the Fourier transform of second order moment or the auto-covariance function is called the linear spectrum,

$$R_{YY}(\tau) = E[Y(t) - m_Y][Y(t+\tau) - m_Y]$$
$$= E[Y(t) \cdot Y(t+\tau)] - m_Y^2. \tag{11.37}$$

Here by the use of the functional expression of $Y(t)$ and $Y(t+\tau)$ as Eq. 11.11 and appropriate variables,

$$R_{YY}(\tau) = \int\limits_{\infty}^{-\infty} \int\limits_{\infty}^{\infty} h_1(s_1) \, h_1(r_1) \, E[X(t-s_1) \cdot X(t+\tau-r_1)] \, ds_1 dr_1$$

$$+ \int\limits_{-\infty}^{\infty} \int\limits_{-\infty}^{\infty} \int\limits_{-\infty}^{\infty} \int\limits_{-\infty}^{\infty} h_2(u_1, u_2) h_2(v_1, v_2) \, E[X(t-u_1) \, X(t-u_2) \, X(t+\tau-v_1) \, X(t+\tau-v_2)]$$
$$du_1 du_2 dv_1 dv_2 - m_Y^2. \tag{11.38}$$

Generally, when X_1, X_2, X_3, X_4 are the probability variables that are from a joint Gaussian distribution, then

$$E[X_1 \, X_2 \, X_3 \, X_4] = M_{12} \, M_{34} + M_{13} \, M_{24} + M_{14} \, M_{23}. \tag{11.39}$$

Here

$$M_{ik} = E[X_i \cdot X_k].$$

From this relation,

$$E[X(t-u_1)\ X(t-u_2)\ X(t+\tau-v_1)\ X(t+\tau-v_2)]$$

$$= R_{XX}(u_1-u_2)\ R_{XX}(v_1-v_2) + R_{XX}(\tau+u_1-v_1)\ R_{XX}(\tau+u_2-v_2)$$

$$+ R_{XX}(\tau+u_1-v_2)\ R_{XX}(\tau+u_2-v_1). \tag{11.39'}$$

When this expression is inserted in Eq. 11.38, the term that comes from the first term of Eq. 11.39' is the same as m_Y^2 in Eq. 11.33 and it cancels with the last term of Eq. 11.38, $-m_Y^2$.

Then from the remainder

$$R_{YY}(\tau) = \int_{-\infty}^{\infty} \int_{-\infty}^{\infty} h(s_1)\ h(r_1)\ R_{XX}(\tau+s_1-r_1)$$

$$+ \int_{-\infty}^{\infty} \int_{-\infty}^{\infty} \int_{-\infty}^{\infty} \int_{-\infty}^{\infty} h_2(u_1,u_2)\ h_2(v_1,v_2)\ R_{XXX}(\tau+u_1-v_1)\ R_{XX}(\tau+u_2-v_2)$$

$$du_1 du_2 dv_1 dv_2$$

$$+ \int_{-\infty}^{\infty} \int_{-\infty}^{\infty} \int_{-\infty}^{\infty} \int_{-\infty}^{\infty} h_2(u_1,u_2)h_2(v_1,v_2)R_{XXX}(\tau+u_1-v_2)R_{XX}(\tau+u_2-v_1)$$

$$du_1 du_2 dv_1 dv_2. \tag{11.40}$$

The terms $h_2(u_1,u_2)$, $h_2(v_1,v_2)$ are symmetrical for u_1, u_2 and v_1, v_2, and the scope of the integral is the same as for $-\infty \to +\infty$ for both the last two terms. Accordingly, the second and third terms are equal. Therefore,

$$s_{YY}(\omega) = \frac{1}{2\pi} \int_{-\infty}^{\infty} R_{YY}(\tau)\ e^{-i\omega\tau}\ d\tau$$

$$= \left| H_1(\omega) \right|^2 s_{XX}(\omega) + \int_{-\infty}^{\infty} \int_{-\infty}^{\infty} \frac{1}{2\pi} \int_{-\infty}^{\infty} \exp[-i\{\omega-(\omega_1+\omega_2)\}\tau]\ d\tau$$

$$\times\ 2H_2{}^*(\omega_1,\omega_2)\ H_2(\omega_1,\omega_2)\ s_{xx}(\omega_1)s_{xx}(\omega_2)\ d\omega_1 d\omega_2. \tag{11.41}$$

Here, using the relation

$$\frac{1}{2\pi} \int_{-\infty}^{\infty} \exp\ [i\{(\omega_1+\omega_2)-\omega\}\tau]\ d\tau = \delta\{(\omega_1+\omega_2)-\omega\} \tag{11.42}$$

δ: Dirac's delta function.

305

in Eq. 11.41 gives

$$s_{YY}(\omega) = |H_1(\omega)|^2 s_{XX}(\omega)$$

$$+ 2 \int\limits_{-\infty}^{\infty} \int\limits_{-\infty}^{\infty} |H_2(\omega_1, \omega_2)|^2 s_{XX}(\omega_1) \ s_{XX}(\omega_2) \delta[\omega_1 - (\omega - \omega_2)] d\omega_1 d\omega_2$$

$$= |H_1(\omega)|^2 s_{XX}(\omega) + 2 \int\limits_{-\infty}^{\infty} |H_2(\omega - \omega_2, \omega_2)|^2 s_{XX}(\omega - \omega_2) s_{XX}(\omega_2) d\omega_2. \quad (11.43)$$

This shows that the linear spectrum $s_{YY}(\omega)$ is the sum of the spectrum of the linear part $|H_1(\omega)|^2 s_{XX}(\omega)$ and the modifying term in Eq. 11.43 defined by the second nonlinear response function $H_2(\omega - \omega_2, \omega_2)$ and the product of two linear spectra $s_{XX}(\omega - \omega_2)$ and $s_{XX}(\omega_2)$.

4. Cross correlation of third moment R_{YXX}; cross bispectrum, $s_{YXX}(\omega)$, and the second order frequency response function $H_2(\omega_1, \omega_2)$.

The cross correlation of the third moment, for example $R_{YXX}(\tau_1, \tau_2)$, is

$$R_{YXX}(\tau_1, \tau_2) \equiv E[\{Y(t) - m_Y\} \ X(t - \tau_1) \ X(t - \tau_2)]$$

$$\equiv E[Y(t)X(t - \tau_1) \ X(t - \tau_2)] - m_Y E[X(t - \tau_1) \ X(t - \tau_2)]. \quad (11.44)$$

Here expressing $Y(t)$ by its functional expression Eq. 11.11 and using the same relation as Eq. 11.39' and Eq. 11.33 for m_Y gives

$$R_{YXX}(\tau_1, \tau_2) \equiv \int\limits_{-\infty}^{\infty} \int\limits_{-\infty}^{\infty} h_2(u_1, u_2) \ E[X(t - u_1) \ X(t - u_2) \ X(t - \tau_1) \ X(t - \tau_2)] \ du_1 du_2$$

$$- m_Y \ R_{XX}(\tau_1 - \tau_2)$$

$$= \int\limits_{-\infty}^{\infty} \int\limits_{-\infty}^{\infty} h_2(u_1, u_2)[R_{XX}(u_1 - u_2) \cdot R_{XX}(\tau_1 - \tau_2)$$

$$+ R_{XX}(\tau_1 - u_1) \ R_{XX}(\tau_2 - u_2) + R_{XX}(\tau_2 - u_1) \ R_{XX}(\tau_1 - u_2)] \ du_1 du_2$$

$$- \int\limits_{-\infty}^{\infty} \int\limits_{-\infty}^{\infty} h_2(v_1, v_2) \ R_{XX}(v_1, v_2) \ dv_1 dv_2 \ R_{XX}(\tau_1 - \tau_2). \quad (11.45)$$

In this equation, the first term and the last term are the same and cancel each other. The second and the third terms are the same, as $h(u_1, u_2)$ is symmetrical with u_1 and u_2, and the range of integrals is from $-\infty \frown +\infty$ for both.

Therefore

$$R_{YXX}(\tau_1, \tau_2) = 2 \int_{-\infty}^{\infty} \int_{-\infty}^{\infty} h_2(u_1, u_2) \, R_{XX}(\tau_1 - u_1) R_{XX}(\tau_2 - u_2) \, du_1 du_2 \qquad (11.46)$$

and

$$S_{YXX}(\omega_1, \omega_2) = \left(\frac{1}{2\pi}\right)^2 \int_{-\infty}^{\infty} \int_{-\infty}^{\infty} R_{YXX}(\tau_1, \tau_2) \exp\left[- i(\omega_1 \tau_1 + \omega_2 \tau_2)\right] d\tau_1 d\tau_2$$

$$= \frac{2}{(2\pi)^2} \int_{-\infty}^{\infty} \int_{-\infty}^{\infty} h_2(u_1, u_2) \, R_{XX}(\tau_1 - u_1) R_{XX}(\tau_2 - u_2) \exp\left[- i(\omega_1 \tau_1 + \omega_2 \tau_2)\right]$$

$$d\tau_1 d\tau_2 \qquad (11.47)$$

$$s_{YXX}(\omega_1, \omega_2) = 2 \, H_2(\omega_1, \omega_2) \, s_{XX}(\omega_1) \cdot s_{XX}(\omega_2) \qquad (11.48)$$

$$H_2(\omega_1, \omega_2) = \frac{s_{YXX}(\omega_1, \omega_2)}{2 s_{XX}(\omega_1) \, s_{XX}(\omega_2)}. \qquad (11.49)$$

Here with the variables ω_1, ω_2 into ω_1', ω_2' inverted by

$$\begin{cases} \omega_1 - \omega_2 = \omega_1' \\ \omega_1 + \omega_2 = \omega_2' \end{cases} \qquad \begin{aligned} \omega_1 &= \frac{1}{2}(\omega_1' + \omega_2') \\ \omega_2 &= \frac{1}{2}(-\omega_1' + \omega_2'), \end{aligned} \qquad (11.50)$$

then

$$s_{YXX}(\omega_1', \omega_2') = s_{YXX}(\omega_1 - \omega_2, \omega_1 + \omega_2) = s_{YXX}(\omega_1, \omega_2) \, J\begin{bmatrix} \omega_1, & \omega_2 \\ \omega_1', & \omega_2' \end{bmatrix}. \quad (11.51)$$

Since Jacobian

$$J\begin{bmatrix} \omega_1, & \omega_2 \\ \omega_1', & \omega_2' \end{bmatrix} = \begin{vmatrix} \dfrac{\partial \omega_1}{\partial \omega_1'} & \dfrac{\partial \omega_2}{\partial \omega_1'} \\ \dfrac{\partial \omega_1}{\partial \omega_2'} & \dfrac{\partial \omega_2}{\partial \omega_2'} \end{vmatrix} = \begin{vmatrix} \dfrac{1}{2}, & -\dfrac{1}{2} \\ \dfrac{1}{2}, & \dfrac{1}{2} \end{vmatrix} = \frac{1}{2}, \qquad (11.52)$$

therefore

$$s_{YXX}(\omega_1', \omega_2') = s_{YXX}(\omega_1, \omega_2) \times \frac{1}{2} \qquad (11.53)$$

and

$$2 \, s_{YXX}(\omega_1 - \omega_2, \omega_1 + \omega_2) = s_{YXX}(\omega_1, \omega_2). \qquad (11.54)$$

Substituting into Eq. 11.49 gives

$$H_2(\omega_1, \omega_2) = \frac{s_{YXX}(\omega_1 - \omega_2, \omega_1 + \omega_2)}{s_{XX}(\omega_1) \, s_{XX}(\omega_2)} \qquad (11.55)$$

307

In the same way, if we use $X^2(t)$ instead of the output process $Y(t)$ and calculate the cross bispectrum $s_{X^2XX}(\omega_1,\omega_2)$,

$$R_{X^2XX}(\tau_1,\tau_2) = E[\{X^2(t) - m_{X^2}\} \cdot X(t-\tau_1)(t-\tau_2)]$$

$$= E[X(t)X(t)\ X(t-\tau_1)\ X(t-\tau_2)] - m_{X^2}E[X(t-\tau_1)\ X(t-\tau_2)]$$

$$= R_{XX}(0)\ R_{XX}(\tau_2-\tau_1) + 2R_{XX}(\tau_1)\ R_{XX}(\tau_2) - m_{X^2}R_{XX}(\tau_2-\tau_1)$$

$$= 2\ R_{XX}(\tau_1)\ R_{XX}(\tau_2), \qquad (11.56)$$

thus $\quad s_{X^2XX}(\omega_1,\omega_2) = \dfrac{2}{(2\pi)^2} \displaystyle\int_{-\infty}^{\infty}\int_{-\infty}^{\infty} R_{XX}(\tau_1)R_{XX}(\tau_2)\exp[-i\{\omega_1\tau_1 + \omega_2\tau_2\}]\ d\tau_1 d\tau_2$

$$= 2\ s_{XX}(\omega_1)s_{XX}(\omega_2). \qquad (11.57)$$

Inserting into Eq. 11.49 gives

$$H_2(\omega_1,\omega_2) = \frac{s_{YXX}(\omega_1,\omega_2)}{s_{X^2XX}(\omega_1,\omega_2)} \qquad (11.58)$$

and inverting the variables as in Eq. 11.55 gives

$$H_2(\omega_1,\omega_2) = \frac{s_{YXX}(\omega_1-\omega_2,\omega_1+\omega_2)}{s_{X^2XX}(\omega_1-\omega_2,\omega_1+\omega_2)}. \qquad (11.59)$$

Both Eqs. 11.49 or 11.55 and Eq. 11.58 or 11.59 can be used for the computation of $H_2(\omega_1,\omega_2)$. However in actual computation, due to the consideration of the window, Eq. 11.58 or 11.59 is much better than Eq. 11.49 or Eq. 11.55.

5. Application of bispectrum analysis.

J. F. Dalzell[55, 56, 57, and 58] applied these theoretical relations (as compiled above in items 1 through 4) to the problem of added resistance of ships in waves. The quadratic process $Y(t)$ is the resistance $D(t)$ of ships in waves and the input process $x(t)$ is the wave height $\eta(t)$ in Eq. 11.1' (when $n = 0 - 2$) and $h_0 = D_0$, as

$$D(t) = D_0 + \int_{-\infty}^{\infty} h_1(\tau)\ \eta(t-\tau)d\tau + \int_{-\infty}^{\infty}\int_{-\infty}^{\infty} h_2(\tau_1,\tau_2)\ \eta(t-\tau_1)\ \eta(t-\tau_2)\ d\tau_1 d\tau_2.$$

Then Eqs. 11.33 and 11.33' are the expression of mean added resistance in waves

$$E[D(t)] = \int_{-\infty}^{\infty} H_2(\omega,-\omega)s_{\eta\eta}(\omega)\ d\omega, \qquad (11.60)$$

and the linear and nonlinear response functions of resistance to waves are Eq. 11.36,

Eq. 11.55, and Eq. 11.59 as

$$H_1(\omega) = s_{D\eta}(\omega)/s_{\eta\,\eta}(\omega)$$

(11.61)

$$H_2(\omega_1,\omega_2) = \frac{s_{D\,\eta\eta}(\omega_1-\omega_2,\omega_1+\omega_2)}{s_{\eta\,\eta}(\omega_1)s_{\eta\eta}(\omega_2)} = \frac{s_{D\,\eta\eta}\ (\omega_1-\omega_2,\omega_1+\omega_2)}{s_{\eta^2\,\eta\eta}\ (\omega_1-\omega_2,\omega_1+\omega_2)}$$

(11.62)

as a special case of Eq. 11.60. Therefore,

$$H_2(\omega,-\omega) = \frac{s_{D\eta\,\eta}(2\omega,0)}{\left|s_{\eta\eta}(\omega)\right|^2} = \frac{s_{D\eta\eta}(2\omega,0)}{S_{\eta^2\,\eta\,\eta}(2\omega,0)}.$$

(11.63)

Dalzell performed a series of tests in a towing tank on resistance increase on encountering head waves, with sea states A, B, and C, where the significant wave heights are in the ratio of 1:2:4. The results were analyzed and the applicability of these theories was made clear.

Figure 11.3 shows the linear frequency response function $[H_1(\omega) = G_1(\sigma)$ in Dalzell's expression] obtained by Eq. 11.61 in real and imaginary parts, and Fig. 11.4 shows the impulse response function $h_1(\tau)$ that is the Fourier transform of $H_1(\omega)$ in the discrete form L_k,

$$h_1\Big\{(\tau = L_k\ \delta(\tau - k\Delta t)\Big\},$$

(11.64)

Δt being the sampling time interval.
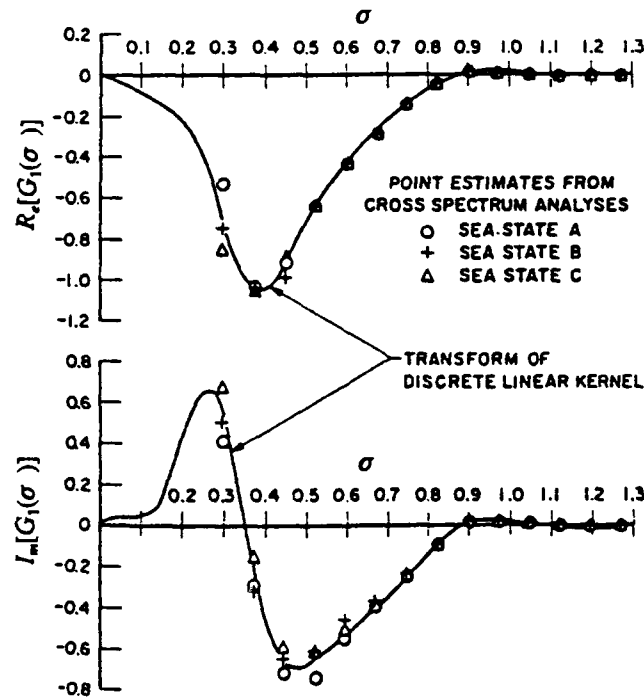
Fig. 11.3. Linear resistance frequency response. (From Dalzell.[55])

309
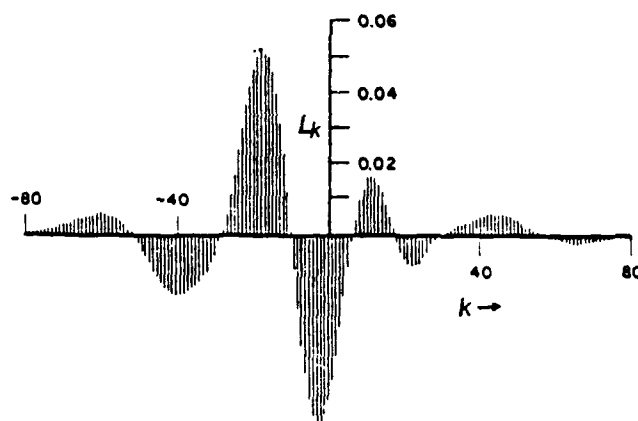
Fig. 11.4. Coefficients L_k of linear resistance impulse response function. (From Dalzell.[55])

Here σ_e is the nondimensional encounter frequency $\sigma_e = \omega_e/\omega_L$, where ω_L is the frequency of the wave with l⌐₋gth equal to the model ship length L, i.e., where $\omega_L = \sqrt{2\pi g/L}$. The added resistance and wave height are also nondimensionalized by the displacement and the length of the model. Figure 11.5 shows the special case of $H_2(\omega_1,\omega_2)$ when $\omega_1 = \omega, \omega_2 = -\omega$. The term $H_2(\omega,-\omega)$ is expressed by Eq. 11.63, and the results obtained in regular wave tests are also shown. The agreement is excellent.
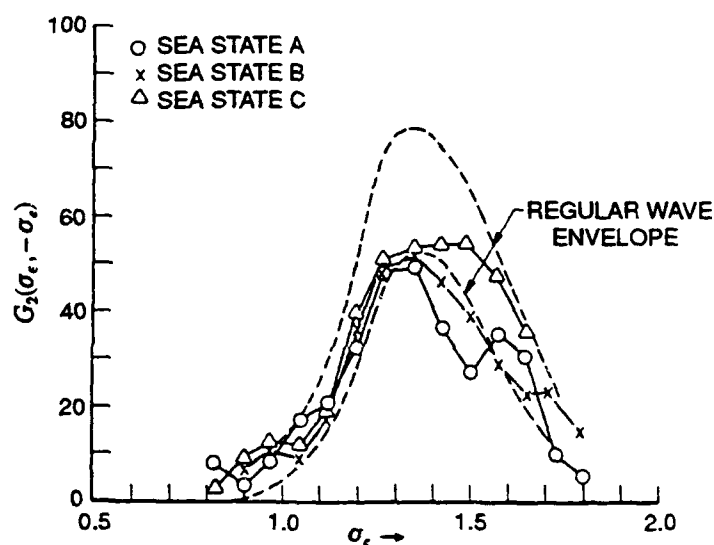
Fig. 11.5. Estimate of $G_2(\sigma_e,-\sigma_e)$ from cross–bispectral analysis, $Fn = 0.15$. (From Dalzell.[55])

310

Figure 11.6 shows an example of the three–dimensional plot of the modulus of a cross bispectrum of wave–wave resistance $s_{D\eta\eta}(\omega_1 \cdot \omega_2)$. Fig. 11.7 shows the plot of the real part of the same cross bispectrum.
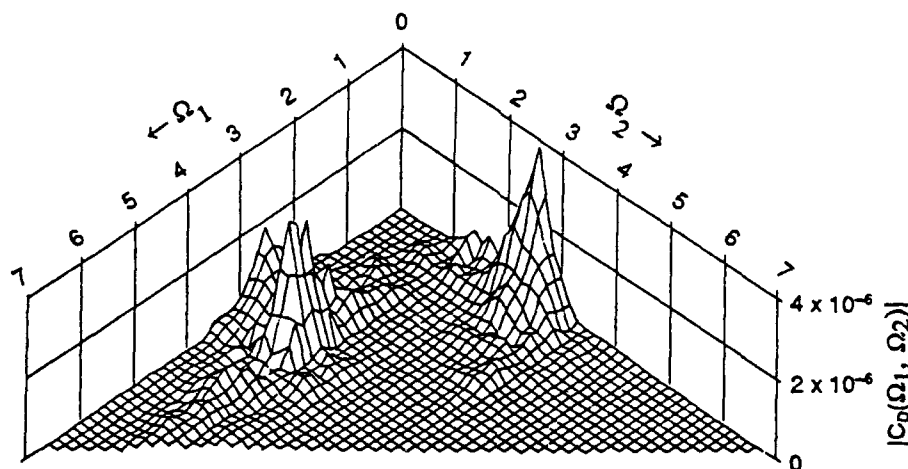
Fig. 11.6. Isometric plot of modulus of wave–wave resistance cross bispectrum, sea state B, $Fn = 0.15$.

(From Dalzell.[55])

The axis Ω_1, Ω_2 used here is $\Omega_1 = \omega_1 - \omega_2$, $\Omega_2 = \omega_1 + \omega_2$. Figure 11.8 shows an example of the real part of $H_2(\omega_1, \omega_2)$ obtained by Eq. 11.62, and Fig. 11.9 shows the second order impulse response function $h_2(\tau_1, \tau_2)$ in discrete form Q_{jk} as

$$h_2(\tau_1, \tau_2) \rightarrow Q_{jk} \, \delta(\tau_1 - j\Delta t) \, \delta(\tau_2 - k\Delta t) \tag{11.65}$$

in the form of weighting functions. These values were obtained from the data in sea state A. Using these weighting functions L_k (Fig. 11.4) and Q_{jk} (Fig. 11.9), obtained from the test data for sea state A, the added resistance was calculated by

$$D(n) = \sum_{j=-m}^{m} L_j \, \eta \, (n-j) + \sum_{j=-p}^{p} \sum_{k=-p}^{p} Q_{jk} \, \eta \, (n-j) \, \eta(n-k) \tag{11.66}$$

for sea states B and C, where the discrete readings $\eta(n-j), \eta(n-k)$ of the time history of wave height $\eta(t)$ for sea states B and C were used. The added resistance thus calculated was compared with the real time history of added resistance in sea states B and C. The results for sea state C are shown in Fig. 11.10 as an example. The agreement of this computed time history with the actually observed time history is surprisingly good. Here, two digital filters, as shown in Fig. 11.11, were used to get rid of the effect of the finite length of the digitized impulse response functions.

311
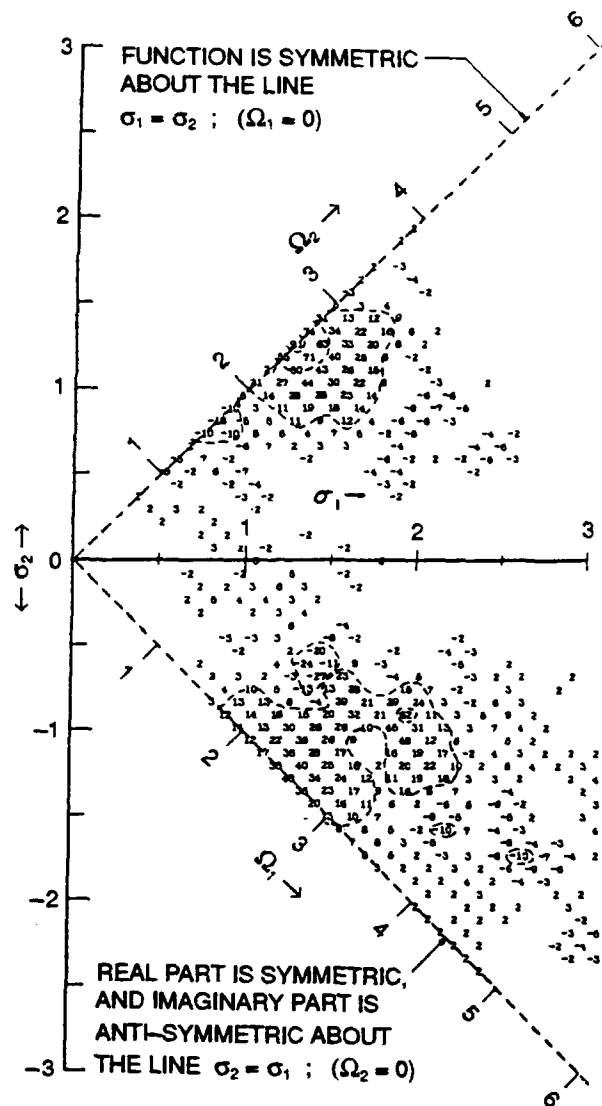
Fig. 11.7. Real part of wave-wave resistance cross spectrum, sea state B, $Fn = 0.15$ (normalization const. $= 3.76 \times 10^{-6}$).

(From Dalzell.[55])
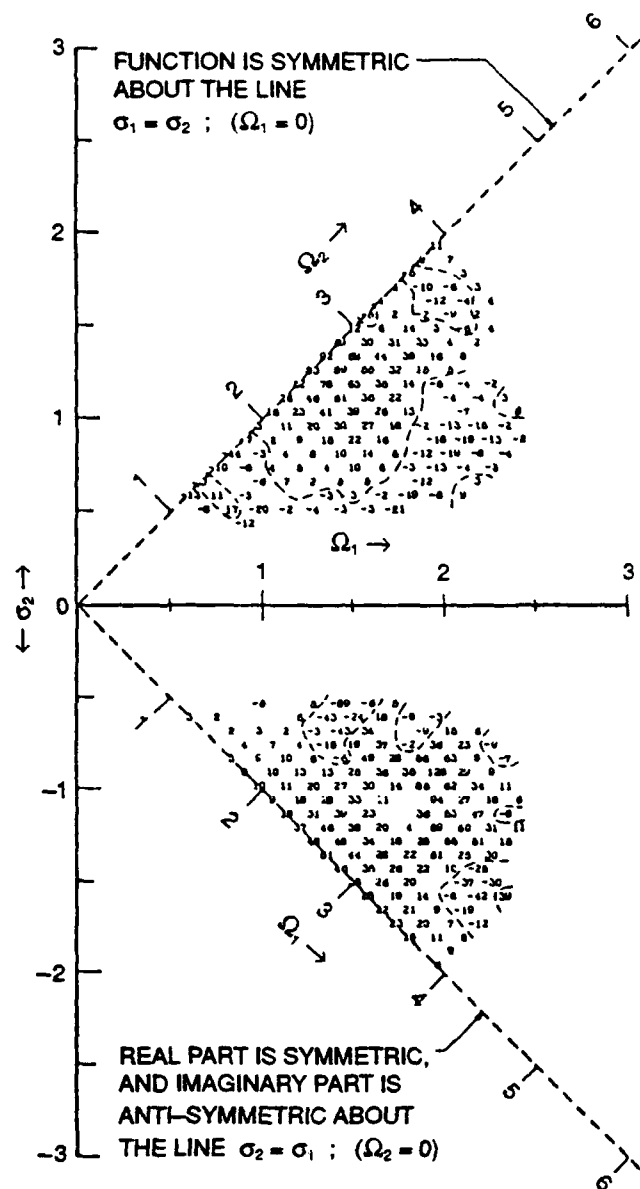
Fig. 11.8. Real part of estimated $G_2(\sigma_e, -\sigma_e)$, sea state B, Fn = 0.15. (From Dalzell.[55])
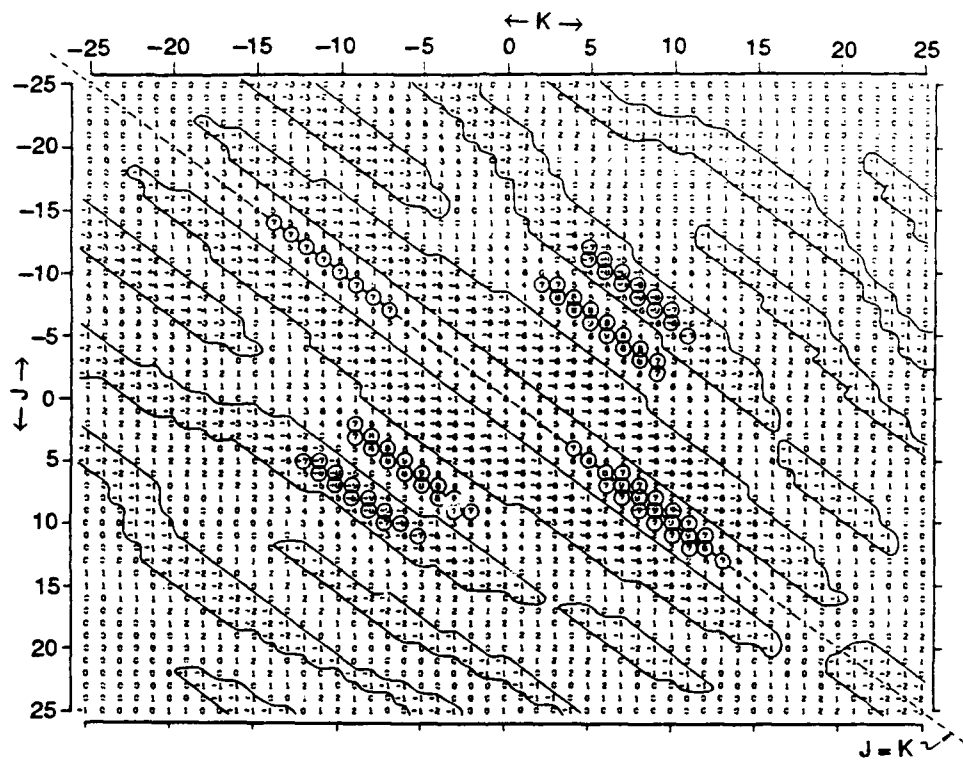
Fig. 11.9. Coefficient Q_{jk} of quadratic resistance impulse response function, values shown are $50\,Q_{jk}$ truncated to integer.
(From Dalzell.[55])
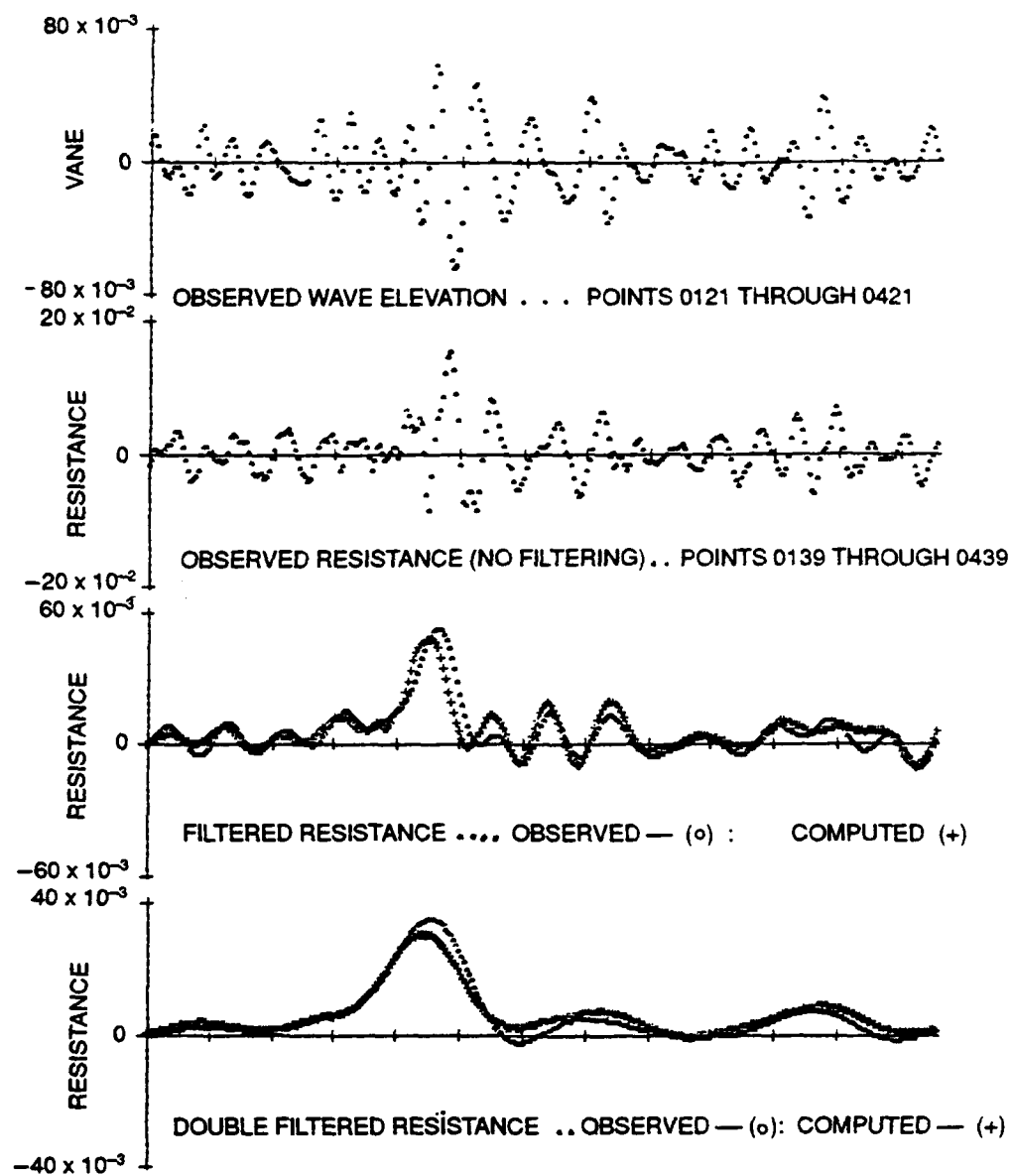
Fig. 11.10. Time history of waves and resistance observed and computed.
(From Dalzell.[55])
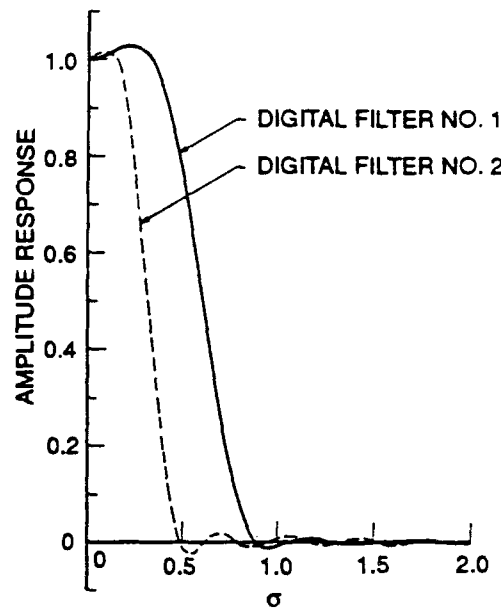
Fig. 11.11. Amplitude response of two digital filters.

(From Dalzell.[55])

11.5 APPLICATION OF THE HIGHER ORDER POLYSPECTRA

When we have to take into account nonlinearities of higher order than quadratic, we need to consider the polyspectra of higher order than the bispectrum. For example, when $Y(t)$ is expressed by

$$Y(t) = \int\limits_{-\infty}^{\infty} h_1(r) \, X(t-r) \, dr + \int\limits_{-\infty}^{\infty} \int\limits_{-\infty}^{\infty} h_2(u_1, u_2) \, X(t-u_1) \, X(t-u_2) du_1 du_2$$

$$+ \int\limits_{-\infty}^{\infty} \int\limits_{-\infty}^{\infty} \int\limits_{-\infty}^{\infty} h_3(q_1, q_2, q_3) \, X(t-q_1) \, X(t-q_2) \, X(t-q_3) dq_1 dq_2 dq_3, \quad (11.67)$$

we have to consider the fourth moment correlation functions and their three–dimensional Fourier transforms, which are called trispectra. In this case, as we did for the quadratic case, we can calculate the statistical values as summarized in the following paragraph.

There, the variables $X_1, X_2, \cdots X_n$ are supposed to follow the joint Gaussian distribution, with $E\{X_n\} = 0$, then as

$$E[X_1] = 0, \quad E[X_1 X_2 X_3] = 0, \quad E[X_1 X_2 \cdots X_5] = 0, \quad \cdots \cdots \quad (11.68)$$

all of the odd moments are zero. Further, as shown in Eq. 11.39

316

$$E[X_1X_2X_3X_4] = M_{12}M_{34} + M_{13}M_{24} + M_{14}M_{23}, \tag{11.69}$$

$$\begin{aligned}
E[X_1X_2X_3X_4X_5X_6] = \ & M_{12}M_{34}M_{56} + M_{12}M_{35}M_{46} + M_{12}M_{36}M_{45}, \\
& + M_{13}M_{24}M_{56} + M_{13}M_{25}M_{36} + M_{13}M_{26}M_{45} \\
& + M_{14}M_{23}M_{56} + M_{14}M_{25}M_{36} + M_{14}M_{26}M_{35} \\
& + M_{15}M_{34}M_{26} + M_{15}M_{32}M_{46} + M_{15}M_{36}M_{24} \\
& + M_{16}M_{34}M_{52} + M_{16}M_{35}M_{42} + M_{16}M_{32}M_{45}, \tag{11.70}
\end{aligned}$$

where $m_{ik} = E[X_i \, X_k]$. These characters as shown in Eqs. 11.68, 11.69, and 11.70 were fully utilized in the calculations of the following together with the symmetry properties of $h_2 (u_1, u_2)$ $h_3(q_1, q_2, q_3)$ in terms of $u_1, u_2; q_1, q_2, q_3$.

1. Mean of $Y(t)$, $m_Y = E[Y(t)]$

$$\begin{aligned}
m_Y &= \int_{-\infty}^{\infty} \int_{-\infty}^{\infty} h_2(u_1, u_2) \; R_{xx}(u_2 - u_1) \; du_1 du_2 \\
&= \int_{-\infty}^{\infty} \int_{-\infty}^{\infty} h_2(u_1, u_2) \int_{-\infty}^{\infty} s_{XX}(\omega) \exp\{- i(\omega u_1 + \omega u_2)\} \; d\omega \cdot du_1 du_2 \\
&= \int H_2(\omega, -\omega) \; s_{XX}(\omega) \; d\omega . \tag{11.71}
\end{aligned}$$

Equation 11.71 is the same expression with Eq. 11.33' for the quadratic process.

2. Second order covariance function, cross spectrum

$$\begin{aligned}
R_{YX}(\tau) &= E[\{Y(t) - m_Y\} \, X(t - \tau)] \\
&= \int_{-\infty}^{\infty} h_1(r)R_{XX}(\tau - r) \; dr \\
&\quad + 3 \int_{-\infty}^{\infty} \int_{-\infty}^{\infty} \int_{-\infty}^{\infty} h_3(q_1, q_2, q_3) \; R_{XX}(q_2 - q_1) \; R_{XX}(\tau - q_3) \; dq_1 dq_2 dq_3. \tag{11.72}
\end{aligned}$$

Therefore

$$\begin{aligned}
s_{YX}(\omega) &= H_1(\omega)s_{XX}(\omega) + 3 \int_{-\infty}^{\infty} H_3(\omega_1, -\omega_1, \omega) \; s_{XX}(\omega_1) \; s_{XX}(\omega) \; d\omega_1 \\
&= s_{XX}(\omega) \; [H_1(\omega) + 3 \int_{-\infty}^{\infty} H_3(\omega_1, -\omega_1, \omega) \; s_{XX}(\omega_1) \; d\omega_1]. \tag{11.73}
\end{aligned}$$

317

The term $s_{YX}(\omega)/s_{XX}(\omega)$ is no longer equivalent to $H_1(\omega)$, but is modified by some term that includes the third order nonlinear frequency response function H_3.

3. Second order autocovariance function, linear spectrum

$$
\begin{aligned}
R_{YY}(\tau) &= E[Y(t) - m_Y][Y(t+\tau) - m_Y] \\
&= E[Y(t) \cdot Y(t+\tau)] - m_Y^2 \\
&= \int_{-\infty}^{\infty} \int_{-\infty}^{\infty} h_1(s_1) h_1(r_1) E[X(t-s_1)X(t+\tau-r_1)] ds_1 dr_1 \\
&\quad + \iint \int_{-\infty}^{\infty} \int h_2(u_1, u_2)\, h_2(v_1, v_2)\, E[X(t-u_1)\, X(t-u_2)\, X(t+\tau-v_1) \\
&\qquad\qquad\qquad\qquad\qquad\qquad\qquad \times X(t+\tau-v_2)]\ du_1 du_2\ dv_1 dv_2 \\
&\quad + \iint \int_{-\infty}^{\infty} \iint h_3(p_1, p_2, p_3) h_3(q_1, q_2, q_3) \\
&\qquad \times E\Big[X(t-p_1)\, X(t-p_2)\, X(t-p_3) \cdot X(t+\tau-q_1)\, X(t+\tau-q_2)\, X(t+\tau-q_3)\Big] \\
&\qquad\qquad\qquad\qquad dp_1 dp_2 dp_3 dq_1 dq_2 dq_3 \\
&\quad - m_Y^2.
\end{aligned}
\tag{11.74}
$$

We take the Fourier transform, and the linear spectrum is, after manipulation,

$$
\begin{aligned}
s_{YY}(\omega) &= s_{XX}(\omega)\ \left| H_1(\omega) + 3 \int_{-\infty}^{\infty} H_3(\omega, \omega_3, -\omega_3)\ s_{XX}(\omega_3)\ d\omega_3 \right|^2 \\
&\quad + 2 \int_{-\infty}^{\infty} \left| H_2(\omega - \omega_2, \omega_2) \right|^2 s_{XX}(\omega - \omega_2)\ s_{XX}(\omega_2)\ d\omega_2 \\
&\quad + 6 \int_{-\infty}^{\infty} \int_{-\infty}^{\infty} \left| H_3(\omega - \omega_2, -\omega_3, \omega_2, \omega_3) \right|^2 s_{XX}(\omega - \omega_2 - \omega_3)\ s_{XX}(\omega_3)\ d\omega_2 d\omega_3.
\end{aligned}
\tag{11.75}
$$

The first term, the term of $s_{XX}(\omega)$ of this Eq. 11.75 is again modified by the cubic response H_3, as was Eq. 11.73 that shows $s_{YX}(\omega)/s_{XX}(\omega)$ is not $H_1(\omega)$ anymore, but is modified by the effect of cubic response $H_3(\omega_1, \omega_2, \omega_3)$. Bedrosian and Rice[80] showed this modification clearly for the case when the input was the sum of sinusoidal waves, and showed the necessity to include the higher order terms in Voltera expansions.

318

4. Third moment cross covariance and cross bispectrum

$$R_{YXX}(\tau_1, \tau_2) = 2 \int\limits_{-\infty}^{\infty} \int\limits_{-\infty}^{\infty} h_2(u_1, u_2)\, R_{XX}(\tau_1 - u_1)\, R_{XX}(\tau_2 - u_2)\, du_1 du_2, \quad (11.76)$$

therefore $\quad\quad S_{YXX}(\omega_1, \omega_2) = 2H_2(\omega_1, \omega_2)\, s_{XX}(\omega_1)\, s_{XX}(\omega_2).$ $\quad\quad$ (11.77)

If we use $X^2(t)$ instead of $Y(t)$, from Eqs. 11.56 and 11.57 we get

$$R_{X^2XX}(\tau_1, \tau_2) = 2R_{XX}(\tau_1)\, R_{XX}(\tau_2) \quad\quad\quad (11.78)$$

$$s_{X^2XX}(\omega_1, \omega_2) = 2s_{XX}(\omega_1)\, s_{XX}(\omega_2) \quad\quad\quad (11.79)$$

as we did in the preceding section for Eq. 11.50, inverting the variables from ω_1, ω_2 into $\omega_1 - \omega_2, \omega_1 + \omega_2$,

$$2\, S_{YXX}\,(\omega_1 - \omega_2, \omega_1 + \omega_2) = s_{YXX}(\omega_1, \omega_2). \quad\quad (11.80)$$

Therefore, the quadratic frequency response function $H_2(\omega_1, \omega_2)$ is obtained by

$$H_2(\omega_1, \omega_2) = \frac{s_{YXX}(\omega_1, \omega_2)}{2s_{XX}(\omega_1)s_{XX}(\omega_2)} = \frac{s_{YXX}(\omega_1, \omega_2)}{s_{X^2XX}(\omega_1, \omega_2)} \quad\quad (11.81)$$

$$= \frac{s_{YXX}(\omega_1 - \omega_2, \omega_1 + \omega_2)}{s_{XX}(\omega_1)\, s_{XX}(\omega_2)} = \frac{s_{YXX}(\omega_1 - \omega_2, \omega_1 + \omega_2)}{s_{X^2XX}(\omega_1 - \omega_2, \omega_1 + \omega_2)}. \quad\quad (11.81')$$

These are the same as Eqs. 11.49, 11.55, 11.58, and 11.59 for the quadratic process and it means that the process to calculate the quadratic response $H_2(\omega_1, \omega_2)$ is the same as for the quadratic nonlinear process, even for this third order nonlinear process.

5. Fourth moment cross correlation and trispectrum

When $Y(t)$ is expressed by Eq. 11.67, which includes the third order nonlinear for the cubic nonlinear process term, the fourth moment cross correlation can be obtained by the same kind of manipulation as in the quadratic nonlinear process as

$$R_{YXXX}(\tau_1, \tau_2, \tau_3) \equiv E[\{Y(t) - m_Y\}\, X(t - \tau_1)\, X(t - \tau_2)\, X(t - \tau_3)]$$

$$= 6 \int\limits_{-\infty}^{\infty} \int\limits_{-\infty}^{\infty} \int\limits_{-\infty}^{\infty} h_3(q_1, q_2, q_3,)\, R_{XX}(\tau - q_1)\, R_{XX}(\tau_2 - q_2)\, R_{XX}(\tau_3 - q_3)$$

$$dq_1 dq_2 dq_3. \quad (11.82)$$

Its three–dimensional Fourier transform is called the trispectrum and is

$$s_{YXXX}(\omega_1, \omega_2, \omega_3) = 6\, H_3(\omega_1, \omega_2, \omega_3)\, s_{XX}(\omega_1)\, s_{XX}(\omega_2)\, s_{XX}(\omega_3). \quad (11.83)$$

If we use $X^3(t)$ instead of $Y(t)$, then

$$R_{X^3XXX}(\tau_1, \tau_2, \tau_3) = 6R_{XX}(\tau_1)R_{XX}(\tau_2)R_{XX}(\tau_3) \quad\quad (11.84)$$

$$s_{X^3XXX}(\omega_1, \omega_2, \omega_3) = 6s_{XX}(\omega_1)s_{XX}(\omega_2)s_{XX}(\omega_3). \quad\quad (11.85)$$

319

Therefore, the third order nonlinear frequency response function is obtained as

$$H_3(\omega_1, \omega_2, \omega_3) = \frac{S_{YXXX}(\omega_1), \omega_2, (\omega_3)}{6S_{XX}(\omega_1)\ s_{XX}(\omega_2)s_{XX}(\omega_3)} = \frac{S_{YXXX}(\omega_1,\ \omega_2,\ \omega_3)}{S_{X^3XXX}(\omega_1,\omega_2,\omega_3)}. \quad (11.86)$$

6. Application of the trispectrum to ship's rolling by Dalzell.

J. F. Dalzell[17] discussed the characters of higher order nonlinear responses in Voltera expansion, especially the interferences between different order nonlinear responses, based on E. Bedrosian and S. O. Rice[80] and also tried to solve the problems encountered on their numerical computations. Besides Dalzell's trial[55-58] on the application of the bispectrum analysis to the added resistance of ships advancing in waves (already referred to in Section 11.4), he also tried[17] an application of trispectrum analysis to the problem of

nonlinear ship's rolling, expressing[81] the nonlinear roll damping by cube of roll angular velocity.

Dalzell expressed the equation of motion as

$$\sum_{j=1}^{3} \left[A_j\{\ddot{Y}(t)\}^j + B_j\{\dot{Y}(t)\}^j + C_j\{Y(t)\}^j \right] = X(t). \quad (11.87)$$

Then, using the so-called incommensurate frequency technique,[80] the relations of $A_j, B_j, C_j(j = 1 - 3)$ and frequency response functions $H_1(\omega)$, $H_2(\omega_1, \omega_2)$, $H_3(\omega_1, \omega_2, \omega_3)$ were derived.

Setting appropriate values for A_1 to C_3, and using the simulated series of wave heights $X(t)$ that have Pierson–Moskowitz type spectra, Dalzell synthesized the roll response $Y(t)$ as shown in Fig. 11.12, using impulse responses $h_1(\tau), h_2(\tau_1, \tau_2)$ and $h_3(\tau_1, \tau_2, \tau_3)$ obtained through $H_1(\omega), H_2(\omega_1, \omega_2)$ and $H_3(\omega_1, \omega_2, \omega_3)$ expressed by A_j, B_j, and $C_j(j = 1 - 3)$.
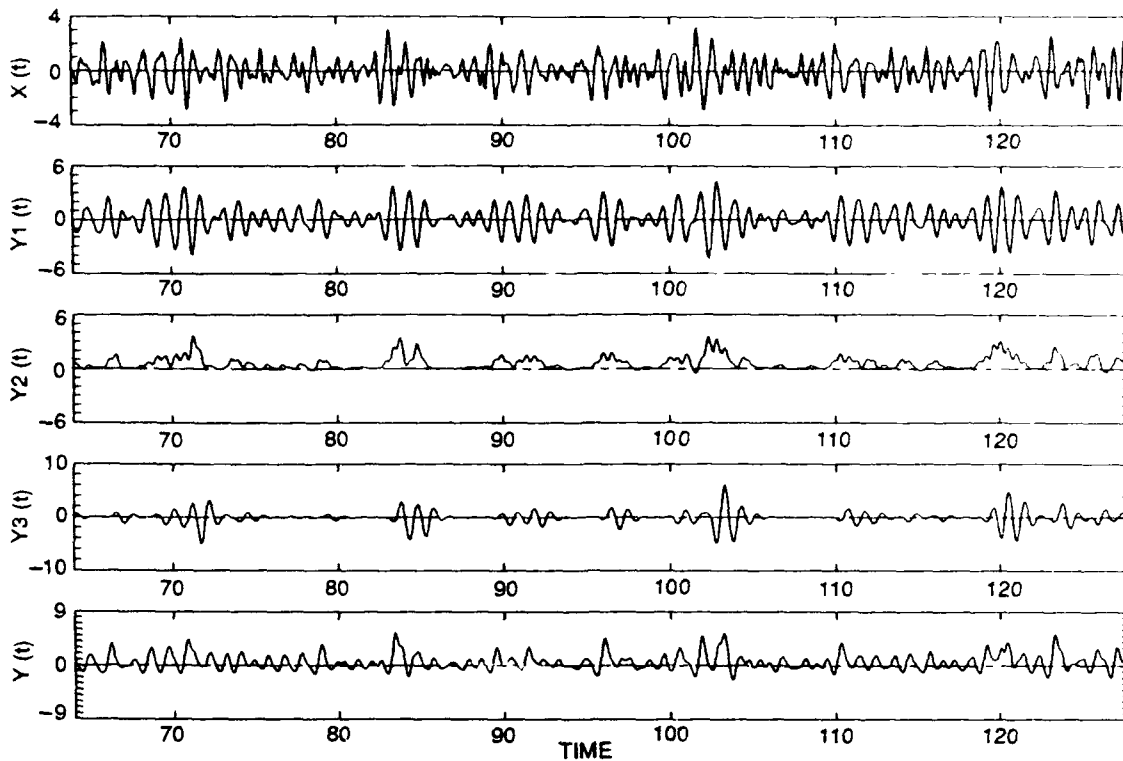
Fig. 11.12. Simulated time histories of linear random excitation $X(t)$ and nonlinear response $Y(t)$, and its components $Y_1(t)$, $Y_2(t)$, and $Y_3(t) \sigma_x = 1.0$.
(From Dalzell.[17])

Here, $Y_1(t)$, $Y_2(t)$, and $Y_3(t)$ show the first, second, and third terms of the Voltera expansion of $Y(t)$ as Eq. 11.67.

Figures 11.13 and 11.14 show the first and second order impulse response functions $h_1(t)$ and $h_2(t_1, t_2)$ in the form of the weighting functions g_j^1, g_{jk}^2 and Fig. 11.15 shows a portion of the third order impulse response function $h_3(t_1, t_2, t_3)$ at the sequence of t_3 values in the form $g_{j\cdot k\cdot l}^3$. It is interesting that impulse responses are obtained quite beautifully by this analysis.
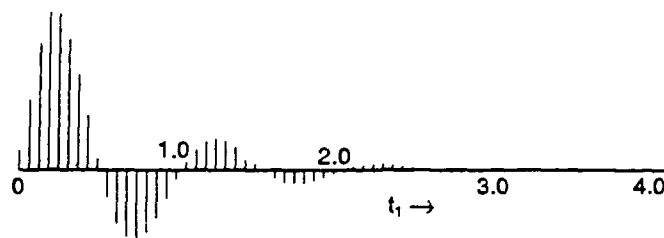
Fig. 11.13. Truncated linear discrete kernel g_j^1.
(From Dalzell.[17])

321

Figure 11.16 compares the observed and the predicted second order moment spectra and also U_1, U_2, and U_3 correspond to the first, second, and third terms of Eq. 11.75. It is rather surprising that the observed value can be almost fully explained theoretically by Eq. 11.75. It is also interesting to find in the upper second figure of Fig. 11.16, that the linear estimated spectrum (shown by solid line) is pretty largely distorted by the existence of cubic frequency response H_3 as are shown by Eq. 11.73 and by the first term of Eq. 11.75, and is modified into $U_1(\omega)$ shown by the dotted line in the same figure.
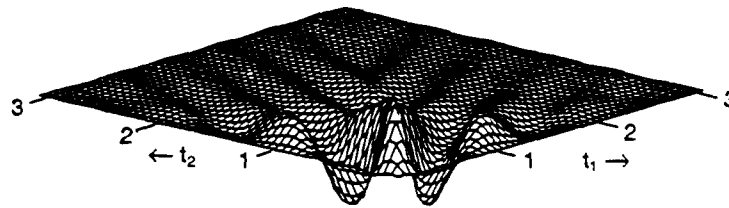
Fig. 11.14. Truncated quadratic discrete kernel g_{jk}^2.
(From Dalzell.[17])
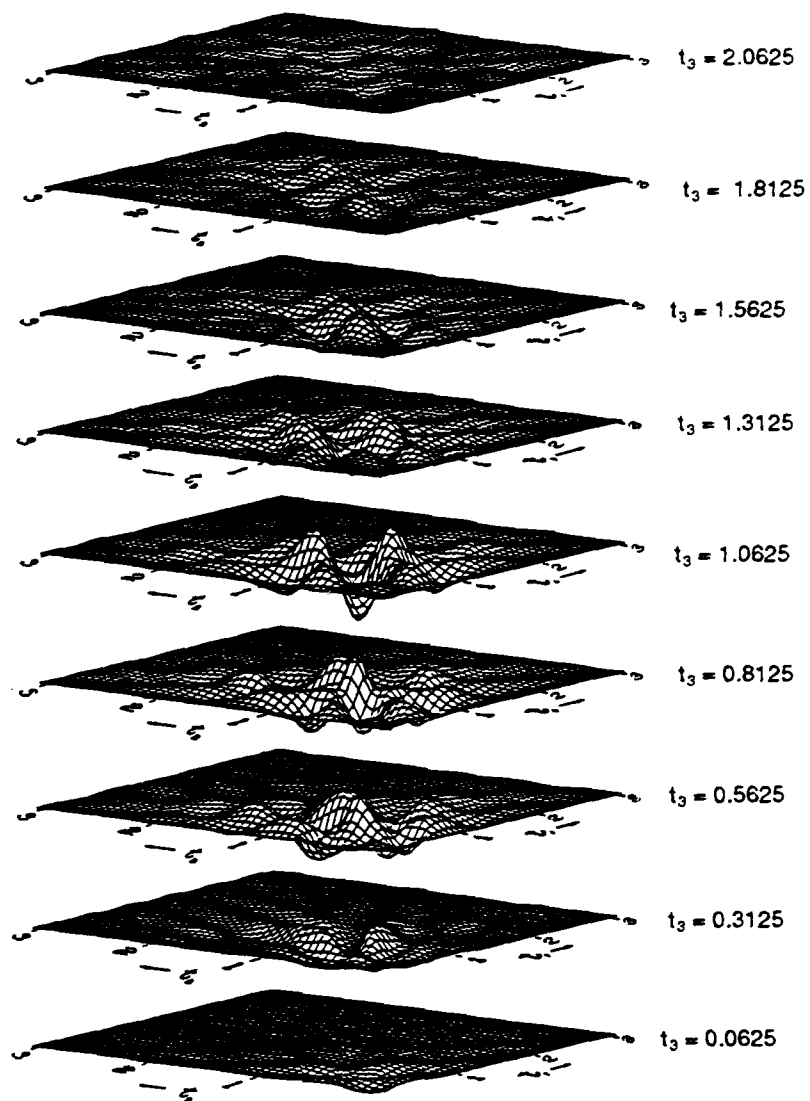
Fig. 11.15. Portions of the truncated cubic discrete kernel g^3_{jkl}. (From Dalzell.[17])
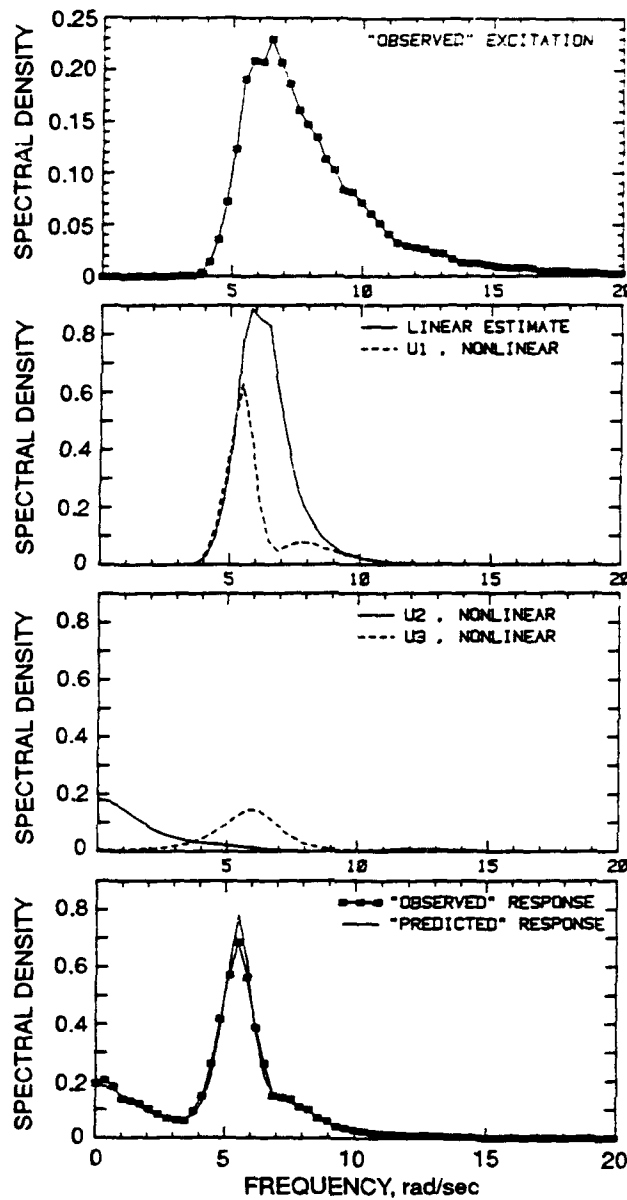
Fig. 11.16. Observed and predicted spectra and the components of spectrum of nonlinear response of the simulated system, nominal $\sigma_x = 1.0$.

(From Dalzell.[17])

7. Expansion to higher order nonlinear process.

By the same procedure as previously used for quadratic and cubic nonlinear processes, we can go on to higher order nonlinearities. For example, from Brillinger,[82]

$$H_m(\omega_1, \omega_2, \cdots \omega_m) = \frac{s_{YXX\cdots X}(\omega_1, \omega_2 \cdots \omega_m)}{m! s_{XX}(\omega_1)\ s_{XX}(\omega_2) \cdots s_{XX}(\omega_m)}. \tag{11.88}$$

324

CHAPTER 12

PROBABILISTIC CHARACTERS OF NONLINEAR RESPONSE PROCESS

12.1 INTRODUCTION

The stochastic or random process can be expressed as a function of time and also as a probabilisitc measure $x(t,s)$. Until Chapter 11, however, we have discussed the characters of the process mostly in the time aspect and, based on the ergodicity, dealt with the correlation functions and spectra and their statistical characteristics. Especially in Chapters 9, 10, and 11, the effects of nonlinearities on these characteristics were studied.

In this chapter, the probability distributions that characterize the response process will be discussed briefly for reference. The main topic in Part III is the nonlinearity of the process. However, general considerations, including the linear cases, will be discussed first.

Generally, the probabilistic character of the random process $X(t)$ can be defined completely by the series of probability distribution density functions as

$p_1(x_1, t_1)dx$: the probability that $X(t)$ is in the range $x_1 \backsim x_1 + dx_1$

at time t_1;

$p_2(x_1, t_1; x_2, t_2)$: the probability that $X(t)$ is in the range $x_1 \backsim x_1 + dx_1$

at time t_1

and in $x_2 \backsim x_2 + dx_2$ at time t_2;

$p_3(x_1, t_1; x_2, t_2; x_3, t_3)$: the probability that $X(t)$ is in the range $x_1 \backsim x_1 + dx_1$

at time t_1,

in $x_2 \backsim x_2 + dx_2$ at time t_2,

and in $x_3 \backsim x_3 + dx_3$ at time t_3.

In the same way p_n is defined for $n=4, 5 \ldots$.

Here   i. $p_n \geq 0$

ii. p_n is symmetrical for $x_1, t_1; x_2, t_2; x_3, t_3; \ldots$

iii.   the marginal probability density function p_m is

$$p_m = \int\limits_{-\infty}^{\infty} \cdots \int\limits_{-\infty}^{\infty} p_n \, dx_{m+1} dx_{m+2} \cdots dx_n. \qquad (12.1)$$

$$\underbrace{\phantom{\int\limits_{-\infty}^{\infty}\cdots\int\limits_{-\infty}^{\infty}}}_{n-m}$$

As was mentioned in Section 2.1, when these probability density functions p_n stay the same when the time t_1 is replaced by t_1+T (T: arbitrary), this process is called stationary. Then $p_1(x_1, t_1)$ is independent of time, and p_2 depends only on the time difference t_2-t_1. Here the concept of the Markov process that is used to classify the random process probability is first introduced.

From the characteristics of these distribution functions, the processes are sometimes classified into three groups: (1) pure random processes, (2) Markov processes, and (3) general processes.

For a pure random process, since the value x_i at time t_i is independent of any values of $x(t)$ at any other times $t_{i-1}, t_{i-2}, \ldots t_2, t_1$, this process can be defined completely by $p_1(x_i, t_i)$, because any higher order joint probability distribution function is

$$p_n(x_1, t_1; x_2, t_2 \cdots x_n, t_n) = \prod_{i=1}^{n} p_1(x_i, t_i) . \qquad (12.2)$$

Accordingly, if only $p_1(x_i, t_i)$ is given, all other joint distribution functions can be derived easily.

12.2 MARKOV PROCESS

When the process is not purely random, but when in addition to p_1 like $p_1(x_i, t_i)$ and $p_1(x_{i-1}, t_{i-1})$, if $p_2(x_{j-1}, t_{j-1}; x_j, t_j)$ is necessary to express the probability characters of the process, the process is called a Markov (or Markovian) (linear) process. The condition that the probability distribution density functions $p_1(x_{i-1}, t_{i-1})$ and $p_2(x_{j-1}, t_{j-1}; x_j, t_j)$ are given is the same as the condition that the conditional probability distribution density functions $p_{c_2}(x_j, t_j - t_{j-1}|x_{j-1})$ are known. Because the conditional probability density function $p_{c_2}(x_j, t_j|x_{j-1}, t_{j-1})$ is the probability distribution density function of this process that x is in the range $x_j \sim x_j + dx_j$ at time t_j, under the condition that the value of this process was in the range of $x_{j-1} \sim x_{j-1} + dx_{j-1}$ at time t_{j-1}, that is $(t_j - t_{j-1})$ prior to t_j, and is expressed by

$$p_{c_2}(x_j, t_j|x_{j-1}, t_{j-1}) = p_{c_2}(x_j, t_j - t_{j-1}|x_{j-1}) = \frac{p_2(x_j, t_j; x_{j-1}, t_{j-1})}{p_1(x_{j-1}, t_{j-1})} . \qquad (12.3)$$

Here, from the characteristics of the probability distribution density function,

i. $p_{c_2}(x_j, t|x_{j-1}) \geq 0$

ii. $\displaystyle\int_{-\infty}^{\infty} p_{c_2}(x_j, t|x_{j-1})dx_j = 1$

iii. $\displaystyle p_1(x_j, t_j) = \int_{-\infty}^{\infty} p_1(x_{j-1}, t_{j-1})p_{c_2}(x_j, t_j - t_{j-1}|x_{j-1})dx_{j-1}.$

Generally, the Markov process is defined as follows, using the conditional probability —— when the probability, that $X(t)$ is in the range $x_j \frown x_j + dx_j$ at t_j, under the condition that

$$
\left\{
\begin{array}{l}
X(t) \text{ is } x_{j-1} \frown x_{j-1} + dx_{j-1}, \text{ at } t_{j-1}, \\[2mm]
x_{j-2} \frown x_{j-2} + dx_{j-2}, \text{ at } t_{j-2}, \\[2mm]
- - - - - - - - - - - - \\[2mm]
x_2 \frown t_2 + dx_2, \text{ at } t_2, \\[2mm]
x_1 \frown x_1 + dx_1, \text{ at } t_1,
\end{array}
\right.
$$

is determined by the conditional probability that $X(t)$ is $x_j \frown x_j + dx_j$, under the condition that at only one preceding time step $t = t_{j-1}$, $x(t)$ is x_{j-1}, —— then this process is called a Markov process. Namely, if

$$p_c(x_j, t_j|x_{j-1}, t_{j-1}; x_{j-2}, t_{j-2}; \ldots ; x_2, t_2; x_1, t_1)$$

$$= p_{c_2}(x_j, t_j|x_{j-1}, t_{j-1}), \tag{12.4}$$

this process $X(t)$ is a Markov process.

From Eq. 12.3 and Eq. 12.4, generally

$$p_n(x_n, t_n; x_{n-1}, t_{n-1}; \ldots x_2, t_2; x_1, t_1) = p_{c_2}(x_n, t_n|x_{n-1}, t_{n-1})$$

$$\times p_{n-1}(x_{n-1}, t_{n-1}; x_{n-2}, t_{n-2}; \ldots x_2, t_2; x_1, t_1). \tag{12.5}$$

Therefore, by the same relation,

$$p_n(x_n, t_n; x_{n-1}, t_{n-1}; \ldots x_2, t_2; x_1, t_1)$$

$$= p_{c_2}(x_n, t_n|x_{n-1}, t_{n-1}) \; p_{c_2}(x_{n-1}, t_{n-1}|x_{n-2}, t_{n-2}) \cdots$$

$$\times p_{c_2}(x_2, t_2|x_1, t_1)p_1(x_1, t_1). \tag{12.6}$$

327

From this expression, the term Markov chain is used. The conditional probability function is also called the transitional probability function.

Also

$$p_2(x_n, t_n; x_{n-2}, t_{n-2}) = \int\limits_{-\infty}^{\infty} p_3(x_n, t_n; x_{n-1}, t_{n-1}; x_{n-2}, t_{n-2}) \, dx_{n-1}$$

and

$$p_2(x_n, t_n; x_{n-2}, t_{n-2}) = p_{c_2}(x_n, t_n | x_{n-2}, t_{n-2}) \, p(x_{n-2}, t_{n-2})$$

$$p_3(x_n, t_n; x_{n-1}, t_{n-1}; x_{n-2}, t_{n-2}) = p_c(x_n, t_n; x_{n-1}, t_{n-1} | x_{n-2}, t_{n-2})$$

$$\times \, p(x_{n-2}, t_{n-2})$$

therefore

$$p_{c_2}(x_n, t_n | x_{n-2}, t_{n-2}) = \int\limits_{-\infty}^{\infty} p_c(x_n, t_n; x_{n-1}, t_{n-1} | x_{n-2}, t_{n-2}) dx_{n-1} \qquad (12.7)$$

this Eq. 12.7 is called a Chapman–Kolomogorov equation or Smoluchowski equation for the transitional distribution of the Markov process. It implies that to go from x_{n-2} at time t_{n-2} to x_n at time t_n, the path x_{n-1} at time t_{n-1} is not important. We can take any path to go to x_n. This characteristic is used to derive the Fokker–Planck equations, shown in the next section.

For example, the AR model of the first order AR(1) as was treated in Chapter 5 is

$$X(t) - aX(t-1) = \epsilon(t), \qquad (12.8)$$

where a is a constant, $\epsilon(t)$ is a pure random process (a Markovian linear process), and so $X(t)$ is statistically determined by the value $X(t-1)$, that is, the value of $X(t)$ at one preceding time step. Accordingly, $X(t)$ is a Markovian process.

12.3 GENERAL PROCESS

If we need the values of a process not only at one preceding time point t_{i-1}, but at two or more preceding time points, i.e., not only p_1 and p_2, but also higher order joint probability functions $p_3, p_4, \ldots$ the process is called a general process. However, among general processes $X(t)$, some can be inverted into vector Markov processes, combining with some other variables and introducing the concept of the state space (Markovian).

Putting aside the concise theory, for example for the second order autoregressive model AR(2) as

$$X(t) - a_1 X(t-1) - a_2 X(t-2) = \epsilon(t), \tag{12.9}$$

we can introduce the vector process $X(t)$ with two elements X_1, X_2 as

$$\begin{cases} X_2(t) = X(t) \\ X_1(t) = a_2 X(t-1)(= a_2 X_2(t-1)). \end{cases} \tag{12.10}$$

Then Eq. 12.9 can be written

$$\underbrace{\begin{bmatrix} X_1(t) \\ X_2(t) \\ \vdots \\ X(t) \end{bmatrix}}_{X(t)} = \begin{bmatrix} 0 & a_2 \\ 1 & a_1 \end{bmatrix} \underbrace{\begin{bmatrix} X_1(t-1) \\ X_2(t-1) \\ \vdots \\ X(t-1) \end{bmatrix}}_{X(t-1)} + \begin{bmatrix} 0 \\ 1 \end{bmatrix} \epsilon(t). \tag{12.11}$$

Here setting

$$\begin{bmatrix} X_1(t) \\ X_2(t) \end{bmatrix} = X(t), \quad \begin{bmatrix} 0 & a_2 \\ 1 & a_1 \end{bmatrix} = a, \quad \begin{bmatrix} 0 \\ 1 \end{bmatrix} \epsilon(t) = \epsilon(t),$$

Eq. 12.11 becomes

$$X(t) = a X(t-1) + \epsilon(t). \tag{12.12}$$

This transformation shows that AR(2) can be inverted into a Markovian linear process or a vector process $X(t) = [X_1(t), X_2(t)]'$.

By the same procedure, the autoregressive process of order n, AR(n), or more generally the autoregressive moving average model ARMA (n, m), can be shown to be invertible into a Markovian process, introducing the matrix of inverting functions.

The characteristics of a Markovian process contribute to the derivation of distribution functions, applying the Fokker–Planck equation, and also for the application of the Kalman filters.

12.4 THE FOKKER–PLANCK EQUATION

To show the behavior of the transitional probability density function p_c of a stochastic process as a Markov process, formally a linear second order partial differential equation called the Fokker–Planck equation is used. This equation was developed by Fokker (1914) and Planck (1917), to indicate the Brownian motion of molecules, and it has also been utilized as the equation of motion to show the behavior of the transitional

probability density function of a stochastic process.[83,84] This equation is, however, not solved analytically in general, except for a few special cases, so special considerations are usually demanded in using it.

Here the conditional or transitional probability density function $p_{c_2}(x, \Delta t|y)$ is expressed merely as p_c, y being the value of process $X(t)$ at a preceding time Δt. The derivation of this equation is given by Caughey.[83]

The Fokker–Planck equation for this transitional probability function is in the form

$$\frac{\partial p_c}{\partial t} = \left[-\frac{\partial}{\partial x} D^{(1)}(x) + \frac{1}{2} \frac{\partial^2}{\partial x^2} D^{(2)}(x) \right] p_c. \qquad (12.13)$$

Here $D^{(1)}(x)$ and $D^{(2)}(x) > 0$ are called the drift coefficient and diffusion coefficient, respectively, and are related to the first and second moments of this distribution as

$$D^{(1)}(x) = \lim_{\Delta t \to 0} \frac{1}{\Delta t} \int_{-\infty}^{\infty} (y - x) p_c(x, \Delta t|y) dy \qquad (12.14)$$

$$D^{(2)}(x) = \lim_{\Delta t \to 0} \frac{1}{\Delta t} \int_{-\infty}^{\infty} (y - x)^2 p_c(x, \Delta t|y) dy. \qquad (12.15)$$

Generally these are functions of time t.

As was stated before, when the general process is inverted into a vector Markov process $X(t)$ of N dimensions as $X(t) = [X_1(t), X_2(t) \ldots X_N(t)]'$, the Fokker–Planck equation is more generally in the form

$$\frac{\partial p_c}{\partial t} = \left[-\sum_{i=1}^{N} \frac{\partial}{\partial x_i} D_i^{(1)}(x) + \frac{1}{2} \sum_{i,j=1}^{N} \frac{\partial^2}{\partial x_i \partial x_j} D_{ij}^{(2)}(x) \right] p_c \qquad (12.16)$$

where

$$D_i^{(1)}(x) = \lim_{\Delta t \to 0} \frac{1}{\Delta t} \left[\int_{-\infty}^{\infty} (y_i - x_i) p_c(x, \Delta t|y) \prod_{i=1}^{N} dy_i \right] \qquad (12.17)$$

$$D_{ij}^{(2)}(x) = \lim_{\Delta t \to 0} \frac{1}{\Delta t} \left[\int_{-\infty}^{\infty} (y_i - x_i)(y_j - x_j) p_c(x, \Delta t|y) \prod_{i=1}^{N} dy_i \right]. \qquad (12.18)$$

x, y are the values of process $X(t)$.

Solving Eqs. 12.13 or 12.16 gives the transitional probability functions. Since these equations are solved analytically only for some restricted types, several methods, such as a simulation method, transformation into a Schrädinger equation, numerical integration, potential method, and so on, are used to obtain the solution.

When, by the elapse of time, the transitional probability function $p_c(x, t|y)$ tends to $p(x)$ as its limit and becomes stationary, independent of time and its initial value, then in the Fokker–Planck Eqs. 12.13 and 12.16, setting $t \to \infty, \frac{\partial p_c}{\partial t} = 0$,

$$\frac{1}{2} \sum_{i=1}^{N} \sum_{j=1}^{N} \frac{\partial^2}{\partial x_i \partial x_j} \left[D^{(2)}(x) \, p(x) \right] - \sum_{i=1}^{N} \frac{\partial}{\partial x_i} [D^{(1)}(x) \, p(x)] = 0, \qquad (12.19)$$

where $p(x)$ obtained as the solution of this equation is an N–dimensional joint distribution related to the N–dimensional state space for this vector process $X(t)$.

Under some considerations and restrictions, these methods can be expanded to deal with nonlinear processes.

For example, following Caughey,[83] consider a nonlinear oscillation with nonlinear restoration under Gaussian (mean = 0) excitation as

$$\ddot{X}(t) + \beta \dot{X}(t) + F\{X(t)\} = f(t) \qquad (12.20)$$

$$E[f(t)] = 0 \qquad (12.21)$$

$$E[f(t_1) \, f(t_2)] = \frac{W_0}{2} \delta(t_1 - t_2) \qquad (12.22)$$

here $W_0/2$ shows the white spectrum of the excitation, and δ is the Dirac's delta function. From the transform

$$\begin{cases} X_1(t) = X(t) \\ X_2(t) = \dot{X}(t) \end{cases} \qquad (12.23)$$

and introducing the vector process

$$X(t) = [X_1(t), \ X_2(t)]' = [X(t), \ \dot{X}(t)]', \qquad (12.24)$$

from Eqs. 12.20 and 12.23

$$\begin{cases} \dot{X}_1(t) = X_2(t) \\ \dot{X}_2(t) = -\beta X_2(t) - F[X_1(t)] + f(t). \end{cases} \qquad (12.25)$$

Coefficients $D_i^{(1)}(x)$, and $D_{ij}^{(2)}(x)$ for the Fokker–Planck equations are, when we insert Eq. 12.23 into Eqs. 12.17 and 12.18,

$$D_1^{(1)} = \lim_{\Delta t \to 0} \frac{E[\Delta X_1]}{\Delta t} = x_2 = \dot{x}$$

$$\qquad (12.26)$$

$$D_2^{(1)} = \lim_{\Delta t \to 0} \frac{E[\Delta X_2]}{\Delta t}$$

$$D_{11}^{(2)} = \lim_{\Delta t \to 0} \frac{E[\Delta X_1^2]}{\Delta t} = 0$$

$$D_{12}^{(2)} = D_{21}^{(2)} = \lim_{\Delta t \to 0} \frac{E[\Delta X_1 \Delta X_2]}{\Delta t} = 0 \qquad (12.27)$$

$$D_{22}^{(2)} = \lim_{\Delta t \to 0} \frac{E[\Delta X_2^2]}{\Delta t}.$$

Substituting Eq. 12.25 for $E[\Delta X_2]$ and $E[\Delta X_2^2]$ and using τ as a dummy variable in t gives

$$D_2^{(1)} = \lim_{\Delta t \to 0} \frac{E\left[\left\{-\beta X_2(t) - F(X_1(t))\right\}\Delta t + \int_t^{t+\Delta t} f(t)dt\right]}{\Delta t}$$

$$= -\beta X_2 - F(X_1) \qquad (12.28)$$

$$D_{22}^{(2)} = \lim_{\Delta t \to 0} \frac{E\left[\left\{ \left\{ -\beta X_2(t) - F(X_1(t)) \right\} \Delta t + \int_t^{t+\Delta t} f(t) d\tau \right\}^2 \right]}{\Delta t}$$

$$= \lim_{\Delta t \to 0} E\left[\left\{ -\beta X_2 - F(X_1) \right\}^2 \Delta t + 2\left\{ -\beta X_2 - F(X_1) \right\} \int_t^{t+\Delta t} f(\tau) d\tau \right]$$

$$+ \lim_{\Delta t \to 0} E\left[\frac{1}{\Delta t} \int_t^{t+\Delta t} \int_t^{t+\Delta t} f(\tau_1) f(\tau_2) d\tau_1 d\tau_2 \right]$$

$$= \frac{W_0}{2} . \tag{12.29}$$

Now, the process is stationary, so with Eq. 12.19, the Fokker–Planck equation becomes

$$\frac{W_0}{4} \frac{\partial^2 p}{\partial x_2^2} - \frac{\partial}{\partial x_1}(x_2 p) + \frac{\partial}{\partial x_2}\left[\left\{ \beta X_2 + F(X_1) \right\} p \right] = 0 . \tag{12.30}$$

This is called the stationary case for Kramer's equation and has been solved by several scholars. Following Caughey–Wu, the solution of Eq. 12.30 is

$$p(x_1, x_2) = p(x, \dot{x}) = C \, \exp\left[-\frac{4\beta}{W_0} \left\{ \frac{x_2^2}{2} + \int_0^{x_1} F(\zeta) d\zeta \right\} \right]. \tag{12.31}$$

Here C is the coefficient for normalization and ζ is a dummy variable for x_1. Equation 12.31 is in the form of

$$p(x, \dot{x}) = C \, \exp\left\{ -4\beta \cdot \frac{E}{W_0} \right\}, \tag{12.32}$$

where E is the total energy per unit mass of this system

333

$$E = \frac{\dot{x}^2}{2} + \int_0^x F(\zeta)d\zeta. \tag{12.33}$$

From Eq. 12.31

$$p(x, \dot{x}) = p(x)p(\dot{x}), \tag{12.34}$$

and

$$p(\dot{x}) = \exp\left\{\frac{-2\beta}{W_0}\dot{x}^2\right\} \tag{12.35}$$

$$p(x) = C \exp\left[-\frac{4\beta}{W_0}\int_0^{x_1} F(\zeta)d\zeta\right], \tag{12.36}$$

we find the probability distribution density function of the velocity $\dot{x}$ is a Gaussian.

More concretely, for a nonlinear spring system, $F\{X(t)\}$ in Eq. 12.20 is

$$F\{X_1(t)\} = F\{X(t)\} = \omega_0^2\Big[X(t) + \epsilon g\{X(t)\}\Big] \tag{12.37}$$

and the equation of oscillation Eq. 12.20 is

$$\ddot{X}(t) + \beta\dot{X}(t) + \omega_0^2\Big[X(w) + \epsilon g\{X(t)\}\Big] = f(t). \tag{12.38}$$

Here for hard spring type, $\epsilon > 0$, and ϵ is on the order of $x(t)/g\{x(t)\}$, $g\{x(t)\} = -g\{-x(t)\}$, and as $|x(t)| > 0$, $x(t)g\{x(t)\} > 0$. Now we define ω_0 as the undamped (when $\beta = 0$) natural frequency of oscillation.

The mean square value of this oscillation is

334

$$E\{X^2(t)\} = \int\limits_{-\infty}^{\infty} x^2 p(x, \dot{x}) dx d\dot{x}$$

$$= \int\limits_{-\infty}^{\infty} \left[x\{x + \epsilon g(x)\} - x\epsilon g(x) \right] p(x) dx. \tag{12.39}$$

From Eq. 12.36 and Eq. 12.37

$$p(x) = C \exp\left\{ -\frac{1}{\sigma_{\dot{x}}^2} \int\limits_0^x F(\zeta) d\zeta \right\} = C \exp\left[-\frac{1}{\sigma_{\dot{x}}^2} \left\{ \frac{x^2}{2} + \epsilon G(x) \right\} \right]$$

$$G(x) = \int\limits_0^x g(\zeta) d\zeta.$$

For a corresponding linear system, $\sigma_{X_0}^2 = \dfrac{W_0}{4\beta\omega_0^2}$

$$\sigma_{\dot{X}_0}^2 = \frac{W_0}{4\beta}.$$

For the linear system, $\epsilon = 0$; therefore from Eq. 12.39,

$$E[X^2(t)] \approx \sigma_{X_0}^2 - \int\limits_{-\infty}^{\infty} x\epsilon g(x) \, p(x) dx$$

$$\approx \sigma_{X_0}^2 - \epsilon \, E\left[x(x) \, g\{x(t)\} \right]. \tag{12.40}$$

For a hard spring system the mean square of the displacement is always smaller than it is for the corresponding linear system.

For the so–called Duffing type system, $g\{X(t)\} = X^3(t)$, and the equation of motion is

$$\ddot{X}(t) + \beta\dot{X}(t) + \omega_0^2 \left\{ X(t) + \epsilon X^3(t) \right\} = f(t). \tag{12.41}$$

335

Therefore from Eq. 12.40

$$E[X^2(t)] \approx \sigma_{x_0}^2 - \epsilon E[X^4(t)].$$ (12.42)

For the Gaussian process $E[X^4(t)] = 3\sigma_x^4$. Therefore in this case, the order is also in

$$E[X^2(t)] \approx \sigma_{x_0}^2 - 3\epsilon\sigma_x^4.$$ (12.43)

It is interesting to find that this approximation is the same type as Eq. 10.17 obtained through the equivalent linearization method and Eq. 10.50 obtained through the perturbation method.

12.5 PROBABILITY CHARACTERISTICS OF AMPLITUDES, MAXIMA AND MINIMA

S. O. Rice[9] has shown that, when the joint probability density function of x and

$\dot{x}$, the values of a stochastic process $X(t)$ at time t, and its derivative $(d/dt)X(t)$, i.e.,

$p(x,\dot{x})$, are known, the frequency of occurrence of any threshold value crossing or zero crossing is easily derived.

For example, the expected value of the frequency of occurrence of the process $X(t)$ for the upward crossing of a threshold of level a, $E[N_+(a)]$, is

$$E[N_+(a)] = \int_0^\infty \dot{x}p(a,\dot{x})d\dot{x}.$$ (12.44)

If $x(t)$ and $\dot{x}(t)$ are independent, $p(x,\dot{x}) = p(x) \cdot p(\dot{x})$, therefore

$$\frac{E[N_+(a)]}{E[N_+(0)]} = \frac{[p(x)]_{x=a}}{[p(x)]_{x=0}}.$$ (12.45)

When the power spectrum is narrow banded, the amplitude of the sample process varies slowly, just like the envelope of sine waves, and as the result, the process is assumed to have an extreme positive value a_p at each cycle of this sine wave.

Then the probability distribution is

$$P_p(a_p > a) = \frac{E[N_+(a)]}{E[N_+(0)]} = 1 - P(a_p \leq a).$$ (12.46)

Therefore, the probability density distribution is

336

$$p_p(a) = -\frac{dP}{da} = -\left(\frac{1}{E[N_+(0)]}\right)\left\{\frac{d(E[N_+(a)])}{da}\right\}. \qquad (12.47)$$

When $X(t)$ and $\dot{X}(t)$ are independent,

$$p_p(a) = -\frac{\left[\dfrac{dp(x)}{dx}\right]_{x=a}}{p(0)}. \qquad (12.48)$$

Expanding this kind of relation, Longuet–Higgins,[12] and Cartwright and Longuet–Higgins,[13] developed the well–known results for the distribution function of extreme values of a general process with various bandwidths.

The probability distribution density function for extreme values of a process $X(t)$, or $\xi_1, \xi_2, \ldots$ normalized by the standard variation of the original process σ_x, as $\xi/m_0^{1/2} = \xi/\sigma_x = \zeta$ was derived as,

$$p(\zeta) = \frac{1}{\sqrt{2\pi}}\left[\epsilon e^{-\frac{\zeta^2}{2\epsilon^2}} + (1-\epsilon^2)^{\frac{1}{2}}\zeta e^{-\frac{\zeta^2}{2}}\int\limits_{-\infty}^{\frac{\zeta(1-\epsilon^2)^{\frac{1}{2}}}{\epsilon}} e^{-\frac{u^2}{2}}\,du\right] \qquad (12.49)$$

as shown in Fig. 12.1, where ϵ is the so–called bandwidth parameter of the spectrum

$$\epsilon = \frac{(m_0 m_4 - m_0^2)}{m_0 m_4}, \qquad (12.50)$$

m_n being the moment of spectrum

$$m_n = \int\limits_{-\infty}^{\infty} \omega^n s(\omega)\,d\omega. \qquad (12.51)$$

When $\epsilon \approx 0$, as for a narrow banded spectrum, $p(\zeta)$ becomes a Rayleigh distribution as is well known,

$$p(\zeta) = \begin{cases} \zeta e^{-\frac{\zeta^2}{2}} & \zeta \geq 0 \\ 0 & \zeta < 0 \end{cases} \qquad (12.52)$$

or

337

or

$$p(\zeta) = \begin{cases} \dfrac{\zeta}{\sigma_x^2} \, e^{-\frac{\zeta^2}{2\sigma_x^2}} & \zeta \geq 0 \\[2ex] 0 & \zeta < 0 \end{cases}.$$ (12.52')

At the other extreme, when $\epsilon = 1$, as when ripples are superimposed on slowly varying waves,

$$p(\zeta) = \frac{1}{\sqrt{2\pi}} \, e^{-\frac{\zeta^2}{2}}$$ (12.53)

$$p(\zeta) = \frac{1}{\sqrt{2\pi}\,\sigma_x} \, e^{-\frac{\zeta^2}{2\sigma_x^2}} = p(x),$$ (12.53')

namely $p(\zeta)$ becomes Gaussian and it is the same as the Gaussian distribution that governs the original process $x(t)$.

When ϵ is between 0 and 1, $p(\zeta)$ is given by Eq. 12.49 and is between the Rayleigh and Gaussian distributions, as shown in Fig. 12.1, and is now popular for us.
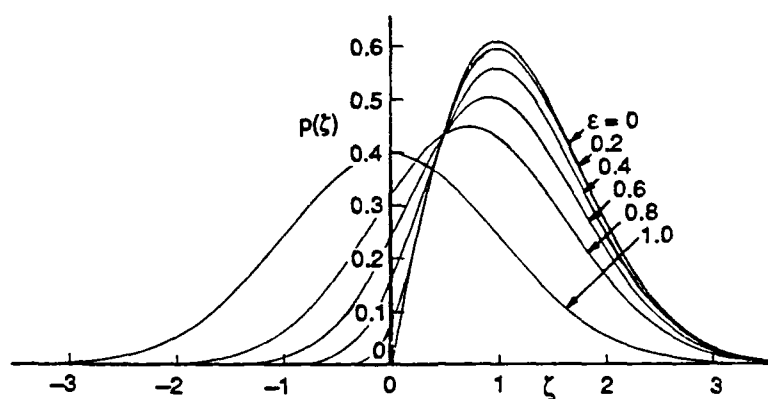
Fig. 12.1. Probability distribution density function of extremes.
(From Cartwright, Longuet–Higgins.[13])

From this distribution, the expected highest value of $1/n$ and the expected highest values of N independent samples have been derived as functions of ϵ. The derivation will not be referred here, as they are well known.

338

Equations 12.46 and 12.47 can be applied to a nonlinear process as long as the process is narrow banded. Crandall[84] analyzed a hardened spring oscillation system, the same as the one analyzed by Caughey[83] utilizing the Fokker–Planck equation, as was shown in Section 12.4. Equation of motion is by Eq. 12.20,

$$\ddot{X}(t) + \beta\dot{X}(t) + F\{X(t)\} = f(t).$$

He obtained the average period $\tau(a)$, the probability distribution function of the peak values $p_p(a)$, and the probability distribution function of the envelope $p_e(a)$ as functions of the amplitude a by introducing the potential energy per unit mass

$$V(x) = \int_0^x F(\zeta)d\zeta. \tag{12.54}$$

The solution of the Fokker–Planck equation, Eq. 12.31 (when $f(x)$ is Gaussian) is

$$p(x,\dot{x}) = C \exp\left[-\frac{1}{\sigma_{\dot{x}}^2}\left\{\frac{\dot{x}^2}{2} + V(x)\right\}\right], \tag{12.55}$$

where C is a normalizing constant that makes

$$\int_{-\infty}^{\infty} \int_{-\infty}^{\infty} p(x,\dot{x}) \, dx \, d\dot{x} = 1.$$

The results are, as for the envelope process $a(t)$,

$$V(a) = \frac{1}{2}\dot{x}^2 + V(x), \tag{12.56}$$

$$P(a_e < a) = 4 \int_0^a dx \int_0^{[2\{V(a)-V(x)\}]^{\frac{1}{2}}} p(x,\dot{x}) \, d\dot{x} \tag{12.57}$$

339

$$p_e(a) = \frac{dP}{da} = 4F(a) \int_0^a \left[2\{V(a) - V(x)\}\right]^{\frac{1}{2}} \, p\left(x, \left[2\{V(a) - V(x)\}\right]^{\frac{1}{2}}\right) \, dx. \quad (12.58)$$

Through manipulation, the following were derived:

$$p_e(a) = C \cdot \tau(a) \cdot F(a) \, \exp\left\{-\frac{V(a)}{\sigma_{\dot{x}}^2}\right\} = p_p(a) v_0^+ \tau(a) \quad (12.59)$$

and also,

$$p_p(a) = F(a) \cdot \sigma_{\dot{x}}^{-2} \exp\left\{-\frac{V(a)}{\sigma_{\dot{x}}^2}\right\}, \quad (12.60)$$

where v_0^+ is the expected number of threshold crossings per unit time of the level $x = 0$ with positive slope, and can be derived as $v_0^+ = C\sigma_{\dot{x}}^2$; $\tau(a)$ is the average period as a function of amplitude a.

Crandall showed the general solution for the following two nonlinear cases:

   i)   for a hard spring Duffing type system,

$$F\{X(t)\} = \omega_0^2 \left\{X(t) + \epsilon X^3(t)\right\}, \quad (12.61)$$

   ii)   for a set–up spring system, as in Fig. 12.2,

$$F\{X(t)\} = \omega_0^2 \left\{X(t) + \epsilon \, sgn \, X(t)\right\}, \quad (12.62)$$
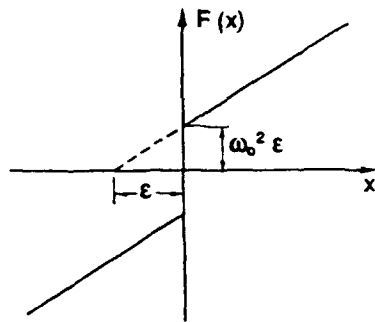
Fig. 12.2. Displacement–force relation of set–up spring.

as are shown in Figs. 12.3 and 12.4. Here σ_x is the standard variation of the linear system

when $\epsilon = 0$. These figures show that the probability distribution of extreme $p_p\left(\dfrac{a}{\sigma_x}\right)$

varies considerably with the extent of nonlinearity, expressed by the value of ϵ.
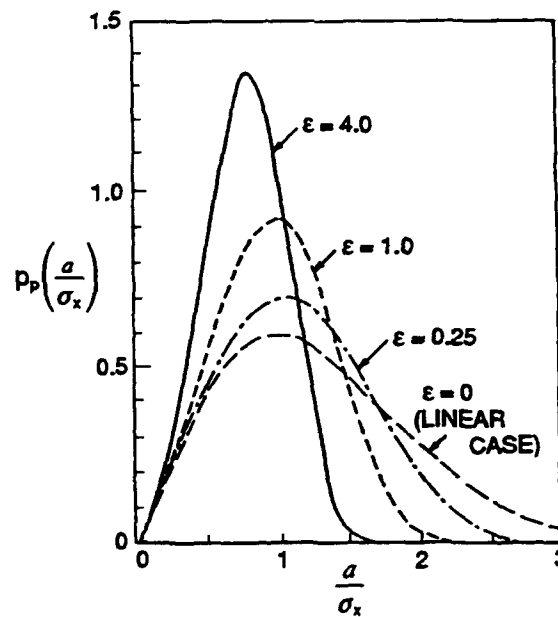
Fig. 12.3. Probability distribution density of the extreme (peak)
values of Duffing type oscillator.
(From Crandall.[84])

341
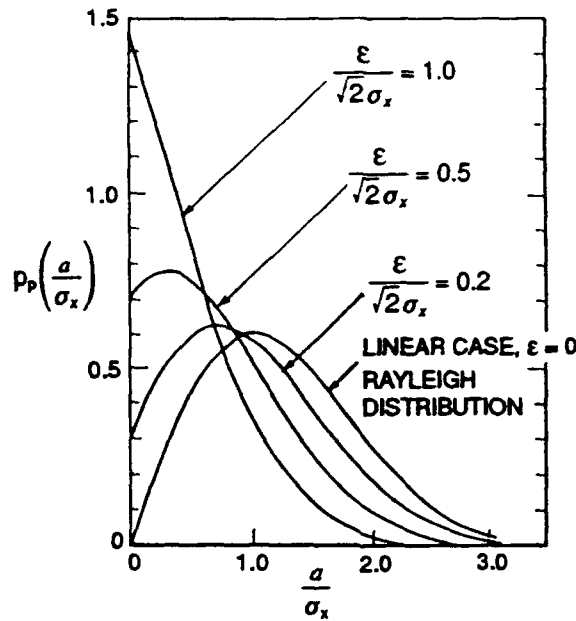
Fig. 12.4. Probability distribution density of the extreme (peak) values of oscillator with set–up springs.

(From Crandall.[84])

12.6 APPLICATION OF THE FOKKER–PLANCK EQUATION FOR THE ANALYSIS OF SEAKEEPING DATA

As has already been mentioned, the Fokker–Planck equations have been solved only for a restricted number of cases, and this has made the applicability of this equation rather difficult in many engineering fields. For example, this method was applied to the nonlinear system with nonlinear restoring terms and with Gaussian white excitation, as shown in the preceding section, but the method has been considered inapplicable to the system with nonlinear damping or with colored noise excitation. A few efforts have been made to overcome these difficulties, for example by J. B. Roberts.[59] His work,[60,61] especially in the analysis of nonlinear seakeeping data, will be summarized briefly.

12.6.1 Nonlinear Analysis of Slow Drift Oscillation of Moored Vessels in Random Seas

Utilizing the known characteristics of the Fokker–Planck equation, Roberts[60] analyzed the statistical behavior of the nonlinear slow drift motion of moored vessels. Assuming that the waves $\eta(t)$ are narrow banded with band width parameter ϵ, and that the drifting force $D(t)$ can be regarded as proportional to the square of the wave height, he modified the expression of wave height $\eta(t)$ and drifting force $D(t)$ to

$$\eta(t) = H(t) \cos [\omega_0 t + \sigma(t)] = hA(t) \cos [\omega_0 t + \sigma(t)]$$

$$= h\left[\left\{a^2(t) + b^2(t)\right\}^{1/2}\right] \cos [\omega_0 t + \sigma(t)]$$

$$= h[a(t) \cos \omega_0 t - b(t) \sin \omega_0 t], \tag{12.63}$$

here ω_0 is the peak frequency of the narrow banded spectrum of the wave, and

$$D(t) = \alpha[H^2(t)] = \alpha'[a^2(t) + b^2(t)] = \overline{D} + k'\xi(t), \qquad (12.64)$$

where $H(t)$, $hA(t)$ are the amplitudes of the envelope; $a(t)$ and $b(t)$ are components of $A(t)$; $\sigma(t)$ is the phase lag; $\overline{D}$ is the mean drifting force; and $\xi(t)$ is the white noise, as will be assumed later.

The equation of swaying motion of the vessel was expressed as

$$(M + m)\ddot{x} + F(x, \dot{x}) = D(t) \qquad (12.65)$$

or

$$\ddot{x} + f(x, \dot{x}) = \beta[a^2(t) + b^2(t)] \qquad (12.66)$$

where $(M + m)$ is the virtual mass of the vessel. Then with $a(t)$, $b(t)$ as the output of white noise $\xi(t)$ through linear filters, the equation of motion was modified to

$$\dot{z} + f(z) = \xi(t). \qquad (12.67)$$

The term z is a vector Markov process with four elements $[x, \dot{x}, a, b]$, and the Fokker–Planck equation of this four–element variable $z(t)$ was then derived. Then since $A(t)$ can be generated as the output of a nonlinear first–order system with a white noise input $\xi(t)$, the process was inverted into a three–element vector Markov process, $y(t)[x(t), \dot{x}(t), A(t)]$, and the Fokker–Planck equation for this process was also derived.

However, the solution of the multidimensional Fokker–Planck equation has a number of difficulties, so Roberts advanced the approximation further, and expressed the drifting force as

$$D(t) \doteq \overline{D} + k'\xi(t), \qquad (12.68)$$

the sum of the mean drifting force $\overline{D}$, that can be approximated as $\alpha'\epsilon$, plus a white noise.

Under these approximations, the equation of swaying motion is

$$\ddot{x} + g(x, \dot{x}) = d + k\xi(t), \qquad (12.69)$$

where $d = \dfrac{\overline{D}}{(M + m)} = \dfrac{\alpha'\epsilon}{(M + m)} = \beta\epsilon,$

$k = \dfrac{k'}{(M + m)}.$

The two–dimensional Fokker–Planck equation was derived as

$$\frac{\partial p}{\partial t} = -\frac{\partial}{\partial Z_1}(Z_2, p) + \frac{\partial}{\partial Z_2}(g, p) + \frac{k^2}{2}\frac{\partial^2 p}{\partial Z_2^2} \qquad (12.70)$$

where $Z_1 = x$, $Z_2 = \dot{x}$, and p is the transitional probability density function.

The stationary solution of p is obtained by $(\partial p/\partial t) = 0$. As $g(x, \dot{x})$ in Eq. 12.69, in its general form

$$g(x, \dot{x}) = \gamma F(x, \dot{x}) + G(x), \qquad (12.71)$$

is used.

Then the joint probability density function of swaying motion $p(x, \dot{x})$ is the solution of Eq. 12.70, when $(\partial p/\partial t) = 0$,

$$p(x, \dot{x}) = C \ \exp\left[-\frac{\gamma}{k^2}Q\left\{\frac{\dot{x}^2}{2} + U(x) - dx\right\}\right] \qquad (12.72)$$

where

$$U(x) = \int_0^x G(\lambda)d\lambda \qquad (12.73)$$

is the potential energy for restoring forces, C is a normalization constant, and

$$Q(v) = \int_0^v \frac{B(\lambda)}{C(\lambda)}d\lambda. \qquad (12.74)$$

Here

$$B(v) = \frac{1}{\sqrt{2}A(v)} \int_R F(x)\sqrt{2(v - U(x))}\,dx \qquad (12.75)$$

$$C(v) = \frac{1}{A(v)} \int_R \sqrt{v - U(x)}\,dx \qquad (12.76)$$

344

$$A(v) = \frac{1}{2} \int\limits_{R} \frac{dx}{\sqrt{v - U(x)}} . \tag{12.77}$$

The integration range R is such that $U(x) < v$. Especially for Duffing type oscillation the equation of motion, Eq. 12.69, is expressed by

$$\ddot{x} + 2\zeta\dot{x} + x + \lambda x^3 = \frac{\beta\epsilon}{\omega_n^2} + \frac{k}{\omega_n^{3/2}} \xi(\tau). \tag{12.78}$$

Here t is replaced by nondimensional time τ, $\tau = \omega_n t$, ω_n being the undamped natural frequency in the linear case ($\lambda = 0$), and the nondimensionalized equation is

$$\ddot{x}' + 2\,\zeta\dot{x}' + x' + \lambda^* \, x'^3 = d^* + 2\,\zeta^{1/2}\xi(\tau), \tag{12.79}$$

where the differentiation is with respect to τ and

$$x' = \frac{x}{\sigma_x}, \quad \lambda^* = \frac{\lambda}{\sigma_x^3}, \quad d^* = \frac{2\beta\epsilon}{k} \left(\frac{\zeta}{\omega_n}\right)^{1/2} = \left[\frac{\zeta(1 + 4\epsilon^{*2})}{\epsilon^*}\right]^{1/2}, \quad \epsilon^* = \frac{\epsilon}{\omega_n}.$$

The joint density distribution for $p(x', \dot{x}')$ and the probability density distribution function $p(x')$ is, from Eq. 12.72,

$$p(x', \dot{x}') = C \, \exp\left[-\left\{\frac{\dot{x}'^2}{2} + \frac{x'^2}{2} + \frac{\lambda^* x'^4}{4} - d^* x'\right\}\right] \tag{12.80}$$

and

$$p(x') = \int\limits_{-\infty}^{\infty} p(x', \dot{x}')dx' \doteq \sqrt{2\pi} \, C \, \exp\left[-\left\{\frac{x'^2}{2} + \frac{\lambda^* x'^4}{4} - d^* x'\right\}\right]. \tag{12.81}$$

Here C is a coefficient for normalization,

$$\int\limits_{-\infty}^{\infty} \int\limits_{-\infty}^{\infty} p(x', \dot{x}')dx'd\dot{x}' = 1.$$

Roberts calculated numerically, for a Duffing type system, with various ζ, λ^*, and ϵ^* and compared them with the simulated results. Figure 12.5 shows an example of his results. He compared $p(x)$ calculated by Eq. 12.81 under the white noise approximation with the result obtained by simulated data and found that the agreement is good and quite different from the Gaussian distribution for $\lambda^* = 0$. Once $p(x)$ of the displacement $x(t)$ is determined, $p(T)$, the probability distribution of tension on the mooring, can be derived as

$$p(T) \approx \frac{p(x)}{\left|\dfrac{dw}{dx}\right|}, \tag{12.82}$$

where the tension is expressed by

$$T = w(x). \tag{12.83}$$
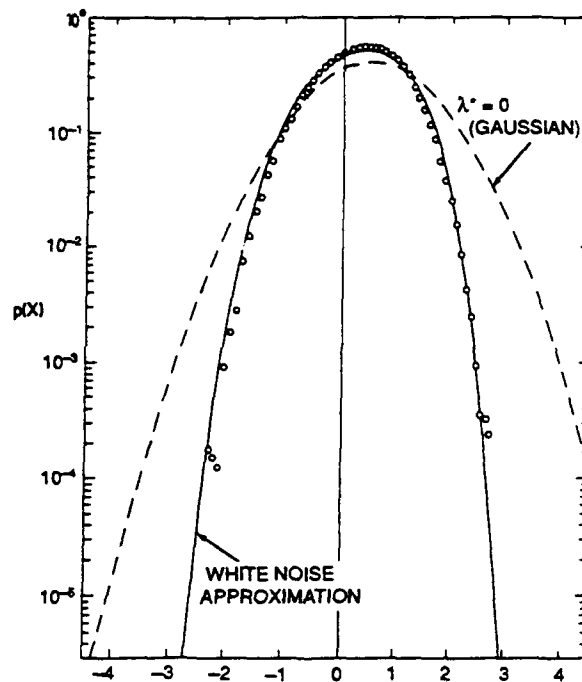
Fig. 12.5. Probability density function for displacement response; $\lambda^* = 0.5, \zeta = 0.05, \epsilon^* = 1.0$, o digital simulation estimate. (From Roberts.[60])

346

12.6.2 Stationary Response of Oscillations with Nonlinear
Damping to Random Excitation

As was mentioned at the beginning of this section, the Fokker–Planck equation has been solved only for restricted cases, such as nonlinear systems with nonlinear restoring forces or systems under white noise excitation. Roberts[59] removed these restrictions and studied the behavior of the Fokker–Planck equation for a system with nonlinear damping. For a nonlinear system with nonlinear damping, the equation of motion is

$$\ddot{x} + \beta F(x, \dot{x}) + G(x) = n(t), \tag{12.84}$$

where β is small, F is an odd function of $\dot{x}$ (odd as was used by Dalzell[81] is more convenient to manipulate), and $n(t)$ is white noise, $G(x)$ being the restoring term.

The two–dimensional Fokker–Planck equation for

$$p(x, \dot{x}) = p(x, y|x_0, y_0; t)$$

is the same as Eq. 12.30, for Eq. 12.20 in the form,

$$\frac{\partial p}{\partial t} = -y\frac{\partial p}{\partial x} + \frac{\partial}{\partial y}\left[\left[\beta F(x, y) + G(x)\right]p\right] + \frac{I}{2}\frac{\partial^2 p}{\partial x^2} \tag{12.85}$$

and is difficult to solve for general $F(x, y)$, so Roberts inverted this two–dimensional Fokker–Planck equation into a one–dimensional Fokker–Planck equation, introducing a physical variable called the energy envelope $V(t)$

$$V(t) = \frac{1}{2}\dot{x}^2 + U(x), \tag{12.86}$$

therefore $\dot{x} = \sqrt{2V(t) - U(t)}$ where $U(x) = \int_0^x G(\xi)d\xi$.

The one–dimensional Fokker–Planck equation for $p(v) = p(v|v_0; t)$ is in the form

$$\frac{\partial p}{\partial t} = \frac{\partial}{\partial v}\left[\left\{\beta B(v) - \frac{I}{2}\right\}p\right] + \frac{I}{2}\frac{\partial^2}{\partial v^2}[C(v)p] \tag{12.87}$$

where I is the strength of excitation as $I = \frac{W_o}{2}$ in Eq. 12.22 or Eq. 12.29, and

$B(v)$, $C(v)$ are as in Eqs. 12.75–12.77

$$B(v) = \frac{1}{\sqrt{2} A(v)} \int_R F\left\{ x \sqrt{2(v - U(x))} \right\} dx$$

$$C(v) = \frac{1}{\sqrt{2} A(v)} \int_R \sqrt{(v - U(x))} \, dx$$

$$A(v) = \frac{1}{2} \int_R \frac{dx}{\sqrt{v - U(x)}}.$$

The integration range R is such that $U(x) < v$. The general stationary solution is given as

$$p(v) = \lim_{t \to \infty} p(v|v_0; t) \approx kA(v) \exp\left\{ -\left(\frac{2\beta}{I} Q(v) \right) \right\} \qquad (12.88)$$

where

$$Q(v) = \int_0^v \frac{B(\xi)}{C(\xi)} d\xi \qquad (12.89)$$

and k is a normalizing constant. Then, from the relation of v, x, $y(= \dot{x})$ and reverting to the original x, y variables,

$$p(x, y) = \lim_{t \to \infty} p(x, y|x_0, y_0; t) = C \, \exp\left\{ -\left(\frac{2\beta}{I} \right) Q\left[\frac{1}{2} y^2 + U(x) \right] \right\}. \qquad (12.90)$$

When the equation of motion is expressed as

$$\ddot{x} + 2\zeta_0 \omega_0 \dot{x}(1 + \epsilon |\dot{x}|^n) + \omega_C^2 \, x = n(t), \qquad (12.91)$$

now ω_0 being the natural frequency of the linear ($\epsilon = 0$) system, Eq. 12.90 becomes

$$p(x, y) = C \, p_0(x, y) \exp\left\{ -\alpha_n \epsilon^* \left[\frac{1}{2} (x^2 + y^2) \right]^{\frac{n+2}{2}} \right\}$$

where

$$\epsilon^* = \epsilon \omega_0^n \sigma_0^n, \quad p_0(x, y) = \frac{1}{2\pi} \exp\left\{ -\frac{1}{2}(x^2 + y^2) \right\} \tag{12.92}$$

$$x = \frac{x(t)}{\sigma_0}, \quad y = \frac{\dot{x}(t)}{\omega_0 \sigma_0}, \quad \sigma_0 = \left(\frac{I}{4} \zeta_0 \cdot \omega_0^3 \right)^{1/2},$$

σ_0 is the standard deviation of response when $\epsilon = 0, \epsilon^* = \epsilon/\omega_0$ is the nondimensional nonlinearity parameter, and $p_0(x, y)$ is the result when $\epsilon^* = 0$ ($C = 1$ when $\epsilon^* = 0$).

From this result, the statistical moments of the response can be calculated. For example, Roberts obtained

$$\frac{\sigma^2}{\sigma_0^2} = 2\theta \left\{ \left[\sqrt{\pi} \ e^{\theta^2}(1 - \text{erf } \theta) \right]^{-1} - \theta \right\} \tag{12.93}$$

$$\theta = \frac{1}{(3\epsilon^*)^{1/2}}.$$

He calculated the equivalent linear damping, as discussed in Section 10.1, using the general expression Eq. 12.91 and calculated

$$\frac{\sigma^2}{\sigma_0^2} = \frac{(\sqrt{1 + 12\epsilon^*} - 1)}{6\epsilon^*} \tag{12.94}$$

for $n = 2$ in Eq. 12.91, which is a closer approximation of σ^2 than Eq. 10.17. He also calculated the corresponding perturbation solution as

$$\frac{\sigma^2}{\sigma_0^2} = 1 - 3\epsilon^*. \tag{12.95}$$

This is slightly different from Eq. 10.50, which was shown for small ϵ. All three results are compared in Fig. 12.6. Robert calls his method, which introduced the energy envelope $V(t)$ as Eq. 12.86, the Markov envelope theory, and indicated in Fig. 12.6 as ME theory.

349
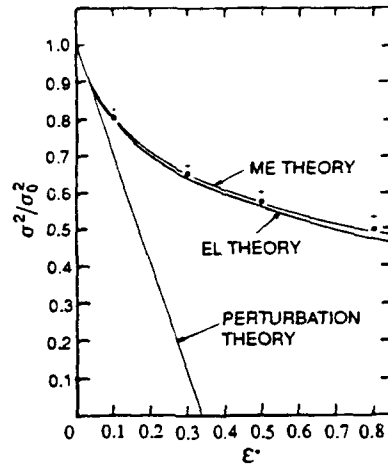
Fig. 12.6. Variation of the mean square of the response with ϵ^*.
Simulation results: $\cdot$ $\zeta_0 = 0.05$, $+$ $\zeta_0 = 0.50$.
(From Roberts.[59])

The equivalent linearization theory is abbreviated as EL theory. In this figure, only the perturbation theory appears different from the rest, but here we have to remember that in the perturbation method this is the first order approximation and we can improve the approximation by increasing the order of the approximation, as indicated in the discussion in Section 10.2.2.

12.6.3 Nonlinear Oscillation in Nonwhite Excitation

Roberts[61] further extended the scope of applicability of this method and solved for nonlinear rolling in nonwhite excitation. The equation of motion is now

$$I\ddot{\phi} + \beta C(\dot{\phi}) + k(\phi) = M(t) \tag{12.96}$$

or

$$\ddot{\phi} + \beta F(\dot{\phi}) + G(\phi) = x(t) \tag{12.96'}$$

where $x(t)$ is a nonwhite excitation, and can have a colored spectrum.

Again, he adopted the total energy envelope as Eq. 12.86

$$V = \frac{\dot{\phi}^2}{2} + U(\phi)$$

where

$$U(\phi) = \int_0^{\phi} G(\xi)d\xi$$

and considered that this was slowly varying.

350

He set

$$\frac{\dot{\phi}^2}{2} = -V\sin^2\theta \qquad\qquad \dot{\phi} = -\sqrt{2}\,V^{\frac{1}{2}}\sin\theta$$

or   (12.97)

$$U(\phi) = V\cos^2\theta \qquad\qquad U(\phi)^{\frac{1}{2}} = V^{\frac{1}{2}}\cos\theta$$

introducing the phase θ as shown in Fig. 12.7. After manipulation of the relations, the equation of motion, Eq. 12.96', was inverted into the equation of $\dot{V}$ and $\dot{\phi}$. When the phase process θ was modified into a process $\lambda(t)$, and the joint process $Z = (V, \lambda)$ was made to converge into a Markovian process, the transitional distribution function $p(Z|Z_0; t)$ was found to be governed by a Fokker–Planck equation of second order. The stationary solution of the Fokker–Planck equation $p(Z)$ was obtained, and from this expression V and λ were found to be uncoupled, and $p(V)$ was calculated. With the relations of V, ϕ and $\dot{\phi}$, $p(V)$ was modified into $p(\phi, \dot{\phi})$.
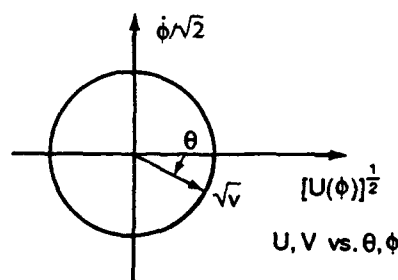
Fig. 12.7. U, V vs. θ, ϕ.
(From Roberts.[61])

For nondimensionalized, nonlinear rolling expressed as

$$\ddot{\phi} + a\dot{\phi} + b|\dot{\phi}|\,\dot{\phi} + \phi - \phi^3 = x(t),$$ (12.98)

Roberts calculated the probability density function of the nondimensionalized amplitude of rolling A by the ME theory and compared it with the Rayleigh distribution obtained by the linear theory as in Fig. 12.8. He[61,86] also compared his results with the nonlinear simulated data obtained by J.F. Dalzell[65] to show the validity of his method. Examples are shown in Figs. 12.9 through 12.11 for a variety of damping coefficients a and b, where $\Omega = \omega_p/\omega_0$, ω_p is the peak frequency of the excitation, and σ_w is standard deviation of the input process $x(t)$. Process 3 in the figures is a wide banded excitation for this example. He showed many other results of comparison for other types of excitation with

351

different bandwidths, named Process 1 and Process 2, used in the simulation by J.F. Dalzell.[85] The deviation from the Rayleigh distribution in Figs. 12.8 to 12.11, and the relation of the standard deviation of roll σ_R to that of input σ_w in Fig. 12.12 shows the extent of nonlinearity. The applicability of the method was also discussed.
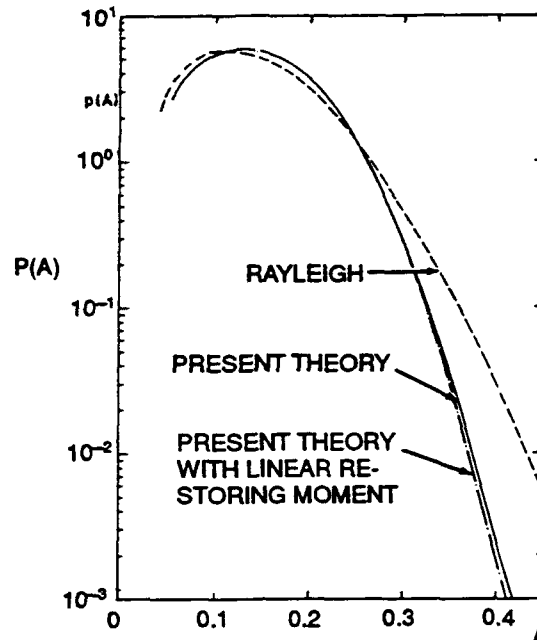
Fig. 12.8. Probability density function for amplitude A:
$a = 0$, $b = 1$, $\sigma_w = 0.036$, $\Omega = 0.90$,
Process 3. (From Roberts.[61])
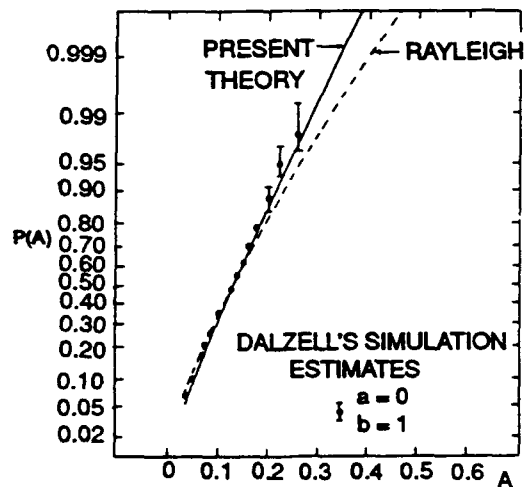
Fig. 12.9. Cumulative probability distribution for amplitude A:
$a = 0$, $b = 1$, $\sigma_w = 0.036$, $\Omega = 0.90$,
Process 3. (From Roberts.[61])

352
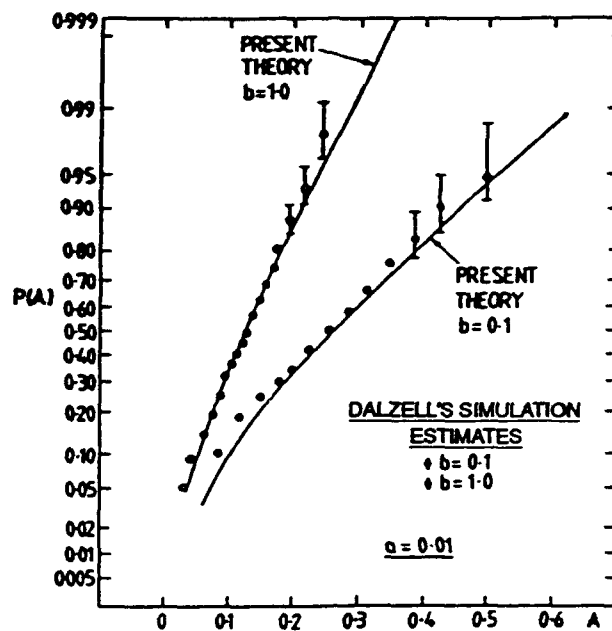
Fig. 12.10. Cumulative probability distribution for amplitude A:
$a = 0.01$, $\sigma_w = 0.036$, $\Omega = 0.90$, $b = 0.1$ and 1.0;
Process 3. (From Roberts.[61])
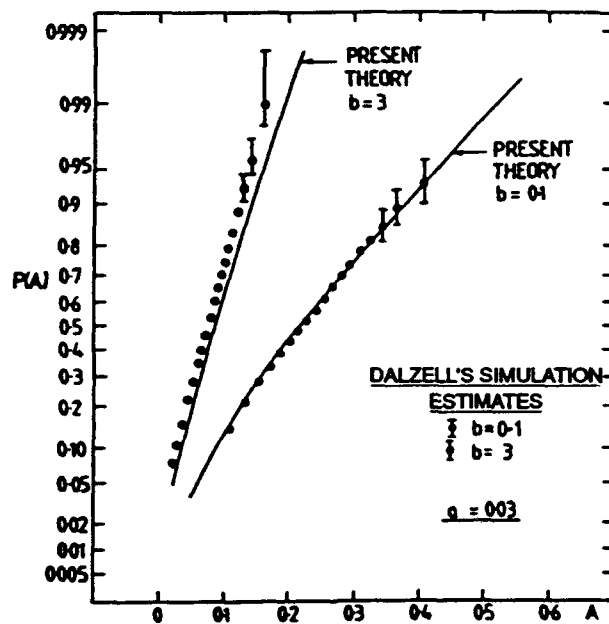
Fig. 12.11. Cumulative probability distribution for amplitude A:
$a = 0.03$, $\sigma_w = 0.036$, $\Omega = 0.90$, $b = 0.1$ and 3.0;
Process 3. (From Roberts.[61])

353
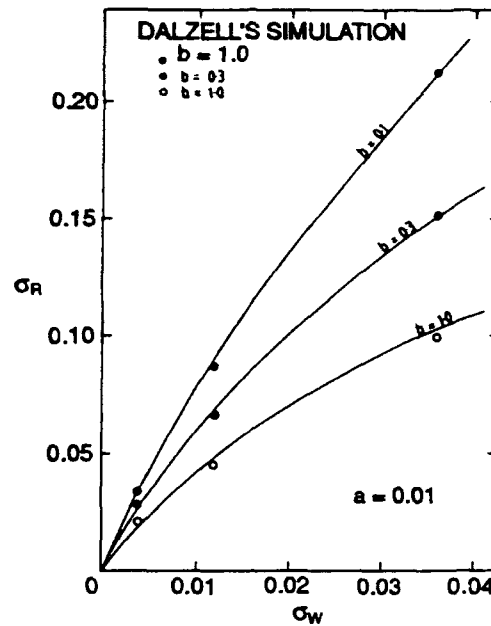
Fig. 12.12. Variation of standard deviation of roll σ_R with standard deviation of wave input σ_w: $a = 0.01$; $\Omega = 0.90$; $b = 0.1, 0.3,$ and 1.0; Process 3. (From Roberts.[61])

12.7 PROBABILITY DENSITY FUNCTIONS OF AMPLITUDES, EXTREME VALUES IN RELATION WITH THE FUNCTIONAL POLYNOMIALS

12.7.1 Narrow–Banded Case

As was mentioned in Section 11.1, when a nonlinear response $z(t)$ was expanded by the Voltera expansions (or functional expansions)

$$z(t) = \sum_{n=1}^{\infty} \underbrace{\iint \ldots \int_{-\infty}^{\infty}}_{n} g_n(\tau_1, \tau_2 \ldots \ldots \tau_n) \; x(t-\tau_1)x(t-\tau_2) \times$$

$$\ldots \ldots x(t-\tau_n) \; d\tau_1 \; d\tau_2 \ldots \ldots d\tau_n, \quad (12.99)$$

the terms for $n \geq 2$ can be considered as the modifying terms of the Taylor expansion of this process around its linear term for $n=1$. If we take until $n=2$, and using small ϵ, sometimes the response $z(t)$ is expressed as

$$z(t) = \int_{-\infty}^{\infty} g_1(\tau) \; x(t-\tau) \; d\tau + \epsilon \int_{-\infty}^{\infty} \int_{-\infty}^{\infty} g_2(\tau_1, \tau_2)x(t-\tau_1)x(t-\tau_2) \; d\tau_1 d\tau_2. \quad (12.100)$$

The derivatives in terms of time is

$$\dot{z}(t) = \int_{-\infty}^{\infty} g_1(\tau) \; \dot{x}(t-\tau) \; d\tau + 2\epsilon \int_{-\infty}^{\infty} \int_{-\infty}^{\infty} g_2(\tau_1, \tau_2)\dot{x}(t-\tau_1)x(t-\tau_2) \; d\tau_1 d\tau_2, \quad (12.101)$$

354

thinking of the symmetry character of $g_2(\tau_1, \tau_2) = g_2(\tau_2, \tau_1)$. On the basis of this expression T. Vinje[87] formulated a general method for getting the probability distribution function of the extreme values, under the assumption that the response $z(t)$ is narrow banded and the input $x(t)$ is Gaussian with variance σ^2. His method is also based on the assumption that the probability distribution function of extreme values can be obtained by the joint distribution function $p(z, \dot{z})$ only.

Now, we start from the statistical moment generating function to get $p(z_1, z_2)$ [here $z_1 = z(t)$, $z_2 = \dot{z}(t)$ z], that is, from the double Fourier transform of $p(z_1, z_2)$,

$$\phi(\theta_1, \theta_2) = E\left[\exp\{i(\theta_1 z_1 + \theta_2 z_2)\}\right]$$

$$= \int_{-\infty}^{\infty} \int_{-\infty}^{\infty} \exp(i\theta_1 z_1 + i\theta_2 z_2) p(z_1, z_2) dz_1 dz_2. \qquad (12.102)$$

Then expanding $\exp(i\theta_1 z_1 + i\theta_2 z_2)$ into a series gives

$$\exp(i\theta_1 z_1 + i\theta_2 z_2) = 1 + \sum_{m,n=0}^{\infty} \frac{z_1^m z_2^n}{m! n!} (i\theta_1)^m (i\theta_2)^n, \qquad (12.103)$$

assuming m, n are positive integers whose sum is greater than zero.
Inserting Eq. 12.103 into Eq. 12.102 gives

$$\phi(\theta_1, \theta_2) = 1 + \sum_{m,n} \frac{\mu_{mn}}{m! n!} (i\theta_1)^m (i\theta_2)^n. \qquad (12.104)$$

Here

$$\mu_{mn} = E[z_1^m, z_2^n] = \int_{-\infty}^{\infty} \int_{-\infty}^{\infty} z_1^m z_2^n \, p(z_1, z_2) dz_1 dz_2. \qquad (12.105)$$

From the Fourier inverse transform of Eq. 12.102,

$$p(z_1, z_2) = \frac{1}{(2\pi)^2} \int_{-\infty}^{\infty} \int_{-\infty}^{\infty} \phi(\theta_1, \theta_2) \exp\{-i(\theta_1 z_1 + \theta_2 z_2)\} d\theta_1 d\theta_2. \qquad (12.106)$$

Putting Eq. 12.104 in Eq. 12.106

$$p(z_1, z_2) = \frac{1}{(2\pi)^2} \int\limits_{-\infty}^{\infty} \int\limits_{-\infty}^{\infty} \sum_{m,n} \frac{\mu_{mn}}{m!n!} (i\theta_1)^m (i\theta_2)^n \exp\{-i(\theta_1 z_1 + \theta_2 z_2)\} d\theta_1 d\theta_2.$$

(12.107)

This Eq. 12.107 shows that $p(z_1, z_2)$ can be calculated if we know all the m,n th order moments of this probability function.

On the other hand, by the definition of the cumulant $k_{m,n}$ and the cumulant generating function $K(i\theta_1, i\theta_2)$,

$$K(i\theta_1, i\theta_2) = \log \phi(\theta_1, \theta_2) = \frac{k_{11}}{1!1!}(i\theta_1)(i\theta_2) + \frac{k_{12}}{1!2!}(i\theta_1)(i\theta_2)^2 + \ldots$$

$$= \sum_{m,n} \frac{k_{mn}}{m!n!} (i\theta_1)^m (i\theta_2)^n.$$

(12.108)

Therefore

$$\phi(\theta_1, \theta_2) = \exp\{K(i\theta_1, i\theta_2)\} = \exp\left\{ \sum_{m,n} \frac{k_{mn}}{m!n!} (i\theta_1)^m (i\theta_2)^n \right\}$$

$$= 1 + \frac{1}{1!} \left\{ \sum_{m,n} \frac{k_{mn}}{m!n!} (i\theta_1)^m (i\theta_2)^n \right\} + \frac{1}{2!} \left\{ \sum_{m,n} \frac{k_{mn}}{m!n!} (i\theta_1)^m (i\theta_n)^n \right\}^2$$

$$+ \frac{1}{3!} \{ \ldots \}^3 + \ldots \quad (12.109)$$

When we insert this $\phi(\theta_1, \theta_2)$ into Eq. 12.106,

$$p(z_1, z_2) = \frac{1}{(2\pi)^2} \int\limits_{-\infty}^{\infty} \int\limits_{-\infty}^{\infty} \exp\{K(i\theta_1, i\theta_2) - i(\theta_1 Z_1 + \theta_2 Z_2)\} d\theta_1 d\theta_2$$

$$= \frac{1}{(2\pi)^2} \int\limits_{-\infty}^{\infty} \int\limits_{-\infty}^{\infty} \exp\left\{ \sum_{m,n} \frac{k_{mn}}{m!n!} (i\theta_1)^m (i\theta_2)^n \right\} \cdot e^{-i(\theta_1 Z_1 + \theta_2 Z_2)} d\theta_1 d\theta_2.$$

(12.110)

From Eqs. 12 104 and 12.109, $k_{m,n}$ and $\mu_{m,n}$ are related as follows:

$$
\begin{cases}
k_{01} = \mu_{01} & \ldots (0) \\
k_{02} = \mu_{02} - \mu_{01}^2 & \ldots (1 + \epsilon^2) \\
k_{03} = \mu_{03} - 3\mu_{01}\mu_{02} + 2\mu_{01}^3 & \ldots (\epsilon + \epsilon^3) \\
\ldots & \ldots \ldots \\
k_{10} = \mu_{10} & \ldots (\epsilon) \\
k_{11} = \mu_{11} - \mu_{10}\mu_{01} & \ldots (0) \\
k_{12} = \mu_{12} - \mu_{10}\mu_{02} - 2\mu_{01}\mu_{11} + 2\mu_{10}\mu_{01}^2 & \ldots (\epsilon + \epsilon^3) \\
\ldots & \ldots \ldots \\
k_{20} = \mu_{20} - \mu_{10}^2 & \ldots (1 + \epsilon^2) \\
k_{21} = \mu_{21} - 2\mu_{10}\mu_{11} - \mu_{01}\mu_{20} + 2\mu_{10}^2\mu_{01} & \ldots (0) \\
\ldots & \ldots \ldots \\
k_{30} = \mu_{30} - 3\mu_{10}\mu_{20} + 2\mu_{10}^3 & \ldots (\epsilon + \epsilon^3)
\end{cases}
\qquad (12.111)
$$

Following these general formulations by Vinje, M. Hineno[67] calculated the probability distribution function of the wave height, treating the wave process as nonlinear, as was mentioned in Section 9.2.1, and will be summarized as follows.

From these relations with μ_{mn} the order of k_{mn} in ϵ's was obtained, which is a smallness parameter that appeared in Eq. 12.100 as is listed in Eq. 12.111. Expanding Eq. 12.110 around $\epsilon = 0$ into a Taylor series and truncating at $0(\epsilon)$ gives

$$
p(z_1, z_2) = \frac{1}{(2\pi)^2} \int \int \exp\left[-\frac{1}{2} k_{20}(0)\theta_1^2 - \frac{1}{2} k_{02}(0)\theta_2^2 \right]
$$

$$
\times \left[1 + k_{10}(0)(i\theta_1) + \frac{\epsilon}{6} k_{30}'(0)(i\theta_1)^3 + \frac{\epsilon}{6} k_{03}'(0)(i\theta_2)^3 \right.
$$

$$
\left. + \frac{\epsilon}{2} k_{12}'(0)(i\theta_1)(i\theta_2)^2 \right] e^{-i(\theta_1 Z_1 + \theta_2 Z_2)} \, d\theta_1 d\theta_2, \qquad (12.112)
$$

where $k_{ij}(0) \equiv k_{ij}\big|_{\epsilon=0}$, $k_{ij}'(0) \equiv \frac{\partial}{\partial \epsilon} k_{ij}\big|_{\epsilon=0}$.

After manipulation,

$$p(z_1, z_2) = \frac{1}{2\pi\sqrt{k_{20}k_{02}}} \; \exp\left(-\frac{z_1^2}{2k_{20}} - \frac{z_2^2}{2k_{02}}\right)$$

$$\times \left[H_0^2 + \frac{k_{10}}{\sqrt{k_{20}}} H_1\left(\frac{z_1}{\sqrt{k_{20}}}\right) + \frac{\epsilon}{6} \frac{k'_{30}}{k_{20}\sqrt{k_{20}}} H_3\left(\frac{z_1}{\sqrt{k_{20}}}\right) + \frac{\epsilon}{6} \frac{k'_{03}}{k_{02}\sqrt{k_{02}}} H_3\left(\frac{z_2}{\sqrt{k_{02}}}\right) \right.$$

$$\left. + \frac{\epsilon}{2} \frac{k'_{12}}{k_{02}\sqrt{k_{20}}} H_1\left(\frac{Z_1}{\sqrt{k_{20}}}\right) H_2\left(\frac{Z_2}{\sqrt{k_{02}}}\right) \right]. \quad (12.113)$$

Here $H_m(x)$ is a Hermite polynomial,

$$H_n(x) = \frac{1}{\sqrt{\pi}} \int\limits_{-\infty}^{\infty} e^{-t^2}(x + i\sqrt{2}\,t)^n dt$$

$$\begin{cases}
H_0(x) = 1 \\
H_1(x) = x \\
H_2(x) = x^2 - 1 \\
H_3(x) = x^3 - 3x \\
\qquad \cdot \\
\qquad \cdot \\
\qquad \cdot \\
H_{n+1}(x) = xH_n(x) - nH_{n-1}(x)
\end{cases} \quad (12.114)$$

convention of (0) is omitted.

Under the assumption that $z_1(t)$ is narrow banded, the number of zero–crossings of an output $z(t)$ is equal to the number of maxima.

Therefore, the expected number of z–up crossings per unit time is given as already shown in Section 12.5, Eq. 12.44,

$$E[N_+(z_1)] = \frac{1}{2} \int\limits_{-\infty}^{\infty} |z_2| \; p(z_1, z_2)dz_2. \quad (12.115)$$

358

Also, the expected number of mean level up-crossings is

$$E[N_+(\bar{z}_1)] = \frac{1}{2} \int_{-\infty}^{\infty} |z_2| \; p(\bar{z}_1, z_2) dz_2. \qquad (12.116)$$

The probability distribution function of a maxima then lies above Z_1 is

$$P(z_1) = \frac{E[N_+(z)]}{E[N_+(\bar{z}_1)]}. \qquad (12.117)$$

Substituting Eq. 12.113 into Eq. 12.115 and carrying on the integration gives

$$E[N_+(z)] = \frac{1}{2\pi} \sqrt{\frac{k_{02}}{k_{20}}} \; \exp\left(-\frac{z^2}{2k_{20}}\right)$$

$$\times \left[1 + \frac{k_{10}}{\sqrt{k_{20}}} H_1\left(\frac{z}{\sqrt{k_{20}}}\right) + \frac{\epsilon}{6} \frac{k'_{30}}{k_{20}\sqrt{k_{20}}} H_3\left(\frac{z_1}{\sqrt{k_{20}}}\right)\right.$$

$$\left. + \frac{\epsilon}{2} \frac{k'_{12}}{k_{02}\sqrt{k_{20}}} H_1\left(\frac{z}{\sqrt{k_{20}}}\right)\right]. \qquad (12.118)$$

As already shown in Eq. 12.111, the cumulants are calculated from the m,nth moment of response, and the m,nth moment can be expressed by using the frequency functions and the input spectrum as some of the examples that were shown in Section 11.4. With the order of each term up to $0\,(\epsilon)$ taken into account, and with the spectrum function, which is a real function, the cumulants can be written as follows:

359

$$k_{10} \equiv \epsilon h_{10} = \epsilon \int_{-\infty}^{\infty} s(\omega) \ G_2(\omega, -\omega) d\omega$$

$$k_{20} = \ h_{20} = \int_{-\infty}^{\infty} s(\omega) \ |G_1(\omega)|^2 d\omega$$

$$k_{02} = \ h_{02} = \int_{-\infty}^{\infty} \omega^2 s(\omega) \ |G_1(\omega)|^2 d\omega$$

$$k_{12} \equiv \epsilon h_{12} = \epsilon \int_{-\infty}^{\infty} \int_{-\infty}^{\infty} (\omega_1 \omega_2 + 2\omega_2^2) \ s(\omega_1) s(\omega_2)$$

$$\times \ [G_1(-\omega_1)G_1(-\omega_2)G_2(\omega_1, \omega_2) \qquad (12.119)$$

$$+ \ G_1^*(-\omega_1)G_1^*(-\omega_2)G_2^*(\omega_1, \omega_2)] \ d\omega_1 d\omega_2$$

$$k_{30} \equiv \epsilon h_{30} = 3\epsilon \int_{-\infty}^{\infty} \int_{-\infty}^{\infty} s(\omega_1)(s\omega_2)$$

$$\times \ [G_1(-\omega_1)G_1(-\omega_2)G_2(\omega_1, \omega_2)$$

$$+ \ G_1^*(-\omega_1)G_1^*(-\omega_2)G_2^*(\omega_1, \omega_2)] \ d\omega_1 d\omega_2,$$

where * indicates a complex conjugate,

$s(\omega)$ is the two–sided spectrum of input $x(t)$,

$G_1(\omega)$ is the linear frequency response function

$$G_1(\omega) = \int_{-\infty}^{\infty} g_1(\tau_1)e^{-i\tau_1\omega}d\tau_1,$$

360

and $G_2(\omega_1, \omega_2)$ is the quadratic response function

$$G_2(\omega_1, \omega_2) = \int\limits_{-\infty}^{\infty} \int\limits_{-\infty}^{\infty} g_2(\tau_1, \tau_2) e^{-\pi_1 \omega_1 - \pi_2 \omega_2} d\tau_1 d\tau_2.$$

Through these manipulations, Hineno obtained his expression for the probability distribution function as

$$P(z) = \exp\left(-\frac{z^2}{2h_{20}}\right)\left[1 + \epsilon\left\{\frac{h_{10}}{h_{20}} + \frac{h_{30}}{6h_{20}^2}\left(\frac{z^2}{h_{20}} - 3\right) + \frac{h_{12}}{2h_{02}h_{20}}\right\}z\right]. \quad (12.120)$$

The probability distribution density function $p(z)$ and the expected $1/n$ highest value $z_{1/n}$ are obtained from the relations

$$p(z) = -\frac{d}{dz}P(z), \quad (12.121)$$

$$\bar{z}_{1/n} = \frac{\displaystyle\int_{z_{1/n}}^{\infty} z\, p(z)dz}{\displaystyle\int_{z_{1/n}}^{\infty} P(z)dz} = n\int_{z_{1/n}}^{\infty} z\, p(z)dz. \quad (12.122)$$

If we use Eq. 12.120 for $P(z)$ and consider that in real calculations, the smallness parameter ϵ is absorbed in the computation of $G_2(\omega_1, \omega_2)$ and does not appear explicitly,

$$p(z) = \exp\left(-\frac{z^2}{2h_{20}}\right)\left[-\frac{h_{10}}{h_{20}} + \frac{h_{30}}{2h_{20}^2} - \frac{h_{12}}{2h_{20}h_{02}} + \frac{1}{h_{20}}\,z\right.$$

$$\left. + \left\{\frac{1}{h_{20}}\left(\frac{h_{10}}{h_{20}} - \frac{h_{30}}{2h_{20}^2} + \frac{h_{12}}{2h_{20}h_{02}}\right) - \frac{h_{30}}{2h_{20}^3}\right\}z^2 + \frac{h_{30}}{6h_{20}^4}\,z^4\right]. \quad (12.123)$$

This is the final expression of the probability distribution density function of the maxima. Using this expression, M. Hineno calculated the probability characteristics of the maxima and minima of the waves that were treated as nonlinear with the quadratic response function, as shown in Eq. 9.10 in Section 9.2.1,

$$G_2(\omega_1, \omega_2) = \frac{1}{2g}\left(\omega_1^2 + \omega_2^2\right)$$

$$G_2(\omega_1, -\omega_2) = -\frac{1}{2g}\left(\omega_1^2 - \omega_2^2\right)$$

with the linear response assumed as $G_1(\omega) = 1$.
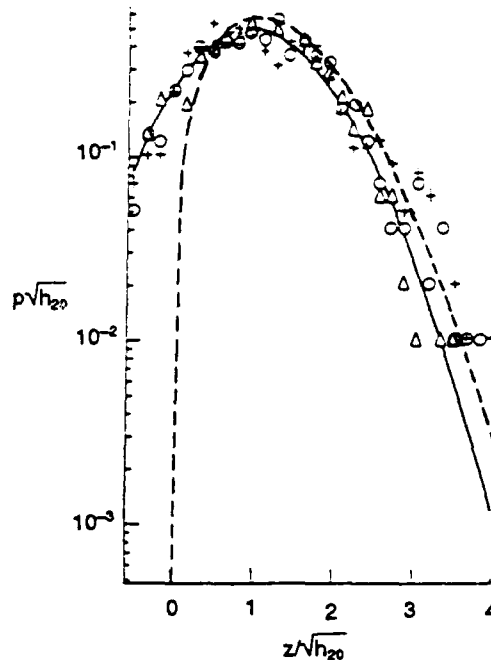
Fig. 12.13. Probability density function of the maxima of waves.
(From Hineno.[67])

Figure 12.13 shows the probability distribution density function for maxima of the waves compared with the experimental data by a certain research worker for model waves with a wave spectrum that is almost of the Pierson–Moskowitz type. In Fig. 12.13, the + marks indicate the experimental data analyzed as nonlinear waves and the other marks (Δ, O) are experimental data analyzed on the assumption of linear waves, the solid line being the theoretical relations as linear for this model waves. Results computed by Eq. 12.123 are shown by a dotted line, and the agreement with + signs is quite good, especially in the larger amplitude range, which is important practically.

Figures 12.14, 12.15, and 12.16 illustrate the calculated results for nonlinear waves, using a modified Pierson–Moskowitz wave spectrum with $H_{1/3} = 11.6$ m, $\overline{T}_{01} = 16.1$ sec as the input. From these figures, we can find the extent of nonlinearity of the waves and also the effects of nonlinearity or the effect of the distortion of the wave forms on the difference of the probability distribution function for maxima and minima.

Hineno[88] also calculated the relative motion of a semi–submersible in this kind of nonlinear wave, assuming a linear response to the excitation by the waves.
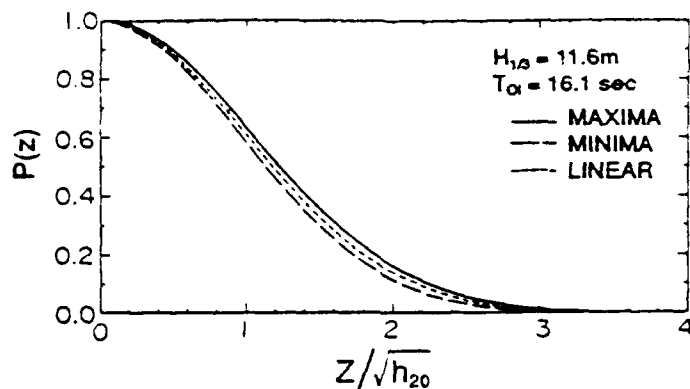
Fig. 12.14. Cumulative probability distribution function of wave amplitude. (From Hineno.[67])
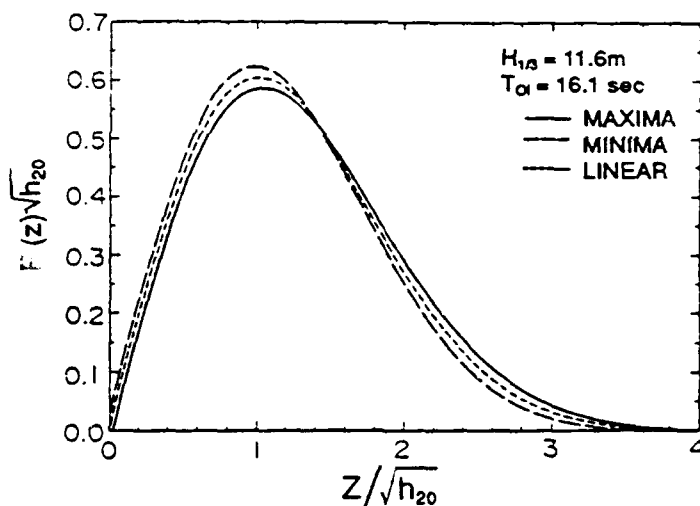
Fig. 12.15. Probability density distribution function of wave amplitude. (From Hineno.[67])

12.7.2 Wide–Banded Case

J. F. Dalzell[56] (1984) extended this technique further. He did not assume narrow bandedness of the response and did not truncate the functional polynomials at n=2 but continued to n=3. He thus formulated the technique for calculating the probability distribution function of extremes of the nonlinear responses to Gaussian inputs. Here the characters of the nonlinear frequency response functions up to degree 3 are assumed to be known from the analysis as discussed in Section 11.5. The nonlinear response $Y(t)$ to Gaussian input $X(t)$ is expressed by
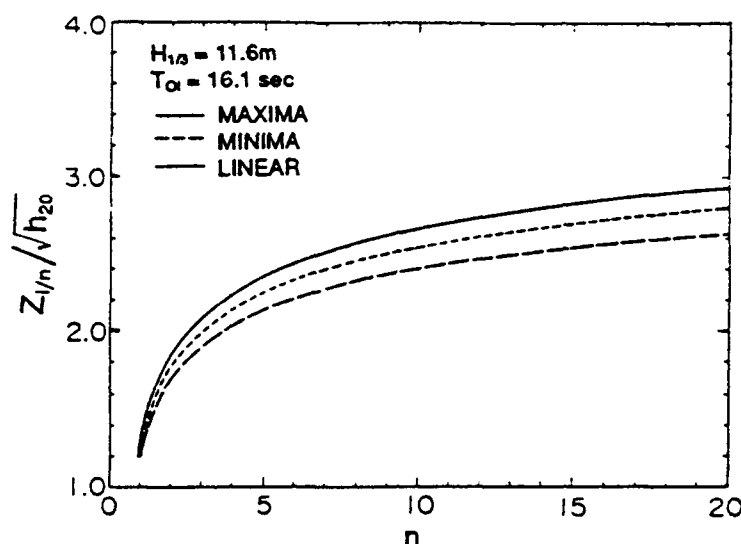
Fig. 12.16. Expected 1/n highest values of wave amplitude.
(From Hineno.[67])

$$Y(t) = \int g_1(\tau_1)\ x(t-\tau_1)\ d\tau_1$$

$$+ \int\int g_2(\tau_1,\tau_2)\ x(t-\tau_1)\ x(t-\tau_2)\ d\tau_1 d\tau_2$$

$$+ \int\int\int g_3(\tau_1,\tau_2,\tau_3)\ x(t-\tau_1)\ x(t-\tau_2)\ x(t-\tau_3)\ d\tau_1 d\tau_2 d\tau_3. \quad (12.124)$$

(Limits of integrals $-\infty \rightharpoonup +\infty$ are omitted throughout this section.)

As was assumed in Section 11.5, here the kernels or the nth degree impulse response functions $g_n(\tau_1,\tau_2 \ldots \tau_n)$ are real, time invariant, completely symmetrical in the variables $g_n(\tau_1,\tau_2 \ldots \tau_n) = g_n(\tau_2,\tau_3 \ldots \tau_n,\tau_1) = \ldots$ for any rearrangement of the variables τ_j, and sufficiently smooth and integrable so that there exist n–fold Fourier transforms,

$$g_n(\tau_1,\tau_2 \ldots \tau_n) = \frac{1}{(2\pi)^n} \underbrace{\int\int \ldots \int}_{n} G_n(\omega_1,\omega_2 \ldots \omega_n)$$

$$\exp\left[i\sum_{j=1}^{n}\omega_j\tau_j\right]d\omega_1 d\omega_2 \ldots d\omega_n \quad (12.125)$$

364

$$G_n(\omega_1, \omega_2 \ldots \omega_n) = \underbrace{\int \int \ldots \int}_{n} g_n(\tau_1, \tau_2, \ldots \tau_n)$$

$$\exp\left[-i\sum_{j=1}^{n} \omega_j \tau_j\right] d\tau_1 d\tau_2 \ldots d\tau_n. \quad (12.126)$$

The function $G_n(\omega_1, \omega_2 \ldots \omega_n)$ is the nth degree frequency response function and is also symmetric in its arguments $G_n(\omega_1, \omega_2 \ldots \omega_n) = G_n(\omega_2, \omega_1, \ldots \omega_n) = \ldots$ for any rearrangement of ω_j because the impulse response functions are real.

$$G_n(-\omega_1, -\omega_2, \ldots -\omega_n) = G_n^*(\omega_1, \omega_2, \ldots \omega_n) \quad (12.127)$$

here the * denotes the complex conjugate.

In Dalzell's paper,[56] the spectrum $S_{xx}(\omega)$ was defined a little differently from those used by this author in Parts I, II, and III. He used 2π times our $s(\omega)$,

$$S_{xx}(\omega) = 2\pi s(\omega), \quad (12.128)$$

and also took the one–sided spectrum

$$U_{xx}[|\omega|] = 2s(\omega) = \frac{1}{\pi} S_{xx}(\omega), \quad \text{for } \omega > 0. \quad (12.128')$$

The initially assumed functional polynomial process was reformulated as the response to a white noise excitation, and a new set of frequency response functions was defined which contains both characteristics of the original frequency response to the excitation and that of the excitation spectrum.

The two–sided spectrum of white noise is

$$S_{ww}(\omega) = 1, \quad (12.129)$$

and the autocorrelation of white noise is a delta function

$$R_{ww}(\tau) = \frac{1}{2\pi} \int \exp[i\omega\tau]d\omega = \delta(\tau). \quad (12.130)$$

We think of the spectrum filter $L(\omega)$ that expresses the spectrum of input $S_{xx}(\omega)$ with the white noise as

$$S_{xx}(\omega) = \sigma_x^2 |L(\omega)|^2 \quad (12.131)$$

365

$$L(\omega) = \frac{[S_{xx}(\omega)]^{1/2}}{\sigma_x}. \qquad (12.131')$$

The linear, quadratic, and cubic frequency response functions connecting the white noise $W(t)$ with the output $Y(t)$ will be

$$\sigma_x H_1(\omega) = \sigma_x L(\omega) G(\omega)$$

$$\sigma_x^2 H_2(\omega_1, \omega_2) = \sigma_x^2 L(\omega_1) L(\omega_2) G_2(\omega_1, \omega_2) \qquad (12.132)$$

$$\sigma_x^3 H_3(\omega_1, \omega_2 \omega_3) = \sigma_x^3 L(\omega_1) L(\omega_2) L(\omega_3) G_3(\omega_1, \omega_2, \omega_3).$$

Then $Y(t)$ can be related to the white noise input $W(t)$ as

$$Y(t) = \sigma_x \int h_1(\tau_1) W(t - \tau_1) d\tau_1$$

$$+ \sigma_x^2 \int \int h_2(\tau_1, \tau_2) W(t - \tau_1) W(t - \tau_2) d\tau_1 d\tau_2$$

$$+ \sigma_x^3 \int \int \int h_3(\tau_1, \tau_2, \tau_3) W(t - \tau_1) W(t - \tau_2) W(t - \tau_3) d\tau_1 d\tau_2 d\tau_3, \quad (12.133)$$

where

$$h_1(\tau_1) = \frac{1}{2\pi} \int H_1(\omega) \exp[i\omega\tau_1] d\omega$$

$$h_2(\tau_1, \tau_2) = \frac{1}{(2\pi)^2} \int \int H_2(\omega_1, \omega_2) \exp[i(\omega_1\tau_1 + \omega_2\tau_2)] d\omega_1 d\omega_2 \qquad (12.134)$$

$$h_3(\tau_1, \tau_2, \tau_3) = \frac{1}{(2\pi)^3} \int \int \int H_3(\omega_1, \omega_2, \omega_3) \exp[i(\omega_1\tau_1 + \omega_2\tau_2 + \omega_3\tau_3)] d\omega_1 d\omega_2 d\omega_3.$$

The derivatives of the output are then

$$\dot{Y}(t) = \sigma_x \int h_1'(\tau_1) W(t - \tau_1) d\tau_1$$

$$+ \sigma_x^2 \int \int h_2'(\tau_1, \tau_2) W(t - \tau_1) W(t - \tau_2) d\tau_1 d\tau_2$$

$$+ \sigma_x^3 \int \int \int h_3'(\tau_1, \tau_2, \tau_3) W(t - \tau_1) W(t - \tau_2) W(t - \tau_3) d\tau_1 d\tau_2 d\tau_3, \quad (12.135)$$

where

$$h_1'(\tau_1) = \frac{1}{2\pi} \int \dot{H}_1(\omega) \exp(i\omega\tau_1)d\omega$$

$$h_2'(\tau_1, \tau_2) = \frac{1}{(2\pi)^2} \int \int \dot{H}_2(\omega_1, \omega_2) \exp[i(\omega_1\tau_1 + \omega_2\tau_2)]d\omega_1 d\omega_2 \qquad (12.136)$$

$$h_3'(\tau_1, \tau_2, \tau_3) = \frac{1}{(2\pi)^3} \int \int \int \dot{H}_3(\omega_1, \omega_2, \omega_3) \exp[i(\omega_1\tau_1 + \omega_2\tau_2 + \omega_3\tau_3)]d\omega_1 d\omega_2 d\omega_3.$$

The terms $\dot{H}_n(\omega)$ are defined as

$$\dot{H}_1(\omega) = i\omega H_1(\omega)$$

$$\dot{H}_2(\omega_1, \omega_2) = i(\omega_1 + \omega_2)H_2(\omega_1, \omega_2) \qquad (12.137)$$

$$\dot{H}_3(\omega_1, \omega_2, \omega_3) = i(\omega_1 + \omega_2 + \omega_3)H_3(\omega_1, \omega_2, \omega_3)$$

and

$$\ddot{Y}(t) = \sigma_x \int \ddot{h}_1(\tau_1)W(t - \tau_1)d\tau_1$$

$$+ \sigma_x^2 \int \int \ddot{h}_2(\tau_1, \tau_2)W(t - \tau_1)W(t - \tau_2)d\tau_1 d\tau_2$$

$$+ \sigma_x^3 \int \int \int \ddot{h}_3(\tau_1, \tau_2, \tau_3)W(t - \tau_1)W(t - \tau_2)W(t - \tau_3)d\tau_1 d\tau_2 d\tau_3, \quad (12.138)$$

where

$$\ddot{h}_1(\tau_1) = \frac{1}{2\pi} \int \ddot{H}_1(\omega) \exp(i\omega\tau_1)d\omega$$

$$\ddot{h}_2(\tau_1, \tau_2) = \frac{1}{(2\pi)^2} \int \int \ddot{H}_2(\omega_1, \omega_2) \exp[i(\omega_1\tau_1 + \omega_2\tau_2)]d\omega_1 d\omega_2 \qquad (12.139)$$

$$\ddot{h}_3(\tau_1, \tau_2, \tau_3) = \frac{1}{(2\pi)^3} \int \int \int \ddot{H}_3(\omega_1, \omega_2, \omega_3) \exp[i(\omega_1\tau_1 + \omega_2\tau_2 + \omega_3\tau_3)]d\omega_1 d\omega_2 d\omega_3,$$

and $\ddot{H}_n$ are defined as

$$\ddot{H}_1(\omega) = -\omega^2 H_1(\omega)$$

$$\ddot{H}_2(\omega_1, \omega_2) = -(\omega_1 + \omega_2)^2 H_2(\omega_1, \omega_2) \qquad (12.140)$$

$$\ddot{H}_3(\omega_1, \omega_2, \omega_3) = -(\omega_1 + \omega_2 + \omega_3)^2 H_3(\omega_1, \omega_2, \omega_3).$$

In addition, the characteristics of the products of white noise were fully utilized as follows:

$$\overline{W_1(t-\tau_1)W(t-\tau_2) \ldots W(t-\tau_N)} = 0 \text{ for } N \text{ odd,}$$

$$\overline{W(t-\tau_1)W(t-\tau_2)} = \delta(\tau_1 - \tau_2) = \delta_{12},$$

$$\overline{W(t-\tau_1)W(t-\tau_2)W(t-\tau_3)W(t-\tau_4)} = \delta_{12}\delta_{34} + \delta_{13}\delta_{24} + \delta_{14}\delta_{23},$$

$$\overline{W(t-\tau_1)W(t-\tau_2)W(t-\tau_3)W(t-\tau_4)W(t-\tau_5)W(t-\tau_6)}$$

$$= \delta_{12}\delta_{34}\delta_{56} + \delta_{12}\delta_{35}\delta_{46} + \delta_{12}\delta_{36}\delta_{45}$$

$$+ \delta_{13}\delta_{24}\delta_{56} + \delta_{13}\delta_{25}\delta_{46} + \delta_{13}\delta_{26}\delta_{45} \qquad (12.141)$$

$$+ \delta_{14}\delta_{23}\delta_{56} + \delta_{14}\delta_{25}\delta_{36} + \delta_{14}\delta_{26}\delta_{35}$$

$$+ \delta_{15}\delta_{34}\delta_{26} + \delta_{15}\delta_{32}\delta_{46} + \delta_{15}\delta_{36}\delta_{24}$$

$$+ \delta_{16}\delta_{34}\delta_{52} + \delta_{16}\delta_{35}\delta_{42} + \delta_{16}\delta_{32}\delta_{45},$$

where $\delta_{ij} = \delta(\tau_i - \tau_j)$.

Eq. 12.141 is the special case of Eqs. 11.68, 11.69, and 11.70 in Section 11.5.

If we do not assume narrow bandedness of the output spectrum, the expected number of maxima of the response Y greater than $Y = \xi$ per unit time is approximated as

$$N_\xi^+ = \int_\xi^\infty \int_{-\infty}^0 |\ddot{Y}| \, p(Y, 0, \ddot{Y}) \, d\ddot{Y} \, dY. \qquad (12.142)$$

Similarly, the expected number of minima of Y less than $Y = \xi$ per unit time is approximated as

368

$$N_\xi^- = \int\limits_{-\infty}^{\xi} \int\limits_{0}^{\infty} |\ddot{Y}|\, p(Y, 0, \ddot{Y})\, d\ddot{Y}\, dY. \qquad (12.143)$$

Then, the expected number of maxima regardless of magnitude per unit time will be

$$N_\infty^+ = \int\limits_{-\infty}^{\infty} \int\limits_{-\infty}^{0} |\ddot{Y}|\, p(Y, 0, \ddot{Y})\, d\ddot{Y}\, dY. \qquad (12.144)$$

Similarly the expected number of minima per unit time will be

$$N_\infty^- = \int\limits_{-\infty}^{\infty} \int\limits_{0}^{\infty} |\ddot{Y}|\, p(Y, 0, \ddot{Y})\, d\ddot{Y}\, dY. \qquad (12.145)$$

Because maxima and minima are paired in the same record of response $N_\infty^+ = N_\infty^-$, from Eqs. 12.142 and 12.144, the probability that a maximum will be less than ξ is approximated

$$\text{Prob[Maximum } \le \xi] = 1 - \left(\frac{N_\xi^+}{N_\infty^+} \right). \qquad (12.146)$$

Similarly,

$$\text{Prob[Minimum } \le \xi] = \left(\frac{N_\xi^-}{N_\infty^-} \right). \qquad (12.147)$$

Then, the probability densities of maxima and minima are obtained by differentiating Eqs. 12.146 and 12.147 with respect to ξ, as

$$p^+(\xi) = \frac{1}{N_\infty^+} \int\limits_{-\infty}^{0} |\ddot{Y}|\, p(\xi, 0, \ddot{Y})\, d\ddot{Y} \qquad (12.148)$$

369

$$p^-(\xi) = \frac{1}{N_\infty^-} \int\limits_0^\infty |\ddot{Y}| \ p(\xi, 0, \ddot{Y}) \ d\ddot{Y}. \qquad (12.149)$$

In the same way as we did for the joint probability density $p(Y, \dot{Y})$ in Section 12.7.1, relations between the joint moment generating function $\phi(it, i\dot{t}, i\ddot{t})$ and the joint cumulant generating function $K(it, i\dot{t}, i\ddot{t})$ were used to give

$$\phi(it, i\dot{t}, i\ddot{t}) = \int \int \int \ p(Y, \dot{Y}, \ddot{Y}) \exp[itY + i\dot{t}\dot{Y} + i\ddot{t}\ddot{Y}] \ dY \ d\dot{Y} \ d\ddot{Y}$$

$$= 1 + \sum_{jkm} \frac{\mu_{jkm}}{j!k!m!} (it)^j \ (i\dot{t})^k \ (i\ddot{t})^m. \qquad (12.150)$$

Here μ_{jkm} is the joint moment

$$\mu_{jkm} = \overline{Y^j \dot{Y}^k \ddot{Y}^m} = \int \int \int \ Y^j \dot{Y}^k \ddot{Y}^m p(Y, \dot{Y}, \ddot{Y}) \ dY \ d\dot{Y} \ d\ddot{Y} \qquad (12.151)$$

$$K(it, i\dot{t}, i\ddot{t}) = \log \ \phi(it, i\dot{t}, i\ddot{t}) = \sum_{jkm} \frac{k_{jkm}}{j!k!m!} (it)^j \ (i\dot{t})^k \ (i\ddot{t})^m. \qquad (12.152)$$

Therefore

$$\phi(it, i\dot{t}, i\ddot{t}) \ = \ \exp \ [K(it, i\dot{t}, i\ddot{t})] \qquad (12.153)$$

where j, k, and m are positive integers whose sum is greater than zero. Therefore, the inverse transform of Eq. 12.150, from Eqs. 12.150 and 12.152, is

$$p(Y, \dot{Y}, \ddot{Y}) = \frac{1}{(2\pi)^3} \int \int \int \exp\left[-\left\{iYt + i\dot{Y}\dot{t} - i\ddot{Y}\ddot{t}\right\}\right] \phi(it, i\dot{t}, i\ddot{t}) \; dt, d\dot{t}, d\ddot{t}$$

$$= \frac{1}{(2\pi)^3} \int \int \int \exp\left[-\left\{iYt + i\dot{Y}\dot{t} - i\ddot{Y}\ddot{t}\right\}\right] \; \exp\left[K(it, i\dot{t}, i\ddot{t})\right] \; dt, d\dot{t}, d\ddot{t}$$

$$= \frac{1}{(2\pi)^3} \int \int \int \exp\left[-iYt - i\dot{Y}\dot{t} - i\ddot{Y}\ddot{t} + K(it, i\dot{t}, i\ddot{t})\right] \; dt, d\dot{t}, d\ddot{t}$$

$$= \frac{1}{(2\pi)^3} \int \int \int \exp\left[(k_{100} - Y) \; it + (k_{010} - \dot{Y}) \; i\dot{t} + (k_{001} - \ddot{Y})i\ddot{t}\right.$$

$$-\frac{1}{2}\left\{k_{200}t^2 + k_{020}\dot{t}^2 + k_{002}\ddot{t}^2 + 2k_{110}t\dot{t} + 2k_{101}t\ddot{t} + 2k_{011}\dot{t}\ddot{t}\right\}$$

$$\left. +\sum_{jkm} \frac{k_{jkm}}{j!k!m!} \; (it)^j \; (i\dot{t})^k \; (i\ddot{t})^m\right] \; dt, d\dot{t}, d\ddot{t}. \tag{12.154}$$

Here j, k, and m are now positive integers whose sum is greater than 2.

The relations between joint moment and joint cumulants are

$$\begin{aligned}
k_{100} &= \mu_{100}\\
k_{010} &= \mu_{010}\\
k_{001} &= \mu_{001}\\
k_{200} &= \text{variance of } Y\\
k_{020} &= \text{variance of } \dot{Y}\\
k_{002} &= \text{variance of } \ddot{Y}.
\end{aligned} \tag{12.155}$$

Nondimensionalizing the variables as follows

$$\begin{aligned}
z &= (Y - k_{100})k_{200}^{1/2}\\
\dot{z} &= (\dot{Y} - k_{010})k_{020}^{1/2}\\
\ddot{z} &= (\ddot{Y} - k_{001})k_{002}^{1/2}
\end{aligned} \tag{12.156}$$

and

$$s = t \, k_{200}^{1/2}$$

$$\dot{s} = \dot{t} \, k_{020}^{1/2} \qquad (12.157)$$

$$\ddot{s} = \ddot{t} \, k_{002}^{1/2}$$

and

$$\lambda_{jkm} = \frac{k_{jkm}}{j! \, k! \, m! \, (k_{200}^{j} \, k_{020}^{k} \, k_{002}^{m})}, \qquad (12.158)$$

$$p(z, \dot{z}, \ddot{z}) = \frac{1}{(2\pi)^3} \int \int \int \exp \left[-izs - i\dot{z}\,\dot{s} - i\ddot{z}\,\ddot{s} \right]$$

$$-\frac{1}{2} \left\{ s^2 + \dot{s}^2 + \ddot{s}^2 + 2\lambda_{110} s \dot{s} + 2\lambda_{101} s \ddot{s} + 2\lambda_{011} \dot{s} \ddot{s} \right\}$$

$$+ \sum_{jkm} \lambda_{jkm} (is)^j \, (i\dot{s})^k \, (i\ddot{s})^m \, ds \, d\dot{s} \, d\ddot{s}. \qquad (12.159)$$

Expanding the characteristics of the moments as shown in Eq. 12.159 into joint moments and modifying them into joint cumulants, Dalzell derived the expression for joint cumulants until the fourth degree from the modified frequency response characteristics $H_1(\omega)$, $H_2(\omega_1, \omega_2)$, $H_3(\omega_1, \omega_2, \omega_3)$, and functions of ω by the same type of style as Eq. 12.119 for the case of $p(z, \dot{z})$. Since these manipulations require many transactions involving the higher order terms in the expansions, he checked the order of magnitude of the functions, suggested the order to truncate the approximations and, by laborious manipulation utilizing Hermite polynomial, he obtained his approximation.

From these expressions, arbitrarily denoting the standardized maxima or minima of response by v he finally derived the expression for $p(v, 0, \ddot{z})$ using the cumulants up to the fourth order and then the probability distribution function for maxima and minima by

$$p^{+}(v) = \frac{1}{N_{\infty}^{+}} \int_{-\infty}^{0} |\ddot{z}| \, p(v, 0, \ddot{z}) \, d\ddot{z}$$

$$= -\frac{1}{N_{\infty}^{+}} \int_{-\infty}^{0} \ddot{z} \, p(v, 0, \ddot{z}) \, d\ddot{z} \qquad (12.160)$$

372

$$p^-(v) = \frac{1}{N_\infty^-} \int_0^\infty |\ddot{z}| \, p(v, 0, \ddot{z}) \, d\ddot{z}$$

$$= \frac{1}{N_\infty^-} \int_0^\infty \ddot{z} \, p(v, 0, \ddot{z}) \, d\ddot{z}. \tag{12.161}$$

Finally he derived the expressions for his first and second approximations $p_1^+(v)$, $p_{\bar{1}}(v)$ and $p_2^+(v)$, $p_{\bar{2}}(v)$ as follows. First, by neglecting the term higher (than 3) order joint cumulants, the first approximation is,

$$p_1^+(v) = \frac{\epsilon}{(2\pi)^{1/2}} \, \exp\left[-\frac{v^2}{2\epsilon^2}\right] + (1-\epsilon^2)^{1/2} \, v \, \exp\left[-\frac{v^2}{2}\right] \phi\left[\frac{v(1-\epsilon^2)^{1/2}}{\epsilon}\right],$$

$$\tag{12.162}$$

$$p_{\bar{1}}(v) = \frac{\epsilon}{(2\pi)^{1/2}} \, \exp\left[-\frac{v^2}{2\epsilon^2}\right] - (1-\epsilon^2)^{1/2} \, v \, \exp\left[-\frac{v^2}{2}\right] \phi\left[-\frac{v(1-\epsilon^2)^{1/2}}{\epsilon}\right],$$

$$\tag{12.163}$$

where $\phi(a)$ is the Gaussian cumulative distribution function and ϵ is the spectrum band width parameter.

The ϵ was introduced in Eq. 12.162 and Eq. 12.163 from the relations as follows that comes from the characters of joint cumulants,

$$-\lambda_{101} = \frac{k_{020}}{(k_{200}k_{002})^{1/2}} = (1-\epsilon^2)^{1/2} \tag{12.164}$$

$$1 - \lambda_{101}^2 = \epsilon^2. \tag{12.165}$$

It is interesting to find that this first approximation, Eq. 12.162, is just the same as the one that Cartwright and Longuet–Higgins[13] derived as shown in Eq. 12.49, and Fig. 12.1 in Section 12.5.

Dalzell's final expressions, including the effect of higher order cumulants (until 3) that take account of the higher order nonlinear response until the third order, are

$$p_2^+(v) = S(v,\epsilon)\ \epsilon\ \frac{\exp\left(-\frac{v^2}{2\epsilon^2}\right)}{(2\pi)^{1/2}}$$

$$+ R(v,\epsilon)\ (1-\epsilon^2)^{1/2}\ \exp\left(-\frac{v^2}{2}\right)\ \phi\left[\frac{v(1-\epsilon^2)^{1/2}}{\epsilon}\right], \quad (12.166)$$

$$p_2^-(v) = S(v,\epsilon)\ \epsilon\ \frac{\exp\left(-\frac{v^2}{2\epsilon^2}\right)}{(2\pi)^{1/2}}$$

$$- R(v,\epsilon)\ (1-\epsilon^2)^{1/2}\ \exp\left(-\frac{v^2}{2}\right)\ \phi\left[-\frac{v(1-\epsilon^2)^{1/2}}{\epsilon}\right]. \quad (12.167)$$

Here

$$S(v,\epsilon) = 1 + v\left[\frac{\lambda_{300}(1+\epsilon^2-5\epsilon^4)}{\epsilon^4} + \frac{\lambda_{003}(1-\epsilon^2)^{1/2}}{\epsilon^4}\right.$$

$$\left. + \frac{\lambda_{102}}{\epsilon^4} + \frac{\lambda_{201}}{\epsilon^4}(1+\epsilon^2)(1-\epsilon^2)^{1/2} - \lambda_{120}\right]$$

$$+ v^3\lambda_{300}, \quad (12.168)$$

$$R(v, \epsilon) = v + \left[\lambda_{120} + \frac{\lambda_{201}}{(1 - \epsilon^2)^{1/2}} + 3\lambda_{300} \right]$$

$$+ v^2 \left[-\lambda_{120} - \frac{\lambda_{201}}{(1 - \epsilon^2)^{1/2}} - 6\lambda_{300} \right]$$

$$+ v^4 \lambda_{300}, \tag{12.169}$$

where ϵ is the so-called band width parameter, as Eq. 12.165.

As referred to in Section 11.5, item 6, Dalzell[56] generated the simulation data of the cubic nonlinear response to check the validity of his tri-spectrum analysis[17] for the Gaussian excitation of the waves, as expressed by the Moskowitz–Pierson type spectrum,

$$U_{xx}(\omega) = 5\sigma_x^2 \omega_0^4 \, \exp \frac{\left[-1.25 \left(\frac{\omega_0}{\omega} \right)^4 \right]}{\omega^5} \tag{12.170}$$

where $U_{xx}(\omega)$ is a one-sided spectrum, σ_x^2 is the spectrum area and variance, and ω_0 is the modal frequency.

Using the same spectrum parameters for nonlinear response as he used before[17] and varying the excitation level by changing σ_x to $\sigma_x = 0.125, 0.25, 0.50, 0.75,$ and $1.0,$ he obtained results for simulated data averaging 10 samples for each case.

He calculated the probability distribution of maxima and minima and compared his results with Eqs. 12.162, 12.163, 12.166, and 12.167.

Figure 12.17 shows the comparison of probability distribution densities of response maxima and minima estimated for the simulations with those of the first and second approximations from Eqs. 12.162, 12.163, 12.166, and 12.167. Here z represents the normalized maxima and minima and was equal to $v - \lambda_{100}, \lambda_{100}$ being the normalized mean and v the standardized maxima and minima as appeared in Eqs. 12.162 through 12.167.

Figures 12.18 and 12.19 compare cumulative distributions of response maxima and minima estimated from the simulations with those of the first and second approximations. In these two figures, the standard deviation of input $\sigma,$ ("SIGMA") is the same, and the band width parameter, $\epsilon,$ ("EPSILON") was different. Here the first approximation is expressed as a straight line (the scale of the cumulative probability is so chosen) and is marked as the fitted distribution.

These figures indicate that the final expression for the second approximation gives excellent results that check the simulated results very well.
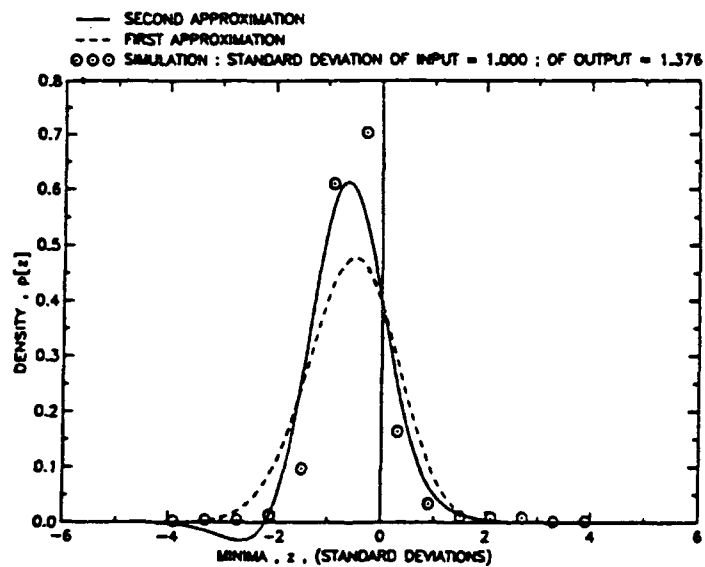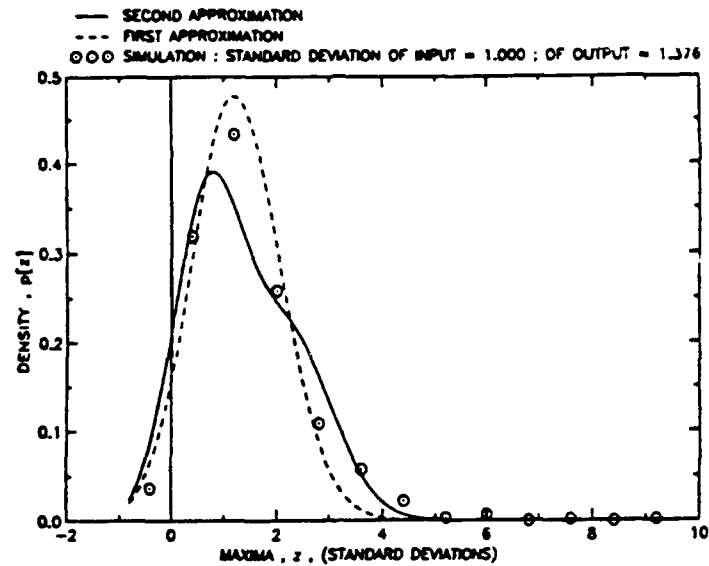
Fig. 12.17. Comparison of densities of response maxima and minima
estimated from the simulations, with those of the
first and second approximations.

(From Dalzell.[56])
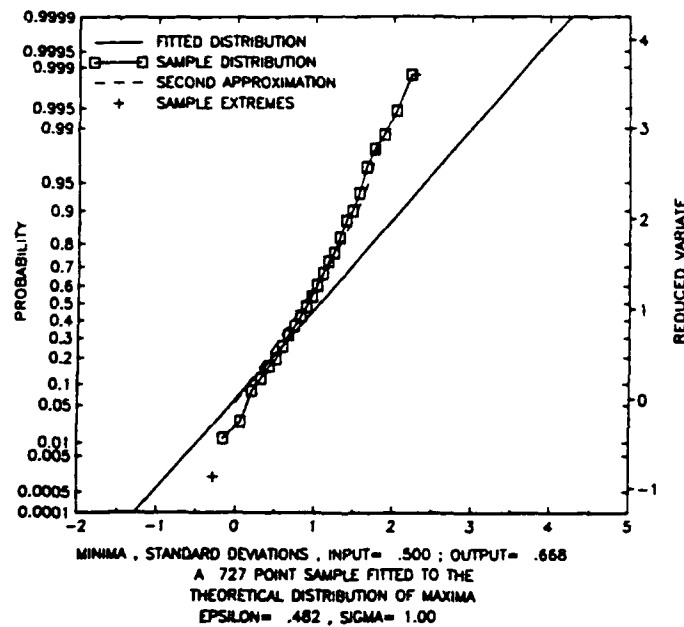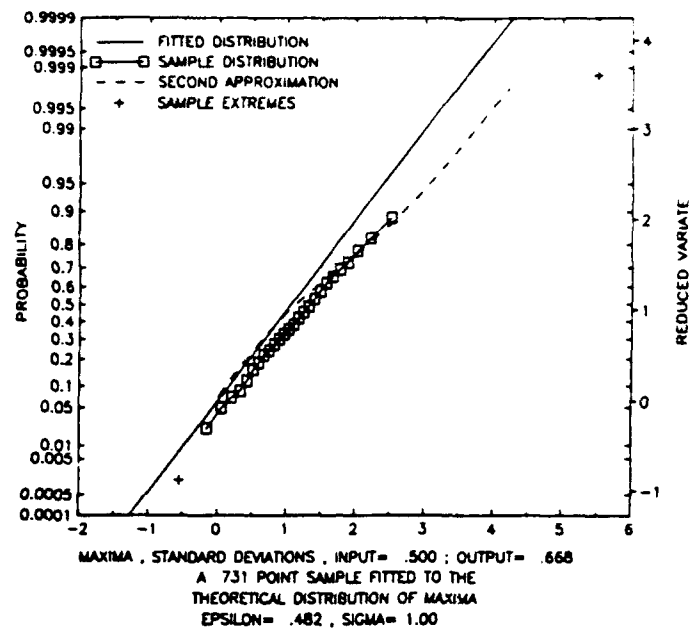
Fig. 12.18. Comparison of cumulative distribution of response maxima and minima estimated from the simulation, with those of the first (fitted distribution) and second approximation – sample 1. (From Dalzell.[56])

377
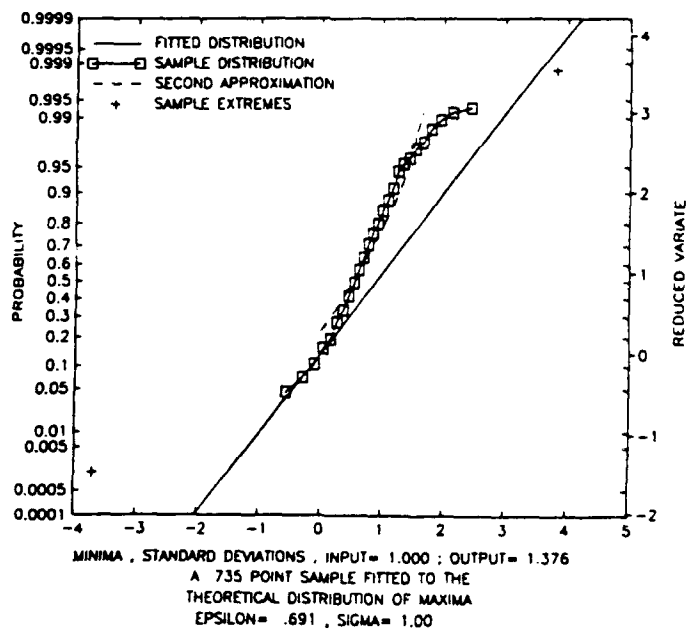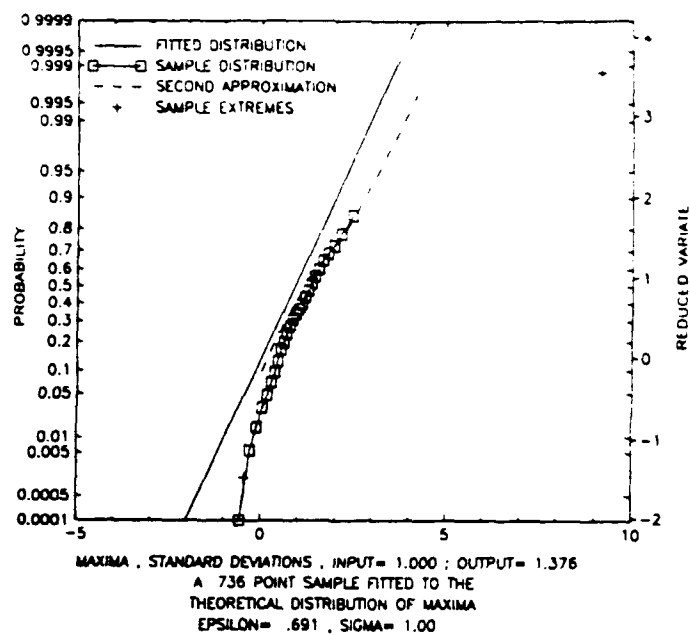
Fig. 12.19. Comparison of cumulative distribution of response maxima and minima estimated from the simulation, with those of the first (fitted distribution) and second approximation – sample 2.
(From Dalzell.[56])

CHAPTER 13

EXTENSION OF MODEL FITTING TECHNIQUES TO NONLINEAR PROCESS

13.1 INTRODUCTION

Suppose we have a discrete random process X_t and a purely random process ϵ_t, and X_t is expressed by

$$X_t = Q_A(X_{t-1}, X_{t-2}, \cdots X_{t-n}) + \epsilon_t. \tag{13.1}$$

When Q_A is a linear function,

$$X_t = a_1 X_{t-1} + a_2 X_{t-2} + \cdots + a_n X_{t-n} + \epsilon_t, \tag{13.2}$$

X_t is called as an autoregressive process (AR) of nth order, as discussed in Part II, Chapter 5.

If X_t is expressed as

$$X_t = Q_M(\epsilon_{t-1}, \epsilon_{t-2}, \epsilon_{t-3}, \epsilon_{t-m}) + \epsilon_t, \tag{13.3}$$

and Q_m is a linear function,

$$X_t = b_1 \epsilon_{t-1} + b_2 \epsilon_{t-2} + \cdots + b_n \epsilon_{t-m} + \epsilon_t, \tag{13.4}$$

then X_t is a moving average model (MA) of mth order, also discussed in detail in Part II, Chapter 5.

When these Q_A or Q_M functions are not linear functions but, for example, the polynomials of X_{t-n} or ϵ_{t-m}, then X_t is no longer a linear process and is called an expanded AR model or an expanded MA model.

A Voltera type process, as we saw in Section 11.1 in Eq. 11.1, is this expanded moving average process. More generally,

$$X_t = Q_A(X_{t-1} X_{t-2}, X_{t-n}) + Q_M(\epsilon_{t-1}, \epsilon_{t-2} \epsilon_{t-m}) + \epsilon_t \tag{13.5}$$

is an expanded ARMA model when Q_A, Q_m are polynomials of variables.

For expanded AR, MA, and ARMA models, there is no general way to solve the process. When the process is expressed as,

$$X_t + a_1 X_{t-1} + a_2 X_{t-2} + \cdots + a_k X_{t-k}$$

$$= \epsilon_t + b_1 \epsilon_{t-1} + \cdots + b_l \epsilon_{t-l} + \sum_{i=1}^{m} \sum_{j=l}^{v} c_{ij} \epsilon_{t-i} X_{t-j}, \tag{13.6}$$

Eq. 13.6 is called a bilinear model. The scope of nonlinear models that have been analytically developed is rather limited. A few efforts have been made along the following models: i) a simple bilinear model, ii) a threshold autoregressive model, and iii) an exponential autoregressive model.

13.2 BILINEAR MODEL

As the simplest example of a bilinear model, we take the first order model

$$X_{t+1} = aX_t + b\epsilon_{t+1} + c\epsilon_t X_t \qquad (13.7)$$

Priestley,[23] in studying the bilinear model, assumed that Eq. 13.7 can be expanded into the form of Voltera functions, Eq. 11.8 as,

$$X_t = \sum_{u=0}^{\infty} g_u U_{t-u} + \sum_{u=0}^{\infty} \sum_{v=0}^{\infty} g_{u,v} U_{t-u} U_{t-v} + \cdots . \qquad (13.8)$$

Here, the general transfer functions are

$$\Gamma_1(\omega_1) = \sum_{u=0}^{\infty} g_u e^{-i\omega_1 u}$$

$$\Gamma_2(\omega_1, \omega_2) = \sum_{u=0}^{\infty} \sum_{v=0}^{\infty} g_{u,v} \, e^{-i\omega_1 u - i\omega_2 v} . \qquad (13.9)$$

Assuming Eq. 13.7 is expanded into the form of Eq. 13.8, he derived $\Gamma_1(\omega)$, setting $\epsilon_t = e^{i\omega t}$ in Eq. 13.7, as

$$\Gamma_1(\omega_1) = \frac{b e^{i\omega_1}}{(e^{i\omega_1} - a)} . \qquad (13.10)$$

Similarly setting $\epsilon_t = e^{i\omega_1 t} + e^{i\omega_2 t}$,

$$\Gamma_2(\omega_1, \omega_2) = \frac{c}{2\left\{ e^{i(\omega_1 + \omega_2)} - a \right\}} \left\{ \Gamma(\omega_1) + \Gamma(\omega_2) \right\}$$

$$= \frac{\frac{1}{2} cb}{\left\{ e^{i(\omega_1 + \omega_2)} - a \right\}} \cdot \left\{ \frac{e^{i\omega_1}}{e^{i\omega_1} - a} + \frac{e^{i\omega_2}}{e^{i\omega_2} - a} \right\} . \qquad (13.11)$$

Particularly along the diagonal $\omega_1 = \omega_2 = \omega$,

$$\Gamma_2(\omega, \omega) = \frac{cb e^{i\omega}}{(e^{2i\omega} - a)(e^{i\omega} - a)} . \qquad (13.12)$$

More generally, Priestley showed that

$$\Gamma_k(\omega, \omega, \cdots \omega) = \frac{c^{k-1} b \, e^{i\omega}}{(e^{i k\omega} - a)(e^{i(k-1)\omega} - a) \cdots (e^{i\omega} - a)} . \qquad (13.13)$$

From these relations, he found that $\Gamma_1(\omega_1, \omega_2)$ included all the a, b, and c of Eq. 13.7. Thus he says, the bilinear process expressed by Eq. 13.7 is invertible to the functional polynomial model of Eq. 13.8.

This bilinear model can also be approximated he says, by the generalized autoregressive model. The first order bilinear model can be expressed by setting $b = 1$ in Eq. 13.7 (without losing generality),

$$X_{t+1} = aX_t + cX_t \ \epsilon_t + \epsilon_{t+1}. \tag{13.14}$$

We can modify this equation to

$$\left[1 + cX_t \ B\right]\epsilon_{t+1} = X_{t+1} - aX_t. \tag{13.15}$$

Here B is the backward shift operator. For small c, Eq. 13.15 can be inverted to

$$\epsilon_{t+1} = \left[1 - c \ X_t \ B\right]\{X_{t+1} - aX_t\}$$
$$= X_{t+1} - aX_t - cX_t^{\ 2} + ca \ X_t \ X_{t-1}. \tag{13.16}$$

This is a generalized autoregressive model. If the product term $X_t \ X_{t-1}$, is neglected, initial estimates of a and c can be obtained by a least squares approach. If the product term is not neglected, a nonlinear least squares approach can be used to get a and c. After initial estimates $\hat{a}_0$ and $\hat{c}_0$ are obtained, $\hat{\epsilon}_t$ can be estimated by

$$\hat{\epsilon}_{t+1} = X_{t+1} - aX_t - cX_t \ \hat{\epsilon}_t \quad \text{for } t = 1, 2, \ \cdots \ N. \tag{13.17}$$

Recursively starting from $\hat{\epsilon}_t = 0$, and using $\{X_t, \hat{\epsilon}_t\}$ for $t = 1, \ \cdots \ N$, new estimates for a and c can be found to minimize

$$\sum_{t=1}^{N} \left\{X_{t+1} - aX_t - cX_t\hat{\epsilon}_t\right\}^2. \tag{13.18}$$

Until the estimates converge, this procedure is repeated. Subba Rao[89] studied this bilinear model and gave several examples.

13.3 THRESHOLD AUTOREGRESSIVE MODEL

The threshold autoregressive model introduced by Tong[90] is generally expressed as

$$X_1 + a_1^{(i)}X_{t-1} + \cdots + a_l^{(i)}X_{t-l} = \epsilon_t^{(i)} \tag{13.19}$$

where $a_1^{(i)} \cdots a_l^{(i)}$ are constants in Region $R^{(i)}$ for

$$(X_{t-1}, \cdots X_{t-l}) \in R^{(i)}, \quad i = 1, \cdots k. \tag{13.20}$$

Region $R^{(i)}$ is in the l–dimensional Euclidean space R^l. For example, the first order threshold autoregressive model TAR(1) is

$$X_t = \begin{cases} a^{(1)}X_{t-1} + \epsilon_t^{(1)}, & \text{if } X_{t-1} < d \\ a^{(2)}X_{t-1} + \epsilon_t^{(2)}, & \text{if } X_{t-1} \geq d \end{cases}, \tag{13.21}$$

where the coefficient a differs by the size of X_{t-1}. Priestley[23] indicates that, if we consider a bilinear system in which the physical input U_t, output X_t, and noise ϵ_t are related by

$$X_{t+1} = aX_t + cU_t \ X_t + \epsilon_{t+1}, \tag{13.22}$$

and if U_t is determined by a feedback mechanism of the form

$$U_t = \begin{cases} +\alpha & \text{if } X_t < d \\ -\alpha & \text{if } X_t \geq d \end{cases} , \tag{13.23}$$

then the model X_t can be expressed by a threshold model

$$X_{t+1} = \begin{cases} a^{(1)} X_t + \epsilon_{t+1}, & \text{for } X_t < d \\ a^{(2)} X_t + \epsilon_{t+1}, & \text{for } X_t \geq d \end{cases} \tag{13.24}$$

where

$$\begin{cases} a^{(1)} = a + \alpha \ c \\ a^{(2)} = a - \alpha \ c. \end{cases} \tag{13.25}$$

This model gives a nonlinear process as shown by Eq. 13.22. It can be called a piece–wise linear approximation. As will be shown later in Section 13.5, Ozaki[91] made it clear that this piece–wise linearization is a special case of his nonlinear threshold autoregressive model.

13.4 EXPONENTIAL AUTOREGRESSIVE MODEL

The nonlinear random vibration system of one degree of freedom is expressed as

$$\ddot{X}(t) + g_1\{X(t)\} \cdot \dot{X}(t) + g_2\{X(t)\} \ X(t) = n(t) \tag{13.26}$$

where $n(t)$ is a random noise excitation.

When

$$\dot{X}(t) = Y(t), \tag{13.27}$$

Eq. 13.26 becomes

$$\dot{Y}(t) = - g_2\{X(t)\} \ X(t) - g_1\{X(t)\} \ Y(t). \tag{13.28}$$

From these two equations and the state space expression as explained in Section 12.3

$$\begin{bmatrix} \dot{X}(t) \\ \dot{Y}(t) \end{bmatrix} = \begin{bmatrix} 0 & 1 \\ -g_2\{X(t)\} & -g_1\{X(t)\} \end{bmatrix} \begin{bmatrix} X(t) \\ Y(t) \end{bmatrix} + \begin{bmatrix} 0 \\ n(t) \end{bmatrix} \tag{13.29}$$

or, in vector notation,

$$\dot{V}(t) = f\{X(t)\} \ V(t) + n(t), \tag{13.30}$$

where

$$V(t) = \begin{bmatrix} X(t) \\ Y(t) \end{bmatrix} = \begin{bmatrix} X(t) \\ \dot{X}(t) \end{bmatrix}. \tag{13.31}$$

So, finding the appropriate expression for $g_1(\cdot)$, $g_2(\cdot)$ in Eq. 13.28 is the same as finding the appropriate function $f\{X(t)\}$ for Eq. 13.30. When these two functions $g_1(\cdot)$, $g_2(\cdot)$ are in

the special forms as follows, the system is called a Duffing type or a Van del Pol type oscillator, respectively, as described in Chapter 10.

Duffing type:

$$g_1\{X(t)\} = c$$

$$g_2\{X(t)\} = \alpha + \beta X^2 \qquad (13.32)$$

Van del Pol type:

$$g_1\{X(t)\} = -c\{1 - X(t)^2\}$$

$$g_2\{X(t)\} = \alpha. \qquad (13.33)$$

For the Duffing type oscillator, under harmonic excitement $F \cos \omega t$,

$$\ddot{X}(t) + c\dot{X} + \alpha X + \beta X^3 = F \cos \omega t. \qquad (13.34)$$

We know that, with harmonic excitement, the response shows damping phenomena, as indicated in Fig. 13.1, and in this case the natural frequency is dependent on amplitude. So we can call this oscillation an amplitude–dependent period shifting oscillation.
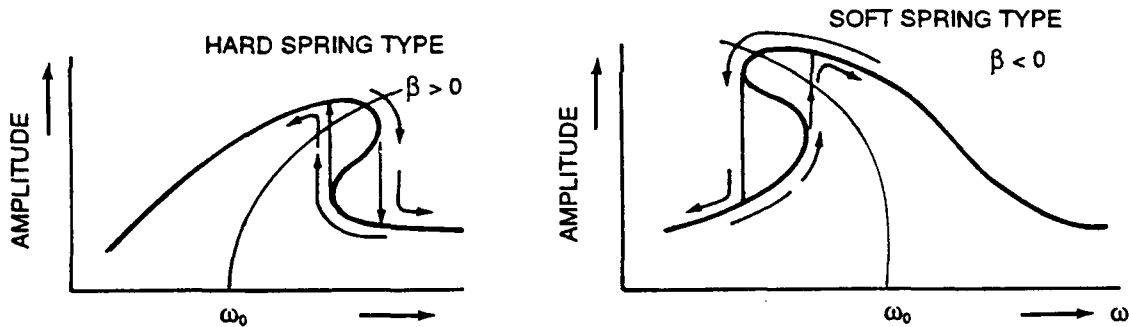
Fig. 13.1. Duffing type oscillator.

For the Van del Pol oscillator,

$$\ddot{X} - c\{1 - X^2\}\dot{X} + \alpha X = 0, \quad \text{for } c > 0, \alpha > 0 \qquad (13.35)$$

the system possesses a limit cycle, because when the amplitude X is small, the damping becomes negative and X starts to diverge, and when $X(t)$ becomes large, the damping becomes positive and the amplitude starts to decay. This system remains in oscillation without any excitation.

When we have random noise excitation $n(t)$

$$\ddot{X} - c(1 - X^2)\dot{X} + \alpha X = n(t), \tag{13.36}$$

the system will produce a perturbed limit cycle.

Ozaki[91-93,96,97] and Haggan and Ozaki[94,95] proposed a new type of nonlinear model called an exponential autoregressive model through the following considerations In Eq. 13.26, when g_1 and g_2 are constants, the system becomes a purely linear oscillator and the equation of motion is expressed as

$$\ddot{X} + c\dot{X} + \alpha X = n(t). \tag{13.37}$$

This expression can be inverted into an ARMA(2.1) model, as was explained in some detail in Section 6.3.2 of Part II, as

$$X_t = \phi_1 X_{t-1} + \phi_2 X_{t-2} + \theta_1 \epsilon_{t-1} + \epsilon_t. \tag{13.38}$$

Here $n(t)$ is a continuous Gaussian white noise and ϵ_t is a discrete Gaussian white noise. The oscillation expressed by Eq. 13.37 is governed by its characteristic equation, as discussed in Section 6.3.2,

$$\mu^2 + c\mu + \alpha = 0 \tag{13.39}$$

and by its roots (or eigenvalues)

$$\mu = -\frac{c}{2} \pm i\sqrt{\alpha - (c^2/4)}. \tag{13.40}$$

We know this model X_t diverges when $c < 0$ and converges when $c > 0$. On the other hand, the model expressed by Eq. 13.38 diverges when the roots of its characteristic equation

$$z^2 - \phi_1 z - \phi_2 = 0 \tag{13.41}$$

are outside the unit circle and converges to a stable process when two roots of Eq. 13.41 are inside the unit circle, as described in some detail in Sections 5.2.4 and 5.2.3 and in Fig. 5.16.

From Eq. 13.41, when $\phi_1^2 \le 4\phi_2$, i.e., when the roots are unequal and complex (conjugate to each other) zone [II] in Fig. 5.16,

$$z = \frac{\phi_1}{2} \pm \frac{1}{2} i\sqrt{-4\phi_2 - \phi_1^2}, \tag{13.42}$$

since $|z|^2 = \phi_2$, when $-\phi_2 > 1$ or $\phi_2 < -1$, this model diverges and when $1 > -\phi_2 > 0$ or $0 > \phi_2 > -1$, this model becomes a stable process.

From the discussion of Green's functions of ARMA(2.1) in Section 5.2.4 or of the autocorrelation of AR(2) in Section 5.2.3, we know that damping is determined by $\sqrt{-\phi_2}$, i.e., by ϕ_2, and the frequency is dependent on ϕ_1.

In the analysis of a ship's nonlinear rolling that comes from the nonlinear restoring moment (the Duffing type), Ozaki and Oda[92] first fitted a nonlinear model of the type

$$X_t = \phi_1 X_{t-1} + \phi_2 X_{t-2} + \pi X_{t-1}^3 + \epsilon_t. \tag{13.43}$$

Equation 13.43 can be transformed into

$$X_t = (\phi_1 + \pi\ X_{t-1}^2)\ X_{t-1} + \phi_2\ X_{t-2} + \epsilon_t. \tag{13.43'}$$

This expression shows that the coefficient of X_{t-1}, the first autoregressive coefficient, changed from ϕ_1 in Eq. 13.38 to $(\phi_1 + \pi\ X_{t-1}^2)$ in Eq. 13.43'. This means the frequency, determined by the coefficient of X_{t-1}, became amplitude dependent. Although this looks fine, Ozaki and Oda found that the time series X_t, defined by the nonlinear autoregressive model Eq. 13.4' was not stable but could be diverged. Therefore, instead of Eq. 13.43, they proposed

$$X_t = (\phi_1 + \pi_1 e^{-X_{t-1}^2})\ X_{t-1} + \phi_2\ X_{t-2} + \epsilon_t. \tag{13.44}$$

This is the exponential type of autoregressive model for a Duffing type oscillator. By expressing it this way, we can make both roots $\lambda(0)$, $\overline{\lambda(0)}$ of the instantaneous characteristic equation, when $X_{t-1} = 0$,

$$\lambda^2 - (\phi_1 + \pi_1) - \phi_2 = 0 \tag{13.45}$$

and also the roots $\lambda(\infty)$, $\overline{\lambda(\infty)}$ of the instantaneous characteristic equation when $X_{t-1} \rightarrow \infty$

$$\lambda^2 - \phi_1\lambda - \phi_2 = 0 \tag{13.46}$$

lie inside the unit circle as shown in Fig. 13.2. Accordingly, with Eq. 13.44 as the model, we can express the amplitude–dependent and stable oscillation under white noise oscillation excitation.
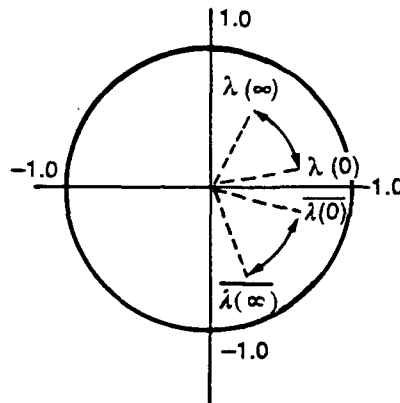
Fig. 13.2. $\lambda(0)$, $\lambda(\infty)$ for stable Duffing type model.

When $\pi_1 > 0$, the model corresponds to a hard spring system and when $\pi_1 < 0$ the model corresponds to a soft spring type oscillator. Haggan and Ozaki (1979)[94] and Ozaki[97-99] showed an example of this type as

$$X_t = (1.5 + 0.28 \; e^{-X_{t-1}^2}) \; X_{t-1} - 0.96 \; X_{t-2} + \epsilon_t \tag{13.47}$$

where $\sigma_\epsilon^2 = 0.025$, namely ϵ_t is $N[0, 0.025]$.

The eigenvalue λ stays $|\lambda|^2 \doteq 0.96$ for $25° \leq$ Arg. $(\lambda) \leq 40°$, and actually moves between $\lambda_0 = 0.89 \pm 0.41i$ and $\lambda_\infty = 0.75 \pm 0.63i$ when $|X_{t-1}|$ changes between 0 and ∞ as schematically shown in Fig. 13.2. The generated time history is shown over $t = 1-100$ in Fig. 13.3. To check the characteristics of this model expressed by Eq. 13.47, the model

$$X_t = (1.5 + 0.28e^{-X_{t-1}^2}) \; X_{t-1} - 0.96 \; X_{t-2} + a_t \tag{13.48}$$

was simulated,[100] where a_t is no longer random but is the form $a_t = \sin\{2\pi \; f(t) \cdot t\}$, where the frequency $f(t)$ changes with time.
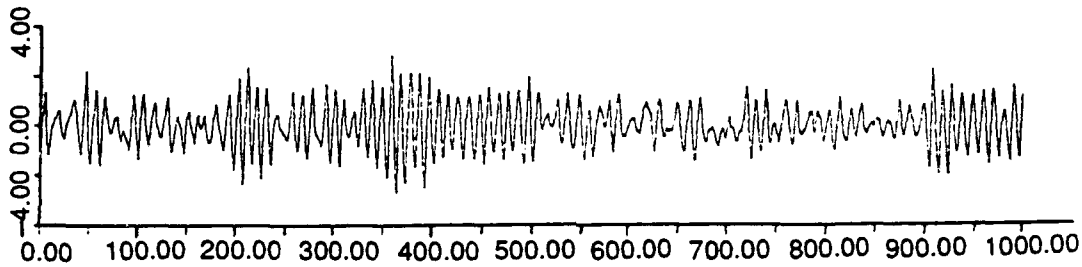
Fig. 13.3. Generated exponential AR model
$$X_t = (1.5 + 0.28e^{-X_{t-1}^2}) \; X_{t-1} - 0.96X_{t-2} + \epsilon_t, \quad \epsilon_t: \; N[0, 0.025] \; .$$
(From Ozaki.[98])

Figures 13.4 and 13.5 show these simulations. In Fig. 13.4, the frequency $f(t)$ increases with time from 0.005 to 0.1, and in Fig. 13.5 the frequency $f(t)$ decreases with time from 0.1 to 0.005. In Fig. 13.4, the amplitude suddenly becomes small at around $f = 0.062$; in Fig. 13.5, the amplitude changes abruptly at around $f = 0.052$ and actually demonstrates the jump phenomenon shown in Fig. 13.1.

In the same way, by making the damping amplitude dependent, Ozaki,[93,98] proposed the model for expressing the Van der Pol type oscillator as

$$X_t = \phi_1 X_{t-1} + (\phi_2 + \pi_2 e^{-X_{t-1}^2}) \; X_{t-2} + \epsilon_1 \tag{13.49}$$

or, more generally,

$$X_t = (\phi_1 + \pi_1 \; e^{-X_{t-1}^2}) \; X_{t-1} + (\phi_2 + \pi_2 e^{-X_{t-1}^2}) \; X_{t-2} + \epsilon_1 . \tag{13.50}$$
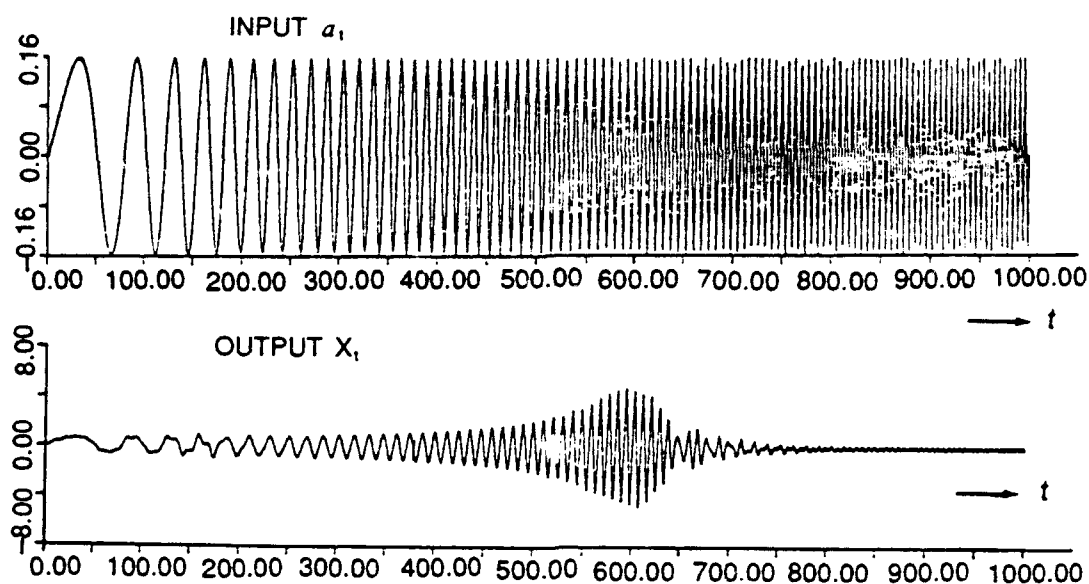
Fig. 13.4. $X_t = (1.5 + 0.28e^{-X_{t-1}^2}) X_{t-1} - 0.96X_{t-2} + a_t$.

Input $a_t = \sin\{\sin\pi \; f(t) \cdot t\}$; $f(t)$ is increasing by time.

(From Ozaki.[98])

In Eq. 13.50, the coefficients $\phi_1, \phi_2, \pi_1, \pi_2$ are to be chosen to make the damping coefficient negative, when the amplitude X_{t-1} is small and the oscillation starts to diverge, and to make the damping coefficient positive, when the amplitude X_{t-1} is large and the oscillation starts to decay. Mathematically

$$\lambda^2 - (\phi_1 + \pi_1)\lambda - (\phi_2 + \pi_2) = 0, \tag{13.51}$$

has roots outside the unit circle, and

$$\lambda^2 - \phi_1\lambda - \phi_2 = 0 \tag{13.52}$$

has roots inside the unit circle, as shown schematically in Fig. 13.6
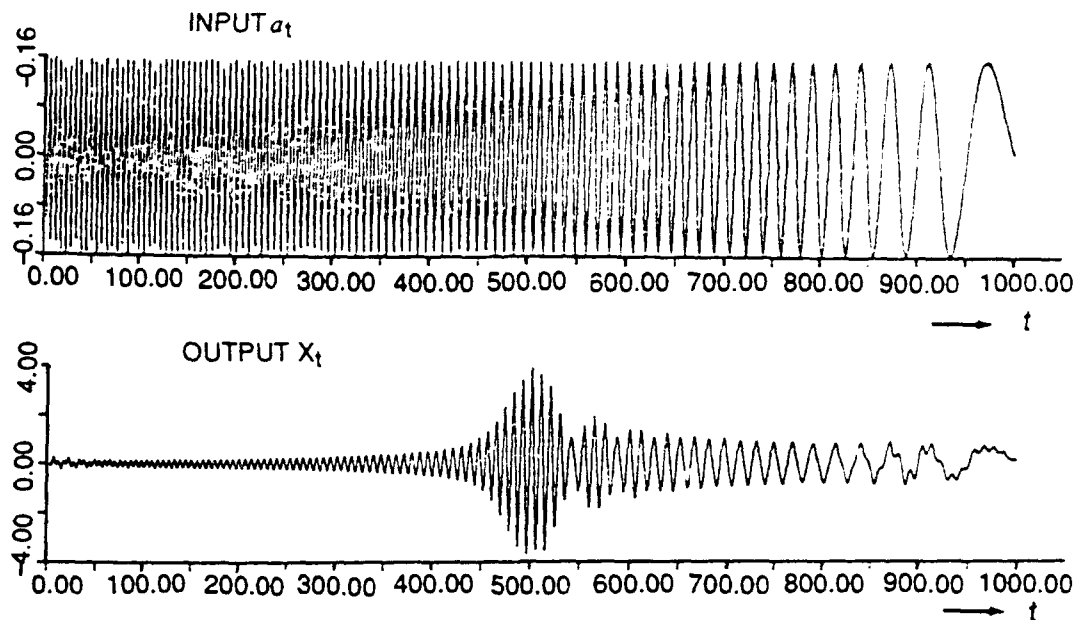
Fig. 13.5. $X_t = (1.5 + 0.28e^{-X_{t-1}^2}) \; X_{t-1} - 0.96X_{t-2} + a_t,$

Input $a_t = \sin\{2\pi \; f(t) \cdot t\}; f(t)$ is decreasing by time.

(From Ozaki.[98]).

As an example, Ozaki showed that, for a model

$$X_t = (1.95 + 0.23 \; e^{-X_{t-1}^2}) \; X_{t-1} - (0.96 + 0.24 \; e^{-X_{t-1}^2}) \; X_{t-2} + \epsilon_t, \qquad (13.53)$$

the characteristic roots are $\lambda_0 = 1.09 \pm 0.109i$ and $\lambda_\infty = 0.975 \pm 0.0968i$, and $|X|^2$ actually moves between $|\lambda_0|^2 = 1.20$ to $|\lambda_\infty|^2 = 0.96$, which shows Van del Pol type oscillation, as shown schematically in Fig. 13.6. Figure 13.7 shows that the model without ϵ_t, which starts with different initial values, approaches to the same limit period. Thus this shows that the model expressed by Eq. 13.53 has a stable limit period.
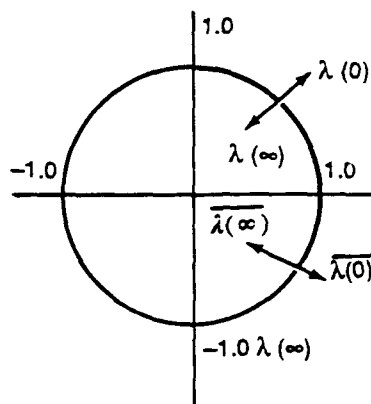
Fig. 13.6. $\lambda(0), \lambda(\infty)$ for Van del Pol type model.

388
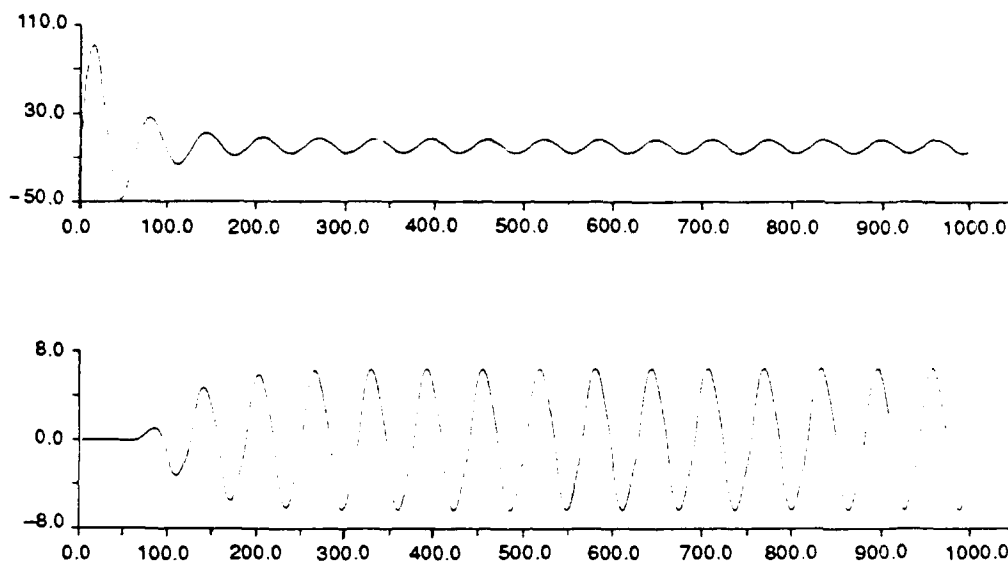
Fig. 13.7. $X_t = (1.95 + 0.23e^{-X^2_{t-1}})X_{t-1} - (0.96 + 0.24e^{-X^2_{t-1}})X_{t-2}$, with different initial values (without white noise).
(From Ozaki.[98])

More generally, Ozaki[98] proposed the higher type Duffing and Van del Pol nonlinear model as

$$X_t = g_1(X_{t-1}) \ X_{t-1} + g_2(X_{t-1}) \ X_{t-2} + \epsilon_t, \tag{13.54}$$

where

$$g_1(X_{t-1}) = \phi_1 + \left(\pi_0^{(1)} + \pi_1^{(1)}X_{t-1} + \pi_2^{(1)}X_{t-1}^2 + \cdots + \pi_{r_1}^{(1)}X_{t-1}^{r_1}\right)e^{-X_{t-1}^2} \tag{13.55}$$

$$g_2(X_{t-1}) = \phi_2 + \left(\pi_0^{(2)} + \pi_1^{(2)}X_{t-1} + \pi_2^{(2)}X_{t-1}^2 + \cdots + \pi_{r_2}^{(2)}X_{t-1}^{r_2}\right)e^{-X_{t-1}^2}. \tag{13.56}$$

The term $g(\cdot)$ is expressed by a constant plus a Hermite type polynomial. When $r_1 = 0, r_2 = 0$ in these equations, an equation of the type of Eq. 13.50 is obtained.

To determine the order, Akaike's criterion (AIC) was shown to be applicable for these nonlinear models, too.

13.5 NONLINEAR THRESHOLD AUTOREGRESSIVE MODEL

Ozaki[99] extended and generalized his model further and proposed his nonlinear threshold autoregressive model and a unified explanation of the nonlinear models.

For example, the exponential autoregressive model that he used as an example of a Van del Pol type nonlinear process, Eq. 13.53,

$$X_t = (1.9^r + 0.23e^{-X_{t-1}^2}) \ X_{t-1} - (0.96 + 0.24e^{-X_{t-1}^2}) \ X_{t-2} + \epsilon_t$$

was shown to be approximated by Tong's linear threshold autoregressive model, as

$$X_t = \begin{cases} 1.95 \ X_{t-1} - 0.96 \ X_{t-2} + \epsilon_t & \text{if } |X_{t-1}| \geq 0.5 \\ 2.18 \ X_{t-1} - 1.20 \ X_{t-2} + \epsilon_t & \text{if } |X_{t-1}| < 0.5. \end{cases} \tag{13.57}$$

The characteristic roots of the model jump from $\lambda_0 \left[|\lambda_0|^2 = 1.2 \right]$ to

$\lambda_\infty \left[|\lambda_\infty|^2 = 0.96 \right]$ or vice versa as in Fig. 13.6 and also shown by a step function in Fig. 13.8. While in the model as is Eq. 13.53, the path of two roots λ_0 and λ_∞ and λ at arbitrary X_{t-1} is specified by a continuous Hermite–type polynomials in the equation, as is shown by a continuous curve in Fig. 13.8.
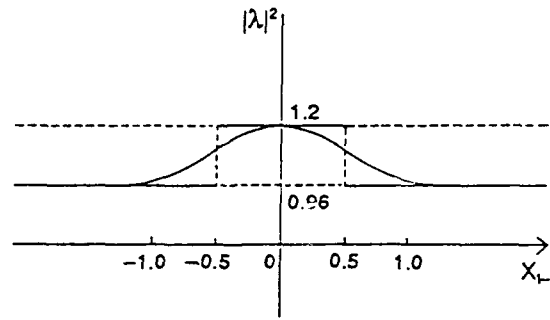
Fig. 13.8. Path of characteristic roots of threshold model and exponential AR model.
(From Ozaki.[99])

Ozaki argued that the threshold linear AR model, however, could not be expected to give a good enough approximation to nonlinear vibration, and appropriate nonlinear threshold AR model must be formulated. His point is, we have to consider the stepwise dynamics of restoring and damping force, but at the same time, the orbitally stableness and independence of the limit cycle of the Van del Pol equation must be maintained.

Instead of the linear step function approximation, nonlinear approximation considered was as follows.

$$X_t = \begin{cases} 1.95 \ X_{t-1} - 0.96 \ X_{t-2} + \epsilon_t \ , & \text{for} \quad |X_{t-1}| \geq 1.0 \\ (2.18 - 0.23 \ X_{t-1}^2) \ X_{t-1} - (1.2 - 0.24 \ X_{t-1}^2) \ X_{t-2} + \epsilon_t \ , \end{cases}$$
$$\text{for} \quad |X_{t-1}| < 1.0. \tag{13.58}$$

Equation 13.58 can give the characteristic roots that move much more smoothly than those of Eq. 13.57. Thus, the general form of the nonlinear threshold autoregressive model for nonlinear vibrations was proposed as,

$$X_t = \begin{cases} \phi_1 X_{t-1} + \cdots + \phi_p \ X_{t-p} + \epsilon_t \ , & \text{for } |X_{t-1}| \geq T \\ f_1(X_{t-1}) \ X_{t-1} + \cdots + f_p(X_{t-p}) \ X_{t-p} + \epsilon_t \ , & \text{for } |X_{t-1}| < T \end{cases} \tag{13.59}$$

where

$$f_i(X) = \phi^{(i)} + \pi_1^{(i)} X + \cdots + \pi_{r_i}^{(i)} X^{r_i}.$$

Schematically, the behavior of the characteristic roots for (1) linear threshold model, (2) nonlinear threshold model, and (3) exponential AR model are expressed as shown in Fig. 13.9.

390
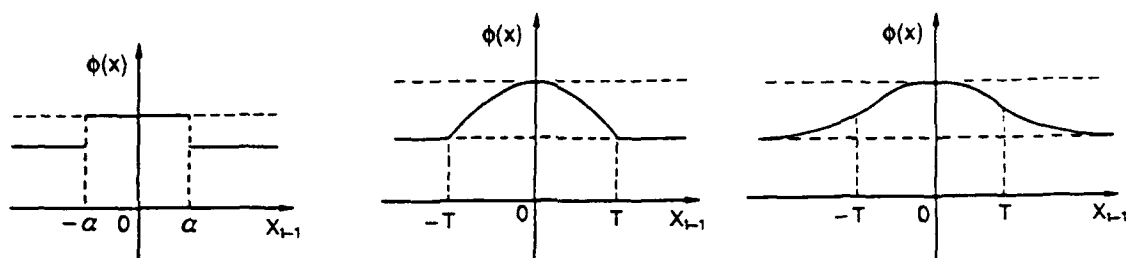
(1) LINEAR THRESHOLD AR MODEL   (2) NONLINEAR THRESHOLD AR MODEL   (3) EXPONENTIAL AR MODEL

Fig. 13.9. Schematical expression of behaviors of characteristic roots by Ozaki.[99]

Ozaki[100] investigated the stability and existence of limit cycles and their relation to the form of the characteristic equation. For example, he showed that a nonlinear threshold model,

$$X_t = \begin{cases} 0.8\ X_{t-1} + \epsilon_t, & \text{for } |X_{t-1}| \geq 1.0 \\ (0.8 + 1.3\ X_{t-i}^2 - 1.3 X_{t-1}^4)\ X_{t-1} + \epsilon_t, & \text{for } |X_{t-1}| < 1.0 \end{cases} \qquad (13.60)$$

has characteristic roots that behave as shown in Fig. 13.10. This model also has three stable singular points and gives a process that fluctuates around one of these points and jumps from one stable singular point to another, depending on the white input, as shown in Fig. 13.11.

With these discussions and examples, Ozaki showed the greater generality of his exponential models.
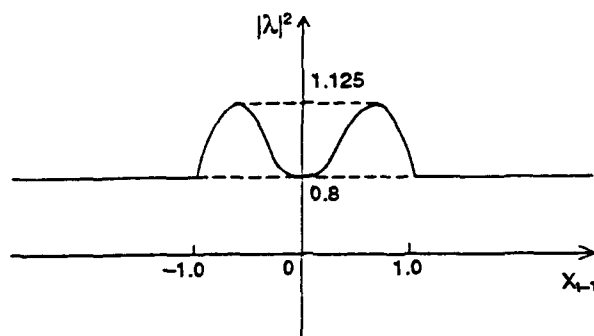
Fig. 13.10. Behavior of characteristic roots of a nonlinear threshold AR model. (From Ozaki.[99])
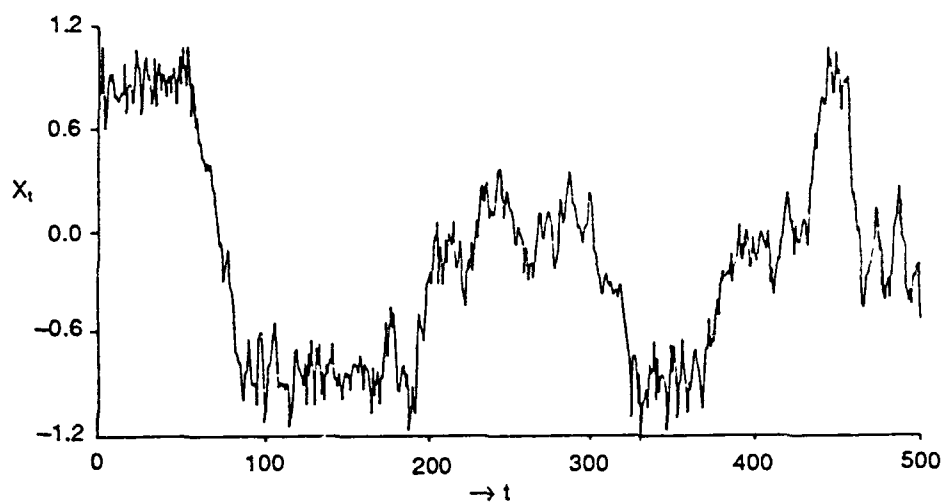
Fig. 13.11. Time history of a nonlinear threshold model that has characteristic roots that behave as Fig. 13.10. (From Ozaki.[99])

CHAPTER 14

CONCLUSIONS FOR PART III

The so–called "spectrum correlation method" discussed in Parts I and II has been shown to be a powerful way in the analysis of stochastic processes, but only when the processes are linear. Many steps in the manipulations in Parts I and II are based on the assumption of linearity of the process.

In the analysis of seakeeping data, as is usual in the general engineering field, many phenomena can be approximated as linear, and so spectrum or correlation analysis has played a significant role in advancing the technique of handling those data. Now, however, the nonlinearity of seakeeping data for ocean vehicles and structures has gradually been introduced, as mentioned in the Introduction.

Here in Part III of this lecture, methods for treating the nonlinearity in the stochastic process analysis were summarized and reviewed. The conclusions obtained here are as follows:

1. Several works on the effect of the nonlinearity of ocean waves on its spectrum were reviewed. It is now clear that, if necessary, we can get the effect of nonlinearity on its spectrum as well as on the probability distribution of the maxima and the minima of its amplitudes. It is also clear that the nonlinearity of ocean waves is usually quite small.

2. Even when the nonlinearity of the waves is small, the response of ocean vehicles and structures might be nonlinear, because of the very low frequency characteristics of their responses that respond rather severely to the higher order nonlinear excitation by waves or because of the nonlinearity in their response characteristics. For these cases, when the nonlinearity is weak and the response characteristics are expressed by weakly nonlinear equations of motions, the equivalent linearization and perturbation methods can be applied if the excitation is approximately linear. The perturbation method was applied by this author rather early to ship's oscillation, and now both methods are well formulated as shown in Chapter 10. These methods are applicable to obtaining the first approximation of weakly nonlinear damping and restoring oscillations under random excitation. To proceed to the second or third order approximation is, however, not necessarily easy.

3. The Voltera or functional expansion is one appropriate way to express the weakly nonlinear response to random excitation, and the polyspectral analysis is a reasonable way to get the higher order nonlinear frequency characteristics. The procedure for this analysis was summarized in Chapter 11.

4. Recently, J. F. Dalzell has engaged in significant efforts on polyspectral analysis. He tried not only bispectrum but even trispectrum analysis in the study of seakeeping in irregular waves, with excellent results, although an enormous amount of careful computation was necessary which at this stage might not be feasible for practical purposes.

5. Probability distribution of the maxima and the minima of the oscillatory motions can also be obtained from the nonlinear frequency responses. The general procedure for obtaining the probability distribution of extremes by calculating the cumulants related to the nonlinear frequency response characters and a few other examples are reviewed in Chapter 12.

6. If the process can be inverted into a vector Markov process by state–space trans-
formations, sometimes the solution of Fokker–Planck equations can be used to estimate
the joint probability distribution function, from which many probability characteristics of
the original process can be derived, even for nonlinear oscillations.

7. Recently, a few applications of this approach have appeared in seakeeping
studies. However, the Fokker–Planck equations have been solved only for some limited
cases, and are not so familiar to engineers. More studies are necessary for naval architects
to become familiar to the application of this method.

8. Some efforts have been made to expand the model fitting method to the nonlin-
ear process. The threshold autoregressive model, the exponential autoregressive model,
and the nonlinear threshold model are examples of expanded models. Some of these mod-
els look promising and some are under active development, but we will have to wait until
they are more fully formulated to accumulate experience in application to practical
problems.

As was mentioned in the Foreword, the contents of this report were summarized at
the time of this author's oral presentation at DTRC in July 1985, reflecting the state of the
art up to 1984, though the written version was completed in August 1987. After these
dates, the state of the art has made considerable progress, especially in the field treated
here in Part III, and this author finds the 'review,' and this conclusion, to be insufficient
because of the recent works of several researchers. In order to update the report, this
author added a Supplement of References 101 through 124, listing publications that have
appeared since 1984, together with some other publications that were not referred to in
the original manuscript.

CHAPTER 15

CONCLUSIONS FOR PART I THROUGH PART III

Part I of this lecture note summarized the conventional procedures for analyzing the irregular time histories of observed data, like irregular ocean waves, and the responses of marine vehicles and structures on the ocean, that can be treated as weakly stationary ergodic stochastic processes. In these analyses, the so-called Wiener's general harmonic analysis technique plays a large role, and the correlation and spectrum functions of the processes were important and included much information on the characteristics of the processes. When the responses of some dynamic systems to random excitation are to be treated, the cross relations of the input (excitation) and the output (response), i.e., the cross correlations and cross spectra, are very important.

The theories of the analysis are complete and rather beautiful. However, in sample computations from practical data, that is, from discrete data sampled at some time interval of finite length, many statistical considerations are necessary in estimating the correlation and spectrum functions to get statistically reliable results. After the general procedures were summarized, the discussion concentrated on that point. In these procedures, this author made several suggestions for improving the reliability (actually the coherencies) and these results were summarized. This author stressed that we should pay more attention to the time–domain characteristics of the functions. For example, the correlogram, that is the diagram of the correlation function and is a function in the time domain, deserves as much attention as is now paid to the spectrum.

Part II is concerned with the parametric analysis of a stationary process, which is really an alternative or more modern method for analyzing the sample random process. This author believes that the characteristics of the function in the time domain play bigger roles in this method than in the nonparametric conventional method, discussed in Part I.

The parametric method fits a statistical model to an observed process and estimates the parameters from the observed data. In Part II, the autoregressive (AR) models, moving average (MA) models, and mixed autoregressive moving average (ARMA) models were introduced. Since these models and the parametric approach are not familiar to most engineers, especially in the field of naval architecture, the author explained them in considerable detail. (He is afraid it was in too much detail.)

Usually a moderate or rather low order finite AR(n), MA(m), or ARMA(n,m) model can be fitted to represent adequately most of the observed processes. The optimum order of these fitted models, n or m, can be estimated by a method called Akaike's information criteria (AIC). This method is based on information theory and enables one to choose the order n or m that maximizes the statistical entropy of the estimate. It is therefore called the "Maximum Entropy Method," although it is different from a similar method already published under the same name. The AIC method can give the optimum order to be adopted. In Part II, in explaining the characteristics of these models, this author generated several fundamental models, the AR(0) (pure random), AR(1), AR(2), ARMA(2.1), MA(2), MA(1), and ARMA(2.2) models, by simulation and analyzed them by the parametric method. The orders were estimated by AIC and, for almost all processes, we succeeded to fit models that coincided with the models used to generate the simulated process. In these demonstrations, the simulated processes were also analyzed by the

nonparametric conventional method (sometimes called the correlation method, or the Blackman–Tukey, BT method), and the spectra were compared with the ones obtained by the parametric method. From these comparisons, we can get an idea of the characteristics of the parametric method. Although they could have very steep peaks, the spectra from the parametric method are smooth, and are free from the erroneous smoothing (blurring) effect of spectral windows in the nonparametric method. They are differently effected by the statistical fluctuations of sample estimation that come from the finiteness of discrete data.

Examples of results obtained by applying this parametric method to the analysis of seakeeping data for marine vehicles and structures were also given to demonstrate the usefulness of this approach in this field.

This author concludes that although this parametric approach is not the ultimate method of course, it is very promising, gives reliable results, and offers a supplement to the nonparametric method explained in Part I. The nonparametric method is, in a sense, a method for estimating infinite or very large number of parameters from finite data, or for estimating their spectrum or correlation functions. The parametric method on the other hand is a method for estimating a finite number of parameters for the same purpose.

The characteristics of a dynamic system, which is usually assumed to be deterministic, must be approximated by a finite number of parameters because the system is usually governed by equations of motions with a certain finite number of parameters. The types and also the order of parametric models are closely related with the order of the equations of motions, so the parametric method can be presumed to be more reasonable in the analysis of response characteristics.

In Parts I and II, the processes were assumed to be linear. In Part III, the method for treating a nonlinear process was summarized and several methods, such as the linearization method, the perturbation method, and the Voltera expansion method (polyspectra method), were reviewed and the relations of these methods to each other were described. Then, in relation to the probability distribution of the extreme amplitudes of nonlinear processes, the application of the Fokker–Planck equation and some examples appearing recently in naval architecture were introduced. The probability distribution of extremes of nonlinear response process were also related to the higher order frequency response functions, and can be connected through the cumulant expressions. The general relations of these functions were summarized. The achievements of J. F. Dalzell on the application of polyspectra and in the derivation of the probability distributions of extremes of seakeeping data were introduced at length. At the end of Part III, as an extension of the model fitting approach treated in Part II, a few trials on nonlinear parametric models proposed by several statisticians were introduced. Some of these trials look promising and are still under active development. However, as has been concluded in Chapter 14, we need more experience with such applications.

ACKNOWLEDGMENTS

THIS PAGE INTENTIONALLY LEFT BLANK

REFERENCES

1. Kan, S., "An Investigation into the Seagoing Qualities of the Single–Screw Cargo Ship *Nissei–Maru* by Actual Ship Experiment" (in Japanese). *J. Soc. Nav. Arch. (Japan)*, Vol. 92, pp. 123–136 (Apr 1952). Also in "Investigation into the Seagoing Qualities of the Single–Screw Cargo Ship *Nissei–Maru* by Actual and Model Ship Experiments" (in English). The First Research Comm., Report No. 1, Shipbuilding Research Association of Japan, Tokyo (Aug 1954).

2. Yamanouchi, Y., "On the Ship Speed–Meter Used in *Nissei–Maru* Experiments," (in Japanese) in: Proceedings of Fourth Annual Meeting, Transportation Tech. Res. Institute (1952).

3. Yamanouchi, Y., "On the Analysis of Ship's Oscillations as a Time Series" (in Japanese), *J. Soc. Nav. Arch. (Japan)*, Vol. 99, pp. 47–64 (Jul 1956). Also (in English) Report of Transportation Technical Research Institute, Report No. 27, Tokyo (Sep 1957).

4. St. Denis, M. and W. J. Pierson, Jr., "On the Motions of Ships in Confused Seas." Trans. *Soc. Nav. Arch. Mar. Eng.*, No. 61, pp. 280–357 (1953).

5. Wiener, N., The Fourier Integral and Certain of its Applications, Cambridge University Press, New York (1933).

6. Wiener, N., Extrapolation, Interpolation, and Smoothing of Stationary Time Series, John Wiley, New York (1949).

7. Doob, J. L., "Time Series and Harmonic Analysis," in: Proceedings of Berkeley Symposium on Mathematical Statistics and Probability, Berkeley, California (1949).

8. Shannon, C. E., "A Mathematical Theory of Communications," *Bell Systems Technical Journal*, Vol. 27, Part I, pp. 379–423 (Jul 1948); Part II, pp. 623–656 (Oct 1948).

9. Rice, S. O., "Mathematical Analysis of Random Noise," *Bell Systems Technical Journal*, Vol. 23, pp. 283–332 (1944); Vol. 24, pp. 46–156 (1945). Also in Selected Papers on Noise and Stochastic Processes, ed. N. Wax, pp. 133–294, Dover, New York (1954).

10. Neumann, G., "On Ocean Wave Spectra and a New Method of Forecasting Wind Generated Sea," Technical Memo, No. 43, Beach Erosion Board (1953).

11. Pierson, W. J., Jr., "An Interpretation of the Observable Properties of Sea Waves in Terms of the Energy Spectrum of the Gaussian Record," Trans. *American Geo. Union*, Vol. 35, No. 5 (1954).

12. Longuet–Higgins, M. S., "On the Statistical Distribution of the Height of the Sea Waves," *J. Mar. Res.*, Vol. XI, No. 3, pp. 245–266 (Dec 1952).

REFERENCES (Continued)

13. Cartwright, D. E. and M. S. Longuet–Higgins, "The Statistical Distribution of Maxima of a Random Function," in: Proceedings of Roy. Soc. A, Vol. 273, pp. 212–232 (1956).

14. Lewis, E.V., "Ship Speed in Irregular Seas," Trans. *Soc. Nav. Arch. and Mar. Eng.*, Vol. 63, pp. 134–202 (1957).

15. Dalzell, J. F. and Y. Yamanouchi, "The Analysis of Model Test Results in Irregular Head Seas to Determine the Amplitude and Phase Relations of Motion to the Waves," in: Proceedings in Second Seminar on Ship Behavior at Sea, Stevens Institute of Technology, ETT Report 708, pp. 97–112, Figs. pp. 152–165 (1958).

16. Dalzell, J. F., "Application on the Functional Polynominal Model to the Ship Added Resistance Problem," in: Proceedings of the Eleventh ONR Symposium on Naval Ship Hydrodynamics, London (1976).

17. Dalzell, J. F., "An Investigation of the Applicability of the Third Degree Functional Polynomial Model to Nonlinear Ship Motion Problem," Technical Report SIT–DL–82–9–2275, Stevens Institute of Technology (Dec 1982).

18. Doob, J. L., Stochastic Process, 654 pages, Wiley, New York (1953).

19. Grenander, U. and M. Resenblatt, Statistical Analysis of Stationary Time Series, 310 pages, Wiley, New York (1957).

20. Davenport, W. B. and W. L. Root, Random Signals and Noise, 389 pages, McGraw Hill, New York (1958).

21. Blackman, R. B. and J. W. Tukey, "The Measurement of Power Spectra from the Point of View of Communications Engineering," *Bell Systems Technical Journal Parts I & II*, Vol. 37, No. 1, pp. 185–282 (Jan 1958), also No. 2, pp. 485–569 (Mar 1958), Dover, New York (1958).

22. Parzen, E., Stochastic Processes, 324 pages, Holden–Day, San Francisco, Calif. (1962).

23. Priestley, M. B., Spectral Analysis and Times Series, Vol. 1. Univariate Series, Vol. 2. Multivariate Series, Prediction and Control, 890 pages, Academic Press, London (1981).

24. Parzen, E., "Mathematical Consideration in the Estimation of Spectra," *Technometrics*, No. 3, pp. 167–190 (1961).

25. Akaike, H., "On the Design of Lag Window for the Estimation of Spectra," in: *Ann. Instit. Stat. Math.*, Tokyo, Vol. 16, No. 1, pp. 1–21 (1964).

26. Tick, L. J., "Conditional Spectra, Linear Systems and Coherency," in: Proceedings of the Symposium on Time Series Analysis, Wiley, New York, pp. 197–203 (1963) .

REFERENCES (Continued)

27. Akaike, H., "On the Statistical Estimation of the Frequency Response Function on a Spectrum having Multiple Input," *Ann. Instit. Stat. Math.*, Tokyo, Vol. 17, No. 2, pp. 185–210 (1965).

28. Enochson, L. D., "Frequency Response Function and Coherency Function for Multiple Input Linear System," Measurement Analysis Corporation NASA Contractor Report CR-32 (1964).

29. Akaike, H. and Y. Yamanouchi, "On the Statistical Estimation of Frequency Response Function," *Ann. Instit. Stat. Math.*, Tokyo, Vol. 14, No. 1, pp. 23–56 (1962).

30. Yamanouchi, Y., "On the Analysis of the Ship Oscillation Among Waves, Part II" (in Japanese), *J. Soc. Nav. Arch. (Japan)*, Vol. 110, pp. 19–29 (Dec 1961).

31. Yamanouchi, Y., "On the Analysis of the Ship Oscillation Among Waves, Part III" (in Japanese), *J. Soc. Nav. Arch. (Japan)*, Vol. 111, pp. 103–115 (Jun 1962).

32. Yamanouchi, Y., "On Some Considerations on the Statistical Analysis of Ship Response in Waves, – On the Statistical Evaluation of the Impulse Response Function and the Effect of Nonlinearity of Response on Calculation of the Spectra"(in Japanese), *J. Soc. Nav. Arch. (Japan)*, Vol. 117, pp. 102–114 (Jun 1965). Also (in English) in "Selected Papers" from the *Soc. Nav. Arch. (Japan)*, Vol. 3, pp. 109–124 (1969).

33. Yamanouchi, Y., "On the Application of Multiple Input Analysis to the Study of Ship's Behavior and an Approach to the Nonlinearity of Responses" (in Japanese), *J. Soc. Nav. Arch. (Japan)*, Vol. 125, pp. 73–87 (1969). Also (in English) in "Selected Papers" from the *Soc. Nav. Arch. (Japan)*, Vol. 7, pp. 92–111 (1971).

34. Takaishi, Y., S. Ando, and H. Kadoi, "Tests on Service Performance of the *M.S. Yamataka–Maru* at North Pacific Route" (in Japanese), *Report S. R. I*, Vol. 2, No. 2, Ship Research Institute, Mitaka, Japan (Mar 1965).

35. Yamanouchi, Y., Y. Takaishi, K. Sugai, and S. Ando, "On the Analysis of the Ship Oscillation among Waves, Part IV, On the Processing of Seakeeping Data" (in Japanese), *J. Soc. Nav. Arch. (Japan)*, Vol. 119, pp. 50–59 (Jun 1966).

36. Pandit, S. M. and S. M. Wu, Time Series and System Analysis with Applications, 586 pages, Wiley, New York (1983).

37. Box, E. P. and G. M. Jenkins, rev. ed., Time Series Analysis: Forecasting and Control, 575 pages, Holden–Day, San Francisco (1976).

38. Harvey, A. C., Time Series Models, 229 pages, Philip Allan Publishers, Oxford (1981).

39. Durbin, J., rev. "The Fitting of Time Series Models," *Institute International Statist. Math.*, Vol. 28, pp. 233–244 (1969).

REFERENCES (Continued)

40. Akaike, H., "Fitting an Autoregressive Model for Prediction," *Ann. Instit. Stat. Math.*, Tokyo,Vol. 21, pp. 243–247 (1969).

41. Akaike, H., · Information Theory and an Expression of the Maximum Likelihood Principle," in: <u>Proceedings of the Second International Symposium on Information Theory</u>, Akademiai Kiado, pp. 267–281 (1973).

42. Akaike, H., "A New Look at the Statistical Model Identification," I.E.E.E. Trans., Automatic Control, AC–19, No. 6, pp. 716–723 (1974).

43. Akaike, H., "Stochastic Theory of Minimal Realization," I.E.E.E. Trans., Automatic Control, AC–19, No. 6, pp. 667–673 (1974).

44. Akaike, H., "Canonical Correlation Analysis of Time Series and the Use of an Information Criterion," <u>Advances and Case Studies in System Identification</u>, eds. R. Mehra and D. G. Lainiotis, Academic Press, New York and London (1976).

45. Akaike, H., "An Entropy Maximization Principle," in: <u>Proceedings of Symposium on Applied Statistics</u>, ed. P. Krishnaiah, North Holland, Amsterdam (1977).

46. Yamanouchi, Y., K. Ohtsu, G. Kitagawa, and H. Oda, "The Recent Trend of Data Analysis (I) – A New Method to Calculate the Spectrum through Model Fitting, (II) A New Method to Calculate the Dynamic Response Characteristics of a System through Model Fitting" (in Japanese), *Bull. Soc. Nav. Arch. (Japan)*, No. 589, pp. 27–34 (Jul 1978), No. 591, pp. 20–31 (Sep 1978).

47. Kullback, S., <u>Information Theory and Statistics</u>, Wiley and Sons, New York (1959).

48. Akaike, H., "A Bayesian Analysis of the Minimum AIC Procedure," *Ann. Instit. Stat. Math.*, Tokyo, Vol. 30, Part A, pp. 9–14 (1978).

49. Akaike, H., "A Bayesian Extension of the Minimum AIC Procedure of Autoregressive Model Fitting," <u>Biometrika</u>, Vol. 66, pp. 237–242 (1979).

50. Shibata, R., "Selection of the Order of an Autoregressive Model by Akaike's Information Criterion," <u>Biometrika</u>, Vol. 63, pp. 117–126 (1976).

51. Akaike, H., "On the Use of a Linear Model for the Identification of Feedback Systems," *Ann. Instit. Stat. Math.*, Tokyo, Vol. 20, No. 3, pp. 429–435 (1968).

52. Yamanouchi, Y., K. Ohtsu, and H. Oda, "Spectrum Estimate through Autoregressive Model Fitting with an Information Criterion Based on he Maximum Entropy Principle," <u>Proceedings of the Eighteenth ITTC</u>, Leningrad, Vol. 2, pp. 139–146 (1981).

53. Oda, H., Y. Yamanouchi, T. Oda, and S. Takanashi, "The New Statistical Method for Estimating Dynamic Behavior of Offshore Structure in Waves" (in Japanese), <u>Mitsui Zosen Tech. Review</u>, No. 117, pp. 1–10 (Jan 1983).

REFERENCES (Continued)

54. Yamanouchi, Y., K. Ohtsu, and H. Oda, "Frequency Response Function Estimate through Multivariate Autoregressive Model," in: *Proceedings of the Seventeenth ITTC*, Göteborg, Vol. 2, pp. 213–216 (1984).

55. Dalzell, J. F., "The Applicability of the Functional Input–Output Model to Ship Resistance in Waves," Report SIT–DL–75–1794, Stevens Institute of Technology (Jan 1975).

56. Dalzell, J. F., "Approximations to the Probability Density of Maxima and Minima of the Response of a Nonlinear System," Report EW–22–84, United States Naval Academy (1984).

57. Dalzell, J. F., "Cross–Bispectral Analysis: Application to Ship Resistance in Waves," *J. Ship Res.*, Vol. 18, No. 1, pp. 62–72 (Mar 1974).

58. Dalzell, J. F., "Estimation of the Spectrum of Nonlinear Ship Rolling: The Functional Series Approach," Davidson Laboratory Report SIT–DL–76–1894 (May 1976).

59. Roberts, J. B., "Stationary Response of Oscillators with Nonlinear Damping to Random Excitation," *J. Sound and Vib.*, Vol. 50, No. 1, pp. 145–156 (1977).

60. Roberts, J. B., "Nonlinear Analysis of Slow Drift Oscillations of Moored Vessels in Random Seas," NMI R85 (Aug 1980), National Maritime Institute. Also *J. Ship Res.*, Vol. 25, No. 2, pp. 130–140 (Jun 1981).

61. Roberts, J. B., "A Stochastic Theory of Nonlinear Ship Rolling in Irregular Seas," *J. Ship Res.*, Vol. 26, No. 4, pp. 229–243 (Dec 1982).

62. Tick, L. J., "A Nonlinear Random Model of Gravity Waves I," *J. Math and Mech.*, Vol. 8, No. 15 (1959).

63. Tick, L. J., "Nonlinear Probability Models of Ocean Waves," *Ocean Wave Spectra*, pp. 163–169, Prentice–Hall (1963).

64. Longuet–Higgins, M. S., "Resonant Interactions between Two Trains of Gravity Waves," *J. Fl. Mech.*, Vol. 12, pp. 321–332 (1962).

65. Longuet–Higgins, M. S., "The Effect of Nonlinearities on Statistical Distributions in the Theory of Sea Waves," *J. Fl. Mech.*, Vol. 17, pp. 459–480 (1963).

66. Phillips, O. M., "On the Dynamics of Unsteady Gravity Waves of Finite Amplitude, Part 1: The Elementary Interactions," *J. Fl. Mech.*, Vol. 9, Part II, pp. 193–217 (1960).

67. Hineno, M., "An Investigation of the Influence of Quadratic Nonlinearities Upon the Statistics of Relative Motion of Semi–submersibles," Report SIT–DL–83–9–2360, Davidson Laboratory, Stevens Institute of Technology (Jul 1983).

REFERENCES (Continued)

68. Hasselman, K., W. Munk, and G. MacDonald, "Bispectrum of Ocean Waves," in: Proceedings of the Symposium on Time Series Analysis, pp. 125–139, John Wiley and Sons, New York (1963).

69. Yamanouchi, Y., "On the Analysis of the Ship Oscillations Among Waves – Part I" (in Japanese), *J. Soc. Nav. Arch. (Japan)*, Vol. 109, pp. 169–183 (1961).

70. Ogilvie, T. F., "Recent Progress Toward the Understanding and Prediction of Ship Motions," in: Proceedings of Fifth ONR Symposium on Naval Hydrodynamics, pp. 3–80 (1964).

71. Hasselman, K., "On Nonlinear Ship Motions in Irregular Waves," *J. Ship Res.*, Vol. 10, No. 1, pp. 64–68, SNAME (Mar 1966).

72. Jacobson, J. S., "Steady Forced Vibration as Influenced by Damping," Trans. ASME, APM–52–15 (1930).

73. Caughey, T. K., "Equivalent Linearization Techniques," *J. Acou. Soc. Am.*, Vol. 35, No. 11, pp. 1706–1711 (1963).

74. Vassilopulos, L. A., "Ship Rolling at Zero Speed in Random Beam Seas with Nonlinear Damping and Restoration," *J. Ship Res.*, Vol. 15, No. 4, pp. 289–294 (Dec 1971).

75. Kaplan, P., "Lecture Notes on Nonlinear Theory of Ship Roll Motion in a Random Seaway," in: Proceedings of Eleventh ITTC, Tokyo, pp. 393–396 (1966).

76. Isserlis, L., "On a Formula for the Product–Moment Coefficient of any Order of a Normal Frequency Distribution in Any Number of Variables," Biometrika, Vol. 12, pp. 134–139 (1918).

77. Crandell, S. H., "Perturbation Techniques for Random Vibration of Nonlinear Systems," *J. Acou. Soc. Am.*, Vol. 35, No. 11, pp. 1700–1705 (1963).

78. Yamanouchi, Y. and K. Ohtsu, "On the Nonlinearity of Ship's Response and the Higher Order Spectrum—Application of the Bispectrum" (in Japanese), *J. Soc. Nav. Arch. (Japan)*, Vol. 131, pp. 115–135 (Jun 1972).

79. Yamanouchi, Y. and K. Ohtsu, "On the Usefulness of Bispectrum, Skewness and Peakedness in the Study of Ship's Response in Waves," in: Proceedings of the Thirteenth ITTC, Hamburg, pp. 189–195 (1972).

80. Bedrosian, E. and S. O. Rice, "The Output Properties of Voltera Systems (Nonlinear Systems with Memory) Driven by Harmonic and Gaussian Inputs," in: Proceedings of the I.E.E.E., Vol. 59, No. 12, pp. 1688–1707 (Dec 1971).

81. Dalzell, J. F., "A Note on the Form of Ship Roll Damping," *J. Ship Res.*, Vol. 22, No. 3, pp. 178–185 (Sep 1978).

REFERENCES (Continued)

82. Brillinger, D. R., "The Identification of Polynominal Systems by Means of Higher Order Spectra," *J. Sound and Vib.*, Vol. 12, pp. 301–313 (1970).

83. Caughey, T. K., "Derivation and Application of the Fokker–Planak Equation to Discrete Nonlinear Dynamic Systems Subjected to White Random Excitation," *J. Acou. Soc. Am.*, Vol. 35, No. 11, pp. 1683–1692 (1963).

84. Crandall, S. H., "Zero Crossings, Peeks, and Other Statistical Measures of Random Responses," *J. Acou. Soc. Am.*, Vol. 35, No. 11, pp. 1693–1699 (1963).

85. Dalzell, J. F., "A Note on the Distribution of Maxima of Ship Rolling," *J. Ship Res.*, Vol. 17, No. 4, pp. 217–226 (Dec 1973).

86. Roberts, J. B., "Comparison between Simulation Results and Theoretical Predictions for a Ship Rolling in Random Beam Waves," *J. Intern. Shipbldg. Prog.*, Vol. 31, No. 359, pp. 168–180 (Jul 1984).

87. Vinje, T., "On the Calculation of Maxima of Nonlinear Wave Forces and Wave Induced Motions," *J. Inter. Shipbldg. Prog.*, Vol. 23, No. 268, pp. 393–400 (Dec 1976).

88. Hineno, M., "The Calculation of the Statistical Distribution of the Maxima of Nonlinear Responses in Irregular Waves," *J. Soc. Nav. Arch. (Japan)*, Vol. 156, pp. 219–228 (1984).

89. Subba Rao, T., "On the Estimation of Bilinear Time Series Models," Tech. Report No. 79, Dept. of Mathematics (Statistics), Univ. of Manchester, Institute of Science and Technology, England (1977).

90. Tong, H., "Threshold Autoregressions, Limit Cycles and Cyclical Data," Tech. Report No. 101, Dept. of Mathematics (Statistics), Univ. of Manchester, Institute of Science and Technology, England (1978).

91. Ozaki, T., "Nonlinear Models for Nonlinear Random Vibrations," Tech. Report No. 92, Dept. of Mathematics (Statistics), Univ. of Manchester, Institute of Science and Technology, England (1978).

92. Ozaki, T., and H. Oda, "Nonlinear Time Series Model Identification by Akaike's Information Criterion," Information and Systems, ed. B. Dubuisson, Pergamon Press (1978).

93. Ozaki, T., "Statistical Analysis of Perturbed Limit Cycle Process Through Nonlinear Time Series Models," Research Memorandum, No. 158, Institute of Statistical Mathematics, Tokyo (1979).

94. Haggan, V. and T. Ozaki, "Modeling Nonlinear Random Vibrating Using an Amplitude–Dependent Autoregressive Time Series Model," Tech. Report No. 115, Institute of Science and Technology, Univ. of Manchester, England (Jun 1979).

REFERENCES (Continued)

95. Haggan, V. and T. Ozaki, "Amplitude-Dependent AR Model Fitting for Nonlinear Random Vibrations," in: Proceedings of International Time Series Meeting, Univ. of Nottingham, England (Mar 1979), ed. O. D. Anderson, North Holland, The Netherlands (1980).

96. Ozaki, T., "Nonlinear Phenomena and Time Series Models," Paper presented at the Forty-Third Session of the International Statistical Institute, Buenos Aires, Argentina (1981).

97. Ozaki, T., "Statistical Analysis of Duffing's Process Through Nonlinear Time Series Models," Research Memorandum No. 151, *Instit. Stat. Math.*, Tokyo (Mar 1979).

98. Ozaki, T., "Nonlinear Vibration and Time Series Model" (in Japanese), *Bull. Instit. Stat. Math.*, Tokyo, Vol. 28, No. 1, pp. 27–40 (1981).

99. Ozaki, T., "Nonlinear Threshold Autoregressive Models for Nonlinear Random Vibrations," Trans. by Applied Probability, Israel, *J. Appl. Prob.*, Vol. 18, pp. 443–451 (1981).

100. Ozaki, T., "Nonlinear Time Series Models and Dynamic Systems," Time Series in the Time Domain, ed. by E. J. Hannan, P. R. Krishmaiah, and M. M. Roo, Handbook of Statistics 5, North–Holland, The Netherlands, pp. 25–83 (1985).

SUPPLEMENT OF REFERENCES

101. Yamanouchi, Y., Some remarks on the "Statistical Estimation of Response Function of a Ship," in: Proceedings of the Fifth Symposium on Naval Hydrodynamics, Bergen, Norway, pp. 97–128 (Sep 1964).

102. Yamanouchi, Y., "Ship's Behavior on Ocean Waves as a Stochastic Process," in: Proceedings of the International Symposium on the Dynamics of Marine Vehicles and Structures in Waves, University College, London, Instit. Mech. Eng., pp. 167–181 (1974).

103. Yamanouchi, Y., "Nonlinear Response of Ships on the Seas," ed. by B. L. Clerkson, in: Proceedings of a Symposium, Pitmans, London, pp. 540–550 (1977).

104. On the Analysis of Random Processes for Engineers in Naval Architecture and Ocean Engineering, (in Japanese), ed. Y. Yamanouchi, Kaibundo, Tokyo, 337 pages (1986).

105. Oda, H., T. Ozaki, and Y. Yamanouchi, "A Nonlinear System Identification in the Analysis of Offshore Structure Dynamics in Random Waves," in: Proceedings of IUTAM Symposium on Nonlinear Stochastic Dynamic Engineering Systems, Innsbruck/Igls, Austria (1987), ed. by F. Ziegler, G. I. Schusller, Springer–Verlag, Berlin, Hidelberg, pp. 87–100 (1988).

106. Newman, J. N., "Second Order, Slowly Varying Forces on Vessels in Irregular Waves," in: Proceedings of the International Symposium on the Dynamics of Marine Vehicles and Structures in Waves, University College, London, Instit. Mech. Eng., pp. 182–186 (1974).

107. Faltinsen, O. M. and A. E. Loken, "Slow Drift Oscillations of a Ship in Irregular Waves," J. of Appl. Ocean Res., Vol. 1, No. 1, pp. 21–31 (1979).

108. Neal, E., "Second–Order Hydrodynamic Force Due to Stochastic Excitation," in: Proceedings of the Tenth Office Naval Research Symposium on Naval Hydrodynamics, Massachusetts Institute of Technology (1974).

109. Kac, M. and A. J. F. Siegert, "On the Theory of Noise in Radio Receivers with a Square Law Detector," J. of Appl. Phys., Vol. 18, pp. 383–397 (Apr 1974).

110. Naess, A., "Statistical Analysis of Second–Order Response of Marine Structures," J. of Ship Res., Vol. 29, No. 4, pp. 270–284 (Dec 1985).

111. Naess, A., "The Statistical Distribution of Second–Order Slowly Varying Forces and Motions," Applied Ocean Research, Vol. 8, No. 2, pp. 110–118 (1986).

112. Naess, A., "On the Statistical Analysis of Slow–Drift Forces and Motions of Floating Offshore," in: Proceedings of the Fifth International Offshore Mechanics and Arctic Engineering (OMAE) Symposium, Tokyo, Vol. 1, pp. 317–329 (1986).

SUPPLEMENT OF REFERENCES (Continued)

113. Naess, A., "The Joint Crossing Frequency of Stochastic Processes and Its Application to Wave Theory," Applied Ocean Research, Vol. 7, No. 1, pp. 35–50 (1985).

114. Naess, A., "Technical Note: On a Rational Approach to Extreme Value Analysis," Applied Ocean Research, Vol. 6, No. 3, pp. 7–18 (1984).

115. Langley, R. S., "A Statistical Analysis of Nonlinear Random Waves," Ocean Engineering, Vol. 14, No. 5, pp. 389–407 (1987).

116. Langley, R. S., "Second Order Frequency Domain Analysis of Moored Vessels," Applied Ocean Research, Vol. 9, No. 1, pp. 7–18 (1984).

117. Vinje, T., "On the Statistical Distribution of Second Order Forces and Motion," International Shipbuilding Progress, Vol. 30, No. 343, pp. 58–68 (1983).

118. Kato, S. and S. Ando, "Statistical Analysis of Low Frequency Responses of a Moored Floating Offshore Structure (1st Report)," Papers of Ship Research Institute, Vol. 23, No. 5, pp. 17–57 (1986).

119. Kinosita, K., S. Kato, and S. Takase, "Non–Normality of Probability Density Function of Total Second Order Responses of Moored Vessels in Random Seas," J. Soc. of Nav. Arch. (Japan), No. 164 (1988).

120. Kinosita, K. and S. Kato, "Nonlinear Response of Moored Floating Structures in Random Waves and Its Stochastic Analysis, Part I, Theory and Model Experiments," Papers of the Ship Research Institute, Vol. 27, No. 4, pp. 1–143 (1990).

121. Kim, K. I. and E. J. Powers, "A Digital Method of Modeling Quadratically Nonlinear Systems with a General Random Input," I.E.E.E. Transactions on Acoustics, Speech, and Signal Processing, Vol. 36, No. 11, pp. 1758–1769 (1988).

122. Kim, S. B., E. J. Powers, R. W. Miksad, F. J. Fischer, and J. Y. Hong, "Spectral Decomposition of Nonlinear TLP Sway Response to Non–Gaussian Irregular Sea," Offshore Technology Conference (OTC) 6134, in: Proceeding of Offshore Technology Conference, pp. 123–128 (1989).

123. Kim, S. B., E. J. Powers, R. W. Miksad, F. J. Fischer, and J. Y. Hong, "Spectral Decomposition of Nonlinear Time Series Analysis Techniques to TLP Model Test Data," Offshore Engineering in: Proceedings of the Seventh International Symposium on Offshore Technology, Rio de Janeiro, Brazil, Pentech Press, London, pp. 238–256 (1990).

124. Huang, N. E. and S. R. Long, "An Experimental Study of the Surface Elevation Probability Distribution and Statics of Wind–Generated Waves," J. Fl. Mech., Vol. 101, Part 1, pp. 179–200 (1980).

INITIAL DISTRIBUTION

Copies

6 OSD
  - 1 DDR&E
  - 1 Dep. Dir. Def. Res. & Engr. (R&AT)
  - 1 Dir. Engr. Tech.
  - 1 Dir. Research & Lab. Mgmt.
  - 1 Dep. Dir. (T&E)
  - 1 Chmn, Defense Sciences Bd.

1 DARPA
  - Dir. Def. Sci. Ofc.

1 DEPT OF THE ARMY
  - U.S. Army Laboratory Command
  - Dir. of Corps. Labs.

2 OFFICE OF THE SECY OF THE NAVY
  - 1 Asst. Secy. of the Navy (RD&A)
  - 1 DASN ASW

15 OCNR
  - 1 10
  - 1 10P
  - 1 11
  - 1 112
  - 1 113
  - 1 12
  - 1 121
  - 1 122
  - 1 20
  - 1 20T
  - 1 21
  - 1 211
  - 1 226
  - 1 233
  - 1 30

Copies

7 CNO
  - 1 096T
  - 1 098
  - 1 982F
  - 1 987L
  - 1 CNO Exec. Panel
  - 1 0911
  - 1 0912

2 NSWC
  - 1 Commanding Officer
  - 1 Technical Director

1 NUWC
  - Technical Director

1 NCCOSC
  - Technical Director

1 NAWC
  - Technical Director

1 NRL

4 USNA
  - 1 Dir. of Research
  - 1 Nav. Sys. Engr. Dept.
  - 1 B. Johnson
  - 1 Lib

2 SPAWAR
  - 1 05
  - 1 051

1 NAVAIR
  - Lib

1 NAVELEX
  - Lib

Copies

Copies					
1	NAVFAC		1	LC/SCI. & TECH. DIV.	
	ENL/Lib		1	MARAD/ADV. SHIP PROG. OFFICE	
10	NAVSEA				
	1	05	1	MMA/TECH. Lib	
	1	05B	1	NASA AMES RESEARCH	
	1	05R		CENTER	
	1	06		R. T. Medan, Ms 221–2	
	1	06R			
	1	50	1	NASA GODDARD SPACE	
	1	51		FLIGHT CENTER	
	1	55		N. E. Huang	

INITIAL DISTRIBUTION (Continued)

Copies

1 NAVFAC
ENL/Lib

10 NAVSEA
  1 05
  1 05B
  1 05R
  1 06
  1 06R
  1 50
  1 51
  1 55
  1 55W
  1 62

2 NADC – 01

3 NOSC
  1 01
  1 013
  1 014

2 NUSC, RI – 10

3 NUSC, CT – 10

2 NPRDC – 03

1 NAVPGSCOL

2 NCEL – L03

1 CAN NAVAL STUDIES GROUP

1 NARDIC

1 USMC (RD)

12 DTIC

1 USCG COMMANDANT
  CAPT D. Whitten

2 USCG R&D CENTER
  1 P. Teabeau
  1 K. Bitting

1 EPA OFFICE OF R&D
  R. Griffiths

Copies

1 LC/SCI. & TECH. DIV.

1 MARAD/ADV. SHIP PROG. OFFICE

1 MMA/TECH. Lib

1 NASA AMES RESEARCH CENTER
  R. T. Medan, Ms 221–2

1 NASA GODDARD SPACE FLIGHT CENTER
  N. E. Huang

1 NASA LANGLEY RESEARCH CENTER

1 NASA/SCI. & TECH. INFO. FACILITY

1 NSF/Eng. Div.

1 Univ. of Bridgeport
  Mech. Engr. Dept.

5 Univ. of California/Berkeley
  College of Engr., NA Dept.
  1 Lib
  1 J. R. Paulling
  1 J. V. Wehausen
  1 W. Webster
  1 R. Yeung

1 Univ. of California/Santa Barbara
  M. Tulin

1 Univ. of California/Scripps

3 CA Inst. of Tech.
  1 A. J. Acosta
  1 T. Y. Wu
  1 Lib

1 Catholic Univ./Mech. Engr.

1 Colorado State Univ.
  Dept. of Civ. Engr.

Copies

		Copies		
1	Univ. of Connecticut Hyd. Research Lab.	1	Univ. of Minnesota St. Anthony Falls R. Arndt	
1	Florida Atlantic Univ. Ocean Engr. Lib	2	City College, CUNY	
1	Univ. of Florida M. Ochi		1 W. J. Pierson, Jr. 1 L. Tick	
1	Harvard Univ./Dept. of Math.	1	Oregon State Univ.	
1	Univ. of Hawaii	1	Penn State Univ. Applied Research Lab.	
1	Univ. of Illinois College of Engr. J. M. Robertson Theoretical & Applied Math.	2 2	SAI/Annapolis Southwest Research Inst. 1 Director 1 Applied Mech. Review	
1	State Univ. of Iowa Iowa Inst. of Hydr. Research – Director	1 2	Stanford Research Inst./Lib Stevens Inst. of Tech. Davidson Lab.	
1	Johns Hopkins Univ. Prof. Owen Phillips		1 Director 1 Lib	
1	Johns Hopkins Univ./APL Tech. Lib	1	Texas A&M	
1	Kansas State Univ. Eng. Exp. Station	1 1	Univ. of Texas/Arlington Utah State Univ./College of Engr. R. W. Jeppson	
1	Lehigh Univ./Fritz Lab. Lib			
1	Long Island Univ. Grad. Dept. of Marine Sci.	3	VPI 1 J. Schetz	
1	Delaware Univ./Math. Dept.		1 A. Nayfeh 1 D. Mook	
4	Massachusetts Inst. of Tech. Dept. of Ocean Engr. 1 J. R. Kerwin 1 J. N. Newman 1 P. Sclavounos 1 T. F. Ogilvie	2	Webb Institute 1 Lib 1 L. W. Ward	
		1	Worcester Poly. Inst. Alden Research Lab.	
3	Univ. of Michigan/Dept. NAME 1 Lib 1 R. Beck 1 A. Troesch	1 1	Woods Hole Ocean Engr. Dept. SNAME	

INITIAL DISTRIBUTION (Continued)

Copies		Copies	
1	Aerojet–General W. C. Beckwith	1	Raytheon Company
1	Analytical Methods Inc.	1	Sperry Systems Mgmt.
1	AT&T Technologies, Inc.	1	TRW Systems Division
1	Bendix Oceanics	1	Westinghouse Electric Corp. B. Kaminsky

Copies

1 Aerojet–General
    W. C. Beckwith

1 Analytical Methods Inc.

1 AT&T Technologies, Inc.

1 Bendix Oceanics

1 Bolt, Beranek & Newman, MA

1 The Glosten Associates
    B. L. Hutchinson

1 CALSPAN, Inc.
    Applied Mech. Dept.

1 Flow Research, Inc.

2 General Dynamics Corp.
  1 Electric Boat Div.
  1 V. T. Boatwright, Jr.

1 Gibbs & Cox, Inc.
    Tech. Info. Control Section

1 Grumman Aircraft Eng. Corp.
    W. P. Carl, Mgr.
    Grumman Marine

1 Hydromechanics, Inc.
    P. Kaplan

4 Lockheed Aircraft Corp.
    Lockheed Missiles & Space
  1 R. L. Waid
  1 R. Lacy
  1 R. Perkins
  1 R. Kramer

1 Martin Marietta Corp./Rias

1 McDonnell–Douglas Corp./DAC
    Lib

1 Newport News Shipbuilding
    Lib

1 North American Rockwell
    Los Angeles Division

Copies

1 Raytheon Company

1 Sperry Systems Mgmt.

1 TRW Systems Division

1 Westinghouse Electric Corp.
    B. Kaminsky

CENTER DISTRIBUTION

Copies	Code	Name
1	01	
1	0112	
1	0113	
1	12	
1	1230	
1	1280	
1	14	
1	15	
1	1504	
1	1506	
1	152	
1	1521	
1	1522	
1	1523	
30	154	
1	1541	
1	1542	
1	1544	
1	156	
1	1561	G. Cox
1	1561	J. Dalzell
1	1561	J. O'Day
1	1562	
1	1563	
1	1564	

INITIAL DISTRIBUTION (Continued)

Copies

1	17	
1	173	
1	1843	
1	341	Publications
1	341	M. Gotthardt
1	341	C. Naas
1	341	A. Phillips
1	342.1	TIC (C)
1	342.2	TIC (A)
10	3432	Reports Control